

Extended Duration Orbiter Medical Project

**Final Report
1989–1995**

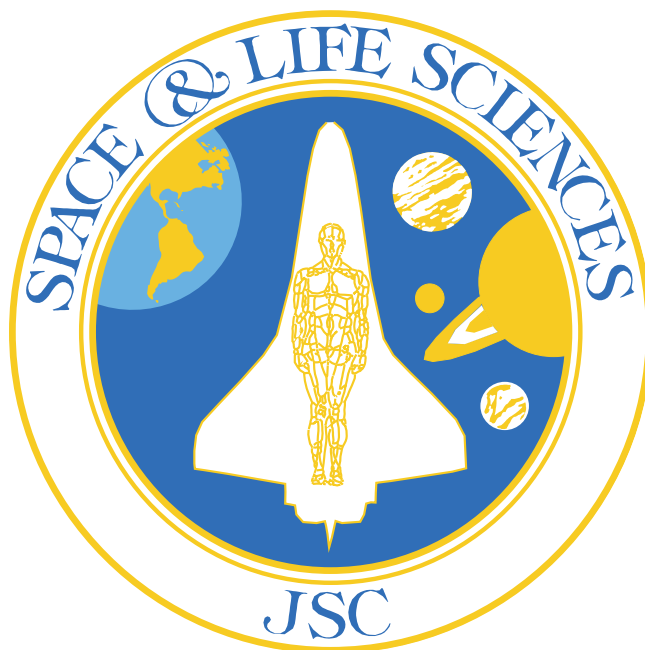


National Aeronautics and
Space Administration

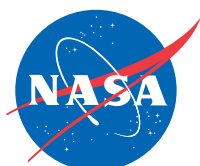
Lyndon B. Johnson Space Center
Houston, Texas

Extended Duration Orbiter Medical Project

Final Report



1989 – 1995



National Aeronautics and
Space Administration

Lyndon B. Johnson Space Center
Houston, Texas

Project Management

J. Travis Brown
Project Manager, EDOMP
NASA Johnson Space Center,
Houston, Texas

Charles F. Sawin, Ph.D.
Project Scientist, EDOMP
NASA Johnson Space Center,
Houston, Texas

Editors

Charles F. Sawin, Ph.D.
Managing Editor

Gerald R. Taylor, Ph.D.
Science Editor

Wanda L. Smith
Editor & Coordinator

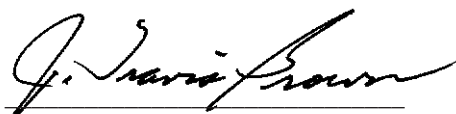
Preface

Biomedical issues have presented a challenge to flight physicians, scientists, and engineers ever since the advent of high-speed, high-altitude airplane flight in the 1940s. In 1958, preparations began for the first manned space flights of Project Mercury. The medical data and flight experience gained through Mercury's six flights and the Gemini, Apollo, and Skylab projects, as well as subsequent space flights, comprised the knowledge base that was used to develop and implement the Extended Duration Orbiter Medical Project (EDOMP).

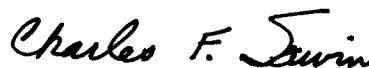
The EDOMP yielded substantial amounts of data in six areas of space biomedical research. In addition, a significant amount of hardware was developed and tested under the EDOMP. This hardware was designed to improve data gathering capabilities and maintain crew

physical fitness, while minimizing the overall impact to the microgravity environment.

The biomedical findings as well as the hardware development results realized from the EDOMP have been important to the continuing success of extended Space Shuttle flights and have formed the basis for medical studies of crew members living for three to five months aboard the Russian space station, Mir. EDOMP data and hardware are also being used in preparation for the construction and habitation of International Space Station. All data sets were grouped to be non-attributable to individuals, and submitted to NASA's Life Sciences Data Archive. They will be integrated into the archive, which is accessible at <http://lsda.jsc.nasa.gov>.



J. Travis Brown
Project Manager, EDOMP
NASA, Johnson Space Center
Houston, Texas



Charles F. Sawin, Ph.D.
Project Scientist, EDOMP
NASA, Johnson Space Center
Houston, Texas

Acronyms and Abbreviations

A/G	air-to-ground	DBP	diastolic blood pressure (mmHg)
ABPM	automatic blood pressure monitor	DFRC	Dryden Flight Research Center
AC	alternating current	DIB	Device Interface Box
ACES	Advanced Crew Escape Suit	DLW	doubly labeled water
AERIS	American Echocardiograph Research Imaging System	DOF	degree of freedom
ALBERT	Advanced Lower Body Extremities Restraint Test	DOME	Device for Orientation and Movement Environments
amu	atomic mass unit	DSO	Detailed Supplementary Objective
ANCOVA	analysis of covariance	DTO	Development Test Objective
ANOVA	analysis of variance	EAFB	Edwards Air Force Base
APAP	appearance of acetaminophen	EC	eyes closed
AOS	Archival Organic Sampler	ECG	electrocardiography
APT	airport passenger transporter	ECLSS	Environmental Control and Life Support System
ASE	American Society of Echocardiography	ECW	extracellular water
ASV	aircraft service vehicle	EDO	Extended Duration Orbiter
BCR	Bar Code Reader	EDOMP	Extended Duration Orbiter Medical Project
BDCF	Baseline Data Collection Facility	EDVI	end diastolic volume index
BERS	Bioelectrical Response Spectrography	EF	ejection fraction
BIP	Biomedical Instrumentation Port	ELOG	Electronic Light Occlusion Goggles
BP	blood pressure	EMI	electromagnetic interference
bpm	beats per minute	EMG	electromyography or electromyogram
BR	Biorack	EO	eyes open
CBPD	Continuous Blood Pressure Device	EOG	electro-oculogram
CCM	credit card memory	ESA	European Space Agency
CCT	Crew Compartment Trainer	ESP	electroshock protection
CE	Cycle Ergometer	ESVI	end systolic volume index
CFU	colony forming unit	EV	exposure value
CH ₄	methane	EVA	extravehicular activity
CHeCS	Crew Health Care System	EVIS	Ergometer Vibration Isolation System
CM	countermeasure	FD	flight day
cm	centimeter	FFT	Full Fuselage Trainer
cm ²	square centimeter	FIR	finite impulse response
CNES	Centre Nationae d'Etudes Spatiales (French Space Agency)	FMK	Formaldehyde Monitoring Kit
CNS	central nervous system	ft	foot
CO	carbon monoxide	FTIR	Fourier Transform infrared spectroscopy
COM	center of mass	g	gravity
CORB	carbon monoxide rebreathing	GBX	materials science glove box
COTS	commercial off-the-shelf	GC/MS	gas chromatograph/mass spectrometer
CP	consistency of procedures	GCM	Generalized Controller Module
CPA	Combustion Products Analyzer	GE	gastric emptying
CRT-TV	Cathode Ray Tube Television	GI	gastrointestinal
CSA	cross-sectional area	gm	gram
CTV	Crew Transport Vehicle	GPWS	General Purpose Work Station
DAS	Data Acquisition System	GRAF	Graphics Research Analysis Facility

GSC	grab sample container	MSFC	George C. Marshall Space Flight Center
² H	deuterium	mph	miles per hour
H ₂	hydrogen	MSIS	Man-Systems Integration Standards
HCl	hydrogen chloride	NBP	neutral body posture
HCN	hydrogen cyanide	NRCCOT	National Research Council Committee on Toxicology
HF	hydrogen fluoride		
HFA	human factors assessment		
HP	Hewlett Packard	¹⁸ O	heavy oxygen
HR	heart rate	OASIS	Operations Acquisition System In-situ
HRF	Human Research Facility	OBS	Orbiter Bioinstrumentation System
HRM	High Rate Multiplexer	OI	Operational Investigation
HRPPC	Human Research Policy and Procedures Committee	OTTR	otolith tilt-translation reinterpretation
Hz	hertz		
		PAC	premature atrial contraction
ICW	intracellular water	PAT	Preflight Adaptation Trainer
IJP	in-flight job performance	PC	personal computer
ILC	integrated logic circuit	PCBA	Portable Clinical Blood Analyzer
IML	International Microgravity Laboratory	PCIS	Passive Cycle Isolation System
ISS	International Space Station	PCR	polymerase chain reaction
IUCA	In-flight Urine Collection Absorber	PDLC	polymer dispersed liquid crystal
IVA	intravehicular activity	PGSC	Payload General Support Computer
IVIS	Inertial Vibration Isolation System	PI	Principal Investigator
IZ	internal Z (axis)	POCC	Payload Operations Control Center
		PRN	post-rotatory nystagmus
JSC	Lyndon B. Johnson Space Center	PSSF	Postflight Science Support Facility
		PVAT	Posture Video Analysis Tool
kg	kilogram	PVC	premature ventricular contraction or polyvinyl chloride
KSC	John F. Kennedy Space Center		
		QD	quick disconnect
l	liter		
lb	pound	RAU	Remote Acquisition Unit
LBNP	lower body negative pressure	RCS	Reuter Centrifugal Sampler
LCD	liquid crystal display	REA	resistive exercise accessories
LCG	Liquid Cooling Garment	REAGS	Re-Entry Anti-Gravity Suit
LCM	Liquid Crystal Display Module	RF	radio frequency
LES	launch and entry suit	RFLP	restriction fragment length polymorphism
LMV	latency to maximum vection	rpm	revolutions per minute
LOV	latency to onset of vection	R-R	R to R interval (pertains to the “QRS” wave of an ECG)
LVMI	left ventricular mass index		
		s	second
μm	micrometer	SAMS	Space Acceleration Measurement System
m	meter	SBP	systolic blood pressure (mmHg)
MANOVA	multivariate analysis of variance	SEM	scanning electron microscopy; standard error of the mean
MAP	mean arterial pressure		
MAS	microbial air sampler	Shuttle	U. S. Space Shuttle
MCTT	mouth-to-cecum transit time	SLD	Subject Load Device
MDM	multiplexer/demultiplexer	SMA	Science Monitoring Area
MET	Mission Elapsed Time	SMAC	spacecraft maximum allowable concentrations
ml	milliliter		
mm	millimeter	SMS	space motion sickness
mmHg	millimeters of mercury	SOP	standard operating procedure
MMD	Microgravity Measuring Device	SOT	Sensory Organization Test
MRI	Magnetic Resonance Imaging	SPS	Shuttle Particle Sampler
ms	milliseconds		

SPM	Shuttle Particle Monitor	$\dot{V}O_2$	volume of oxygen consumed (in liters)
SSAS	Solid Sorbent Air Sampler	$\dot{V}O_{2max}$	maximum oxygen consumed
STE	stimulated echo	$\dot{V}O_{2peak}$	peak volume of oxygen consumed per unit of time
STS	Space Transportation System	VOC	volatile organic contaminant
SVI	stroke volume index	VOR	vestibulo-ocular reflex
TBP	total body protein	VS	visual-spatial or visual scene
TCT	task completion time	VSIZE	visual scene versus internal Z axis overall
TEE	total energy expenditure	VSIZE	visual scene versus internal Z axis time of transition
TF	training fidelity	VTR	video tape recorder
TPRI	total peripheral resistance index	VVOR	visually assisted vestibulo-ocular reflex
TTD	Tilt Translation Device	W	watt
UCD	Urine Collection Device	WCS	Waste Collection System
UCLA	University of California/Los Angeles	WETF	Weightless Environment Test Facility
USML	United States Microgravity Laboratory	WHO	World Health Organization
UTAF	Usability Testing and Analysis Facility	W&P	(total body) water and (total body) protein
UTC	User Time Clock	XRF	X-ray fluorescence
VAC	volts alternating current	Y	year
$\dot{V}CO_2$	volume of carbon dioxide output		
VDC	volts direct current		
VHM	voluntary head movement		

Contents

	Page
Preface	iii
Acronyms and Abbreviations	v
Tables	xiii
Figures	xv
Introduction	xxiii
Section 1 Cardiovascular Deconditioning	1-1
Background	1-1
Goal 1 - Descriptive Studies	1-1
Introduction	1-1
Methods and Materials	1-1
Results	1-2
Conclusions	1-4
Goal 2 - Mechanistic Studies	1-6
Introduction	1-6
Methods and Materials	1-6
Results	1-6
Conclusions	1-10
Goal 3 - Countermeasure Studies	1-10
Introduction	1-10
Methods and Materials	1-10
Results	1-13
Conclusions	1-15
Discussion	1-16
Summary	1-17
Recommendation	1-18
References	1-18
Section 2 Regulatory Physiology	2-1
Background	2-1
Methods and Results	2-3
Energy and Metabolic Requirements for Extended Duration Space Flight (DSO 612)	2-3
In-flight Assessment of Renal Stones (DSO 610)	2-4
Gastrointestinal Function During Extended Duration Space Flight (DSO 622)	2-4
Assessment of Circadian Shifting in Astronauts by Bright Light (DSO 484)	2-5
Evaluation of a Portable Clinical Blood Analyzer (DSO 492)	2-6
Evaluation of an In-flight Urine Collection Absorber (DSO 328)	2-7
Discussion	2-7
References	2-8
Section 3 Functional Performance Evaluation	3-1
Introduction	3-1
Part 1 - Skeletal Muscle Adaptations of Space Flight	3-1
Purpose	3-1
Background	3-2

Skeletal Muscle Performance (DSOs 477 & 617)	3-3
Skeletal Muscle Biopsies (DSO 475)	3-8
Quantifying Muscle Size by Magnetic Resonance Imaging (MRI) (DSO 606)	3-10
Part 2 - The Effect of In-flight Exercise on Postflight Exercise Capacity and Orthostatic Function	3-10
Purpose	3-10
Background	3-11
Exercise In Flight and the Effects on Exercise Capacity at Landing (DSOs 476 & 608)	3-11
Sub-Maximal Exercise In Flight and Cardiac Performance at Landing (DSO 624)	3-12
Effects of Intense Exercise Before Landing on Aerobic Capacity and Orthostatic Function at Landing (DSO 618)	3-14
Part 3 - Changes in Body Composition in Space and the Effects on Exercise Performance	3-18
Purpose	3-18
Background	3-18
Changes in Body Composition after EDO Flights	3-18
Changes in Protein and Fluid Volumes and the Effects on Performance	3-19
Summary and Recommendations	3-20
Skeletal Muscle Performance	3-20
Exercise Capacity and Orthostatic Function	3-20
Body Composition and Exercise	3-21
References	3-21

Section 4 Environmental Health **4-1**

Background	4-1
Critical Questions	4-1
Approach	4-1
Methods	4-4
Investigations Using Existing Hardware	4-4
Investigations Requiring Equipment Development	4-4
Setting 30-Day Spacecraft Maximum Allowable Concentration (SMAC) Values	4-6
Results and Discussion	4-7
Accumulation of Chemical Air Pollutants	4-7
Assessment of Particulate Air Pollutants	4-7
Assessment of Accidental Chemical Releases	4-7
Microbial Contamination	4-8
Setting 30-Day Spacecraft Maximum Allowable Concentration (SMAC) Values	4-8
Countermeasures/Potential Countermeasures	4-9
Chemical Contaminant Countermeasures	4-9
Microbial Countermeasures	4-10
References	4-11

Section 5 Neurovestibular Dysfunction **5.1-1**

Part 5.1 - Overview of Studies Conducted	5.1-1
Introduction	5.1-1
Operational Investigations	5.1-1
Design and Definition of Protocols	5.1-4
Summary	5.1-4
References	5.1-5
Part 5.2 - Visual-Vestibular Integration: Motion Perception Reporting (DSO 604 OI-1)	5.2-1
Background	5.2-1
Methods	5.2-2
Results and Discussion	5.2-4

Summary	5.2-6
References	5.2-7
Figures	5.2-8
Part 5.3 - Visual-Vestibular Integration as a Function of Adaptation of Space Flight and Return to Earth (DSO 604 OI-3)	5.3-1
Background	5.3-1
Methods	5.3-6
Results and Discussion	5.3-10
References	5.3-18
Figures	5.3-22
Part 5.4 - Recovery of Postural Equilibrium Control Following Space Flight (DSO 605)	5.4-1
Background	5.4-1
Methods	5.4-3
Results and Discussion	5.4-6
Conclusion	5.4-9
References	5.4-10
Figures	5.4-12
Part 5.5 - Effects of Space Flight on Locomotor Control (DSO 614)	5.5-1
Background	5.5-1
Methods	5.5-4
Results	5.5-13
Discussion	5.5-22
References	5.5-31
Figures	5.5-37
Section 6 Assessment of Human Factors	6-1
Introduction	6-1
Space Human Factors Topics	6-1
Ergonomic Evaluations of Microgravity Gloveboxes	6-1
Lower Body Negative Pressure (LBNP) System	6-2
Stowage, Restraints, Deployment and Cables	6-3
Crew Productivity – Task and Timeline Analysis	6-4
Touchscreen Usability in Microgravity	6-5
Electronic Procedures	6-5
Vibration Evaluation in Microgravity	6-5
Acoustic Noise Environment	6-6
Lighting Assessment	6-9
Translation Through a Transfer Tunnel	6-9
Neutral Body Posture	6-11
Questionnaires	6-12
Summary	6-13
References	6-13
Section 7 Facilities	7-1
Landing Site Medical Facilities	7-1
Background	7-1
Edwards Air Force Base (EAFB)	7-1
Kennedy Space Center (KSC)	7-2
Crew Transport Vehicle (CTV)	7-2
Johnson Space Center (JSC)	7-3

Section 8 Hardware	8-1
Introduction	8-1
Specific Flight Hardware and Ground Support Items	8-2
Ambulatory Cardiovascular Monitoring Assembly	8-2
Lower Body Negative Pressure (LBNP) System	8-2
Data Acquisition System (DAS)	8-5
Operations Acquisition System In-situ (OASIS)	8-5
American Echocardiograph Research Imaging System (AERIS)	8-5
Re-entry Anti-gravity Suit (REAGS)	8-6
Bar Code Reader	8-6
Urine Collection Kit	8-7
In-flight Urine Collection Absorber (IUCA)	8-7
Saliva Collection Kit	8-7
Breath Sample Kits	8-8
Doubly Labeled Water (DLW) Dose Kits	8-8
Performance Test Unit	8-8
Actilume	8-8
Glucometer Kit	8-8
Drug Administration Kit	8-8
Heart Rate Watch Assembly	8-8
Microbial Air Sampler	8-9
Combustion Products Analyzer	8-9
Archival Organic Sampler	8-10
Formaldehyde Monitor Kit	8-10
Shuttle Particle Sampler (SPS) and Shuttle Particle Monitor (SPM)	8-10
Visual-Vestibular Data System (Superpocket)	8-11
Locker-Mounted Video Camera System	8-12
Cycle Ergometer	8-12
Ergometer Vibration Isolation System (EVIS)	8-13
Passive Cycle Isolation System (PCIS)	8-14
Inertial Vibration Isolation System (IVIS) for the Cycle Ergometer	8-14
Microgravity Measuring Device (MMD)	8-15
EDO Treadmill	8-15
EDO Rower (MK-1 and MK-2)	8-17
Conclusion	8-18
Section 9 Project Summary and Conclusions	9-1
Cardiovascular Deconditioning	9-3
Regulatory Physiology	9-4
Functional Performance Evaluation	9-4
Environmental Health	9-5
Neurovestibular Dysfunction	9-5
Human Factors	9-6
Gloveboxes	9-6
Lower Body Negative Pressure (LBNP)	9-6
Stowage, Restraints, Deployment and Cables	9-6
Touchscreen Usability in Microgravity	9-6
Vibration in Flight	9-6
Acoustic Noise Environment	9-6
Facilities	9-6
Hardware	9-7
Conclusions	9-7
Appendices	
EDOMP Medical DSOs Listed by Discipline	A-1
EDOMP Subject Participation	B-1
EDOMP Publications	C-1

Tables	Page
Section 1 Cardiovascular Deconditioning	1-1
1-1 Cardiovascular EDOMP studies	1-2
1-2 Cardiovascular measurements (mean ± SEM) before and after short-duration spaceflight	1-5
1-3 Measurements from all subjects on all test days	1-7
1-4 Subjects grouped according to relative orthostatic tolerance judged by cardiovascular parameters	1-8
1-5 Supine measurements from all subjects on all test days	1-12
1-6 Comparison of landing day values for presyncopal vs. non-presyncopal astronaut subjects	1-14
Section 2 Regulatory Physiology	2-1
2-1 EDOMP regulatory physiology investigations	2-3
2-2 Energy intake and expenditure, and fluid intake and turnover, from 13 men before and during 8- to 14-day spaceflights	2-3
2-3 Renal stone risk-assessment profile for six male astronauts before, during, and after 11- to 16-day space shuttle missions	2-5
2-4 Pharmacokinetics of acetaminophen after a 650-mg oral dose in two crew members	2-6
Section 3 Functional Performance Evaluation	3-1
3-1 Investigations constituting the functional performance evaluation of the Extended Duration Orbiter Medical Project	3-2
3-2 DSO 477 mean skeletal muscle strength performance on landing day vs. preflight	3-6
3-3 Measurements from all subjects on all test days (DSOs 476, 608, 618, 624)	3-11
3-4 Flight duration and “exercise volume” (%HRmax × min/week) for DSOs 476 and 608	3-13
Section 4 Environmental Health	4-1
4-1 Accumulation of dichloromethane in spacecraft air	4-7
4-2 Formaldehyde concentrations in spacecraft air	4-7
4-3 Particle masses from the SPS on STS-32 and STS-40	4-7
4-4 Air contamination incidents in the Space Shuttle	4-8
4-5 Decreases in selected SMAC values for the EDOMP	4-10
Section 5 Neurovestibular Dysfunction	
Part 5.1 Neuroscience investigations: an overview of studies conducted	5.1-1
5.1-1 Extended Duration Orbiter Medical Project (EDOMP) neuroscience discipline implementation team members	5.1-4
5.1-2 EDOMP neuroscience investigations	5.1-5
Part 5.2 Visual-vestibular integration motion perception reporting (DSO 604 OI-1)	5.2-1
5.2-1 Evaluation of education/demonstration components of the PAT program	5.2-6

Part 5.3	Visual-vestibular integration as a function of adaptation to space flight and return to Earth (DSO 604 OI-3)	5.3-1
5.3-1	Operational investigations (OI) performed on designated flights and total number of subjects	5.3-6
5.3-2	Types of eye movements required for pursuit tracking	5.3-10
5.3-3	Classification of Stark types	5.3-16
Part 5.4	Recovery of postural equilibrium control following space flight (DSO 605)	5.4-1
5.4-1	DSO 605 experiment test schedule	5.4-4
5.4-2	Subject demographic information	5.4-7
5.4-3	Preflight and postflight data for the six experiment test conditions	5.4-8
Part 5.5	Effects of space flight on locomotor control (DSO 614)	5.5-1
5.5-1	Experiment conditions	5.5-6
5.5-2	Number of significant differences in preflight and postflight variables	5.5-12
5.5-3	ANOVA results of phaseplane variability as a function of stride epoch and flight	5.5-15
5.5-4	Frequency distribution of preflight-to-postflight muscle activation correlation coefficients for the combination of the right and left lower limbs	5.5-16
5.5-5	Frequency distribution of right vs. left lower limb muscle activation correlation coefficients combined for preflight and postflight conditions	5.5-16
5.5-6	Onset and duration (as percent of stride cycle) of muscle activation before and after space flight	5.5-17
5.5-7	Offset and duration (as percent of stride cycle) of tibialis anterior activations before and after space flight	5.5-18
5.5-8	Subject classification based on kinematic measurements	5.5-20
5.5-9	Stiffness and damping in second order model	5.5-21
5.5-10	Second order response parameters	5.5-22
Section 6	Assessment of Human Factors	6-1
6-1	EDOMP human factors engineering Detailed Supplementary Objective (DSO) 904 topics	6-1
6-2	Approximations of microgravity experiment crew time usage (STS-40/SLS-1)	6-4
6-3	Comparison of measured sound levels for STS-40, STS-50 and STS-57	6-7
Section 7	Facilities No tables in this section	
Section 8	Hardware	8-1
8-1	Ground-based EDOMP hardware	8-1
Section 9	Project Summary and Conclusions	9-1
9-1	Initial EDOMP concerns that led to significant findings and resulted in countermeasures and flight rules for space shuttle missions	9-1

Figures

Page

Section 1 Cardiovascular Deconditioning	1-1
1-1 Heart rate and arterial pressure before, during, and after flight.	1-3
1-2 Intrasubject standard deviations of heart rate and arterial pressure before, during, and after flight.	1-3
1-3 Premature atrial and ventricular contractions before, during, and after flight.	1-4
1-4 Systolic and diastolic pressure response to entry, landing, and egress.	1-4
1-5 Heart rate response to entry and landing.	1-4
1-6 Carotid baroreceptor vagal-cardiac reflex responses before flight and on landing day.	1-7
1-7 Preflight and landing day differences between standing and supine systolic and diastolic pressures and heart rate.	1-8
1-8 Preflight-to-postflight (landing day) changes of operational points and systolic pressure responses to standing.	1-9
1-9 Comparisons of preflight to landing day changes between 2 groups identified by cluster analysis.	1-9
1-10 Three-dimensional plot of power spectra of R-R intervals during controlled frequency breathing for 12 subjects, all days.	1-9
1-11 R-R interval spectral power: average total power, power in 0.05- to 0.15-Hz band, 0.2- to 0.3-Hz band, and ratio of low- to high-frequency power.	1-9
1-12 Arterial pressure responses during Valsalva maneuvers preflight, on landing day, and 3 days after landing.	1-10
1-13 Blood pressure and heart rate responses of 2 subjects during Valsalva maneuvers.	1-11
1-14 Supine and standing plasma norepinephrine and epinephrine concentrations before and after spaceflight.	1-11
1-15 Beat-to-beat blood pressure and heart rate during stand tests.	1-13
1-16 Heart rate, systolic blood pressure, and diastolic blood pressure during LBNP test preflight and in flight at maximum level of LBNP for four astronauts.	1-15
1-17 Postflight stand test with g-suit inflated.	1-15
1-18 Effect of fludrocortisone on plasma volume losses.	1-16
Section 2 Regulatory Physiology No figures in this section	
Section 3 Functional Performance Evaluation	3-1
3-1 A subject undergoes strength and endurance testing with the LIDO® dynamometer.	3-4
3-2 U.S. Space Shuttle treadmill.	3-5
3-3 Examples of force-velocity curves for concentric strength, eccentric strength, and concentric endurance tests.	3-6
3-4 Changes in strength of the knee, lower leg, and trunk on landing day in those who exercised on a treadmill during flight versus those who did not.	3-7
3-5 DSO 617 changes in elbow (3-5 a) and wrist (3-5 b) strength after space flight in crew members who conducted EVA during flight versus one who did not.	3-8
3-6 Preflight vs. postflight, percent change by skeletal muscle fiber type of the vastus lateralis.	3-9
3-7 Changes in the distribution of Type I and Type II muscle fibers in the vastus lateralis on landing day after 11 days or 5 days of space flight.	3-9
3-8 Percent change of mean number of capillaries per fiber type following 11 days of space flight.	3-10

3-9	Preflight-to-postflight changes in VO_{2peak} for 40 participants in DSOs 476 and 608.	3-13
3-10	DSO 624 subjects who performed identical work rates before and after flight.	3-14
3-11	In-flight exercise patterns appear to influence the degree of oxygen consumption change at the termination workload (85% age-predicted HR max) following flight.	3-14
3-12	Heart rate and arterial pressure responses to preflight and landing day stand tests.	3-16
3-13	Aerobic capacity of DSO 618 subjects.	3-16
3-14	Pre- and in-flight heart rate responses of DSO 618 subjects.	3-17
3-15	Changes in body weight, fat-free mass, total body water, intracellular water, total body mineral, and total body protein in 10 astronauts after 7- to 16-day flights.	3-17
3-16	Percent decreases in muscle volumes, measured by magnetic resonance imaging, from three EDO Shuttle missions.	3-19
3-17	Influence of fluid volumes and protein on aerobic capacity before and after space flight.	3-20
Section 4 Environmental Health		4-1
4-1	Air sampling devices.	4-2
4-2	Microbial quantitation of spacecraft air.	4-9
4-3	Microorganisms isolated from in-flight air samples.	4-10
4-4	Bacteria and fungi isolated from ten U.S. Space Shuttle surface sites.	4-11
Section 5 Neurovestibular Dysfunction		
Part 5.1 Neuroscience Investigations An Overview of Studies Conducted		5.1-1
5.1-1	Stimulus and response make-up of spatial orientation with a schematic of the neural substrate.	5.1-2
Part 5.2 Visual-Vestibular Integration Motion Perception Reporting (DSO 604 OI-1)		5.2-1
5.2-1	Percent of astronauts who reported self and/or surround motion associated with making voluntary head/body movements while fixating near and far visual targets in flight, during entry and at wheels stop.	5.2-8
5.2-2	Percent of astronauts who reported self motion and surround motion associated with making voluntary pitch, roll, and yaw head/body movements while fixating near and far visual targets on-orbit, during entry and at wheels stop.	5.2-8
5.2-3	Percent of astronauts on short and medium duration missions who reported self vs. surround motion associated with making voluntary head/body movements in flight and during the entry and immediate postflight periods.	5.2-9
5.2-4	Percent of astronauts who reported gain, temporal, and path input-output disturbances in flight and during the entry and immediate postflight periods.	5.2-9
5.2-5	Percent of internal Z-axis and visuo-spatial astronauts on short and medium duration missions who reported self and/or surround motion in flight and during the entry and immediate postflight periods.	5.2-9
5.2-6	Percent of self motion in the roll plane postflight, during exposure to the tilt-translation device, reported by internal Z-axis and visuo-spatial astronauts on short and medium duration missions.	5.2-10
5.2-7	Average number of reports (across all roll motion profiles in the tilt-translation device) of asymmetries in the perceived roll amplitude experienced postflight for the internal Z-axis and the visuo-spatial astronauts.	5.2-10
5.2-8	Average number of reports (across all roll motion profiles in the tilt-translation device) of asymmetries in the perceived roll amplitude experienced postflight for the internal Z-axis and the visuo-spatial astronauts on short and medium duration missions.	5.2-10

5.2-9	Average number of reports (across all roll motion profiles in the tilt-translation device) of visual disturbances (e.g., oscillopsia, blurring or tilting of the stripes inside the device) preflight and postflight.	5.2-10
5.2-10	Mean onset to vection latency (sec) preflight (produced by the device for orientation and motion environments) for astronauts who transitioned from a visual to an internal orientation rest frame early, mid, and late in flight.	5.2-11
5.2-11	Mean latency to the onset of vection preflight (produced by the device for orientation and motion environments) for the internal Z-axis, the visuo-spatial, and the mixed rest frame of reference astronauts.	5.2-11
5.2-12	Mean latency to the onset of vection and to maximum vection preflight and postflight (produced by the device for orientation and motion environments) for the internal Z-axis, the visuo-spatial, and the mixed rest frame of reference astronauts.	5.2-11
5.2-13	Mean latency to the onset of vection and to maximum vection preflight and postflight (produced by the device for orientation and motion environments) for the rookie and veteran astronauts.	5.2-12
5.2-14	Mean latency to the onset of vection and to maximum vection preflight and postflight (produced by the device for orientation and motion environments) for astronauts on short, medium, and long duration missions.	5.2-12

**Part 5.3 Visual-Vestibular Integration as a Function of Adaptation to Space
Flight and Return to Earth (DSO 604 OI-3)**

		5.3-1
5.3-1	Representation of target location on tangent screen.	5.3-22
5.3-2	Unpredictable pursuit tracking: ramp stimulus.	5.3-22
5.3-3	Predictable smooth pursuit: sinusoidal stimulus.	5.3-22
5.3-4	Vertical and horizontal eye calibration.	5.3-22
5.3-5	Various calibration curves applied to a vertical target acquisition eye movement response.	5.3-23
5.3-6	Dynamic, fixed-gaze eye calibration curve – vertical.	5.3-23
5.3-7	Geometrical gaze correction.	5.3-24
5.3-8	Vertical smooth pursuit: eyes only.	5.3-24
5.3-9	Horizontal smooth pursuit: eyes only.	5.3-24
5.3-10	Cumulative time foveation is off target.	5.3-25
5.3-11	Loss of acuity with target displacement from foveal center.	5.3-25
5.3-12	Total number saccades: horizontal and vertical smooth pursuit.	5.3-25
5.3-13	Total catch-up saccades: horizontal and vertical smooth pursuit.	5.3-25
5.3-14	Total anticipatory saccades: horizontal and vertical smooth pursuit.	5.3-26
5.3-15	Cumulative gaze error time (%): horizontal and vertical smooth pursuit.	5.3-26
5.3-16	Horizontal – smooth pursuit (eyes only).	5.3-27
5.3-17	Vertical – smooth pursuit (eyes only).	5.3-27
5.3-18	Vertical pursuit tracking with head and eyes.	5.3-28
5.3-19	Total number saccades: horizontal and vertical head/eye pursuit.	5.3-29
5.3-20	Total catch-up saccades: horizontal and vertical head/eye pursuit.	5.3-29
5.3-21	Total anticipatory saccades: horizontal and vertical head/eye pursuit.	5.3-30
5.3-22	Cumulative gaze error time (%): horizontal and vertical head/eye pursuit.	5.3-30
5.3-23	Horizontal – eye-head tracking.	5.3-31
5.3-24	Vertical – eye-head tracking.	5.3-31
5.3-25	L-10 Unpredictable pursuit tracking: Low velocity (15°/sec) ramp tracking with eye ramp moving rightward.	5.3-32
5.3-26	R+0 Unpredictable pursuit tracking: Low velocity (15°/sec) ramp tracking with eye ramp moving rightward.	5.3-32

5.3-27	L-10 Unpredictable pursuit tracking: Low velocity (30°/sec) ramp tracking with eye ramp moving rightward.	5.3-33
5.3-28	R+0 Unpredictable pursuit tracking: Low velocity (30°/sec) ramp tracking with eye ramp moving rightward.	5.3-33
5.3-29	L-120 Unpredictable pursuit tracking: High velocity (30°/sec) ramp tracking with both head and eye ramp moving leftward.	5.3-34
5.3-30	R+0 Unpredictable pursuit tracking: High velocity (30°/sec) ramp tracking with both head and eye ramp moving leftward.	5.3-34
5.3-31	Pre and postflight target acquisition in vertical plane.	5.3-35
5.3-32	Upward target acquisition nearing the end of mission (EOM).	5.3-35
5.3-33	An illustration of how delays of head and eye movements are designated for quantification of the five different Stark types.	5.3-35
5.3-34	Stark type I.	5.3-35
5.3-35	Stark type II.	5.3-36
5.3-36	Stark type IIIa.	5.3-36
5.3-37	Stark type IIIb.	5.3-36
5.3-38	Stark type IV.	5.3-36
5.3-39	Preflight acquisition of target beyond the EOM.	5.3-36
5.3-40	Postflight acquisition of a target beyond the EOM.	5.3-36
5.3-41	Gaze plane showing preflight total gaze error and VOR gain	5.3-37
5.3-42	Gaze plane showing postflight total gaze error and VOR gain.	5.3-37
5.3-43	Preflight gaze error.	5.3-37
5.3-44	Postflight gaze error.	5.3-37
5.3-45	Integrated gaze error over time.	5.3-37
5.3-46	Changes in gaze error during flight for target displacement and recovery following flight.	5.3-37
5.3-47	Postflight performance based on preflight gaze error.	5.3-38
5.3-48	Postflight performance based on in-flight gaze error.	5.3-38
5.3-49	Postflight performance based on gaze error.	5.3-38
5.3-50	Gaze stabilization as a function of flight phase.	5.3-38
5.3-51	Postflight gaze stabilization with associated saccadic activity.	5.3-39
5.3-52	Sinusoidal head shakes: peak-to-peak displacement with vision during voluntary head shakes in the vertical plane.	5.3-39
5.3-53	Displacement in the yaw plane during pitch head shakes: effects of flight phase and vision.	5.3-39
5.3-54	Phase plane for 0.2 Hz vertical head shake with vision.	5.3-39
5.3-55	Phase plane for 0.3 Hz vertical head shake with vision.	5.3-39
5.3-56	Phase plane for 0.8 Hz vertical head shake with vision.	5.3-39
5.3-57	Phase plane for 2.0 Hz vertical head shake with vision.	5.3-40
5.3-58	Phase plane for 0.2 Hz vertical head shake without vision.	5.3-40
5.3-59	Phase plane for 0.3 Hz vertical head shake without vision.	5.3-40
5.3-60	Phase plane for 0.8 Hz vertical head shake without vision.	5.3-40
5.3-61	Phase plane for 2.0 Hz vertical head shake without vision.	5.3-40
5.3-62	Horizontal head calibration, velocity: subject 1.	5.3-41
5.3-63	Horizontal head calibration, position: subject 2.	5.3-41
5.3-64	Horizontal head velocity, calibration: subject 1.	5.3-41
5.3-65	Horizontal head calibration, velocity: subject 2.	5.3-41

Part 5.4 Recovery of Postural Equilibrium Control Following Space Flight (DSO 605)	5.4-1
5.4-1 Link segment biomedical model.	5.4-12
5.4-2 Preflight and postflight antero-posterior (a-p) center of gravity sway time series traces for each of the six sensory organization test conditions for a typical subject.	5.4-12
5.4-3 Preflight and postflight stabilograms corresponding to the a-p center of gravity sway traces of figure 5.4-2.	5.4-13
5.4-4 Preflight and postflight cumulative distribution functions of the peak to peak (p-p) a-p center of gravity sway for the 34 subjects of each of the six sensory organization test conditions.	5.4-13
5.4-5 Mean (\pm s.e.m.) p-p a-p center of gravity sway for each of the six sensory organization tests preflight and postflight.	5.4-14
5.4-6 Mean (\pm s.e.m.) p-p a-p center of gravity sway data demonstrating the independent roles of sensory inputs to balance control.	5.4-14
5.4-7 Mean (\pm s.e.m.) p-p a-p center of gravity sway data demonstrating the interactions among the independent variables between the main effects.	5.4-15
5.4-8 Model of postflight balance control recovery dynamics.	5.4-15
5.4-9 Phase plane representations of hip sway responses to support surface translations after space flight for a typical subject.	5.4-16
5.4-10 Comparison between rookie and veteran astronauts on preflight and postflight performances of the six sensory organization tests.	5.4-16
Part 5.5 Effects of Space Flight on Locomotor Control (DSO 614)	5.5-1
5.5-1 The convention for joint angle measurements.	5.5-37
5.5-2 Map view of the experiment set up.	5.5-37
5.5-3 Subject head sets used in the locomotor spatial orientation study.	5.5-37
5.5-4 Sagittal plane body model.	5.5-37
5.5-5 One degree of freedom, second order model of vertical (Z) COM motion following impact.	5.5-37
5.5-6 Waveforms from one subject showing the relationship between vertical translation of the trunk and corresponding pitch angular head movement for the NEAR target condition during pre- and postflight locomotion.	5.5-38
5.5-7 To show the step-to-step variability, each cycle in the waveforms depicting vertical trunk translation and compensatory pitch head movements were aligned at the point of heel strike in one subject.	5.5-38
5.5-8 Mean (\pm 1 S.E.) pre- and postflight coherence values relating vertical trunk translation and corresponding pitch head movement for all subjects combined, for both FAR and NEAR target conditions.	5.5-39
5.5-9 One pre- and postflight example of Fourier amplitude spectra of pitch head angular displacement for the NEAR target condition for one subject during locomotion.	5.5-39
5.5-10 Individual mean pre- and postflight changes in the magnitude of the predominant peak of pitch head movements for the FAR and NEAR target conditions.	5.5-40
5.5-11 Mean (\pm 1 S.E.) magnitude of the predominant peak of pitch head movements for all subjects for the FAR and NEAR target conditions during both pre- and postflight testing.	5.5-40
5.5-12 Comparison between first- and multi-time fliers of the mean (\pm 1 S.E.) magnitude of the predominant peak of pitch head movements during the FAR and NEAR target conditions.	5.5-41
5.5-13 Waveforms showing pitch angular head displacement for 5 individual subjects during the eyes open and eyes closed epochs of the IV condition obtained during one preflight trial.	5.5-42

5.5-14	(a) Pre- and postflight mean (± 1 S.E.) predominant frequency amplitude for all subjects during the alternate 5 second eyes open/closed epochs of the IV Condition. (b) Pre- and postflight mean (± 1 S.E.) head tilt relative to vertical in the sagittal plane for all subjects during the alternating 5 second eyes open/closed epochs.	5.5-43
5.5-15	Mean and standard deviation of the preflight and postflight trial stride time for each of the seven subjects plotted as a function of subject height.	5.5-44
5.5-16	Preflight and postflight mean duty factor presented for each subject as a function of subject height.	5.5-44
5.5-17	Exemplar phase portraits of three lower limb joints. These data are from one subject and illustrate 15 consecutive cycles of one preflight and one postflight trial.	5.5-45
5.5-18	Box plots of phase plane variability as a function of stride epoch, from right heel strike to right heel strike.	5.5-46
5.5-19	Box plots of phase plane variability of the preflight and postflight toe off and heel strike events for the hip, knee, and ankle angles.	5.5-47
5.5-20	Box plots of the system stability index for the preflight and postflight toe off and heel strike events.	5.5-47
5.5-21	Grand ensemble average preflight and postflight wave forms for biceps femoris, rectus femoris, gastrocnemius, and tibialis anterior.	5.5-48
5.5-22	Differences in relative amplitude between preflight and postflight grand ensemble reduced wave forms at each 5% gait cycle epoch for: biceps femoris, rectus femoris, gastrocnemius, and tibialis anterior.	5.5-49
5.5-23	Preflight versus postflight latency average (± 1 S.D.) difference for each subject between GA offset and TA onset.	5.5-50
5.5-24	Example of preflight and postflight walking trajectories (eyes closed condition).	5.5-51
5.5-25	Comparison of preflight and postflight joint angle phase-plane portraits for hip, knee and ankle.	5.5-52
5.5-26	Comparison of preflight and postflight COM motion for postflight-compliant subject S-1.	5.5-52
5.5-27	Average preflight and postflight maximum joint flexion values for nine astronaut subjects.	5.5-53
5.5-28	COM displacement.	5.5-55
5.5-29	Modeled COM vertical motion using stiffness and damping estimated for representative pre- and postflight for P-C subject S-1.	5.5-56
5.5-30	Mean preflight and postflight model vertical stiffness.	5.5-57

Section 6 Assessment of Human Factors 6-1

6-1	Percentage of time primary crewmembers spent in each posture category.	6-3
6-2	Laptop computer and touchscreen.	6-5
6-3	Comparison of touchscreen to trackpoint with respect to reaction time and error rate, versus task type and object site.	6-6
6-4	Simulation of crew member preferred and maximum communication distances in the Spacelab under typical background noise conditions.	6-8
6-5	Luminance measurements in the Orbiter.	6-9
6-6	Luminance measurements in the SpaceHab.	6-10
6-7	Transfer tunnels and their interior dimensions.	6-11
6-8	The Neutral Body Posture model.	6-12
6-9	Female crew member with leg and foot posture deviating from the MSIS model.	6-13

Section 7 Facilities	7-1
7-1 Postflight Science Support Facility (PSSF) at Dryden.	7-1
7-2 Examination room at PSSF.	7-2
7-3 Baseline Data Collection Facility (BDCF) at KSC.	7-2
7-4 Crew Transport Vehicles (CTVs).	7-3
Section 8 Hardware	8-1
8-1a Ambulatory Cardiovascular Monitoring Assembly.	8-2
8-1b HOBO Temperature Monitoring Device.	8-2
8-2a Lower Body Negative Pressure (LBNP) device.	8-4
8-2b LBNP Controller.	8-4
8-2c LBNP Controller schematic.	8-4
8-2d Controller data flow diagram.	8-5
8-3 American Echocardiograph Research Imaging System (AERIS).	8-6
8-4 Re-entry Anti-gravity Suit (REAGS).	8-6
8-5 Bar Code Reader.	8-7
8-6 Urine Collection Kit.	8-7
8-7 Heart Rate Watch Assembly.	8-9
8-8a Biotest Microbial Air Sampler (MAS) with accessories.	8-9
8-8b Burkhard Microbial Air Sampler (MAS).	8-9
8-9 Combustion Products Analyzer (CPA).	8-9
8-10 Archival Organic Sampler (AOS).	8-10
8-11 Formaldehyde Monitor.	8-10
8-12 Shuttle Particle Sampler (SPS) and Shuttle Particle Monitor (SPM).	8-11
8-13 Superpocket System.	8-11
8-14 Locker-mounted Video Camera System.	8-12
8-15 Cycle Ergometer.	8-13
8-16 Passive Cycle Isolation System (PCIS).	8-14
8-17 Cycle Ergometer with Inertial Vibration Isolation System (IVIS) boxes attached.	8-15
8-18 Microgravity Measuring Device (MMD) mounted in middeck locker.	8-15
8-19 Subject using EDO Treadmill on KC-135.	8-16
8-20 Subject using MK-2 Rower on KC-135.	8-17
Section 9 Project Summary and Conclusions No figures in this section	

Section 1

Cardiovascular Deconditioning

EXTENDED DURATION ORBITER MEDICAL PROJECT

Cardiovascular Deconditioning

*John B. Charles, Janice M. Fritsch-Yelle, Peggy A. Whitson, Margie L. Wood,
Troy E. Brown, and G. William Fortner, Cardiovascular Laboratory,
Johnson Space Center, Houston, TX*

BACKGROUND

Spaceflight causes adaptive changes in cardiovascular function that may deleteriously affect crew health and safety [1, 2, 3, 4, 5]. Over the last three decades, symptoms of cardiovascular changes have ranged from post-flight orthostatic tachycardia and decreased exercise capacity to serious cardiac rhythm disturbances during extravehicular activities (EVA). The most documented symptom of cardiovascular dysfunction, postflight orthostatic intolerance, has affected a significant percentage of U.S. Space Shuttle astronauts [6, 7, 8, 9]. Problems of cardiovascular dysfunction associated with spaceflight are a concern to NASA. This has been particularly true during Shuttle flights where the primary concern is the crew's physical health, including the pilot's ability to land the Orbiter, and the crew's ability to quickly egress and move to safety should a dangerous condition arise.

The study of astronauts during Shuttle activities is inherently more difficult than most human research [8]. Changes in diet, sleep patterns, exercise, medications, and fluid intake before and during spaceflight missions are difficult to control. Safety restrictions make many standard research protocols inadvisable. Data collections must occur without disruption of primary mission objectives. Hardware malfunctions during in-flight data collections affect the quantity and/or quality of resulting data. Concurrent investigations may confound interpretation of both studies. Consequently, sample sizes have been small and results have lacked consistency. Before the Extended Duration Orbiter Medical Project (EDOMP), there was a lack of normative data on changes in cardiovascular parameters during and after spaceflight. The EDOMP for the first time allowed studies on a large enough number of subjects to overcome some of these problems.

There were three primary goals of the Cardiovascular EDOMP studies. The first was to establish, through descriptive studies, a normative data base of cardiovascular changes attributable to spaceflight. The second goal was to determine mechanisms of cardiovascular changes resulting from spaceflight (particularly orthostatic hypotension and cardiac rhythm disturbances). The third

was to evaluate possible countermeasures. The Cardiovascular EDOMP studies involved parallel descriptive, mechanistic, and countermeasure evaluations (Table 1-1).

GOAL 1 – DESCRIPTIVE STUDIES

Introduction

Before EDOMP, data describing changes in basic cardiovascular parameters during and after spaceflight were sparse and equivocal, and were sometimes only reported as case studies. Because of the competition for in-flight resources, many experiments were often scheduled on the same crew members, even though one study may have interfered with the measurements of another. Because of these limitations, reports were inconsistent, and a good representative data base did not exist. Even such a basic parameter as heart rate had been reported to be increased, decreased, and unchanged during spaceflight. The main objective of the EDOMP cardiovascular descriptive studies was to correct this deficit by collecting data; and by monitoring heart rate, blood pressure, cardiac dysrhythmias, cardiac function, and orthostatic intolerance, consistently and with a large enough number of subjects to make meaningful conclusions.

Methods and Materials

The first descriptive study was conducted as Detailed Supplementary Objective (DSO) number 463. This study employed 24-hour Holter monitor recordings before flight, during flight, and after flight on five crew members to document any occurrence of in-flight cardiac dysrhythmias [10].

The second descriptive study (DSO 602) employed Holter monitors as well as automatic blood pressure devices to monitor heart rate, cardiac arrhythmias, and arterial pressure for 24-hour periods before, during, and after flight [10]. The subjects were 12 astronauts who flew missions lasting from 4 to 14 days. During data collections the electrocardiogram was recorded continuously, using the Holter monitor, and blood pressure was taken automatically every 20 minutes when the subjects were awake,

Table 1-1. Cardiovascular EDOMP studies

<i>Descriptive Studies</i>	<i>Mechanistic Studies</i>	<i>Countermeasure Evaluations</i>
In-flight Holter Monitoring (463) 5 Subjects PI1	Baroreflex Function (467) 16 Subjects PI1	In-flight Lower Body Negative Pressure (478) 13 Subjects PI1
In-flight Arterial Pressure and Holter Monitoring (602) 12 Subjects PI2	Baroreflex/Autonomic Control of Arterial Pressure (601) 16 Subjects PI2	LBNP Countermeasure (623) 12 Subjects PI1
Cardiac Function (466) 32 Subjects PI1	Neuroendocrine Responses to Standing (613) 24 Subjects PI3	Hyperosmotic Fluid Countermeasure (479) 23 Subjects PI1
Orthostatic Function during Entry, Landing and Egress (603) 34 Subjects PI1	Cardiovascular and Cerebrovascular Responses to Standing (626) 40 Subjects PI2	In-flight Use of Fludrocortisone (621) 16 Subjects PI2

Key to Principal Investigators:

- PI1 John B. Charles
- PI2 Jan M. Fritsch-Yelle
- PI3 Peggy A. Whitson

and every 30 minutes during sleep. Subjects maintained normal routines, both on the ground and in flight.

In the third descriptive study (DSO 466), 32 astronauts on short duration missions (4-5 days in space) were studied with two-dimensionally directed M-mode echocardiography to determine the effects of spaceflight on cardiac volume, cardiac function, and cardiac mass [11]. Heart rate, blood pressure, and echocardiograms were obtained in the supine and standing positions before and after flight. M-mode echocardiograms were interpreted according to American Society of Echocardiography (ASE) measurement conventions [12]. Cardiac volumes and ejection fraction were derived by using the Teichholz formula [13]. Myocardial mass index was subsequently determined from a modification of the ASE basic formula for left ventricular mass. The mean velocity of circumferential fiber shortening was estimated by the method of Cooper et al. [14].

In the fourth descriptive study (DSO 603), the standard Shuttle launch and entry pressure suit (LES) was modified to include a biomedical instrumentation port that would allow physiological signals to be monitored while the LES was being worn. An automatic blood pressure/heart rate monitor was used to measure the electrocardiogram continuously and to determine heart rate and arterial pressure at 2-minute intervals. In most cases, three 1-axis accelerometers were used to provide reference acceleration levels. A fourth accelerometer was

attached to the upper torso of the LES to document changes in body posture. The following parameters were derived from the collected data: (1) heart rate, (2) systolic, diastolic, and mean arterial pressure, and (3) pulse pressure. These values were compiled for several time periods during the preflight and in-flight testing period. These were (1) preflight seated and standing values with the g-suit inflated to the expected in-flight level, (2) in flight prior to onset of gravity, (3) at the onset of gravity, (4) at peak gravity during entry, (5) at touchdown, and (6) seated and standing measurements during the first stand [15].

Results

There were several important findings in the first two studies (DSO 463 and 602). First, heart rate, diastolic pressure, and their variabilities were reduced during spaceflight (Figures 1-1 and 1-2). Second, the diurnal variations of both heart rate and diastolic pressure were reduced during spaceflight. Third, monitoring records demonstrated that spaceflight did not increase dysrhythmias (Figure 1-3). These data are unique because they were obtained during normal 24-hour routines, rather than as a part of any in-flight experiment intervention. Therefore, they are important for establishing a normative data base for cardiovascular parameters during short duration spaceflight.

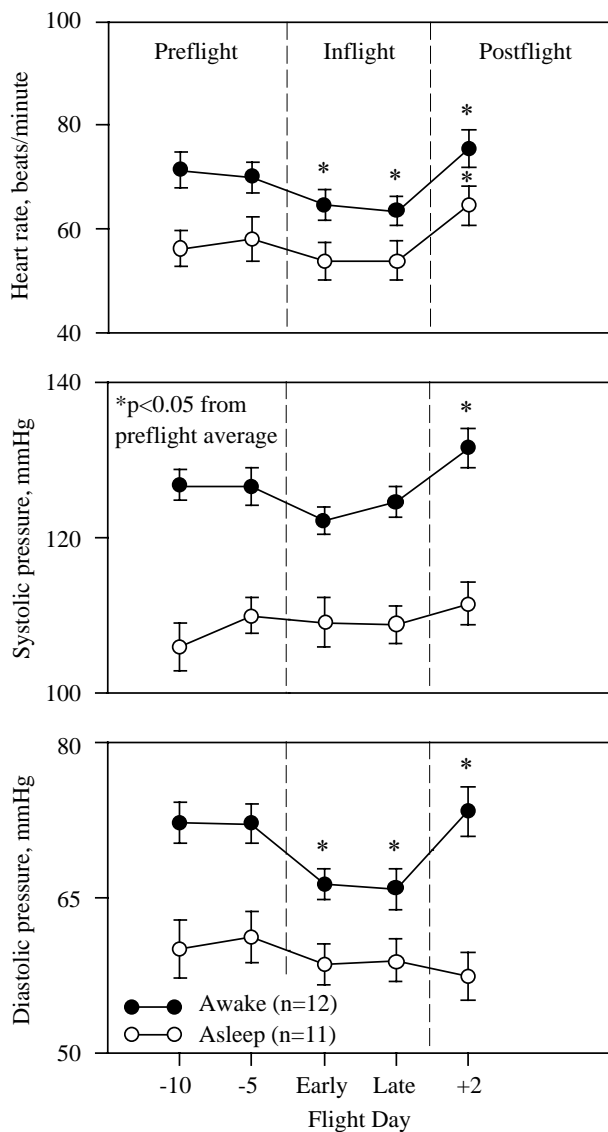


Figure 1-1. Heart rate and arterial pressure before, during, and after flight.

In the third study (DSO 466) (Table 1-2), the supine left ventricular end diastolic volume index (EDVI) diminished by 11% ($P < 0.0006$) on landing day when compared with preflight. Similar to EDVI, supine left ventricular stroke volume index (SVI) diminished by 17% ($P < 0.006$) on landing day compared with preflight. Overall standing EDVI was less than supine, but no significant changes occurred between test days. Left ventricular end systolic volume index (ESVI) did not significantly change for position or time. Total peripheral resistance index (TPRI) was significantly greater in the standing position than the supine position on all test days except landing day. Similarly, the TPRI orthostatic response was less on landing day. Ejection fraction and velocity of circumferential fiber shortening did not change significantly, suggesting that spaceflight of this

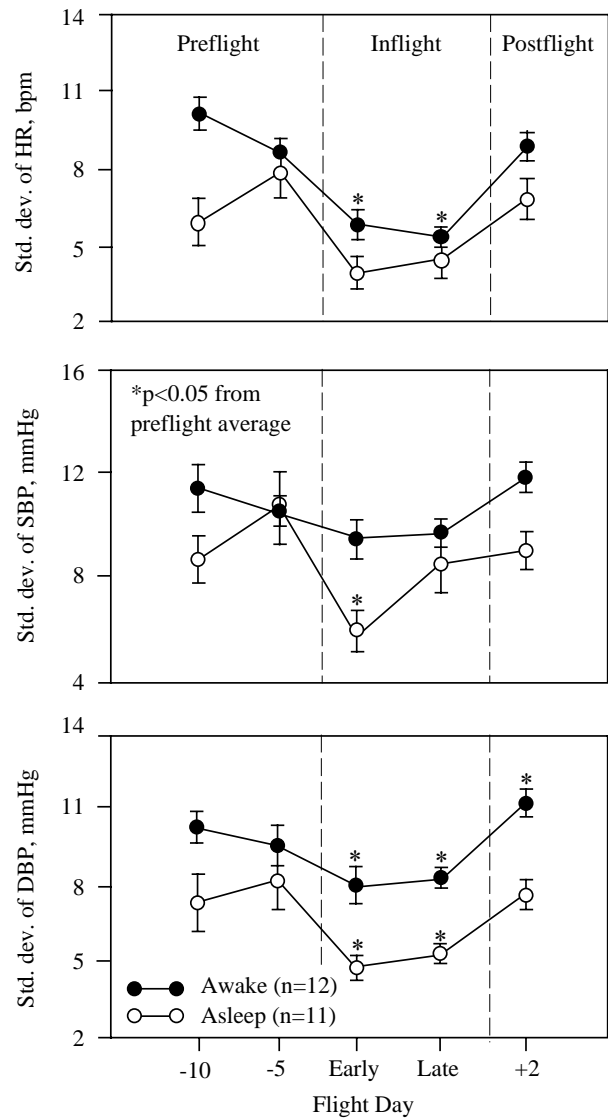


Figure 1-2. Intrasubject standard deviations of heart rate and arterial pressure before, during, and after flight.

duration has no effect on myocardial contractility. Left ventricular wall thickness and myocardial mass index also showed no significant changes (data not shown).

Arterial pressures and heart rates were monitored in the fourth study (DSO 603) during landing and egress from the Orbiter. Arterial pressure responses are shown in Figure 1-4. During spaceflight, both systolic and diastolic pressure were elevated relative to preflight baseline values throughout the recording period, reaching their highest values at peak gravity during entry, and on touch-down. Standing upright for the first time after landing was associated with a significant decrease, from the seated value, in systolic pressure. In seven cases, the drop was greater than 20 mmHg. This occurred in 22% of the subjects on landing day, but did not occur in any subjects before flight.

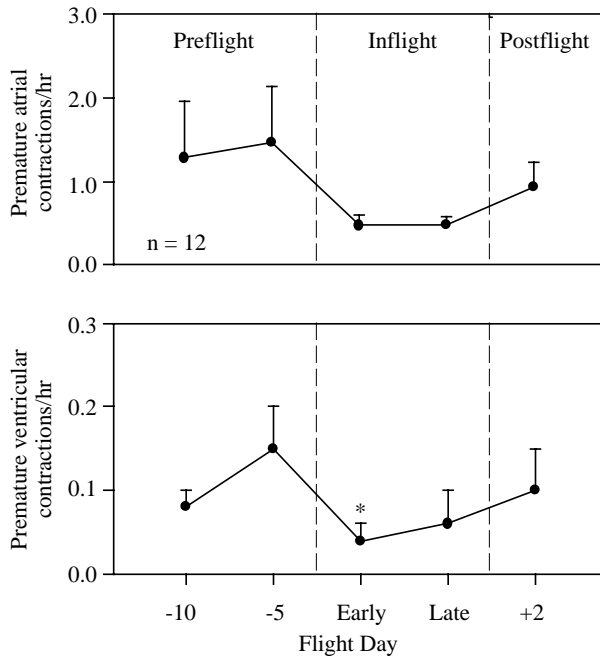


Figure 1-3. Premature atrial and ventricular contractions before, during, and after flight.

When the subjects stood after touchdown, diastolic pressures also decreased relative to values while the subjects were seated. During standing in the laboratory before flight, systolic and diastolic pressures exhibited small increases. There were differences in arterial pressure and heart rate attributable to use of the g-suit when crew members who inflated the g-suit (n=24) were compared with those who did not (n=8). Most notably, diastolic pressure was more adequately maintained in the g-suit-inflated group during the post-touchdown standing maneuver, compared to the non-inflated g-suit group ($P < 0.006$) (data not shown).

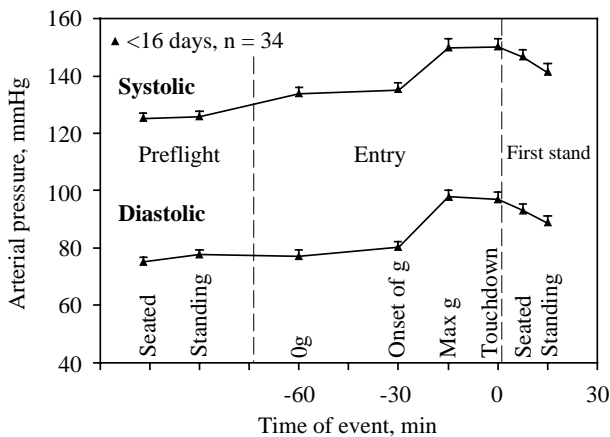


Figure 1-4. Systolic and diastolic pressure response to entry, landing, and egress.

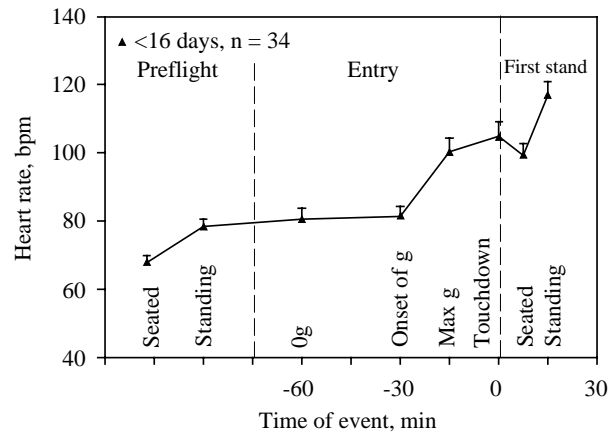


Figure 1-5. Heart rate response to entry and landing.

Heart rate also reached high values at peak gravity and touchdown. The maximum value was obtained during the first stand (Figure 1-5). Although there was large inter-individual variability in seated and standing heart rates, crew members generally showed a substantial increase in heart rate upon standing after touchdown. There was a 70% increase in heart rate upon standing compared to the increase seen before flight. Four crew members had heart rate values on standing that were equal to, or greater than, their maximal heart rate responses during preflight lower body negative pressure tests. The highest heart rate observed for any crew member was 160 bpm. Both systolic pressure and heart rate returned quickly to preflight values during the first hour after landing, although substantial differences frequently remained.

Conclusions

In the first two descriptive studies, the results indicate that heart rate, blood pressure, and cardiac dysrhythmias decreased during spaceflight when compared to preflight norms. This suggests that living in a microgravity environment did not cause a constant stress to the cardiovascular system. However, the adaptive changes that occurred in response to the microgravity environment left the astronauts ill-prepared for the cardiovascular stresses associated with return to Earth.

In the third study, changes in cardiac function occurred after short duration (4 to 5 day) spaceflights. These changes included decreased left ventricular end diastolic volume and decreased stroke volume indices, with compensatory increased heart rate and increased maintenance of cardiac output. In addition, altered total peripheral vascular resistance occurred, with an apparent reduction in the ability to augment peripheral vascular tone on assumption of upright posture. Changes in cardiovascular measurements resolved within 7 days of landing. There were no significant changes in left ventricular contractility or cardiac mass after short

Table 1-2. Cardiovascular measurements (mean \pm SEM) before and after short-duration spaceflight

	L-10		L-5		L+0		L+(7-10)	
HR								
Supine	57	(1.8)	58	(2.0)	70*	(2.2)	57	(1.8)
Standing	75	(2.6)	75	(2.7)	101**	(3.6)	78	(2.2)
SBP								
Supine	105	(2.1)	106	(2.2)	109	(2.0)	106	(2.2)
Standing	110	(1.7)	114†	(1.7)	111	(2.2)	112	(2.0)
DBP								
Supine	64	(2.1)	61	(2.1)	68	(2.6)	64	(2.7)
Standing	79	(1.7)	79	(1.3)	81	(1.6)	80	(1.2)
MAP								
Supine	77	(1.9)	76	(2.0)	82	(2.2)	78	(2.4)
Standing	89	(1.5)	91	(1.2)	91	(1.5)	91	(1.3)
PP								
Supine	41	(1.9)	45	(1.5)	41	(2.2)	43	(1.8)
Standing	31	(1.8)	35	(1.7)	31	(2.1)	32	(1.8)
EDVI								
Supine	59.4	(2.7)	56.1	(3.3)	52.6††	(2.7)	56.7	(2.6)
Standing	41.3	(2.4)	42.6	(4.5)	35.8	(2.7)	43.0	(2.4)
ESVI								
Supine	20.9	(1.2)	18.6	(2.0)	20.5	(1.6)	19.6	(1.6)
Standing	17.3	(1.8)	16.2	(3.3)	13.4	(1.6)	17.6	(1.9)
SVI								
Supine	38.5	(1.8)	37.5	(1.9)	32.1	(1.8)	37.1	(1.6)
Standing	24.0	(1.5)	26.4	(1.9)	22.3	(1.5)	25.4	(1.1)
TPRI								
Supine	38.4	(2.2)	38.9	(2.6)	39.7	(2.5)	39.4	(2.5)
Standing	51.7	(3.8)	49.0	(6.7)	41.8	(2.0)	47.0	(2.1)
EF								
Supine	65	(1.3)	68	(2.1)	62	(2.0)	66	(1.6)
Standing	59	(3.3)	64	(5.6)	63	(2.5)	60	(2.2)
LVMI								
	63.3	(2.5)	59.6	(2.4)	61.1	(2.2)	60.9	(2.1)

P* 0.0005, cf of L-10 supine *P* 0.0001, cf of L-10 standing †*P* 0.04, cf of L-10 standing
††*P* 0.0006, cf of L-10 supine *P* 0.006, cf of L-10 supine
HR = heart rate (bpm)
SBP = systolic blood pressure (mmHg)
DBP = diastolic blood pressure (mmHg)
MAP = mean arterial pressure (mmHg)
PP = pulse pressure (mmHg)
EDVI = left ventricular end-diastolic volume index (ml/m²)
ESVI = left ventricular end-systolic volume index (ml/m²)
TPRI = total peripheral vascular resistance index (mmHg, l/min/m²)
EF = ejection fraction (%)
LVMI = left ventricular mass index (g/m²)
L- = launch minus
L+ = landing plus

duration spaceflight. Echocardiography provided a useful noninvasive technique for evaluation of cardiovascular physiology after spaceflight.

Analysis of results from the fourth study showed that entry, landing, and seat egress after Shuttle flights were associated with drops in systolic pressure and increases in heart rate. These results describe a cardiovascular system under significant stress during nominal entry, landing, and seat egress, and indicate that the cardiovascular system was performing at or near its maximum capacity in a significant fraction (20%) of the study population. While these crew members were never clinically hypotensive, their swings in arterial pressure and heart rate indicate that they were unable to buffer arterial pressure changes as well as before flight. It is questionable whether sufficient reserve capacity remained to permit unaided emergency egress by these individuals.

GOAL 2 – MECHANISTIC STUDIES

Introduction

The series of EDOMP cardiovascular mechanistic studies was undertaken to test the hypothesis that orthostatic hypotension following spaceflight is due, at least in part, to a disruption of autonomic control of the cardiovascular system. The series consisted of four studies. The first study was a simple evaluation of carotid baroreceptor cardiac reflex function before and after 4 to 5 days in space. The second study tested carotid baroreflex function after 8 to 14 day spaceflights, and added measurements of resting plasma catecholamine levels, Valsalva maneuvers, and spectral analyses of arterial pressure and heart rate. The third study evaluated the relationship between plasma catecholamine levels and total peripheral resistance changes upon standing. The fourth study looked at integrated cardiovascular and cerebrovascular responses to standing, as well as the effect of reduced postflight plasma volume on orthostatic tolerance. All of these studies used data only from crew members who had not taken vasoactive or autonomic medications within 12 hours, or caffeine within 4 hours of the study.

Methods and Materials

The first mechanistic study (DSO 467) tested 16 astronaut subjects before and after 4 to 5 day spaceflight missions [7, 16]. Subjects were studied 10 and 5 days before launch, on landing day, and up to 10 days after landing. The protocol consisted of a 20-minute supine rest period, followed by carotid baroreceptor stimulation. A stepping motor-driven bellows was connected to a neck chamber to deliver stepped pulses of pressure and suction to the neck. During held expiration, the pressure was increased to 40 mmHg and held for 5 seconds. With the

next seven heart beats, the pressure stepped down sequentially to 25, 10, -5, -20, -35, -50, and -65 mmHg. R-R intervals were plotted against carotid distending pressure, derived by subtracting the neck chamber pressure from the systolic pressure. The following variables were taken from the stimulus-response relationship: maximum slope, R-R interval range of response, minimum and maximum R-R intervals, and operational point. The operational point was the R-R interval at zero neck pressure which represented the relative hypotensive versus hypertensive buffering capacity of the reflex.

The second mechanistic study (DSO 601) repeated the above measurements before and after spaceflight missions lasting 8 to 14 days [8]. In addition, 5 minutes of continuous ECG data were taken for spectral analyses of R-R intervals, and blood samples were drawn before the neck stimuli for analysis of plasma catecholamine levels. Two Valsalva maneuvers were performed at 30 mmHg expired pressure for 15 seconds, and two were performed at 15 mmHg expired pressure for 15 seconds. Sixteen astronaut subjects participated in this activity, using the same schedule as the previous study.

The third mechanistic study (DSO 613) measured catecholamine levels and cardiovascular responses to standing in 24 astronauts before and after spaceflight [17]. Studies were performed 10 days before launch, on landing day, and 3 days after landing. Arterial pressure, heart rate, and cardiac output were measured. Blood samples, drawn at the end of a 20-minute supine rest period and after 5 minutes of standing, were tested for catecholamines and plasma renin activity.

The fourth mechanistic study (DSO 626) sought to define differences in physiological responses of astronauts who did or did not become presyncopal on landing day [18]. This study was performed on 40 astronauts before and after Shuttle missions of up to 16 days. The protocol consisted of a 20-minute supine rest period, followed by a blood draw for analyses of plasma catecholamine and plasma renin activity. Plasma volume was then measured by the carbon monoxide rebreathing (CORB) technique. An enhanced stand test was then performed, and included the following: (1) echocardiographic measurements to obtain aortic cross sectional area, (2) continuous wave Doppler for aortic flow, and (3) beat-to-beat arterial pressure and ECG. All measurements were continued for 5 more minutes supine and 10 minutes standing. A final blood sample was drawn at the end of standing. This entire protocol was performed 30 and 10 days before launch, on landing day, and 3 and 10 days after landing. Data were analyzed to document differences between presyncopal and non-presyncopal astronauts.

Results

In the first study of short duration flights (DSO 467), the following summary data were obtained on landing

day and compared to the preflight norm (Table 1-3, Figure 1-6): resting R-R intervals and standard deviations; the slope, range, and position of operational points on the carotid distending pressure; and R-R interval response relation. These variables were all reduced on landing day relative to preflight. Stand tests on landing day revealed two separate groups, differentiated by their ability to maintain standing arterial pressure. This maintenance of arterial pressure was determined by evaluating preflight slopes, operational points, and supine and standing R-R intervals, and by preflight-to-postflight changes in standing systolic pressures, body weights, and operational points (Table 1-4, Figures 1-7, 1-8, and 1-9).

In the second study, involving longer duration flights (DSO 601), the following changes between preflight and landing day were found: (1) orthostatic tolerance decreased, (2) R-R interval spectral power in the 0.05 to 0.15-Hz band increased (Figures 1-10 and 1-11), (3) resting plasma norepinephrine and epinephrine levels increased, (4) the slope, range, and operational point of the carotid baroreceptor cardiac reflex response decreased (Table 1-5), and (5) blood pressure and heart rate responses to Valsalva maneuvers were altered (Figures 1-12 and 1-13). Carotid baroreceptor cardiac reflex response changes persisted for several days after landing (Table 1-5).

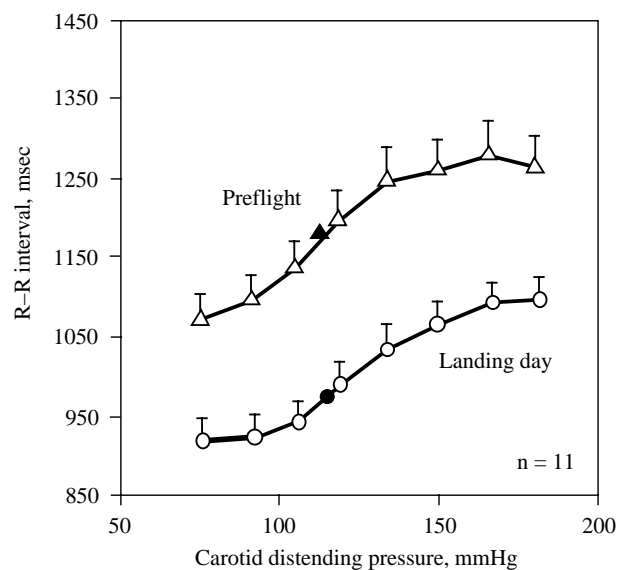


Figure 1-6. Carotid baroreceptor vagal-cardiac reflex responses before flight and on landing day. Closed symbols, position of operational points. Average operational point was reduced significantly on landing day, but slope and range were not.

Table 1-3. Measurements from all subjects on all test days

	Preflight	Landing Day	Postflight Day		
			2	3	8-10
Systolic pressure, mmHg	116±2	116±2	117±2	116±2	116±2
Diastolic pressure, mmHg	75±1	73±2	72±2	73±2	74±2
R-R interval, ms	1,123±42	965±25*	1,069±38	1,134±39	1,069±31
Standard deviation of R-R, ms	62±6	40±4*	58±6	55±5	47±5
Body weight, kg	75.6±4.0	74.4±2.4*	75.2±2.4	75.3±2.4	75.4±2.1
<i>Baroreflex measurements</i>					
Maximum slope, ms/mmHg	5.0±1.0	3.4±0.5	3.6±0.6*	3.90±0.6*	3.9±0.6*
Operational point, %	48.9±3.5	29.4±4.2†	39.8±3.6	52.4±4.7	42.4±6.0
R-R interval, ms					
Range	243±47	182±25	177±20*	192±102*	189±27*
Minimum	1,081±43	923±30*	1,036±39	1,084±35	1,037±31
Maximum	1,324±68	1,104±31*	1,213±41*	1,275±43	1,226±38*
Carotid distending pressure, mmHg					
At minimum R-R	80±4	83±4	92±9	82±7	75±2
At maximum R-R	153±8	172±4	160±6	157±7	161±5

Values are means ± SE. All comparisons between landing day and preflight measurements used only 11 subjects; those between landing day and measurements taken 8-10 days after landing used only 12 subjects.

* $P < 0.05$; † $P < 0.01$.

Table 1-4. Subjects grouped according to relative orthostatic tolerance judged by cardiovascular parameters

	10 Days Before Launch		Landing Day	
	More resistant	Less resistant	More resistant	Less resistant
Weight, kg	74.30±3.3	77.20±2.9	73.86±3.3	75.76±2.9
Age, yr	42.1±2.4	43.1±1.8		
<i>Stand tests</i>				
Systolic pressure, mmHg				
Supine	110.4±3.4	106.4±3.0	110.3±3.7	117.9±3.9
Standing	121.4±3.4	118.9±2.0	124.3±4.0	114.0±2.9
Diastolic pressure, mmHg				
Supine	66.0±3.0	68.6±3.2	71.8±3.8	80.9±3.8
Standing	81.0±2.6	84.7±2.0	87.7±3.4	87.7±9.1
Heart rate, beats/min				
Supine	58.6±2.3	51.3±2.6	67.0±2.4	66.7±2.6
Standing	76.9±3.0	66.9±3.0*	98.3±3.7	104.4±4.2
R-R interval, m				
Supine	1,032±10	1,205±11*	901±9	931±10
Standing	791±10	912±11*	640±9	613±12
<i>Baroreflex measurements</i>				
Maximum slope, ms/mmHg	3.7±1.5	5.9±2.3*	3.2±1.2	5.0±2.0*
R-R range, ms	194±9	232±13	177±8	225±12
Operational point, %	45.8±3.3	54.4±3.4*	32.4±3.3	27.7±4.1

Values are means ± SE for 11 subjects. * $P \leq 0.05$ between groups.

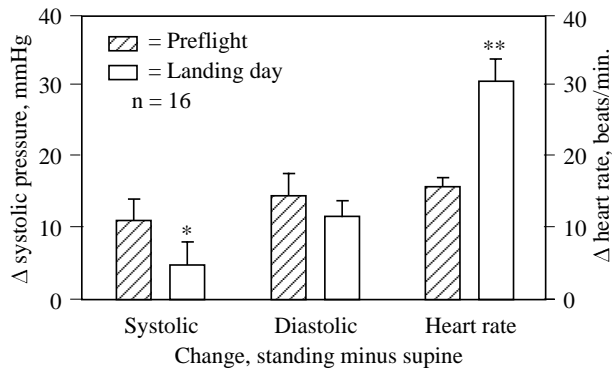


Figure 1-7. Preflight and landing day differences between standing and supine systolic and diastolic pressures and heart rate. Significant difference between groups: * $P < 0.05$; ** $P < 0.01$.

The third study (DSO 613) showed that on landing day supine plasma norepinephrine and epinephrine levels were increased 34% and 65%, respectively, from the preflight norm, and standing norepinephrine and epinephrine levels were increased 65% and 91% (Figure 1-14). Supine

and standing norepinephrine levels remained elevated 3 days after landing while epinephrine levels returned to preflight levels. On landing day, supine heart rate and systolic blood pressure were elevated 18% and 8.9%, respectively, when compared to the preflight norm. Standing heart rate and diastolic blood pressure were elevated 38% and 19%, respectively (data not shown).

In the fourth study (DSO 626), 40 crew members were tested. However, 11 were excluded for violations of test constraints or contamination of blood samples. Of the remaining 29 astronauts, 8 could not complete their stand tests on landing day because they became presyncopal. These subjects displayed arterial pressure and heart rate responses to standing that were similar to those seen in adrenergic failure (Figure 1-15). On landing day, their standing norepinephrine levels were significantly lower than the norepinephrine levels of the astronauts who did not become presyncopal (Table 1-6a). The failure of the sympathetic nerves to increase norepinephrine release with standing translated into lower peripheral vascular resistance and ultimately presyncope. Plasma volumes were not different between groups either before or after flight.

There were also significant preflight differences between the presyncopal and non-presyncopal groups

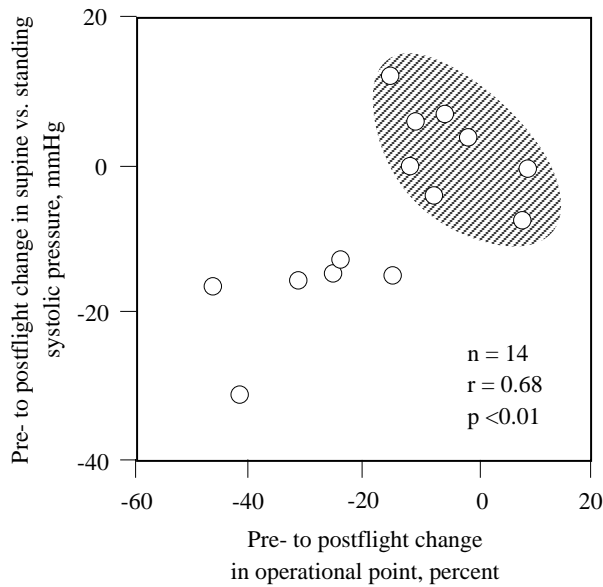


Figure 1-8. Preflight-to-postflight (landing day) changes of operational points and systolic pressure responses to standing. Linear regression correlation coefficients are for all data. Cluster analysis of these data identified 2 distinct groups, which have been termed less and more resistant to postural change. Hatched area, more resistant group.

(Table 1-6b). While still well within normal ranges, the group that became presyncopal on landing day had lower preflight supine and standing diastolic pressures and peripheral vascular resistance than the non-presyncopal group. The supine heart rates of the presyncopal group were also higher and their standing systolic pressures were lower. Three days after landing, norepinephrine levels and diastolic pressure were again similar in the two groups (Table 1-6c). However, peripheral vascular resistance and systolic pressure were lower in the presyncopal group during standing.

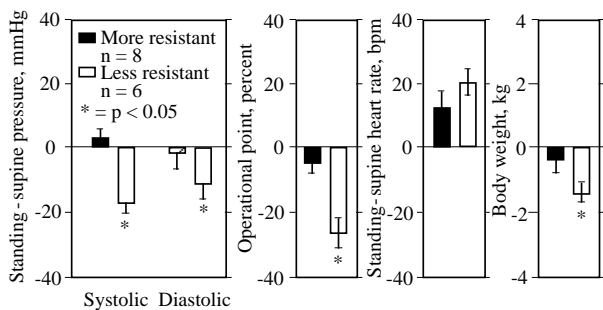


Figure 1-9. Comparisons of preflight to landing day changes between 2 groups identified by cluster analysis. * $P < 0.01$.

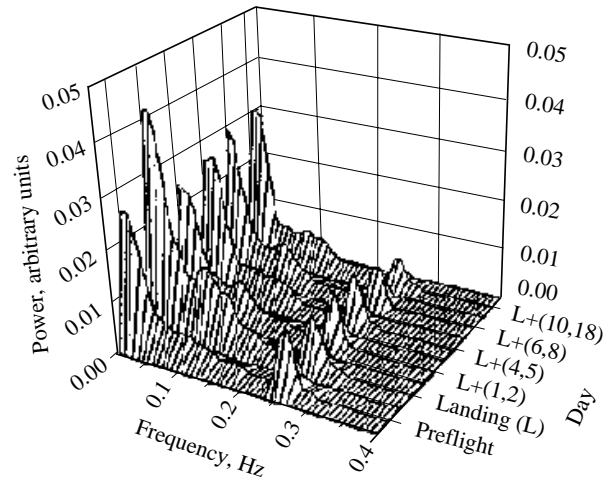


Figure 1-10. Three-dimensional plot of power spectra of R-R intervals during controlled frequency breathing for 12 subjects, all days.

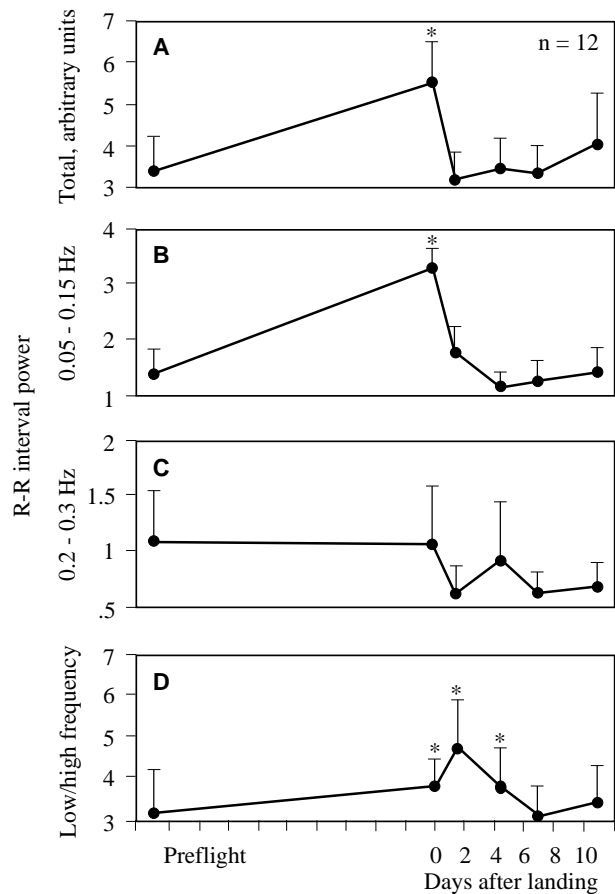


Figure 1-11. Average total power (A), power in 0.05- to 0.15-Hz band (B), 0.2- to 0.3-Hz band (C), and ratio of low- to high-frequency power (D) throughout study. n , no. of subjects. * $P < 0.025$ compared with preflight.

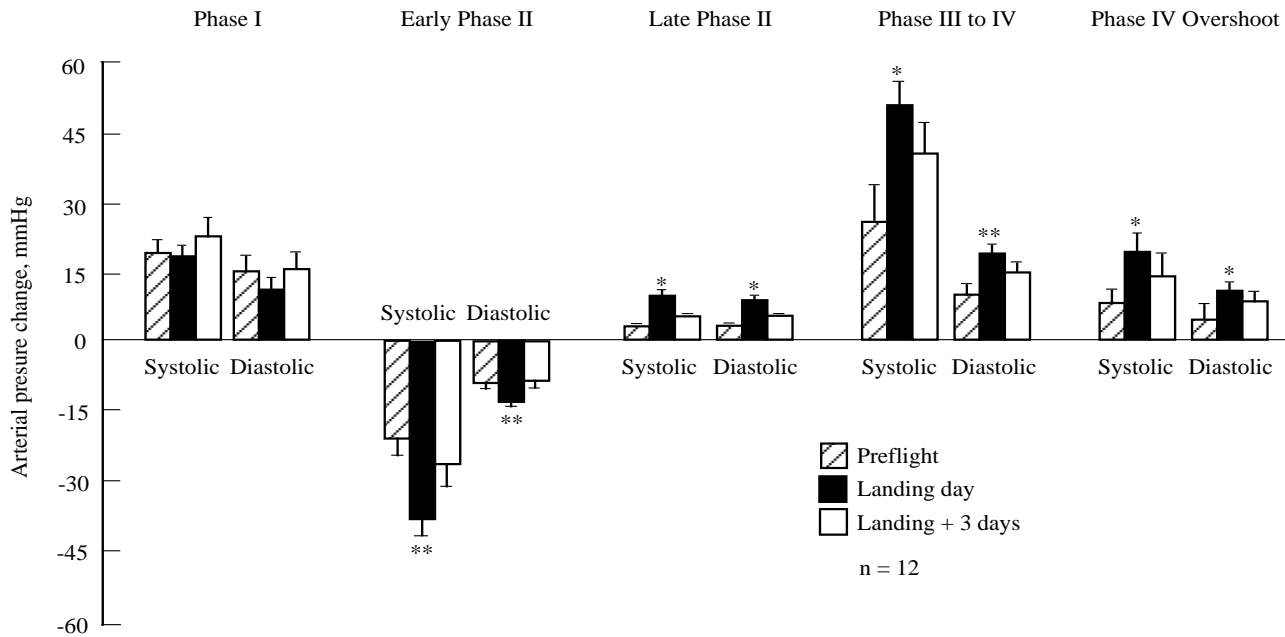


Figure 1-12. Arterial pressure responses during Valsalva maneuvers preflight, on landing day, and 3 days after landing. * $P < 0.025$ compared with preflight. ** $P < 0.01$ compared with preflight.

Conclusions

The results from the first two studies show that short duration spaceflight leads to significant reductions in vagal control of heart rate that may contribute to orthostatic intolerance. The results from long duration flights (10 days or longer) provide further evidence of functionally relevant postflight disruption of autonomic regulation of arterial pressure and heart rate.

The results from the third study showed an apparent uncoupling between sympathetic nerve activity and peripheral resistance. Responses of presyncopal and non-presyncopal astronauts were not compared in this study.

The results of the fourth study have both spaceflight and Earth-bound importance. They suggest that spaceflight caused changes in central modulation of baroreflex function which were manifested as a hypoadrenergic response to standing. Furthermore, drastically differing susceptibilities to postflight orthostatic intolerance were observed in the astronaut population. This study also suggests that there was a subset of the astronaut population that had orthostatic responses well within normal ranges before flight, but was nevertheless predisposed to experience presyncope during upright posture after spaceflight. Data obtained from the preflight stand test show promise in predicting which crew members might be susceptible to postflight orthostatic intolerance. The flight surgeons may use this information to identify individuals who may be most likely to benefit from the application of an in-flight countermeasure.

GOAL 3 – COUNTERMEASURE STUDIES

Introduction

Orthostatic intolerance is a well-documented consequence of spaceflight. Causes could be postflight hypovolemia and/or autonomic dysfunction. Although preventive measures of fluid-load and use of a g-suit are required of every crew member, they have not been successful in totally preventing this problem [18]. Before EDOMP, the standard operational countermeasure in the U.S. Space Program was 8 gm salt, mixed in approximately 1 liter of water to provide isotonic saline [1]. New countermeasures to postflight orthostatic intolerance were evaluated during EDOMP. These included ingestion of hypotonic and hypertonic saline solutions before landing, in-flight use of fludrocortisone to expand plasma volume, and in-flight use of lower body negative pressure while ingesting isotonic saline to unload cardiopulmonary receptors and expand plasma volume.

Methods and Materials

In the first countermeasure study (DSO 478), the orthostatic tolerance and presyncopal symptoms of each crew member were documented at least 2 months before flight, using lower body negative pressure (LBNP) tolerance tests [19]. In this protocol, LBNP was applied in stepped decrements of 10 mmHg until the crew member

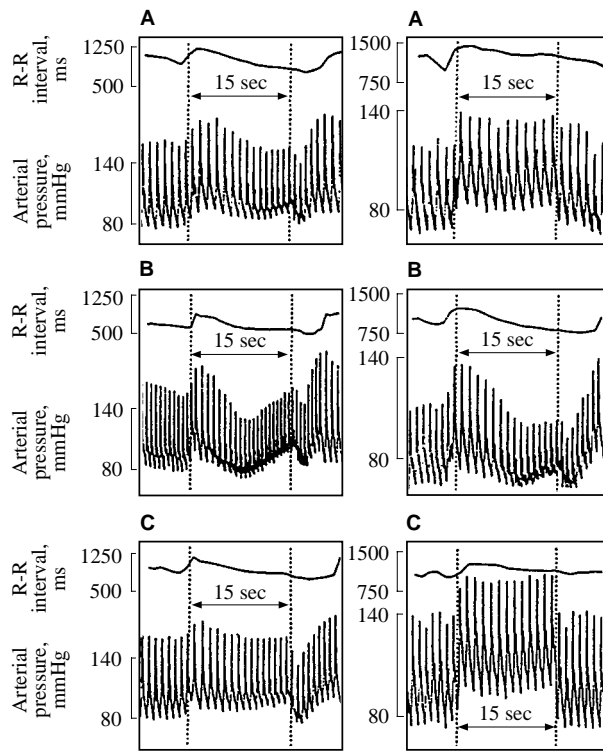


Figure 1-13. Left: blood pressure and R-R interval responses of 1 subject during Valsalva maneuvers preflight (A), on landing day (B), and 3 days after landing (C). Right: blood pressure and heart rate responses of different subject during Valsalva maneuvers preflight (A), on landing day (B), and 3 days after landing (C). This individual was a square-wave responder preflight.

exhibited evidence of presyncope, such as a sudden decrease in heart rate (a change of more than 15 bpm within 1 minute), or a systolic pressure less than 70 mmHg.

Baseline heart rate and arterial pressure data were also collected on each crew member using a preflight LBNP "ramp" test. The LBNP ramp test protocol began with 30 minutes of supine baseline data collection, followed by consecutive 5-minute stages at 0 (atmospheric pressure), -10, -20, -30, -40, -50, and -60 mmHg decompressions, and a 5-minute recovery stage at atmospheric pressure. Heart rate and arterial pressure were measured at least once each minute. Changes in leg circumference were measured continuously with a mercury-in-silastic strain gauge positioned over the largest area of the calf. Ultrasound echocardiographic measurements of heart dimensions and aortic blood flow velocity were also acquired on four missions, for correlation with similar in-flight measurements.

A collapsible LBNP device, developed for use aboard the Shuttle, was used for all in-flight LBNP

exposures. A modified clinical automatic blood pressure monitor measured heart rate and arterial pressure once per minute and provided analog signals for telemetry to the ground station. A modified clinical ultrasound echocardiograph was used on four missions to document changes in heart volume and blood flow during LBNP.

The LBNP treatment protocol (called a soak) began with a stepwise decompression to -50 mmHg, followed by about 3.5 hours of decompression at -30 mmHg below ambient pressure. One liter of water or artificially sweetened fruit drink, and 8 gm of sodium chloride, were ingested during the first hour of -30 mmHg decompression. The treatment was evaluated by comparing heart rate and arterial pressure responses to the in-flight ramp

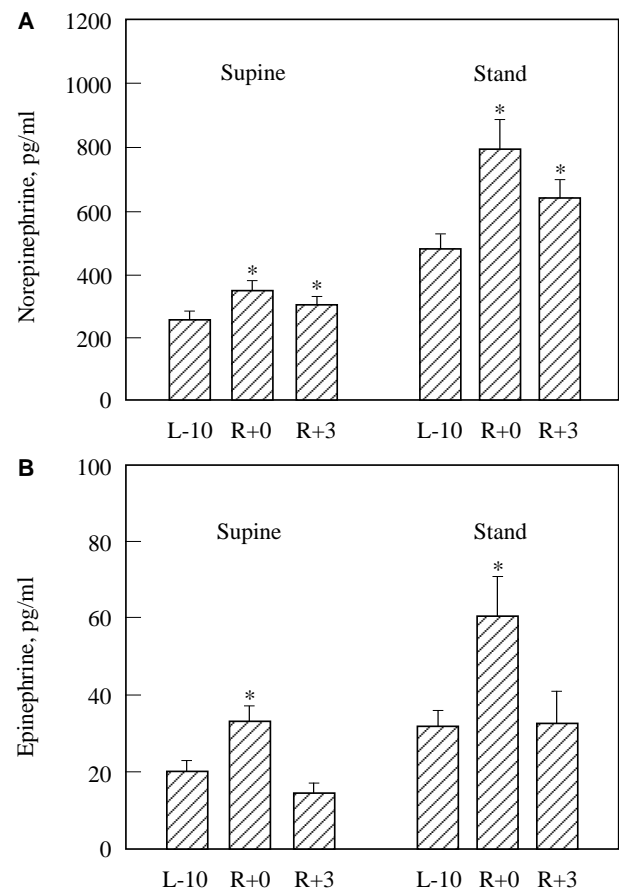


Figure 1-14. Supine and standing plasma norepinephrine and epinephrine concentrations before and after spaceflight. Norepinephrine and epinephrine were quantified from samples obtained 10 days before flight (L-10), on landing day (R+0), and 3 days after flight (R+3). A: supine (n = 24) and standing (n = 16) norepinephrine levels. B: supine (n = 23) and standing (n = 15) epinephrine levels. *Significantly different from corresponding L-10 value, $P < 0.05$ (analysis of variance; Dunnett's test).

Table 1-5. Supine measurements from all subjects on all test days

	Preflight	Landing Day	Days Postflight				
			1-2	3	4	6-8	10-18
<i>Baseline measurements</i>							
Systolic pressure, mmHg	110±2	115±2*	112±2	112±2	114±1	112±2	112±2
Diastolic pressure, mmHg	73±1	75±2	74±2	74±2	73±2	73±1	74±2
R-R interval, ms	1,159±49	1,003±51 [†]	1,024±45 [†]	1,132±54	1,088±48	1,069±53	1,020±43
Body wt, kg	78.5±3.7	76.0±3.8*	76.5±3.5	76.9±3.8	77.2±3.7	77.1±3.6	77.4±3.5
Norepinephrine, pg/ml	290±35	332±39*		303±23			
Epinephrine, pg/ml	27±5	36±6*		22±3			
<i>Baroreflex measurements</i>							
Maximum slope, ms/mmHg	4.7±0.4	4.0±0.4*	3.8±0.4*	4.7±0.6	4.4±0.5	5.6±0.6	3.4±0.6
R-R range, ms	244±23	186±17*	181±16 [†]	233±24	214±21	245±22	233±24
Operational point, %	36.3±3.8	29.8±4.7	34.2±3.9	36.9±4.9	35.0±3.6	32.0±3.9	31.0±4.2
Minimum R-R, ms	1,080±42	968±48*	980±86*	1,090±50	1,008±42	1,022±51	979±40
Maximum R-R, ms	1,323±54	1,154±51*	1,162±51*	1,323±61	1,222±53	1,267±61	1,212±51
Carotid distending pressure at minimum R-R, mmHg	75±2	80±4	75±3	75±3	76±2	75±3	78±3
Carotid distending pressure at maximum R-R, mmHg	162±4	165±5	161±4	159±5	165±4	160±4	168±3

Values are means ± SE; n=16 subjects, n = 12 subjects used for all comparisons between landing day and preflight measurements and those between landing day and days 10-18 measurements. * $P < 0.025$; [†] $P < 0.01$.

tests, at 3-day intervals before, and 1 or 2 days after, the soak treatment. The stepwise decompression at the beginning of the treatment also provided information on cardiovascular function immediately before treatment.

The second countermeasure study (DSO 623) sought to determine if the soak treatment described above, performed 24 hours before landing, would preserve orthostatic tolerance after landing [19]. In this study, the orthostatic tolerance and presyncopal symptoms of each participating crew member were documented during two LBNP tolerance tests occurring between 120 and 90 days before launch. Baseline heart rate and arterial pressure were measured on each crew member, using a ramp test on two preflight sessions between 90 and 30 days before launch. During each test, heart rate and arterial pressure were measured once per minute, along with continuous recordings of electrocardiogram and noninvasive, beat-to-beat, finger blood pressure using the Finapres™ device. Ultrasound echocardiographic measurements of heart dimensions and aortic blood flow were also acquired on two crew members for correlation with similar in-flight measurements. Crew member subjects also performed a preflight stand test to measure baseline orthostatic responses.

In flight, “active” crew member subjects participated in a single 4-hour soak treatment on the nominal day before landing. The average heart rate (HR), systolic (SBP) and diastolic pressures, mean arterial pressure (MAP), pulse

pressure, tolerance index (MAP/MAP baseline)/ (HR/HR baseline), and shock index (SBP/HR) were determined at each stage of decompression. Results from subjects who performed the soaks (active subjects) were compared with those who did not perform the soaks (inactive subjects).

In the third countermeasure study (DSO 479), 23 astronauts from five Shuttle flights each consumed one of three fluid loading solutions 1 to 2 hours before landing. The solution choices were: (1) hyperosmotic (1.07%) salt tablets/water solution, (2) isotonic saline solution, and (3) salt tablets and water to equal isotonic saline solution. These solutions had previously been evaluated in ground-based studies for their efficacy in increasing plasma volume [20]. Each crew member performed a stand test two times before flight, on landing day to assess the effectiveness of the candidate fluid loading countermeasure, and three days after landing to verify return to preflight baseline status.

In the fourth countermeasure study (DSO 621), fludrocortisone was tested as a means to expand plasma volume and improve postflight orthostatic tolerance. The following regimens for fludrocortisone were used: (1) 0.2 mg twice daily (B.I.D.) for the last 5 days of flight, (2) 0.1 mg B.I.D. for the last 5 days of flight, or (3) a single dose of 0.3 mg taken 7 hours before landing. Supine blood volume, supine and standing heart rate and arterial pressure, and plasma catecholamines were measured before and after flight.

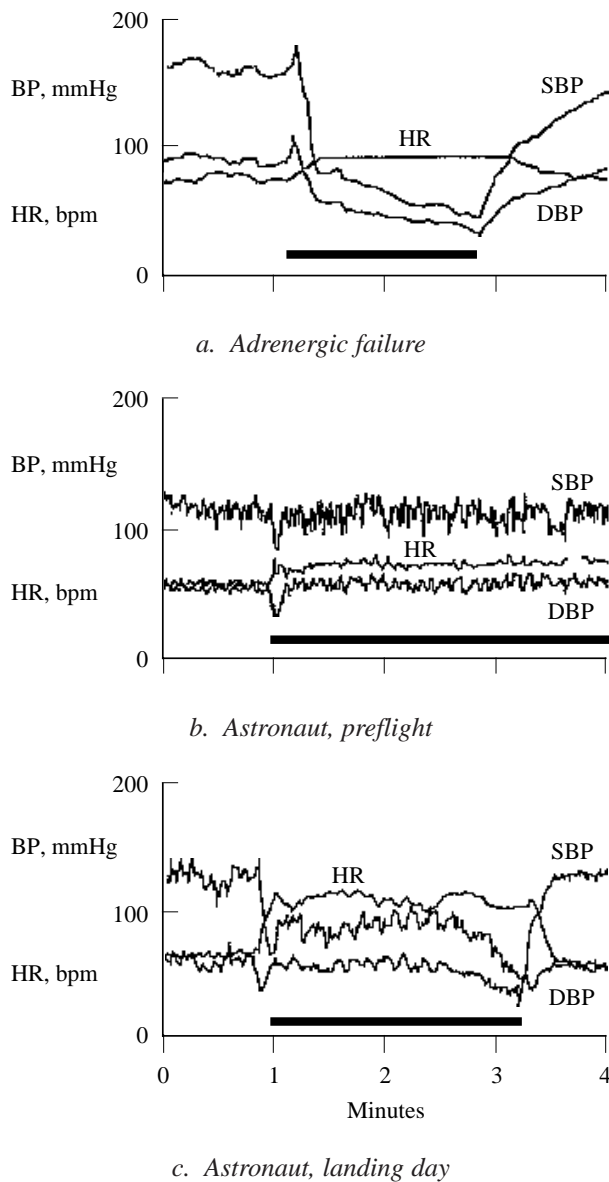


Figure 1-15. Beat-to-beat blood pressure and heart rate during stand tests.

Results

In the first countermeasure study (DSO 478), data applicable to the evaluation of the LBNP countermeasure were obtained for 4 of the 13 crew member subjects. The protective effect of the LBNP and concurrent saline ingestion were evaluated by comparison of heart rate and systolic and diastolic pressures at maximum decompression. Two of the four subjects did not reach the maximum planned level of decompression (-50 mmHg) at least once during flight. However, they did achieve the -40 mmHg level at each session. Therefore, for those two subjects, the

reported heart rate and arterial pressure responses are from -40 mmHg decompression preflight and in flight.

The heart rate and systolic and diastolic pressures during maximum LBNP before and during flight, both before and after the soak treatment, are shown in Figure 1-16. Heart rate increased significantly between preflight and early in-flight tests (flight days 3 to 5), but thereafter plateaued between the mid-flight and late in-flight tests before treatment. One day after the soak treatment, the heart rate response to maximum LBNP was significantly less than before the soak, indicating that the soak had a beneficial effect. Two days after treatment, the heart rate response to LBNP was returning toward the pre-soak value, indicating that the beneficial effect was lost (Figure 1-16a). Neither systolic nor diastolic pressures during LBNP differed across all preflight and in-flight values (Figures 1-16b, 1-16c).

In the second study (DSO 623), which was an actual trial of the countermeasure, data were obtained from five crew members who underwent the soak on the day before landing, and seven crew members (including one who participated in LBNP ramp tests but not the soak) from the same missions who did not participate in other countermeasure studies. Data from two crew members whose landing was delayed by one day were pooled with data from three crew members who landed as planned on the day after LBNP treatment. There was no practical possibility of repeating the treatment on a wave-off day because of crew time constraints.

Data collected shortly after landing, during the Orbiter stand test with g-suit inflated, show a difference between the crew members using, or not using, LBNP during the flight. Diastolic pressure was lower in LBNP subjects, both seated and standing, than in non-LBNP subjects (Figure 1-17a). The non-LBNP subjects showed a greater tendency for systolic pressure to decrease after standing than the LBNP subjects (data not shown). Finally, the LBNP subjects showed a lower heart rate both seated and standing than the non-LBNP subjects (Figure 1-17b). There were no differences between LBNP and non-LBNP subjects in red blood cell volume, plasma volume, or heart rate and arterial pressures during stand tests 1 to 3 hours after landing (data not shown).

In the fourth countermeasure study (DSO 621), the results indicate that fludrocortisone, as administered by the first two protocols, was not tolerated by the crew members. None of the protocols restored blood volume. The percent change in plasma and red blood cell volume from preflight to postflight was not significantly different in the fludrocortisone vs. non-fludrocortisone group (Figure 1-18). Fludrocortisone subjects did not have greater orthostatic tolerance than control subjects on landing day. Participation in protocols was incomplete and limited by subjective evaluation of the medication; therefore, only limited conclusions could be made.

Table 1-6. Comparison of landing day values for presyncopal vs. non-presyncopal astronaut subjects

a. Landing day measurements

	Presyncopal on Landing Day (n = 8)			Nonpresyncopal on Landing Day (n = 21)		
	Supine	Standing	Standing-supine	Supine	Standing	Standing-supine
Plasma norepinephrine, pg/ml	330 ± 67	420 ± 46*	105 ± 41*	278 ± 18	618 ± 88*	340 ± 62*
Peripheral vascular resistance, mmHg • l ⁻¹ • min	16.0 ± 1.3	22.9 ± 2.5*	6.4 ± 2.9	21.1 ± 1.6	33.8 ± 2.7*	12.6 ± 2.6
Diastolic pressure, mmHg	74 ± 4	61 ± 4†	-14 ± 7†	76 ± 2	81 ± 2†	3 ± 2†
Systolic pressure, mmHg	110 ± 4*	80 ± 3†	-28 ± 4†	120 ± 2*	109 ± 3†	-11 ± 3†
Heart rate, beats/min	72 ± 5*	114 ± 8†	41 ± 6*	62 ± 2*	91 ± 4†	29 ± 3*
Stroke volume, ml	78 ± 4	28 ± 2	-51 ± 5	77 ± 5	32 ± 9	-44 ± 5
Cardiac output, l/min	5.5 ± 0.3	3.3 ± 0.3	-2.4 ± 0.3	4.7 ± 0.3	2.9 ± 0.2	-1.8 ± 0.3
Mean flow velocity (middle cerebral artery), cm/s	52.4 ± 4.7	40.0 ± 2.9	-12.4 ± 2.2	47.6 ± 2.3	39.7 ± 1.6	-7.5 ± 1.2
Cerebral vascular resistance, mmHg • cm ⁻¹ • s	1.7 ± 0.3	1.1 ± 0.1†	-0.7 ± 0.2	2.0 ± 0.1	1.6 ± 0.1†	-0.4 ± 0.1
Plasma epinephrine, pg/ml	42 ± 5	66 ± 12	20 ± 13	23 ± 2	48 ± 6	25 ± 7
Plasma renin activity, ng • ml ⁻¹ • h ⁻¹	2.7 ± 1.2	3.4 ± 1.5	1.3 ± 0.6	2.2 ± 0.3	3.7 ± 0.6	1.5 ± 0.3
Plasma volume, liters	2.7 ± 0.2			3.2 ± 0.2		

Values are means ± SE, n, no. of subjects. Supine, standing, and standing-supine difference measurements for all variables (plasma volume was only measured supine) are separated into presyncopal and nonpresyncopal groups on landing day. *P < 0.05 between groups. †P < 0.01 between groups

b. Preflight measurements

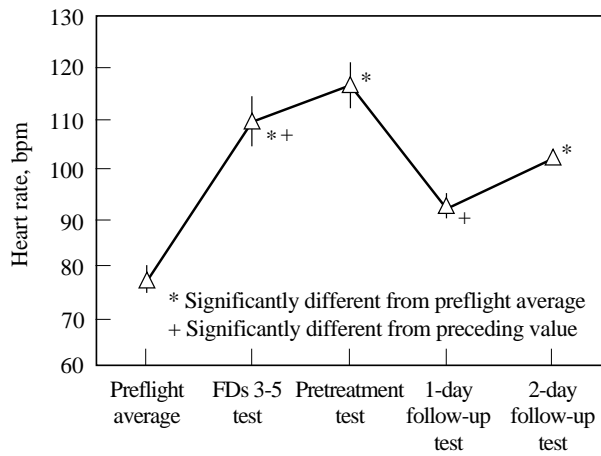
	Presyncopal on Landing Day (n = 8)			Nonpresyncopal on Landing Day (n = 21)		
	Supine	Standing	Standing-supine	Supine	Standing	Standing-supine
Plasma norepinephrine, pg/ml	213 ± 28	467 ± 42	254 ± 37	209 ± 15	466 ± 44	257 ± 38
Peripheral vascular resistance, mmHg • l ⁻¹ • min	15.5 ± 0.9*	22.9 ± 1.8*	7.4 ± 1.5	21.2 ± 1.9*	31.8 ± 2.3*	10.6 ± 1.9
Diastolic pressure, mmHg	66 ± 2†	69 ± 4†	3 ± 3	73 ± 2†	77 ± 2†	4 ± 1
Systolic pressure, mmHg	109 ± 3*	99 ± 4†	-10 ± 2*	114 ± 2*	108 ± 3†	-5 ± 2*
Heart rate, beats/min	62 ± 2†	81 ± 5†	19 ± 5	54 ± 1†	71 ± 2†	17 ± 2
Stroke volume, ml	86 ± 5	45 ± 5	-41 ± 3	83 ± 4	41 ± 2	-43 ± 3
Cardiac output, l/min	5.3 ± 0.5*	3.6 ± 0.4*	-1.7 ± 0.2	4.4 ± 0.2*	2.9 ± 0.2*	-1.6 ± 0.2
Mean flow velocity (middle cerebral artery), cm/s	58.9 ± 5.7	51.2 ± 2.5*	-7.5 ± 1.6	53.4 ± 5.5	43.1 ± 2.1*	-11.4 ± 2.3
Cerebral vascular resistance, mmHg • cm ⁻¹ • s	1.5 ± 0.2	1.1 ± 0.2*	-0.4 ± 0.1	1.9 ± 0.1	1.5 ± 0.1*	-0.4 ± 0.1
Plasma epinephrine, pg/ml	19 ± 3	30 ± 3	12 ± 2	24 ± 3	38 ± 4	14 ± 4
Plasma renin activity ng • ml ⁻¹ • h ⁻¹	1.7 ± 0.4	2 ± 0.5	0.3 ± 0.2	1.3 ± 0.2	1.6 ± 0.2	0.2 ± 0.1
Plasma volume, liters	3.2 ± 0.2			3.4 ± 0.1		

Values are means ± SE, n, no. of subjects. Supine, standing, and standing-supine difference measurements for all variables (plasma volume was only measured supine) are separated into presyncopal and nonpresyncopal groups before flight (average of 2 preflight data sessions). *P ≤ 0.05 between groups. †P ≤ 0.01 between groups

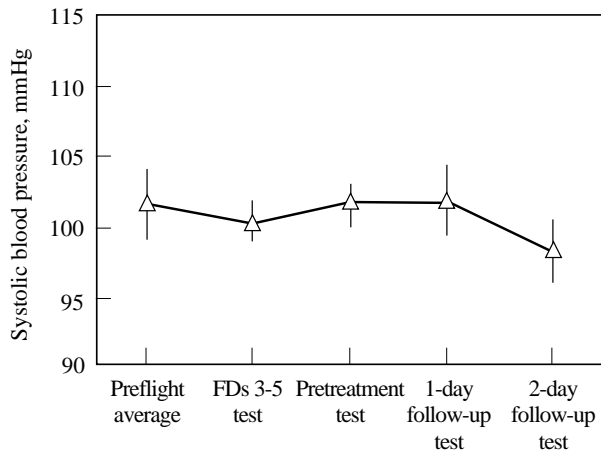
c. Measurements 3 days after landing

	Presyncopal on Landing Day (n = 8)			Nonpresyncopal on Landing Day (n = 21)		
	Supine	Standing	Standing-supine	Supine	Standing	Standing-supine
Plasma norepinephrine, pg/ml	234 ± 36	552 ± 86*	318 ± 57	252 ± 23	509 ± 53*	256 ± 39
Peripheral vascular resistance, mmHg • l ⁻¹ • min	16.3 ± 0.9	23.9 ± 0.9†	7.6 ± 2.5*	21.5 ± 1.9	36.4 ± 2.5†	14.9 ± 2.0*
Diastolic pressure, mmHg	68 ± 2†	71 ± 4†	3 ± 3	77 ± 1†	81 ± 2†	5 ± 2
Systolic pressure, mmHg	110 ± 7*	96 ± 5†	-14 ± 4*	118 ± 2*	114 ± 3†	-5 ± 2*
Heart rate, beats/min	60 ± 2*	83 ± 6	23 ± 5	57 ± 2*	75 ± 2	20 ± 2
Stroke volume, ml	87 ± 8	54 ± 7	-42 ± 7	83 ± 5	37 ± 3	-46 ± 4
Cardiac output, l/min	5.1 ± 0.3	3.6 ± 0.4	-1.5 ± 0.3	4.7 ± 0.3	2.8 ± 0.2	-1.9 ± 0.2
Mean flow velocity (middle cerebral artery), cm/s	63.3 ± 7.2	57.0 ± 6.8	-6.3 ± 1.2	50.6 ± 3.0	46.1 ± 3.0	-3.9 ± 1.3
Cerebral vascular resistance, mmHg • cm ⁻¹ • s	1.4 ± 0.2	1.1 ± 0.2	-0.4 ± 0.1	1.9 ± 0.1	1.5 ± 0.1	-0.4 ± 0.1
Plasma epinephrine, pg/ml	18 ± 4	25 ± 4*	7 ± 5	25 ± 4	38 ± 4*	14 ± 4
Plasma renin activity ng • ml ⁻¹ • h ⁻¹	1.9 ± 0.7	1.7 ± 0.8	0.4 ± 0.2	1.2 ± 0.2	1.4 ± 0.3	0.3 ± 0.08
Plasma volume, liters	3.5 ± 0.2			3.6 ± 0.1		

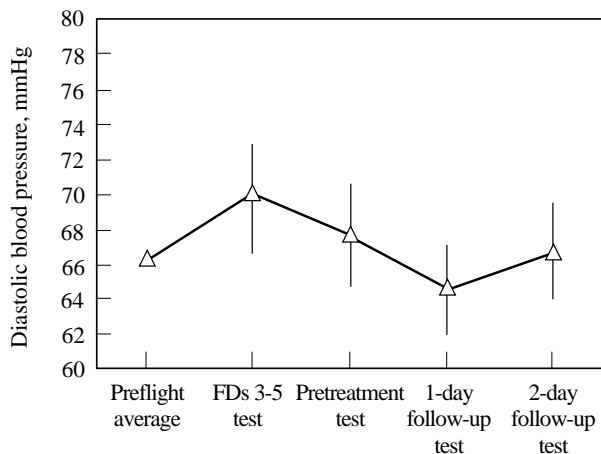
Values are means ± SE, n, no. of subjects. Supine, standing, and standing-supine difference measurements for all variables (plasma volume was only measured supine) are separated into presyncopal and nonpresyncopal groups three days after landing. *P ≤ 0.05 between groups. †P ≤ 0.01 between groups.



a.

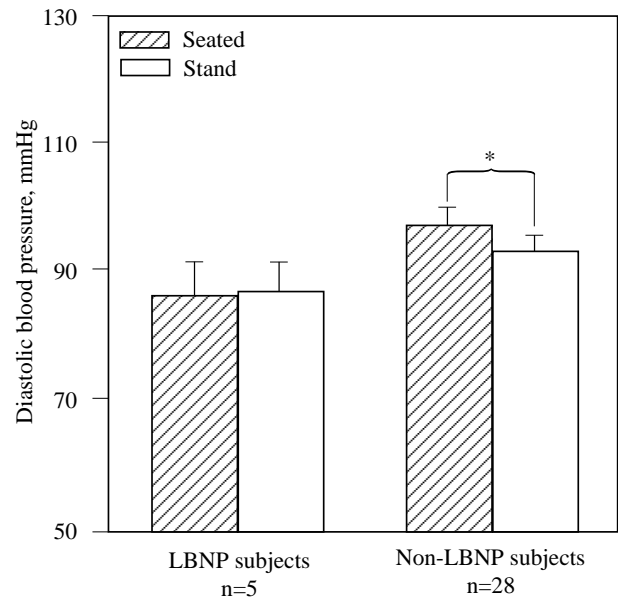


b.

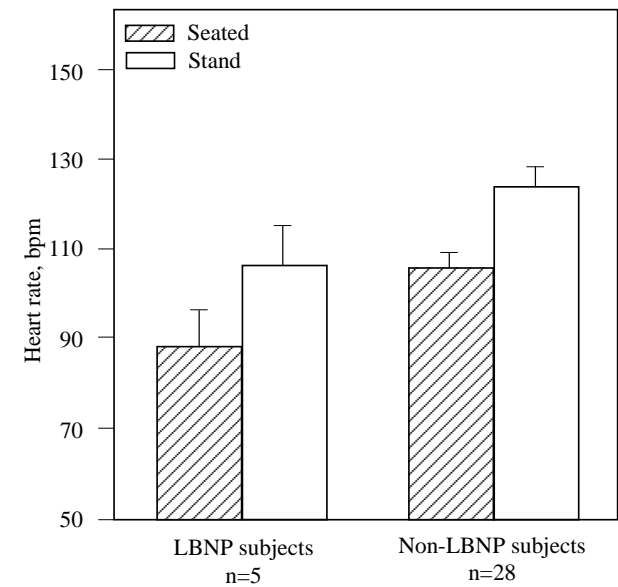


c.

Figure 1-16. Heart rate, systolic blood pressure, and diastolic blood pressure during LBNP test preflight and in flight at maximum level of LBNP for four astronauts.



a. Diastolic blood pressure



b. Heart rate

Figure 1-17. Postflight stand test with g-suit inflated.

Conclusions

In-flight heart rate, during -40 to -50 mmHg lower body ramp decompressions, increased until the day of the LBNP soak. One day after LBNP soak, the heart rate response to -40 to -50 mmHg lower body decompression indicated that the soak had a protective effect. Two days after the combined countermeasure, the effect was gone. These data were obtained in flight as part of DSO 478.

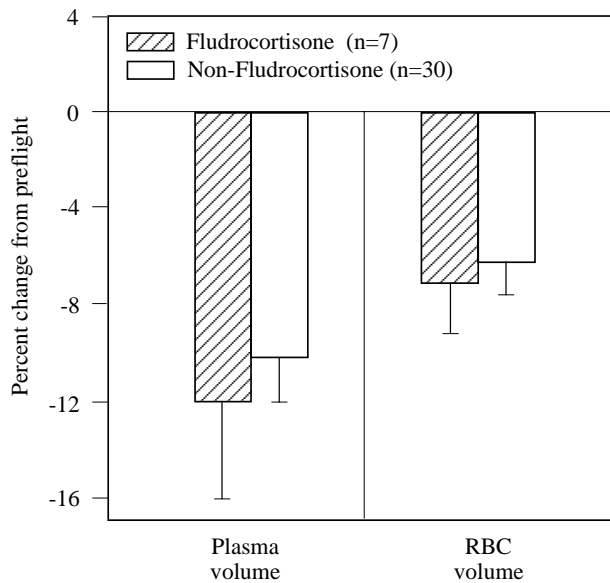


Figure 1-18. Effect of fludrocortisone on plasma volume losses.

The combination of LBNP with ingestion of fluid and salt is a potentially efficacious countermeasure against postflight orthostatic intolerance. Early in-flight loss of orthostatic capacity was documented in this study. This suggests that the significant cardiovascular deficit observed after long duration missions is already well developed after much shorter flights of 10 days or less. We would infer that the same type of protective or ameliorative measures envisaged for long duration crew members should also be made available to their short duration counterparts. However, in terms of a cost/benefit analysis, the soak has not been accepted for general operational applications, since approximately 5 hours are required to treat one subject.

In the third countermeasure study (DSO 479), evaluation of the relative efficacy of the different candidate fluid loading solutions was difficult due to the existence of several factors that compromised data quality. These factors were: (1) a flight rule requiring crew members to repeat half of the fluid load protocol in the event of a one revolution wave-off of landing, (2) variations in the amount of solution ingested, (3) subsequent uncontrolled fluid ingestion after completion of the fluid loading protocol, which, in effect, diluted the prescribed solutions, and (4) use of fluids other than water, as prescribed, which altered not only the conditions of the investigation but also the efficacy of the countermeasure.

Evaluation of the candidate fluid loading countermeasure solutions and their ability to maintain orthostatic function after spaceflight was terminated without providing a conclusive answer to the question of the efficacy of a hypertonic solution as an end-of-mission rehydration

countermeasure. Results from in-flight use of fludrocortisone led us to conclude that fludrocortisone, as administered, had no effect on orthostatic intolerance.

DISCUSSION

Cardiovascular deconditioning was observed in astronauts early in the manned spaceflight program [21]. A component of deconditioning included a cephalid fluid shift and resultant loss of fluid [22]. Bed rest studies revealed the usefulness of oral rehydration in providing a degree of protection against orthostatic intolerance [23]. One of the early DSO studies showed some improvement in cardiovascular deconditioning by using fluid loading as a countermeasure [1]. Subsequently, oral fluid and salt loading was adopted as an operational countermeasure for all Shuttle crew members. Nevertheless, virtually every astronaut returning from space continued to suffer from some degree of orthostatic intolerance. Returning astronauts typically developed orthostatic intolerance attributable to autonomic dysfunction when subjected to upright posture [7, 8, 18, 24]. Signs and symptoms include tachycardia, nausea, vomiting, lightheadedness (presyncope), and fainting (syncope). Common treatments for orthostatic intolerance, such as blood volume expansion (oral fluid loading) or shock trousers (anti-gravity suits), when modified to protect astronauts, have not been completely effective [18, 25]. Orthostatic intolerance in returning astronauts normally resolves without treatment in 1 to 2 days.

Various cardiac dysrhythmias have been reported throughout the U.S. spaceflight experience. These have occurred during activities both inside and outside the space vehicle [21]. In flight, Holter monitoring of astronauts showed the incidence of dysrhythmias to be no greater during flight than before flight, leading to the conclusion that spaceflight alone does not cause an increase in the incidence of dysrhythmias [10].

Documented responses to landing day activities show that the cardiovascular system is under significant stress during entry, landing, and seat egress [15]. No differences were found that were related to flight duration between 4 to 14 days. Nominal entry, landing and seat egress are associated with blood pressure decreases and heart rate increases. The cardiovascular systems of about 30% of the subjects were compromised during the landing period.

Immediately after Shuttle landing, the cardiovascular system was challenged to support arterial pressure, resulting in standing heart rates as high as 160 bpm and systolic pressure drops by as much as 25 mmHg [15]. Landing day studies conducted one to two hours after landing have shown that heart rates, arterial pressures, and supine and standing plasma catecholamine levels all were elevated, but increases in peripheral vascular resistance per unit increase in circulating norepinephrine were reduced.

Changes in autonomic regulation affect postflight cardiovascular function. Attenuation of the vagally mediated carotid baroreceptor cardiac reflex response may begin early in flight and persist for about a week postflight. On landing day, reductions in this reflex correlate directly with lower standing systolic pressures. Decreases in heart rate and arterial pressure during flight were reversed on landing day, and the frequency of cardiac dysrhythmias decreased in flight, compared to preflight values. These reports suggest that sympathetic activity may be low during spaceflight, but they do not support the conclusion that loss of plasma volume was the primary cause of postflight orthostatic hypotension.

There was a wide range of individual susceptibility to orthostatic intolerance after spaceflight. Some individuals had severe symptoms, while others were less affected [7, 8]. These data, taken as a whole, provide convincing evidence that the precipitating factor for orthostatic intolerance after spaceflight was a hypoadrenergic response to orthostatic stress. The parallel insufficient levels of plasma norepinephrine, diastolic pressure, and peripheral vascular resistance strongly support this.

These data suggest that human cardiovascular adaptations to the microgravity encountered during spaceflight included changes in central modulation of baroreceptor inputs that contributed to a hypoadrenergic response to orthostasis and presyncope in 25% of returning astronauts. The idea of changes in central modulation is supported by other symptoms, including retention/incontinence; diarrhea; constipation; changes in vision, taste, smell, thirst, and appetite; and hypesthesias as well as parasthesias in the feet.

These data not only suggest a mechanism for postflight orthostatic intolerance, but also show clear differences between susceptible and non-susceptible individuals. The data, for the first time, also raise the possibility of predicting susceptible individuals before launch. The intergroup differences before flight suggest that there was a subset of the normal population with orthostatic responses within the normal range before flight that was somehow predisposed to postflight orthostatic intolerance. In this subgroup, the norepinephrine responses to standing were normal both before and 3 days after flight. However, during every test session the subgroup tended to have somewhat lower vascular resistance and arterial pressures, and higher heart rates than the other group. This suggests possible preflight intergroup differences in venous compliance or vascular responsiveness. Spaceflight somehow caused this subgroup to have greatly subnormal adrenergic responses after they landed, while their norepinephrine responses to standing were very similar to those in patients with autonomic dysfunction known to be centrally modulated.

A number of countermeasures to prevent orthostatic intolerance have been studied. Fluid loading has shown

some benefits as mentioned earlier. A second trial procedure has been the LBNP soak, which typically decompresses the legs and abdomen by up to -30 mmHg and allows fluid to pool in the legs and abdomen [26, 27]. Brief decompression of up to -50 mmHg (ramp) was used as a gravity-independent test of orthostatic capacity. Longer decompression (soak), either alone or in combination with salt and water ingestion, has been used as a countermeasure trial in an attempt to restore orthostatic tolerance. One day after LBNP soak, decreased heart rate response to -40 to -50 mmHg lower body decompression indicated in flight (DSO 478) that the soak provided a protective effect. Diastolic blood pressure was lower in LBNP subjects, both seated and standing, than in non-LBNP subjects, suggesting that the LBNP subjects required a smaller increase in total peripheral resistance to maintain adequate blood pressure. The non-LBNP subjects showed a greater tendency for systolic blood pressure to decrease after standing than did the LBNP subjects. The LBNP subjects showed a lower heart rate both seated and standing than the LBNP subjects. This suggests that the LBNP subjects treated by the soak procedure had a greater reserve capacity to increase heart rate if required by the metabolic demand. However, these differences were not statistically significant.

A third countermeasure under study was fludrocortisone, which causes renal retention of sodium with consequent plasma volume expansion. Fludrocortisone has shown some ability to restore plasma volume and orthostatic tolerance at the end of bed rest [23]. The use of fludrocortisone did not restore blood volume when used in flight by astronauts, using the single-dose regimen noted. Further, fludrocortisone subjects did not seem to have greater orthostatic tolerance than control subjects on landing day.

SUMMARY

Findings from the Cardiovascular EDOMP studies include:

1. Changes in central modulation of baroreceptor inputs result in a hypoadrenergic response to orthostasis and presyncope in 25% of returning astronauts, as documented by a 10-minute clinical stand test.
2. Spaceflight alone does not increase the incidence of dysrhythmias, nor does it constitute a significant cardiovascular stress.
3. Landing poses a significant cardiovascular stress.
4. There are clear differences between susceptible and non-susceptible individuals.
5. Susceptibility of individuals to postflight orthostatic intolerance may be predicted before launch.

RECOMMENDATION

With the conclusion of the EDOMP, the Cardiovascular Laboratory at JSC has reported some significant findings that might be quickly translated into countermeasure trials for postflight orthostatic intolerance. A comparison of presyncopal and non-presyncopal astronaut responses to standing has shown significant differences between the two groups on landing day. The most fundamental intergroup difference was the low standing norepinephrine levels in the presyncopal group, which ultimately resulted in inadequate cerebral perfusion and presyncope. The failure to increase norepinephrine translated into lower peripheral vascular resistance, lower arterial pressures, and lower heart rate responses to decreasing systolic pressure in the presyncopal group. Crew members who became presyncopal on landing day also showed some differences before launch, such as lower peripheral vascular resistance, and lower systolic and diastolic pressures with standing.

This loss of the pressor response suggests that a pharmacological countermeasure could be utilized to combat orthostatic intolerance. A systematic study using pressor agents could prove the efficacy of the pharmacological approach. Coupling a successful pressor agent with the at-risk crew members, diagnosed as described above, would allow flight surgeons to more effectively manage postflight orthostatic intolerance in astronauts.

REFERENCES

1. Bungo MW, Charles JB, Johnson PC Jr. Cardiovascular deconditioning during space flight and the use of saline as a countermeasure to orthostatic intolerance. *Aviat Space Environ Med* 1985; 56(10):985-990.
2. Charles JB, Bungo MW, Fortner GW. Cardio-pulmonary function. In: Nicogossian AE, Huntoon CL, Pool SL, editors. *Space physiology and medicine*. 3rd ed. Philadelphia: Lea & Febiger; 1994; 286-304.
3. Charles JB, Lathers CM. Cardiovascular adaptation to spaceflight. *J Clin Pharm* 1991; 31:1010-1023.
4. Johnson RL, Hoffler GW, Nicogossian AE, Bergman SA Jr, Jackson MM. Lower body negative pressure: third manned Skylab mission. In: Johnston RS, Dietlein LF, editors. *Biomedical results from Skylab (NASA SP-377)*. Washington: U.S. Government Printing Office; 1977; 284-312.
5. Michel EL, Rummel JA, Sawin CF, Buderer MC, Lem JD. Results of Skylab medical experiment M171-metabolic activity. In: Johnston RS, Dietlein LF, editors. *Biomedical results from Skylab (NASA SP-377)*. Washington: U.S. Government Printing Office; 1977; 372-387.
6. Blomqvist CG, Nixon JV, Johnson RL Jr, Mitchell HH. Early cardiovascular adaptation to zero gravity simulated by head-down tilt. *Acta Astronaut* 1980; 7:543-553.
7. Fritsch JM, Charles JB, Bennett BS, Jones MM, Eckberg DL. Short-duration spaceflight impairs human carotid baroreceptor-cardiac reflex responses. *J Appl Physiol* 1992; 73:664-671.
8. Fritsch-Yelle JM, Charles JB, Jones MM, Beightol LA, Eckberg DL. Spaceflight alters autonomic regulation of arterial pressure in humans. *J Appl Physiol* 1994; 77(4):1776-1783.
9. Robertson D, Biaggioni I, Mosqueda-Garcia R, Robertson RM. Orthostatic hypotension of prolonged weightlessness: clinical models. *Acta Astronaut* 1992; 27:97-101.
10. Fritsch-Yelle JM, Charles JB, Crockett MJ, Wood ML. Microgravity decreases heart rate and arterial pressure in humans. *J Appl Physiol* 1996; 80(3): 910-914.
11. Mulvagh SL, Charles JB, Riddle JM, Rehbein TL, Bungo MW. Echocardiographic evaluation of the cardiovascular effects of short-duration spaceflight. *J Clin Pharm* 1991; 31:1024-1026.
12. Sahn DJ, DeMaria A, Kisslo J, Weyman A. The committee on m-mode standardization of the American Society of Echocardiography: Results of a survey of echocardiographic measurements. *Circulation* 1978; 58:1072-1083.
13. Teichholz LE, Kreulen T, Hermand MV, Gorlin R. Problems in echocardiographic volume determinations: echocardiographic-angiographic correlations in the presence or absence of asynergy. *Am J Cardiol* 1976; 37:7-11.
14. Cooper RH, O'Rourke RA, Karliner JS, Peterson KL, Leopold GR. Comparison of ultrasound and cineangiographic measurement of the mean velocity of circumferential fibre shortening in man. *Circulation* 1972; 46:914-922.
15. Jones MM, Charles JB. Human blood pressure and heart rate changes during space shuttle landing and crew egress. (Abstract) *FASEB* 1993; 7:A665.
16. Eckberg DL, Fritsch JM. Human autonomic responses to actual and simulated weightlessness. *J Clin Pharm* 1991; 31:951-954.
17. Whitson PS, Charles JB, Williams WJ, Cintron NM. Changes in sympathoadrenal response to standing in humans after space flight. *J Appl Physiol* 1995; 79:428-433.
18. Fritsch-Yelle JM, Whitson PA, Bondar RL, Brown TE. Subnormal norepinephrine release relates to presyncope in astronauts after space flight. *J Appl Physiol* 1996; 81(5):2134-2141.

19. Charles JB, Lathers CM. Summary of lower body negative pressure experiments during space flight. *J Clin Pharm* 1994; 36:571-583.
20. Frey MAB, Riddle J, Charles JB, Bungo MW. Blood and urine responses to ingesting fluids of various salt and glucose concentrations. *J Clin Pharm* 1991; 31:880-887.
21. Bungo MW, Johnson PC Jr. Cardiovascular examinations and observations of deconditioning during the space shuttle orbital flight test program. *Aviat Space Environ Med* 1983; 54:1001-1004.
22. Thornton WE, Hoffler GW, Rummel JA. Anthropometric changes and fluid shifts. In: Johnston RS, Dietlein LF, editors. *Biomedical results from Skylab (NASA SP-377)*. Washington: U.S. Government Printing Office; 1977; 324-338.
23. Vernikos J, Dallman MF, van Loon G, Keil LC. Drug effects on orthostatic intolerance induced by bedrest. *J Clin Pharm* 1991; 31:974-984.
24. Mulvagh SL, Charles JB, Fortney SM, Bungo MW. Changes in peripheral vascular resistance may account for orthostatic intolerance after space flight. (Abstract) *Circulation* 1990; 82:Supp III, 515.
25. Bungo MW. The cardiopulmonary system. In: Nicogossian AE, Huntoon CL, Pool SL, editors. *Space physiology and medicine*. 2nd ed. Philadelphia: Lea & Febiger; 1989; 179-201.
26. Wolthius RA, Bergman SA, Nicogossian AE. Physiological effects of locally applied reduced pressure in man. *Physiol Rev* 1974; 54(3):566-595.
27. Johnson PC, Driscoll TB, Leblanc AD. Blood volume changes. In: Johnston RS, Dietlein LF, editors. *Biomedical results from Skylab (NASA SP-377)*. Washington: U.S. Government Printing Office; 1977; 235-241.

Section 2

Regulatory Physiology

EXTENDED DURATION ORBITER MEDICAL PROJECT

Regulatory Physiology

Helen W. Lane, Peggy A. Whitson, Lakshmi Putcha, Ellen Baker, Scott M. Smith, and Karen Stewart of the Johnson Space Center, Houston, TX; Randall J. Gretebeck and R. R. Nimmagudda of the Universities Space Research Association; Dale A. Schoeller of The Committee on Human Health Nutrition and Nutritional Biology, University of Chicago Department of Medicine, Chicago, IL; Janis Davis-Street, Robert A. Pietrzyk, and Diane E. DeKerlegand of KRUG Life Sciences, Houston, TX; Charles Y. C. Pak of Southwestern Medical School, Dallas, TX; D.W.A. Bourne of the University of Oklahoma, Oklahoma City, OK

BACKGROUND

As noted elsewhere in this report, a central goal of the Extended Duration Orbiter Medical Project (EDOMP) was to ensure that cardiovascular and muscle function were adequate to perform an emergency egress after 16 days of spaceflight. The goals of the Regulatory Physiology component of the EDOMP were to identify and subsequently ameliorate those biochemical and nutritional factors that deplete physiological reserves or increase risk for disease, and to facilitate the development of effective muscle, exercise, and cardiovascular countermeasures. The component investigations designed to meet these goals focused on biochemical and physiological aspects of nutrition and metabolism, the risk of renal (kidney) stone formation, gastrointestinal function, and sleep in space. Investigations involved both ground-based protocols to validate proposed methods and flight studies to test those methods. Two hardware tests were also completed.

The first of the Regulatory Physiology studies was designed to relate nutritional status to the definition and maintenance of energy balance, with the primary focus on determining energy requirements during flight. Maintaining energy balance is an integral part of meeting the goals of the EDOMP because any crew member who is in negative energy balance (i.e., whose energy expenditure exceeds energy intake) will lose lean body mass regardless of the type, frequency, or intensity of exercise regimens [1,2] or protein consumption [3].

Results from Skylab suggest that crew members can and do lose weight during flight despite the consumption of adequate calories (energy) and protein [4]. The weight lost as a result of microgravity exposure generally consists of body fluids and electrolytes [5], red blood cells [6], and muscle or lean tissue [7]. A significant portion of in-flight weight loss, even during relatively brief missions (up to 10 days) is thought to be due to loss of lean body mass [4]. One important cause of loss of lean body mass is being in

negative energy balance [1]. Loss of lean body mass reduces muscle work capacity and promotes loss of electrolytes, especially potassium, both of which affect muscle and cardiovascular function. Detailed Supplementary Objective (DSO) 612 was designed to (1) measure total energy expenditure (TEE) during spaceflight, (2) compare those measurements with calculations of energy intake, and (3) compare those results with traditional estimates of energy requirements for healthy, active adults. The ultimate goal of this effort was to prevent loss of lean body mass and electrolytes by ensuring that crew members' energy intake was equivalent to their energy utilization.

A second aim of the Regulatory Physiology investigations was to assess how the physiological reactions to microgravity exposure affect the risk of forming renal stones. Renal stone risk can be assessed by characterizing the key factors that contribute to stone formation, including metabolic, environmental, and physicochemical factors [8]. Metabolic factors, so named because a change in their excretion is usually of metabolic origin, include urinary calcium, oxalate, uric acid, citrate, and pH. Risk factors that can be influenced by environmental factors include total urine volume and urinary sodium, sulfate, phosphorus, and magnesium. These metabolic and environmental factors are used to calculate physicochemical risk factors, e.g., the supersaturation of calcium oxalate, brushite (calcium phosphate), monosodium urate, undissociated uric acid, and struvite. These factors are compared to values from normal populations to assess the risk of stone formation relative to those populations.

Several of the physiological changes that take place during human exposure to microgravity are thought to affect the factors that contribute to the risk of renal stone formation, especially changes in urine volume or urinary calcium, phosphate, potassium, and sodium excretion. For example, urinary calcium concentrations begin to increase within 24 hours of exposure to microgravity [9]; urinary phosphate levels also tend to be higher during flight than

before. Both of these imbalances probably reflect the bone-demineralization process, and both increase the urinary saturation of calcium oxalate and calcium phosphate. Additional factors that could aggravate the potential for stone formation in astronauts include diets high in animal protein, frequent exercise, loss of lean body mass, and varying degrees of dehydration.

A precursor to DSO 610 involved analyzing urine samples from crew members before and immediately after spaceflight, and using those results to estimate risk profiles [10]. Although those results were limited by the lack of in-flight measurements, they did indicate that some metabolic reactions to spaceflight could increase the risk of renal stone formation, and that the risk could increase as the duration of flight increased [10]. DSO 610 was undertaken to characterize the risk of stone formation directly during flight. A secondary goal was to assess the influence of diet on the risk factors for stone formation.

The third segment of the Regulatory Physiology investigations concerned gastrointestinal (GI) function. The GI tract plays a central role in maintaining energy balance by absorbing nutrients from food and other consumed substances in forms that the body can use. Changes in GI motility and gastric secretion can result in decreased appetite [11] as well as malabsorption of amino acids, fats, vitamins, fluids, electrolytes, and many medications, which in turn affects the bioavailability of these substances [12-15]. GI motility, a central aspect of GI function, therefore plays a key role in the absorption and disposition of nutrients and drugs. The absence of a gravity vector in spaceflight, coupled with the corresponding changes in body posture and fluid distribution, may reduce GI motility.

GI motility has two distinct components: (1) gastric emptying (GE) rate, which is the rate at which the stomach contents empty into the small intestine, and (2) intestinal transit time, which is the rate at which the intestinal contents move from the small bowel to the cecum. GE rate is known to be slower in supine subjects [16,17]. A head-down bed-rest study was performed to determine whether the associated fluid redistribution, which mimics that of spaceflight, would alter GI motility; DSO 622 focused on measuring GE rate and intestinal transit time before and during spaceflight.

The fourth component of the Regulatory Physiology investigations focused on circadian rhythms, an important component of performance, during spaceflight. Efforts to maximize crew time during flight have included shifting work-rest schedules before flight to allow around-the-clock operations during missions. People who work in 24-hour operations consistently demonstrate drowsiness, fatigue, sleep disturbances, and impaired performance and mood [18-21]. The complexity and demanding nature of many spaceflight tasks dictate that any performance decrements arising from shift-change work must be minimized whenever possible.

Human circadian patterns can be altered by different methods: modifying the sleep period gradually over time with corresponding shifts in the work schedule or shifting by periodic timed exposures to bright light (7,000-12,000 lux). Bright light can shift cycles of body temperature, cortisol and melatonin release, markers of circadian patterns [22].

Plasma melatonin is a good indicator of shifts in human circadian rhythms [23-25]. The endogenous melatonin cycle is known to be sensitive to light and darkness, and seems to cycle in synchrony with core body temperature as well [26]. DSO 484 was designed to test the effectiveness of a timed bright-light treatment in combination with sleep shifting over a 7-day period before flight and during flight. The effectiveness of this shift was monitored daily by measuring melatonin and cortisol in saliva and urine samples.

Two new hardware devices also were tested as part of this effort: a Portable Clinical Blood Analyzer (PCBA) manufactured by the i-STAT Corporation of Princeton, NJ (DSO 492), and an In-flight Urine Collection Absorber (IUCA) device (DSO 328). Research on human adaptation to weightlessness often involves collecting biological samples, which typically are stored during flight and analyzed on return to Earth. This process presents several problems, including the inability to analyze and interpret data during the mission, the need for in-flight refrigeration or freezing, and the potential instability of the samples during storage. Real-time analysis of electrolytes, pH, and ionized calcium in blood samples would provide valuable information for physicians who provide health care to astronauts or other remote populations.

We assessed several performance characteristics of the PCBA on the ground and during spaceflight. A ground-based study involved comparisons of capillary (fingerstick) and venous blood, control solutions vs. blood samples, and PCBA vs. traditional laboratory methods. The flight study (DSO 492), on the other hand, involved real-time analyses of control solutions and capillary samples with the PCBA, and comparisons among preflight, in-flight, and postflight sample periods.

Also developed and tested was a prototype device for collecting and storing small volumes of urine during flight for experiments involving excretion of stable (non-radioactive) isotopes. The urine collection devices used for non-Spacelab missions were cumbersome, tended to leak, could not be used by women, and required considerable storage space. The IUCA was developed as an alternative that would facilitate the collection of small-volume urine samples for metabolic studies that did not require measurements of void volume.

The IUCA consisted of a small, conical piece of high-absorbency filter paper that could be placed in urine-collection funnels, which themselves were attached to the Shuttle waste collection system. This assembly could be used by men and women, and could be used on the

Table 2-1. EDOMP Regulatory Physiology investigations

DSO Number	Title	PI
612	Energy and Metabolic Requirements for Extended-Duration Space Flight Assessment	H.W. Lane
610	In-Flight Assessment of Renal Stones	P.A. Whitson
622	Gastrointestinal Function during Extended-Duration Spaceflight	L. Putcha
484	Assessment of Circadian Shifting in Astronauts by Bright Light	L. Putcha
492*	Evaluation of a Portable Clinical Blood Analyzer	H.W. Lane
328*	Evaluation of an In-Flight Urine Collection Absorber	H.W. Lane

*Assessment of flight hardware

Shuttle middeck. Ground-based evaluations focused on potential effects of the absorbent filter on the analysis of deuterium (^2H) and “heavy oxygen” (^{18}O), two stable isotopes that are used to measure energy expenditure, water metabolism, and body composition. DSO 328 was performed to evaluate the ease with which men and women could use this system during flight.

Table 2-1 lists the DSOs that were flown for the Regulatory Physiology section of the EDOMP. Methods and results from investigations of nutritional status, especially energy and hydration deficits, renal-stone formation risk, gastrointestinal changes, and circadian-rhythm shifting, are reviewed below.

METHODS AND RESULTS

Energy and Metabolic Requirements for Extended-Duration Space Flight (DSO 612)

The specific aim of this study was to measure energy intake and expenditure in healthy men during brief (<14-day) spaceflights, and to compare these measurements with estimates of energy requirements for healthy, active adults. Earlier estimates of energy requirements for spaceflight relied on results from metabolic balance studies and food intake records [4,27]. For this study, total energy expenditure was calculated by indirect calorimetry from a modified version of a doubly labeled water protocol [28], from records of food and fluid intake [29], and from

estimates of energy requirements published by the World Health Organization (WHO) [30].

Subjects were 13 men on six Shuttle flights between 1992 and 1994. Details of the study protocol are described elsewhere [31]. Briefly, each subject completed two 5-day test sessions, one before and the other during flight. Test sessions involved consuming a dose of doubly labeled water ($^2\text{H}^{18}\text{O}$), providing urine and saliva samples periodically, and recording food and fluid intake, as well as exercise and use of medications. These data were used to calculate water turnover, amount and nutrient content of consumed food, and total energy expenditure. Each crew member served as his own control, and the preflight assessment was the control period. One-way repeated-measures ANOVA was used to identify any differences between energy intake and expenditure in the preflight vs. in-flight periods and the WHO determination of energy requirements. The Student-Newman-Keuls test was used for post hoc comparisons. Paired t-tests were used to detect any differences in dietary intake between the preflight and in-flight periods. TEE was corrected for body weight and fat-free mass, and was tested similarly to detect differences between reported intake and expenditure.

Results

Results from this study are summarized in Table 2-2. Energy expenditures calculated by using the doubly labeled water technique were similar before and during flight, and also were similar to the WHO estimates for required energy. Thus, the WHO estimates were predictive of dietary energy requirements for this group of subjects, both before and during spaceflight. Both energy and fluid intake were lower during flight than before, and probably contributed to the overall weight loss for this group (mean -1.5 kg, range +1.0 to -3.9 kg) (mean -3.3 lb, range +2.2 to -8.6 lb).

Table 2-2. Energy intake and expenditure, and fluid intake and turnover, from 13 men before and during 8- to 14-day spaceflights

	Before Flight	During Flight
Energy intake, MJ/d	11.38±2.06 ^a	8.76±2.26 ^b
Energy expenditure, MJ/d	12.40±2.83 ^a	11.70±1.89 ^a
WHO-predicted energy requirement, MJ/d	12.64±0.51 ^a	12.68±0.49 ^a
Fluid intake, l/d	2.7±0.4	2.2±0.5*
Water turnover, l/d	3.8±0.5	2.7±0.6*

^aValues are means ± s.d.

^bEnergy results with different superscripts are significantly different from one another, $p < 0.001$.

*Significantly different from preflight values, $p < 0.05$.

In-flight Assessment of Renal Stones (DSO 610)

The specific aim of this study was to assess urinary components and dietary factors in order to clarify which variables contribute to a putative increase in the risk of renal stone formation associated with microgravity exposure. Details of this flight study and a previous ground-based investigation, are available elsewhere [10,32].

Six male astronauts, who flew on Shuttle missions lasting 11 to 16 days, participated in this study. Each subject collected urine during two 24-hour periods before flight, the last within 10 days of launch. During flight, void-by-void samples were collected over two 24-hour periods and aliquots were placed into tubes containing either 0.05% thymol or 0.1% thimerosal, once between flight days 3 and 4 and again within 4 days of landing. Preflight and postflight samples were collected into containers and stored at about 4°C. At the end of each period, the contents were mixed and decanted into graduated cylinders for total volume and pH measurements. A 10-ml aliquot was removed for biochemical analyses. A second 10-ml aliquot was acidified with 6 molar (M) hydrochloric acid (HCl) for the analysis of citrate, oxalate, and sulfate; two additional aliquots were removed and thymol and thimerosal added to serve as controls for the room temperature storage of the in-flight controls.

Before and after flight, crew members also maintained daily handwritten logs of food and fluid consumption for four 48-hour periods, beginning 24 hours before the urine collection periods and continuing throughout those 24-hour periods. During flight, food and fluid intake was tracked with an automated barcode scanning system. Neither diet nor activity level differed from the crew members' usual routines. Fluid intake was ad lib during all sampling periods; however, all crew members consumed the equivalent of normal saline about 90 minutes before landing as part of an established countermeasure against orthostatic intolerance. Urinary factors associated with renal stone formation were analyzed according to the methods described in Ref. 10.

Results

Urinary risk factors for the six crew members in this study are listed in Table 2-3. Changes in the chemical environment of the urine increased the risk of forming calcium oxalate and calcium phosphate stones in this group. Urine volume after landing was equivalent to that before flight; in-flight volume may have been less than preflight volume, but this difference was not significant at the 0.05 level. Urinary pH was no different during flight than before, but did drop significantly ($p < 0.05$) on landing day, as did landing day values for a previous study of 150 astronauts [10]. Urinary calcium excretion increased slightly by the late in-flight period and was still greater than preflight values on landing day. Urinary potassium

levels dropped during flight ($p < 0.05$) and returned to preflight levels after landing. Citrate excretion tended to decline during flight, but the difference was not statistically significant for this small group. However, previous studies have indicated that landing day citrate levels tend to be lower than preflight values [10].

Relative supersaturation ratios for calcium oxalate, brushite (calcium phosphate), sodium urate, and uric acid indicated increased-risk range (>2.0) for renal-stone formation during the early in-flight period, and calcium-oxalate remained significantly elevated throughout the remainder of the flight. Calcium-oxalate supersaturation remained in the high-risk range (>2.0) on landing day, but was not statistically different from preflight. The risk of brushite stone formation followed the same pattern as that of calcium oxalate. The risk of sodium urate and uric acid stone formation reached the high-risk range during flight, but the change was not statistically significant.

Dietary intake of fluid, energy, protein, potassium, phosphorus, and magnesium all were significantly less during flight than before or after flight (data not shown). However, records on landing day may have been incomplete because of scheduling constraints on those days.

Gastrointestinal Function During Extended Duration Space Flight (DSO 622)

The specific aim of this study was to evaluate the effect of spaceflight on two components of GI motility, gastric-emptying (GE) rate and intestinal-transit time. GE rate can be measured by following blood or saliva concentrations of acetaminophen as it is absorbed through the intestinal wall; the absorption rate of acetaminophen after oral administration has been shown to be directly proportional to GE rate [33]. GE rate was determined by salivary concentration of acetaminophen, and the urinary concentration of its metabolites, after an oral dose. Intestinal transit time was measured indirectly by using a noninvasive technique, the $G\text{E}t_{50}$ with the breath test [51,34,39]. In this test, subjects consume lactulose, a nondigestible sugar, that passes undigested through the small intestine. Bacteria in the colon ferment the lactulose, producing hydrogen that is exhaled by the subject. The period between the ingestion of lactulose and peak rise in breath hydrogen represents mouth-to-cecum transit time [40,41] Since gastrointestinal motility depends on the rate of gastric emptying, performing both tests (breath-hydrogen for GI motility and acetaminophen for GE rate) allows the assessment of intestinal transit time to be assessed indirectly by subtracting GE time from the overall GI transit time.

These methods were validated with six subjects in a 10-day head-down bed-rest study, and then tested with two crew members. Both subjects completed the protocol 3 times before launch (L-60, L-45, and L-30 days), once during flight (flight day 5), and once after landing (R+9 days).

Table 2-3. Renal stone risk-assessment profile for six male astronauts before, during, and after 11- to 16-day space shuttle missions†

	<i>Before Flight</i>		<i>Early in Flight</i>		<i>Late in Flight</i>		<i>Landing Day</i>		<i>7-10 Days after Landing</i>	
Total volume (l/d)	1.676	(0.09)	0.797	(0.08)	1.303	(0.17)	1.524	(0.35)	1.572	(0.31)
pH	6.01	(0.18)	5.95	(0.19)	5.92	(0.13)	5.14	(0.05)*	6.09	(0.14)
Calcium (mg/d)	166.2	(32.7)	131.8	(22.0)	221.8	(34.4)	245.2	(70.2)*	227.1	(50.0)
Phosphate (mg/d)	884.8	(110)	822.8	(170)	920.5	(104)	678.0	(165)	933.2	(166)
Oxalate (mg/d)	32.1	(4.6)	27.2	(2.7)	31.0	(2.4)	23.4	(3.6)	28.5	(5.4)
Sodium (mg/d)	2597	(443)	1807	(104)	2127	(285)	1704	(410)	4029	(654)*
Potassium (mg/d)	2620	(308)	1439	(256)*	1675	(177)*	1713	(395)	2157	(331)
Magnesium (mg/d)	93.5	(6.6)	89.2	(6.0)	101.8	(10.3)	71.2	(13.3)	97.8	(9.7)
Citrate (mg/d)	717.7	(115)	468.8	(109)	522.3	(66)	456.3	(82)	671.3	(148)
Sulfate (mmol/d)	20.8	(1.7)	13.3	(1.8)	20.7	(2.4)	21.9	(3.9)	17.0	(2.2)
Uric Acid (mg/d)	593.5	(49.0)	321.6	(32.3)	454.3	(72.4)	267.2	(74.2)*	556.2	(63.7)
Creatinine (mg/d)	1621	(159)	1237	(182)	1408	(61)	1598	(195)	1710	(152)
<i>RELATIVE SUPERSATURATION VALUES</i>										
Calcium Oxalate	1.52	(0.40)	2.95	(0.65)*	2.78	(0.47)*	2.07	(0.40)	1.60	(0.28)
Brushite	1.11	(0.32)	2.20	(0.32)*	2.10	(0.43)*	0.32	(0.07)	1.92	(0.31)
Sodium Urate	1.83	(0.47)	2.66	(0.50)	1.77	(0.42)	0.66	(0.42)	3.59	(0.88)
Struvite	1.29	(0.78)	3.46	(1.44)	0.99	(0.28)	0.05	(0.04)	1.05	(0.32)
Uric Acid Saturation	1.96	(0.69)	2.31	(0.75)	1.68	(0.31)	2.84	(0.76)	1.21	(0.38)

Asterisks indicate significant differences relative to before flight, $p < 0.05$.

Values for before flight are the means (\pm SEM) from two separate preflight urine-collection sessions. All other values are the average of 6 subjects (except for early in flight, when $n=5$).

†Data were published in Whitson, et al. [32].

After the sleep period, crew members provided baseline breath, saliva, and urine samples, next consumed a prescribed low-fiber breakfast, and then ingested 20 g of lactulose and 650 mg of acetaminophen, both in liquid dosage forms. After ingesting the doses, crew members provided breath samples every 15 minutes for 4 hours, and saliva samples every 15 minutes for the first hour and then at 2, 3, 5, 4, 6, and 8 hours.

Saliva samples were analyzed for acetaminophen, and urine samples for acetaminophen, acetaminophen glucuronide, and acetaminophen sulfate, by high performance liquid chromatography [42]. The saliva and urine concentrations with respect to time were analyzed with the BOOMER pharmacokinetic program [43], which provided an indication of gastric emptying rate. Mouth-to-cecum transit time (MCTT) was calculated from peak hydrogen concentrations in the breath samples [15].

Results

Pharmacokinetic variables, calculated from the levels of acetaminophen in saliva and its metabolites in urine, are

shown in Table 2-4. The substantial variability and the small number of subjects preclude reaching any conclusions until more subjects can be tested. However, acetaminophen seemed to have been absorbed quickly during flight, since peak saliva concentrations were reached by 15 minutes after the dose was taken (data not shown). With regard to intestinal transit time, peak breath-hydrogen levels were greater during flight than before (data not shown); however, a trend of increased transit time during flight was noticed.

Assessment Of Circadian Shifting In Astronauts By Bright Light (DSO 484)

The specific aim of this study was to test whether bright-light treatment over a 7-day preflight period could produce a 9- to 12-hour phase shift in crew member circadian rhythms. Details of this study can be found in Ref. 44. The ultimate goal was to optimize sleep patterns and performance in preparation for a launch

Table 2-4. Pharmacokinetics of acetaminophen after a 650-mg oral dose in two crew members

	Subject 1			Subject 2		
	Before Flight	During Flight	After Flight	Before Flight	During Flight	After Flight
C _{max} , µg/ml	16.40	10.58	26.90	8.91	16.10	7.68
AUC, µg/ml/h	30.35	24.10	37.50	46.37	63.50	46.90
Elimination half-life, h	3.18	2.10	1.95	4.07	6.24	4.71

C_{max}, peak concentration of acetaminophen (in saliva)
AUC, area under the [saliva-acetaminophen concentration over time] curve

Subjects for this study were eight Shuttle astronauts (5 men and 3 women) from three missions. All subjects underwent a combination of sleep shifting and bright-light treatment; all provided saliva and urine samples before and during the treatment for analysis of cortisol and melatonin rhythms.

Two types of sleep shifts were attempted. The first group (n = 3) was instructed to sleep on treatment days 2 through 7 from 10:00 a.m. to 6:00 p.m. The second group (n = 5) was instructed to go to bed progressively later, and sleep later, over the same 6-day period. All subjects were exposed to bright light (7,000 - 12,000 lux), delivered via special ceiling lights in the crew quarters at JSC and KSC, for 2 to 6 hours daily before their scheduled sleep periods. Crew members in the first group (the ‘abrupt’ sleep shift group) were instructed to wear dark goggles, or remain in a dimly lit area, for several hours before bedtime so that their light-dark cycles were the same as those for the other sleep-shift group. Compliance with the treatment protocols was neither monitored nor recorded. Melatonin and cortisol rhythms were measured in saliva and urine as described in Ref. 44, and compared to results from 15 control subjects with normal sleep-wake cycles (data not shown).

After this initial study was completed, two additional crew members were tested with an expanded protocol that included in-flight assessments of ambient light, sleep duration, and sleep quality. These variables were measured with the Actillum device (described in the Hardware chapter), a wristwatch-type device worn continuously during flight. The activity data generated by the Actillum were auto-scored for sleep, and illumination levels were analyzed for patterns of light exposure on all flight days. The participating crew members also kept manual logs of sleep and medication use throughout the flight period.

Results

At the beginning of the sleep-shift protocol, cortisol and melatonin acrophases (peaks) in the original group of eight subjects were within 2.5 hours of those of the control group. During the first 4 days of bright-light exposure, melatonin production was suppressed, but cortisol did not change; moreover, the melatonin rhythm (as a function of time of day) diminished during this period, but the cortisol rhythm was preserved. By the end of the 7-day treatment period, the peak melatonin concentrations were the same as they had been before the treatment, and they appeared within 2 hours of the expected 12-hour phase delay. The more gradual change in the melatonin acrophase of the second group paralleled the more gradual change in that group’s prescribed sleep-wake times. Cortisol acrophases were similar to melatonin acrophases except for one subject in the second sleep-shift group. With this one exception, all subjects achieved the expected circadian shift within the 7-day treatment period. Phase delays were 11-15 hours for subjects in the first group, and 7-12 hours for those in the second.

With regard to the later in-flight tests, results generated by the Actillum indicated that the ambient light in the cabin was much lower than the ambient light on the ground. Saliva melatonin peaks were higher during flight than before. Performance during shift work in flight was comparable to that during a preflight normal (non-shift) work schedule.

Evaluation of a Portable Clinical Blood Analyzer (DSO 492)

Details of the entire evaluation, which included verification of instrument calibration, assessments of precision, comparisons of methods, and statistical analyses, are given in Ref. 45.

As noted in the introduction to this chapter, the ground-based portion of this study involved comparisons of capillary (finger-stick), venous blood, and control solutions measured by PCBA vs. by traditional laboratory methods. The flight study involved only PCBA analysis of control solutions and capillary samples, with comparisons made across test periods (before, during, and after flight).

The PCBA, a hand-held, battery-powered device, was tested with approximately 85 µl of whole blood to analyze electrolytes, glucose, and hematocrit. Electrolytes (sodium, potassium, and ionized calcium) are determined by ion-selective electrode potentiometry; glucose by amperometry; hematocrit by conductometrics; and pH through direct potentiometry. Hemoglobin is calculated from hematocrit, and is not measured directly.

Subjects for the flight studies were 21 astronauts (18 men, 3 women) on five Space Shuttle missions. The subjects collected capillary samples from each other by finger-stick with a lancing device and balanced heparin

capillary tubes (radiometer). Blood was transferred quickly to the cartridge for PCBA analysis. Samples obtained before and after flight were collected either by the crew members or by medical technologists. Blood samples were scheduled to be collected 3 times before flight, twice during flight, and 3 times after flight (the latter on R+0, R+3, and R+6 days). Control samples were run every day that blood samples were collected.

Differences between ground and flight values (control samples) and data obtained before, during, and after flight (subject data) were investigated with repeated-measures ANOVA with *a priori* contrasts (i.e., contrasts planned before data analysis was undertaken). Data were missing on one flight day from 5 subjects. To maximize sample size, the in-flight data were averaged, and *a priori* contrasts were used to compare data obtained before, during (average in flight), and after flight (3 postflight days).

Results

PCBA performance in microgravity was similar between ground vs. in-flight for control solutions of all analytes except sodium, which was lower in flight than before [45]. However, this difference was within the performance limits set by the Clinical Laboratories Improvement Act (CLIA), and probably does not reflect any analytical problems in microgravity. Thus, measurements provided by the PCBA in microgravity, for the analytes tested, are probably no different from those obtained on the ground.

With regard to subject data, in-flight values of potassium were greater and ionized calcium were lesser during flight relative to preflight. In-flight glucose results were variable, probably because fasting state was not controlled in this experiment. Landing-day measurements of potassium, ionized calcium, and pH were lower than preflight values. However, these values returned to preflight levels by R+3 days (pH and ionized calcium) or by R+6 days (potassium).

Evaluation of an In-Flight Urine Collection Absorber (DSO 328)

The purpose of this project was to develop and evaluate a means of collecting small-volume urine samples that could be used in flight (on the Shuttle mid-deck or in other constrained areas) by male and female astronauts.

The In-flight Urine Collection Absorber (IUCA) was a conical, 75 cm² filter that fit into the urine-collection funnel. The filter material could absorb 20.4 gm of water per 100 cm², and weighed approximately 20 gm empty and 35 gm full. By comparison, the urine-collection device (UCD) assembly, which could be used only by men, weighed 65 gm empty and 300-400 gm when full. Theoretically, as the crew member voided, the vortex action created by the Shuttle's vacuum system would allow urine to saturate the

IUCA. When the void was complete, the IUCA could be removed, placed in a double-ziplock bag, and stored in an absorber containment bag for return. This technology could be used only for experiments that did not require void volume to be measured.

Two ground-based tests were conducted to assess whether the absorbent material would affect the analysis of deuterium (²H) and heavy oxygen (¹⁸O). In the first test, tap water samples were spiked with known amounts of ²H and ¹⁸O, and aliquots were placed in UCDs and in unassembled IUCAs. The UCDs and IUCAs were stored at room temperature and sampled after 1, 2, and 3 weeks. Each sample was either processed (extracted with charcoal then filtered) or unprocessed (filtered only). Samples were weighed periodically to monitor gross evaporative loss. Processed and unprocessed samples were stored at -20°C until mass-spectrometric analysis of the stable isotopes. Results from this test indicated that evaporative losses were minimal from the IUCA samples and were far less than those from the samples stored in the UCD. Stable isotope enrichment was similar in both the IUCA and UCD samples.

For the second ground-based test, urine samples obtained from a subject who had ingested ²H- and ¹⁸O-labeled water as part of a protocol to measure energy expenditure and total body water, were collected and stored in either standard containers, UCDs, or IUCAs. Again, samples were processed and stored at -20°C until mass spectrometric analysis. Results from this test indicated little difference among the three storage conditions in terms of energy expenditure and total body water measurements. For a follow-up study in which two subjects collected urine, the variance among urine collected in a cup, in a flight urine-collection bag, or in an IUCA was within the 5% error characteristic of calculating energy expenditure and total body water from doubly labeled water.

The flight study involved asking male and female crew members to verify the performance of the IUCA during flight. Five crew members (3 men and 2 women) used the device on STS-67 and STS-70 to collect random urine samples over 2- to 4-day periods. The volumes recovered during flight ranged from 11 to 13 ml, with no difference between the male vs. female subjects.

DISCUSSION

Results from DSO 612 indicate that most of the 13 astronauts tested were in negative energy balance (a catabolic state) during spaceflight, and consumed inadequate fluid.

Although energy utilization was unchanged during spaceflight, energy (caloric) intake was lower during flight than before. The resulting negative energy balance probably was responsible for some of the weight loss present at landing day in almost all of the crew members

tested. The similarity between measures of energy utilization and the WHO calculation for predicting energy utilization was remarkable, and suggests that the WHO calculation can be used to estimate the energy (dietary) needs for space crews.

The reduction in fluid intake observed during flight (Table 2-2) may have produced dehydration, which in terms of urine concentration may foster renal stone formation. The importance of maintaining adequate food and fluid intake should be emphasized to avoid conditions that contribute to flight-induced deconditioning. This information also will be important for identifying requirements for the food system(s) on board future missions.

With regard to renal stone risk (DSO 610), this preliminary report of six male crew members revealed that renal stone risk increased as a result of changes in urinary composition during flight. Factors that contributed to increased potential for stone formation during flight were significant reductions in urinary pH and increases in urinary calcium. Urinary output (volume) and citrate, a potent inhibitor of calcium-containing stones, were slightly reduced during flight. Additional subjects should be assessed, with particular attention directed toward fluid, food, and medication intake, to minimize the risk of forming renal stones during and after flights. With regard to potential countermeasures, one logical recommendation would be for crew members to ingest at least 2.5 liters of water per day. In this way, the urinary concentration of stone-forming salts could be diluted, and the potential for crystal nucleation and renal-stone formation may well be reduced.

Results from the gastrointestinal-function investigation (DSO 622), which involved only two subjects, are too few to draw definitive conclusions. However, the acetaminophen results suggest that liquid dosage forms may be better absorbed during flight than solid forms such as tablets. Recommendations for future evaluations include (1) simultaneously measuring hydrogen concentrations in the spacecraft air and in the subject's breath, (2) collecting several baseline breath samples before the subject ingests the lactulose, and (3) continuing to collect breath samples for longer than 4 hours after lactulose ingestion. Further studies are needed to evaluate the effect of prolonged exposure to microgravity on gastrointestinal function. This information will be useful in developing pharmaceutical and nutritional countermeasures for future missions.

With regard to in-flight circadian rhythms (DSO 484), the number of participants in the study was too small and the number of treatments too large to generate definitive recommendations. However, a 7-day period of sleep-shifting and bright light treatment before flight successfully shifted melatonin and cortisol rhythms in the eight crew members tested. Data from two subjects who were tested before and during flight suggested that sleep quality was poor before flight, even after the bright-light treatment.

Anecdotal reports suggest that sleep quality also was poor during the first few days after return. Future studies should include measurements of body-temperature cycles as well as cognitive performance and alertness over time. Rest-activity cycles and absolute illumination levels also should be recorded systematically during flight.

The PCBA (DSO 492) was highly reliable for measuring sodium, potassium, ionized calcium, pH, and glucose in real time, both on Earth and during spaceflight. Some of the variability noted between capillary (fingerstick) blood vs. venous (whole) blood in the ground-based comparisons probably reflects the fact that capillary blood more closely resembles arterial rather than venous blood. The success of the PCBA in measuring ionized calcium is of particular interest, given the importance of being able to follow changes in bone and calcium homeostasis during long spaceflight. In summary, the PCBA is a reliable device with which to measure most analytes and is being flown routinely to assist flight surgeons in evaluating crew health.

Finally, the IUCA (DSO 328) offered a lightweight means of collecting urine samples, from either men or women, during flight when urine volume measurements were not required. These devices can be used on Shuttle flights or on International Space Station.

REFERENCES

1. Woo R, Daniels-Kush R, Horton ES. Regulation of energy balance. *Ann Rev Nutr* 1985; 5: 411-33.
2. Rasvussin E, Bogardies C. Relationship of genetics, age, and physical fitness to daily energy expenditure and fuel utilization. *Am J Clin Nutr* 1989; 49:968-75.
3. Anderson HL, Heindel MB, Linkswiler H. Effect on nitrogen balance of adult man of varying sources of nitrogen and level of caloric intake. *J Nutr* 1969; 99:82-87.
4. Leonard JI, Leach CS, Rambaut, PC. Quantitation of tissue loss during prolonged space flight. *Am J Clin Nutr* 1983; 38:667-79.
5. Leach CS, Alfrey CP, Suki WN, et al. Regulation of body fluid compartments during short-term space flight. *J Appl Physiol* 1996; 81(1):105-16.
6. Alfrey CP, Udden MM, Leach-Huntoon C, et al. Control of red blood cell mass in space flight. *J Appl Physiol* 1996; 81(1):98-104.
7. Rambaut PC, Smith MC, Leach CS, et al. Nutrition and responses to zero gravity. *Federation Proceedings* 1977; 36:1678-82.
8. Pak CYC. Medical management of nephrolithiasis. *J Urol* 1982; 128(6):1157-64.

9. Whedon GD, Lutwak L, Rambaut PC, Whittle MW, Smith MC, Reid J, Leach C, Stadler CR, Sanford DD. Mineral and nitrogen metabolic studies—experiment M071. In: Johnston RS, Dietlein LF, editors. *Biomedical Results from Skylab, NASA SP-377*. Washington DC: NASA; 1977. p 165-74.
10. Whitson PA, Pietrzyk RA, Pak CYC, Cintron NM. Alterations in renal risk factors after space flight. *J Urol* 1993; 150:803-07.
11. Nicholl CG, Polak JM, Bloom SR. The hormonal regulation of food intake, digestion, and absorption. *Ann Rev Nutr* 1985; 5:213-39.
12. Holgate AM, Read NW. Relationship between small bowel transit time and absorption of a solid meal. Influence of metachlorpromide, magnesium sulfate, and lactulose. *Dig Dis Sci* 1983; 28:812-19.
13. Meyer JH, Gu YG, Elashoff J, Reedy T, Dressman J, Amidon G. Effect of viscosity and flowrate on gastric emptying of solids. *Am J Physiol* 1986; 250:G161-G164.
14. Meyer JH, Mayer EA, Jehn D, Gu Y, Fink AS, Fried M. Gastric processing and emptying of fat. *Gastroenterology* 1986; 90:1176-87.
15. Bond JH, Levitt MD. Investigation of a small bowel transit time in man utilizing pulmonary hydrogen measurements. *J Lab Clin Invest* 1972; 85:546-55.
16. Nimmo WS, Prescott LF. The influence of posture on paracetamol absorption. *Br J Clin Pharm* 1978; 5:348.
17. Thomas JE. Mechanics and regulation of gastric emptying. *Physiol Rev* 1957; 37:453-74.
18. Akerstedt T, Torsvall L, Gillberg M. Sleepiness and shift work: field studies. *Sleep* 1982; 5:S95-S106.
19. Gold DR, Rogacz S, Bock N, Tosteston TD, Baum TM, Speizer FE, Czeisler CA. Rotating shift work, sleep, and accidents related to sleepiness in hospital nurses. *Am J Public Health* 1992; 82:1011-14.
20. Englund CE, Ryman DH, Naitoh P, Hodgdon JA. Cognitive performance during successive sustained physical work episodes. *Behav Res Methods Instru Computers* 1985; 17:75-85.
21. Reinberg A, Migraine C, Apfelbaum M, et al. Circadian and ultradian rhythms in the feeding and nutrient intakes of oil-refinery operators with shift work every 3-4 days. *Diabete Metab* 1979; 5:33-41.
22. Czeisler CA, Allan JS, Strogatz SH, Ronda JM, Sanchez R, Rios CD, Freitag WO, Richardson GS, Kronauer RE. Bright light resets the human circadian pacemaker independent of the timing of the sleep-wake cycle. *Science* 1986; 233:667-71.
23. Lewy AJ, Wehr TA, Goodwin FK, Newsom DA, Markey SP. Light suppresses melatonin secretion in humans. *Science* 1980; 210:1267-69.
24. McIntyre IM, Norman TR, Burrows GD, Armstrong SM. Melatonin rhythm in human plasma and saliva. *J Pineal Res* 1987; 4(2):177-83.
25. Arendt J. Melatonin and rhythmic functions in mammals: Therapeutic and commercial potential. In: Reinberg A, Smolensky MH, Labrecque G, editors. *Annual Review of Chronopharmacology Vol 6*. London: Pergamon Press; 1990. p 137-53.
26. Shanahan TL, Czeisler CA. Light exposure induces equivalent phase shifts of the endogenous circadian rhythms of circulating plasma melatonin and core temperature in men. *J Clin Endocrinol Metab* 1991; 73:227-35.
27. Lane HW. Energy requirements for space flight. *J Nutr* 1992; 122:13-18.
28. Schoeller DA, Leitch CA, Brown C. Doubly labeled water method: in vivo oxygen and hydrogen isotope fractionation. *Am J Physiol* 1986; 251:R1137-R1143.
29. Gretebeck RJ, Schoeller DA, Gibson EK, Lane HW. Energy expenditure during antiorthostatic bed rest (simulated microgravity). *J Appl Physiol* 1995; 78:2207-11.
30. WHO. Energy and protein requirements. Report of a joint FAO/WHO/UNU expert consultation. World Health Organization Tech Report Services 1985; p 724.
31. Lane HW, Gretebeck RJ, Schoeller DA, et al. Comparison of ground-based and space flight energy expenditure and water turnover in middle-aged healthy male U.S. astronauts. *Am J Clin Nutr* 1997; 65:4-12.
32. Whitson PA, Pietrzyk RA, Pak CYC. Renal-stone risk assessments during Space Shuttle flights. *J Urol* 1997; 158:2305-2310.
33. Clements JA, Heading RC, Nimmo WS, Prescott LF. Kinetics of acetaminophen absorption and gastric emptying in man. *Clin Pharmacol Ther* 1978; 24:420-31.
34. Read NW, Miles CA, Fisher D, Holgate AM, Kime ND, Mitchell MA, Reeve AM, Roche TB, Walker M. Transit of a meal through the stomach, small intestine, and colon in normal subjects and its role in the pathogenesis of diarrhea. *Gastroenterology* 1980; 79:1272-82.
35. Read NW, Al-Janabi MN, Bates TE, Holgate AM, Cann PA, Kinsman RI, McFarlane A, Brown CH. Interpretation of the breath hydrogen profile obtained after ingesting a solid meal containing unabsorbable carbohydrate. *Gut* 1985; 26:839-42.
36. Scarpello JHB, Greaves M, Sladen GE. Small intestinal transit in diabetes. *Br J Med* 1976; 2:1225-26.

37. Shafer RB, Prentiss RA, Bond JH. Gastrointestinal transit in thyroid disease. *Gastroenterology* 1984; 86:852-55.
38. Metz G, Gassull MA, Leeds AR, Blendis LM, Jenkins DJA. A simple method of measuring breath hydrogen in carbohydrate malabsorption by end-respiratory sampling. *Clin Sci Mol Med* 1976; 50:237-40.
39. Corbett CL, Thomas S, Read NW, Hobson N, Bergman I, Holdsworth CD. Electrochemical detector for breath hydrogen determination measurement of small bowel transit time in normal subjects and in irritable bowel syndrome. *Gut* 1981; 22(10): 836-40.
40. Van Wyk M, Sommers DK, Steyn AGW. Evaluation of gastrointestinal motility using the hydrogen breath test. *Br J Clin Pharmacol* 1985; 20:479-81.
41. Ladas SD, Latoufis C, Giannopoulou H, et al. Reproducible lactulose hydrogen breath test as a measure of mouth-to-cecum transit time. *Dig Dis Sci* 1989; 34:919-24.
42. Jung D, Zafar NL. Micro high performance liquid chromatographic assay of acetaminophen and its metabolite in plasma and urine. *J Chromatogr* 1985; 339:199-202.
43. Bourne DWA. BOOMER, a simulation and modeling program for pharmacokinetic and pharmacodynamic data analysis. *Computer Meth Prog Biomed* 1989; 29:191-95.
44. Whitson PA, Putcha L, Chen YM, et al. Melatonin and cortisol assessment of circadian shifts in astronauts before flight. *J Pineal Res* 1995; 81:141-47.
45. Smith SM, Davis-Street JE, Fontenot TB, et al. Assessment of a portable clinical blood analyzer during space flight. *Clin Chem* 1997; 43:1056-65.

Section 3

Functional Performance Evaluation

EXTENDED DURATION ORBITER MEDICAL PROJECT

Functional Performance Evaluation

*Michael C. Greenisen, Judith C. Hayes, Steven F. Siconolfi,
and Alan D. Moore of the
Johnson Space Center, Houston, TX*

INTRODUCTION

The Extended Duration Orbiter Medical Project (EDOMP) was established to address specific issues associated with optimizing the ability of crews to complete mission tasks deemed essential to entry, landing, and egress for spaceflights lasting up to 16 days. The main objectives of this functional performance evaluation were to investigate the physiological effects of long-duration spaceflight on skeletal muscle strength and endurance, as well as aerobic capacity and orthostatic function. Long-duration exposure to a microgravity environment may produce physiological alterations that affect crew ability to complete critical tasks such as extravehicular activity (EVA), intravehicular activity (IVA), and nominal or emergency egress. Ultimately, this information will be used to develop and verify countermeasures. The answers to three specific functional performance questions were sought: (1) What are the performance decrements resulting from missions of varying durations? (2) What are the physical requirements for successful entry, landing, and emergency egress from the Shuttle? and (3) What combination of preflight fitness training and in-flight countermeasures will minimize in-flight muscle performance decrements?

To answer these questions, the Exercise Countermeasures Project looked at physiological changes associated with muscle degradation as well as orthostatic intolerance. A means of ensuring motor coordination was necessary to maintain proficiency in piloting skills, EVA, and IVA tasks. In addition, it was necessary to maintain musculoskeletal strength and function to meet the rigors associated with moderate altitude bailout and with nominal or emergency egress from the landed Orbiter. Eight investigations, referred to as Detailed Supplementary Objectives (DSOs) 475, 476, 477, 606, 608, 617, 618, and 624, were conducted to study muscle degradation and the effects of exercise on exercise capacity and orthostatic function (Table 3-1).

This chapter is divided into three parts. Part 1 describes specific findings from studies of muscle strength, endurance, fiber size, and volume. Part 2 describes results from studies of how in-flight exercise

affects postflight exercise capacity and orthostatic function. Part 3 focuses on the development of new noninvasive methods for assessing body composition in astronauts and how those methods can be used to correlate measures of exercise performance and changes in body composition.

PART 1 – SKELETAL MUSCLE ADAPTATIONS TO SPACEFLIGHT

Purpose

Adaptation to the microgravity environment of spaceflight involves muscular deconditioning. Changes in muscle morphology and function could affect motor function and control. Decrements in motor performance could impair the successful completion of many tasks associated with EVA, IVA, and emergency or routine landing and egress. Prior to EDOMP, the scope of the deconditioning process and the extent to which it may affect performance had not been established. In particular, changes in skeletal muscle performance and morphology during extended duration Shuttle flights had not been determined.

The four studies described in Part 1 (DSOs 475, 477, 606, and 617) constituted a comprehensive investigation of skeletal muscle function and atrophy associated with the physiological adaptation to spaceflight. The associated measurements were important because: (1) a timeline for muscle function changes had not been established, (2) critical periods of muscle atrophy and deconditioning had not been identified, and (3) losses of functional levels of muscle strength and endurance had not been assessed. The results from these investigations were expected to provide the knowledge needed to support development of future preflight conditioning, in-flight countermeasures, and postflight rehabilitation activities, all of which are essential in maintaining operational effectiveness.

Table 3-1. Investigations constituting the functional performance evaluation of the Extended Duration Orbiter Medical Project

<i>DSO No.</i>	<i>Title</i>	<i>Investigators</i>
DSO 475	Direct assessment of muscle atrophy and biochemistry before and after short spaceflight.	VR Edgerton, ML Carter, and MC Greenisen
DSO 476	Aerobic exercise in flight and recovery of cardiovascular function after landing.	SF Siconolfi and JB Charles
DSO 477	Evaluating concentric and eccentric skeletal muscle contractions after spaceflight.	JC Hayes, BA Harris, and MC Greenisen
DSO 606	Assessing muscle size and lipid content with magnetic resonance imaging (MRI) after spaceflight.	AD LeBlanc
DSO 608	Effects of space flight on aerobic and anaerobic metabolism during exercise: The role of body composition.	SF Siconolfi and AD Moore
DSO 617	Evaluating functional muscle performance after spaceflight.	JC Hayes and MC Greenisen
DSO 618	Effects of intense in-flight exercise on postflight aerobic capacity and orthostatic function.	AD Moore and MC Greenisen
DSO 624	Cardiorespiratory responses to sub-maximal exercise before and after flight.	AD Moore and MC Greenisen

Background

Scientific and technological advancements in spaceflight have necessitated the development of ways to maximize the ability of flight crews to perform during increasingly long missions. Optimizing crew capability, both during flight and upon return to a terrestrial environment, is essential for successful completion of and recovery from long missions.

NASA has established the development, construction, and operation of a permanently occupied space station in low Earth orbit as a definitive goal. Constructing an International Space Station (ISS) is expected to exacerbate the physiological stresses on flight crews, both from increasingly longer stays in space and from the physical demands associated with construction activities. In order to accomplish the objectives associated with longer spaceflights safely and efficiently, the life sciences community was charged with establishing reliable means of ensuring crew proficiency for such flights.

EDOMP was established to address the issue of how best to protect the ability of crews to complete mission tasks deemed essential to entry, landing, and egress for spaceflights lasting up to 16 days [1]. A major component of this effort was the development and verification of in-flight countermeasures to offset any physiological adaptations that could negatively affect the ability to complete those tasks. Effective countermeasures also could speed the rate of recovery after landing, i.e., the rate at which crew members return to their preflight baselines.

Microgravity exposure is known to affect neuromuscular and musculoskeletal function in ways that could affect the ability to complete critical operational tasks [2]. Maintaining adequate motor coordination and function is essential for operational success, which can be defined as being able to preserve proficiency in tasks associated with piloting, EVA, and IVA. Musculoskeletal strength and function also must be maintained to help crews meet the physical rigors associated with nominal or emergency egress.

Egress from the Orbiter, even under nominal conditions, places physical demands on the major muscle groups of the arms, legs, and torso. The current launch and entry suit (LES) weighs 51 pounds (23 kg) and must be worn during all landing and egress procedures. In addition, a parachute pack weighing an additional 26 pounds (12 kg) must be worn with the LES in the event of emergency bailouts. The excess weight could well impair operational performance during landing and egress, especially in emergencies which require lifting, pushing, pulling, jumping, climbing, and running. For example, in an expedited contingency landing, one of the crew members must deploy a 45 pound (20 kg) flight package, which includes an inflatable slide that must be lifted up against the side hatch and locked into designated slots before inflation and egress. Another somewhat less likely scenario involves exiting through the top window on the flight deck, which would require climbing out of the top window and rappelling down the side of the Orbiter [3].

Maintaining physical fitness during flight has been proposed as one way of minimizing the physiological effects of adaptation to microgravity during flight, thereby protecting the ability to function effectively upon return to a gravity environment and perhaps speeding the postflight recovery process [4]. The complexity of the adaptation process, which involves shifts in the cardiovascular, respiratory, musculoskeletal, neurosensory, and other systems, requires that baseline measures be established against which the effects of intervention can be compared. Some aspects of the musculoskeletal adaptation process are briefly described below.

Muscles become deconditioned as a result of chronic disuse. Insufficient functional loads, whether engendered by immobilization, bed rest, or spaceflight, result in atrophy, reduced strength, and reduced endurance [5-9]. Rats flown on Spacelab-3 (STS-51B) lost 36% of the mass and 30% of the cross sectional area of the soleus after only one week of spaceflight [10]. Pre-flight-to-postflight comparisons of skeletal muscle volume by magnetic resonance imaging (MRI) revealed 4 to 10% reductions in selected muscles and muscle groups from the crew of Spacelab-J (STS-47) [11]. Cosmonauts on Mir flights have shown reductions of up to 18% in lower limb and back muscle mass. The implications of these findings for performance are significant, since loss of muscle mass is directly related to movement control. If less muscle mass is available, then less tension is produced when these muscles are maximally activated. Thus, functional adjustments in performance would have to be made in order to maintain appropriate movement responses and postural control [12]. Loss of movement control has operational impacts during IVA and EVA, but also may have important implications for landing and egress tasks, especially in emergencies.

Skeletal muscle contractions involve either shortening or lengthening of muscle fibers. Muscle tensions that accelerate a lever arm and shorten the muscle fibers are defined as concentric contractions. Such contractions often are labeled "positive work." Conversely, muscle tensions that decelerate a lever arm and lengthen muscle fibers are termed eccentric contractions, or negative work. Isokinetic contractions are dynamic muscle activities, performed at a fixed angular velocity and with variable resistance, conditions that accommodate the ability of the muscle to generate force [13]. Eccentric and concentric muscular contractions contribute equally to the functional activities of daily living. Running, jumping, throwing, and maintaining postural balance all require eccentric strength and endurance. Many activities associated with EVA and IVA, routine or rapid egress, and piloting a space vehicle upon return to Earth, also involve eccentric capabilities.

Postflight isokinetic strength testing has provided an important means of quantifying musculoskeletal deconditioning. Concentric strength of Skylab crews was

tested with a Cybex isokinetic dynamometer before and after flight. Postflight tests conducted with the Skylab 2 crew, which took place 5 days after their 28-day flight, revealed losses of approximately 25% in leg extensor strength. Declines in arm strength were not as severe [9]. Moreover, these crew members likely had experienced some recovery in strength during the 5 days between landing and testing. The Skylab 3 and 4 crews also lost leg strength after their 59- and 84-day missions, respectively, but to a lesser extent than the Skylab 2 crew, presumably because of the emphasis on in-flight exercise during the two longer missions [8,9].

Evidence of microgravity-induced changes in motor performance has been reported by Russian investigators. Biomechanical analysis of ambulation patterns showed that adaptation to space flight affected the motor skills associated with walking after return to Earth [14]. Gross motor skills, as assessed by long and high jumps, were diminished after a 63-day Russian mission [14]. Skeletal muscle strength, measured with concentric isokinetic dynamometry after long (110 to 237 days) and short (7 days) flights, declined by as much as 28% in both isometric and isokinetic modes [15]. Significant changes in the torque-velocity relationship were apparent in the gastrocnemius/soleus, anterior tibialis, and ankle extensors of 12 crew members after only 7 days of flight on Salyut 6. Losses in the sural triceps ranged from 20 to 50% after missions lasting 110 to 235 days. Decrements in isokinetic strength properties of the sural triceps were similar after long or short missions [15], although loss of strength was not uniform throughout the velocity spectrum tested.

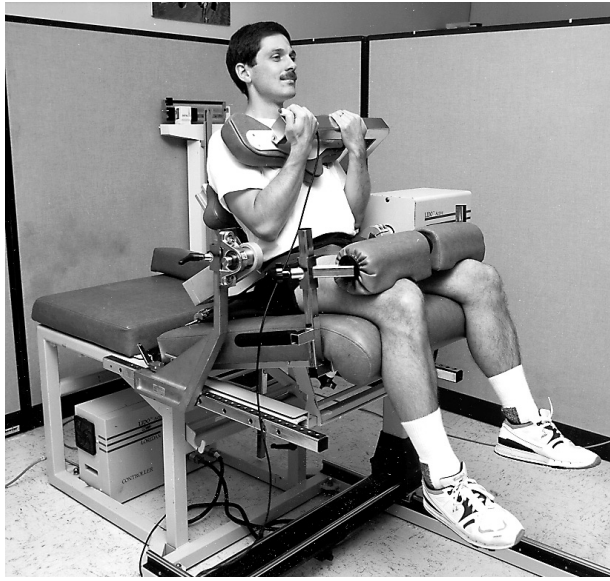
Aspects of neuromuscular function that affect contractility and the electrical efficiency of muscles also may adapt to microgravity in ways that would affect performance upon return to 1-g. However, the mechanisms underlying such space deconditioning are unclear.

In summary, flight crews must preserve muscle strength and endurance in order to maintain their ability to carry out operational tasks during and after flight. The EDOMP provided an opportunity to quantify flight-induced changes in skeletal muscle mass and function. This information is operationally relevant to the development of future preflight, in-flight, and postflight exercise prescriptions and countermeasures because the effectiveness of proposed countermeasures cannot be evaluated without information on normal changes in skeletal muscle.

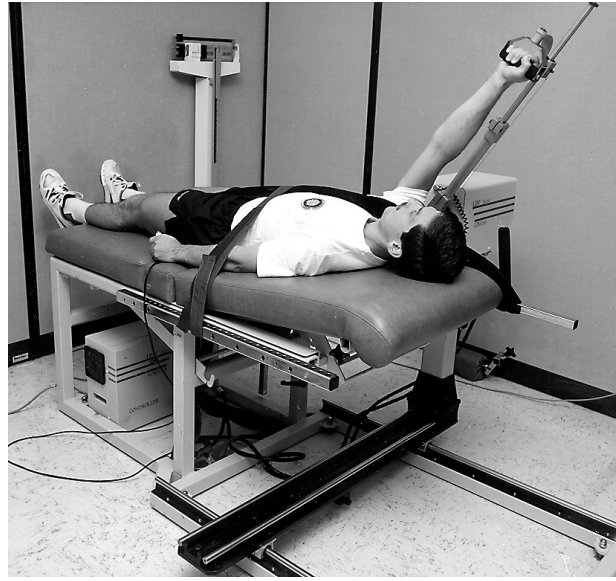
Skeletal Muscle Performance (DSOs 477 & 617)

Specific Aim

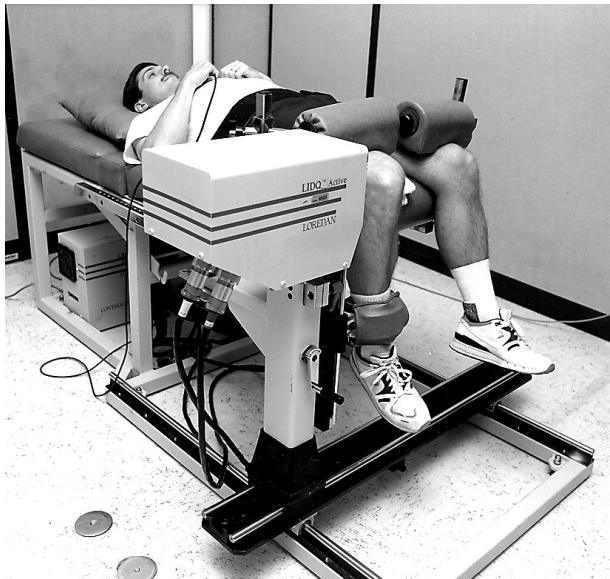
The specific aim of DSOs 477 and 617 was to evaluate functional changes in concentric and eccentric strength (peak torque) and endurance (fatigue index) of the trunk, upper limbs, and lower limbs of crew members before and after flight.



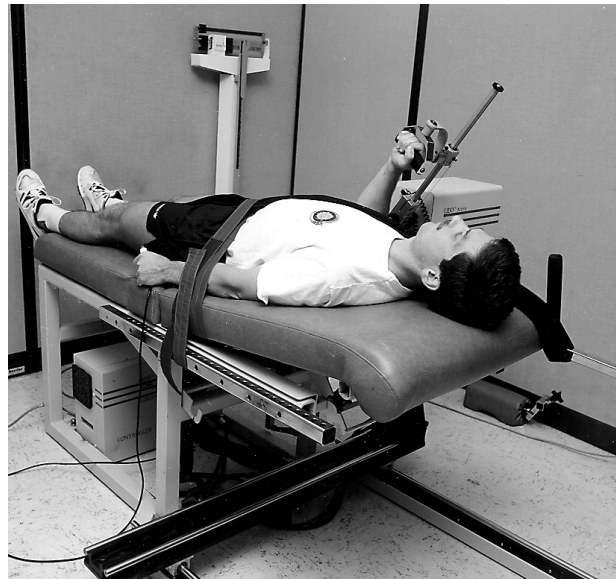
a. Trunk



b. Ankle



c. Knee



d. Shoulder

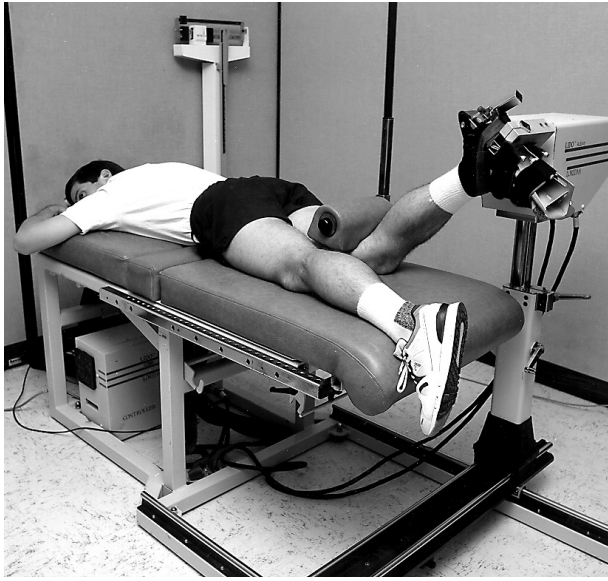
Figure 3-1. A subject undergoes strength and endurance testing with the LIDO® dynamometer.

Methods

Muscle function was tested before and after flight in the Exercise Physiology Laboratory at the Johnson Space Center (JSC). The landing-day tests took place at the Orbiter landing site in the Baseline Data Collection Facility (BDCF) at the Kennedy Space Center (KSC) or the Postflight Science Support Facility (PSSF) at the Dryden Flight Research Center (DFRC).

LIDO® dynamometers were used to evaluate concentric and eccentric contractions before and after flight. In all, three LIDO® Active Multi-Joint Isokinetic Rehabilitation

Systems [16] were used to assess muscle performance. Each dynamometer was upgraded by the manufacturer to increase the eccentric torque maximum to 400 ft lbs. Each test facility (JSC, KSC, and DFRC) was equipped with identical dedicated systems. Test subjects were crew members on Shuttle missions ranging from 5 to 13 days in duration. All subjects were instructed to abstain from food for 2 hours before testing, from caffeine for 4 hours before testing, and from exercise for 12 hours before testing. The dynamometers were calibrated externally and internally (electronically) before each test session. Joint



e. Elbow

Figure 3-1. Concluded.

configurations and ranges of motion were recorded for each subject and reproduced for each test session (Figure 3-1). All testing (except for the trunk) was unilateral with the dominant limb, unless otherwise contraindicated (i.e., previous injury). Concentric and eccentric strength were tested in the trunk and upper and lower limbs. Concentric endurance was tested in the knee. Verbal instructions were

1. Tread
2. Pulleys
3. Flywheel
4. Brake
5. Speed Control
6. Speedometer
7. Control
8. Tachometer
General

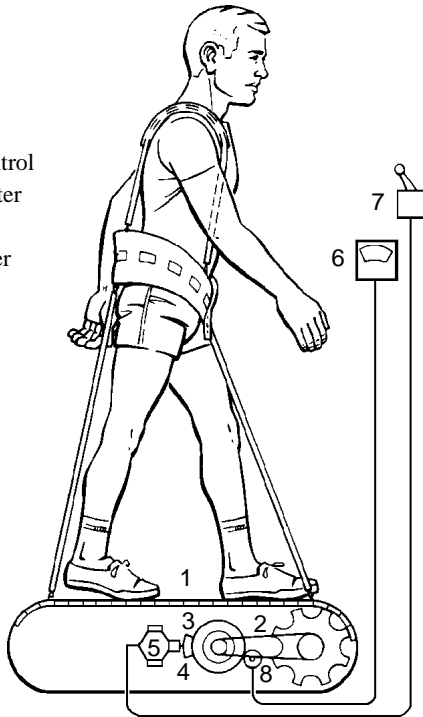


Figure 3-2. U.S. Space Shuttle treadmill.

consistent and given before each joint test. No verbal encouragement was given during the tests.

Test subjects in this study exercised during flight as part of separate investigations (DSOs 476 or 608). Those subjects ran on the original Shuttle treadmill (Figure 3-2) for various durations, intensities, and number of days in flight. Exercise protocols included continuous and interval training, with prescriptions varying from 60% to 85% of preflight maximum oxygen consumed ($\dot{V}O_{2\max}$) as estimated from heart rate. However, several subjects reported difficulty in achieving or maintaining these target heart rates during flight. The speed of this passive treadmill was controlled at seven braking levels by a rapid-onset centrifugal brake. A harness and Bungee tether system was used to simulate body weight by providing forces approximately equivalent to a 1-g body mass. This nonmotorized treadmill required subjects to run at a positive percentage grade in microgravity to overcome mechanical friction.

Test subjects were familiarized with the LIDO[®] test protocol and procedures 30 days before flight (L-30), after which six test sessions were held. Three sessions took place before launch (L-21, L-14, and L-8 days) and three after landing (landing day, R+2, and R+7-10 days).

Data Reduction and Analysis

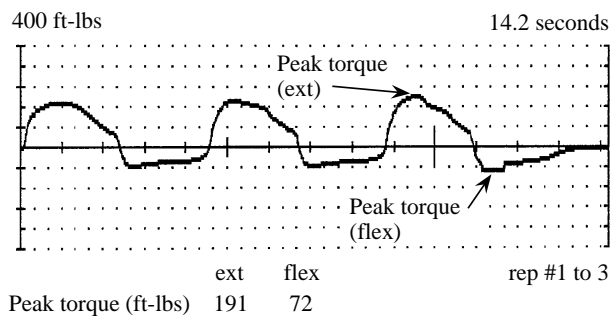
Torque and work data were reduced from the force-velocity curves (Figure 3-3). Statistical analyses of strength, endurance, and power were conducted separately for each muscle group tested. Repeated-measures analysis of variance was used to test the null hypothesis (i.e., no effect of spaceflight on mean peak responses). Peak torque, total work, and fatigue index measurements were compared among the three preflight test sessions; when no differences were found among sessions, values from the three preflight sessions were averaged and this average used to compare preflight values with those on landing day and thereafter. When the overall effect of spaceflight was significant, dependent (paired) t-tests were performed to compare the preflight response to each postflight response.

Skeletal-muscle strength was defined as the peak torque generated throughout a range of motion from 3 consecutive voluntary contractions for flexion and extension (Figures 3-3a, 3-3b).

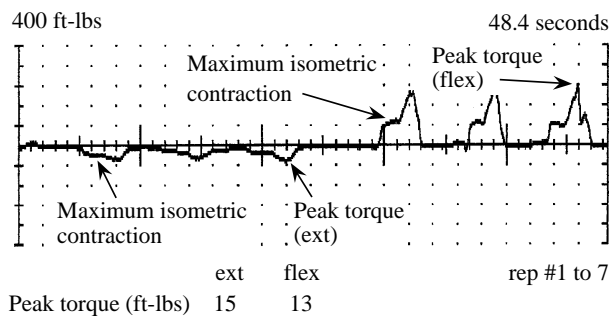
Skeletal-muscle endurance was defined as the total work generated during 25 repetitions of concentric knee exercise (Figure 3-3c), as determined from the area under the torque curve for a set of exercise. Work also was compared between the first 8 and last 8 repetitions. Endurance parameters were measured during concentric knee flexion and extension activity only.

Results

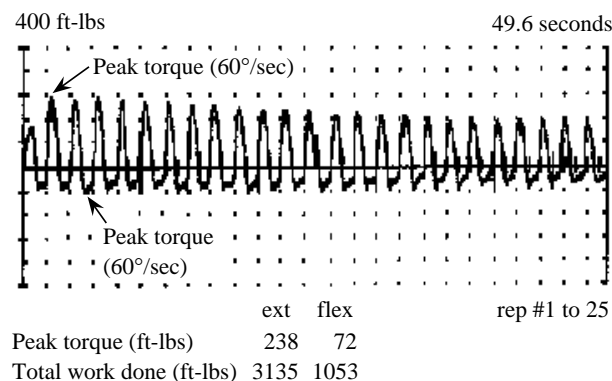
With the exception of concentric strength in the quadriceps, results from the three preflight test sessions were found to be statistically equal by univariate



a. Isokinetic concentric tests consisted of 3 maximal voluntary contractions.



b. Isokinetic eccentric tests included 3 maximal voluntary contractions with a 2-second pause between directions to allow a maximal isometric contraction to precede the onset of each eccentric action.



c. Skeletal-muscle endurance was tested during 25 repetitions of isokinetic concentric (flexion-extension) exercise of the knee.

Figure 3-3. Examples of force-velocity curves for concentric strength (3-3 a), eccentric strength (3-3 b), and concentric endurance (3-3 c) tests.

repeated-measures ANOVA for all muscle groups. Therefore, means of the three preflight sessions were compared to results on landing day (R+0) and on the seventh day after landing (R+7).

Table 3-2. DSO 477 mean skeletal muscle strength performance on landing vs. preflight (n=17)

*Pre > R+0 (p<0.05)

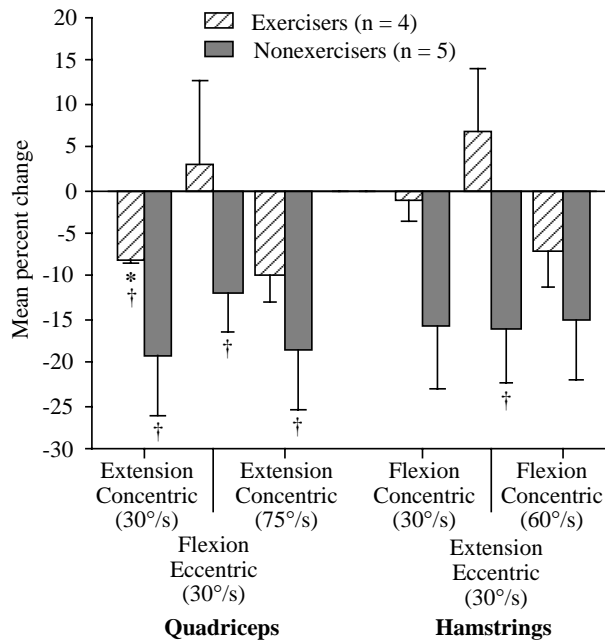
Muscle Group	Test Mode	
	Concentric	Eccentric
Back	-23 (± 4)*	-14 (± 4)*
Abdomen	-10 (± 2)*	-8 (± 2)*
Quadriceps	-12 (± 3)*	-7 (± 3)
Hamstrings	-6 (± 3)	-1 (± 0)
Tibialis Anterior	-8 (± 4)	-1 (± 2)
Gastroc/Soleus	1 (± 3)	2 (± 4)
Deltoids	1 (± 5)	-2 (± 2)
Pects/Lats	0 (± 5)	-6 (± 2)*
Biceps	6 (± 6)	1 (± 2)
Triceps	0 (± 2)	8 (± 6)

Strength: On landing day, significant decreases in concentric and eccentric strength were shown in the back and abdomen relative to the preflight means (Table 3-2). Concentric back extension and eccentric dorsiflexion were still significantly less than preflight values on R+7. Recovery (i.e., an increase in peak torque from R+0 to R+7) was demonstrated for the eccentric abdomen and the concentric and eccentric back extensors.

Endurance: Most of the decrease in total work by the quadriceps on R+0 probably reflects significant loss in the first third of the exercise bout (-11%). The declines in peak torque at the faster endurance-test velocities are consistent with changes seen at the slower angular velocity used during the strength tests. Torque for the quadriceps at 75°/s was 15% less than preflight values, but for the hamstrings was 12% less than the preflight mean at 60°/s. Endurance data showed little difference between preflight and R+7 tests, suggesting that crew members had returned to baseline by one week after landing.

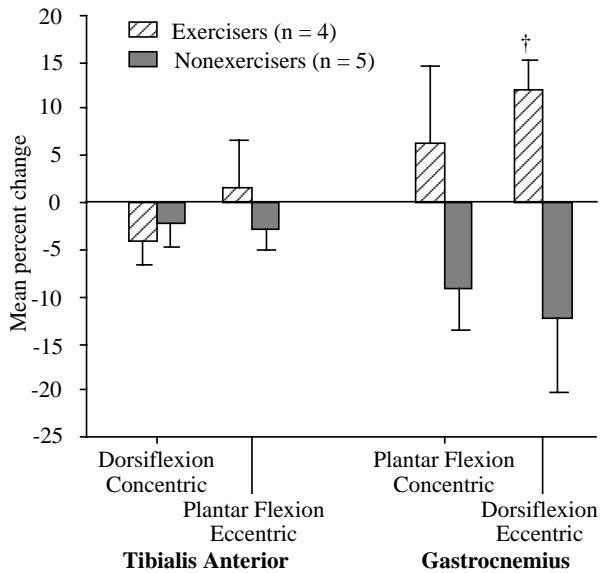
In-Flight Treadmill Exercise: Subjects who exercised during flight (as part of a separate study) tended to have slightly higher preflight peak torques than those who did not exercise during flight. At landing day, no significant differences were found between exercisers and nonexercisers, except for concentric strength of the quadriceps (Figure 3-4a, 3-4b). Exercisers had greater concentric leg extension strength on landing day than did nonexercisers (224.0 vs. 131.0 ± 61.9 ft-lbs, respectively).

Subjects who exercised during flight had significant (p<0.05) losses within 5 hours of landing in concentric and eccentric strength of the abdomen, eccentric strength of the gastrocnemius/soleus, and concentric strength of the quadriceps (30°/sec), relative to the respective preflight values. No aspect of endurance changed for this group.



a. Percent changes in upper leg strength following space flight

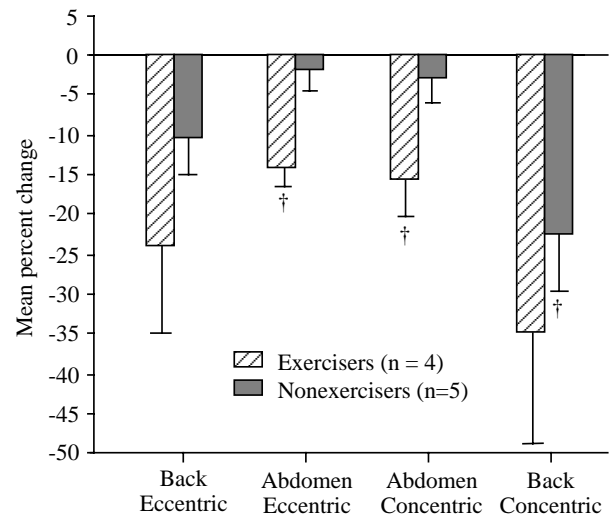
*Nonexercisers change > exercisers on R+0
 †Preflight > R+0 ($p < 0.05$)



b. Percent change in lower leg strength following space flight; exercisers vs. nonexercisers

†Pre < R+0 ($p < 0.05$)

Subjects who did not exercise in flight also had significant ($p < 0.05$) losses within 5 hours of landing in concentric strength of the back, concentric and eccentric strength of the quadriceps (30°/sec), and eccentric strength of the hamstrings, relative to the respective preflight values. Nonexercisers also had significantly less



c. Percent change in trunk strength following space flight; exercisers vs. nonexercisers

†Pre > R+0 ($p < 0.05$)

Figure 3-4. Changes in strength of the knee (3-4 a), lower leg (3-4 b), and trunk (3-4 c) on landing day in those who exercised on a treadmill during flight versus those who did not.

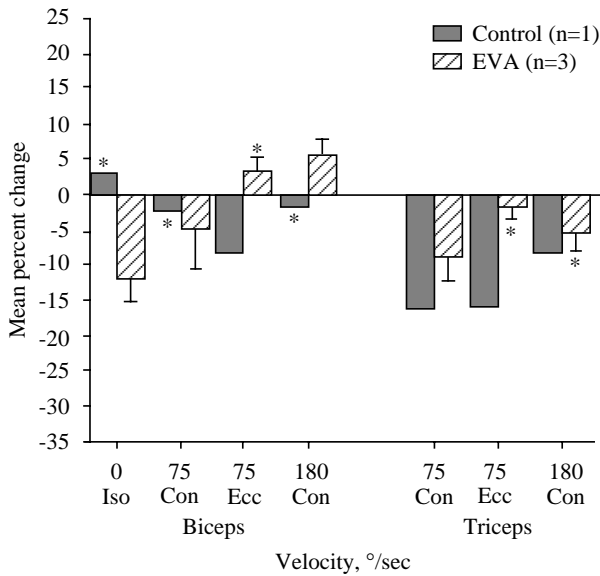
concentric strength of the quadriceps at 75°/sec, and lower total work extension, work first-third flexion, and work last-third extension, immediately after landing, than before flight. These results indicate that muscles are less able to maintain endurance and resist fatigue after spaceflight, and that exercise may avert decrements in these aspects of endurance.

Although the in-flight exercise group had lost more strength at landing, when the changes were expressed as percentages (Figure 3-4c), preflight strength in trunk flexion and extension was substantially greater in the exercising group. These results imply that treadmill exercise did not prevent decrements in trunk strength after 9-11 days of spaceflight, and that preservation of muscle integrity may be limited to only those muscles exercised.

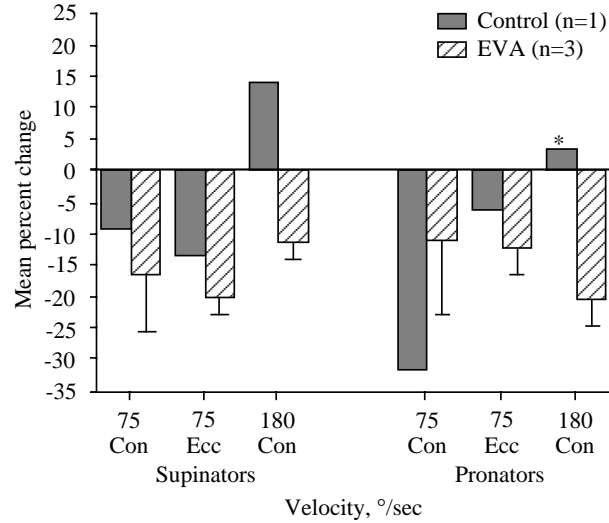
EVA: Early attempts to evaluate the effect of EVA on strength in the elbow (Figure 3-5a) and wrist (Figure 3-5b) over several functional velocities demonstrated some significant losses (>10%) in arm-musculature strength. Although these losses imply a tendency toward deconditioning and fatigue, they could not be verified statistically. Therefore, the effects of EVA on performance require further study.

Estimates of Risk

Loss of muscle mass is associated with loss of muscle function. Less efficient ambulation is the major consequence, as the lower limb muscles are most at risk. Loss of the ability to ambulate effectively would delay



a. Percent change in elbow strength; EVA vs. control
*Preflight variability > percent change



b. Percent change in wrist supination and pronation strength; EVA vs. control
*Preflight variability > percent change

Figure 3-5. DSO 617 changes in elbow (3-5 a) and wrist (3-5 b) strength after space flight in crew members who conducted EVA during flight versus one who did not.

the crew member's return to normal status and would negatively affect the crew member's ability to vacate an Earth-landing vehicle in the event of an emergency egress. Loss of muscle mass during long-duration spaceflight may affect the ability to carry out in-flight operational tasks such as EVA. Additionally, skeletal muscle damage could contribute to decreases in functional ability, as well as predispose a crew member to a higher risk of injury while performing nominal operational tasks.

Because no risk-of-injury analogs had been identified for space deconditioning, rehabilitation clinical standards for injured or postoperative individuals were used to assess musculoskeletal risk. With this model, the predicted percentage of the astronaut population at increased risk for back injury exceeded 40%, and about 20% were at risk for upper and lower leg injury. Because these predictions were based on a single muscle group, this analysis represents a fairly conservative estimate of musculoskeletal injury risk in astronauts after landing. Space-induced changes in skeletal muscle occur systematically, affecting many major muscle groups simultaneously. Loss of muscle performance and volume, coupled with changes in neuromuscular function and potential muscle damage, increases the risk of musculoskeletal injury immediately after landing. Additionally, the requirement of wearing the 51-lb. (23 kg) LES during landing may further compromise the safety of some crew members by increasing the musculoskeletal demands of routine egress.

Most of the crew members tested returned to near-baseline status by 7 to 10 days after landing. Thus, many

of the losses described above were transitory after relatively short flights, and the risk of injury decreased rapidly as the crew members readapted to the Earth environment. However, the time course of reconditioning after spaceflight has yet to be defined for long duration flights (i.e., aboard Mir or the International Space Station) or for those flights that incorporate operational countermeasures.

Skeletal Muscle Biopsies (DSO 475)

Specific Aim

The specific aim of this investigation was to define the morphologic and biochemical effects of spaceflight on skeletal muscle fibers.

Methods

Biopsies were conducted once before flight (L->21 days) and again on landing day (R+0). Preflight biopsies were conducted at the JSC Occupational Health Clinic. R+0 biopsies were conducted at the Orbiter landing site either in the BDCF at KSC or the PSSF at DFRC.

Subjects were eight crew members, three from a 5-day mission and five from an 11-day mission. Biopsies were taken with a 6 mm biopsy needle equipped with a suction device. Other materials included Betadine (a topical antiseptic/microbiocide), alcohol wipes, #11 scalpel, 23 gauge hypodermic needle, 3 ml syringe, and 2% xylocaine. Liquid nitrogen and freon were used to freeze and store samples.

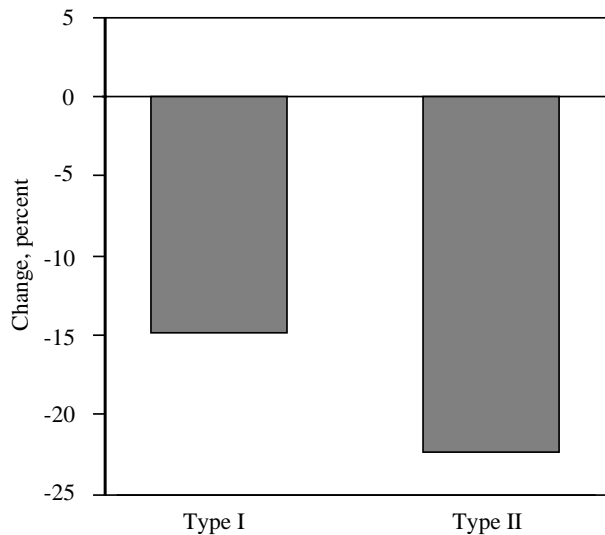


Figure 3-6 Preflight vs. postflight, percent change by skeletal muscle fiber type of the vastus lateralis (n=8).

Samples were obtained from the mid-portion of the vastus lateralis, using the needle as follows: The sample site was identified as being 40% of the distance from the lateral condyle of the distal femur to the femoral trochanter. The site was prepared by shaving and cleaning with Betadine. The site was anesthetized by subcutaneous injections of 2% xylocaine, followed by in-depth injections just below the muscle fascial plane. Once anesthetized, the muscle fascial plane was pierced with a scalpel. The biopsy needle was inserted and suction applied for tissue extraction. Samples were withdrawn, the site was cleaned, and butterfly adhesive bandages were applied to the incision. The samples were quick-frozen in liquid nitrogen and maintained at -70°C. Samples

were split, packaged, and transported for analysis to the University of California/Los Angeles (UCLA), Washington State University, and the Karolinska Institute in Stockholm.

Data Reduction and Analysis

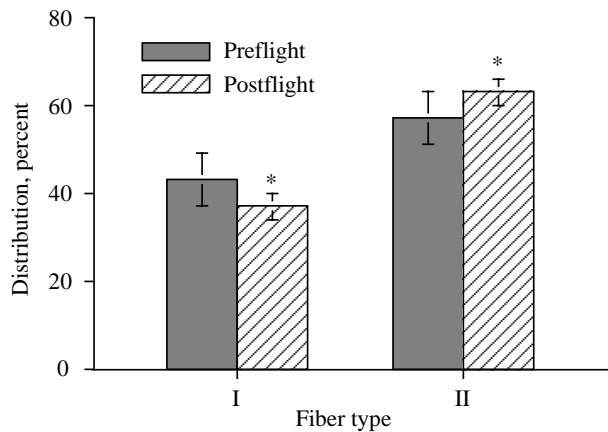
A one-tailed paired t-test was used to identify significant differences ($p < 0.05$) between the mean values of fiber cross-sectional area (CSA), fiber distribution, and number of capillaries of all crew members before flight compared to the mean value for all crew members after flight.

Results

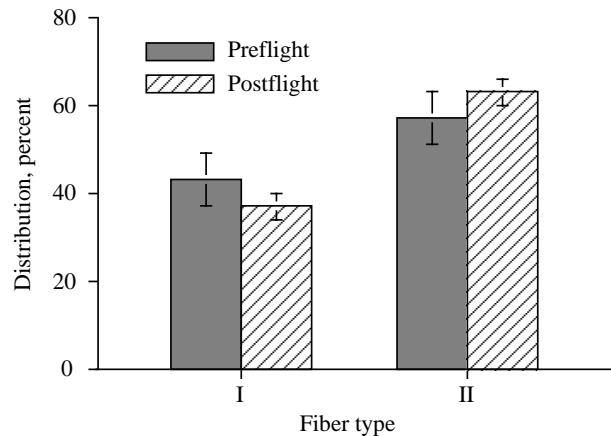
Of all the variables measured, the one with the greatest implications from a physiological standpoint was CSA of the muscle fibers. The CSA of slow-twitch (Type I) fibers after flight was 15% less than before; the CSA of fast-twitch (Type II) fibers was 22% less after flight than before (Figure 3-6). However, these mean values do not reflect the considerable variation among the eight astronauts tested. At least some of this variation probably resulted from differences in the types and amounts of preflight and in-flight countermeasures (exercise or LBNP) in the group.

The relative proportions of Type I and II fibers were different after the 11-day mission than before (Figure 3-7a); the fiber distribution also seemed to follow the same trend after the 5-day mission (i.e., more Type II and less Type I fibers after than before), but the sample size was too small to reach statistical significance (Figure 3-7b).

The number of capillaries per fiber was significantly reduced after 11 days of flight (Figure 3-8). However, since the mean fiber size was also reduced, the number of capillaries per unit of CSA of skeletal-muscle tissue was unchanged.



a. Fiber type distribution following 11 days of space flight (n=5). * $p < 0.05$



b. Fiber-type distribution following 5 days of space flight (n=3).

Figure 3-7. Changes in the distribution of Type I and Type II muscle fibers in the vastus lateralis on landing day after 11 days (3-7 a) or 5 days (3-7 b) of space flight.

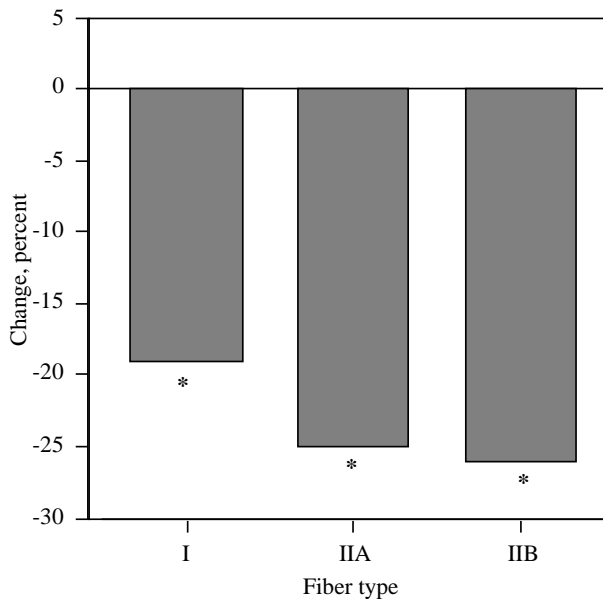


Figure 3-8. Percent change of mean number of capillaries per fiber type following 11 days of space flight (n=5). * $p < 0.03$.

Quantifying Skeletal Muscle Size by Magnetic Resonance Imaging (MRI) (DSO 606)

Specific Aim

The purpose of this investigation was to noninvasively quantify changes in size, water, and lipid composition in antigravity (leg) muscles after spaceflight.

Methods

Eight Space Shuttle crew members, five from a 7-day flight and three from a 9-day flight, participated as test subjects. The subjects underwent one preflight and two postflight tests on days L-30 or L-16 days and on R+2 and R+7 days. Testing involved obtaining an MRI scan of the leg (soleus and gastrocnemius) at The University of Texas-Houston Health Science Center, Hermann Hospital. Equipment consisted of: (1) a General Electric Signa whole-body MRI scanner, operated at 1.5 Tesla, with spectroscopy accessory, (2) a 2T MR imager/spectrometer with a 25 cm clear horizontal bore magnet, and (3) an HP 4193A Vector impedance bridge for the RF coil design.

Test subjects were positioned supine inside the magnetic bore for approximately one hour. A 15 cm cage resonator was used for radio frequency transmission and signal reception. Multi-slice axial images of the leg were obtained to identify and locate various muscle groups. Image-guided localized proton spectroscopy of individual muscle groups used stimulated echo (STE) sequence. Spectral analysis was obtained with an echo time of 15 ms and mixing time of 7.8 ms. All MR studies were performed on the soleus and gastrocnemius

muscles. Water and lipid peak areas were computed to quantify concentrations. The proton sample was obtained from a standard placed within the field of view. Concentrations of tissue water and lipid in the soleus and gastrocnemius were expressed relative to a standard sample placed in the field of view. Changes in water and lipid content were measured, in addition to CSA, to distinguish changes in fluid versus tissue volumes. Multiple slices were measured by computerized planimetry.

Data Reduction and Analysis

The time in milliseconds required for protons to reach a resting state after maximal excitation is the relaxation time. Two types of relaxation time (T1 and T2) were used to detect changes in the water and lipid content of tissue. Skeletal-muscle volume was assessed in terms of CSA. Thirty to forty 3 to 5 mm slices were acquired in 256 x 128 or 256 x 246 matrices. Multiple slices were measured by computerized planimetry.

Results

CSA and volume of the total leg compartment, soleus, and gastrocnemius were evaluated to assess skeletal muscle atrophy. The volumes of all three compartments were significantly smaller ($p < 0.05$) after both the 7- and 9-day Shuttle flights, relative to preflight, with 5.8% lost in the soleus, 4.0% lost in the gastrocnemius, and 4.3% lost in the total compartment. These decreases represent true skeletal muscle tissue atrophy, not fluid shift. No recovery was apparent by 7 days after landing (data not shown).

PART 2 – THE EFFECT OF IN-FLIGHT EXERCISE ON POSTFLIGHT EXERCISE CAPACITY AND ORTHOSTATIC FUNCTION

Purpose

Exposure to the microgravity environment of spaceflight causes loss of the gravity-induced hydrostatic pressure gradients normally present in the body, thus allowing blood volume to move away from the lower extremities and toward the upper body [17]. Changes in orthostatic function observed immediately after spaceflight have been attributed to orthostatic intolerance [18]. Four investigations (DSOs 476, 608, 618, and 624) were conducted to study the effects of exercise on aerobic capacity and orthostatic function before, during, and after spaceflight.

Both bed rest and microgravity induce cardiovascular deconditioning and affect exercise capacity [19-21]. Less tolerance of orthostatic stress on the day of return from spaceflight has been shown to be common and has been attributed mostly to reduced blood plasma volume and depressed baroreflex response.

Findings from the Apollo era (n=27) demonstrated that oxygen consumption, at work loads that elicited heart rates (HR) of 160 beats per minute, was reduced by an average of 19.2% on the first day after flight, and that this decrease was largely mitigated 24 hours later [20, 21]. The relative contributions of postflight change in vascular volume versus classical “aerobic deconditioning” were unclear. However, it is known that regular aerobic exercise during bed rest can maintain both vascular volume and aerobic capacity [22, 23]. Three investigations were conducted (DSOs 476, 608 and 624) to document the degree of exercise deconditioning after flight and to investigate the use of aerobic exercise during flight to reduce the severity of postflight deconditioning (Table 3-1).

Intense exercise has been shown to expand plasma volume 24 hours thereafter [24, 25]. Intense exercise near the end of a bed-rest study also has been shown to reverse the depression of the vagally mediated baroreflex function [26]. A maximal or near-maximal exercise bout before return from spaceflight could minimize the effects of renewed exposure to gravity on the cardiovascular system [19, 27]. These findings prompted an investigation (DSO 618) of the acute effects of exercise on aerobic capacity and orthostatic function.

Background

Aspects of the four EDOMP investigations of how in-flight exercise affects postflight exercise capacity and orthostatic function are compared in Table 3-3. The original intent of DSO 476, which began before EDOMP, was to examine the effect of aerobic exercise performed during flight on cardiac echocardiographic measurements of left-ventricular end-diastolic volume at rest. Exercise capacity was measured two days after landing. Because EDOMP focused on the ability to carry out landing and egress, DSO 608, in which exercise capacity was to be measured on landing day, was conducted to replace DSO 476. The preflight and postflight exercise tests were similar for the two investigations, but DSO 608 included a body-composition component.

Manifesting equipment and recruiting subjects for DSOs 476 and 608 proved to be challenging for several reasons. First, the preflight and postflight tests involved maximal exercise, during which subjects were monitored continuously with electrocardiography (ECG). Second, the tests were designed to be conducted with a treadmill, for the reason that emergency egress would require crew members to walk or run away from the Shuttle. After occasional reports of delayed muscular soreness after the R+0 test, which was severe in one case, the exercise test device for DSO 608 was changed from treadmill to cycle ergometer so that tests would be given on the same type of device provided for exercise during flight. Yet another challenge was the relatively long period on landing day needed for all of the DSO 608 activities. Finally, DSO 608 was

Table 3-3. Measurements from all subjects on all test days

<i>Experiment</i>	<i>First Postflight Test on</i>	<i>Exercise to Maximum?</i>	<i>Testing to Modality</i>
DSO 476	R+2	Yes	Treadmill
DSO 608	R+0	Yes	Mixed*
DSO 618	R+0	Yes	Cycle
DSO 624	R+0	No	Cycle

*Originally treadmill: later changed to match the device used for exercise during flight.

modified after its initiation to allow several in-flight exercise prescriptions and modalities to be studied.

DSO 624, which was limited to sub-maximal exercise, was proposed as an alternative to DSO 608 with the objective of increasing crew participation. DSO 624 involved preflight and postflight sub-maximal tests on a cycle ergometer. Workloads were calculated to elicit 85% of each participant’s age-predicted maximum HR. Subjects participating in DSO 624 were not assigned specific in-flight exercise prescriptions, but logged all in-flight exercise and monitored their heart rates during that exercise.

DSO 618 was designed to study how a single bout of intense exercise, performed 24 hours before landing, affected postflight orthostatic function and aerobic capacity. Maximal exercise testing was required before, during, and after flight. DSO 618 also required a long data collection session on landing day. Results from 10 subjects were collected to assess the efficacy of this potential countermeasure.

Exercise In Flight and the Effects on Exercise Capacity at Landing (DSOs 476 & 608)

Specific Aim

The specific aim of DSOs 476 and 608 was to document exercise capacity, measured as peak oxygen consumption ($\dot{V}O_{2\text{peak}}$), after spaceflight in crew members who exercised during flight compared to those who did not.

Methods

Exercise Tests: All exercise tests, except for those performed on landing day, were conducted at the Exercise Physiology Laboratory at JSC. Landing day tests were conducted in either in the BDCF at KSC or the PSSF at DFRC. All exercise tests were similar for the two studies (DSOs 476 and 608) except as noted. Forty-two astronauts (38 men and 4 women, ages 40.3 ± 4.8 y, weight 74.7 ± 9.6 kg) participated in the exercise portion of the two studies. Each subject completed one or two

graded exercise tests to volitional fatigue 10 to 30 days before and 0 to 10 days after spaceflight. Subjects in DSO 476 (n=24) were tested on R+2 or R+3. Subjects in DSO 608 were tested on R+0.

HR and rhythm were monitored continuously during exercise tests with a Q-5000 ECG (Quinton Instruments, Seattle, WA). Blood pressure was recorded at rest and during the last minute of each exercise stage. Volume of oxygen consumed ($\dot{V}O_2$) and volume of carbon dioxide output ($\dot{V}CO_2$) were analyzed continuously during exercise tests held at JSC with a Q-Plex system (Quinton Instruments, Seattle, WA), modified and interfaced with a mass spectrometer (MGA-1100, Marquette Electronics, St. Louis, MO). The Q-Plex provided the ventilatory measurements and computational software, and the MGA-1100 provided measures of the composition of expired gases. Tests on landing day were conducted with a standard Q-Plex system that used zirconium oxide and infrared sensors to measure expired gas composition. Verification tests of both systems showed no differences in metabolic measurements obtained with the two systems. The metabolic gas analysis systems were calibrated before and after each test with a calibrated syringe and calibration gases that were certified as accurate to $\pm 0.03\%$.

Thirty-two astronauts completed graded exercise tests on a treadmill. The remaining 10 performed cycle-ergometer tests before and after flight. Thirteen of the treadmill subjects (DSO 476) completed tests that included five sub-maximal steady-state exercise stages of 3 minutes each at 4.0, 4.5, 5.0, 6.0, and 7.0 mph, followed by grade increases of 2.5% each minute until the subject reported volitional fatigue. Tests for the remaining 19 treadmill subjects included three sub-maximal steady-state exercise stages of 3 minutes each at 5.0, 6.0, and 7.0 mph, followed by grade increases of 3.0% each minute until the subject reported volitional fatigue. This shorter protocol was adopted to reduce the amount of time needed for landing day tests. Because preliminary analyses revealed greater decreases in treadmill determined aerobic capacity in the crew members who used the cycle ergometer during flight, and because of the muscular soreness experienced during postflight treadmill exercise as mentioned earlier, cycle ergometry tests were used for the remaining subjects. The cycle ergometer test included three sub-maximal steady-state exercise stages of 3 minutes each at 100, 125 and 150 watts (w) at 60 rpm, followed by increases of 25w each minute until the subject reported volitional fatigue. These subjects also exercised during flight on the cycle ergometer.

In-flight Exercise: Most of the subjects who participated in exercise tests also completed one of three prescribed exercise protocols (continuous, interval, or high interval) during spaceflight. The continuous protocol consisted of three stages, lasting 8 to 10 minutes each, at heart rates (HR) elicited by 60, 70, and 80% of the subject's preflight $\dot{V}O_{2\text{peak}}$. This protocol was conducted on

the treadmill only. The interval protocol consisted of five stages of work at a HR corresponding to 65% of the preflight $\dot{V}O_{2\text{peak}}$ for 4 minutes followed by 2 minutes at a HR corresponding to 50% $\dot{V}O_{2\text{peak}}$. Subjects completed this protocol on the treadmill, rower, or cycle ergometer. The high interval protocol was a modification of the interval protocol. This protocol had five stages, each consisting of 4 minutes of high and 2 minutes of low exercise. The first two high/low stages were at HRs corresponding to 65 to 50% of the preflight $\dot{V}O_{2\text{peak}}$. The next two stages were at HRs corresponding to 75 to 50% of preflight $\dot{V}O_{2\text{peak}}$. The last stage was at the HR elicited by 85% of preflight $\dot{V}O_{2\text{peak}}$. All protocols began and ended with a 3-minute warm-up and cool-down period. One cycle-ergometer subject performed a continuous exercise protocol of his own design, but averaged 70 to 80% of the $\dot{V}O_{2\text{peak}}$ estimated by HR for all sessions. A Polar Vantage XL heart rate monitor (Polar CIC, Inc., Port Washington, NY) recorded HRs and provided real-time visual feedback to the exercising astronauts.

The amount of in-flight exercise was quantified as follows. HR was used as an indicator of exercise intensity. The duration of exercise performed for each session was recorded, as was the number of times that the crew member exercised. "Exercise volume" was calculated as the product of exercise intensity (% of HR_{max}), minutes exercised per session (time), and number of exercise sessions per week.

Results

The amount of exercise performed by the participants both before and during flight varied greatly (Table 3-4). Participants who used the cycle ergometer during flight tended to be on longer missions. Preflight-to-postflight changes in aerobic capacity (quantified by $\dot{V}O_{2\text{peak}}$) are illustrated in Figure 3-9. Subjects who did not exercise and subjects who used the in-flight cycle-ergometer protocols had significant ($p < 0.05$) reductions in aerobic capacity. Those subjects who exercised with the treadmill or rower showed no significant change from preflight aerobic capacity. Flight duration and the extent of decline in $\dot{V}O_{2\text{peak}}$ were not correlated.

Sub-Maximal Exercise In Flight and Cardiac Performance at Landing (DSO 624)

Specific Aim

The purpose of DSO 624 was to evaluate the usefulness of sub-maximal aerobic exercise during flight in reducing the severity of postflight deconditioning, as assessed by heart rate and $\dot{V}O_2$ measurements during postflight exercise.

Methods

Exercise Tests: Thirty-nine Shuttle crew members (35 men and 4 women), assigned to missions lasting 8 to 16 days, were subjects for this study. Two subjects

Table 3-4. Flight duration and “exercise volume” (%HR_{max} × min/week) for DSOs 476 and 608 (mean ± S.D.)

Exercise Modality	Flight Duration, days	“Exercise Vol” Before Flight	“Exercise Vol” During Flight	“Exercise Vol” During/Before
No exercise	10	8.7 ± 1.9	NA	NA
Cycle	16	12.1* ± 3.2	20,737 ± 19,429	20,127 ± 20,206
Rower or treadmill	9	7 ± 1.7	17,799 ± 8,097	12,665 ± 6,688
Treadmill, continuous	7	8.6 ± 1.1	15,858 ± 6,993	16,893 ± 6,848

Cycle significantly ($p < 0.05$) longer flights than other groups.

Note: The crew member who completed his own continuous cycle protocol during flight was included in the cycle group: one member of the no-exercise group was evaluated before and after flight on a cycle ergometer and was added to the No Ex group.

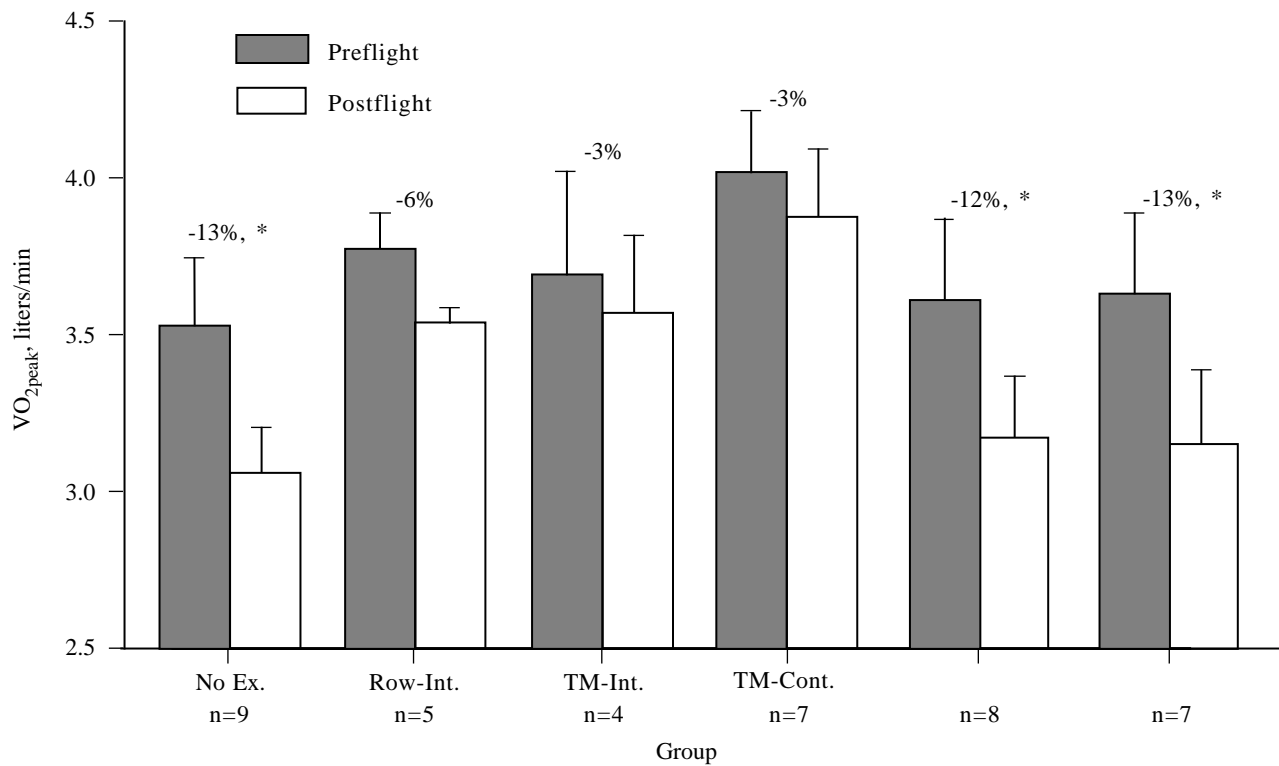


Figure 3-9. Preflight-to-postflight changes in $\dot{V}O_{2peak}$ for 40 participants in DSOs 476 and 608. Subjects are categorized by type of exercise device used and protocol performed during flight: No Ex = nonexercisers; Row = rower; TM = treadmill; Cycle = cycle/ergometer; Int = interval; Cont = continuous; Hi Int = high intensity.

*Postflight < Preflight ($p < 0.05$).

participated twice, on separate missions. All exercise tests took place on an upright cycle ergometer. The upright, as opposed to supine, position was selected because of the operational nature of EDOMP. Even though an orthostatic component of postflight deconditioning could exaggerate HR during postflight exercise, gravitational effects on the cardiovascular responses to exercise also would be present during contingency egress.

Exercise tests were conducted twice before flight (L-30 and L-10 days) and again on landing day. The L-30 test was designated a familiarization trial, and L-10 data were used for subsequent preflight-to-postflight comparisons. Tests consisted of exercise that increased by 50 w every 3 minutes until the subject completed the first workload that elicited a HR 85% of his or her age-predicted maximum HR. At the end of a stage, if the participant’s HR

was ≤ 5 beats per minute of their 85% age-predicted maximum HR, the workload was increased 25 w for the final stage. HR was recorded every 15 seconds during the test with a Polar Vantage XL heart rate monitor (Polar CIC, Inc., Port Washington, NY). Metabolic gases were analyzed continuously with the same systems described above for DSOs 476 and 608. Oxygen consumption ($\dot{V}O_2$) attained during the last minute of the final exercise stage was used as an index of cardiovascular exercise performance to compare preflight and postflight results.

In-flight Exercise: Subjects in DSO 624 were not given specific in-flight exercise prescriptions, but all exercised on the cycle ergometer during flight. Subjects wore the Polar HR monitor during exercise, and recorded the number and duration of exercise sessions. The HR monitor recorded and stored HR once every 15 seconds during exercise in up to eight data files. These data were retrieved and down-loaded onto a personal computer after landing. One mission did include both the cycle ergometer and the EDO treadmill, but only one DSO 624 subject performed two exercise sessions on the treadmill. In-flight exercise was quantified on the basis of exercise frequency, intensity (HR as % of age-predicted maximum), and duration of the in-flight exercise sessions.

Results

Heart rate and $\dot{V}O_2$ responses for the 25 subjects who achieved 50, 100, and 150 w work rates before and after flight are presented in Figure 3-10. Not all subjects completed these three levels of exercise, because several terminated exercise sessions on landing day at 125 w. Both the $\dot{V}O_2$ and HR results confirmed that cardiovascular stress, as indicated by elevated HR, was increased during the postflight activity. The elevation in HR response resulted in the test being terminated at a lower work rate on landing day relative to preflight tests. Subjects who exercised three or more times per week during flight, at a HR $>70\%$ of their age-predicted maximum HR and for more than 20 minutes per session, experienced smaller decrements in $\dot{V}O_2$ at test termination on landing day than did subjects who exercised less frequently or at lower intensities (Figure 3-11). Again, no correlation was found between amount of decline in $\dot{V}O_2$ and flight duration.

Effects of Intense Exercise Before Landing on Aerobic Capacity and Orthostatic Function at Landing (DSO 618)

Specific Aim

This investigation was designed to study the influence of a single bout of maximal exercise, conducted 24 hours before landing, on aerobic capacity and orthostatic function at landing. Aerobic capacity was assessed from peak oxygen consumption during cycle ergometer tests, and orthostatic function from HR and blood pressure (BP) responses to a stand test.

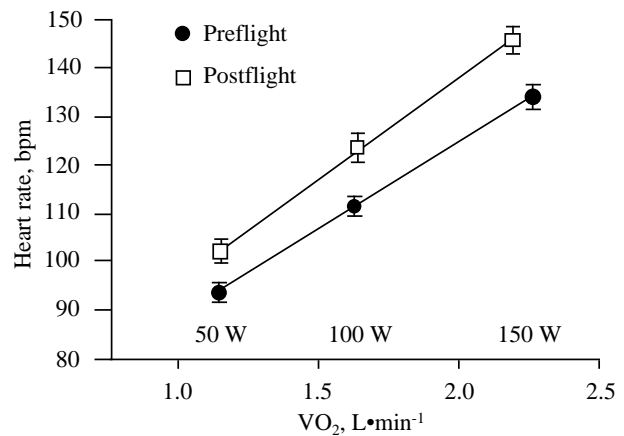
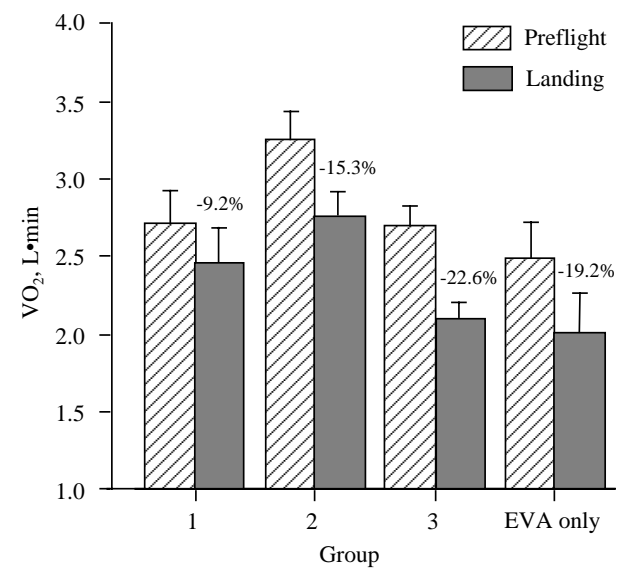


Figure 3-10. DSO 624 subjects ($n=25$) who performed identical work rates before and after flight demonstrated increased cardiovascular stress by an increased HR, with no change in $\dot{V}O_2$, within each exercise stage on landing day.



Group 1 ($n=11$): Exercised $>3x$ /week. HR $>70\%$ age-predicted, ≥ 20 min/session (“regular” exercise group)

Group 2 ($n=10$): Exercised $>3x$ /week. HR $<70\%$ age-predicted, ≥ 20 min/session (“low intensity” exercise group)

Group 3 ($n=14$): Exercised $<3x$ /week. HR and min/session variable (“minimal” exercise group)

EVA Only ($n=4$): Subjects performed EVAs. Minimal other exercise performed during flight (Hubble mission)

Figure 3-11. In-flight exercise patterns appear to influence the degree of oxygen consumption change at the termination workload (85% age-predicted HR max) following flight.

Methods

Subjects: Ten Shuttle crew members (9 men and 1 woman), assigned to missions lasting 8 to 14 days, were the subjects for DSO 618. Six of the subjects, designated the countermeasure (CM) group, were instructed to perform a maximal exercise session 18 to 24 hours before the scheduled landing time of their flight. The other four subjects acted as controls. Each subject was to perform a test of orthostatic function (stand test) and a test to measure $\dot{V}O_{2\text{ peak}}$ before and after flight.

Although 10 subjects participated in the study, mission constraints dictated that data from fewer subjects could be used. One CM participant performed the in-flight exercise session to volitional fatigue 24 hours before scheduled landing time, but landing was postponed for an additional 24 hours and the subject could not repeat the exercise. Thus, the landing-day data collected from this subject could not be used for preflight-to-postflight comparisons. Another CM participant was not allowed to perform the stand test or the exercise tests on landing day because that participant had exceeded the maximum 18-hour duty day limit [28] by that time. Two other participants, one CM and one control, performed the stand test on landing day, but did not perform the exercise test, in one case because of duty day constraints and in the other because of extreme fatigue. Thus, the final data set for DSO 618 allowed comparison of eight subjects (four control and four CM) for orthostatic function and only six subjects (two control and four CM) for aerobic capacity measures.

Orthostatic-Function (Stand) Test: Stand tests were conducted twice before flight, at about L-20 and L-10 days, and once 1.5 to 3.0 hours after landing. The L-30 test was designated a familiarization trial, and L-10 data were used for subsequent preflight-to-postflight comparisons. Preflight tests were conducted in the morning, 2 to 4 hours after subjects had consumed a light breakfast. Subjects were asked not to consume alcohol, caffeine, or cold medications, and to avoid smoking or strenuous exercise for 24 hours before testing. The exception to this rule was the exercise session by the CM group before landing. All subjects completed a NASA-required fluid loading protocol [29] about 2 hours before landing, during which approximately eight salt tablets were consumed with approximately 912 ml of water (actual amount was based on subject's weight). Subjects were asked to not consume additional fluids after the fluid load until after the stand test.

For the stand test, subjects rested supine for 6 minutes, after which two assistants helped them move quickly into a standing position. Subjects were instructed to let the technicians move them rather than making active movements themselves. Subjects stayed still once they reached the standing position, with feet approximately 25 cm apart, and remained in that position for 10 minutes. HR and rhythm were monitored continuously

with a defibrillator monitor (Lifepak8™, Physiocontrol, Inc., Redmond, WA) throughout the test. HR was recorded during the last 15 seconds of each minute. BP was recorded every 60 seconds from the left arm, at the level of the heart, with a calibrated aneroid sphygmomanometer. Mean HR and BP during the last 3 minutes in each posture were computed and used for subsequent analyses.

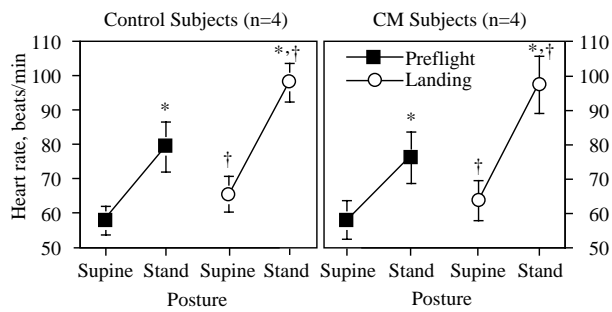
Preflight and Postflight Exercise Tests: All subjects performed two exercise tests on a Monarch cycle ergometer during the month before flight, and one test on landing day. Subjects were asked to maintain a 75 revolutions per minute (rpm) rotation rate, beginning at 50 w and increasing by 50 w increments every 3 minutes until they either could not maintain the cycling cadence or indicated that they could not continue the test. When the test was completed, subjects continued to pedal at 50 w for at least 5 minutes. During these tests, HR and rhythm were monitored continuously with a Q-5000 ECG (Quinton Instruments, Seattle, WA). Blood pressure was recorded while the subjects were seated at rest, and during the last minute of each exercise stage. Metabolic gases ($\dot{V}O_2$ and $\dot{V}CO_2$) were analyzed continuously during the exercise tests as described above for DSOs 476 and 608. The " $\dot{V}O_{2\text{ peak}}$ " was considered to be the highest value attained during any 60-second period during the test.

In-flight Exercise Constraints and Tests: All in-flight exercise was performed on a cycle ergometer designed for use in microgravity. The ergometer was calibrated before flight and verified as unchanged after each flight. Because a NASA flight rule required that exercise take place on all missions lasting more than 10 days, all subjects were allowed to exercise in flight. However, because of the potential for confounding the experiment, the investigators limited that exercise as follows: (1) intensity of < 60% of the maximum work rate attained before flight, (2) duration of no more than 20 minutes per session, and (3) frequency of no more than 3 times in a 7-day period. Subjects recorded HR during exercise with the Polar HR monitor. No exercise, other than the maximum session by the CM subjects, was allowed during the last 48 hours of flight.

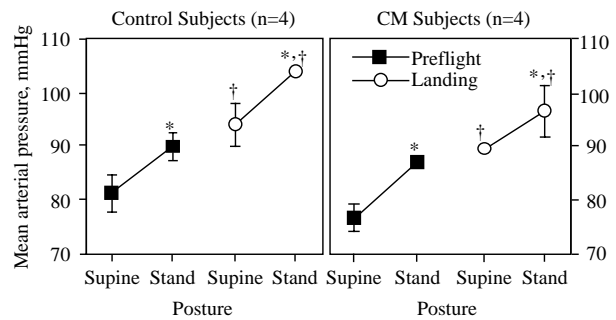
The maximum session for the CM subjects was similar to the exercise test and was conducted 18 to 24 hours before scheduled landing. In order to ensure high-quality data and voice transfer, subjects contacted the Mission Control Center in Houston before beginning the exercise and again before beginning the stage that corresponded to their peak preflight exercise level. The ECG was monitored via the Shuttle's bioinstrumentation system. Heart rates and rhythms were monitored in the Mission Control Center. Metabolic gas data were not collected during flight.

Results

Orthostatic Function: Stand-test results revealed no systematic differences between the CM (n=4) and control (n=4) subjects. Both groups demonstrated



a. Stand test heart rates in the DSO 618 subject groups. *Standing HR was significantly greater than supine HR ($p < 0.01$); †landing HR > preflight HR ($p < 0.01$)



b. Stand test mean arterial pressures in DSO 618 subject groups. *Standing HR was significantly > supine HR ($p < 0.01$); †landing HR > preflight HR ($p < 0.01$)

Figure 3-12. Heart rate and arterial pressure responses to preflight and landing day Stand tests.

approximately equivalent HR responses to standing after flight (Figure 3-12a). The BP responses also changed after flight, but no differences were evident between groups. Mean arterial BP was elevated, compared to preflight values, on landing day in both the horizontal and standing positions (Figure 3-12b) for both groups. None of the subjects in either group exhibited symptoms of orthostatic intolerance, such as dizziness or presyncope, on landing day.

Intense In-flight Exercise and Postflight Aerobic Capacity: Aerobic capacity declined 18% in the CM subjects versus 21% in the two control subjects who performed exercise tests on landing day (Figure 3-13). The HR responses for those participants who performed an exercise test before and during flight (the full set of CM subjects) are illustrated in Figure 3-15. HR response to exercise during flight was not statistically ($p = 0.12$) different than that recorded before flight (Figure 3-14).

Discussion

DSOs 476, 608, and 624 were steps in assessing the efficacy of exercise countermeasures with regard to preserving aerobic capacity for egress on landing day. Tasks associated with landing and egress also required maintaining orthostatic function. The remaining study, DSO 618, was an evaluation of a potential exercise countermeasure to improve orthostatic function and exercise capacity on landing day.

Aerobic Capacity: The results demonstrate clearly that performing minimal or no exercise countermeasures during flight negatively affects the ability to perform aerobic exercise on landing day. The postflight $\dot{V}O_{2\text{peak}}$ dropped 13% in the control (no exercise) group for DSO 608, and 18 to 21% for subjects in DSO 618. Moreover,

those DSO 624 participants who performed only minimal exercise during flight had the largest drop in $\dot{V}O_2$ (22.6%) of any subject group at the test termination HR.

These results also indicate that regular aerobic training attenuates microgravity effects on aerobic performance after flight. Treadmill exercise during flight was associated with only a 3% reduction in $\dot{V}O_{2\text{peak}}$, and rowing during flight resulted in a 6% reduction after flight. Cycle ergometer exercise was associated with a 12 to 13% reduction in aerobic capacity after flight, which was equivalent to the drop seen for DSOs 476 and 608 control subjects. However, these results also include the confounding factor of the time at which postflight testing

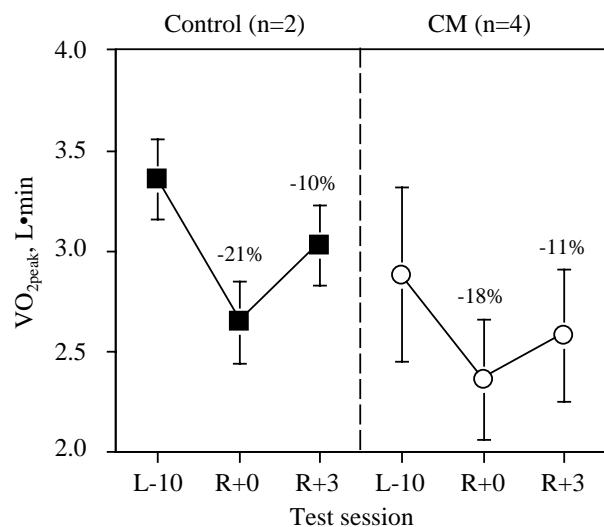


Figure 3-13. Aerobic Capacity of DSO 618 Subjects.

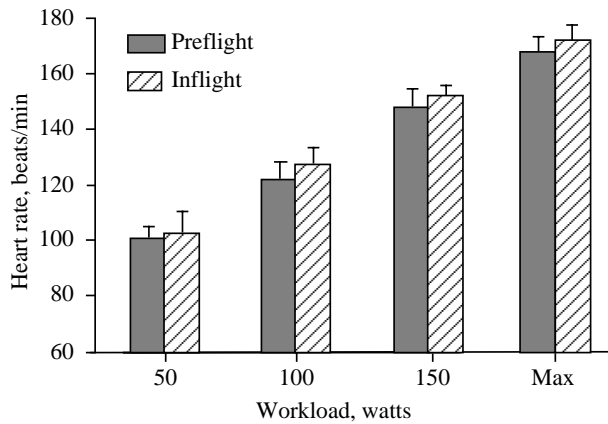


Figure 3-14. Pre- and in-flight heart rate responses of DSO 618 subjects ($n=6$). Although HR increased with work rate ($p<0.01$), there were no statistical differences between the pre- vs. in-flight values ($p=0.12$).

took place (on R+0 or on R+2 or R+3). Subgroups that were tested on landing day (R+0) for DSOs 476 and 608 were as follows:

- No Exercise, 44% (four of nine subjects)
- Treadmill or Rower Interval Subjects, 22% (two of nine)
- Treadmill Continuous Subjects, 0% (zero of seven)
- Cycle Ergometer subjects, 67% (10 of 15)

The preservation of $\dot{V}O_{2\text{ peak}}$ among the treadmill or rower group may not have been as marked if more subjects had been tested on R+0. This hypothesis is supported by the results from DSO 618, which showed $\dot{V}O_{2\text{ peak}}$ to be reduced on R+3, but to a lesser extent than on R+0 (from a 20% to a 10% reduction). To date, no consensus of opinion has been reached as to the optimal exercise device, or protocol, for maintaining aerobic capacity.

The results from DSO 624 also verify the benefit of in-flight exercise. Subjects who exercised regularly, that is, more than three times a week, for more than 20 minutes, at an intensity eliciting greater than 70% of their age-predicted HR maximum, experienced smaller declines in $\dot{V}O_2$ measured immediately after flight than did those subjects who performed less exercise. Subjects who exercised regularly, but at lower intensities, experienced greater reductions in their termination $\dot{V}O_2$ on landing day. Finally, those subjects who exercised the least during flight showed the largest reduction in test-termination $\dot{V}O_2$. Thus, exercise intensity has been shown to be an important factor to consider in developing exercise prescriptions.

Intense Exercise and Orthostatic Function: The crew members tested with the intense exercise countermeasure did not seem to be protected against orthostatic intolerance after flight. This finding contrasts with results from other investigations [28, 29] because of the lack of difference in orthostatic tolerance between the control and experimental groups.

DSO 618 was useful in exposing potential difficulties associated with an end-of-mission countermeasure. For example, the subject whose mission was delayed for 24 hours could not unpack the exercise and monitoring hardware to repeat the exercise session. This situation would be even more difficult if several crew members were scheduled for repeat exercise sessions. Another useful finding was that the HR response to exercise on the cycle ergometer during flight was similar to preflight values. Some astronauts, mostly those from flights on which the original Shuttle treadmill was flown, have commented on the difficulty in achieving sufficient HR during flight. The results from DSO 618 indicate that such difficulty was related more to the exercise device than to any physiological changes associated with microgravity exposure.

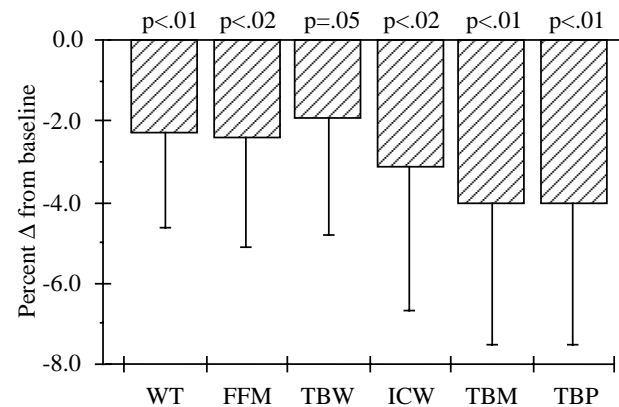


Figure 3-15. Changes in body weight (WT), fat-free mass (FFM), total body water (TBW), intracellular water (ICW), total body mineral (TBM), and total body protein (TBP) in 10 astronauts after 7- to 16-day flights. Variables were measured or derived from underwater weighing and the BERS model.

PART 3 – CHANGES IN BODY COMPOSITION IN SPACE AND THE EFFECTS ON EXERCISE PERFORMANCE

Purpose

Spaceflight is thought to affect aspects of body composition such as total body protein [11, 32-36], mineral and bone mineral content [37-41], and various body-water compartments [42-45]. To some extent, changes in compositional variables reflect the process by which humans adapt to the spaceflight environment, but can also result from inadequate nutrition, exercise, or fluid intake. Changes in these variables may well limit the safe duration of human space exploration through their putative effects on muscle performance, orthostatic tolerance, and crew safety.

A simple, reliable way of monitoring changes in protein, bone mineral, and fluid volumes before and after spaceflight would allow flight surgeons, crew medical officers, and investigators to monitor crew health and the effectiveness of nutrition, exercise, and fluid countermeasures. One of the goals of DSO 608 was to develop such a method.

Background

One of the EDOMP goals was to integrate measures of body composition with measures of performance so that they could be used to evaluate the efficacy of countermeasures. Accordingly, simple, reliable techniques were developed that could be used during spaceflight to measure the four basic components of body composition: fat, water, protein, and mineral. A new body-composition model, the bioelectrical response spectrography or BERS model, was also developed to noninvasively measure blood and plasma volume [46-51]. The new methods were evaluated by measuring changes in body composition during spaceflight and by relating changes in protein and fluid volume to the performance variable $\dot{V}O_{2\text{peak}}$.

Development of a body-composition measurement technique for use in space took place in several steps. The first step was to select an appropriate body-compositional model from existing equations used to estimate amounts of fat, water, protein, and mineral. The results generated by the selected model were then compared with those generated by standard techniques such as dilution of isotopically labeled water, dual X-ray absorptiometry, and underwater weighing. This comparison verified that total body mineral, bone mineral content, and total body protein could be assessed from total body water and body density with a three-compartment model (fat, water, and dry lean mass), and that this approach was suitably simple for use in spaceflight.

The next step in completing the new model was to find ways of measuring body mass, body volume, and total body water during spaceflight. Body mass has been measured during flight since Skylab [52], and new methods that involve smaller and more accurate instruments are currently being evaluated on the Shuttle by other investigators. Therefore, we focused our attention on ways of easily and noninvasively assessing body volume and total body water in space.

To measure body volume, a series of air-displacement volumeters were developed [50]. To measure total body water, a new circuit model was developed that relied on BERS [53-61]; this model was used to estimate blood and plasma volumes. These important components of total body water typically are measured from dilution of radio-labeled albumin (^{125}I) or red blood cells (^{51}Cr) [62-64], carbon monoxide [65], or inert dyes such as Evans blue [66]. The usefulness of these techniques for spaceflight is limited by the need for multiple blood samples, the time needed for tracers to equilibrate within the vascular compartment, and the potential risks from use of radiolabeled compounds. Preliminary results (data not shown) suggest that BERS could serve as a good noninvasive alternative to these techniques for assessing vascular volumes. The new body-composition method was used to measure changes in crew member body composition before and after spaceflight. Additionally, potential changes in protein and fluid volume were related to changes in $\dot{V}O_{2\text{peak}}$.

Changes in Body Composition After EDO Flights

Specific Aim

The purpose of this investigation, a component of DSO 608, was to use the new body-composition method to assess weight, total body water, extracellular water, intracellular water, fat, fat-free mass, total body mineral, and total body protein in astronauts after 7- to 16-day flights.

Methods

Previous measurements of changes in body composition after spaceflight have been limited to weight, total body water, and extracellular water (ECW). These variables, plus changes in intracellular water (ICW), fat, percent fat, fat-free mass, total body mineral, and protein were examined in 10 astronauts before and 2 days after flights that lasted 7 to 16 days. All measures were derived from body weight, body water, and body density. Body density was calculated from underwater weights with correction for residual lung volume. Body fluids were estimated with a previously validated, multi-frequency bioelectrical response spectrograph model [49]. The change in each variable was analyzed with dependent t-ratios.

Results

Changes in body weight, fat-free mass, total body water, intracellular water, total body mineral, and total

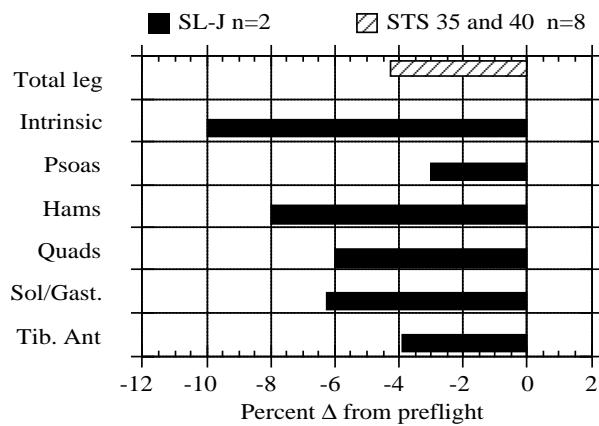


Figure 3-16. Percent decreases in muscle volumes, measured by magnetic resonance imaging, from three EDO Shuttle missions.

body protein, illustrated as percent change from preflight values, are shown in Figure 3-15. No physiologically significant changes were present in body fat or ECW. The decrease in body weight was due primarily to loss of fat-free mass. All three components of fat-free mass (water, protein, and mineral) were reduced after flight. The decrease in water was due primarily to loss of ICW, which in turn may have been a response to decreases in protein and nonosseous (~17% of the total body mineral) mineral levels within the muscles and other tissues. Since the results from Skylab showed postflight changes in serum osmolality [67], and probably no postflight change in ECW osmolality, we assume that reduction of cellular protein (and glycogen) and mineral would cause a decrease in intracellular water in order to maintain normal osmotic pressure gradients between the cells and interstitial fluids.

Decreases in cellular protein (decreased muscle volume) after Shuttle flights (Figure 3-16) have been reported previously [11, 68]. The average decrease in muscle volume was 6%, and the average decrease in total body protein was 4% (Figure 3-16). We conclude that decreases in total body protein and mineral after spaceflight contributed to the loss of water from cells and that the combination of these reductions resulted in decreased fat-free mass. These decreases may affect physical and metabolic performance or health of astronauts during or after spaceflight.

Changes in Protein and Fluid Volumes and the Effects on Performance

Specific Aim

Muscle atrophy, measured by various means, after spaceflight [32-36] has been linked with postflight declines in aerobic capacity ($\dot{V}O_{2\text{peak}}$, in $\text{ml}\cdot\text{kg}^{-1}\cdot\text{min}^{-1}$) [46]. However, no one has reported how decreases in

muscle mass might affect specific aspects of performance. Therefore, we sought to determine whether post-flight decreases in performance ($\dot{V}O_{2\text{peak}}$) were associated with decreases in protein, water, or both.

Methods

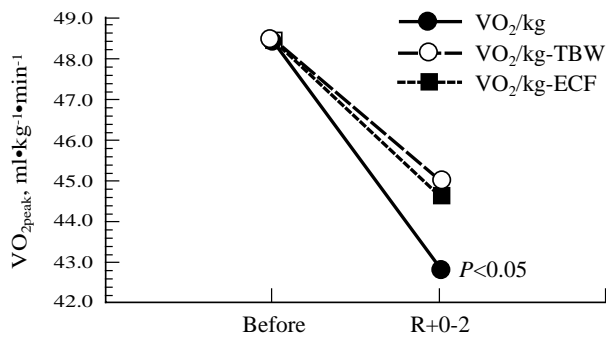
Eight astronauts who completed flights of 7 to 16 days were the subjects for this study. $\dot{V}O_{2\text{peak}}$ was measured during a graded treadmill test to volitional fatigue [46]. Subjects also underwent underwater weighing, residual-volume, and body-mass measurements, which were used to calculate body density, and BERS, which was used to calculate body fluid volumes. Astronaut subjects completed the testing about 10 days before flight and again 0 to 2 days after flight. Body-composition analysis always preceded measures of aerobic capacity on the same day. Total body protein was calculated from body density and water [47].

To statistically remove the effect of the covariate (body-composition variables) from the performance response, an analysis of covariance was computed with the aerobic capacity data, using total body water, extracellular fluid, total body protein, or the sum of total body water plus protein as the covariates. Any significant decrease in aerobic capacity observed after the removal of the covariate would indicate that another mechanism was contributing to the loss of performance.

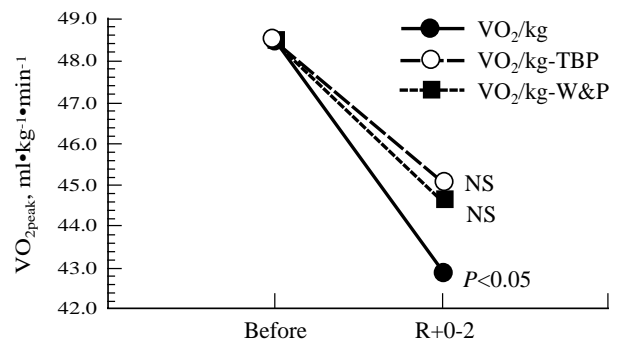
Results

Aerobic capacity declined by 12% ($p < 0.05$), total body water by 2% ($p < 0.05$), and protein by 4% ($p < 0.05$). A 1.5% decrease in extracellular fluid was not significant. Removing the effects of the decrease in extracellular fluid and total body water reduced the decrease in aerobic capacity from ~12% to 9.5% and 8.6%, respectively (Figure 3-17a). These adjusted postflight aerobic performance values were still significantly lower than preflight measures. This finding probably reflects the fact that 8 of the 10 subjects were evaluated 2 days after landing, when fluid volumes had returned to near-preflight levels [42,43].

In contrast, removing the effects of the decrease in total body protein (TBP) significantly reduced the decrease in aerobic capacity from 12% to 7.4% (Figure 3-17b). Removing the effects of both total body protein and total body water (W&P) also significantly reduced the decrease in aerobic capacity from 12% to 8.0% (Figure 17a). Adding water-plus-protein as a covariate was no better than protein alone in reducing the decrease in aerobic capacity. The decrease in protein probably resulted from a reduction in muscle mass, since the observed 4% decrease was similar to the decrease in muscle volume (4-6%) measured by magnetic resonance imaging [11, 68]. The smaller muscle mass would contribute to a decrease in performance.



a. Decreases in aerobic capacity ($\dot{V}O_{2peak}$) without (solid line, closed circles) and with covariate adjustments for total body water (dashed line, open circles) or extracellular fluid (dotted line, closed boxes). Removing the effects of loss of fluid did not significantly reduce the observed decreases in performance.



b. Decreases in aerobic capacity ($\dot{V}O_{2peak}$) without (solid line, closed circles) and with covariate adjustments for total body protein (TBP: dashed line, open circles) or the sum of total body protein and water (W&P: dotted line, closed boxes). Removing the effects of protein significantly reduced the observed decreases in performance. However, adding water to protein did not improve this finding.

Figure 3-17. Influence of fluid volumes and protein on aerobic capacity ($\dot{V}O_{2peak}$) before and after space flight.

Conclusion

We conclude that the decreases in aerobic performance were due at least in part to a reduction in TBP, and that the protein loss probably represents a reduction of muscle mass. This study also highlights the importance of measuring changes in body composition in order to better understand changes in other physiological systems.

SUMMARY AND RECOMMENDATIONS

Skeletal Muscle Performance

Exposure to microgravity, even for 5 days or less, evokes changes in skeletal muscle performance and morphology. These changes, being part of the microgravity-induced deconditioning process, may have negative implications for completing critical operational tasks. NASA seeks to minimize the consequences of this deconditioning by providing countermeasures that optimize in-flight physical performance, ensure suitable return to a terrestrial environment, and ensure nominal postflight recovery.

The test battery described to monitor skeletal muscle performance is an efficient and objective way of validating preflight, in-flight, and postflight exercise countermeasures. Such countermeasures include preflight training protocols, in-flight exercise hardware such as the treadmill, rower, cycle, resistive exercise device, and other equipment, and postflight rehabilitation regimens. This test battery includes clinical tests such as MRI to

evaluate changes in muscle volume; biochemical markers, such as creatine kinase and myoglobin, to assess muscle damage; and isokinetic muscle-function tests to determine overall muscle performance. This test battery is an important step in assessing crew health and in validating countermeasure interventions.

Exercise Capacity and Orthostatic Function

The results from DSOs 476, 608, 618, and 624 offer insight into the development of countermeasures against declines in aerobic capacity and orthostatic function on landing day. Conclusions and recommendations for future study are given below.

Exercise intensity, frequency, and duration are all important factors to consider in prescribing activities to maintain aerobic exercise capacity after flight. We recommend that crew members exercise at least three times a week, for more than 20 minutes per session, at work rates high enough to elicit 70% or more of their maximum HR. Preflight maximum exercise testing also is recommended for determining maximum HR and work rates, which will be vital in developing exercise prescriptions tailored to individuals. Age-predicted maximum HR is too conservative and shows too much variation. Interval protocols, if used, can be prescribed more accurately from work rates rather than from HR.

The modality for in-flight exercise may be important as well. Findings from DSO 608 are too limited in this regard to generate firm recommendations. Additional landing day data should be collected as to how well

aerobic exercise capacity is maintained after in-flight use of the cycle ergometer versus the treadmill versus the rower.

Crew reports of inability to reach target HR came mostly from crew members who used the original treadmill. Considerable attention has been focused on a new treadmill designed for the International Space Station (ISS). Speeds, length of the running surface, and loads on the subject from an improved restraint system have been evaluated carefully so that this device can deliver appropriate work rates.

Maximal exercise performed on the treadmill on landing day was associated with delayed onset muscle soreness. Maximal exercise tests on cycle ergometers have not produced these effects. Maximal testing is considered necessary for accurate assessment of aerobic capacity. However, values estimated from sub-maximal tests are acceptable for operational programs. If maximal testing is used on or near landing day, the cycle ergometer should be used to minimize the risk of muscle injury.

Data regarding use of maximal exercise at the end of flight to counter loss of orthostatic function on landing day were equivocal. However, the number of subjects tested was small, and the effects of fluid loading plus return of subjects to the test facility in the seated position may have confounded these findings.

In the future, if an end-of-mission countermeasure is proposed, we recommend that studies be conducted regarding the length of time after administration that the countermeasure remains effective. This will aid NASA by determining when a repeat session is absolutely necessary in the event of a landing delay. The decision on acceptable weather for landing is usually made less than 24 hours, and on many flights is postponed until minutes, before the deorbit burn is scheduled. An established plan of action is critical regarding the need for, and practicality of, repeating the countermeasure.

The time course for recovery of aerobic capacity after spaceflight has not been well documented. This information will be necessary to plan effective postflight rehabilitation protocols for longer missions, such as those planned for the ISS.

Body Composition and Exercise

Spaceflight is thought to affect aspects of human body composition such as protein, mineral, and various compartments of body water. Changes in these variables can reflect the adaptation process, but they also can reflect inadequate nutrition, exercise, or fluid intake. We developed a simple, reliable way of monitoring changes in protein, bone mineral, and fluid volumes before and after spaceflight.

Changes in body composition after spaceflight revealed that decreases in TBP and mineral contributed

to the loss of water from tissue. The combination of these reductions resulted in decreased fat-free mass. These decreases may affect physical and metabolic performance or health of astronauts during or after spaceflight.

An analysis of changes in body composition and their relation to $\dot{V}O_{2\text{peak}}$ revealed that decreases in aerobic performance were due at least in part to a reduction in TBP and that the protein loss probably represented a reduction of muscle mass. This study also highlighted the importance of measuring changes in body composition in order to better understand changes in other physiological systems.

REFERENCES

1. Extended Duration Orbiter Medical Project Plan. Houston: Johnson Space Center; December 1988.
2. Convertino VA. Physiological adaptations to weightlessness: Effects on exercise and work performance. *Exercise & Sports Sci Rev* 1990; 8:119-66.
3. Crew escape system overview. NASA document WG-5/NASA/CTC/NPO E/5030. Houston: Johnson Space Center; April 1994.
4. Extended Duration Orbiter Medical Project: Investigation Requirements Document. Houston: Johnson Space Center, July 1990.
5. Booth FW. Effect of limb immobilization on skeletal muscle. *J Appl Physiol: Respirat Environ Exer Physiol* 1982; 52(5):1113-8.
6. Greenleaf JE, Van Beaumont W, Convertino VA, Starr JC. Handgrip and general muscular strength and endurance during prolonged bedrest with isometric and isotonic leg exercise training. *Aviat Space Environ Med* 1983; 54:696-700.
7. LeBlanc A, Gogia P, Schneider V, Krebs J, Schonfeld E, Evans H. Calf muscle area and strength changes after five weeks of horizontal bedrest. *Am J Sports Med* 1988; 16(6):624-9.
8. Thornton WE. Rationale for exercise in space flight. In: Parker, JF, Lewis CS, Christensen DG, editors. *Conference Proceedings: Spaceflight and Physical Fitness*, January 8-10, 1981 (NASA 3469). Falls Church, VA: Biotechnology Inc; 1981. p 13-80.
9. Thornton WE, Rummel JA. Muscular deconditioning and its prevention in space flight. In: Johnston RS, Dietlein LF, editors. *Biomedical Results of Skylab (NASA SP 377)*. Washington, DC: U.S. Government Printing Office; 1977. p 191-7.
10. Martin TP, Edgerton VR. Some factors that influence the neuromuscular response to space flight and simulation models of space flight. *Space Life*

- Sciences Symposium: Three Decades of Life Science Research in Space. Washington, DC: NASA; 1987.
11. LeBlanc AD, Rowe R, Schneider VS, Evans HJ, Hedrick T. Regional muscle loss after short duration space flight. *Aviat Space Environ Med* 1995; 66:1151-4.
 12. Edgerton VR. Exercise issues related to the neuromuscular function and adaptation to microgravity. NASA Conference Publication 3051; 1986. 77-8.
 13. Watkins MP, Harris AH. Evaluation of isokinetic muscle performance. *Clinics in Sports Medicine* 1983; 2(1):37-53.
 14. Chekirda IF, Yeremin AV. Dynamics of cyclic and acyclic locomotion of the Soyuz-18 crew after a 63-day space mission. *Kosm Biol i Aviakosm Med* 1977; 11(4):9-13.
 15. Grigoryeva LS, Koslovskaya IB. Effect of weightlessness and hypokinesia on velocity and strength properties of human muscles. *Kosm Biol i Aviakosm Med* 1987; 21(1):27-30.
 16. LIDO® Active Operations Manual, 1988.
 17. Charles JB, Frey MA, Fritsch-Yelle JM, Fortner GW. Cardiovascular and cardiorespiratory function (Chapter 3). In: Huntoon CL, Antipov W, Grigoriev AI, editors. *Space Biology and Medicine, Volume III: Humans in Spaceflight*. Washington, DC: American Institute of Aeronautics and Astronautics; 1997. p 63-88.
 18. Charles JB, Bungo MW, Fortner GW. Cardiopulmonary function (Chapter 14). In: Nicogossian AE, Huntoon CL, Pool SL, editors. *Space Physiology and Medicine*, 3rd ed. Philadelphia: Lea & Febiger; 1994. p 286-304.
 19. Convertino VA. Physiological adaptations to weightlessness: effects on exercise and work performance. In: Pandolf KB, Holloszy JO, editors. *Exercise and sports science reviews*. Baltimore: Williams & Wilkins; 1990.
 20. Rummel JA, Sawin CF, Michel EL. Exercise response. In: Johnston RS, Dietlein LF, Berry CA, editors. *Biomedical Results of Apollo (NASA SP-368)*. Washington, DC: National Aeronautics and Space Administration; 1975. p 265-75.
 21. Rummel JA, Michel EL, Berry CA. Physiological responses to exercise after space flight-Apollo 7 through Apollo 11. *Aerosp Med* 1973; 44(3):235-8.
 22. Greenleaf JE, Vernikos J, Wade CE, Barnes PR. Effect of leg exercise training on vascular volumes during 30 days of 6° head-down bed rest. *J Appl Physiol* 1992; 72(5): 1887-94.
 23. Greenleaf JE, Bernauer EM, Ertl AC, Trowbridge TS, Wade CE. Work capacity during 30 days of bed rest with isotonic and isokinetic exercise training. *J Appl Physiol* 1989; 67(5):1820-6.
 24. Green HJ, Jones LL, Painter DC. Effects of short-term training on cardiac function during prolonged exercise. *Med Sci Sports Exerc* 1990; 22(4):488-93.
 25. Green HJ, Thomson JM, Ball ME, Hughson RL, Sharratt MT. Alterations in blood volume following a short term supramaximal exercise. *J Appl Physiol: Respirat Environ Exerc Physiol* 1984; 56:145-9.
 26. Convertino VA, Doerr DF, Guell A, Marini JF. Effects of acute exercise on attenuated vagal baroreflex function during bedrest. *Aviat Space Environ Med* 1992; 63(11):999-1003.
 27. Convertino VA. Potential benefits of maximal exercise just prior to return from weightlessness. *Aviat Space Environ Med* 1987; 58(6):568-72.
 28. Space Shuttle Operational Flight Rules Annex. NSTS Document #18308, 1995. Note: This document is updated every flight; the document listed was effective for STS-72.
 29. Bungo MW, Charles JB, Johnson PC. Cardiovascular deconditioning during space flight and the use of saline as a countermeasure to orthostatic tolerance. *Aviat Space Environ Med* 1985; 56:985-90.
 30. Baisch FAN, Beck LEJ, Blomqvist CG, Karemaker JM. Lower body fluid pooling does not fully explain postflight orthostatic intolerance. In: Sahm PR, Keller MH, Schiewe B, editors. *Scientific Results of the German Spacelab Mission D-2*. Köln, Germany: Deutsche Agentur für Raumfahrtangelegenheiten (DARA); 1994. p 682-7.
 31. Blomqvist CG, Lane LD, Wright SJ, Meny GM, Levine BD, Buckley JC, Peshock RM, Gaffney FA, Watenpaugh DE, Arbeille P, Baisch FA. Cardiovascular regulation at microgravity. In: Sahm PR, Keller MH, Schiewe B, editors. *Scientific Results of the German Spacelab Mission D-2*. Köln, Germany: Deutsche Agentur für Raumfahrtangelegenheiten (DARA); 1994. p 688-90.
 32. Kozlovskaya IB, Kreidich YuV, Rakhmanov AS. Mechanisms of the effects of weightlessness on the motor system of man. *Physiologist* 1981;24(6, Suppl.): S59-S64.
 33. Edgerton VR, Saltin B, Gollnick P. Adaptation of human muscle to short duration space flight. Final Report of detailed supplementary objective #475 to NASA Johnson Space Center. Available from the Space Biomedical Research Institute, NASA JSC, Houston, TX 77058; 1992.

34. Martin TP, Edgerton VR, Grindeland RE. Influence of space flight on rat skeletal muscle. *J Appl Physiol* 1988; 65:2318-25.
35. Miu B, Martin TP, Roy RR, Oganov VS, Ilyina-Kakueva EI, Martin JF, Bodine-Fowler SC, Edgerton VR. Metabolic and morphological properties of single fibers in the rat after space flight: Cosmos 1887. *FASEB J* 1990; 4:64-72.
36. Ohira Y, Jiang B, Roy RR, Oganov VS, Ilyina-Kakueva EI, Martin JF, Edgerton VR. Rat soleus muscle fiber responses to 14 days of space flight and hindlimb suspension. *J Appl Physiol* 1992; 73(2 Suppl):51s-57s.
37. Vogel JM, Whittle MW. Bone mineral changes: the second manned Skylab mission. *Aviat Space Environ Med* 1976; 47:396-400.
38. Stupakov GP, Kazeykin VS, Kozloskiy AP, Korolev VV. Evaluation of changes in human axial skeletal bone structures during long-term space flight. *Kosm Biol Aviakosm Med* 1984; 18:33-7.
39. Oganov VS, Cann C, Rakmanov AS, Ternovoy SK. Computer tomography measurement of vertebral bones and muscles following extended manned space missions. *Kosm Biol Aviakosm Med* 1990; 24:20-22.
40. Schneider VS, LeBlanc AD, Taggart LC. Bone and mineral metabolism. In: Nicogossian AE, Huntoon CL, Pool SL, editors. *Space physiology and medicine*, 3rd ed. Philadelphia: Lea & Febiger; 1994. p 327-33.
41. Vico L, Novikov VE, Very JM, Alexander C. Bone histomorphometric comparison of rat tibial metaphysis after 7-day tail suspension vs. 7-day space flight. *Aviat Space Environ Med* 1991; 62:26-31.
42. Leach CS, Alexander WC, Johnson PC. Endocrine, electrolyte, and fluid volume changes associated with Apollo missions. In: Johnston RS, Dietlein LF, Berry CA, editors. *Biomedical results of Apollo*, NASA SP-368. Washington DC: U.S. Government Printing Office; 1975. p 163-84.
43. Leach CS, Inners LD, Charles JB. Changes in total body water during space flight. In: *Results of Life Sciences DSOs Conducted aboard the Space Shuttle*. Houston: National Aeronautics and Space Administration; 1987.
44. Johnson PD, Driscoll TB, LeBlanc AD. Blood volume changes. In: Johnston RS, Dietlein LF, editors. *Biomedical Results from Skylab*, NASA SP-377. Washington DC: National Aeronautics and Space Administration; 1977. p 235-41.
45. Michel EL, Rummel JA, Sawin CF. Results of Skylab medical experiment M-171, Metabolic activity. In: Johnston RS, Dietlein LF, editors. *Biomedical results of Skylab*, NASA SP-377. Washington DC: National Aeronautics and Space Administration; 1977. p 372-87.
46. Siconolfi SF, Charles JB, Moore AD Jr, Barrows LH. Comparing the effects of two in-flight aerobic exercise protocols on standing heart rates and O_{2peak} before and after space flight. *J Clin Pharmacol* 1994; 34:590-5.
47. Siconolfi SF, Gretebeck RJ, Wong WW. Assessing total body mineral, bone mineral content, and total body protein from total body water and body density. *J Appl Physiol* 1995; 79:1837-43.
48. Siconolfi SF, Gretebeck RJ. The effects of body fluid shifts on single and multi-frequency bioelectrical analyses. *Med Sci Sports Exer* 1994; 26:S202.
49. Siconolfi SF, Gretebeck RJ, Wong WW, Pietrzyk RA, Suire SS. Assessing total body and extracellular water from bioelectrical response spectroscopy. *J Appl Physiol* 1997; 82:704-10.
50. Siconolfi SF. Evaluation of new body-composition techniques in variable gravity. NASA Technical Memorandum 104745. Houston: National Aeronautics and Space Administration; November 1991.
51. Siconolfi SF, Nusynowitz ML, Suire SS, Moore AD Jr, Rogers A. Assessing total blood (TBV), plasma volume (PV), Δ TBV, and Δ PV from bioelectrical response spectroscopy (BERS). *FASEB J* 1994; 8:A15.
52. Thornton WE, Ord J. Physiological mass measurements in Skylab. In: Johnston RS, Dietlein LF, editors. *Biomedical results from Skylab*, NASA SP-377. Washington DC: National Aeronautics and Space Administration; 1977. p 175-83.
53. Lohman TG. *Advances in body composition assessment*. Champaign, IL: Human Kinetics Publishers; 1992. p 7-23.
54. Perry RH, editor. *Engineering manual: A practical reference of data and methods in architectural, chemical, civil, electrical, mechanical, and nuclear engineering*. 2nd ed. New York: McGraw-Hill; 1959. p 7-6 to 7-11.
55. Deurenberg P, Schouten FJM, Andreoli A, deLorenzo A. Assessment of changes in extra-cellular water and total body water using multi-frequency bioelectrical impedance. In: Ellis KJ, Eastman JD, editors. *Human body composition: in vivo methods, models, and assessments*. Basic Life Sciences Volume 60. New York: Plenum Press; 1993. p 129-32.
56. Kushner RF, Schoeller DA. Estimation of total body water by bioelectrical impedance analysis. *Am J Clin Nutr* 1986; 44:417-24.

57. Lukaski HC, Bolonchuk WW. Estimation of body fluid volumes using tetrapolar bioelectrical impedance measurements. *Aviat Space Envir Med* 1988; 59:1163-9.
58. Schoeller DA, Ravussin E, Schutz Y, Acheson KJ, Baertschi P, Jequier E. Energy expenditure by doubly-labeled water: validation in humans and proposed calculations. *Am J Physiol* 1986; 250:R823-30.
59. Schoeller DA, Kushner RF. Determination of body fluids by the impedance technique. *IEEE Engin Med Biol Mar* 1989; 19-21.
60. Segal KR, Burastero S, Chun A, Coronel P, Pierson RN Jr, Wang J. Estimation of extracellular and total body water by multiple-frequency bioelectrical-impedance measurement. *Am J Clin Nutr* 1991; 54:26-9.
61. Van Loan MD, Maycline PL. Use of multi-frequency bioelectrical impedance analysis for the estimation of extracellular fluid. *Eur J Clin Nutr* 1992; 46:117-24.
62. Nusynowitz ML, Blumhardt R. Estimation of true red cell volume from RISA red cell volume. *Am J Roentgen* 1974; 120:549-52.
63. Nusynowitz ML, Blumhardt R, Volpe J. Plasma volume in erythremic states. *Am J Med Sciences* 1974; 267:31-4.
64. Nusynowitz ML, Strader WJ, Waliszewski JA. Predictability of red cell volume from RISA blood volume. *Am J Roentgen* 1970; 109:829-32.
65. Thomsen JK, Fogh-Andersen N, Bulow K, Devantier A. Blood and plasma volumes determined by carbon monoxide gas, 99m TC-labeled erythrocytes, 125I-albumin and the T 1824 technique. *Scand J Clin Lab Invest* 1991; 51:185-90.
66. Lawson HC, Overby DT, Moore JC, Shadle OW. Mixing of cells, plasma and dye T-1824 in the cardiovascular system of barbitalized dogs. *Am J Physiol* 1947; 151:282-9.
67. Leach CS, Rambaut PC. Biochemical responses in the Skylab crewmen: An overview. In: Johnston RS, Dietlein LF, editors. *Biomedical Results from Skylab, NASA SP-377*. Washington DC: National Aeronautics and Space Administration; 1977. p 204-16.
68. Jaweed MM. Muscle structure and function. In: Nicogossian AE, Huntoon CL, Pool SL, editors. *Space physiology and medicine*. 3rd ed. Philadelphia: Lea & Febiger; 1994. p 320-6.

Section 4

Environmental Health

EXTENDED DURATION ORBITER MEDICAL PROJECT

Environmental Health

*Duane Pierson, John James, Dane Russo, Thomas Limero, Steve Beck,
and Theron Groves, Medical Sciences Division,
Johnson Space Center, Houston, TX*

BACKGROUND

The Environmental Health activity for the Extended Duration Orbiter Medical Project (EDOMP) was formed to develop an overall strategy for safeguarding crew members from potential airborne hazards anticipated on missions of extended duration. These efforts were necessary because of major modifications to the air revitalization system of the U.S. Space Shuttle and an increased potential for environmental health risks associated with longer space flights.

Degradation of air quality in the Shuttle during a space flight mission has the potential to affect the performance of the crew not only during piloting, landing, or egress, but also during space flight. It was anticipated that the risk of significant deterioration in air quality would increase with extended mission lengths and could result from: (1) a major chemical contamination incident, such as a thermodegradation event or toxic leak, (2) continual accumulation of volatile organic compounds to unacceptable levels, (3) excessive levels of airborne particles, (4) excessive levels of microorganisms, or (5) accumulation of airborne pathogens.

CRITICAL QUESTIONS

The critical questions addressed by the EDOMP Environmental Health activity were: (1) Do the concentrations of particulate and chemical pollutants, or airborne bacteria and fungi, accumulate to unacceptable levels during long duration flights? Do the levels increase continuously as a function of mission duration, or are stable levels reached after a few days of space flight? (2) Do changes in the population dynamics of microorganisms occur as the mission proceeds, resulting in changes in bacterial and fungal species present in the air and on surfaces? (3) What chemical pollutants should be monitored as a result of a contingency event, such as an accidental release of a pollutant from an experiment or a fluid system, or from overheating of onboard electronics? (4) What are the appropriate crew member exposure limits to chemical pollutants for long duration (up to

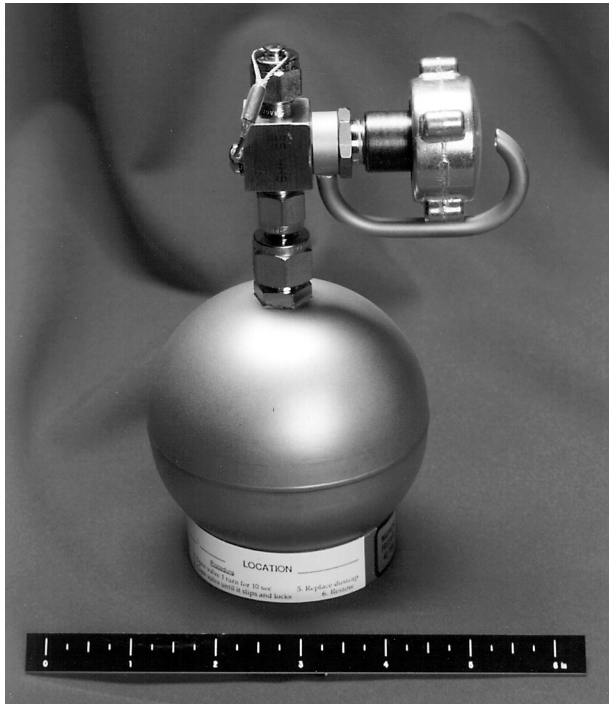
30 days) Shuttle flights? (5) What are the best air sampling techniques for monitoring particulates, chemical pollutants, and microorganisms in the Shuttle during long duration space flights?

Originally, the EDOMP was conceived to focus on 28-day orbital missions. Later, when the focus was reduced to flights of 16 days, the criticality of the questions listed above diminished. However, each remained important because of the potential for the space craft environment to affect crew health in subtle ways.

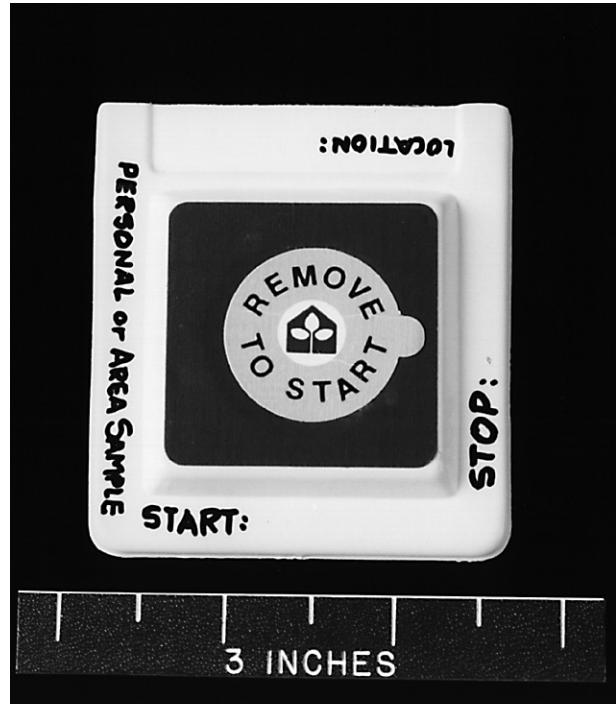
APPROACH

The EDOMP Environmental Health activity was conducted as three investigations explained below. Each was conducted as a Detailed Supplementary Objective (DSO). DSO 471 was conducted on two Shuttle missions to characterize respirable airborne particulate matter in the Shuttle atmosphere. DSO 488 was conducted on one Shuttle flight to measure formaldehyde, using passive dosimetry. DSO 611 was conducted on nine Shuttle flights to evaluate innovative air monitoring instrumentation and to characterize the Shuttle atmosphere. Principal investigators for these studies were: DSO 471, Dane Russo; DSO 488, John James; and DSO 611, Duane Pierson.

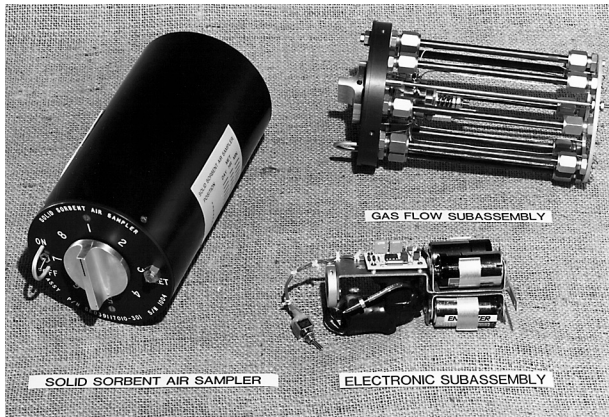
The accumulation of chemical pollutants was evaluated by sampling air contaminants periodically during each extended flight and determining whether concentrations were increasing with time. Instantaneous samples were obtained with grab sample containers (GSC). Each GSC was used to collect a 0.35 liter air sample (Figure 4-1a). Time integrated samples were obtained with the Solid Sorbent Air Sampler (SSAS). The SSAS method employed a concentration technique, whereby volatile organic compounds from larger volumes (1 to 2 liters) of air were trapped onto the sorbent resin (Figure 4-1b). Therefore, the SSAS provided greater sensitivity for specific pollutants. On the other hand, the GSC could trap volatile contaminants that were poorly adsorbed on the SSAS. Consequently, these methods complemented each other.



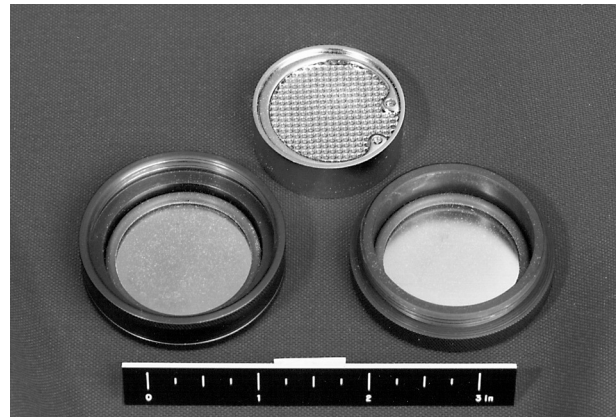
a. Grab Sample Container (GSC)



c. Formaldehyde Monitor



b. Solid Sorbent Air Sampler (SSAS)



d. Archival Organic Sampler (AOS)

Figure 4-1. Air sampling devices.

Formaldehyde, an important pollutant for measurement, was not quantified well by either method. Therefore, a badge specific for trapping formaldehyde was developed for use in the Shuttle. This badge formed the basis for a Formaldehyde Monitoring Kit (FMK), developed for this investigation. A single monitor is pictured in Figure 4-1c. An archival organic sampler (AOS) was developed to provide a lightweight, passive device capable of obtaining a time integrated sample of volatile organic air pollutants (Figure 4-1d).

The question of the concentration, composition, and size distribution of airborne particles led to the

development of two instruments by the Particle Technology Laboratory at the University of Minnesota [1]. These instruments were the Shuttle Particle Sampler (SPS) and Shuttle Particle Monitor (SPM). Two SPSs and one SPM were flown on each of two Space Transportation System (STS) missions, STS 32 and STS 40. Each SPS employed a multistage impactor and filtering system to separate and trap particles, over a 24-hour sampling period, into fractions of $<2.5 \mu\text{m}$, 2.5 to $10 \mu\text{m}$, 10 to $100 \mu\text{m}$, and $>100 \mu\text{m}$. After the devices were returned to the laboratory, the particulate mass in each size range was determined gravimetrically, and the elemental



e. Combustion Products Analyzer (CPA)

Figure 4-1. Continued.

composition of the two smaller particle fractions was determined by X-ray fluorescence. The SPM provided a real time, in situ measurement of particulate concentration by nephelometry, employing photometric detection of light scatter. The instruments complemented each other because the SPS facilitated size distribution studies averaged over time, and the SPM facilitated measurement of temporal changes in particle concentrations, but recorded only particles of less than 100 μm and was blind to the size distribution.

Technologies currently available for sampling airborne microorganisms were assessed in ground based tests of office buildings. Off-the-shelf air samplers were evaluated for technical performance and compatibility with space flight applications. Following extensive ground based testing [2], the candidate samplers were flight certified and flight tested aboard the Shuttle. Air samples were collected with Microbial Air Samplers (MAS) from the middeck, flight deck, and in the Spacelab (when present) two days before launch and at least three times during flight. The goal was to collect two samples, one each for bacteria and fungi, at the three locations in the Shuttle/Spacelab every other day during

the mission. The microbial contaminants in the air were collected and allowed to grow during the mission, and returned to the laboratory at the Johnson Space Center (JSC), where each bacterial and fungal species was identified and quantified. This approach provided the needed information to assess the levels and species of airborne bacteria and fungi as a function of time in orbit.

The risk associated with accidental chemical releases was addressed by the development of a Combustion Products Analyzer (CPA) shown in Figure 4-1e. Experience with nominal Shuttle flights has shown that the greatest threat to air quality comes from accidents involving over-heating or pyrolysis of electronic components [3]. The CPA was designed to quantify carbon monoxide (CO), hydrogen fluoride (HF), hydrogen chloride (HCl), and hydrogen cyanide (HCN) at concentrations that could pose a threat to crew member health after thermodegradation of electronic components. The CPA was jointly developed by the Space and Life Sciences Directorate and the Shuttle Program Office at JSC.

The need for long term spacecraft maximum allowable concentrations (SMACs) was addressed by placing the 30-day EDOMP effort into an activity already

underway to set 180-day SMACs for the International Space Station (ISS). Air pollutants were prioritized, and documentation of the limits was prepared by JSC toxicologists. Each document and SMAC was reviewed and approved by the National Research Council's Committee on Toxicology (NRCCOT).

METHODS

Investigations Using Existing Hardware

Solid Sorbent Air Sampler (SSAS)

The SSAS consisted of eight tubes filled with approximately 0.5 gm Tenax adsorbent through which air could be pumped at rates that permitted sampling of volumes from 0.5 liters to 2.0 liters in 24 hours. Preparations before flight included thermal cleaning and proof testing of each tube, using a gas chromatograph/mass spectrometer (GC/MS) to verify that no pollutants remained trapped on the sorbent. The rate of air flow through each tube was measured with a bubble flow meter. During flight, a crew member turned on the device and set the selector knob to one of the sorbent tube positions. A sample was normally taken for 24 hours and the device returned to the park position and turned off. The cycle could be repeated once for each of the seven available tubes in the SSAS. After the flight, each tube was thermally desorbed, and the released contaminants were quantified using GC/MS. The air flow through each tube was measured again to confirm that it had not changed significantly during the flight. Specific procedures evolved during the EDOMP. Details of the latest method were documented by the JSC Toxicology Laboratory [4].

Grab Sample Containers (GSC)

Grab sample containers were flown on all Extended Duration Orbiter (EDO) flights and used primarily to obtain instantaneous samples near the end of a mission. The canisters, SUMMA®-treated to minimize wall effects, were originally cylindrical, but were replaced during the EDOMP with spherical canisters of 0.35 liter volume. Before flight, these canisters were thoroughly evacuated, cleaned, and proofed using the GC/MS. During flight, a crew member opened the valve so that spacecraft air could enter the GSC until a pressure equilibrium occurred. The valve was then closed and the sample stowed and returned to the JSC Toxicology Laboratory for analysis. Analytical procedures included GC/MS and a separate GC procedure to quantify highly volatile compounds including methane (CH₄), carbon monoxide (CO), and hydrogen (H₂). Specific details of the procedure changed during the EDOMP. The latest procedures are illustrated in NASA standard operating procedures [5, 6].

Investigations Requiring Equipment Development

Shuttle Particle Monitor (SPM)

The SPM was flown on STS-32 and STS-40. Minor modifications were made between the flights to eliminate the need for continuous battery power to the data logger and to improve the resolution and detection limits. The minimum, maximum, and average particle concentrations were recorded continuously in 15-minute intervals during the operational time in flight. Preflight and postflight checks of the instrument zero confirmed that it did not drift during the handling and flight process. During flight and before deployment, the instrument was subjected to a zero set procedure involving its response to clean air delivered from a zero module system. The SPM was calibrated by calculating its average voltage response during the period when it was operated alongside the SPS, and comparing this SPM voltage to the mass of particles found in all size ranges in the SPS.

Shuttle Particle Sampler (SPS)

Two SPSs were flown on STS-32 and STS-40. The SPSs obtained particle samples in four size ranges over sampling periods of approximately 24 hours each. During postflight analyses, the largest particles were vacuumed from the 100 µm inlet filter onto a weighed filter, and the remaining three fractions were trapped directly on filters inside the sampler. The weight differences before and after particle loading determined the mass of each particulate fraction. Elemental analysis in the range of 11 to 82 atomic mass units (amu) was performed on the two smallest particle collections by x-ray fluorescence (XRF), a nondestructive method. Individual particles in the two largest particulate fractions were assessed by scanning electron microscopy (SEM) for morphology and elemental composition by energy dispersive spectroscopy. Both of these latter two methods were destructive.

Combustion Products Analyzer (CPA)

The CPA, flown on every Shuttle flight since late 1989, consisted of four electrochemical sensors designed to measure HCl, HF, HCN, and CO in the event of a combustion problem during a mission. A comprehensive evaluation of the CPA was performed at the White Sands Test Facility before flight tests. This evaluation involved exposure of the CPA to thermodegradation products from selected materials used in the Shuttle, including wiring insulation, polyurethane foam insulation, circuit boards, and materials containing polyvinyl chloride. Before flight, each of the sensors was zeroed and calibrated in a dynamic flow chamber. During flight, crew members took daily readings to account for any baseline drift in the sensors. This was especially important for the CO sensor which responded to hydrogen as it accumulated in the spacecraft



f. Reuter Centrifugal Sampler (RCS)

Figure 4-1. Continued.

air. In the event of a suspected combustion problem, flight rules indicated the use of the CPA in conjunction with other criteria to assess whether the atmosphere posed a risk to crew member health. After flight, the instrument was evaluated to determine the stability of the zero and calibration settings.

Formaldehyde Monitor Kit (FMK)

Formaldehyde was not detected by any of the methods described above unless it was at extremely high concentrations. The 30-day SMAC limit for formaldehyde was set at 0.05 mg/m³ based on its irritant properties. After assessing several methods, it was found that a badge made by Air Quality Research (Durham, NC) could detect airborne formaldehyde at concentrations below the SMAC limit if sample times were at least 8 hours. Before flight, monitors from a specific lot were evaluated for their formaldehyde uptake rate and for satisfactory background (blank) levels. During flight, a crew member removed a seal and either placed the badge in an area of the spacecraft with adequate air flow, or wore the badge during waking hours. At the end of the sampling period, the sampling orifice was resealed and the device stowed for return

to the JSC laboratory. Formaldehyde trapped by the badge, and in appropriate controls, was quantified by the Chromotropic Acid Procedure [7].

Archival Organic Sampler (AOS)

An effort was undertaken to develop, evaluate, and test during flight, a small, lightweight passive sampler for the collection of volatile organic contaminants (VOC). The utility of the AOS was its simplicity and ability to be used as a personal monitor or placed at various locations within a spacecraft for spatial variation studies. Ground based and flight tests were conducted to compare results obtained by the AOS and the SSAS [2].

Microbial Air Sampler (MAS)

From ground based evaluations of microbial air samplers [2], emerged three instruments that were the most promising candidates for use in the Shuttle. These three air samplers were: (1) a Reuter Centrifugal Sampler (RCS) (Figure 4-1f), (2) an RCS Plus (Biotest Diagnostics Corp., Denville, NJ) (Figure 4-1g), and (3) the Burkard air sampler (Burkard Manufacturing Co., Ltd., Rickmansworth, Hertfordshire, U.K.) (Figure 4-1h). All



g. Reuter Centrifugal Sampler Plus (RCS Plus)



h. Burkhard Air Sampler

Figure 4-1. Concluded.

three air samplers were small, portable, and battery powered. The RCS and RCS Plus were centrifugal impactors in which airborne microbes impacted onto a growth medium contained in 34 plastic wells on a plastic strip. The Burkhard air sampler used an impactor with 100 holes of 1 mm diameter and a 90 cm Petri dish to collect airborne microorganisms. In addition to rigorous ground based testing, each of these samplers was used in flight on one or more EDO missions.

Air sample locations in flight consisted of the flight deck and middeck of the Shuttle, and in the Spacelab, when present, in the payload bay. Each air sampler used was set to collect 100 liters of air. Air sampling was scheduled every other day during the mission at a low activity time to minimize disturbance of airborne particulate and microbe levels. In all air samplers, trypticase soy agar was used for growth of bacteria, and rose bengal agar was used to culture fungi. Sample strips, or Petri plates in the case of the Burkard sampler, were incubated at ambient temperature on the middeck of the crew compartment for 2 to 13 days until return to Earth for analysis. Upon receipt of the samples in the laboratory, the bacterial and fungal colonies were quantified and subcultured for identification procedures. Bacterial isolates were subcultured on trypticase soy agar, and fungal isolates were subcultured on Sabouraud's agar. Identification of the bacterial isolates was completed using the Vitek AutoMicrobic System (BioMerieux, France) or the Biolog Automated System (Biolog Inc., Hayward, CA).

Surface sampling for microorganisms was also conducted before and after EDO missions because bacteria and fungi recovered from surfaces reflected the microbial content of the air. Calcium alginate swabs were used to sample 10 to 15 selected surfaces in the crew compartment of the Shuttle and the Spacelab. Each swab, moistened with phosphate buffered saline, was used to sample a 25 cm² area, then placed into a tube containing 2 ml of trypticase soy broth for return to the JSC laboratory where it was analyzed for bacteria and fungi.

Setting 30-day Spacecraft Maximum Allowable Concentration (SMAC) Values

For a given compound, the process used to set exposure limits for long missions, including EDO flights, started with a search of the toxicological literature for all data available on the inhalation toxicity of that compound. If inhalation data were lacking, information from noninhalation routes of exposure and from structurally similar compounds was used. The resulting information was assembled and the most important studies reviewed for quality and completeness. A document reviewing the literature and providing explicit rationale for each SMAC limit was prepared, based on guidelines provided by the NRCCOT. The rationale included methods for species extrapolation, time extrapolation, cancer modeling, pharmacokinetics, and other factors for the effects of spaceflight on susceptibility to chemical toxicity. Each document was reviewed by members of the NRCCOT and the supporting rationale was presented at a meeting of the NRCCOT. Changes were made, as appropriate, prior to publication by the NRCCOT. These limits were used to assess the air quality during EDO flights according to published methods [8].

RESULTS AND DISCUSSION

Accumulation of Chemical Air Pollutants

Data collected during the EDOMP indicate that VOCs in the cabin atmosphere were generally below their SMAC limits. Moreover, the data clearly indicate that most pollutants reached an equilibrium concentration within the first few days of a mission. Exceptions to this were hydrogen, methane, and dichloromethane. Of these three, only dichloromethane, with a 30-day SMAC of 20 mg/m³, has significant toxic properties. Data from STS-40, 42, 45, and 49 show accumulations of up to 0.79 mg/m³ in missions of 2 weeks or less (Table 4-1). In view of the 30-day SMAC of 20 mg/m³, this accumulation is of no concern for missions of less than one month.

There is no evidence at this time that nominal levels of VOCs typically seen in the cabin air during extended duration missions are detrimental to crew members. However, a VOC of particular concern was formaldehyde, found to be present in spacecraft air at concentrations above the 30-day SMAC limit of 0.05 mg/m³ for each of the three EDO missions in which the monitors were flown (Table 4-2).

It was hoped that sampling of VOCs could be simplified by application of a passive device. However, pilot studies with the AOS indicated that results were not comparable to those obtained with the SSAS [2]. The Teflon seals used in the AOS were found to be inadequate, resulting in contamination during unexposed periods. This contamination was significant, and alternate sealing materials were studied. Ultimately it was determined that leakage around the seals could only be prevented by a total redesign. This effort was discontinued.

Assessment of Particulate Air Pollutants

The total mass of particles averaged 56 mg/m³ on STS-32 and 35 mg/m³ on STS-40 (Table 4-3). In neither mission was there a temporal increase in the particulate concentration. As expected, the size distribution showed a strong enrichment in the heavier particles that did not settle out of the spacecraft atmosphere. Elemental analysis suggested that most of the particles were organic in origin [1], which is reasonable given the high density of human occupation of the spacecraft.

Assessment of Accidental Chemical Releases

Although accidental air contamination problems originated from a variety of sources, the dominant source was thermodegradation of electronic devices (Table 4-4). Burning of electronic circuits or wiring could have serious effects on air quality because of the toxic fumes generated from pyrolysis of materials such as Teflon, Kapton, and epoxy resin. Of the nine toxicological incidents occurring from STS-35 to STS-55, four were the

Table 4-1. Accumulation of dichloromethane in spacecraft air (mg/m³)

STS Mission	SSAS Sample Number						
	1	2	3	4	5	6	7
40	0.09	0.10	0.14	0.13	0.17	—	0.32
42	0.32	0.40	0.44	0.46	0.56	0.50	0.70
45	0.27	0.49	0.51	0.60	0.71	—	—
49	0.17	0.53	0.79	0.75	0.65	0.71	0.56

Table 4-2. Formaldehyde concentrations in spacecraft air (mg/m³)

STS Mission	Type of sample	Range of Concentrations
56	area	0.037 - 0.065
	personal	0.048 - 0.056
59	area	0.049 - 0.072
	personal	0.056 - 0.080
67	area	0.033 - 0.039
	personal	0.042 - 0.074

Table 4-3. Particle masses from the SPS on STS-32 and STS-40

Particle Size (μm)	Mass Concentration (μg/m ³)		Normalized percent	
	STS-32	STS-40	STS-32	STS-40
<2.5	2	2	4	7
2.5 to 10	19	5	33	13
10 to 100	5	3	10	9
>100	30	25	53	71
Totals	56	35	100	100

result of electronic burns. These incidents are summarized in a report by J. T. James *et al.* [3]. The need for real-time monitoring of critical combustion products was established several years ago as evidenced by the aforementioned incidents. This need culminated in the development of the Combustion Products Analyzer that has flown on every Shuttle mission since October 1989.

Table 4-4. Air contamination incidents in the space shuttle

STS Mission	Contamination Concern	Analytical Results
28	Teleprinter cable short	SSAS sample showed nothing unusual
31	High benzene in preflight sample	Benzene, found at 0.5 mg/m ³ in preflight sample, was scrubbed down to 0.01 mg/m ³ late in mission
35	Odor of burning electronics near the data display units (2 failures)	SSB sample showed 0.01 mg/m ³ benzene, which was later reproduced from ground pyrolysis of identical electronic components
37	Odors in galley area	SSB showed no unusual contaminants
40	Noxious odors from refrigerator/freezer	SSB sample showed no clear evidence of contamination. Ground studies of burned motor showed released ammonia and formaldehyde
49	Odor from airlock after EVA	Acetaldehyde (0.6 mg/m ³) was unusually high in SSB sample
50	Burning odor near American Echo Research Imager	SSB sample showed unusually high concentration of dichloromethane
53	Crew experienced nasal congestion possibly due to air contaminant	No unusual contaminants found in SSB sample
54	Odors in area of waste control system	Two incompletely identified organic compounds were found
55	Noxious odors from contingency waste container	Three dimethyl sulfides found at concentrations that would produce a noxious odor

Microbial Contamination

Air samples were collected during the flight phase of 14 Shuttle flights. The mission duration ranged from 5 days to 16 days, with four different Shuttle vehicles being used in the study. Quantification results of airborne bacteria and fungi recovered during four different missions (STS-42,

47, 58, and 65) are shown in Figure 4-2. In general, bacterial levels increased moderately as the mission proceeded, whereas the fungal levels tended to decrease. Bacterial levels ranged from a few hundred colony forming units per cubic meter of air (CFU/m³) early in the mission to more than 1000 CFU/m³ in the final days of the STS-47 and 58 missions. The fungi ranged from undetectable levels, usually late in the mission, to a few hundred CFU/m³ in samples taken early in the mission.

The identities of bacteria and fungi recovered from the air samples are shown in Figure 4-3. Fifteen species or groups of bacteria were recovered from the samples collected during flight. It is probable that many of the bacterial genera were of human origin. Bacteria commonly found in the gastrointestinal tract (*Enterococcus faecalis*) and the respiratory tract (*Klebsiella pneumoniae*) were recovered during some missions. *Staphylococcus* spp., *Micrococcus* spp., *Enterobacter* spp., and *Bacillus* spp. were recovered from the air in the crew compartment during more than 85% of the missions. *Staphylococcus aureus* was recovered during 57% of the missions. Even though fungal levels were generally low, *Aspergillus* spp. and *Penicillium* spp. were recovered in 60% or greater of the missions. Eleven other species or groups of fungi were recovered one or more times.

The results of bacteria recovered from 10 surface sites in the crew compartment, during each of 13 space flight missions, are shown in Figure 4-4a. Again, those typically associated with humans were among the most common bacteria isolated from Shuttle surfaces. In examining the data from more than 70 missions, 40% of the surface sampling sites exhibited a tenfold or more increase during the mission [9]. The results of fungi isolated from the same 10 surface sites during the same 13 space flight missions are shown in Figure 4-4b. As in the air, *Aspergillus* spp. and *Penicillium* spp. were the most common genera found on interior surfaces. Unlike bacteria, fungi were not as commonly found on surfaces and rarely exhibited increased numbers during the mission. Pierson *et al.* [9, 10] have previously reported using DNA fingerprinting technology, such as restriction fragment length polymorphism (RFLP) analysis and repeated sequence polymerase chain reaction (PCR), to demonstrate transmission of *Staphylococcus aureus* and *Candida albicans* between Shuttle crew members. DNA fingerprinting may also be used to assess the dissemination of microbes throughout the internal environment.

Setting 30-day Chemical Spacecraft Maximum Allowable Concentration (SMAC) Values

As part of the EDOMP, approximately fifty 30-day SMACs were set and documented by JSC toxicologists in cooperation with the NRCCOT. In many cases new data and methods of risk analysis led to 30-day SMACs that were far below existing 7-day SMACs (Table 4-5).

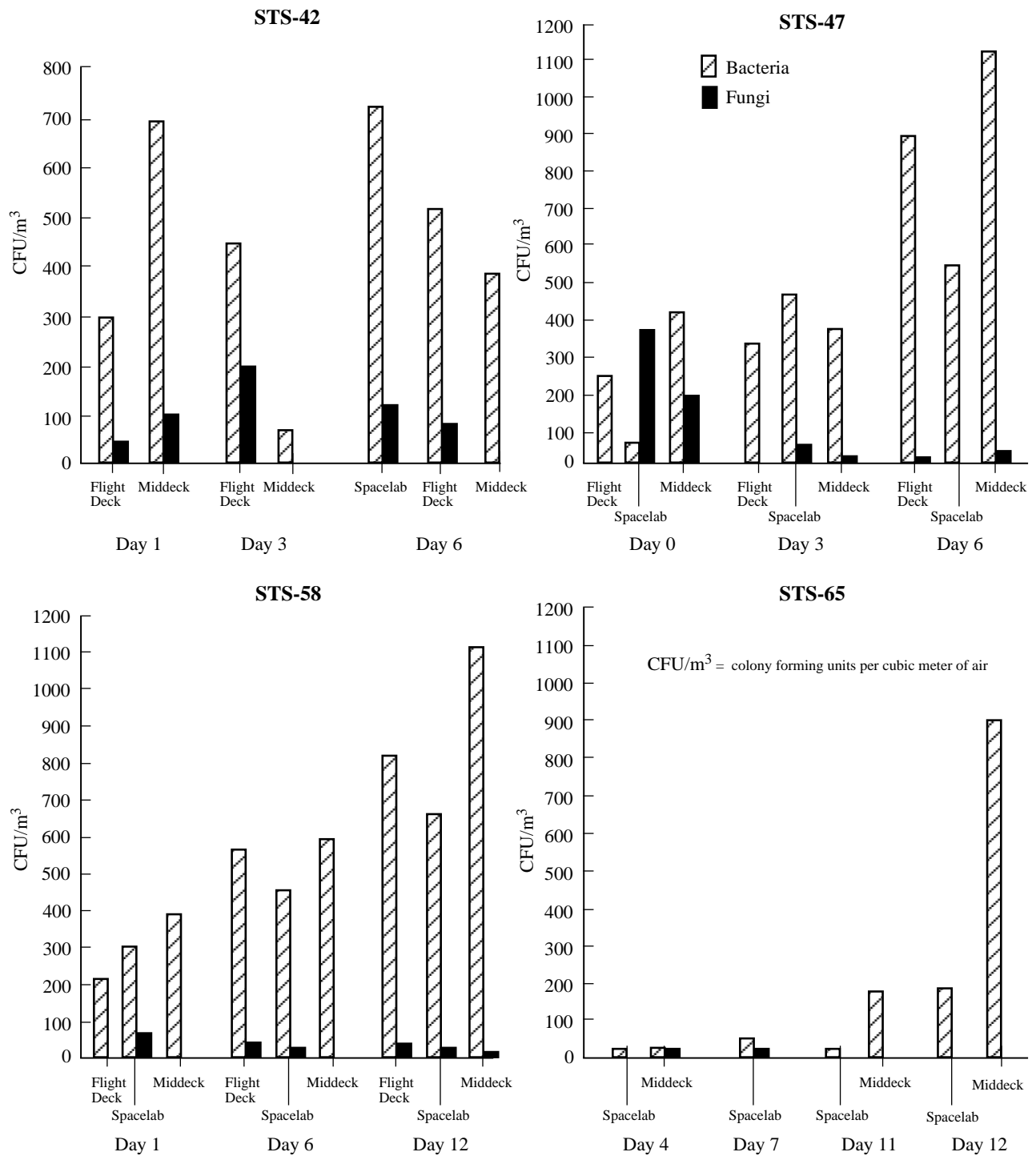


Figure 4-2. Microbial quantitation of spacecraft air.

COUNTERMEASURES/ POTENTIAL COUNTERMEASURES

Chemical Contaminant Countermeasures

The major finding from the EDOMP chemical contamination study was that formaldehyde concentrations

exceeded the SMAC limit for 30 days of exposure. The sources of formaldehyde were thought to be a small contribution from crew metabolism and a major contribution from equipment off-gassing. To reduce the latter contribution, a method was implemented to detect formaldehyde during hardware off-gas acceptance testing. With that method, formaldehyde was quantified in gaseous samples

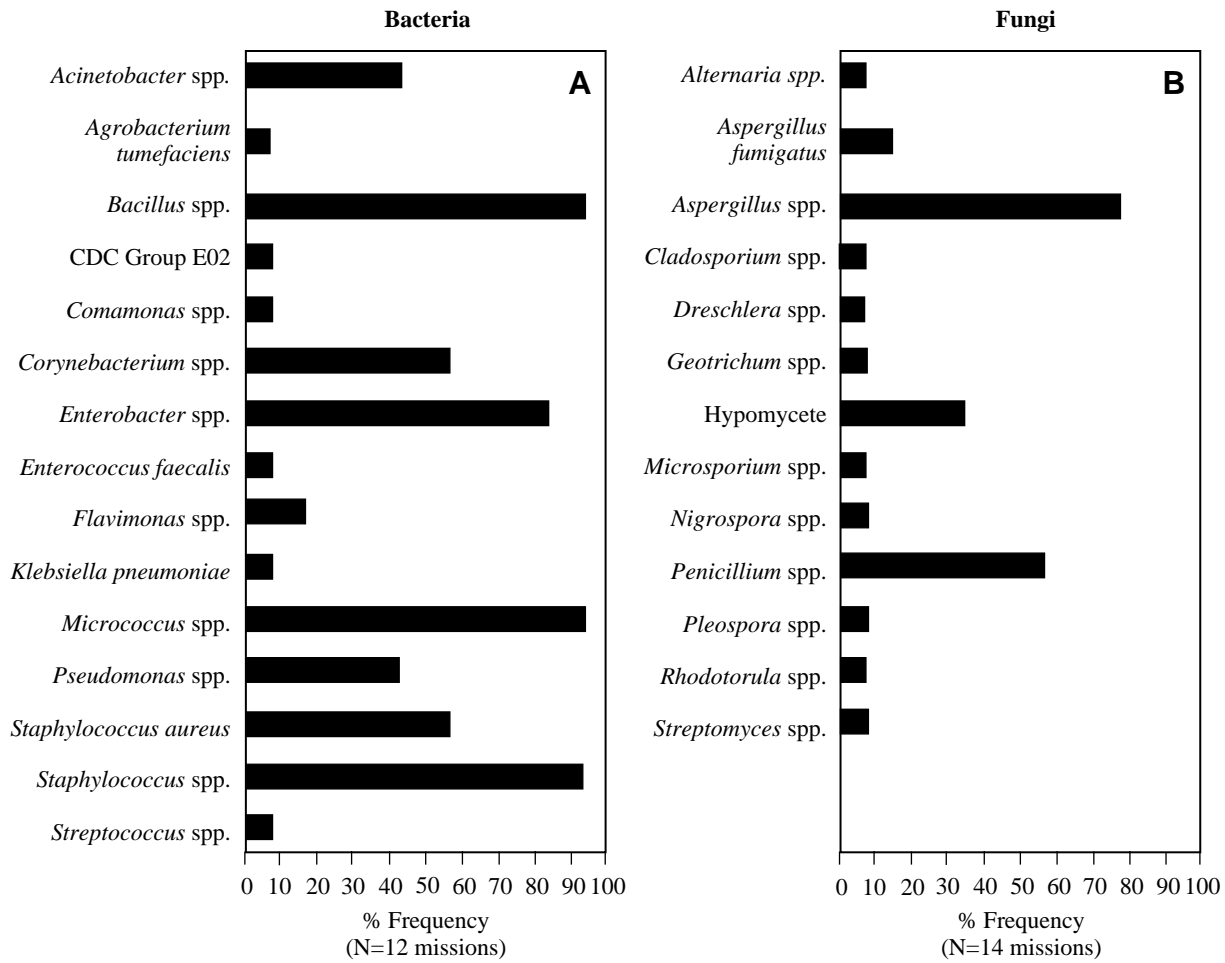


Figure 4-3. Microorganisms isolated from inflight air samples.

by Fourier Transform infrared spectroscopy (FTIR) at a wavelength of 3.45 μm . Since adding this method to the standard off-gas test procedure, several items of flight equipment have been rejected based on high releases of formaldehyde during the test. Results from CPA measurements following a thermodegradation incident could provide useful real-time data to the crew and entire incident management team. A new flight rule, which includes the use of CPA readings, has been written to aid in the management of a thermodegradation incident.

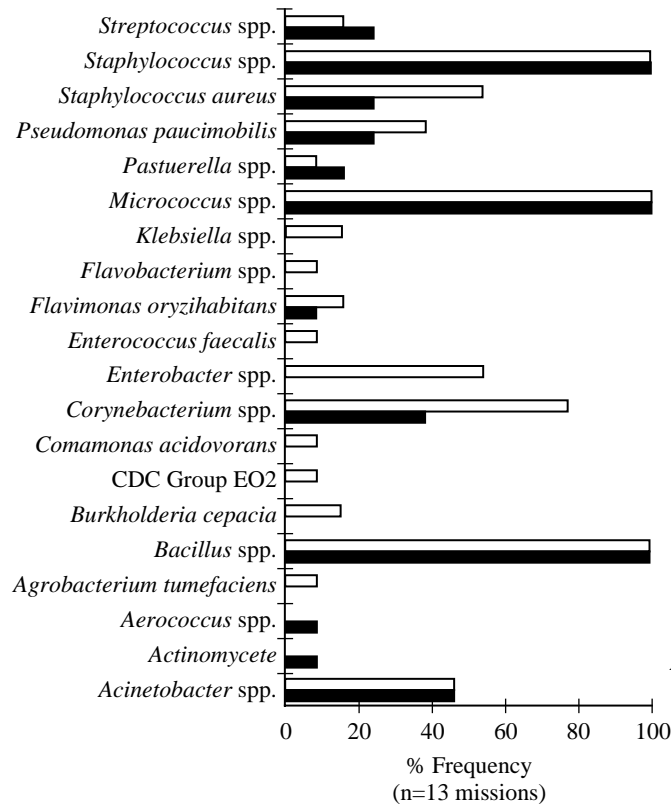
Microbial Countermeasures

Airborne bacterial levels tended to increase and fungal levels tended to decrease as the mission proceeded. Not uncommonly, the levels of airborne bacteria exceeded the ISS acceptability limit of 1000 CFU/m³. The fungal levels were routinely low, but occasionally fungi also exceeded the ISS acceptability limit. The planned environmental control system for ISS incorporates microbial air filters, with 99.97% retention of particulates 0.3 μm and larger, to ensure biologically safe

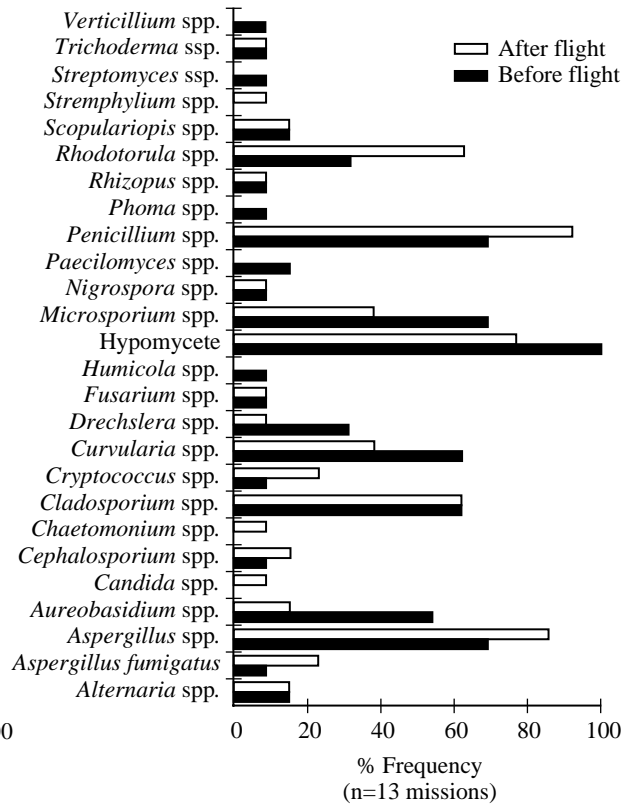
air. The Shuttle environmental control system employed stainless steel mesh that allowed particulates smaller than 70 μm in diameter to pass through. Bacteria and fungal spores range from less than 1 μm to as much as 10 μm

Table 4-5. Decreases in selected SMAC values for the EDOMP

Compound	Previous 7-day SMAC (mg/m ³)	New 30-day SMAC (mg/m ³)
acetaldehyde	84	4
acetone	700	50
carbon monoxide	30	10
1,2-dichloroethane	40	2
ethylene glycol	130	13
methanol	50	9
methyl ethyl ketone	60	30
dichloromethane	90	20



a. Bacteria isolated from ten U.S. Space Shuttle surface sites



b. Fungi isolated from ten U.S. Space Shuttle surface sites

Figure 4-4.

in diameter. Whereas many were entrapped in the stainless steel mesh, some microbes were clearly small enough to pass through the filtration system. The addition of microbial filtration material could easily be incorporated into a filter configuration that would remove greater than 90% of airborne bacteria, fungi, particulates, dust mite antigen, pollen, and other allergens. Clearly, such modification to the air filtration system on the Shuttle would greatly improve the biological air quality in the crew compartment.

REFERENCES

1. Liu BY et al. Airborne particle measurement in the space shuttle. JSC-26786 Space Life Sciences;1: 5-7 through 5-29. Houston, TX: National Aeronautics and Space Administration; 1994.
2. Mehta SK, Mishra SK, Pierson DL. Evaluation of three portable samplers for monitoring airborne fungi. Appl Environ Microbiol 1996; 62(5):1835-8.
3. James JT et al. Volatile organic contaminants found in the habitable environment of the space shuttle: STS-26 to STS-55. Aviat Space Environ Med 1994; 65:851-7.
4. JSC Toxicology Laboratory standard operating procedure F1 - Measurements of VOCs in Spacecraft Air Using the SSAS, 1995. Located at JSC Toxicology Laboratory.
5. JSC Toxicology Laboratory standard operating procedure F2 - Measurement of VOCs in Spacecraft Air Using Grab Sample Containers, 1995. Located at JSC Toxicology Laboratory.
6. JSC Toxicology Laboratory standard operating procedure F3 - Gas Chromatography Analysis of Methane, Hydrogen, and Carbon Monoxide in Spacecraft Air Collected in GSCs, 1995. Located at JSC Toxicology Laboratory.
7. JSC Toxicology Laboratory standard operating procedure F5 - Measurement of Formaldehyde in

- Spacecraft Air Using Passive Monitors, 1995. Located at JSC Toxicology Laboratory.
8. James JT. JSC 20584 Spacecraft maximum allowable concentrations for airborne contaminants. Houston: JSC Printing Office; 1995.
 9. Pierson DL, Mehta SK, Magee RR, Mishra SK. Person-to-person transfer of *Candida albicans* in the space environment. J Med & Vet Mycol 1994; 33: 145-50.
 10. Pierson DL, Chidambarum M, Heath JD, Mallery L, Mishra SK, Sharma B, Weinstock GM. Epidemiology of *Staphylococcus aureus* during space flight. FEMS Imm & Med Micro 1996; 16:273-281.

Section 5.1

Neurovestibular Dysfunction

Neuroscience Investigations An Overview of Studies Conducted

*Millard F. Reschke
Johnson Space Center
Houston, TX*

INTRODUCTION

The neural processes that mediate human spatial orientation and adaptive changes occurring in response to the sensory rearrangement encountered during orbital flight are primarily studied through second and third order responses. In the Extended Duration Orbiter Medical Project (EDOMP) neuroscience investigations, the following were measured: (1) eye movements during acquisition of either static or moving visual targets, (2) postural and locomotor responses provoked by unexpected movement of the support surface, changes in the interaction of visual, proprioceptive, and vestibular information, changes in the major postural muscles via descending pathways, or changes in locomotor pathways, and (3) verbal reports of perceived self-orientation and self-motion which enhance and complement conclusions drawn from the analysis of oculomotor, postural, and locomotor responses.

In spaceflight operations, spatial orientation can be defined as situational awareness, where crew member perception of attitude, position, or motion of the spacecraft or other objects in three-dimensional space, including orientation of one's own body, is congruent with actual physical events.

Perception of spatial orientation is determined by integrating information from several sensory modalities (Figure 5-1). This involves higher levels of processing within the central nervous system that control eye movements, locomotion, and stable posture. Spaceflight operational problems occur when responses to the incorrectly perceived spatial orientation are compensatory in nature. Neuroscience investigations were conducted in conjunction with U. S. Space Shuttle flights to evaluate possible changes in the ability of an astronaut to land the Shuttle or effectively perform an emergency post-landing egress following microgravity adaptation during space flights of variable length. While the results of various sensory motor and spatial orientation tests could have an impact on future space flights, our knowledge of sensorimotor adaptation to spaceflight is limited, and the future application of effective countermeasures depends, in large part, on the results from appropriate neuroscience investigations. Therefore, the objective of the neuroscience investigations

was to define spaceflight related adaptive changes within a narrowly defined subset of the sensorimotor systems that could have a negative effect on mission success.

The Neuroscience Laboratory, Johnson Space Center (JSC), implemented three integrated Detailed Supplementary Objectives (DSO) designed to investigate spatial orientation and the associated compensatory responses as a part of the EDOMP. The four primary goals were (1) to establish a normative database of vestibular and associated sensory changes in response to spaceflight, (2) to determine the underlying etiology of neurovestibular and sensory motor changes associated with exposure to microgravity and the subsequent return to Earth, (3) to provide immediate feedback to spaceflight crews regarding potential countermeasures that could improve performance and safety during and after flight, and (4) to take under consideration appropriate designs for preflight, in-flight, and postflight countermeasures that could be implemented for future flights.

OPERATIONAL INVESTIGATIONS

Motion Perception Reporting (DSO 604 OI-1)

Preflight, in-flight, and postflight self- and surround-motion perception and motion sickness reports were collected from crew members, using a standardized Sensory Perception Questionnaire [1-2] and Motion Sickness Symptom Checklist. These reports included quantitative estimates of perceived self motion and surround motion associated with (1) voluntary head/body movements in flight, during entry, and immediately postflight, and (2) exposure to motion profiles in a Tilt Translation Device (TTD), and in a Device for Orientation and Movement Environments (DOME) located in the Preflight Adaptation Trainers (PAT) Laboratory at JSC [3]. Verbal descriptions of perceived self motion and surround motion were reported in flight, during entry, and at wheels stop, using a microcassette voice recorder.

This investigation involved four experiment protocols. One protocol using the TTD-PAT device and a second using the DOME-PAT device were performed before

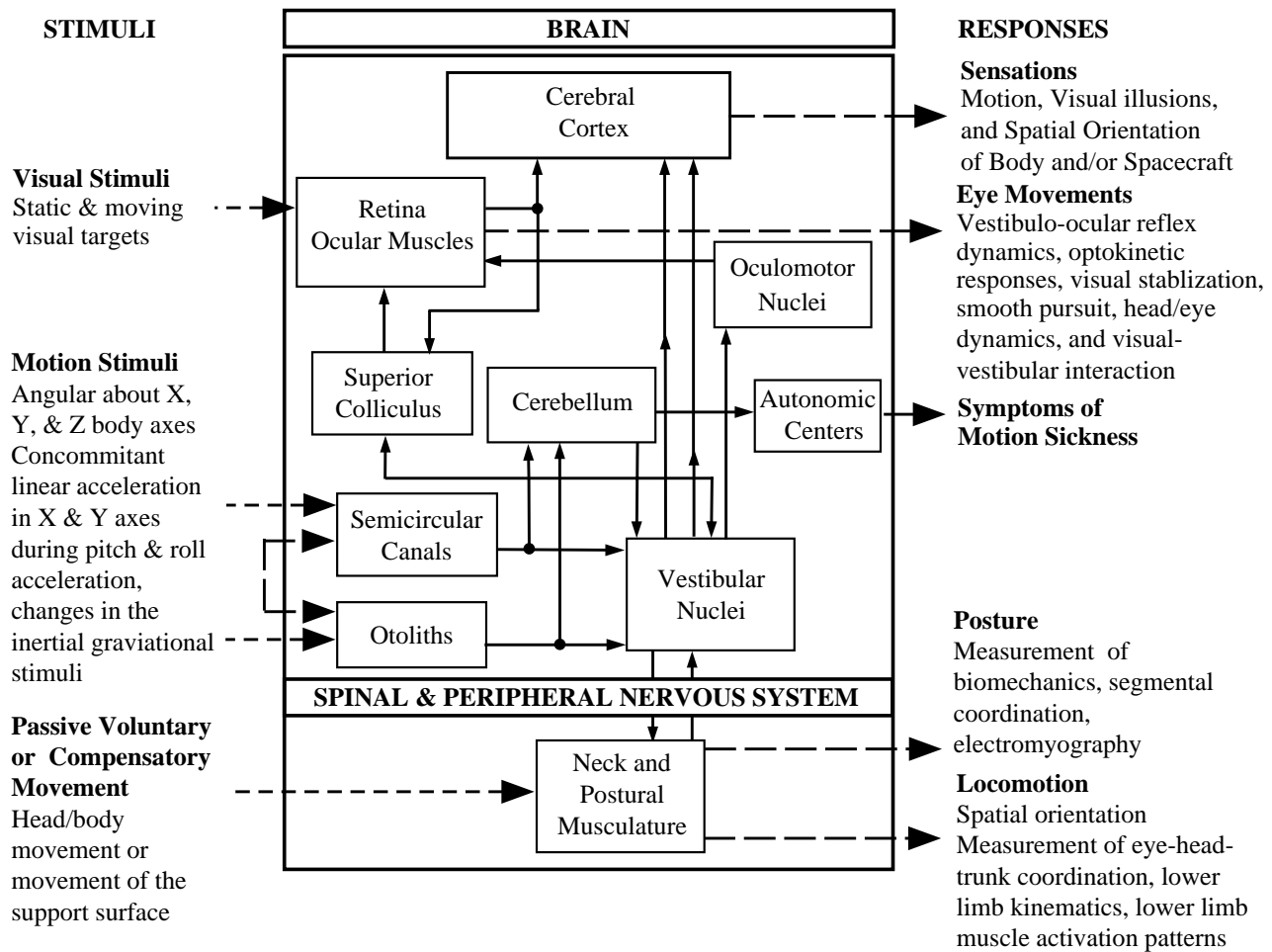


Figure 5.1-1. Stimulus and response make-up of spatial orientation with a schematic of the neural substrate.

flight for training and data collection, and again after flight for data collection. A third protocol, involving voluntary head/torso movements, was performed during flight and immediately after wheels stop at landing. A fourth, head-only movement, protocol was performed during the Shuttle entry phase of the mission.

Self-motion and surround-motion perception and motion sickness reports were collected from crew members, before, during, and after flight, using a standardized Sensory Perception Questionnaire [1-2] and Motion Sickness Symptom Checklist.

Visual-Vestibular Integration (Gaze) (DSO 604 OI-3)

A number of experiment paradigms, classified as voluntary head movements (VHMs), in which the head was unrestrained and free to move in all planes during all phases of the study, were standardized. The investigations included the performance of (1) target acquisition, (2) gaze stabilization, (3) pursuit tracking, and (4) sinusoidal head oscillations. Where possible, each of these four protocols

was performed on all subjects during all phases of the spaceflight.

Target acquisition protocols used a cruciform tangent system where targets were permanently fixed at predictable angular distances in both the horizontal and vertical planes. To facilitate differentiation, each target was color coded ($\pm 20^\circ$ green, $\pm 30^\circ$ red, etc.) corresponding with the degree of angular offset from center. For all target acquisition tasks, the subject was required, using a time optimal strategy, to look from the central fixation point to a specified target indicated by the operator (right red, left green, up blue, etc.) as quickly and accurately as possible, using both the head and eyes to acquire the target. When target acquisition was performed in flight, measurements were obtained using a cruciform target display that attached to the Shuttle middeck lockers. In all cases, surface electrodes were placed appropriately on the face, and eye movements were obtained with both horizontal and vertical electrooculography (EOG). Head movements were detected with a triaxial rate sensor system mounted on goggles that were fixed firmly to the head. Both head movements (using a head-mounted laser)

and eye movements were calibrated using the color coded horizontal position targets.

The gaze stabilization protocol used transient rotational displacement of the head following occlusion of vision while the subject consciously attempted ocular fixation on a just viewed wall-fixed target. With this simple paradigm, verbal instruction controlled the subject's conscious intent, while the brief stimulus favored constancy of mental set during the testing regime. The short transient stimuli in this protocol had the added merit of simulating natural patterns of head movement and minimizing long term adaptive effects.

Pursuit tracking, performed as preflight and postflight trials, used two separate protocols: (1) smooth pursuit and (2) pursuit tracking with the head and eye together. In addition, these protocols were followed using predictable, sinusoidal stimuli and unpredictable stimuli with randomly directed velocity steps. These protocols were selected to study the smooth pursuit eye movement system and to evaluate how this system interacted with the vestibulo-ocular reflex (VOR). The sinusoidal pursuit tracking tasks were performed at moderate (0.333 Hz) and high (1.4 Hz) frequencies to investigate alterations in the strategy used to dictate the relative contributions of eye and head movement in maintaining head-free gaze. The unpredictable pursuit tracking used position ramps that varied in direction, maximal displacement, and velocity. Sinusoidal head oscillations (head shakes) in both the horizontal and vertical plane were made at 0.2, 0.8, and 2.0 Hz with (1) vision intact, in which the subject maintained a fixation point in the primary frontal plane, and (2) vision occluded, where the subject imagined the fixation point available with vision.

Unless indicated otherwise, all 604-OI3 protocols were completed a minimum of three times prior to flight, two times in flight, and up to five times following flight. The last preflight test session was typically within ten days of flight. In-flight measurements were performed within 24 hours following orbital insertion and again within 24 hours of landing. After flight, the first measurement was about 2 hours after wheels stop. Subsequent postflight measurements were obtained 3, 5, 8, and 12 days after landing. The 5, 8, and 12 day postflight tests were completed only when the subjects had not returned to preflight baseline values.

Recovery of Postural Equilibrium Control (DSO 605)

To accomplish DSO 605, two experiment protocols were performed by 40 crew members before, during, and after Shuttle missions of varying duration. The first of these protocols focused primarily on reactive responses by quantifying the reflex (open loop) response to sudden, stability threatening, base of support perturbations. The second protocol focused on sensory integration by quantifying the

postural sway during quiet upright stance with normal, reduced, and altered sensory feedback. All participating subjects performed the two protocols on at least three occasions before flight to provide an accurate, stable set of 1-g control data from which postflight changes could be determined. All subjects also performed the two paradigms on up to five occasions after flight to capture the full sensory motor readaptation time course. Postflight tests began on landing day, as soon after Orbiter wheels stop as possible, and were scheduled on an approximately logarithmic time scale over the subsequent eight days.

Of the 40 astronaut subjects studied, 11 were from short duration (4-7 day) missions, 18 from medium duration (8-10 day) missions, and 11 from long duration (11-16 day) missions. Seventeen of the subjects were first time (rookie), and 23 were experienced (veteran) fliers. The effect of spaceflight on neural control of posture was inferred from differences between preflight and postflight performance in all subjects. The effect of mission duration was inferred from statistical comparison between the performance of the short, medium, and long duration mission subjects. The effect of previous spaceflight experience was inferred from statistical comparison between the performance of the rookie and veteran fliers.

Effects of Spaceflight on Locomotor Control (DSO 614)

Five primary protocols were employed to accomplish the goals of DSO 614. The first protocol was designed to determine if exposure to the microgravity environment of spaceflight induced alterations in eye-head-trunk coordination during locomotion. In this protocol, astronaut subjects were asked to walk (6.4 km/h, 20 s trials) on a motorized treadmill while visually fixating on a centrally located earth-fixed target positioned either 2.0 m or 0.30 m from the eyes. In addition, some trials were also performed during periodic visual occlusion. Head and trunk kinematics during locomotion were determined with the aid of a video-based motion analysis system.

Also using a treadmill, the second protocol sought to investigate strategies used for maintaining gaze stability during postflight locomotion by examining the lower limb joint kinematics recorded during preflight and postflight testing and the contribution of the lower limb movement on the head-eye-trunk coordination obtained in the first protocol.

The third protocol was designed to provide a systematic investigation of potential adaptations in neuromuscular activity patterns associated with postflight locomotion. Both before and after flight, the subject was tasked with walking on the treadmill at 6.4 km/h while fixating a visual target 30 cm away from the eyes. Surface electromyography was collected from selected lower limb muscles, and normalized with regard to mean amplitude and temporal relation to heel strike. Protocol 4 investigated changes in spatial orientation ability and walking

performance following spaceflight. The subject was asked, before and after flight, to perform a goal-directed locomotion paradigm consisting of walking a triangular path with and without vision. This paradigm involved inputs from different sensory systems and allowed quantification of several critical parameters during a natural walking task. These included orientation performance, walking velocities, and postural stability. The fifth protocol examined the ability of a subject to jump from a height of 18 cm with either eyes open or closed. Three trials in each visual condition were conducted. Body segment measurements were obtained with the aid of a video-based motion analysis system.

DESIGN AND DEFINITION OF PROTOCOLS

The protocols outlined above were established by the Neuroscience Laboratory at JSC, under the guidance of a standing international neuroscience Discipline Implementation Team (DIT), listed in Table 5.1-1. Table 5.1-2 outlines the tests and protocols that were the final product generated through association with the DIT. The DIT participated in semiannual reviews of the science and results of the ongoing neuroscience EDOMP investigations. Where appropriate, the investigations were modified to conform to suggestions and recommendations from DIT members.

Very few subjects on a mission participated in each neuroscience DSO, thus limiting comparisons between investigations (Appendix B). This limitation was partially overcome by the relatively large number of subjects participating in each of the investigations.

SUMMARY

A complete and detailed review of each of the DSOs summarized in this introductory section is presented in the pages that follow. Overall, the results across and within neuroscience investigations show that spaceflight has a profound effect on sensory-motor function. Gaze is disturbed during target acquisition and during locomotion. Dynamic postural responses show clearly a link between duration of flight and prior spaceflight experience, and the magnitude/duration of postural ataxia. Thanks to the EDOMP we have gained valuable knowledge which allows us to obtain a better understanding of the neural substrate controlling sensory-motor function and the effects of spaceflight on that neural substrate. Importantly, the results of the neurosensory investigations have helped define our need for sensory-motor countermeasures. Overall, NASA's commitment to the EDOMP represents perhaps the most advanced set of operational investigations in support of our crew members' health and safety.

Table 5.1-1. Extended Duration Orbiter Medical Project (EDOMP) neuroscience discipline implementation team members

David J. Anderson, Ph.D.
University of Michigan
Ann Arbor, MI

Alain F. Berthoz, Ph.D.
Collège de France
Centre National de la Recherche Scientifique
Paris, France

F. Owen Black, M.D.
Good Samaritan Hospital
Portland, OR

Bernard Cohen, M.D.
Mount Sinai Medical Center
New York, NY

Stefan Glasauer, Ph.D.
Ludwig-Maximilians-Universität München
Munich, Germany

Fred Guedry, Jr., Ph.D.
University of West Florida
Pensacola, FL

Robert S. Kennedy, Ph.D.
Essex Corporation
Orlando, FL

R. John Leigh, M.D.
Case Western Reserve University
Cleveland, OH

Donald E. Parker, Ph.D.
University of Washington
Seattle, WA

Laurence R. Young, Sc.D.
Massachusetts Institute of Technology
Department of Aeronautics and Astronautics
Cambridge, MA

James W. Wolfe, Ph.D.*
Universities Space Research Association
San Antonio, TX

*Observer

Table 5.1-2. EDOMP neuroscience investigations

<i>Operational Investigation</i>	<i>Mission</i>
DSO 604 OI-1: Mission Perception Reporting (22)	STS-41 (1), STS-39 (1), STS-48 (1), STS-44 (1), STS-45 (2), STS-49 (1), STS-46 (1), STS-52 (1), STS-53 (1), STS-54 (2), STS-57 (3), STS-70 (2), STS-73 (2), STS-74 (2), STS-72 (1)
DSO 604 OI-3: Visual-Vestibular Integration as a Function of Adaptation DSO 604 OI-3A: Preflight, In-flight, Entry, Wheels Stop, Postflight (3) DSO 604 OI-3B: Pre-/Postflight (26) DSO 604 OI-3C: Preflight, Inflight, Postflight (10)	STS-43 (1), STS-44 (1), STS-49 (1), STS-52 (2), STS-53 (1), STS-54 (1), STS-57 (2), STS-51 (1), STS-58 (1), STS-61 (3), STS-62 (4), STS-59 (2), STS-65 (2), STS-68 (2), STS-64 (3), STS-66 (2), STS-67 (3), STS-69 (3), STS-73 (2), STS-72 (2)
DSO 605: Recovery of Postural Equilibrium Control Following Space Flight (40)	STS-28 (1), STS-36 (2), STS-41 (2), STS-35 (3), STS-40 (2), STS-43 (3), STS-44 (2), STS-49 (3), STS-52 (3), STS-53 (1), STS-54 (3), STS-56 (2), STS-51 (1), STS-58 (2), STS-62 (1), STS-65 (2), STS-68 (1), STS-64 (1), STS-67 (2), STS-69 (2), STS-73 (1)
DSO 614: The Effects of Space Flight on Eye, Head, and Trunk Coordination During Locomotion DSO 614A: Head/Gaze Stability (32) DSO 614B: Locomotor Path Integration (9)	STS-43 (2), STS-48 (2), STS-44 (2), STS-45 (4), STS-49 (3), STS-50 (2), STS-46 (4), STS-47 (3), STS-53 (2), STS-57 (3), STS-58 (1), STS-62 (2), STS-65 (2), STS-68 (2), STS-64 (3), STS-66 (2), STS-67 (2)

() Denotes number of subjects

*Does not include those subjects for which only partial data were collected.

REFERENCES

1. Harm DL, Parker DE. Perceived self-orientation and self-motion in microgravity, after landing and during preflight adaptation training. *J Vestib Res, Equil & Orient* 1993; 3:297-305.
2. Reschke MF, Bloomberg JJ, Paloski WH, Harm DL, Parker DE. Physiologic adaptation to space flight: neurophysiologic aspects: sensory and sensory-motor function. In: Nicogossian AE, Leach CL, Pool SL, editors. *Space Physiology and Medicine*. Philadelphia: Lea & Febiger; 1994. p 261-85.
3. Harm DL, Parker DE. Preflight adaptation training for spatial orientation and space motion sickness. *J Clinical Pharmacology* 1994; 34:618-27.

Section 5.2

Neurovestibular Dysfunction

Visual-Vestibular Integration Motion Perception Reporting

(DSO 604 OI-1)

*Deborah L. Harm and Millard R. Reschke of the Johnson Space Center, Houston, TX;
Donald E. Parker of the University of Washington, Seattle, WA*

BACKGROUND

Our perception of how we are oriented and moving is dependent on the transduction and integration of sensory information from visual, vestibular, proprioceptive, somatosensory, and auditory systems. Attention levels and expectations about position and movement also influence perception. Perceptual errors are most commonly due to one or more of the following: (1) limitations of sensory modalities in transducing position and motion information from environmental stimuli, particularly inertial and visual, (2) loss of information from one or more of the sensory modalities due to pathology or absence of an effective stimulus, and (3) incorrect integration of multi-modal sensory signals. Illusory self-orientation, self-motion, and visual scene or object motion are evidence of perceptual errors. Almost 200 years ago, Purkinje [1] wrote of how perceptual errors provide insight into the mechanisms underlying perceptual and sensorimotor functions that make normal performance possible.

Perceptual errors may lead to inappropriate motor commands to control systems involved in eye-head, eye-hand, eye-head-hand coordination, and postural and locomotor stability. The effects of perceptual errors cover a wide range and can be: (1) merely interesting or fun, such as illusions of self-motion produced by large screen cinemas, (2) annoying, as with reaching errors and knocking objects on the floor or unnecessary postural adjustments, (3) severely inappropriate postural adjustments, resulting in falls and physical injury, or (4) inappropriate control of a vehicle, such as a car or aircraft, resulting in serious injury or death. Perceptual errors are considered to be the primary cause of approximately 10% of fixed wing and helicopter military accidents, and for approximately 35% of all general aviation fatalities [2].

The absence of an effective gravity vector in spaceflight rearranges the relationships of signals from visual, skin, joint, muscle, and vestibular receptors, initiating adaptive changes in sensorimotor and perceptual systems. Return to Earth normal gravity requires readaptation. Adaptation occurs as the result of sensory compensation and/or sensory reinterpretation. In the absence of an appropriate

graviceptor signal during spaceflight, information from other spatial orientation receptors, such as the eyes, the vestibular semicircular canals, and the neck position and somatosensory receptors, can be used by astronauts to maintain spatial orientation and movement control. Alternatively, signals from graviceptors may be reinterpreted by the brain. On Earth, otolith signals may be interpreted as linear motion or head tilt with respect to gravity. Because stimulation from gravity is absent during spaceflight, interpretation of the graviceptor signals, such as tilt, is inappropriate. Therefore, during adaptation to microgravity the brain reinterprets all otolith graviceptor inputs to indicate translation. This is the otolith tilt-translation reinterpretation (OTTR) hypothesis [3, 4].

A spatial orientation perceptual-motor system that is inappropriately adapted for the inertial environment can lead to spatial disorientation, motion sickness, and errors during: (1) spaceflight activities, such as visual capture of operationally relevant targets, switch throws, satellite capture, object location, and manipulation of objects, (2) entry, such as acquiring information from instrumentation, switch throws, activities requiring eye/head/hand coordination, attitude control procedures, pursuit of a moving object, and pursuit and capture of visual, tactile, or auditory targets, and (3) nominal egress activities, such as visual target acquisition, pursuit of a moving object, and emergency egress. The risk of operational performance errors and motion sickness is thought to be related to prior spaceflight experience, flight duration, and circumstance, such as unusual Orbiter attitude, smoke, darkness, or crew complement. The transition between microgravity and Earth, when the perceptual and sensory motor systems are inappropriately adapted to the inertial environment, poses potential risks to space travelers. Therefore, the development of countermeasures for these disturbances was important to EDOMP.

Detailed Supplementary Objective (DSO) 604 Operational Investigation-1 (OI-1) was conducted to investigate the following hypotheses:

1. Adaptation to microgravity and readaptation to Earth normal gravity is indicated by the initial appearance

and gradual resolution of motion sickness symptoms and perceptual illusions of self/surround-motion produced by voluntary head/body movements during spaceflight and after return to Earth.

2. Vision and/or tactile cues attenuate the illusory self-motion associated with voluntary head/torso movements during spaceflight and upon return to Earth.

3. Adaptation to microgravity is revealed initially by reliance on visual scene orientation cues and subsequently by reliance on internally generated orientation cues.

4. Postflight motion sickness, perceptual disturbances, and readaptation time constants increase as mission length increases. These disturbances occur more frequently, are more intense, and take longer to resolve as mission duration increases.

METHODS

Motion perception and motion sickness reports were collected from crew members before, during, and after spaceflight, using a standardized Sensory Perception Questionnaire [5, 6] and a Motion Sickness Symptom Checklist. These reports included quantitative estimates of perceived self-motion and surround-motion associated with: (1) voluntary head/body movements in flight, during entry and immediately after flight, and (2) exposure to motion profiles in both the Tilt Translation Device (TTD) and the Device for Orientation and Movement Environments (DOME), which are located in the Preflight Adaptation Trainers (PAT) Laboratory at the Johnson Space Center [7]. Verbal descriptions of perceived self/surround-motion were reported during flight, during entry, and at wheels stop using a microcassette voice recorder.

This investigation involved four experiment protocols. Protocols using the TTD-PAT device and the DOME-PAT device were performed before flight for training and data collection, and after flight for data collection. A third protocol, involving voluntary head/torso movements, was performed during flight and immediately after wheels stop at landing. A fourth head movement only protocol was performed during the Shuttle entry phase of the mission.

Education consisted of a 1-hour course on neurosensory functional anatomy and physiology, perceptual processes, perceptual illusory phenomena, spatial orientation disturbances, and a specific vocabulary for describing and reporting perceived self-motion and surround-motion. Perceptual illusory phenomena were demonstrated by exposing crew members to a variety of motion profiles in the TTD-PAT for 30 minutes. Ten of the 18 crew members were also exposed to motion profiles in the DOME-PAT for 30 minutes. Crew members were exposed to the TTD and DOME on two separate occasions before their mission.

Preflight Protocols

Before flight, crew member subjects were: (1) briefed on the purpose and objectives of the investigation, (2) provided with descriptions of the functional anatomy of the vestibular and visual systems, perceptual processes, types of illusory self- and surround-motion, and hypotheses concerning sensory adaptation to microgravity, (3) taught a set of vocabulary terms and the body coordinate system used in describing perceptions of self- and/or surround-motion induced by voluntary head movements or passive motion, (4) provided an opportunity to practice using vocabulary terms used to describe motion perceptions during exposure to a variety of stimulus rearrangements produced by the PAT devices, and (5) provided demonstrations and an opportunity to practice voluntary head/torso movement protocols to be performed during different phases of the mission.

TTD-PAT Apparatus and Protocol

This device was a one degree of freedom (DOF) tilting platform on which the subject was restrained in a car seat. In the pitch configuration, the axis of tilt rotation was approximately aligned with the subject's interaural axis, whereas in the roll configuration the axis of rotation was approximately aligned with the subject's nasooccipital axis. A visual surround, mounted on the platform, moved linearly parallel to the subject's X body axis in the pitch configuration and to the subject's Y body axis in the roll configuration. Surround-motion provided a visual stimulus that translated with respect to the subject. In the pitch configuration, the subject faced the end wall and the surround translated toward and away from the subject. In the roll configuration the subject faced the side wall and the surround translated left and right of the subject. The visual surround was a 2.74 m × 0.89 m × 0.91 m (approximately 9 ft × 3 ft × 3 ft) white box with three-dimensional vertical black stripes on the inside walls and horizontal stripes on the ceiling. Four successively smaller outlined black squares and a solid black square in the center were attached to the inside of the end walls. The line width and separation between lines was progressively smaller from the outer to the inner square to produce the appearance of a tunnel. This tunnel effect produced a visual stimulus distance ambiguity which was designed to allow the subject to scale perceived distance to the walls so that the expanding and contracting optic flow and looming pattern matched the simulated physical acceleration stimulus provided by the tilting base [8]. The linear translation of the visual surround was designed to elicit linear vection (self-motion). The amplitude, frequency, phase, and wave form shape of the tilt base and surround translation were independently controlled by a microcomputer.

Crew members were exposed to four pitch and five roll motion profiles, the order of which was alternated across data collection sessions. The visual surround

displacement amplitude was held constant at ± 60 inches maximum displacement in each direction for all pitch and roll motion profiles. Tilt displacement amplitude for the pitch configuration was $\pm 4^\circ$ with a -4° rearward offset, and $\pm 4^\circ$ for the roll configuration. Each motion profile was presented for approximately 3 minutes. During exposure to the various motion profiles, crew members were instructed to describe their perceived self-motion and/or surround-motion using the standard vocabulary. The subject was prompted, when appropriate, to ensure that all aspects of the motion were described.

All quantitative estimates of self-motion and/or surround-motion were hand recorded on data spread sheets; and all quantitative and qualitative descriptions of perceived self-motion and/or surround-motion, motion path, visual disturbances, and motion sickness symptoms were voice recorded on a microcassette recorder. Data were subsequently entered onto spread sheets for tabular summary and, where appropriate, statistical analyses.

DOME-PAT Apparatus and Protocols

This device was a 3.7 m (12 ft) diameter spherical dome, with a 1.8 m (6 ft) diameter hole in the bottom. The inner surface was painted white and served as a projection surface for two Triuniplex video projectors with custom wide angle optics. The projectors, along with an adjustable trainee restraint assembly, were mounted on a 1.8 m (6 ft) diameter rotating base that filled the hole in the bottom of the dome. However, rotation was not used in this investigation. The trainee restraint adjusted for positioning the subject to: (1) sit upright, (2) lie on either the left or right side, or (3) lie supine. For the first two positions, the projectors' optical axes were horizontal, and for the supine test, the images were projected on the dome top. The field of view for the trainee was $100^\circ \times 170^\circ$, with 0.1° between adjacent pixels or scan lines. This provided a very wide field of view with moderate to coarse resolution.

The visual data base was a set of polygons representing the visible surfaces in the interior of a closed environment. This was unlike the usual data base for aircraft flight simulators that only represent the outside surface of objects. The operator could select environments and interpretation of trainee controls for different training protocols. The trainee could be placed inside a closed visual environment that represented the Shuttle middeck, flight deck, Spacelab, or a checkerboard room.

A crew member was restrained in the seated upright position and the virtual room was rotated continuously at $35^\circ/\text{second}$ in pitch, roll and yaw with respect to the subject. For pitch, the room moved so that the subject view changed from ceiling to wall to floor to wall to ceiling and so on. For roll, the crew member looked at a wall that rotated in roll with respect to the subject. For yaw, the crew member looked from wall to wall to wall with feet toward the floor. The walls, ceiling and floor of the room

were designed in a checkerboard pattern where each surface had a different color of squares alternating with black squares. Polar cues in the virtual room included a door, windows, a printed sign and several stick-man figures standing on the floor. Each rotation axis was presented in the \pm direction with each axis-direction combination presented once in each of three sets of six trials each for a total of 18 trials.

The experiment trials within and across sets were systematically randomized for each crew member. This allowed a unique presentation order for each subject such that each trial followed every other trial at least once, but not necessarily an equal number of times. This was similar to a repeated Latin square design where more than one Latin square was created, and each subject had a dedicated random assignment of systematically randomized trials. The crew member began each trial with eyes closed. Eyes were opened upon instruction from the operator. Using a hand-held event switch, the crew member indicated the following: (1) eyes open, (2) onset of self-motion (vection), and (3) saturation or maximum percent self-motion achieved. The crew member then reported the axis and direction of self-motion, the perceived rate of rotation in degrees/second, percent self- versus percent surround-motion, and if present, the magnitude (in degrees) and direction of paradoxical body tilt. Data were subsequently entered onto spread sheets for tabular summary and, where appropriate, statistical analysis.

The event switch signal was recorded as a square wave using a National Instruments Data Acquisitions Board driven by Data4th software, sampled at 40 Hz. Latency to the onset of self-motion and to maximum self-motion was derived from the event switch signal with a Matlab algorithm script that automatically located the leading edge of the first square wave (indicating eyes open) and calculated the time (seconds) from this point to the leading edge of each of the next two square waves (onset and maximum self-motion, respectively). All crew comments were voice recorded.

Flight Protocol

In the Shuttle middeck, crew members performed voluntary head/torso movements about the pitch, roll, and yaw axes with the axis of rotation being about the waist, and in a feet-to-the-floor orientation. The peak-to-peak head displacement amplitude was approximately 40° and was performed as a step input motion. The crew members, having been instructed to keep their heads aligned with their torsos during all movements to minimize neck proprioceptive inputs, slowly moved to the -20° from vertical position, quickly rotated to the $+20^\circ$ position, and paused until any perceived lag or persistence of motion subsided. The procedure was repeated starting from the -20° position and rotating to the $+20^\circ$ position. Each axis of motion was repeated for three to four cycles, and each

set of repetitions was performed with the eyes open (EO) and once with the eyes closed (EC). During the eyes open condition, the crew member performed each axis of motion once while fixating on a far visual target (approximately 100 cm) and once while fixating on a near target (approximately 30 cm). All of these conditions were performed once with the feet in restraints and once free floating. Following each axis of voluntary head/torso movements, and/or surround-motion were recorded in terms of: (1) linear and angular amplitude, (2) velocity, (3) lag (in seconds) between input and output (real-perceived) motion, (4) persistence (in minutes or seconds) of perceived self-motion and/or surround-motion after real motion stopped, (5) directional differences, and (6) the perceived overall motion path. Whenever possible, the head/torso protocols were videotaped.

Shuttle Entry Protocol

During entry, crew members performed $\pm 20^\circ$, head only, sinusoidal motions at approximately 0.25 Hz in pitch, roll and yaw. Each axis of motion was repeated for three to four cycles, and each set of repetitions was performed once with eyes open while fixating on a visual target, and once with eyes closed. Depending on seat position, the target distance ranged from 2.5 to 3.0 ft (76.2 to 91.5 cm). Following each axis of head movement, perceptions of self-motion and/or surround-motion were recorded as during flight. This protocol was waived for crew members returning on the flight deck.

After Wheels Stop Protocol

Crew members repeated the in-flight voluntary head/torso movement protocol. In some cases, a crew member performed the wheels stop protocol as soon as possible after flight in the Crew Transport Vehicle (CTV) or in the data collection facility.

Postflight Protocol

A videotaped debrief was performed on landing day, with an additional debrief on R+1 or 2 days. The landing day debrief was used to review perceptual experiences associated with the voluntary head movement protocol as well as perceptual experiences not directly associated with the protocol. The debrief performed on R+1 or 2 was used to: (1) clarify descriptions of self- and/or surround-motion recorded in flight and/or during the landing day debrief, and (2) assess perceptual disturbances associated with normal postflight activities. In addition, TTD-PAT and DOME-PAT protocols were repeated after the flight on days R+1 or 2, R+4, and on R+8 if perceptual responses remained different from those recorded before flight.

RESULTS AND DISCUSSION

Perceptions Associated with In-Flight Voluntary Head/Body Movements

The data in Figure 5.2-1 reveal that approximately 70% of the participating astronauts reported illusions of self- and/or surround-motion associated with head/body movements in flight. This value was approximately 80% during entry, and in the early postflight period was approximately 90%. In flight, there were significantly more reports of surround (target) motion than self-motion, associated with both near and far target conditions, whereas during entry and after flight, surround-motion was reported only slightly more often than self-motion (Figure 5.2-1). The strength or compellingness of perceived self/surround-motion was generally reported by crew members to be greatest during entry, somewhat less at wheels stop, much less late in the flight, and the least early in the flight.

Reports of perceived self/surround-motion were more often associated with pitch and roll head movements than with yaw head movements. Of those who reported illusory self-motion, all reported illusory pitch self-motion in flight (far target condition). During entry and wheels stop, there were more reports of illusory self roll motion than pitch or yaw (Figure 5.2-2). When surround-motion was produced by a head movement, crew members frequently reported a perceived lag in the surround-motion of 0.05 to 2.00 seconds and persistence of the motion for 2.00 seconds or more. Crew members reported that smaller head movements tended to produce surround-motion in the same direction as the head movement, whereas larger head movements tended to produce surround-motion in the opposite direction. Perceptions of self/surround-motion during head movements made during flight were described by crew members as stronger and having larger displacement amplitudes when performed under eyes closed and untethered conditions. Larger and/or faster head/body movements were more likely to produce perceptions of self/surround-motion than smaller and/or slower head movements. In general, self-motion and/or surround-motion was reported more frequently during and following medium duration missions compared to short duration missions (Figure 5.2-3).

Crew member descriptions of motion perception illusions associated with voluntary movement provided the information required to develop a useful framework to quantify and categorize motion perception disturbances. Three primary categories of input-output motion perception disturbances were identified: (1) gain (amplitude and rate), (2) temporal (lag and persistence), and (3) path (direction and axis). The most frequent type of disturbance reported both in flight and during the entry/postflight periods was gain disturbance. The most interesting findings were related to temporal disturbances, because three times more temporal lag disturbances were reported during the

flight than during the entry/postflight period. However, more than twice as many reports of temporal persistence disturbances were reported during the entry/postflight period than in flight (Figure 5.2-4).

Classification of Individual Astronaut In-Flight Rest Frame of Reference

Previously, two types of astronauts were identified, based on the spatial orientation “resting frame” they adopted [5]. These were: (1) visual-spatial (VS) crew members (50%) who tended to increase the weighting of visual-spatial cues/information to compensate for the absence of a gravitational “down” cue” and (2) internal Z axis (IZ) crew members (42%) who increased the weighting assigned to internally generated Z axis orientation vectors and appeared to ignore visual polarity information, and down was wherever their feet pointed. Eight percent of the crew members weighted VS and IZ information equally.

In the current study, a more systematic approach to rating crew members on the IZ-VS “rest frame” of reference continuum was developed. Transcripts of the two postflight debriefings were analyzed independently by two observers using verbal protocol analysis techniques, to determine the microgravity spatial orientation rest frame of each subject. Each transcript was assigned two scores, one for visual scene versus internal Z axis overall (VSIZO), and the other for visual scene versus internal Z axis time of transition (VSIZT). VSIZO scores were assigned from 1 (primarily internal Z axis) to 3 (primarily visual scene). VSIZT scores, which indicated the time during a mission when the astronaut transitioned from a visual scene to an internal Z axis rest frame, were assigned from 1 (early in flight) to 3 (late in flight or never). Scores were assigned for the purpose of classification.

Transcripts were evaluated using the following VS criteria: (1) rates self as using visual scene rest frame, (2) prefers working in flight in a nominal 1g orientation, (3) greater sense of well-being if 1g orientation is adopted in flight, (4) may perceive self as upside down, sideways, etc. in flight, (5) reports difficulty in switching orientation references and performing coordinate transformations, (6) adopts visual scene as truth, (7) space motion sickness (SMS) disturbances worse with eyes closed, or (8) reports loss of orientation when coming out of airlock. IZ criteria included: (1) self rating as IZ, (2) sense of well-being in any orientation, (3) head defines up, feet define down, (4) easily perceives walls as floor or ceiling, ceiling as floor, etc., depending on current orientation, (5) attributes real self-motion to surround / Orbiter, (6) easily manipulates coordinates (switches references), or (7) reports that the visual scene may be upside down. The data indicate that astronaut perceptual reports can be reliably classified along a VS-IZ dimension. Collapsed across VSIZO and VSIZT ratings, reliability between the people doing the rating was $r_s = 0.83462$; $p < 0.0007$.

In flight there was no difference in the percent of crew reports of self/surround-motion when the rest frame type and mission duration were compared. The one exception was that all of the IZ type astronauts on medium duration missions, but only 25% of the IZ type astronauts on short duration missions, reported self-motion (Figure 5.2-5a). During the entry/postflight period, both IZ and VS type crew members on medium duration missions consistently reported more self-motion and surround-motion than those on short duration missions (Figure 5.2-5b). Finally, VS type crew members on short duration missions tended to report more self-motion and surround-motion than IZ type crew members on short duration missions, in flight and during the entry/postflight period (Figure 5.2-5a and b).

Motion Perception in the TTD-PAT Device

After flight, in the TTD, both IZ and VS type crew members on medium duration missions reported a higher percentage of self-motion than IZ and VS crew members on short duration missions. In addition, postflight in the TTD, VS type crew members on short duration missions reported a much higher percentage of self-motion than IZ type crew members on short duration missions (Figure 5.2-6). Differences in preflight to postflight perceptions of self/surround-motion were generally resolved within four days after landing (R+4).

Overall, asymmetries in perceived angular displacement amplitude right/left (roll) in the TTD were reported much more frequently two days after landing (R+2) than before flight. Also, they were reported significantly more often by VS type than IZ type crew members (Figure 5.2-7). Postflight reports of perceived roll asymmetries were about the same for IZ and VS type crew members on short duration missions. However, IZ type astronauts on medium duration missions reported fewer roll asymmetries postflight than did those on short duration missions. VS type astronauts on medium duration missions reported more roll asymmetries postflight than did those on short duration missions (Figure 5.2-8), suggesting an interaction between spatial orientation type and mission duration.

Finally, in roll configuration the visual surround effectively presented a horizontal, slow optokinetic stimulus. Before flight, crew members never reported visual disturbances, such as blurring or tilting of the stripes or oscillopsia, associated with the stimulus. However, after the flight, there was an average of three reports of visual disturbances across all five profiles (Figure 5.2-9).

Motion Perception in the DOME-PAT Device

Angular vection (self-motion perception) responses were elicited and calculated as described above for the DOME Protocol. Two parameters were calculated: latency to the onset of vection (LOV), and latency to maximum vection (LMV). There were no significant differences in

these parameters across axes or between directions within axes. Therefore, all subsequent analyses of variance (ANOVAs) were performed on data collapsed across axes and directions.

Spearman rank order (r_s) correlations were performed to examine the relationship between rest frame of reference and time to transition from VS to IZ, and LOV (Figure 5.2-10). The data indicate that VS-IZ scores were significantly related to vection latencies determined before and after flight (Figure 5.2-11). VSIZO and VSIZT were inversely related to vection onset latency ($r_s = -0.56$; $p < 0.0001$ for VSIZO and $r_s = -0.68$, $p < 0.0001$ for VSIZT). That is, the VS crew members and those who transitioned late or never had shorter latencies to the onset of vection than did IZ crew members.

Both the LOV and LMV were greater for the IZ crew members compared to the VS or the Mixed, which did not differ in latencies (Figure 5.2-12). Similarly, rookies had longer LOV and LMV values than veterans (Figure 5.2-13). Finally, LOV and LMV values were longer for crew members on long duration missions compared to those on short or medium duration missions (Figure 5.2-14).

Countermeasure Evaluation

Findings from behavioral medicine programs, designed to manage chronic medical disorders, suggest that educational components of the treatment program can lead to some improvement in the patient's condition. Therefore, we predicted that the education and demonstration components of PAT should result in fewer reports of SMS. Motion sickness symptom reports from a group of 14 crew members who participated in OI-1 PAT education were compared with reports from a group of 40 non-participating crew members. The comparison revealed a 33.5% improvement in a group of six SMS symptoms in the educated group (Table 5.2-1). It should be noted that 52.5% of those who received no education and 44.4% of those who received education took anti-motion sickness medication in flight.

SUMMARY

Self-orientation and self/surround-motion perception derive from a multimodal sensory process that integrates information from the eyes, vestibular apparatus, proprioceptive and somatosensory receptors. Results from short and long duration spaceflight investigations indicate that: (1) perceptual and sensorimotor function was disrupted during the initial exposure to microgravity and gradually improved over hours to days (individuals adapt), (2) the presence and/or absence of information from different sensory modalities differentially affected the perception of orientation, self-motion and surround-motion, (3) perceptual and sensorimotor function was initially disrupted

Table 5.2-1. Evaluation of education/demonstration components of the PAT program

Symptom	Percent of Crewmembers Reporting Symptom(s)		
	No Education (N=40)	Education (N=18)	% Improvement With Education
Impaired Concentration	23	11.1	51.7
Headache	55	27.7	49.6
Malaise	38	22.2	41.6
Stomach Awareness	65	44.4	31.7
Vomiting	48	38.9	19.0
Nausea	60	55.6	7.3
Mean:			33.5

upon return to Earth-normal gravity and gradually recovered to preflight levels (individuals readapt), and (4) the longer the exposure to microgravity, the more complete the adaptation, the more profound the postflight disturbances, and the longer the recovery period to preflight levels. While much has been learned about perceptual and sensorimotor reactions and adaptation to microgravity, there is much remaining to be learned about the mechanisms underlying the adaptive changes [9], and about how intersensory interactions affect perceptual and sensorimotor function during voluntary movements.

During space flight, SMS and perceptual disturbances have led to reductions in performance efficiency and sense of well-being. During entry and immediately after landing, such disturbances could have a serious impact on the ability of the commander to land the Orbiter and on the ability of all crew members to egress from the Orbiter, particularly in a non-nominal condition or following extended stays in microgravity [10].

An understanding of spatial orientation and motion perception is essential for developing countermeasures for SMS and perceptual disturbances during spaceflight and upon return to Earth. Countermeasures for optimal performance in flight and a successful return to Earth require the development of preflight and in-flight training to help astronauts acquire and maintain a dual adaptive state. Despite the considerable experience with, and use of, an extensive set of countermeasures in the Russian space program, SMS and perceptual disturbances remain an unresolved problem on long-term flights [11].

Reliable, valid perceptual reports are required to develop and refine stimulus rearrangements presented in

the PAT devices currently being developed as countermeasures for the prevention of motion sickness and perceptual disturbances during spaceflight, and to ensure a less hazardous return to Earth. Prior to STS-8, crew member descriptions of their perceptual experiences were, at best, anecdotal. Crew members were not schooled in the physiology or psychology of sensory perception, nor were they exposed to the appropriate professional vocabulary. However, beginning with the STS-8 Shuttle flight, a serious effort was initiated to teach astronauts a systematic method to classify and quantify their perceptual responses in space, during entry, and after flight. Understanding, categorizing, and characterizing perceptual responses to spaceflight has been greatly enhanced by implementation of that training system.

REFERENCES

1. Purkinje J. Boebachtungen und Versuche Zyr Physiologie der Sinne. II Neu Beitrage Zur kenntnis des sehens in subjectiver Hinsicht. Berlin; 1825.
2. Benson AJ. Sensory functions and limitations of the vestibular system. In: Warren R, Wertheim AH, editors. Perception and control of self-motion. Hillsdale, New Jersey: Lawrence Erlbaum; 1990. p 145-70.
3. Parker DE, Reschke MF, Arrott AP, Homick JL, Lichtenberg BK. Otolith tilt-translation reinterpretation following prolonged weightlessness: implications for preflight training. *Aviat Space Environ Med* 1985; 56: 601-6.
4. Young LR, Oman CM, Watt DGD, Money KE, Lichtenberg BK. Spatial orientation in weightlessness and readaptation to Earth's gravity. *Science* 1984; 225: 205-8.
5. Harm DL, Parker DE. Perceived self-orientation and self-motion in microgravity, after landing and during preflight adaptation training. *J Vestib Res* 1993; 3:297-305.
6. Reschke MF, Harm DL, Parker DE, Sandoz G, Homick JL, Vanderploeg JM. Physiologic adaptation to space flight: neurophysiologic aspects: space motion sickness. In: Nicogossian AE, Leach CL, Pool SL, editors. Space physiology and medicine. Philadelphia: Lea & Febiger; 1994. p 228-60.
7. Harm DL, Parker DE. Preflight adaptation training for spatial orientation and space motion sickness. *J Clin Pharm* 1994; 34:618-27.
8. Harm DL, Zografos LM, Skinner NC, Parker DE. Changes in compensatory eye movements associated with simulated stimulus conditions of space flight. *Aviat Space Environ Med* 1993; 64:820-26.
9. Young LR. Space and the vestibular system: what has been learned? *J Vestib Res Equilibrium & Orientation* 1993; 3:203-6.
10. Reschke MF, Bloomberg JJ, Paloski WH, Harm DL, Parker DE. Physiologic adaptation to space flight: neurophysiologic aspects: sensory and sensory-motor function. In: Nicogossian AE, Leach CL, Pool SL, editors. Space physiology and medicine. Philadelphia: Lea & Febiger; 1994. p 261-85.
11. Kovalenko Ye A, Kasyan II. On the pathogenesis of weightlessness. *Patol Fiziol Eksp Ter* 1989; 3:9-18.

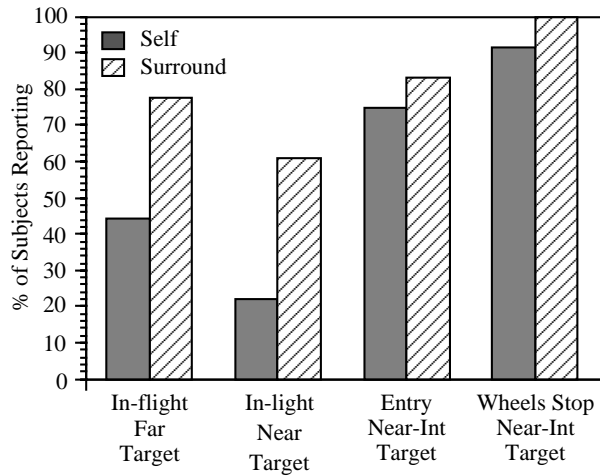


Figure 5.2-1. Percent of astronauts who reported self and/or surround motion associated with making voluntary head/body movements while fixating near and far visual targets in-flight, during entry and at wheels stop.

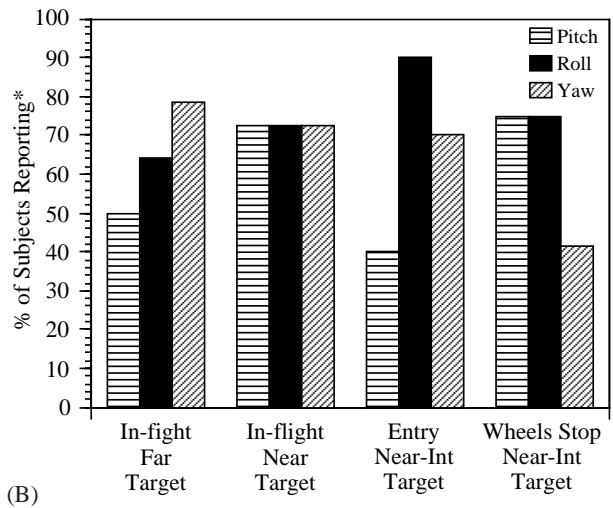
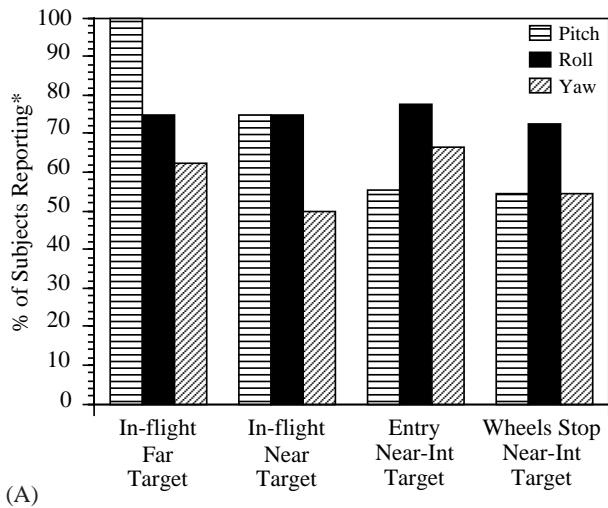


Figure 5.2-2. (A) Percent of astronauts who reported self motion and (B) surround motion associated with making voluntary pitch, roll, and yaw head/body movements while fixating near and far visual targets on-orbit, during entry and at wheels stop.

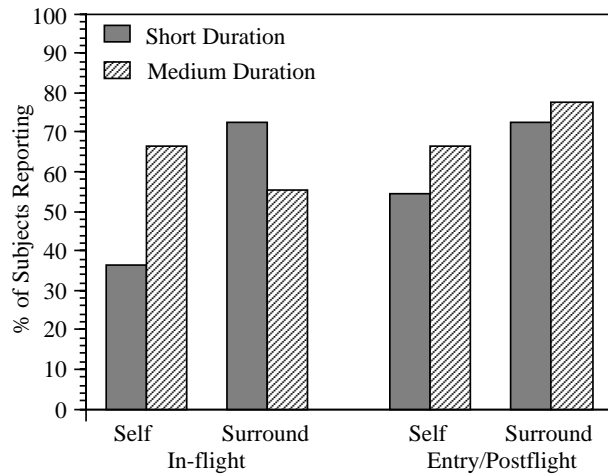


Figure 5.2-3. Percent of astronauts on short and medium duration missions who reported self vs. surround motion associated with making voluntary head/body movements in-flight and during the entry and immediate postflight periods.

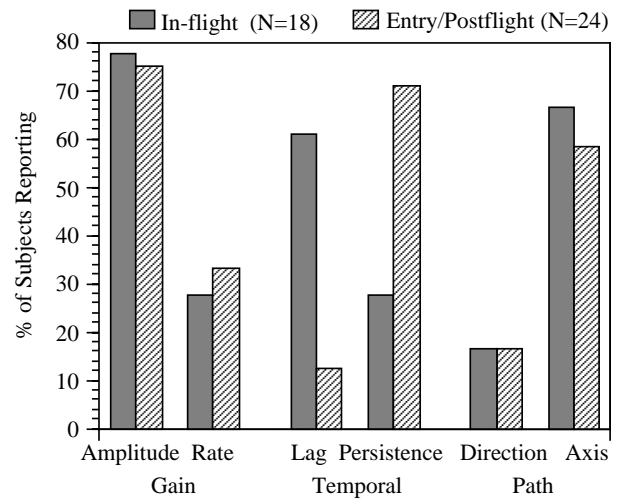
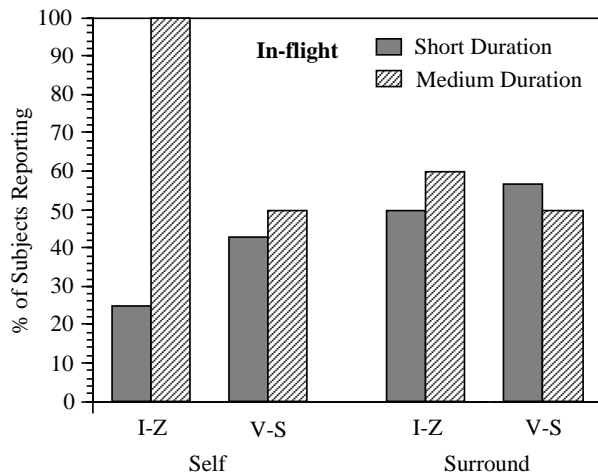
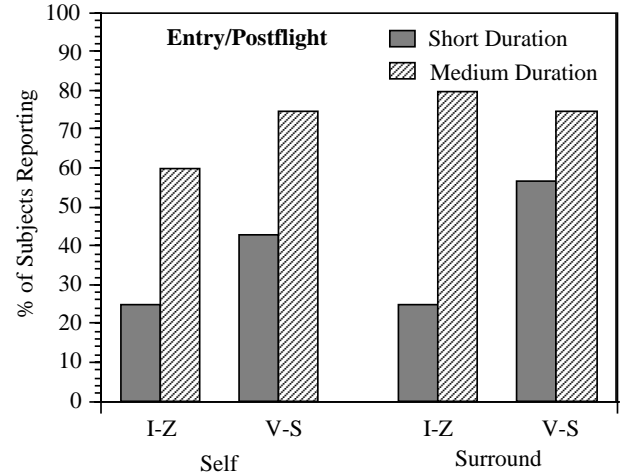


Figure 5.2-4. Percent of astronauts who reported gain, temporal and path input-output disturbances in-flight and during the entry and immediate postflight periods.



(A)



(B)

*Reports associated with voluntary head/body movements while fixating a visual target.

Figure 5.2-5. Percent of internal Z-axis (IZ) and visuo-spatial (VS) astronauts on short and medium duration missions who reported self and/or surround motion (A) in-flight and (B) during the entry and immediate postflight periods.

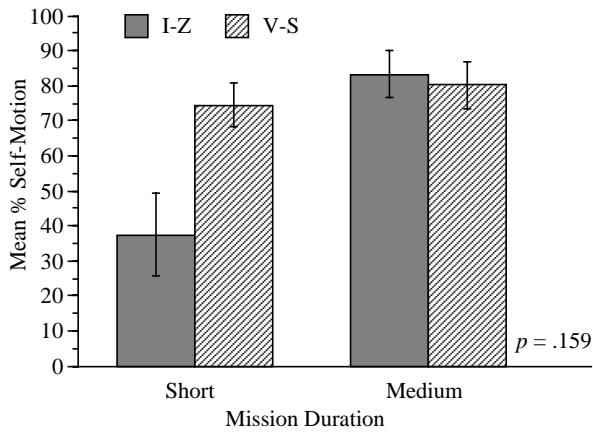


Figure 5.2-6. Percent of self motion in the roll plane postflight, during exposure to the tilt-translation device (TTD), reported by internal Z-axis (IZ) and visuo-spatial (VS) astronauts on short and medium duration missions.

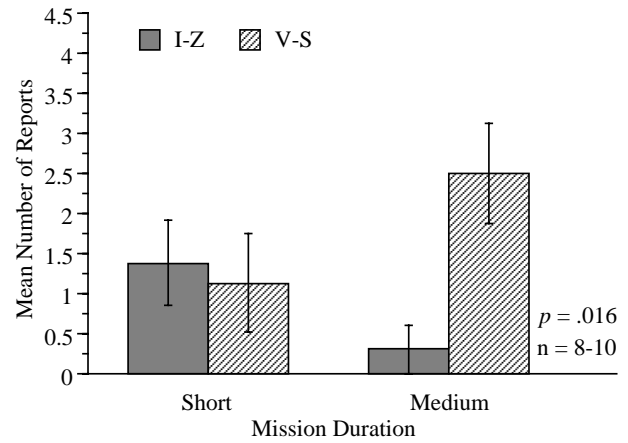


Figure 5.2-8. Average number of reports (across all roll motion profiles in the tilt-translation device [TTD]) of asymmetries in the perceived roll amplitude experienced postflight for the internal Z-axis (IZ) and the visuo-spatial (VS) astronauts on short and medium duration missions.

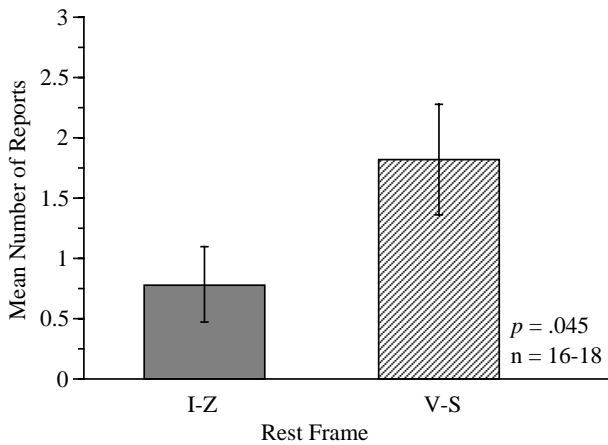


Figure 5.2-7. Average number of reports (across all roll motion profiles in the tilt-translation device [TTD]) of asymmetries in the perceived roll amplitude experienced postflight for the internal Z-axis (IZ) and the visuo-spatial (VS) astronauts.

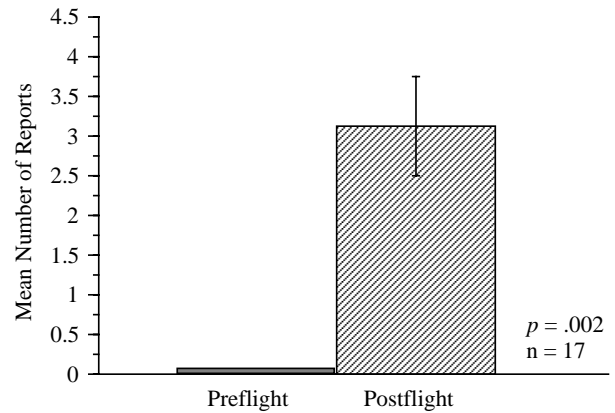


Figure 5.2-9. Average number of reports (across all roll motion profiles in the tilt-translation device [TTD]) of visual disturbances (e.g. oscillopsia, blurring or tilting of the stripes inside the device) preflight and postflight.

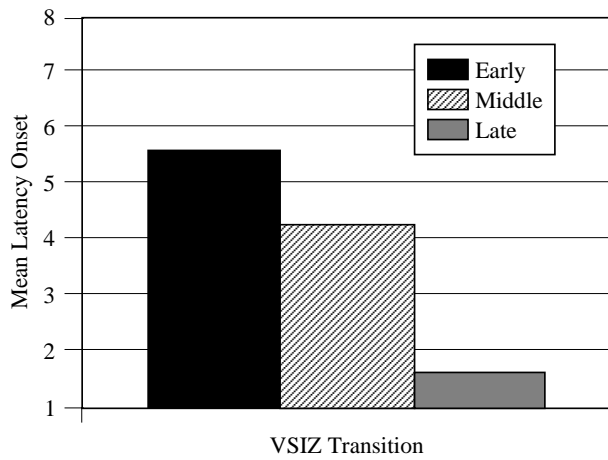


Figure 5.2-10. Mean onset to vection latency (sec) preflight (produced by the device for orientation and motion environments [DOME]) for astronauts who transitioned from a visual to an internal orientation rest frame early, mid and late in-flight.

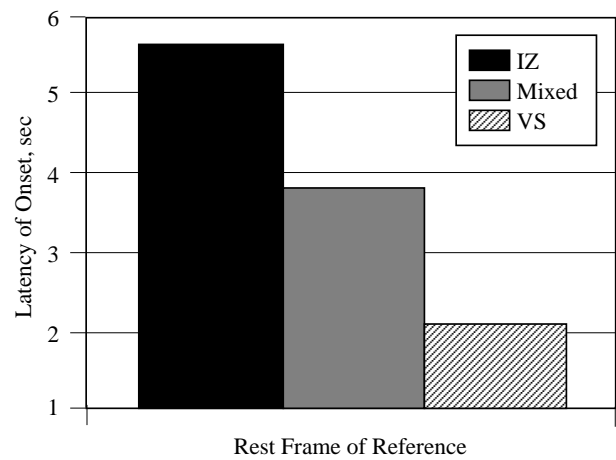


Figure 5.2-11. Mean latency to the onset of vection preflight (produced by the device for orientation and motion environments [DOME]) for the internal Z-axis (IZ), the visuo-spatial (VS) and the mixed rest frame of reference astronauts.

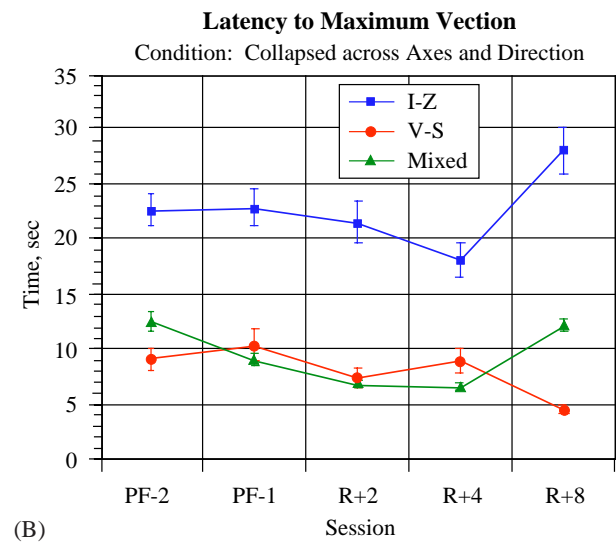
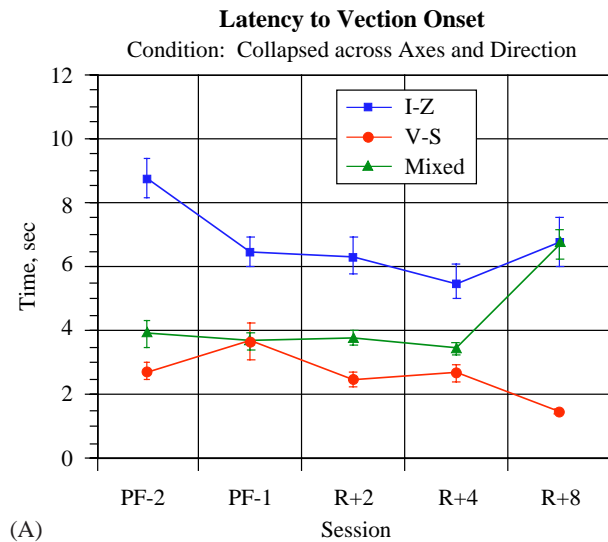


Figure 5.2-12. Mean latency to the onset of vection (A) and to maximum vection (B) preflight and postflight (produced by the device for orientation and motion environments [DOME]) for the internal Z-axis (IZ), the visuo-spatial (VS) and the mixed rest frame of reference astronauts.

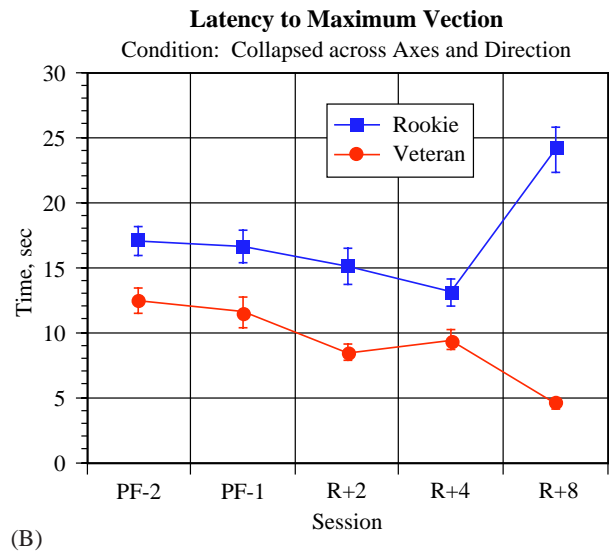
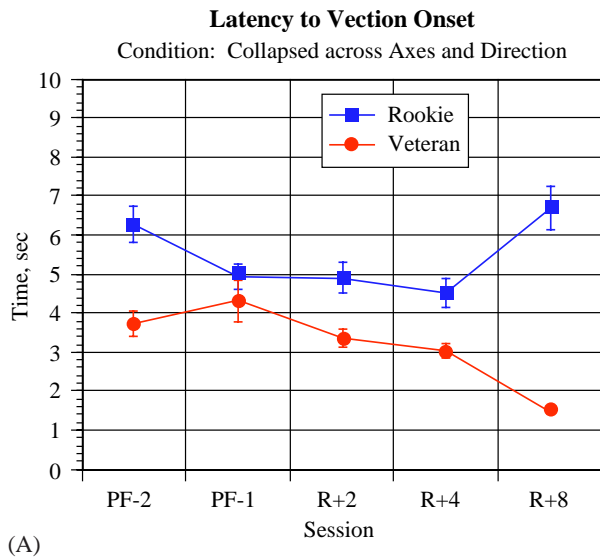


Figure 5.2-13 Mean latency to the onset of vection (A) and to maximum vection (B) preflight and postflight (produced by the device for orientation and motion environments [DOME]) for the rookie and veteran astronauts.

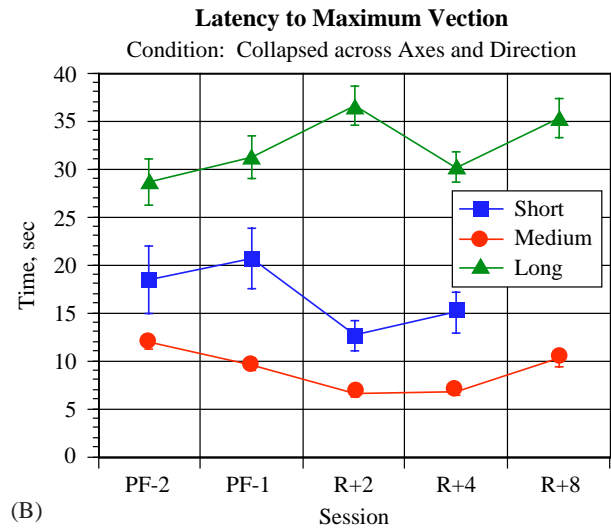
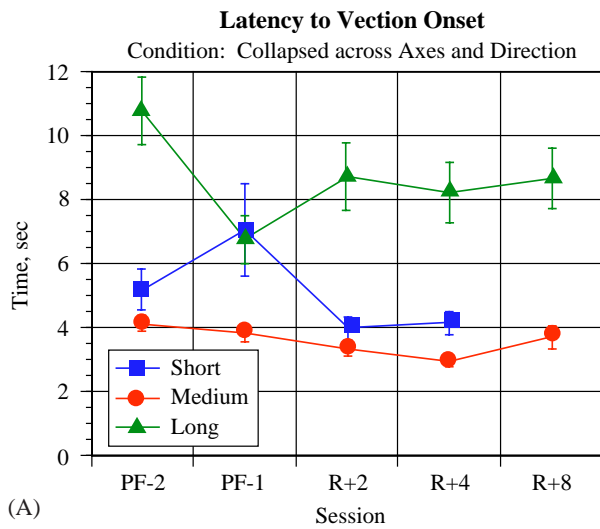


Figure 5.2-14. Mean latency to the onset of vection (A) and to maximum vection (B) preflight and postflight (produced by the device for orientation and motion environments [DOME]) for astronauts on short, medium and long duration missions.

Section 5.3

Neurovestibular Dysfunction

Visual-Vestibular Integration as a Function of Adaptation to Space Flight and Return to Earth

(DSO 604 OI-3)

Millard R. Reschke, Jacob J. Bloomberg, Deborah L. Harm, William P. Huebner, Jody M. Krnavek, and William H. Paloski of the Johnson Space Center, Houston, TX; Alan Berthoz of the Laboratoire de Physiologie de la Perception et de L'Action, College de France, Paris

BACKGROUND

Research on perception and control of self-orientation and self-motion addresses interactions between action and perception [1]. Self-orientation and self-motion, and the perception of that orientation and motion are required for and modified by goal-directed action. Detailed Supplementary Objective (DSO) 604 Operational Investigation-3 (OI-3) was designed to investigate the integrated coordination of head and eye movements within a structured environment where perception could modify responses and where response could be compensatory for perception. A full understanding of this coordination required definition of spatial orientation models for the microgravity environment encountered during spaceflight.

The central nervous system (CNS) must develop, maintain, and modify as needed, neural models that may represent three-dimensional Cartesian coordinates for both the self (intrinsic) and the environment (extrinsic). Extrinsic coordinate neural models derive from the observer's ability to detect up/down vector signals produced by gravity (g) and visual scene and polarity (VS). Horizontal coordinates are incompletely specified by the up/down vector. Additional complexity is introduced because extrinsic coordinate models derive from multimodal processes. For example, detection of gravity is mediated by graviceptors at several locations in the body, including the vestibular apparatus (Gves), somatic receptors (Gs), and visceral receptors (Gvic) [2, 3]. Intrinsic coordinate models must be more complex because they may be eye centric, head centric, torso centric, and so on [4]. Intrinsic coordinate models also should differ from those for extrinsic coordinates in that X-, Y-, and Z-axis vectors are all nonarbitrary and physiologically specified [5].

Effective action in the normal environment requires mapping of relationships between models for intrinsic coordinates relative to the model for extrinsic coordinates. The resulting maps may be used in at least two ways: perception of body orientation, and determination (settings) of initial conditions for central motor control command system(s). Eye/head movements during visual target acquisition, limb movements during reaching for targets, and locomotion toward goals all require motor control.

While earlier studies suggested a common (shared) central motor command system, more recent research suggests parallel command pathways, at least for the head and eye during visual target acquisition control [6].

Recent advances in neuroscience suggest that central neural processing involves activity in multiple, parallel pathways, also known as distributed functions or distributed networks [7]. Based on these advances, and the evidence for parallel motor control systems, we postulated multiple, parallel maps relating intrinsic and extrinsic coordinate neural models. These parallel maps may be associated with different processes, including perception of whole body motion, limb target acquisition, and head/eye target acquisition. For effective reaching or locomoting toward a target, the map that provides initial conditions for the limb motor control system would require weighting of the intrinsic Z body axis. For effective looking for a target, the map that provides initial conditions for head/eye motor control would require weighting of the intrinsic Z head and retinal meridian axes.

Self-orientation and self-motion perception derives from a multimodal sensory process that integrates information from the eyes, vestibular apparatus, and somatosensory receptors. Perhaps due to these underlying multimodal processes, self-orientation perception is not referred to any single receptor or body location [8] in the sense that a tactile stimulus is referred to a location on the body surface, or that visual stimuli are referred to the eyes. For example, self-orientation with respect to gravitationally defined vertical can be reported employing numerous procedures such as setting a luminous line, positioning a limb in darkness, or verbally reporting perceived head position in darkness.

Useful reviews of spatial orientation research by Howard and Templeton [9], Guedry [10], and Howard [4, 11] include the following:

1. Observers are able to report perceived orientation with respect to extrinsic reference vectors (axes) defined by gravity, visual scene polarity, and tactile polarity, and to intrinsic reference vectors such as the eye, head, or torso Z axes (Z_e , Z_h , and Z_t , respectively).
2. Reports can be obtained verbally as well as by movements of the eyes, movements of the limbs, manipulation

of a tactile stimulus (rod) and movement of a visual line, and report accuracy can be judged with respect to the reference vectors.

3. Reports indicate a compromise when visual and gravitational reference vectors are not parallel, as in rod and frame studies, and tilted room experiments.

4. Studies show that discrepancies between gravity and internal Z-axis vectors may also influence reports. For example, reported tilt of a truly vertical line in the direction opposite to the head tilt implies that the subjective visual vertical is tilted in the same direction as the head tilt. This A (Aubert) effect predominates when body tilt is large ($> 60^\circ$) [4], and can be understood by relating extrinsic G- and intrinsic Z-axis vectors [12, 13].

5. Observers are able to estimate accurately rotational displacement solely on the basis of semicircular canal cues within known limits of rotational velocity and amplitude [10]. Consequently, whole body rotation can be used in microgravity, analogous to static head tilt on Earth, to produce a disturbance, compensation for which indicates weighting of neural signals that indicate extrinsic VS and intrinsic Zt reference vectors as well as changes in their weighting during microgravity adaptation [14].

Reviews of recent research concerning sensorimotor adaptation in microgravity [15-18] suggest that in the absence of a gravitational reference axis (G), astronauts initially exhibit increased reliance on visual reference axes derived from VS coordinates [15, 19], and that during prolonged microgravity exposure, reliance may shift toward intrinsic reference vectors, including Ze, Zh, Zt [20-22]. Alteration of sensory processing, such as labyrinthectomy, or rearrangement of environmental features, as in prolonged exposure to microgravity, requires adaptation for effective motor control. One aspect of adaptation may involve re-mapping of intrinsic and extrinsic coordinate relationships. In the normal adapted state, parallel maps are likely to be congruent. During adaptation, these maps may differ and adaptation may be complete when the parallel maps are once again congruent.

Perceptual and oculomotor response discrepancies, observed during adaptation to stimulus rearrangements, support these concepts. Except in the case of ocular torsion and perceived tilt [23], perceptual and oculomotor responses are normally approximately congruent [10]. However, response incongruence has been noted during adaptation to unilateral loss of vestibular function when the spinning sensation gradually subsides, while peripheral asymmetry, as revealed by eye movement records, remains [24]. Similar response incongruence has been observed following exposure to stimulus rearrangements, including the inertial visual stimulus rearrangement produced by microgravity.

Perhaps the most dramatic case of perceptual oculomotor response incongruence was reported by Oman et al. [25]. After 1 to 3 hours of wearing goggles that

produced a left-right reversal of the visual field, subjects exposed to a moving stripe display reported illusory self rotation in the same direction as the observed stripe motion. However, no subject showed evidence of reversal of the VOR slow phase component. More recently Oman and Balkwell [26] reported that during microgravity, a nystagmus dumping procedure consisting of a 90° forward head pitch following a sudden stop from $120^\circ/\text{sec}$ rotation, resulted in an almost instantaneous termination of perceived self rotation. However, post-rotatory nystagmus durations were as long as those observed before and after spaceflight when the head was held erect (no dumping). These and related observations led Peterka and Benolken [24] to suggest that the neural mechanisms underlying central compensation may not be fully shared by vestibular reflex and self-motion perception systems. Our suggestion of re-mapping the relationships between intrinsic and extrinsic coordinate neural models appears to be a variation of their hypothesis.

If the fully adapted state is characterized by congruence among parallel maps, one implication is that different re-mapping processes may occur across different time intervals during adaptation. Given that the re-mapping processes suggested here would be a form of sensorimotor learning, that would almost certainly be true. Of the conditions that facilitate sensorimotor learning, active, voluntary motion is among the most important [27]. The rate of re-mapping would be dependent upon the classes of voluntary actions performed. If an observer were to engage only in head/eye target acquisition behaviors, one might expect that the map serving the head/eye motor control system would be altered sooner than would the map serving limb motor control.

The vestibulo-ocular reflex (VOR) serves to maintain a clear image on the retina by producing eye movements that compensate for perturbations of the head. The VOR is mediated by vestibular information relying on appropriate canal-otolith interaction for effective gaze stabilization. On Earth, the direction of the gravity vector sensed by the otoliths is thought not to vary during yaw head oscillations [28]. Several investigations of the effects of microgravity on yaw VOR have been conducted. In-flight experiments have relied on voluntary head oscillations at frequencies ranging from 0.25 to 1 Hz [29-33]. Passive rotation has also been employed before and after spaceflight [33]. Head oscillations were performed with eyes open fixating a wall target where gain was presumably 1.0, and with eyes open in darkness or eyes closed while imagining a wall-fixed target. Few studies have detected significant preflight or postflight changes in yaw VOR [29, 32, 33]. When changes were noted, the direction of the change varied between subjects [34].

In an experiment conducted aboard the U.S. Space Shuttle, a subject who was instructed to use an imaginary wall-fixed target during head oscillations, exhibited decreased VOR gain at 0.25 Hz on his first test six hours

into the mission [31]. VOR recovered to preflight levels by flight day 7. This finding of decreased VOR gain early in microgravity was consistent with the parabolic flight and centrifuge results of others who have demonstrated decreased VOR gain with decreasing gravity [35, 36]. Since no phase shift accompanied the in-flight reduction in VOR, suppression of vestibular input by the subject may have occurred. The subject was trained as a pilot, so suppression to avoid sensory conflict could have been learned. It is also possible that the subject could not imagine a wall-fixed target in the absence of gravity [31].

Parabolic experiments by DiZio and colleagues [37, 38] demonstrated that the apparent time constant of post-rotatory nystagmus (PRN) in yaw and pitch was shortened during, but not after, acute exposure to microgravity. Yaw axis PRN to a step velocity rotation, using a hand-spun rotating chair, was monitored in flight in one crew member on a Shuttle mission. The results indicated no change in gain and were suggestive of a shortened time constant in flight. The nystagmus dumping phenomenon appeared during flight, suggesting that it could be triggered by processes related to the active head movement rather than by gravity *per se* [39].

Comparisons of preflight and postflight PRN among nine Shuttle astronauts have shown a residual shortening of the apparent time constant, but no consistent change in the magnitude of the initial peak slow phase velocity response during the first several days after return from a week-long flight [40, 41]. The effects were thus qualitatively similar to those observed by DiZio et al. [37, 38] in parabolic flight. Responses gradually returned to preflight norms during the first week after landing. Oman et al. [42] have speculated that as a consequence of the altered gravireceptive input in microgravity, the CNS may have reduced the vestibular component driving central velocity storage in favor of visual inputs.

In contrast to yaw, pitch head oscillations in normal gravity produce changes in the direction of the gravity vector sensed by the otoliths. The microgravity environment offers an ideal way to investigate the contribution of the otoliths to pitch VOR [28]. In-flight investigations of pitch VOR have employed voluntary head oscillations at frequencies comparable to those described above for yaw. While in-flight and postflight changes have not been observed in some instances [32], other investigations have noted alterations in the vertical VOR. Two subjects exposed to pitch oscillation at 1 Hz demonstrated significantly increased VOR gain in tests 14 hours after landing, compared to day 5 and 7 during flight [28]. In these experiments, an increased phase lag was present during the in-flight tests. However, the change in vertical VOR gain and phase relationship was not statistically significant due to high dispersion of data.

A decrease in vertical VOR gain for 0.25 Hz pitch oscillations was observed with a subject tested on STS-51G [31]. His gain was diminished for the first four days

in flight, after which the gain slowly returned to preflight levels. The results of both experiments conflicted with the increased VOR gain observed during the zero-gravity portions of parabolic flight aboard the KC-135 for pitch oscillation at 0.25 Hz [43]. Possible explanations for these conflicting results include: (1) learned suppression of vestibular input by the STS-51G subject [31], (2) occurrence of adaptation before in-flight measurements on Spacelab-1 (SL-1), (3) testing at a frequency (1 Hz) for which the canals were dominant, or (4) the potential difficulty in imagining a wall-fixed target during spaceflight in the same manner as on Earth [28].

It is hypothesized, based on the work of Guedry [44, 45], Benson and Bodin [46], and Bodin [47] that the differences anticipated between the horizontal and vertical canals are based on differing organizations of the compensatory responses to angular motion about the yaw (Z) axis when compared to the responses in pitch (Y) and roll (X) axes. In the normal upright position, motion in yaw occurs typically without any major changes in the direction of the gravity vector. During oscillation in the other two axes, there is concordant information supplied to the CNS by the vertical canals and otoliths. In a microgravity environment, the canals continue to supply input about the direction and magnitude of rotation while the otoliths, depending on their resting sensitivity level, will not provide the expected information, leading to alteration in VOR function.

Gaze is the direction of the visual axis with respect to space. It is defined as the sum of eye positions with respect to the head, and head position with respect to space. Coordinated eye-head movements toward an offset visual target usually consist of a combined saccadic eye and VOR response that shifts gaze onto target. It has been previously demonstrated that exposure to microgravity of spaceflight induces modification in eye-head coordination during target acquisition [48, 49] and ocular saccadic performance [50]. To achieve this sensorimotor transformation, current models of eye-head coordination postulate that a vestibular signal, specifying head movement relative to space, serves as an integral component underlying saccadic spatial programming during head-free gaze shifts [51, 52]. In these models, desired gaze position is compared to an internal representation of actual gaze position. Actual gaze position is derived by summing an efferent copy of eye position in the head with a vestibularly derived reconstruction of current head position. The difference between desired and actual gaze position produces a gaze position error signal that drives saccadic motor output until the error signal is nullified and eye movement stops.

Recent studies support these models by demonstrating that saccadic eye movements generated in total darkness successfully acquire a just-seen Earth-fixed target after cessation of head angular [53, 54] and linear displacement [55]. Such saccadic eye movements are spatially targeted using remembered semicircular and

otolithic vestibular information. The demonstration of this capability indicates that a functionally meaningful vestibular signal has access to the saccade generating mechanism and may, therefore, play a pivotal role in eye-head gaze shifts.

Given these documented disruptions that occur in VOR function during spaceflight and the putative vestibular coding underlying saccadic spatial coding, the first goal of this study was to investigate components of the eye and head target acquisition system during and following adaptation to microgravity.

Using a special oculomotor mechanism located within the brain, it is possible to fixate the eyes on a small object of interest that is moving relative to a fixed background and follow it voluntarily, without moving the head (smooth pursuit response). This mechanism is primarily driven by differences between the velocity of the object (target) and the instantaneous eye velocity. However, we normally track moving objects of interest with a combination of eye and head movements to keep the object near the center of our field of view and our eyes centered within the skull's orbit. When we rotate our head to track a target, a different reflexive mechanism, driven by the signals initiated within the vestibular system, called the vestibulo-ocular reflex (VOR), acts to counter-rotate the eyes in an attempt to keep unchanged the gaze position, defined as the position of the eye with respect to space. In order to track the moving target during a concurrent head motion, the eye movement command signal from the VOR must in some way be nulled to allow gaze position to change with target position. Studies have shown that the primary signal responsible for cancellation of the VOR during eye-head tracking originates within the smooth pursuit system [56-58], although other signals may also contribute [59-61], and the internal gain of the VOR may be somewhat attenuated [58, 62]. The saccadic system provides a mechanism, anatomically represented by the foveal portion of the retina, that rapidly corrects for gaze position errors by coding ballistic eye movement commands based upon perceived position differences between the target and the center of focus. These saccadic eye movements can be used to correct gaze for limitations in the ability of the smooth pursuit system to provide sufficient eye movement command signals to cancel the command signals from the VOR.

In results reported by Russian investigators [63], changes in pursuit tracking of vertical pulsed movements of a point stimulus were manifested early in flight, on days 3 and 5, by decreased eye movement amplitude (under-shooting) and the appearance of correction saccades. Also during flight, pursuit of a vertically or diagonally moving point stimulus deteriorated while associated saccadic movements were unchanged. The effects of microgravity on the pursuit function were most pronounced early in flight on day 3, after long exposure to microgravity on flight days 50, 116, and 164, and also after flight. Pursuit

was found to be improved following in-flight execution of active head movements, indicating that the deficiencies in pursuit function noted in microgravity may have been of central origin [63]. Further analyses of these data indicate that, although postflight tracking seemed to provide gaze changes comparable to target motion, the relative contributions of saccades and smooth pursuit eye movements to the overall gaze changed relative to preflight values. Postflight gaze relied much more heavily upon saccadic contributions, generated due to position errors, that were both more frequent and of larger amplitude. Also, slow phase eye velocity was actually in the opposite direction of head motion, indicating that the VOR was incompletely canceled by the smooth pursuit system. The latter suggests that adaptation to spaceflight caused either an appreciable change in the gain of the VOR, a reduction in the efficacy of the smooth pursuit system, or both.

In contrast, tests of two cosmonauts in the Mir Station, during the ARAGATZ mission, showed that horizontal and vertical smooth pursuit were unchanged in flight [64]. However, results of corresponding saccadic tasks showed: (1) a tendency toward over-shooting of a horizontal target early in flight with high accuracy later in flight, (2) increased saccade velocity, and (3) a trend toward decreased saccade latency.

The stability of the visual world during voluntary eye and head movements depends upon a complex physiological integration of stimuli and perception that is interrupted by the brain in response to changes in the inertial environment. Performance of the ocular motor system undergoes constant recalibration and adjustment to assure optimal visual capability during adaptation to microgravity and subsequent return to Earth. Adaptation of vestibulo-ocular motor motility in one inertial environment is not appropriate for proper physiological function in another inertial environment. Further, erroneous perception of self-motion or surround motion drives compensatory eye movements that are inappropriate for the new inertial environment. This leads to an additional degradation of sensory-motor function.

Physiological failure of eye movement is best defined by considering function. The vestibular, optokinetic, and visual fixation systems act to hold images of the seen world steady on the retinal fovea. Their function is to hold gaze steady. Saccades, smooth pursuit, and vergence work together to acquire and hold objects of interest on the fovea. Their function is to shift gaze. DSO 604 OI-3 was designed to investigate the ability of spaceflight crew members to perform both of these functions. Specifically, physiologic failure of eye movement function occurs during and immediately following a gravito-inertial transition, such as exposure to microgravity and return to Earth. At such times the ability to perform one or more of the following functions has been compromised: (1) hold an image on the retina when the head is stationary, (2) hold an image on the retina during brief head movements, (3)

hold an image on the retina during sustained rotation of self or surround, (4) hold the image of a moving target on the retina, (5) bring images of objects of interest onto the fovea, or (6) maintain accurate perceptions of self-motion and surround motion. The final common pathway of dysfunction in all of these responses is failure to acquire and/or maintain an image of interest on the fovea.

A vestibulo-ocular sensory-motor system that is inappropriately adapted for the inertial environment can result in errors during spaceflight activities, including errors in spatial orientation, delays in visually capturing operationally relevant targets, switch throws, satellite capture, object location, or manipulation of objects. During reentry, errors can occur in acquiring information from instrumentation, switch throws, eye/head/hand coordination, attitude control, perception of altitude, pursuit of an object that is either moving or stationary relative to the crew member, or delays in pursuit and capture of visual, tactile, or auditory targets. Errors during nominal egress activity may include difficulty with visual target acquisition, pursuit of a moving object, or inappropriate perceptions that can result in inappropriate head stabilization strategies, which in turn can affect postural stability and locomotion. Errors during emergency egress may cause problems that could result in personal injury.

Risk of operational failure is hypothesized to be related to: (1) flight duration—the longer the flight the higher the risk, (2) smoke, darkness, crew complement, and circumstances where the Shuttle is in an unusual attitude, and (3) prior spaceflight experience. Risk is the end product of inappropriate response patterns leading to failure in an operational setting. Eye movements must be accurate and precise or the crew member will become susceptible (i.e., at risk) to the dangers of the flight environment. Greater risk is associated with environments that require constant vigilance, timely responses, and accurate visual target identification and/or location. Therefore, risk is defined in terms of the ability of the crew members to correctly perceive their orientation in three-dimensional space. Specifically, orientation is considered to involve the correct determination of the dynamic position and attitude of self or spacecraft in three-dimensional space. The key word here is “dynamic,” implying full knowledge of self-motion, or motion of the spacecraft, as well as the static position of instruments and a geographical point of reference.

Crew member loss of veridical orientation is operationally defined as spatial disorientation. For convenience, and consistency of nomenclature designators of spatial disorientation in the spaceflight environment, spatial disorientations are assigned to one of two categories. Spatial disorientations in the Type I category refer to loss of orientation without the knowledge of the crew member. In this case crew members fail to sense correctly their position in space, may improperly locate instrumentation and geographical references, and then may act on erroneous perceptions. In the Type II disorientation category, crew

members recognize that they are disoriented and can resolve the sensory conflict. It is important to recognize that it is possible, indeed highly likely, that spatial disorientation can and does occur without the knowledge of either the pilot/commander or other members of the crew. Even when crew members are entirely cognizant of the immediate consequence of their spatial disorientation, and recognize that with head movements vision is blurred or that they have thrown an incorrect switch, it is frequently assigned less importance than it merits, and the importance declines with distance from the incident. In part, avoidance of spatial disorientation requires accurate and timely foveation of visual targets. Anatomical, physiological, and physical parameters define the minimal criteria for performance that will maximize foveation and veridical perception of true spatial orientation.

Anatomically, the fovea of the eye has variously been reported to subtend a visual angle ranging from $\pm 0.25^\circ$ to $\pm 4.0^\circ$, depending on the author or measurement technique. However, it is clear that a linear function (as described psychophysically) shows that by the time gaze has deviated by as little as 1.0° from absolute foveal center, visual acuity falls off by a factor of two to three. Therefore, clear unambiguous perception requires that the selected target be maintained within approximately $\pm 0.5^\circ$ relative to central foveal gaze. Physiologically, time to foveate a target depends upon the command process issued for target acquisition. Typically, only about one ten-thousandth of our visual field is clearly seen, but we are not at a loss because our eyes continually move (small saccades) to point the area of the central fovea toward the object of interest. However, physiologically, the cost of the small corrective saccades is approximately 200 msec/saccade. Physically, target acquisition depends upon the location (distance and direction the head and eye must be rotated to foveate the target) and the type (spatial frequency) of the target.

A number of investigators have assessed the role of vestibular-based subsystems both during and immediately following exposure to microgravity [17, 18, 65]. While these assessments provide information specific to one or more sensorimotor subsystems, there is little documentation of changes in the strategies used for coordination among subsystems or for those strategies supporting performance of natural, goal-directed behaviors. Among the several strategies selected for use during the process of adaptation to microgravity are: (1) reduced use of head movements during early phases of the mission, (2) reliance on either an internal coordinate system (intrinsic) or environmental coordinates (extrinsic) during different phases of space flight for spatial orientation, and (3) compensation for the changing role of proprioceptive information during flight. Strategies developed during spaceflight are transferred to behavior immediately following a return from orbit. The newly acquired behavior is not appropriate, and responses, particularly in off-nominal situations, will result

in performance decrements. These strategies can be evaluated using goal-directed head and eye coordination tasks. Therefore, the primary objective of this study was to investigate the emergence or alteration of goal-oriented strategies required to maintain effective gaze when the interactive sensorimotor systems required for this function were modified following exposure to the stimulus rearrangement of spaceflight, and to relate changes in the newly developed strategy to changes in parameters that would degrade performance.

METHODS

A number of experiment paradigms classified as voluntary head movements (VHMs) were selected and designed to investigate changes in spatial orientation and strategies as a function of exposure to the stimulus rearrangement encountered during spaceflight. The primary protocols of DSO 604 OI-3 included target acquisition, gaze stabilization, pursuit tracking, and sinusoidal head oscillations. In all cases, participating crew members completed, as a minimum, each protocol three times before flight and three times after flight. When OI-3 was performed in flight, an additional two sessions were required before flight so that protocols could be practiced and data collected within the training mockups of the Shuttle middeck. When collected in flight, data were obtained at least twice—less than 48 hours after launch, and approximately 24 hours before landing. Additionally, data were collected to measure gaze stabilization during entry, starting at Shuttle entry interface minus 5 minutes, and immediately following wheels stop, before seat egress.

The astronauts who volunteered to participate in each of the protocols were provided with informed consent agreements, given a briefing on the intent and purposes of each protocol, and were free to withdraw from the study at any time. All subjects had completed a recent Air Force Class II physical examination, were free from any central nervous system problems, and had normal vestibular function. For those with visual correction, all protocols were completed with the correction in place. The number of subjects participating in each of the three OI-3 protocols are listed in Table 5.3-1 by flight.

Target Acquisition

Acquisition targets were permanently fixed to a tangent screen at predictable angular distances in both the horizontal ($\pm 20^\circ$, $\pm 30^\circ$, and $\pm 60^\circ/68^\circ$) and vertical ($\pm 15^\circ$, $\pm 20^\circ$, and approximately $\pm 55^\circ$) planes (Figure 5.3-1). To easily differentiate between targets, each was color coded ($\pm 20^\circ$ green, $\pm 30^\circ$ red, etc.), corresponding to the degree of angular offset from center.

Table 5.3-1. Operational investigations (OI) performed on designated flights and total number of subjects

Mission	OI-3a	OI-3b	OI-3c
STS-43		1	
STS-44	1		
STS-49		1	
STS-52		2	
STS-53		1	
STS-54	1		
STS-57		2	
STS-51	1		
STS-58		1	
STS-61		3	
STS-62		4	
STS-59		2	
STS-65		1	1
STS-68			2
STS-64		3	
STS-66		2	
STS-67			3
STS-69		3	
STS-73			2
STS-72			2
<i>Totals</i>			
20	3	26	10

OI-3a - Preflight, In-flight, Entry, Wheels Stop, Postflight

OI-3b - Preflight, Postflight

OI-3c - Preflight, In-flight, Postflight

For all target acquisition tasks, the subject, using a time optimal strategy, was required to look from the central fixation point to a specified target indicated by the operator as quickly and accurately as possible, using both the head and eyes to acquire the target. Each of the 12 targets was acquired a minimum of two times. When target acquisition was performed during flight, measurements were obtained using a cruciform target display on the mid-deck lockers. In all cases eye movements were obtained with both horizontal and vertical electro-oculogram (EOG). Head movements were detected with a triaxial rate sensor system mounted on goggles that could be fixed firmly to the head. Both the head (using a head-mounted laser) and eye movements were calibrated using the color coded acquisition targets.

Gaze Stabilization

Ocular stabilization of a stationary target, during active yaw and pitch head movements, was investigated using a gaze stabilization paradigm with the following steps: (1) the subject visually fixated a wall-fixed target with head in a central position, (2) when the goggles became opaque and vision occluded, the subject rotated

the head while maintaining pursuit. When the gaze seen wall-fixed target, (3) when the goggles became clear, the subject refixated the target, if necessary, with eyes only, and (4) the head was rotated back to center, keeping eyes on the target. During testing before and after spaceflight, and during flight, subjects performed a minimum of six trials in ya
pitc

stabilization protocol was performed during entry, horizontal and vertical trials were alternated. A single fixation point was affixed to the Shuttle forward middeck lockers, directly in front of the subject at a neutral gaze position. The trials began at the Shuttle entry interface and continued nonstop until 5 minutes had elapsed or the Shuttle had landed. Following Shuttle roll-out (wheels stop), the gaze stabilization trials, patterned after those accomplished during entry, were performed for 5 minutes. The entry and wheels stop protocols were difficult because the head movements were performed inside of the helmet, using special goggle devices to assist in recording head and eye movements. As expected, the helmet restricted head movement amplitude.

Pursuit Tracking

Pursuit tracking studies, designed to measure the effectiveness of both smooth pursuit eye movements and combined eye-head tracking in acquiring and maintaining gaze on a moving target, were conducted before and after flight. All trials required the crew member to track the apparent smooth movement of a laser projected on a blank neutral gray tangent screen, first with just the eyes (smooth pursuit), and subsequently using eye movements in concert with active, self-generated head movements (combined eye-head tracking). The subject was positioned 86 cm from, and facing, the tangent screen. Two types of target motion trials, unpredictable and predictable, were presented for each plane of motion.

For stimuli requiring unpredictable target tracking, the target was initially stationary in the center of the field of view (Figure 5.3-2). At an unpredictable time, the target began to move at constant velocity, either to the right, left, up, or down [66] as determined by a schedule of systematic randomization. The target traveled at either 15°/sec or 30°/sec, through a minimum displacement of 30° horizontally or 20° vertically. The onset time of target motion, direction of motion, target velocity, and final target displacement were randomized to eliminate the possible effects of predictive mechanisms, known to affect pursuit tracking responses [67, 68].

In trials involving predictable target motion, the target initially moved horizontally with respect to the subject, then repeated using vertical target motion (Figure 5.3-3). The target oscillated sinusoidally at two separate and individual frequencies at rates that held peak velocity essentially constant at approximately 63°/sec. The frequencies

were 0.333 Hz through $\pm 30^\circ$ horizontally and $\pm 20^\circ$ vertically, and 1.4 Hz through $\pm 7.14^\circ$ horizontally and vertically. Each trial of sinusoidal tracking was performed twice with a minimum of 6 cycles per trial.

Sinusoidal Head Oscillations (Head Shakes)

To perform this test, the subject was first positioned with the wall-fixed target located at the center of the visual field. The subject then attempted to maintain visual fixation on the target while smoothly oscillating the head in either the horizontal or vertical plane, in cadence with an audio tone (1-2k Hz) that was sinusoidally modulated at each of either three or four frequencies (0.2, 0.3, 0.8, and 2.0 Hz). Angular displacement of head oscillation was selected by the subject. Following a collection of responses to a minimum of 10 cycles at each frequency, the visual field was occluded by activating the Electronic Light Occlusion Goggles (ELOGs) with a control voltage, making them opaque. Immediately upon occlusion of the visual field, the subject repeated head movements at each of the individual frequencies while attempting to maintain visual fixation on the remembered target. Subjects repeated this entire procedure in each plane for each visual condition twice for a total of three trials. Special attention was paid to cross-axes head movements, corresponding compensatory eye movements, and changes in head movement control.

Calibration of Head Position in Space

Head position measurements were calibrated by activating a low power laser mounted on the browpiece of the plastic web cap firmly affixed to the subject's head. The cap and laser were adjusted so that the laser was located centrally on the forehead, between the eyes. With the subject's head in the zero or neutral position, the laser was adjusted within a swivel mount to align with the 0° target. Visual feedback from the laser allowed the subject to accurately align the head with a given calibration target. Movements were made successively between the central target and each calibration target in both the horizontal and vertical planes. At least two trials to all targets were performed at the beginning of each experiment, and repeated if for any reason the plastic web cap had been disturbed or removed.

Measurement of Head Position

Active head movements were measured using a triaxial rate sensor bundle integrated on the same plastic web cap that housed the positioning laser. The rate sensor was located approximately on the apex of the skull, and adjusted prior to each test session, to minimize cross talk between the yaw, pitch, and roll axes. Software was developed to remove any residual cross talk. Three rate sensors separately transduced yaw, pitch, and roll head velocity movements. From these sensors, horizontal (yaw), vertical

(pitch), and roll head position wave forms were obtained using digital integration techniques, following initial processing performed to remove any offset signal in the rate sensors.

Occlusion of Vision

Because the corneo-retinal potential changes with drastic shifts in illumination and effects EOG measurements, special Electronic Light Occlusion Goggles (ELOGs) were developed, using a polymer dispersed liquid crystal or PDLC. In its normal state, the PDLC was opaque and transmitted up to 98% of the light, much like frosted glass. When an appropriate voltage was applied across this plastic, it became transparent. Transformation from opaque to visible was virtually instantaneous, did not significantly change the relative illumination level to the subject, or alter the measured EOG gains. When vision was occluded with the ELOGs, the visual “scene” was featureless and provided no fixed visual reference.

Eye Movement Measurement and Calibration

Eye positions were measured during all phases of the test, using standard electro-oculography. Disposable infant non-polarizing ECG electrodes were applied to the outer canthus of each eye to measure horizontal eye movements. Vertical electrodes were applied above and below the right eye, equally distant from the pupil during straight ahead gaze, to capture vertical eye movements. A ground electrode was applied to a neutral surface behind the right ear. During flight, signals were amplified with a gain of 4000 and recorded on tape. Before and after flight, signals were directly digitized with a sampling rate of 500 Hz. To remove extraneous high frequency noise, the measured wave forms were digitally filtered before processing with a finite impulse response (FIR) low pass Hamming window filter, with a nominal cutoff frequency [-3 decibel (dB) point] of 30 Hz. Data were passed through the filter twice, once forward in time and once backward in time, to eliminate all phase shifts and double the stop-band attenuation.

Eye movements were calibrated with a tangent screen before and after flight, and with a locker-mounted cruciform target display in flight. The subject was instructed to acquire the target with rapid eye movements and the head held stationary, from the central target (0°) to the $\pm 20^\circ$, $\pm 30^\circ$ targets in the horizontal plane, and to the $\pm 15^\circ$, $\pm 20^\circ$, $\pm 30^\circ$ targets in the vertical plane. At least two trials to all targets were performed at specific intervals during the experiment, to allow characterization of possible variations in EOG eye movement gain.

Because of the well-known drawbacks of using standard EOG, two novel processing techniques were used: (1) a method for determining and constraining a piecewise quadratic curve derived from the nonlinear response

characteristics of vertical EOG, allowing quantitative calibration of the vertical EOG, and (2) an alternate, dynamic technique for generating horizontal and vertical EOG calibration curves by measuring the EOG signals generated when the eyes move to maintain fixation on a stationary target, while the subject slowly oscillates the head in either the horizontal or vertical plane.

Eye Calibration Using Multiple Fixed Targets

Vertical EOG (Figure 5.3-4a), unlike horizontal EOG (Figure 5.3-4b), is characterized by the volts-to-degrees relationships being generally nonlinear, showing dramatically different voltage outputs for identical upward and downward eye movements. In previous attempts to model this relationship, different investigators have used functions such as third order polynomials or piecewise linear curves joined at zero. Both of these functions may introduce large calibration errors because they are either under (cubic) or over (piecewise linear) constrained. The optimization of function and fit was empirically determined by measuring eye movement responses between zero and multiple targets along the vertical axis spanning the oculomotor range necessary to characterize the data obtained for this DSO. The best approximation to the measured volts-to-degrees relationship came from using a piecewise quadratic function, joined at zero degrees, but not constrained to be zero volts there, and having a continuous first derivative through the connection. This curve matched DSO data through the entire oculomotor range, and essentially the same curves were obtained when calculated using only those targets available to the DSO protocol. As expected, the piecewise linear curve did a satisfactory job of characterizing the data midway between the upper and lower ranges, at the expense of errors near zero and at the oculomotor extremes. The cubic curves usually did a satisfactory job of modeling the dense data. However, when the more sparse data sets were used for calculation, the curves were occasionally less “well-behaved” at the ends of the range and could not be used.

Figure 5.3-5 summarizes the effects of using piecewise linear, piecewise quadratic, and piecewise quadratic with continuous first derivative vertical eye calibration curves on a crew member’s target acquisition trial of combined head and eye movements used to acquire a stationary eccentric target. As can be predicted from the corresponding calibration curves, the piecewise linear curve (Figure 5.3-5a) caused the eye movement response to undershoot for low displacements and to overshoot for higher amplitude displacements. Thus, although a piecewise linear structure for the vertical EOG calibration curve accounted for vertical calibration asymmetries, it provided an unrealistic calibration mapping for the data, resulting in considerable differences (errors) in the calculated response wave forms. To obtain a better fit for the calibration segments, the calibration components were

allowed to assume second order curve characteristics (quadratic). As can be seen from Figure 5.3-5b, this technique was better equipped to accurately map the conversion from measured volts to displayed degrees. However, this piecewise continuous curve near zero had a considerable discontinuity in slope, with the negative displacements approaching zero almost linearly while the small positive displacements rapidly “bulged” in displacement for small changes in input voltage above zero. This rapid change in slope was not characteristic of a physiological system in which changes in calibration mapping, due to system nonlinearity, are probably more gradual. For this reason, we constrained the piecewise quadratic curves to have a continuous first derivative (Figure 5.3-5c). As expected, the differences due to these latter two techniques were small except at low displacements where the response from the curve with unconstrained slopes at zero caused a slight increase in displayed displacement. It is for this reason that we scaled all of our vertical EOG data using piecewise quadratic calibration curves with continuous first derivatives at zero.

Eye Calibration Using Fixed Target and Head Movements

An alternate, dynamic technique for generating horizontal and vertical EOG calibration curves was developed. This technique measured the EOG signals generated when eyes were moved to maintain fixation on a stationary target while the subjects slowly oscillated their heads in either the horizontal or vertical plane. As the head rotated through a certain angle, the eyes generally counter-rotated back through the same, but opposite, angle to maintain fixation. Based on this relationship, angular head position was used to determine the expected eye position required to maintain fixation. These expected eye positions were compared with the corresponding measured EOG voltages to yield the volts-to-degrees relationship necessary for calculating a calibration curve (Figure 5.3-6). Satisfactory fits of the calibration data were obtained from cubic polynomials, although we chose to fit the data with polynomials of lower orders when possible. There were two main advantages of using this dynamic calibration technique:

1. A calibration curve was constructed from hundreds, or even thousands, of data points, whereas calibration curves determined from static calibration data normally were based on 20 points or less.
2. Because each subject individually controlled the peak amplitude of head oscillation, a curve was generated to span each subject’s complete oculomotor range. In this way, subjects were not required to view targets outside of their oculomotor range or to view targets that did not reach the limits of their oculomotor range. This is particularly important because it is at the extremes of the oculomotor range that the largest EOG nonlinearities occur in the vertical plane.

EOG Signal Drift

Aside from the nonlinearity of the vertical EOG, another drawback to using EOG was the problem associated with signal drift. Processing software was developed to optimally and simultaneously scale wave forms (calibration trials) and remove drift. This method was based on a “pseudo-inverse” least squares technique, in which the drift over a trial segment was modeled as an arbitrary order, first order default polynomial. A set of polynomial coefficients and a constant wave form scale factor were calculated, over response regions selected by the operator, to optimally match the measured eye position wave form with the expected eye position wave form that was calculated from the known target and measured head positions. This method was much more robust and reliable than techniques that either ignored the drift or separately calculated the underlying drift characteristics and the calibration scale factor.

Head and Eye Geometry Effects

The geometric effects that the eccentric position of the eyes in the head had on the processing of our target-directed eye and head movement data were considered. Although many laboratories have facilities that allow “far” target viewing, in which geometric considerations have little consequence, space constraints have forced the visual targets to be close to the subject, so that the eccentric position of the eye in the head may no longer be considered negligible. Tests of astronauts on the Shuttle were conducted with extreme spatial constraints, the nominal distance from subject to target display surface being 86 cm.

Oculomotor researchers have historically calculated gaze (the angle of the eye with respect to space) as the simple sum of eye and head wave forms. However, because the axes of head rotation and eye rotation are different, and because the subject was closer than optical infinity relative to the targets, the relative locations of these rotational axes, as well as the magnitude of the rotation about the axes, were considered when interpreting gaze values. This was further complicated because the axis from which target positions were specified did not coincide with either the head or eye rotation axes. Several investigators have demonstrated the dangers of assuming that visual targets lie at optical infinity, and they note the importance of considering the eccentric position of the eyes in the head [58, 69-74]. Clearly, gaze displacement and target displacement were not equal, even if the subject maintained fixation on the target, due to eye eccentricity.

Two basic approaches to analyzing data were used to deal with this geometry issue. The first technique involved comparing measured eye movements with expected eye movements, while considering the geometric relationships between the eye, head, and target. This approach allowed for the direct evaluation of oculomotor performance without modifying the measured eye or head wave forms by

calculating the position of the target with respect to the eye, no matter where the eye was in its plane of motion. This same calculation also provided for the spatial relationships between the eye and head, and between the head and target. The second approach involved adjusting the measured eye movement data to compensate for different axes of head and eye rotation [58]. This technique standardized the measured eye (gaze) position data by mathematically relocating the apparent eye position to the center of head rotation. In this way, eye eccentricity effects were eliminated. This approach provided more data analysis flexibility. Direct comparisons of response wave forms were made from multiple trials, both within and between subjects, by inherently accounting for trial-to-trial variations in head or target motion. Both techniques were used to analyze active eye and head movement data.

The information in Figure 5.3-7 demonstrates that when the head was required to rotate during a trial, it was important to consider the location of the eye in the head when processing eye and head movement data. A trial of Gaze Stabilization is depicted in Figure 5.3-7. The subject fixated a centrally located target. When vision was occluded, the subject rotated the head a comfortable but significant amount while attempting to maintain fixation on the stationary target. When vision was regained, the subject generated a refixation saccade to reacquire the target. Because eye movements were recorded using EOG, a cyclopean eye geometry was assumed, and it was appropriate for the eye to be at zero while fixating a zero target with the head at zero. The panel on the left (Figure 5.3-7a) shows gaze calculated as the simple sum of measured eye and head rotations. The refixation saccade took gaze off target rather than back on target as expected, because gaze was calculated and referenced with respect to the location of the eye in space. Because the rightward rotation moved the cyclopean eye rightward in space, it was appropriate for gaze to deviate leftward to reacquire the stationary target. However, this sort of analysis was not particularly intuitive, and the amplitude of the calculated gaze displacement depended upon the amplitude of the corresponding head movement. To facilitate analysis and interpretation and to remove the effects of eye eccentricity, the geometry considerations to calculate gaze were used as though the measurement was from the location of the cyclopean eye, with the head at zero (Figure 5.3-7b). In this example, gaze drifted off target during vision-occluded head rotation. When vision was again restored, gaze reassumed the expected position at zero. This technique was routinely used to standardize measured signals so that data collected from different subjects or under different conditions could be directly compared.

Verbal Responses

Following each experiment trial, crew members were asked to provide verbal quantitative descriptions of

perceived self-motion and/or visual surround motion, or changes in orientation/position. Primarily, they were asked to specify distinct differences between preflight, in-flight, and postflight sensations. Specifically, they were asked to describe the perceived amplitude and rate of the rotational and/or translational components of self/surround motion following head movements.

RESULTS AND DISCUSSION

Sinusoidal Pursuit Tracking

Sinusoidal pursuit tracking data were used to ascertain the relationships between at least three distinct, functional eye movement systems, as well as how the effects of spaceflight changed these relationships. Neural commands drive eye movements to either: (1) rapidly redirect the line of sight (gaze) to different objects within, or outside of, the field of view, using the saccadic system, (2) track targets moving smoothly relative to the person, such as when tracking the “Ball-Bar” navigation system during entry, using the smooth pursuit system, or (3) maintain gaze on stationary objects of interest, such as cockpit switches, despite head motions, using the VOR. These three systems work together in an attempt to provide the appropriate eye movement command signals to allow the maintenance of fixation on targets despite head or target motion. To tease out the relative contributions from each of these ocular motor systems, we considered the differences in their origins. Table 5.3-2 summarizes which of the fundamental eye movement systems can be expected to contribute to a given test wave form collected in response to a given tracking task.

The saccadic system responds to retinal position errors and is the only fundamental eye movement system that relies primarily on position information. Thus, to determine the contribution to overall gaze from the saccadic system, gaze position errors were compared with gaze velocity errors. If gaze position errors were minimal, but gaze errors were substantially greater when represented in velocity, we concluded that the saccadic system was playing a major

Table 5.3-2. Types of eye movements required for pursuit tracking

<i>Tracking Task</i>	<i>Test Waveform</i>	<i>Component Systems</i>
Smooth Pursuit	Gaze Position	SP, Sacc
Smooth Pursuit	Gaze Velocity	SP
Eye-Head Tracking	Gaze Position	SP, VOR, Sacc
Eye-Head Tracking	Gaze Velocity	SP, VOR

SP = Smooth Pursuit System, Sacc = Saccadic System, VOR = Vestibulo-ocular Reflex

role in supplementing the other eye movement systems to keep the eyes directed toward the target. On the other hand, the smooth pursuit system responds to retinal velocity errors. As long as the head was stationary, we could evaluate the efficacy of the smooth pursuit system by comparing gaze velocity with target velocity. Differences (errors) were attributed to reduced performance of the smooth pursuit system.

Performance of the vestibulo-ocular reflex can be evaluated by inference, through its interaction with the smooth pursuit system during eye-head tracking. During sinusoidal eye-head tracking, the subject tracks a sinusoidally moving target with both the head and eyes, rather than with the eyes alone as during smooth pursuit. Because the VOR responds to head motion and is responsible for maintaining fixed gaze despite head motion, the ability to track moving targets with combinations of eye and head movements requires that the reflexive command signals from the VOR in some way be canceled or suppressed to allow gaze to change along with the target. For cases of eye-head tracking, the VOR is actually an unwanted neurological command signal that must be overcome. Although several possible mechanisms exist to overcome the VOR command signal during eye-head tracking, it is believed that under normal conditions a major contribution to VOR cancellation is the command signal from the smooth pursuit system. Thus, gaze errors observed during eye-head tracking may be due to incomplete cancellation of the VOR by the smooth pursuit system, which could result from (1) reduced efficacy of the smooth pursuit system in providing the necessary cancellation signal, (2) increased VOR gain to a level beyond which a normal smooth pursuit cancellation signal can operate, or (3) some combination of the two.

To assess the effects of spaceflight on the interactions of these three ocular motor subsystems, crew member tracking responses were compared before and after spaceflight. To facilitate comparison of the measured responses, the global gain and phase characteristics of measured gaze responses and their separate eye and head components were calculated relative to their corresponding sinusoidal target counterparts. A gain of 1.0 and a phase of 0.0 indicated ideal overall tracking performance, while deviations from these values indicated changes in performance or tracking strategy. Gain and phase values were calculated for gaze position and velocity wave forms, collected in response to both sinusoidal smooth pursuit and combined eye-head tracking tasks, and for target motion in both the horizontal and vertical planes.

Smooth Pursuit – Saccades and Gaze Error

Figure 5.3-8 shows a typical example of smooth pursuit tracking recorded across subjects when the trial called for pursuing the small laser dot in the horizontal plane at a frequency of 0.33 Hz. Of interest is the change in eye amplitude and the increased number and amplitude of

saccades. The panel on the left shows smooth pursuit approximately 10 days prior to spaceflight. The eye, head, and target are represented by the red, green, and blue traces respectively. Horizontal smooth pursuit was similar, but saccadic activity tended to vary somewhat more across subjects. The panel on the right shows pursuit activity obtained approximately 2 hours after landing. Saccadic activity, composed primarily of what we have termed “catch-up” saccades, was increased. That is, rather than anticipating the position (or velocity) of the target, the subject lagged behind the pursuit stimulus.

Figure 5.3-9 shows smooth pursuit tracking in the horizontal plane. The panel on the left indicates tracking 10 days before flight (L-10). Tracking on landing day (R+0) is on the right panel. From the top to the bottom are presented the target wave form, the horizontal eyes, eye velocity, eye error velocity, and eye error position. Eye error velocity was derived by taking the difference between eye velocity and target velocity, and eye position from target position. The increase in saccadic activity is clearly visible between preflight and postflight values. For the most part, the saccadic activity present in the postflight trace represents anticipatory saccades, when the subject was capable of anticipating target position and velocity. Of particular interest is the large error observed in the velocity and position error traces. This error results primarily from saccadic activity. When error was applied in the position domain, it was possible to infer the amount of time the subject spent on the target.

The position error from Figure 5.3-9 is plotted in Figure 5.3-10. It shows integrated cumulative error (total area/time) as a function of the amount of time the smooth pursuit target was not within $\pm 1^\circ$ of foveal center. The postflight (R+0) retinal error was more than twice that observed before flight (L-10). Figure 5.3-11, adapted from Leigh and Zee [75], shows the degradation in acuity with target distance from foveal center. From this figure it is clear that acuity decreases by more than 50% when the target falls beyond the $\pm 1^\circ$ band.

Smooth Pursuit, Eyes Only – Summary Gaze Error and Saccadic Activity

Figures 5.3-12, 5.3-13, 5.3-14, and 5.3-15 show the relationship between saccadic activity and gaze error for four representative subjects. These subjects were selected because they represented examples of a relatively large change through modest or no change. Figure 5.3-12 shows the total number of saccades, both anticipatory and catch-up, observed over three complete cycles at 0.33 Hz of smooth pursuit for both the horizontal and vertical planes. Also shown are the averages of the four subjects with associated standard error of the mean (SEM). While not all subjects showed an increase in total saccades between preflight baseline and postflight measurements, and some actually showed a decrease, there was an overall trend toward increased saccadic activity after flight. It is

interesting to note that there were considerably more saccades in the vertical plane than in the horizontal plane, and that three of the four subjects showed an increase in vertical saccades.

The total saccade count, illustrated in Figure 5.3-12, is composed of both anticipatory saccades, where eye movements jump ahead of the predictable target, and catch-up saccades, with eye movements that lag and must move rapidly to lock on to target once the target has advanced ahead of the pursuit eye movement. Figure 5.3-13 shows the total number of catch-up saccades for horizontal and vertical pursuit tracking during preflight and postflight measurement sessions. Note that overall, the number of catch-up saccades increased by as many as 15 between horizontal plane testing before and after flight. Interestingly, there were more preflight catch-up saccades in the vertical plane than in the horizontal plane before and after flight. However, there was a slight decrease in catch-up activity between preflight and postflight saccades in the vertical plane, across all four subjects.

The relationship between catch-up and anticipatory saccades can be seen in Figures 5.3-13 and 5.3-14. While the total number of catch-up and anticipatory saccades was independent, there was a tendency to decrease anticipatory saccades when catch-up saccadic activity was high. The inverse was also observed. Note that this relationship is evident between catch-up and anticipatory saccades in the vertical plane.

Both the total number of saccades and their amplitude combine over time to create cumulative gaze error. Figure 5.3-15 shows the dramatic increase in cumulative retinal error between preflight and postflight testing in both the horizontal and vertical plane. For cumulative gaze error time calculations, deviations of $\pm 2^\circ$ from estimated foveal center were used, rather than the $\pm 1^\circ$ band width illustrated in Figure 5.3-9. Note that there were substantial increases in total error between preflight and postflight measurements, and that the increases, as expected, were greater in the vertical than in the horizontal plane. The immediate operational impact of increased gaze error was reduced visual acuity. Referring to Figure 5.3-11, and using the $\pm 2^\circ$ error band, these four subjects, on average, were off target over 50% of the time, and visual acuity was reduced by more than 75% from that expected based on preflight measures.

Smooth Pursuit – Gain and Phase

The position results, depicted in Figures 5.3-8 and 5.3-9, indicate the efficacy of the saccadic and smooth pursuit systems acting together to maintain gaze on target. The preflight gains were all near 1.0, and the only apparent phase differences were from small head movements which had insignificant gain. The postflight position gains were slightly reduced (Figure 5.3-9), suggesting that the saccadic system did contribute somewhat to the reduction of gaze position errors, but it could not contribute enough

to maintain gaze on target after flight, and may have contributed to pulling gaze away from the target (Figure 5.3-15). These observations are summarized for four subjects in Figure 5.3-16.

When the saccades were removed by processing the data in the velocity domain, the efficacy of the smooth pursuit system acting alone was observed. Before flight, the performance of the smooth pursuit system was comparable to that observed when saccades were available, indicating that there was a very small saccadic contribution to the horizontal maintenance of gaze during eyes only (smooth pursuit) tracking. After flight, there was a much larger (as much as 50%) decrement in the gain of the gaze wave form, indicating that the saccadic system was necessary to augment the postflight smooth pursuit response and reduce gaze position errors.

From the vertical smooth pursuit results depicted in Figure 5.3-17, it is apparent that gaze position was well maintained on target by contributions from both the saccadic and smooth pursuit systems. However, when saccades were removed, the performance of the smooth pursuit system alone was revealed (Figure 5.3-17b). Significant decreases in gain indicate that for vertical smooth pursuit, the smooth pursuit system relied on contributions from the saccadic system to keep the eyes directed toward the target, even before flight. This decrement in vertical plane performance, relative to horizontal tracking, is generally observed among the normal population. After flight, there was a larger attenuation of gain (as much as 80%), suggesting that there was an even stronger reliance on the availability of the saccadic system to generate eye movements to match the line-of-sight with the target. Even with the saccadic system available, postflight position gains depicted wide variability. This suggests that crew members, especially subject B, adopted different head stationary tracking strategies postflight that relied on the saccadic system in varying ways.

Eye and Head Sinusoidal Tracking

Figure 5.3-18a illustrates the effect of spaceflight on pursuing a predictable target of changing velocity, with both head and eyes. During sinusoidal eye-head tracking, the subject tracks a sinusoidally moving target with both the head and eyes, and the vestibulo-ocular reflex responds to head motion and is responsible for maintaining fixed gaze despite head motion. Therefore, the ability to track moving targets with combinations of eye and head movements requires that the reflexive command signals from the VOR in some way be canceled or suppressed to allow gaze to change along with the target. For cases of eye-head tracking, the VOR is actually an unwanted neurological command signal that must be overcome. However, phasic differences between the head and the target often make use of the VOR. In Figure 5.3-18a the left panel shows preflight tracking of the laser point stimulus at 0.33 Hz, 20° peak. Target, head, eye, and gaze are

represented by the black, red, blue, and green traces, respectively. The VOR is present before flight, and gaze only slightly lags the target. It is also apparent that the VOR is functional, and that gain is close to unity, evident not only in the gaze peak amplitude, but also in the lack of saccadic activity in the gaze trace. After flight (R+0) the saccadic activity was apparent, driven by both the catch-up and anticipatory saccades observed during smooth pursuit results (Figure 5.3-18a right panel). Spaceflight clearly increased both gaze error and gain, whereas phase lagged.

Figure 5.3-18b shows a single cycle from a subject different than that illustrated in Figure 5.3-18a. The primary difference between these two examples is the suppression of the VOR during the preflight (L-10) testing (Figure 5.3-18b). Postflight, gaze may in fact be maintained because the VOR compensated for the reduced peak-to-peak displacement (reduced velocity and gain) of the head.

Smooth Pursuit, Eyes and Head – Saccades and Gaze Error

Figure 5.3-19 shows the total number of saccades, before and after flight, over three complete cycles of the sinusoidally moving laser point stimulus, with a 20° peak displacement in the vertical and a 30° peak displacement in the horizontal planes. The same four subjects analyzed above in eyes-only smooth pursuit were used. Vertical bars, superimposed on the average of the four subjects, represent SEM. In keeping with the eyes-only smooth pursuit results, there was an overall average increase in saccadic activity after flight. Also in the horizontal plane there was an average of 35 saccades after flight as compared to 19 before flight. Figure 5.3-20 shows the number of catch-up saccades, and Figure 5.3-21 the number of anticipatory saccades, over three complete cycles. In both cases there was an overall increase in both types of saccadic activity, in both planes and across spaceflight conditions postflight, compared to the preflight value. However, unlike the saccadic activity in the eyes-only pursuit, most of the activity with the head and eyes acting together was clearly related to catch-up saccades. Not surprisingly, most of the overall saccadic activity, both before and after flight, was in the vertical plane. With eye and head sinusoidal tracking at 0.33 Hz, the postflight cumulative gaze error in the horizontal plane increased for two subjects and decreased for two. The overall effect was a slight decrease across all four subjects, with large variability. Gaze error was considerably larger in the vertical than in the horizontal plane (Figure 5.3-22).

Eye and Head Pursuit Tracking – Gain and Phase

Figure 5.3-23 depicts the gaze gains and phase differences with respect to the target, as well as the corresponding eye and head movement gain and phase components of gaze. For horizontal eye-head tracking before flight, the

minimal differences between the gaze position and velocity data indicate that saccadic contributions to eye-head tracking were small. On-target gaze data were obtained from a strategy that combined head movements (which led the target) with lower amplitude eye movements (which lagged behind the target). This head-lead/eye-lag strategy was a general trend with considerable variability among subjects. The postflight position data were quite similar to the preflight position data, although there was a slight tendency after flight toward larger contributions to gaze from head, and consequently less contributions from eye.

Two interesting observations can be made from the postflight velocity data. First, the slight decrease in gain for gaze velocity after flight, compared to before flight, can be attributed to an increase in the contributions from the saccadic system. Second, the significant eye velocity phases (~90-180°) indicate that the combined eye movement contributions from the VOR and the smooth pursuit system caused the eye to move opposite of the target and the head. This is important because eye velocity counter to that of head velocity is indicative of a residual VOR command signal that is not being sufficiently canceled by the smooth pursuit system. Thus, for eye-head tracking after flight, there was a residual VOR that was not being completely canceled by the smooth pursuit system. This presumably occurred either because of decrements in the ability of the smooth pursuit system to generate “normal” VOR cancellation signals, or because VOR gain had increased to a point where normal VOR cancellation signals were no longer effective in providing complete cancellation.

Preflight, vertical eye-head tracking gains (Figure 5.3-24) indicated that subjects were able to match sinusoidal target motion fairly well using the full complement of smooth pursuit, VOR, and saccadic eye movements. Again, the major contribution to gaze came from head movements, while eye movements played a lesser role in supplementing the head and correcting for head tracking errors. By comparing preflight position and velocity data it is apparent from the decrease in gaze gain that the saccadic system is necessary to correct for position errors. The position errors apparently result from incomplete tracking with the combination of head movements, smooth pursuit eye movements, and the VOR during vertical tracking tasks.

Postflight, position gains were reduced slightly in three subjects, with most of the gaze tracking contribution coming from head movement. Subject B had a large head phase lead and thus needed a higher gain eye lag to compensate. The dramatic reduction in overall gaze gain, with the saccades removed in the velocity domain, shows that saccades played an important role in maintaining gaze position on target. Also, the large phase shifts (~180°) of the eye velocity signals show that the smooth (non-saccadic) eye movements were driven in a direction opposite of the head (and target), suggesting incomplete VOR

cancellation or suppression. Incomplete attenuation of the VOR signal during horizontal tracking suggests that either (1) the smooth pursuit signal was no longer capable of canceling the normal VOR command signal, (2) the VOR gain had increased to a level where even a normally adequate smooth pursuit cancellation signal was no longer effective, or (3) a combination of the two occurred.

All of these data indicate that saccades were important to maintain gaze directed toward the target during postflight tracking of a sinusoidally moving target, both with the head stationary and with the head assisting in tracking. Because sequences of saccades are generated in more or less a "stair-step" pattern, using them in any significant way to track smoothly moving targets results in periods of clear vision intermixed with intervals in which the eyes are stationary while the target moves (e.g., Figure 5.3-24, R+0). The latter circumstance results in slip of the target image on the retina and thus, reduced visual acuity. The significant postflight reliance on the saccadic system suggests that crew members were not seeing with a clear, smooth vision, but rather in time-displaced "snapshots," sampled at the conclusion of each saccade.

Finally, the large phase shifts associated with the eye velocity data during eye-head tracking after flight, show that the VOR was not being adequately canceled or suppressed. Either there was a reduction in overall efficacy of the smooth pursuit system during this task, or a substantial increase in VOR gain. If the latter were true, one might expect that some crew members would adopt a tracking strategy that moved the head in the opposite direction of the target, thereby using the increased gain VOR as a tracking mechanism to actively drive the eyes toward the target. At this point, none of the data suggest such a counter-directional head movement strategy.

Pursuit Tracking of an Unpredictable Velocity Ramp

The sinusoidal pursuit tasks discussed above are predictive in nature, each being a recurring cycle that once began, continues in the same fashion until the trail ends. The pursuit tracking of velocity ramps was an unpredictable task, with the velocity, peak displacement, and plane of the ramps counterbalanced, using a systematic randomization scheme. The end result was that they were clearly unpredictable in terms of direction of movement, velocity, and peak amplitude. Unlike the predictable sinusoidal trials, where velocity was constantly changing although peak velocity remained constant, the velocity steps maintained a constant velocity until peak amplitude was reached. The constant velocity factor may have been a significant component in the results obtained with this stimulus. Information illustrated in Figures 5.3-25-5.3-30 is from a single subject, representative of all subjects tested with this protocol.

Figures 5.3-25 and 5.3-26 illustrate pursuit tracking with the eyes only, using a low velocity (15°/sec), large displacement (30°) position ramp stimulus to the subject's

right in the horizontal plane. Before flight (Figure 5.3-25), the subject easily tracked the ramp stimulus (black trace) with the eyes (blue trace) while the head was held stationary (green trace). There was a characteristic delay in the eye movement following initiation of the target stimulus, after which the eye quickly locked onto the target. After the target reached its maximum amplitude, the eye continued to move briefly in the direction of previous target displacement and was returned to the final target position with a small accurate saccade. After flight (Figure 5.3-26), the response pattern was qualitatively the same as that observed before flight, showing no difference in response due to microgravity exposure. This same response pattern was noted when a much higher velocity stimulus was used (30°/sec) with a final target displacement of 30° (Figures 5.3-27 and 5.3-28).

Figures 5.3-29 and 5.3-30 illustrate pursuit tracking, with both the eyes and head, using unpredictable large displacements and velocities (30° and 30°/sec respectively) to the subject's left in the horizontal plane. The primary difference between the eyes only and head plus eyes tracking was a constant deviation of the eye position (red trace) that did not return to 0°. The difference between preflight and postflight response when both the head and eye tracked the ramp target was a decrease in head velocity, requiring a compensatory eye saccade to maintain gaze on the target during the postflight testing.

Target Acquisition

Typically, an orienting gaze movement, initiated to bring a selected part of the visual world onto the fovea, consists of an eye movement saccade and a head movement followed by a reflexive compensatory eye movement driven by the VOR. In the usual sequence, a saccade directs the eye either onto the target for targets with a small angular displacement or toward the target when the angular displacement exceeds either the physical or physiological limits of eye rotation. The head, being a larger mechanical object with greater inertia compared with the eye, typically moves after the eye has moved in the orbit. The head movements excite the semicircular canals and produce an eye movement through the VOR that is opposite in direction and velocity to that of the head. The compensatory VOR returns the eye to the primary straight ahead position in the skull's orbit, exchanging the head's final angular position for the initial eye saccade. Most observations before flight used a normal sequence of head and eye movements to assist in target acquisition. Immediately after flight, strategies were used to bring gaze onto a target that did not necessarily correspond to those observed by other investigators who have studied changes in strategies associated with verbal instructions and target predictability.

After flight, there was a consistent trend (Figure 5.3-31) for the head movement to the target to be delayed for

those targets near or beyond the effective oculo-motor range ($\pm 50^\circ$), as defined by Guitton and Volle [76]. Such a delay could result in a VOR following the initial eye saccade that would tend to pull gaze off target. Figure 5.3-31a shows head, eye, and gaze position in the left-most panel, and velocity traces for each of these parameters in the rightward panel for preflight acquisition of a vertical target in the upward direction that is beyond the EOM. Figure 5.3-31b shows the same parameters for a postflight (R+0) target acquisition. When the preflight parameters are compared with those obtained, several clear differences are apparent. First, postflight the head movement to the target is delayed relative to preflight, and the final position of the head, as well as the head's velocity, are reduced. As a consequence, the VOR was initiated at an inappropriate time, pulling gaze off target during the postflight measurement. This postflight delay (and low velocity head movement) induced a series of large anti-compensatory saccades that were required to direct gaze back onto the target.

Figure 5.3-32 illustrates the acquisition of a target beyond the EOM, in the vertical plane throughout all flight phases. As can be seen in the preflight trial, the subject used the eyes to attempt acquisition of the target. The eyes were moved prior to the head, and gaze was established with the eyes' position. Once the head began to move, the visually assisted vestibulo-ocular reflex (VVOR) was established and the reflex pulled gaze off the target. Both the head and a corrective eye saccade were then used to maintain gaze. During the flight, a different strategy was developed. The eye was still used to establish gaze, but the head movement was greatly reduced in both velocity and displacement (flight days 1 and 8). The number of saccades made by the eyes and the velocity of these saccades did not represent a typical VVOR response, but had a higher than normal gain. The responses for R+0 and R+1 days show most of the strategy components, such as attainment of target with eyes, low head velocity, and multiple saccades, developed during the flight. A return to preflight levels was observed by R+4.

A preliminary attempt was made to combine data across trials and subjects. The results obtained on a randomly-selected five subjects follows; however, because the strategies selected by each astronaut were different, traditional descriptive and multivariate statistical analysis washed out individual trends. Traditional analysis was therefore abandoned in favor of attempting to establish strategy groups. One approach was to place responses in groups identified by head and eye movement patterns identified by Zangemeister and Stark [77].

For horizontal gaze shifts, the delay between the start of eye and head movements was significantly different only for the 68° target (preflight 0.010 ± 0.076 sec vs. postflight 0.070 ± 0.102 sec, $p=0.015$; indicates head leads eye). For vertical target acquisition, this delay was again only significant for targets approaching the limits of the EOM

range ($\pm 50^\circ$), and only for targets in the upwards direction (preflight 0.042 ± 0.077 sec vs. postflight 0.177 ± 0.184 sec; $p=0.045$). For all other targets in the vertical plane, including those in the downward direction, there was a strong but insignificant trend for the head to be delayed during postflight testing. There was a significant difference in two of the five subjects for both horizontal and vertical targets within the EOM range, resulting in an average head delay of approximately 50 msec, when data from all five subjects were pooled.

The maximal eye and head velocities determine the time to bring gaze on target when the eye and head movement strategies function correctly and the interaction between the saccadic and VOR eye motion is sequenced correctly. After flight, the eye and head maximal velocities were found to be consistently below those observed before flight. For small target displacements ($\leq 20^\circ$) the difference was not significant, but showed the same trend observed for eye and head velocities made to targets beyond the EOM range. For the 30° targets both eye and head velocities were only 80% of the preflight value (preflight: head = $127 \pm 35^\circ/\text{sec}$ vs. postflight $105 \pm 32^\circ/\text{sec}$, $p=0.037$; eye = $329 \pm 46^\circ/\text{sec}$ vs. postflight $274 \pm 71^\circ/\text{sec}$, $p=0.007$). For the 68° target in the horizontal plane, a reduction of more than 30% was observed for both head and eye velocity (preflight: head = $196 \pm 36^\circ/\text{sec}$ vs. postflight $150 \pm 44^\circ/\text{sec}$, $p=0.003$; eye = $305 \pm 35^\circ/\text{sec}$ vs. postflight $208 \pm 60^\circ/\text{sec}$, $p=0.0005$).

The overall means of the final horizontal eye and head amplitudes before flight were not significantly different than after flight. However, postflight the eyes tended to contribute more to gaze displacement than preflight. Three of the five subjects showed smaller head amplitudes ($>20\%$) during postflight testing for targets beyond the EOM range. Vertical velocities for upward target acquisition trials also decreased, although significance levels were smaller. No differences were found for the 15° target. For the 20° target head velocity remained the same, but eye, and hence gaze, velocity decreased (gaze = preflight $343 \pm 76^\circ/\text{sec}$ vs. postflight $274 \pm 90^\circ/\text{sec}$, $p=0.021$; eye = preflight $330 \pm 82^\circ/\text{sec}$ vs. postflight $244 \pm 88^\circ/\text{sec}$, $p=0.038$). Both eye and head velocities decreased with targets beyond the EOM range, but were more variable than those within the EOM range. These differences occurred only for upward movements. For the near target (15°), mean eye and corresponding gaze velocity increased after flight (eye: preflight $308 \pm 82^\circ/\text{sec}$ vs. postflight $351 \pm 238^\circ/\text{sec}$), while head velocity remained the same.

One method of illustrating and qualitatively describing the changes in strategy, rather than pooling subject data, involves determining the type of gaze movement evoked. Zangemeister and Stark [77] have attempted to do this by determining the timing sequence between the command to move the head and the command to move the eyes. They have determined that gaze shift movements fall into four distinct types with respect to eye-head

latencies. In an attempt to group gaze shift strategies in the target acquisition task, we adopted a method developed by Wolfgang Zangemeister and Lawrence Stark. This method identifies five distinct groupings, called Stark Types, that are differentiated by the latency of eye movement onset, specifically the difference between the time of eye muscle stimulation (tEs) and the time of neck muscle stimulation (tHs), relative to head movement onset.

Because head or eye EMG were not measured, the time of eye and neck muscle stimulation were derived from measured values of eye movement onset (tEo) and head movement onset (tHo). To do this, the relative mass of the eye and head were taken into account. Since the mass of the eye is small, we assumed that the time of eye muscle stimulation and time of measured eye movement onset is simultaneous, and that the latency between the two is negligible ($tEo - tEs = 0$). However, the head has a much larger mass and does not move instantaneously after neck EMG excitation. Zangemeister and Stark found that the time of neck muscle stimulation (tHs) and time of head movement onset (tHo), are delayed by 50 msec. Therefore, 50 msec must be subtracted from the measured time of head movement onset ($tHo - 50 \text{ msec} = tHs$) to get time of neck muscle stimulation (Figure 5.3-33).

The latency information, obtained from the formula ($tEs - tHs$), can be used to group each gaze shift into either Stark Type I, II, IIIa, IIIb, or IV, depending upon where the latency falls in the time ranges defined by Zangemeister and Stark (Table 5.3-3). Table 5.3-3 shows times of EMG latencies that define each Stark Type. However, because these are physiological systems and neck and eye EMG are not being measured, it is highly unlikely that the latency will be exactly equal to zero. Therefore we have chosen a time window, Δt , of ± 25 msec around tHs where differences in tEs and tHs are effectively equal. So to be a Stark Type I, the difference between neck and eye muscle stimulation must fall within the ± 25 msec Δt time window (Figure 5.3-34). Stark Type II is defined as a late head movement, where the difference between neck and eye muscle stimulation falls before the ± 25 msec Δt time window (Figure 5.3-35). This type was seen very rarely in our study because the subject was instructed to move eyes and head as quickly, but accurately, as possible to acquire the target. Stark Type IIIa is defined as an early head movement where the latency of neck and eye stimulation must be in the range following

Table 5.3-3. Classification of Stark types

Type	Electromyogram (tEs - tHs)
I	0
II	Negative
IIIa	0 - 150 msec
IIIb	150 - 500 msec
IV	>500 msec

the $+\Delta t$ time window to 150 msec (Figure 5.3-36). This means that the head is commanded to move up to 150 msec before the eye is commanded. This is the most common type that occurred in our study, with occasional appearance of Type IIIb. Stark Type IIIb is also defined as an early head movement relative to the eye, but the head is commanded to move 150 msec to 500 msec before the eye is commanded (Figure 5.3-37). This type usually produces an initial eye movement in the opposite direction of the head before a saccade brings the eye toward the target. Stark Type IV is defined as a gaze shift where head movement completely governs the eye movement (Figure 5.3-38). It can be either a suppression of the VOR where the eye is carried to the target by the head, or without suppression of the VOR where the head first reaches the target and gaze is shifted to target with a late eye saccade. This gaze shift type, never seen in our study, would mean that the crew member was not doing the task correctly. When the Stark gaze shift types are represented in either the phase plane or parametric plots, it is possible to generate gaze plane representations that clearly allow the establishment of gaze shift errors. One of the most useful gaze shift errors to examine is that generated as a function of time. Figures 5.3-39 through 5.3-45 illustrate the process of establishing gaze-shift error.

Figures 5.3-39 and 5.3-40 show two different gaze shift strategies that were used to obtain a target beyond the EOM. Figure 5.3-39 was generated from data obtained before flight and shows a head movement that begins synchronous with, or perhaps just slightly before, movement of the eye towards the target. This type of movement corresponds to a Stark Type I strategy. The target acquisition illustrated in Figure 5.3-40 was obtained after flight and shows an eye movement towards the target just prior to movement of the head (Stark Type III). The primary difference between the preflight and postflight strategies is clearly seen in the velocity of the head, the final position of the head, and the number of saccades generated prior to gaze stability. Before flight, the eye made a major saccade toward the target, assisted by the movement of the head. A normal VVOR was established with a gain just slightly greater than one. After flight, there were multiple saccades prior to final gaze position, and the gain of these saccades was much greater than unity, indicating that they were not a component of the VVOR.

The difference between these two responses is clearly illustrated when gaze is plotted as a phase plane (Figures 5.3-41 and 5.3-42). Total gaze error can be derived from integrating the area represented in blue (head position 0° to maximum gaze displacement). However, gaze error is a function of time and can be best illustrated by Figures 5.3-43 and 5.3-44. Three major factors contribute to gaze error. These are: (1) response latency, (2) time taken to achieve final gaze position, and (3) the number of saccadic eye movements generated. The area bounded by red in both figures represents the area to be integrated. The preflight gaze error (Figure 5.3-43) was approximately

$20^\circ \times \text{sec}$ and the postflight gaze error (Figure 5.3-44) was $54^\circ \times \text{sec}$. Another way of illustrating gaze error as a function of time is presented in Figure 5.3-45.

Figure 5.3-46 represents the gaze error for a representative subject who displayed large gaze error as a function of flight days. The shaded area is the average total gaze error before flight, the day of landing (R+0), and six days later (R+6). Total gaze error over time increased dramatically on R+0, and on R+6 was still above that observed before flight. Absolute values of gaze error at R+6 were as much as 40% above the preflight values, particularly for the targets beyond the EOM. Figure 5.3-46 also clearly demonstrates that total gaze error was greatest for those targets that were beyond the EOM, and that as postflight recovery occurred, the differences between the targets beyond the EOM and those within the EOM became less.

Perhaps one of the most important aspects of determining total gaze error as a function of time is its use as an index of performance. When it is critically important to obtain a target in the shortest amount of time, large gaze errors result in less accurate target acquisition responses over time. It may also be used to predict postflight or in-flight performance using preflight behavior. This hypothesis was tested by determining the absolute gaze error as a function of time from preflight trials, using only those targets beyond the EOM, then relating the absolute gaze error to the head and eye velocity in the vertical plane for a specific trial obtained during target acquisition. In relating gaze error to head and eye velocity, the error was categorized in terms of either a large or small gaze error, with a small gaze error being the smallest value relative to a typical Stark Type III response.

Figure 5.3-47 shows preflight gaze error as a function of the head and eye velocity associated with the target acquisition response where the gaze error was associated. Based on this information it is not possible to use preflight gaze error to predict postflight performance. When the gaze error derived from the in-flight responses was evaluated as a function of vertical head and eye velocities measured postflight (Figure 5.3-48), a slight trend was apparent. Although large gaze errors appeared to be associated with lower vertical eye velocities, the absolute gaze errors did not clearly separate into distinct groups.

When absolute gaze errors as a function of time were associated with postflight vertical head and eye velocities, a clear trend was apparent (Figure 5.3-49). Large gaze errors were more likely to be associated with lower head and eye velocities, while small gaze errors were related to higher head and eye velocities. Among other things, this finding suggests that the neural strategies adopted during adaptation to microgravity may not have been optimal for postflight performance. Astronauts adopting a strategy of higher head and eye velocities may have had less difficulty and reduced gaze error.

Gaze Stabilization

Several parameters of gaze stabilization were computed, such as VVOR gain which was expressed by the slope of eye versus head velocity after saccade removal, gaze error after the head movement, and maximal velocities and amplitudes of eye and head. Only the decrease in vertical head peak velocity for downward movements showed a significant difference (preflight $80.9 \pm 15.4^\circ/\text{sec}$ vs. postflight $64.0 \pm 18.7^\circ/\text{sec}$). In general, postflight performance required a large saccadic eye movement to bring the eye back on target once vision was restored for the first trial or two. The saccadic correction is illustrated by comparing the preflight response (Figure 5.3-50a) with the postflight response (Figure 5.3-50b). Subsequent postflight trials showed an immediate trend, in all planes and directions, toward preflight baseline values, usually returning to normal within four gaze stabilization trials. Postflight performance was also often disturbed by saccadic eye movements (Figure 5.3-51). Subjects often locked their eyes in the head when starting a head movement. This required following saccades to bring the eye back on target, even when vision was not present.

The early in-flight gaze stabilization trials were similar to those observed before flight. However, measurements taken late in flight were more analogous to those obtained immediately after flight. Gaze stabilization was also the only VHM performed during entry, landing, and immediately after landing, while crew members were still in the space craft and in their space suits. During orbit to maximal sustained gravity (Figure 5.3-50c), the phase of entry where the change in gravitational forces was the greatest, there was not a corresponding VOR for the head movement in both the horizontal and vertical planes. It was at this stage of flight that small head movements frequently evoked sensations of either self-motion or surround motion that were linear in response to an angular input. One probable explanation for the lack of VOR and subsequent gaze drift is that the eye movement was compensating for the perception of self-motion and surround motion.

Sinusoidal Head Shakes

During sinusoidal head shakes, the subject maintained visual fixation on the target, or when vision was occluded, the subject attempted to maintain fixation on the target while smoothly oscillating the head in either the horizontal or vertical plane, in cadence with an audio tone that was sinusoidally modulated at each of four frequencies (0.2, 0.3, 0.8, and 2.0 Hz). Angular displacement of head oscillation was selected by the subject for comfort. When performing the analysis of the head shakes, special attention was paid to cross axes head movements, corresponding compensatory eye movements, and changes in head movement control. Figure 5.3-52 demonstrates the yaw cross

axes head movements when the head was pitched at each of the four different frequencies. While small, there was considerable secondary cross axis yaw movement. As expected, the greatest cross axis yaw movements occurred at the lowest frequency, and decreased as frequency was increased to 2.0 Hz (Figure 5.3-53). The larger overall cross-axis movement, when the subject had visual feedback regarding head position, was not expected. With the exception of 0.20 Hz, the postflight performance between vision and no vision was reversed relative to preflight values, indicating that after flight the removal of visual feedback resulted in the maintenance of head plane to the primary axis. There was no significant evidence of roll head movements when the head was pitched.

Figures 5.3-54 through 5.3- 61 illustrate the pitch head shakes in phase plane plots. Presented in this fashion, it is easy to see peak to peak displacement, velocity, head precession, and cycle-to-cycle consistency. Figures 5.3-54 through 5.3-57 show head shakes with vision before (L-10) and after space flight (R+0) at each of the four frequencies, when the subject had a visual reference. Displacement was greatest for the lower frequencies and decreased as the frequency increased. The inverse was true for velocity. There was very little evidence of precession, as the head did not progressively move from its original peak displacements, centered around up and down during the head shakes, to seek a new center. With the exception of the 0.20 Hz head shake, there was little change in either amplitude or velocity as a function of the flight phase.

Figures 5.3-58 through 5.3-61 show the results when vision was removed (occluded with the eyes open). Like the head shakes with vision, those without vision showed a progressive decrease in displacement with an increase in head shake frequency, and an increase in velocity as frequency increased. Unlike the head shakes with vision, there was a consistent trend to decrease head shake velocity, more strongly evidenced at the lower frequencies, immediately after space flight (R+0). There was also evidence, again at the lower frequencies, for precession to occur. Precession is important because it points to a loss or change in crew member spatial orientation. The strongest trend for precession occurred at the higher frequencies.

Head Movement Control

As evidenced by investigations of changes in the major postural muscles [16], spaceflight is believed to have a major impact on the sensory-motor systems responsible for balance and locomotion. Driven by the stimulus rearrangement of the flight environment, the newly adapted postural control is more suitable for microgravity than the Earth's gravitational forces. Loss of muscle mass and subsequent decreases in strength may also play a role in the changes observed in sensory-motor control as a function of spaceflight. All of these factors that may affect the major postural

muscles may also affect control of the neck muscles. Specifically, there is a possibility that sensory/motor nerve terminals may undergo changes that would make control of the neck more difficult in the Earth's environment following spaceflight. One possible way to investigate these changes is to examine head movement control after flight and compare it to preflight functional performance.

Figure 5.3-62 shows horizontal head position as a function of time during calibration procedures of the rate sensors used to measure the head position in space. The green trace shows a preflight trial (L-10). The red trace represents data obtained during the first head movement calibration trial immediately after flight (R+0), and shows that head position overshoot the calibration target. This overshoot reflects the lack of head control, and suggests that motor performance was compromised as a result of: (1) changes in descending vestibular information, and/or (2) a change in the substrate of the sensory-motor physiology. Figure 5.3-63 shows data for a second subject that did not display the changes evident in Figure 5.3-62. The differences could be due to head velocity, assuming that changes in the sensory-motor substrate were equal for both subjects. Also, the velocity of head movements could be different; the higher the velocity, the less control is available. Figure 5.3-64 depicts the velocity for head position shown in Figure 5.3-62. Figure 5.3-65 shows the velocity for head position plotted in Figure 5.3-63. The postflight velocity shown in Figure 5.3-65 was approximately 40% less than that depicted in Figure 5.3-64 for a different subject.

REFERENCES

1. Shaw RE, Kugler PN, Kinsella-Shaw J. Reciprocities of intentional systems. In: Warren R, Wertheim AH, editors. Perception and control of self-motion. Hillsdale, New Jersey: Lawrence Erlbaum; 1990. p 579-620.
2. Mittelstaedt H, Fricke E. The relative effect of sacular and somatosensory information on spatial perception and control. *Adv Oto-Rhino-Laryngol* 1988; 42:24.
3. von Gierke HE, Parker DE. Differences in otolith and abdominal viscera graviceptor dynamics: Implications for motion sickness and perceived body position. *Aviat Space Environ Med* (in press).
4. Howard IP. Human visual orientation. New York: John Wiley & Sons; 1982.
5. Cornilleau-Peres V, Droulez J. Three-dimensional motion perception: sensorimotor interactions and computational models. In: Warren R, Wertheim AH, editors. Perception and control of self-motion. Hillsdale, New Jersey: Lawrence Erlbaum; 1990. p 81-100.

6. Bock O. Coordination of arm and eye movements in tracking of sinusoidally moving targets. *Behav Brain Res* 1987; 24:3-100.
7. Calvin WH. *The cerebral symphony*. New York: Bantam Books; 1989.
8. Parker DE, Parker KL. Adaptation to the simulated stimulus rearrangement of weightlessness. In: Crampton GH, editor. *Motion and space sickness*. Boca Raton, FL: CRC Press; 1990. p 247-62.
9. Howard IP, Templeton WB. *Human spatial orientation*. London: John Wiley & Sons; 1966.
10. Guedry, F. Psychophysics of vestibular sensation. In: Held R, Liebowitz HW, Tuerber HL, editors. *Handbook of sensory physiology; vestibular system part 2: psychophysics and applied aspects and general interpretations*. Berlin: Springer Verlag; 1974. p 3-154.
11. Howard IP. The perception of posture, self motion, and the visual vertical. In: Boff KR, Kaufman L, Thomas JP, editors. *Handbook of perception and human performance, vol 1*. New York: John Wiley & Sons; 1986. p 18-1 to 18-62.
12. Mittelstaedt H. A new solution to the problem of subjective vertical. *Naturwissenschaften* 1983; 70:272-81.
13. Parker DE, Poston RL. Tilt from a head-inverted position produces displacement of visual subjective vertical in the opposite direction. *Perception & Psychophysics* 1984; 36:461-5.
14. Parker DE, Poston RL, Gullledge WL. Spatial orientation: visual-vestibular-somatic interaction. *Perception & Psychophysics* 1983; 33:139-46.
15. Young LR, Oman CM, Merfeld D, Watt D, Roy S, DeLuca, C, Balkwell D, Christie J, Groleau N, Jackson DK, Law G, Modestino S, Mayer W. Spatial orientation and posture during and following weightlessness: Human experiments on Spacelab Life Sciences 1. *J Vestib Res* 1993; 3:231-9.
16. Reschke MF, Harm DL, Parker DE, Sandoz G, Homick JL, Vanderploeg JM. Physiologic adaptation to space flight: neurophysiologic aspects: space motion sickness. In: Nicogossian AE, Leach CL, Pool SL, editors. *Space physiology and medicine*. Philadelphia: Lea & Febiger; 1994. p 228-60.
17. Reschke MF, Bloomberg JJ, Paloski WH, Harm DL, Parker DE. Physiologic adaptation to space flight: neurophysiologic aspects: sensory and sensory-motor function. In: Nicogossian AE, Leach CL, Pool SL, editors. *Space physiology and medicine*. Philadelphia: Lea & Febiger; 1994. p 261-85.
18. Clément G, Reschke MF. Neurosensory and sensory-motor function. In: Moore D, Bie P, Oser H, editors. *Biological and medical research in space*. Berlin: Springer-Verlag; 1996. p 178-258.
19. Paloski WH, Black FO, Reschke MF. Vestibular ataxia following shuttle flights: effects of transient microgravity on otolith-mediated sensorimotor control of posture. *Am J Otolaryngol* 1993; 1:9-17.
20. Friederici AD, Levelt WJM. Resolving perceptual conflicts: the cognitive mechanisms of spatial orientation. *Aviat Space Environ Med* 1987; 58(9 Suppl):A164-9.
21. Harm DL, Parker DE. Perceived self-orientation and self-motion in microgravity, after landing and during preflight adaptation training. *J Vestib Res* 1993; 3:297-305.
22. Mittelstaedt H, Glasauer S. Crucial effects of weightlessness on human orientation. *J Vest Res* 1993; 3:307-14.
23. Wolfe JM, Held R. Eye torsion and visual tilt are mediated by different binocular processes. *Vis Res* 1979; 19:917-20.
24. Perterka RJ, Benolken MS. Relation between perception of vertical axis rotation and vestibulo-ocular reflex symmetry. *J Vest Res* 1992; 2:59-70.
25. Oman CM, Bock OL, Huang JK. Visually induced self-motion sensation adapts rapidly to left-right visual reversal. *Science* 1980; 209:706-8.
26. Oman CM, Balkwill MD. Horizontal angular VOR, nystagmus dumping, and sensation duration in Space-lab SLS-1 crewmember. *J Vest Res* 1993; 3:315-30.
27. Welch RB. Adaptation of space perception. In: Boff KR, Kaufman L, Thomas JP, editors. *Handbook of Perception and Human Performance, vol 1*. New York: John Wiley & Sons; 1986. p 24-1 to 24-45.
28. Berthoz A, Grantyn A. Neuronal mechanisms underlying eye-head coordination. *Prog Brain Res* 1986; 64:325-43.
29. Thornton WE, Biggers WP, Thomas WG, Pool SL, Thagard NE. Electronystagmography and audio potentials in space flight. *Laryngoscope* 1985; 95:924-32.
30. Thornton WE, Uri JJ, Moore T, Pool S. Studies of the horizontal vestibulo-ocular reflex in space flight. *Arch Otolaryngol Head Neck Surg* 1989; 115:943-9.
31. Vieville T, Clement G, Lestienne F, Berthoz A. Adaptive modifications of the optokinetic vestibulo-ocular reflexes in microgravity. In: Keller EL, Zee DS, editors. *Adaptive processes in visual and oculomotor systems*. New York: Pargamon Press; 1986. p 111-20.
32. Watt DGD, Money KE, Bondar RL, Thirsk RB, Garneau M, Scully-Power P. Canadian medical experiments on shuttle flight 41-G. *Can Aeronaut Space J* 1985; 31:215-26.

33. Benson AJ, ViÈville T. European vestibular experiments on the Spacelab-1 mission: 6. Yaw axis vestibulo-ocular reflex. *Exp Brain Res* 1986; 64:279-83.
34. Grigoriev AL, et al. Medical results of the Mir year-long mission. *Physiologist* 1991; 34:S44-48.
35. Vesterhaug S, Mansson A, Johansen TS, Zilstorff K. Oculomotor response to voluntary head rotations during parabolic flights. *Physiologist* 1982; 25:S117-18.
36. Lackner JR, Graybiel A. Variations in gravito-inertial force level affect the gain of the vestibulo-ocular reflex: implications for the etiology of space motion sickness. *Aviat Space Environ Med* 1981; 52:154-58.
37. DiZio P, Lackner JR, Evanoff JN. The influence of gravito-inertial force level on oculomotor and perceptual responses to sudden stimulation. *Aviat Space Environ Med* 1987; 58:A224-30.
38. DiZio P, Lackner JR. The effects of gravito-inertial force level and head movements on post-rotational nystagmus and illusory after-rotation. *Exp Brain Res* 1988; 70:485-95.
39. Oman CM. Personal communication. 1991.
40. Oman CM, Kulbaski M. Spaceflight affects the 1-g postrotatory vestibulo-ocular reflex. *Adv Oto-Rhino-Laryng* 1988; 42:5-8.
41. Oman CM, Weigl H. Postflight vestibulo-ocular reflex changes in space shuttle/Spacelab D-1 crew. *Aviat Space Environ Med* 1989; 60:480.
42. Oman CM, Lichtenberg, BK, Money KE. Space motion sickness monitoring experiment: Spacelab 1. In: Crampton GH, editor. *Motion and space sickness*. Boca Raton, FL: CRC Press; 1990. p 217-46.
43. Clément G, Reschke MF, Verrett CM, Wood SJ. Effects of gravito-inertial force variations on optokinetic nystagmus and on perception of visual stimulus orientation. *Aviat Space Environ Med* 1992; 63:771-77.
44. Guedry FE. Orientation of the rotation-axis relative to gravity: Its influence on nystagmus and the sense of rotation. *Acta Otolaryng* 1965; 60:30-48.
45. Guedry FE. Psychophysiological studies of vestibular function. In: Neff WD, editor. *Contribution to Sensory Physiology*. New York: Academic Press; 1965.
46. Benson AJ, Bodin MA. Comparison of the effect of the direction of the gravitational acceleration on post-rotational responses in yaw, pitch and roll. *Aerospace Medicine* 1966; 37:889-97.
47. Bodin MA. The effect of gravity on human vestibular responses during rotation in pitch. *J Physiol* 1968; 196:74-75.
48. Kozlovskaya IB, et al. The effects of real and simulated microgravity on vestibulo-oculomotor interaction. *The physiologist* 1985; 28(6):51-56.
49. Thornton WE, Moore TP, Uri JJ, Pool SL. Studies of the vestibulo-ocular reflex on STS 4, 5 and 6. NASA Technical Memorandum 1988; 100 (461):42.
50. Uri JJ, Linder BJ, Moore TP, Pool SL, Thornton WE. Saccadic eye movements during space flight. NASA Technical Memorandum 1989; 100(475):9.
51. Laurutis VP, Robinson DA. The vestibulo-ocular reflex during human saccadic eye movement. *J Physiol (Lond)* 1986; 373:209-233.
52. Guitton D, Volle M. Gaze control in humans: eye head coordination during orienting movements to targets within and beyond the oculomotor range. *J Neurophysiol* 1987; 58:427-59.
53. Bloomberg J, Melvill Jones G, Segal B, McFarlane S, Soul J. Vestibular-contingent voluntary saccades based on cognitive estimates of remembered vestibular information. *Adv Oto-Rhino-Laryng* 1988; 41:71-75.
54. Bloomberg J, Melvill Jones G, Segal B. Adaptive modification of vestibularly perceived self-rotation. *Exp Brain Res* 1991; 84:47-56.
55. Israel I, Berthoz A. Contribution of the otoliths to the calculation of linear displacement. *J Neurophysiol* 1989; 62:247-63.
56. Barnes G.R. Visual-vestibular interaction in the coordination of eye and head movements. In: Fuchs & Becker, editors. *Progress in oculomotor research*. New York: Elsevier; 1981. p 299-308.
57. Halmagyi GM, Gresty MS. Clinical signs of visual-vestibular interaction. *J Neurol Neurosurg Psychiatry* 1979; 42: 934-39.
58. Huebner WP, Leigh RJ, Thomas CW. An adjustment to eye movement measurements which compensates for the eccentric position of the eye relative to the center of the head. *J Vestib Res* 1992; 2:167-73.
59. Robinson DA. A model of cancellation of the vestibulo-ocular reflex. In: Lennerstrand G, Zee DS, Keller EL, editors. *Functional Basis of Ocular Motility Disorders*. New York: Pergamon Press; 1982. p 5-13.
60. Cullen KE, Chen-Huang C, McCrea RA. Firing behavior of brain stem neurons during voluntary cancellation of the horizontal vestibuloocular reflex. II. Eye movement related neurons. *J. Neurophysiol* 1993; 70(2):844-56.
61. Cullen KE, McCrea RA. Firing behavior of brain stem neurons during voluntary cancellation of the

- horizontal vestibuloocular reflex. I. Secondary vestibular neurons. *Neurophysiol* 1993; 70(2):828-43.
62. McKinley PA, Peterson BW. Voluntary modulation of the vestibulo-ocular reflex in humans and its relation to smooth pursuit. *Exp Brain Res* 1985; 60: 454-64.
 63. Kornilova LN, et al. Pathogenesis of sensory disorders in microgravity. *Physiologist* 1991; 34:S36-39.
 64. André-Deshays C, Israel I, Charade O, Berthoz A, Popov K, Lipshits M. Gaze control in microgravity: I. Saccades, pursuit, eye-head coordination. *J Vest Res* 1993; 3:331-43.
 65. Young LR. Space and the vestibular system: what has been learned. *J Vestib Res Equilibrium & Orientation* 1993; 3:203-06.
 66. Rashbass C, Russell GFM. Action of a barbituate drug (Amylobarbitone Sodium) on the vestibulo-ocular reflex. *Brain* 1961; 84:329-35.
 67. Kowler E, Martins AJ, Pavel M. The effect of expectations on slow oculomotor control-IV. Anticipatory smooth eye movements depend on prior target motions. *Vision Res* 1984; 24:197-210.
 68. Robinson DA, Gordon JL, Gordon SE. A model of the smooth pursuit eye movement system. *Biol Cybern* 1986; 55:43-57.
 69. Blakemore C, Donaghy M. Coordination of head and eyes in the gaze changing behavior of cats. *J Physiol (Lond)* 1980; 300:317-35.
 70. Collewijn H, Conijn P, Tamminga EP. Eye-head coordination in man during the pursuit of moving targets. In: Lennerstrand G, Zee DS, Keller E, editors. *Functional basis of ocular motility disorders*. Oxford: Pergamon Press; 1982. p 369-78.
 71. Wist ER, Brandt T, Krafczak S. Oscillopsia and retinal slip. Evidence supporting a clinical test. *Brain* 1983; 106:153-68.
 72. Virre E, Tweed D, Milner K, Vilis T. A reexamination of the gain of the vestibuloocular reflex. *J Neurophysiol* 1986; 56:439-50.
 73. Hine T, Thorn F. Compensatory eye movements during active head rotation for near targets: effects of imagination, rapid head oscillation and vergence. *Vision Res* 1987; 27:1639-57.
 74. Collewijn H, Erkelens CJ, Steinman RM. Binocular coordination of human horizontal saccadic eye movements. *J Physiol (Lond)* 1988; 404:157-82.
 75. Leigh RJ, Zee DS. *The neurology of eye movements*. Philadelphia: F.A. Davis Co.; 1991.
 76. Guitton D, Volle M. Gaze control in humans; eye-head coordination during orienting movements to targets within and beyond the oculomotor range. *J Neurophysiol* 1989; 58:427-59.
 77. Zangemeister WH, Stark L. Gaze latency; variable interactions of head and eye latency. *Exp Neurol* 1982; 75:389-406.

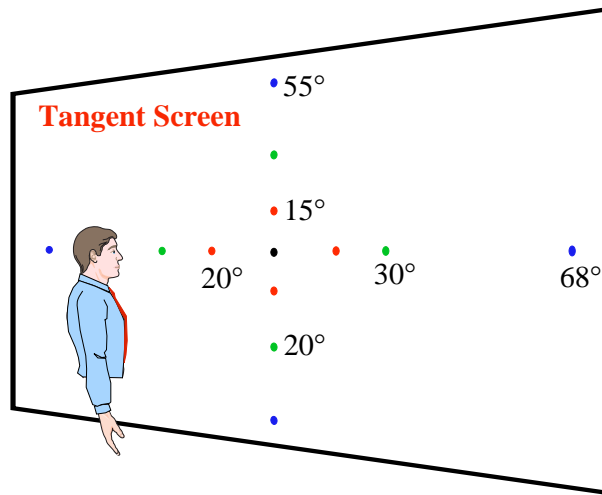


Figure 5.3-1. Representation of target location on tangent screen.

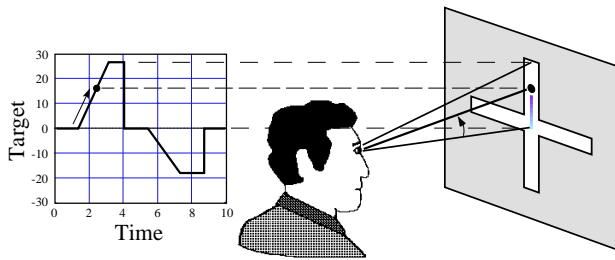


Figure 5.3-2. Unpredictable pursuit tracking: ramp stimulus.

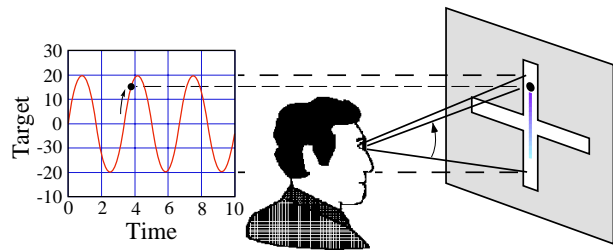


Figure 5.3-3. Predictable smooth pursuit: sinusoidal stimulus.

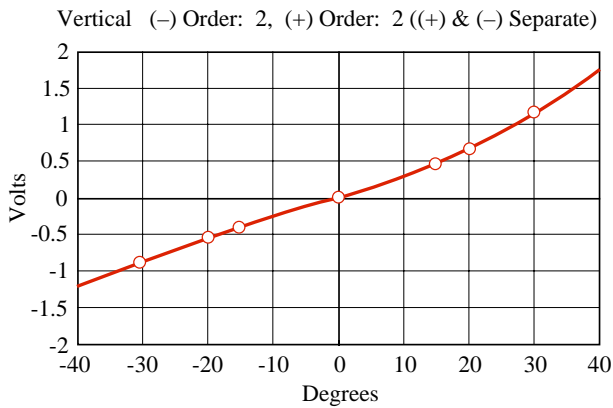


Figure 5.3-4a. Vertical eye calibration.

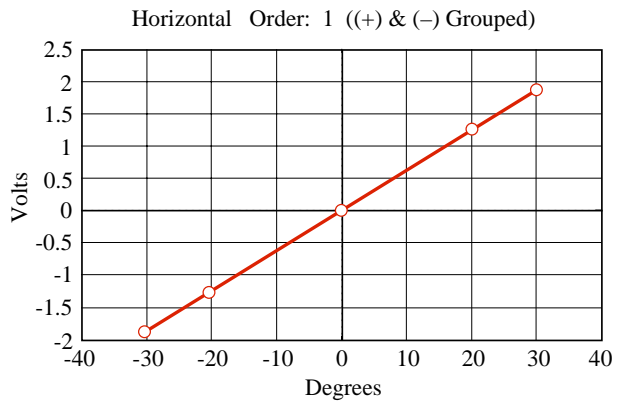


Figure 5.3-4b. Horizontal eye calibration.

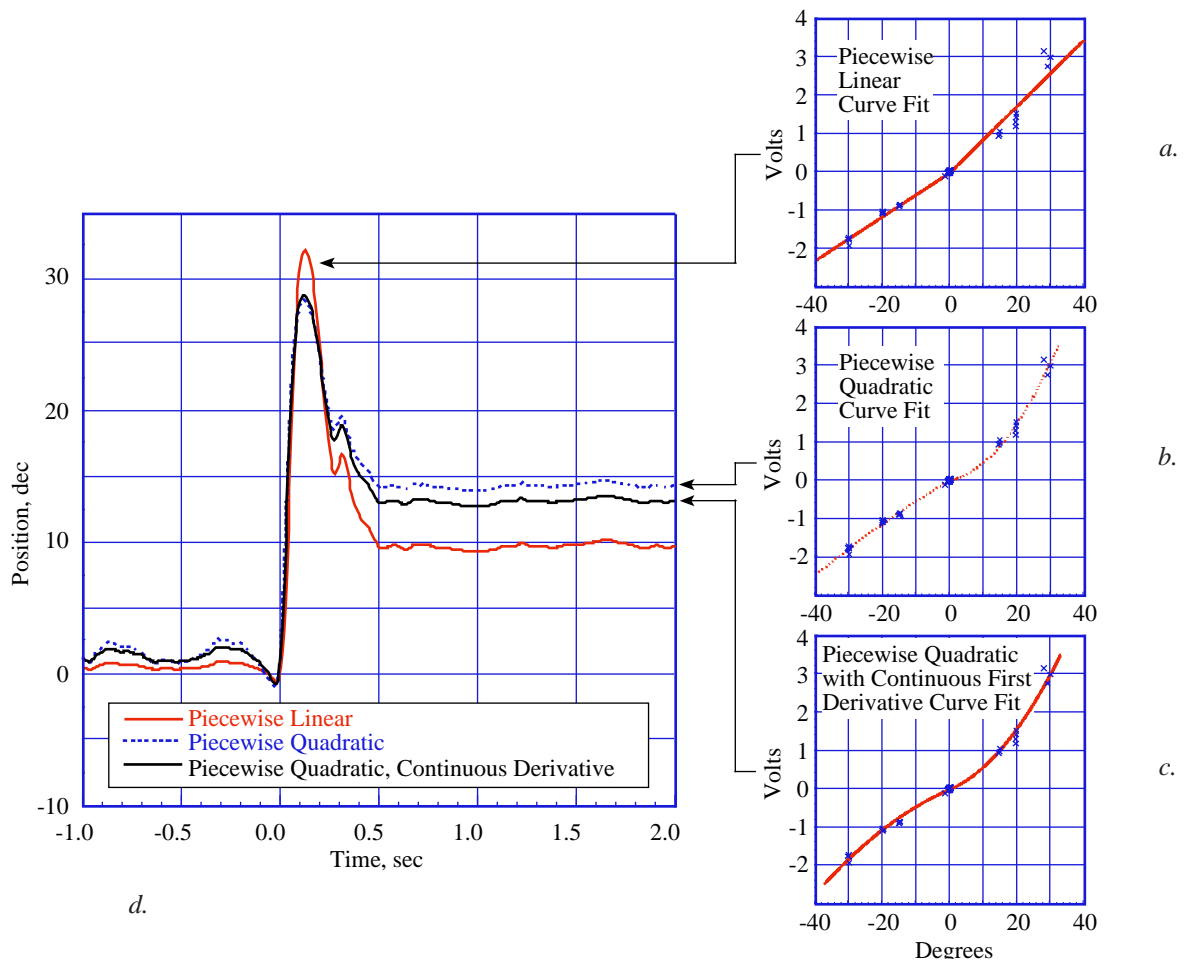


Figure 5.3-5. Various calibration curves applied to a vertical target acquisition eye movement response.

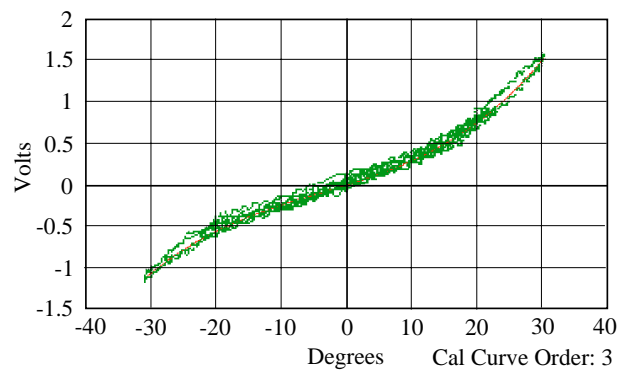
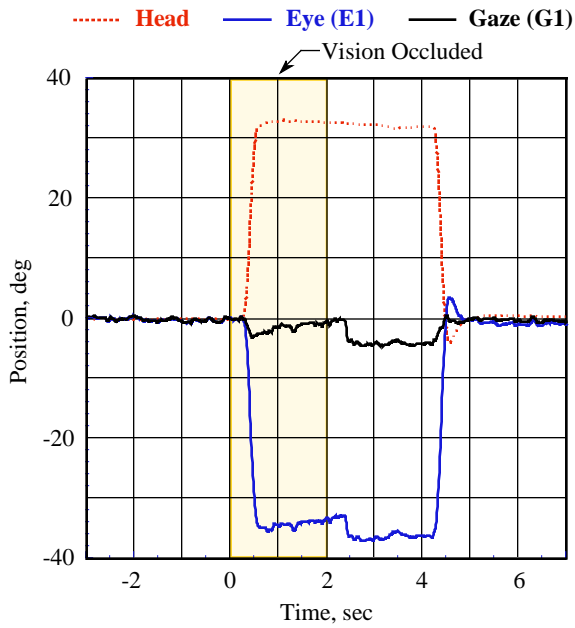


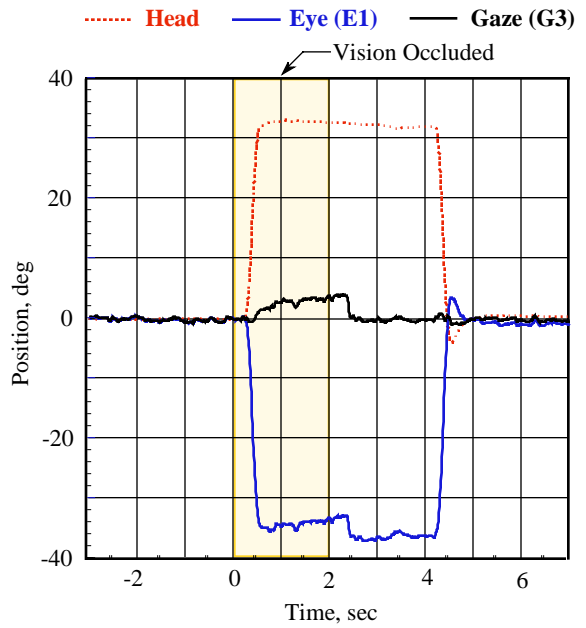
Figure 5.3-6. Dynamic, fixed-gaze eye calibration curve – vertical.

Simple Calculation of Gaze ($G = E + H$):
 Gaze Referenced to Displaced Location of Eye in Space



a.

Geometry of Eye Eccentricity Considered in Calculation of Gaze:
 Gaze Referenced to Primary Eye Position with Head at Zero



b.

Figure 5.3-7. Geometrical gaze correction.

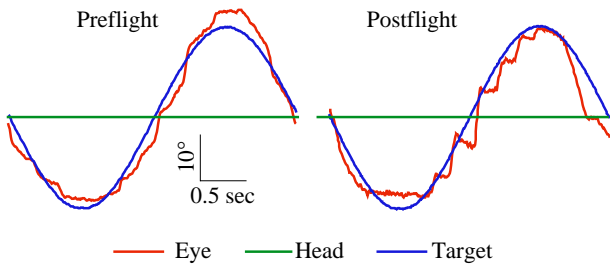
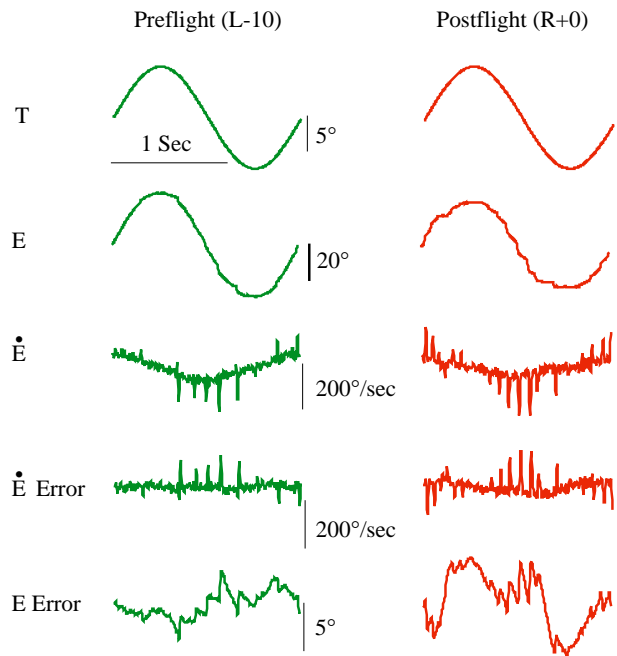


Figure 5.3-8. Vertical smooth pursuit: eyes only.



T = Target Wave Form
 E = Horizontal Eyes
 \dot{E} = Eye Velocity
 \dot{E} Error = Eye Error Velocity
 E Error = Eye Error Position

Figure 5.3-9. Horizontal smooth pursuit: eyes only.

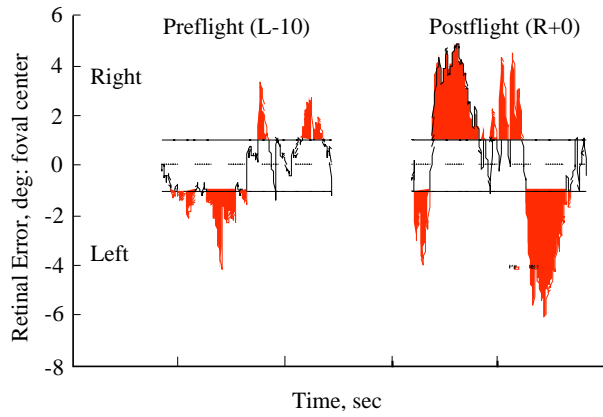


Figure 5.3-10. Cumulative time foveation is off target.

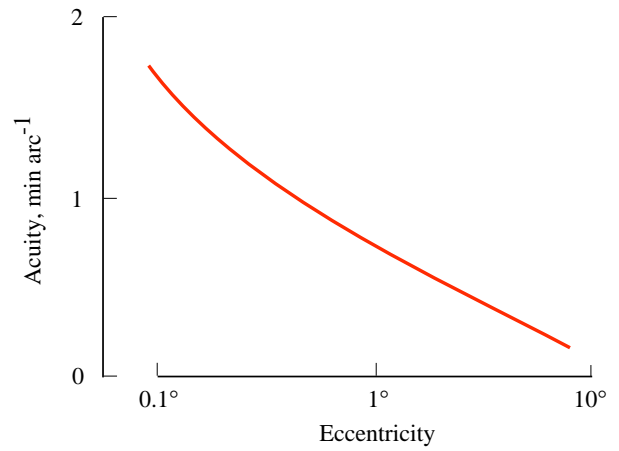


Figure 5.3-11. Loss of acuity with target displacement from foveal center.

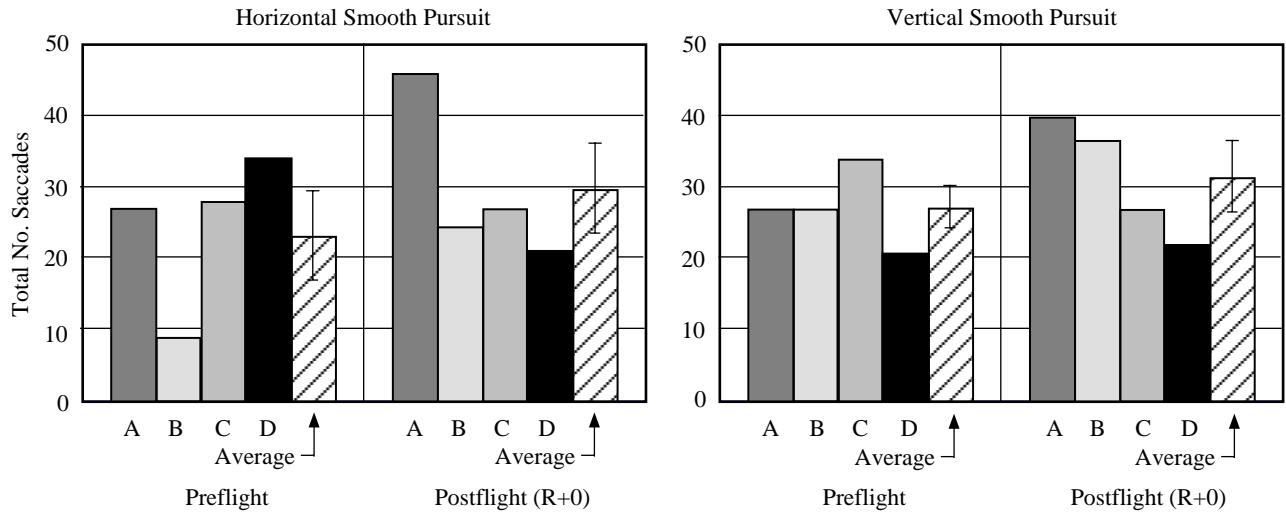


Figure 5.3-12. Total Number of Saccades.

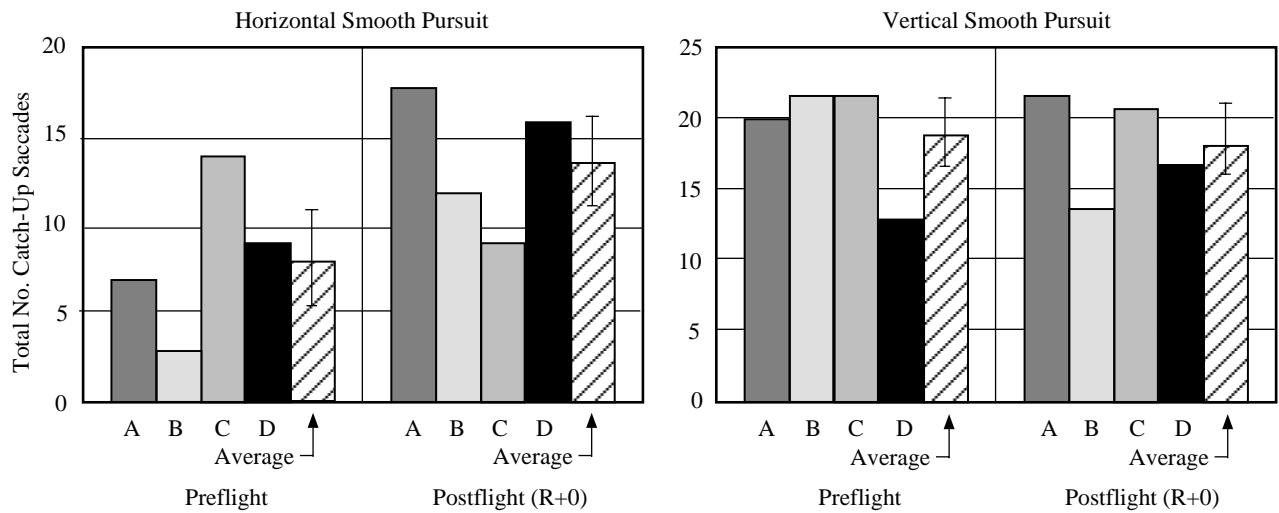


Figure 5.3-13. Total Catch-up Saccades.

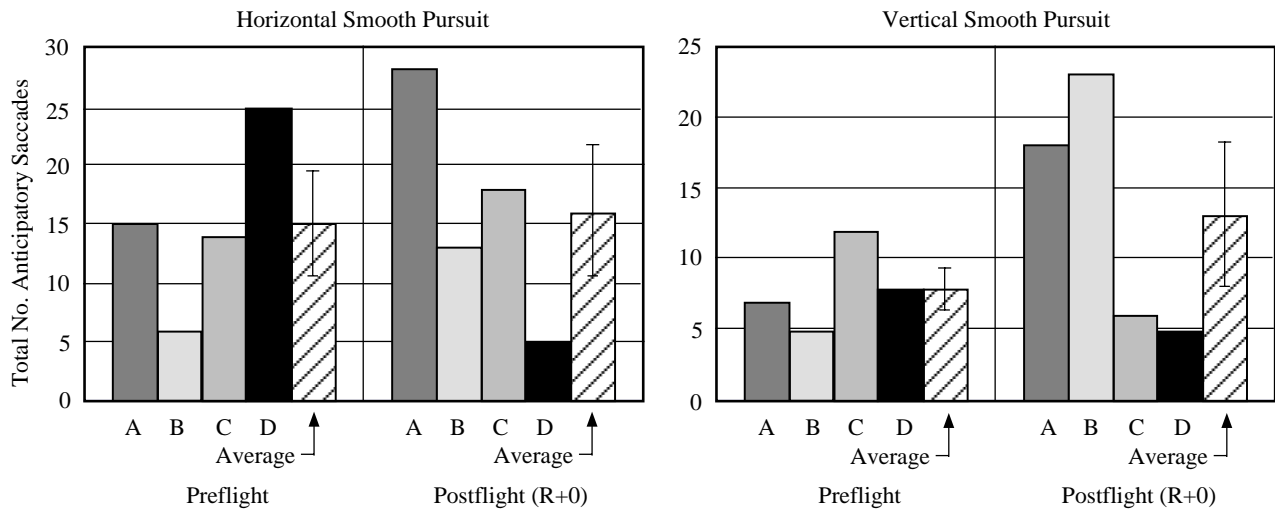


Figure 5.3-14. Total Anticipatory Saccades.

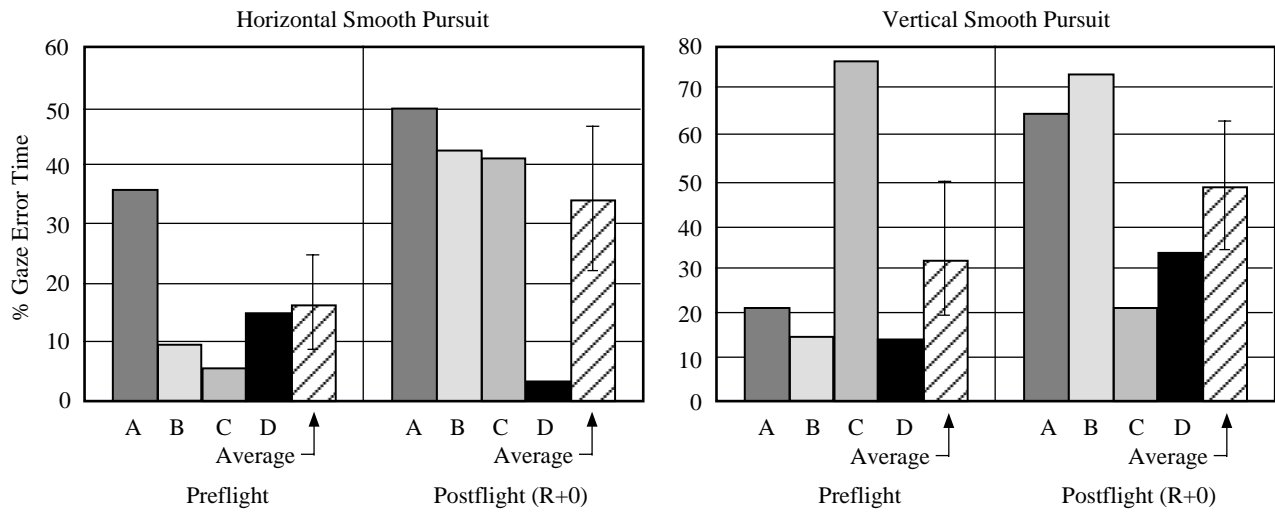


Figure 5.3-15. Cumulative gaze error time (%).

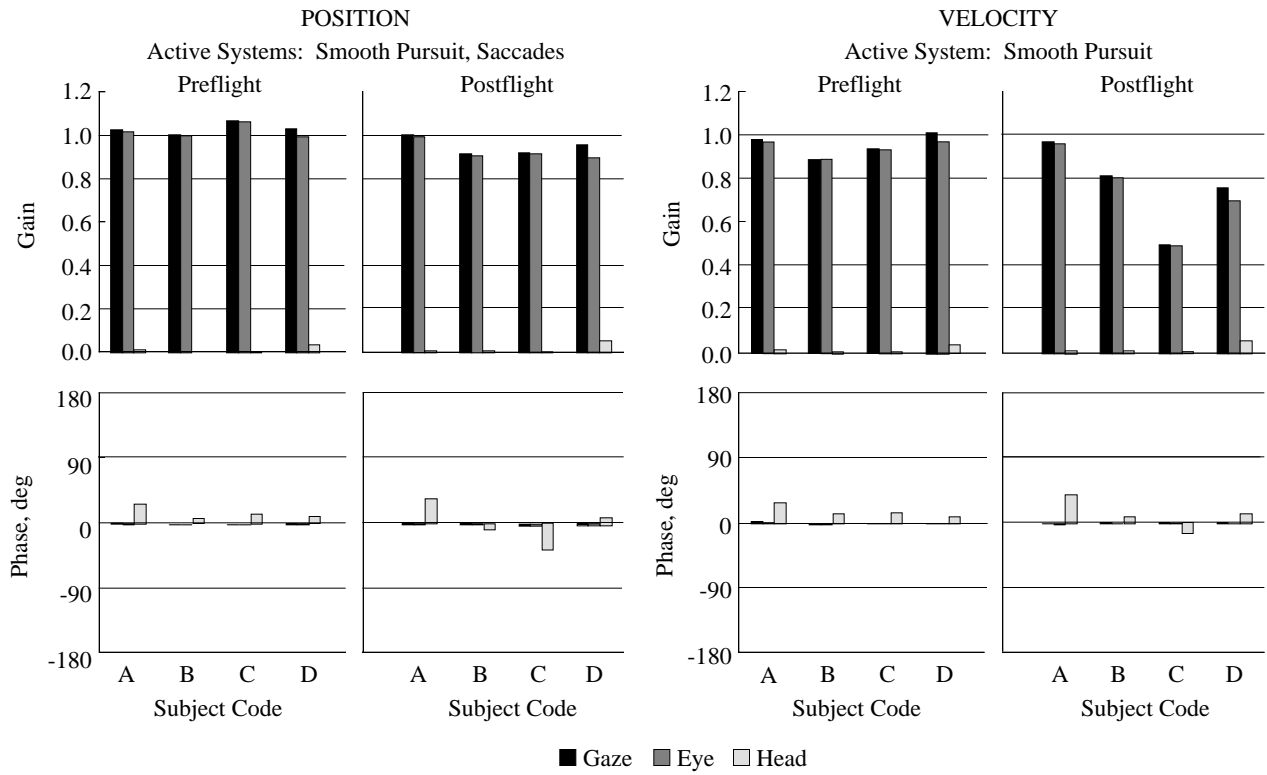
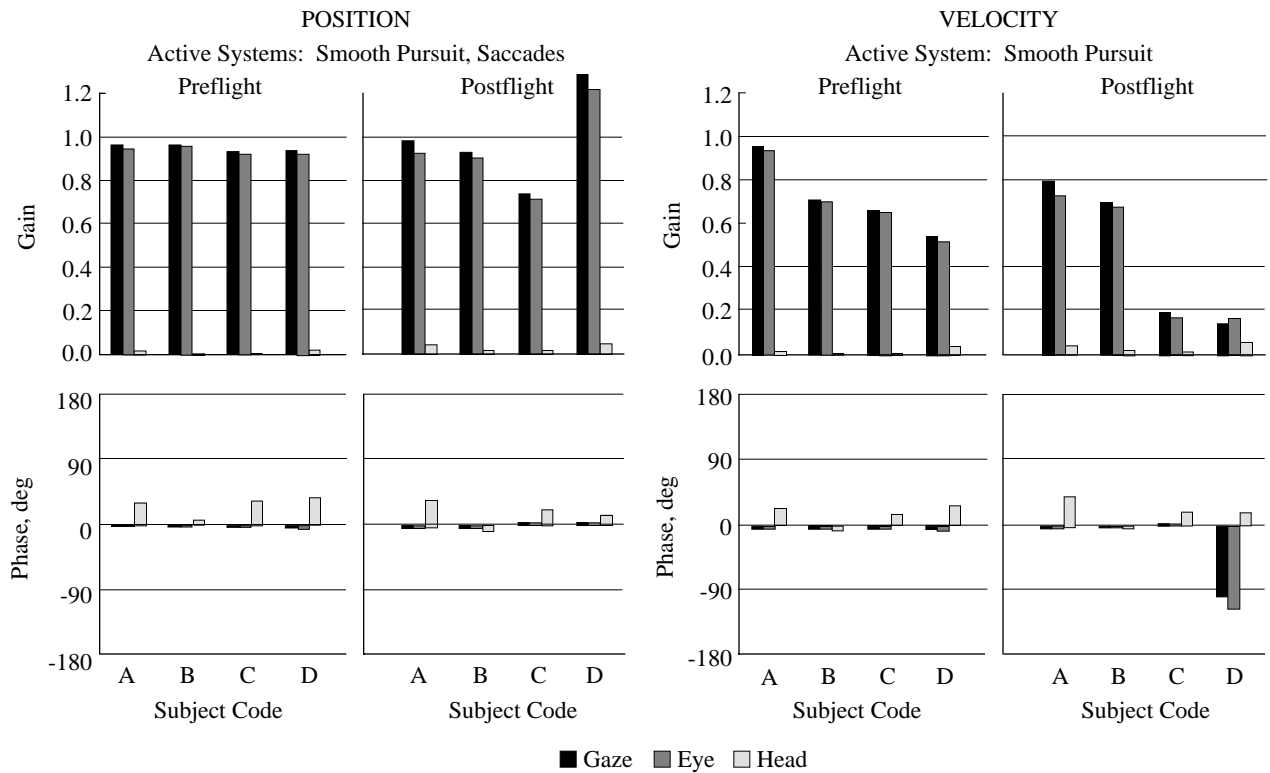


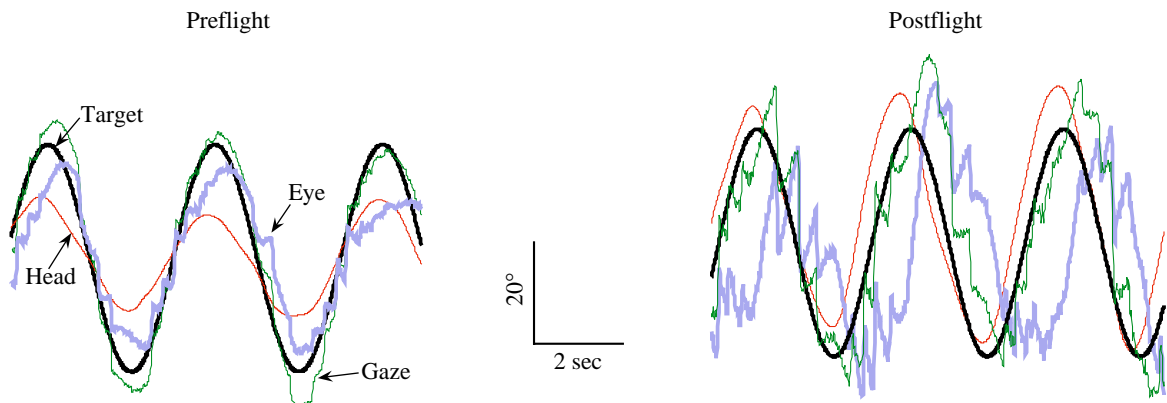
Figure 5.3-16. Horizontal – smooth pursuit (eyes only).



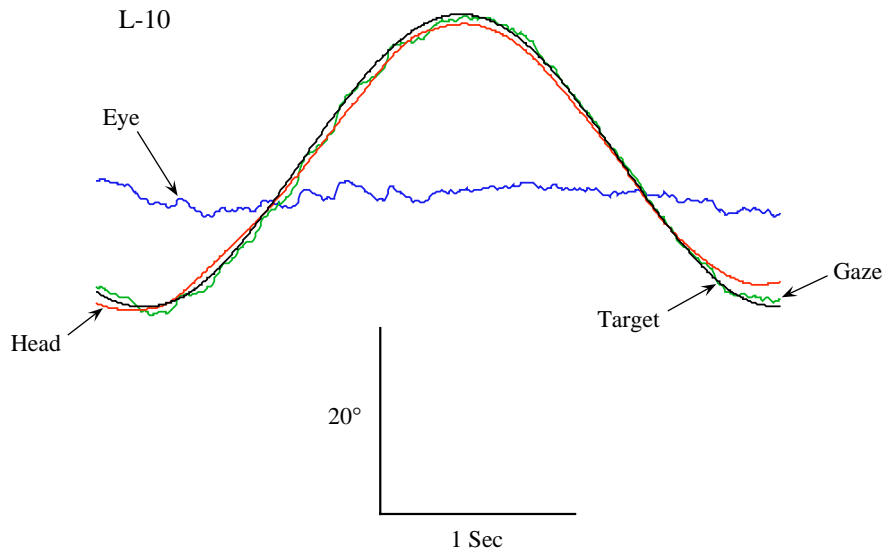
a.

b.

Figure 5.3-17. Vertical – smooth pursuit (eyes only).



a.



b.

Figure 5.3-18. Vertical pursuit tracking with head and eyes.

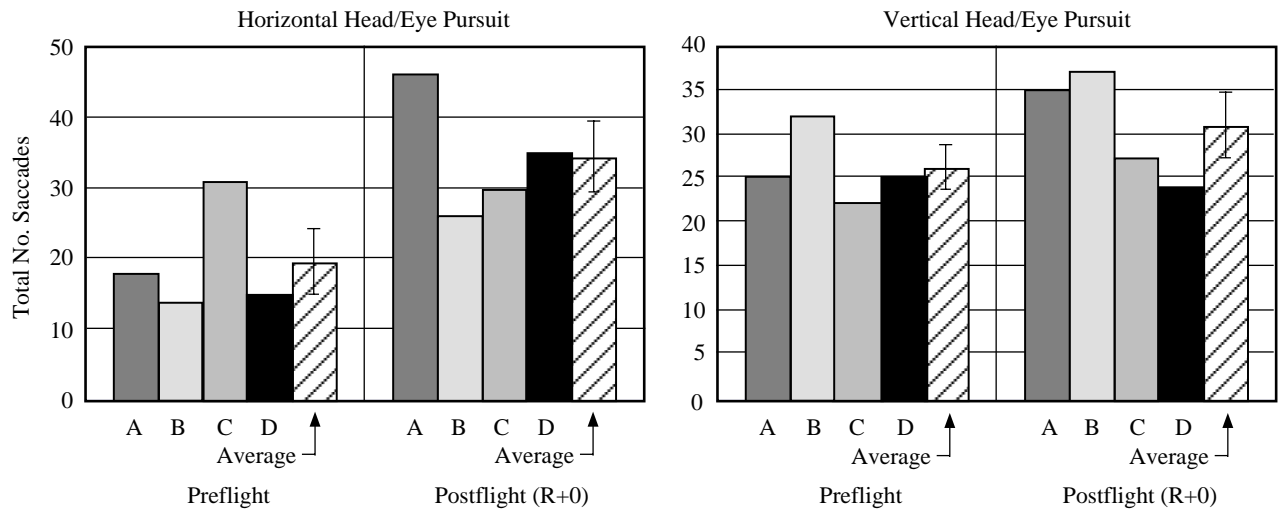


Figure 5.3-19. Total Number of Saccades.

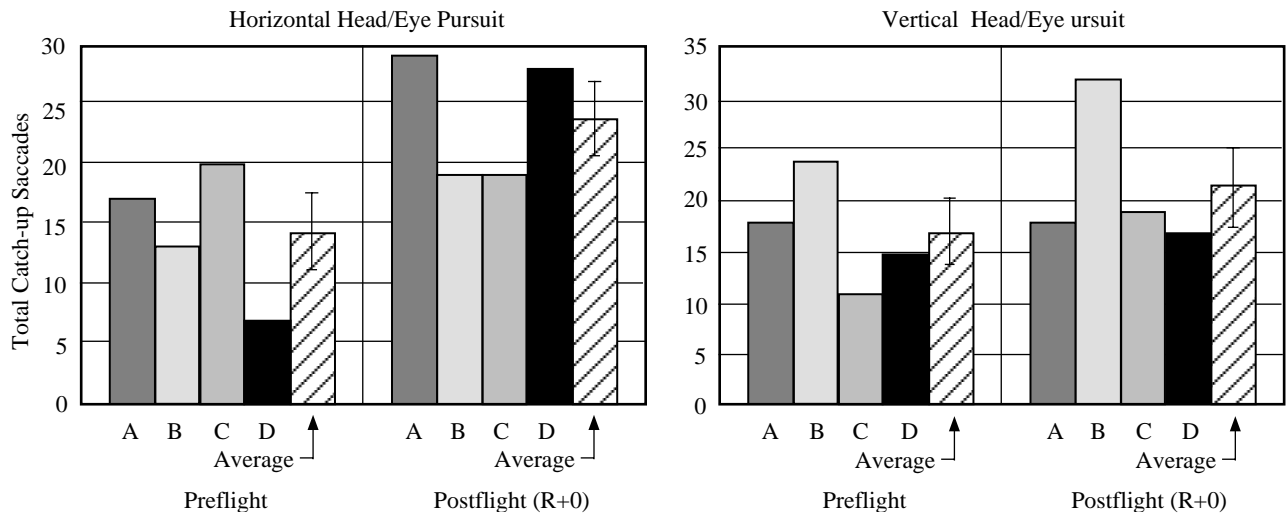


Figure 5.3-20. Total Catch-Up Saccades.

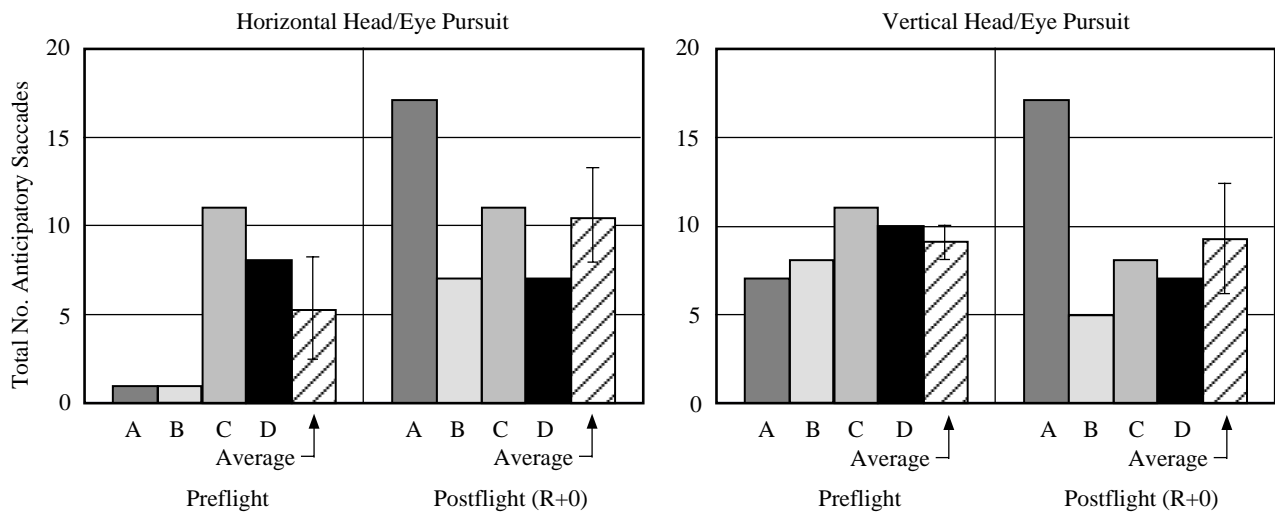


Figure 5.3-21. Total Anticipatory Saccades.

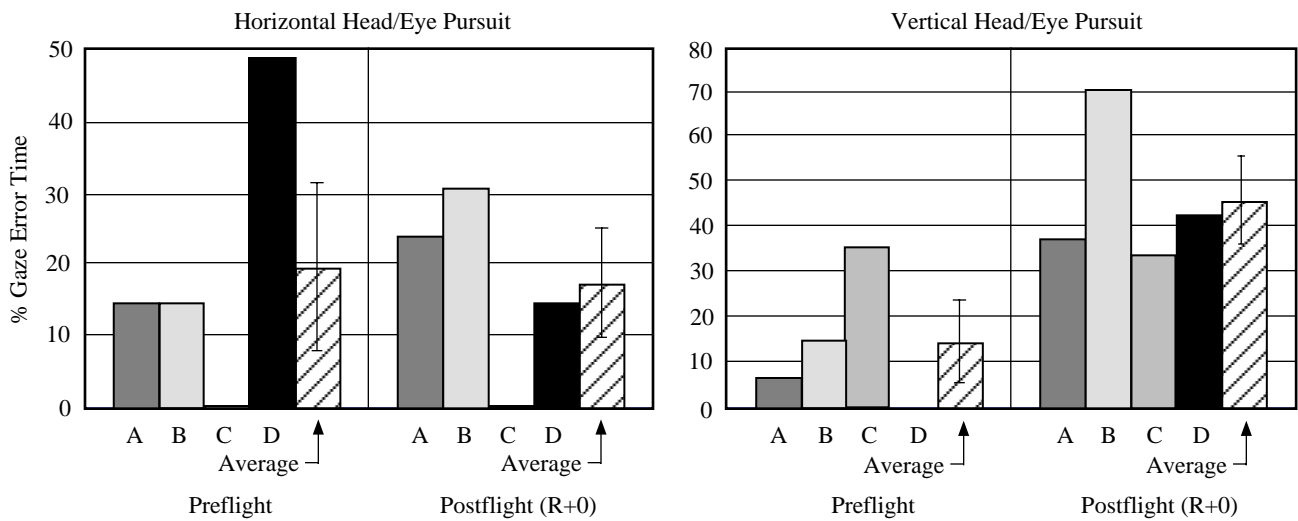


Figure 5.3-22. Cumulative gaze error time (%).

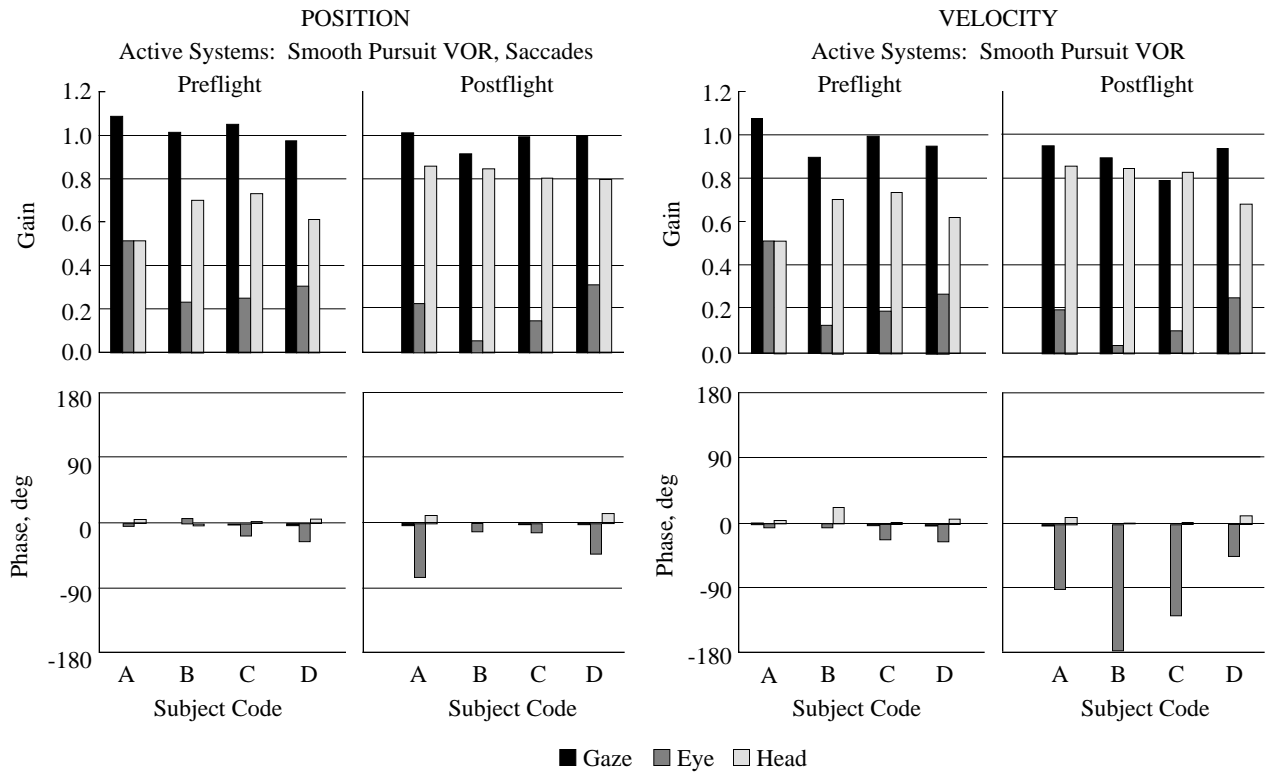


Figure 5.3-23. Horizontal – eye-head tracking.

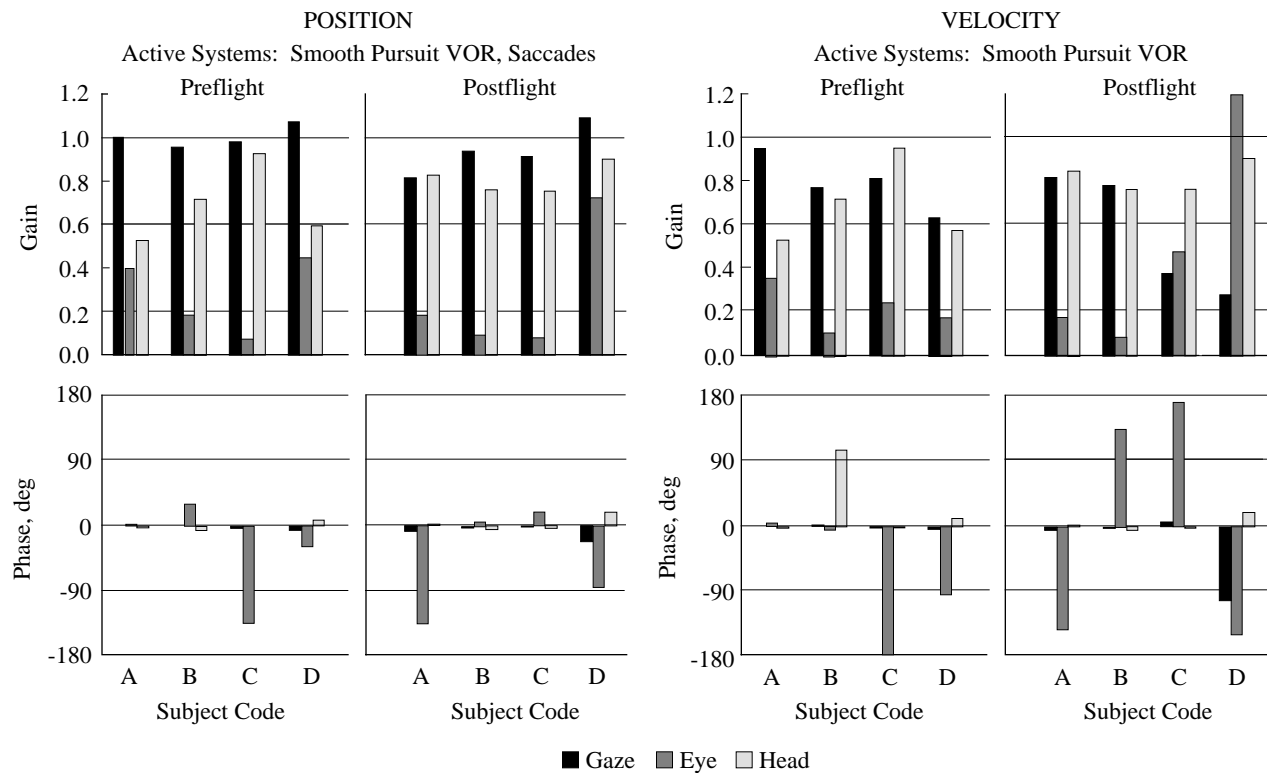


Figure 5.3-24. Vertical – eye-head tracking.

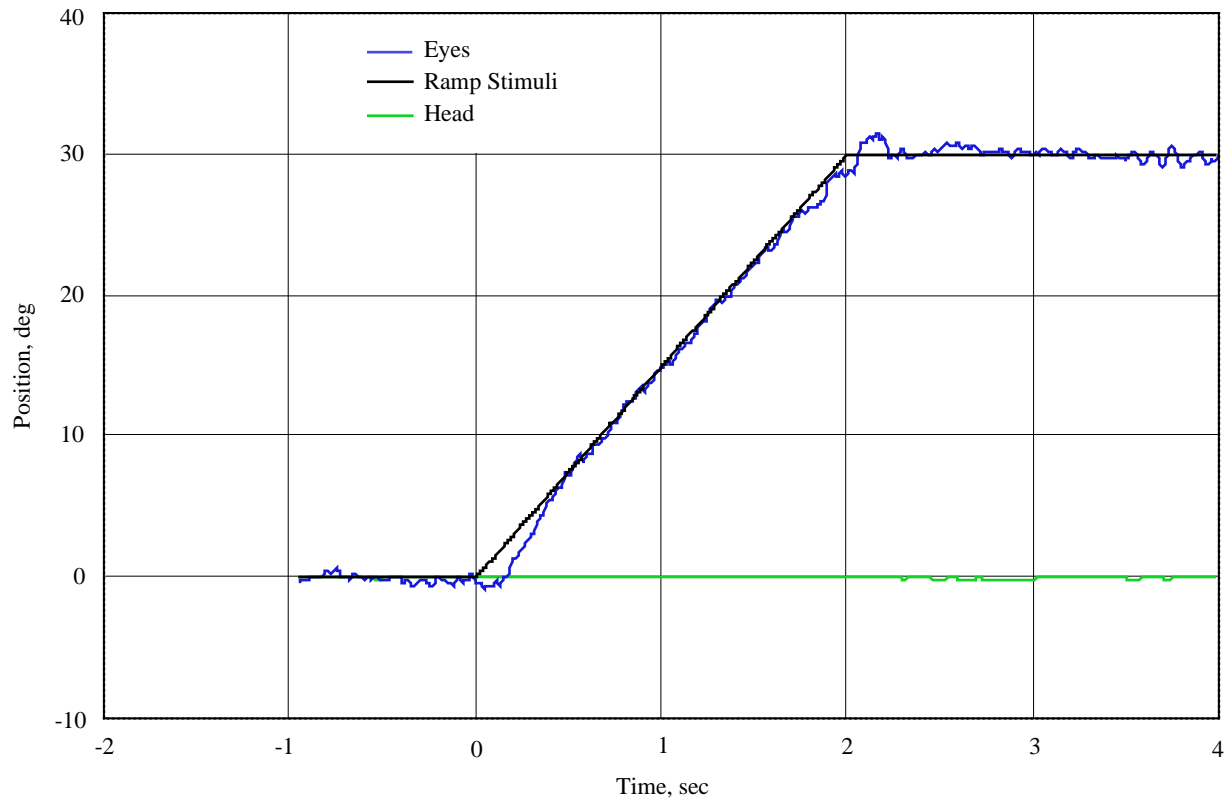


Figure 5.3-25. L-10 Unpredictable pursuit tracking: Low velocity ($15^\circ/\text{sec}$) ramp tracking with eye ramp moving rightward.

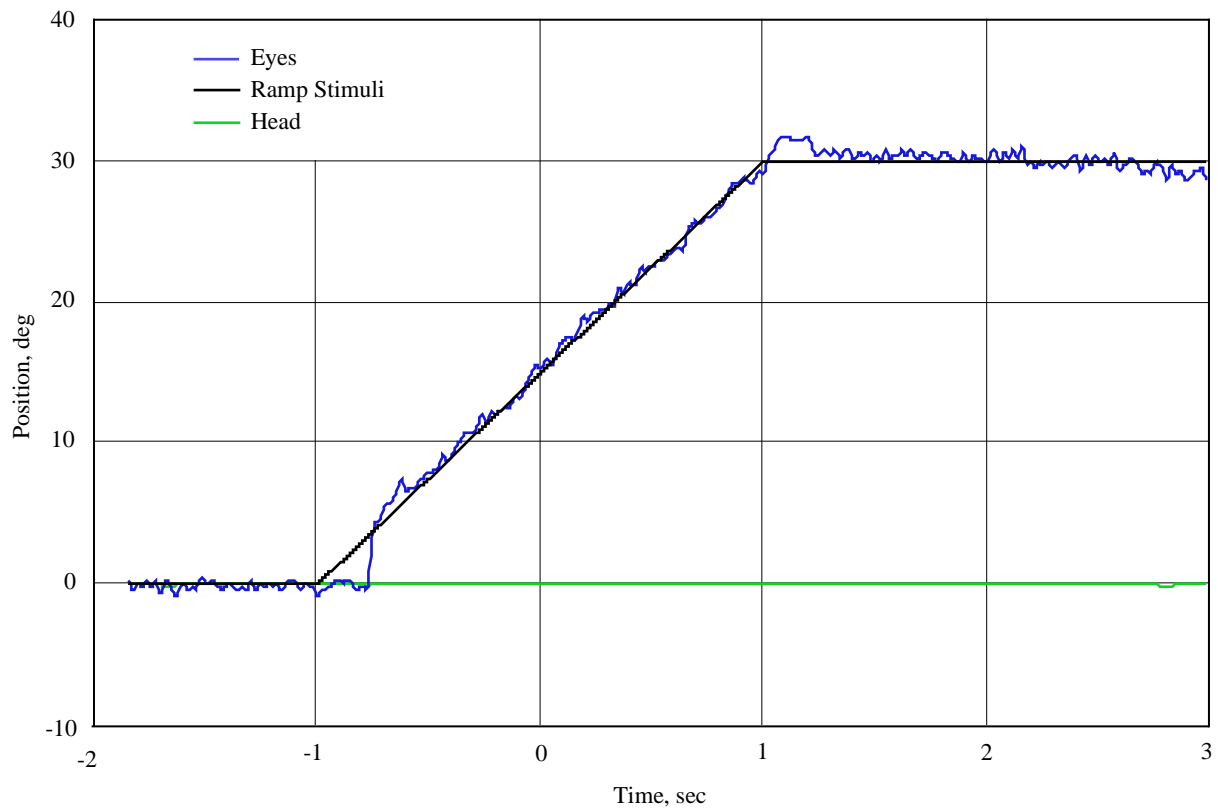


Figure 5.3-26. R+0 Unpredictable pursuit tracking: Low velocity ($15^\circ/\text{sec}$) ramp tracking with eye ramp moving rightward.

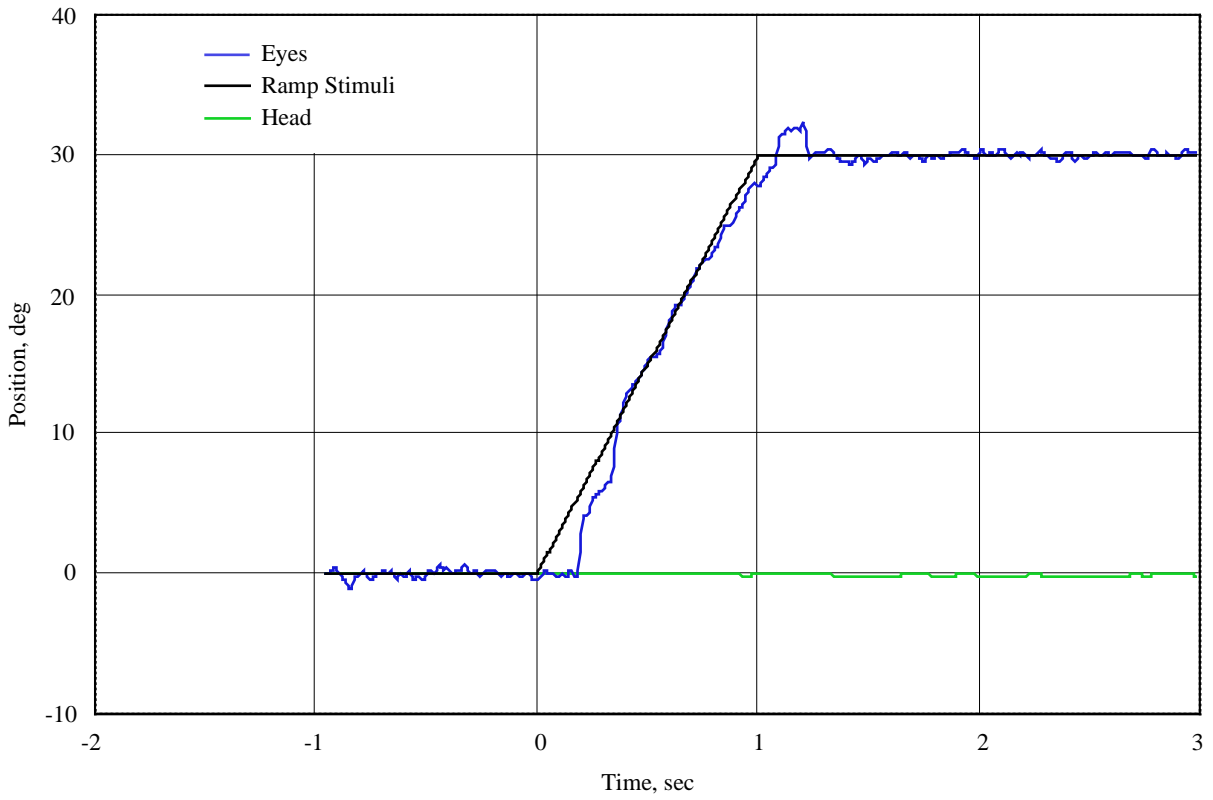


Figure 5.3-27. L-10 Unpredictable pursuit tracking: Low velocity (30°/sec) ramp tracking with eye ramp moving rightward.

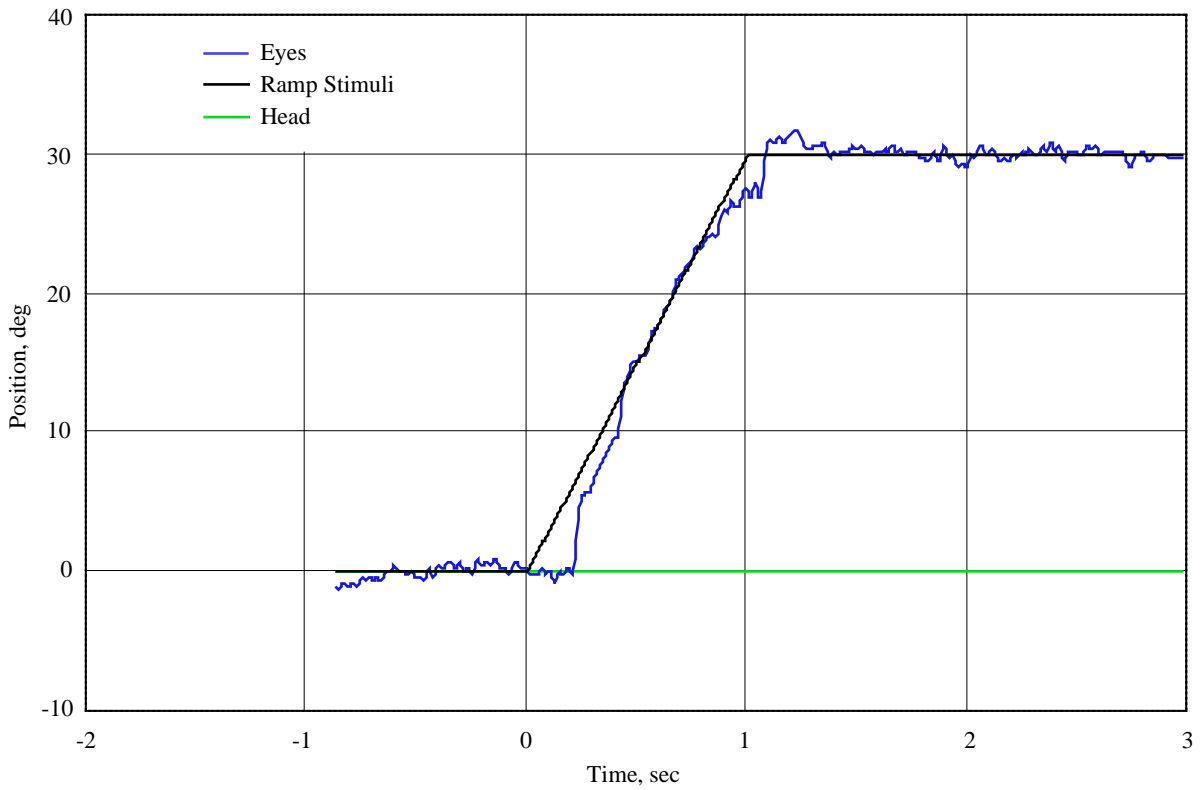


Figure 5.3-28. R+0 Unpredictable pursuit tracking: Low velocity (30°/sec) ramp tracking with eye ramp moving rightward.

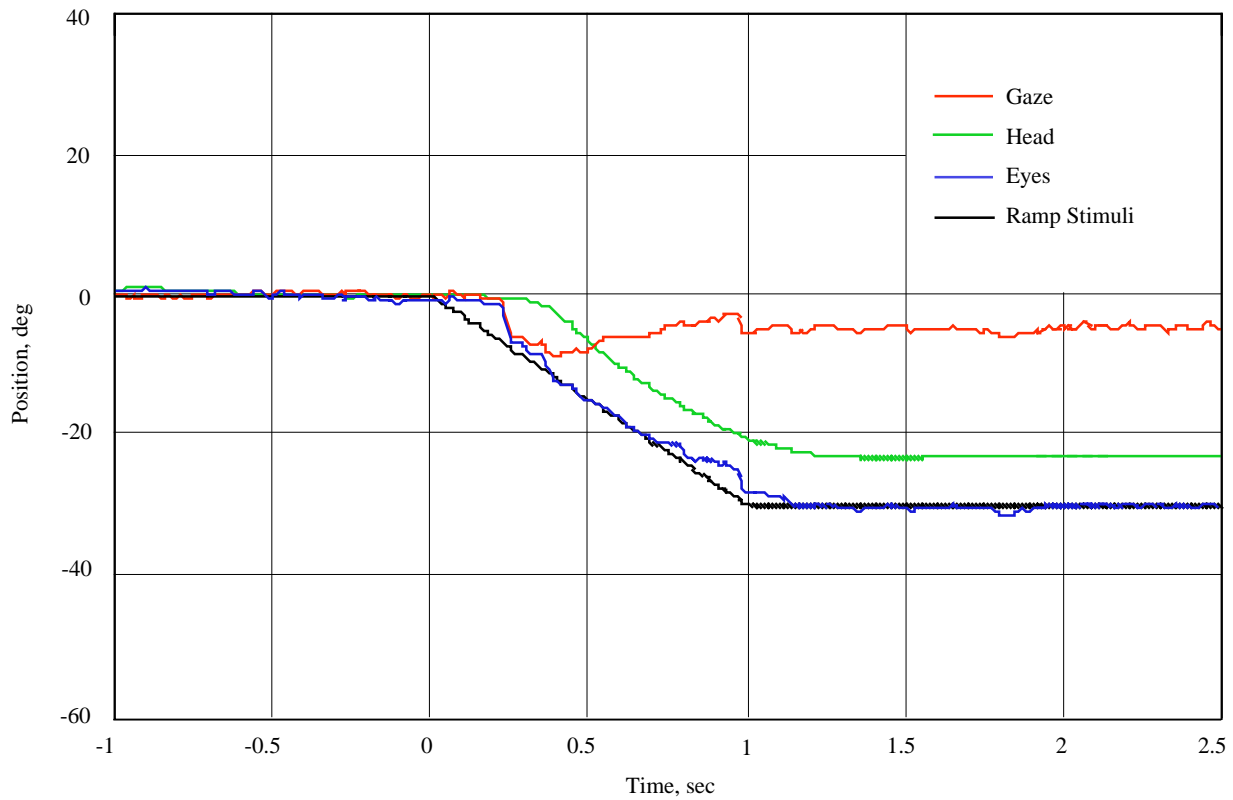


Figure 5.3-29. L120 Unpredictable pursuit tracking: High velocity ($30^\circ/\text{sec}$) ramp tracking with both head and eye, with a ramp moving leftward.

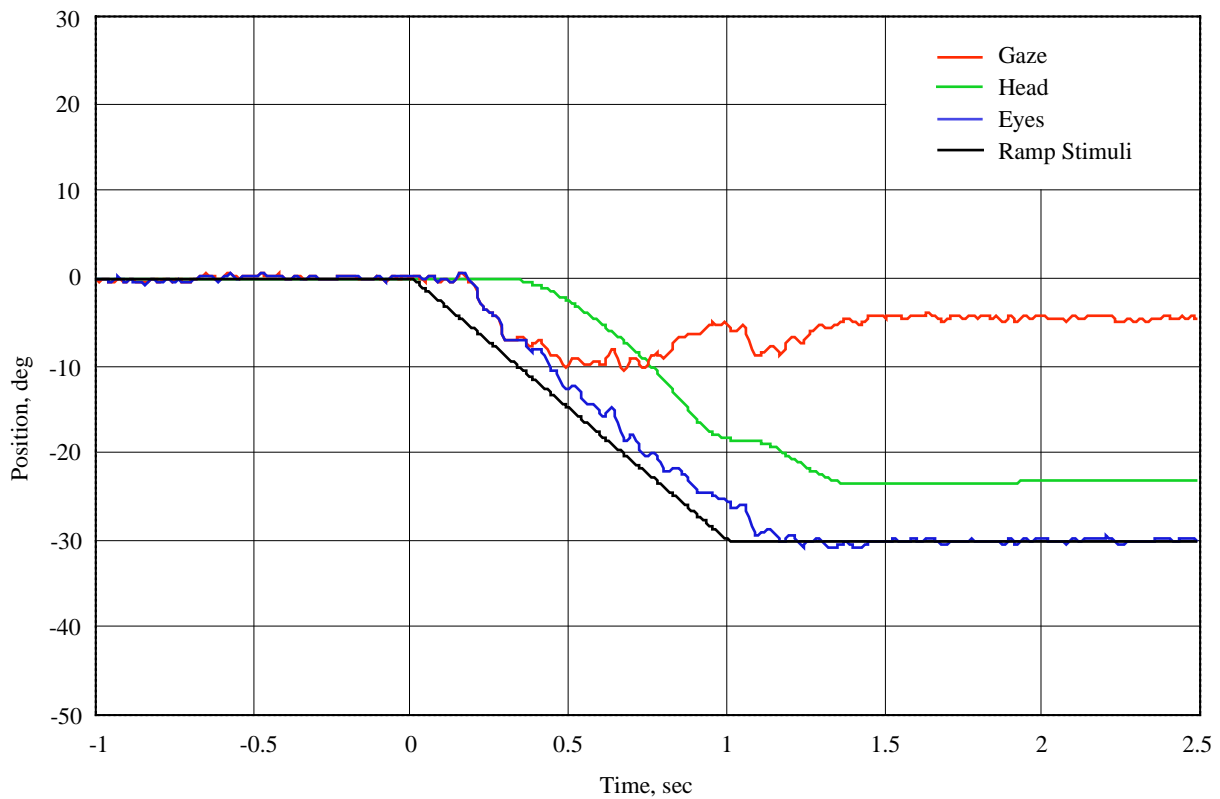


Figure 5.3-30. R+0 Unpredictable pursuit tracking: High velocity ($30^\circ/\text{sec}$) ramp tracking with both head and eye, with a ramp moving leftward.

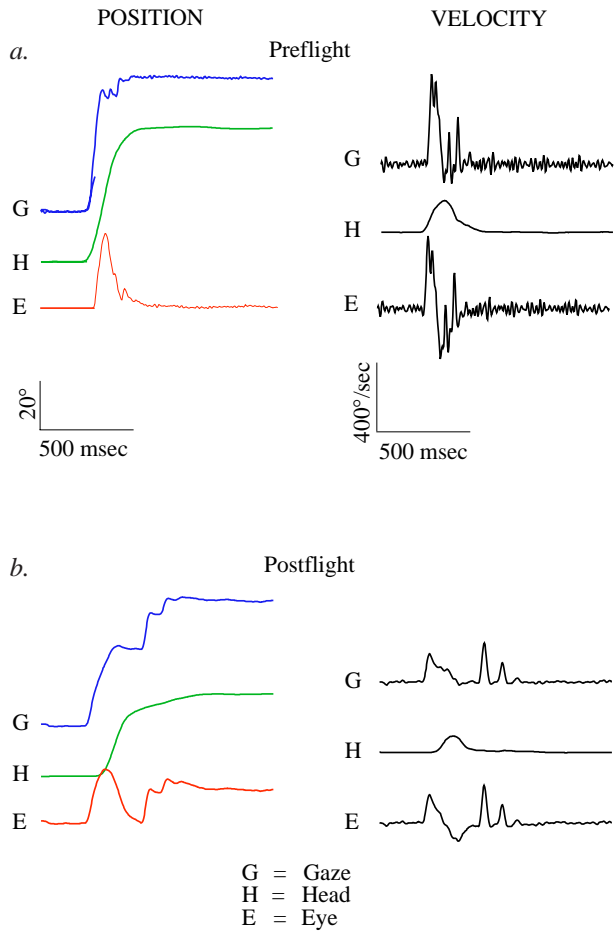


Figure 5.3-31. Pre and postflight target acquisition in vertical plane.

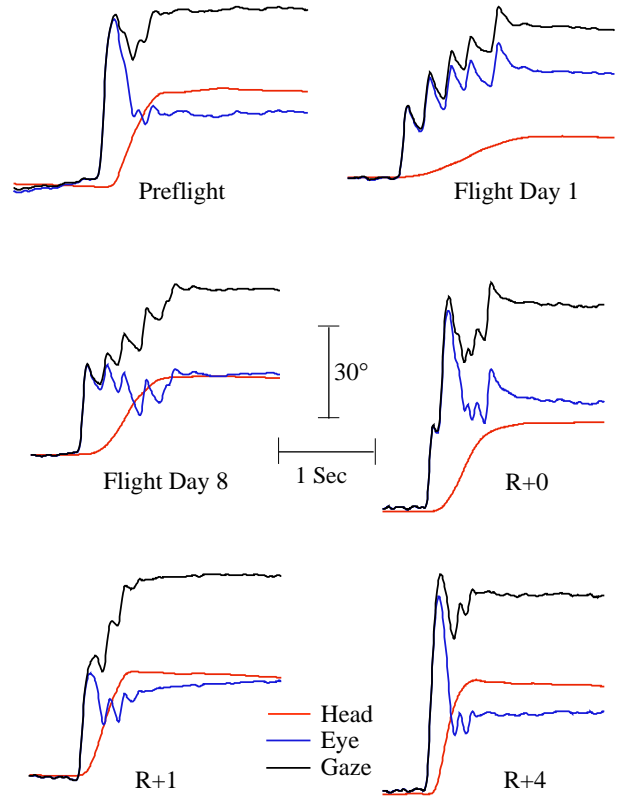


Figure 5.3-32. Upward target acquisition nearing the EOM (+50°).

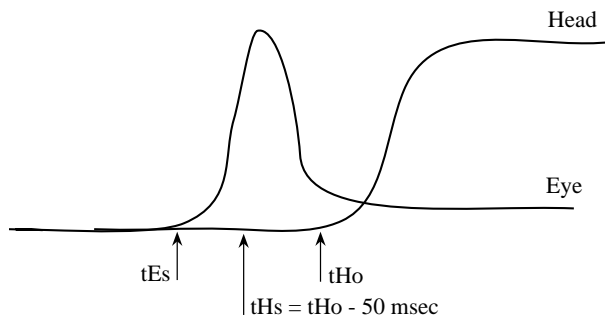


Figure 5.3-33. An illustration of how delays of head and eye movements are designated for quantification of the five different Stark types.

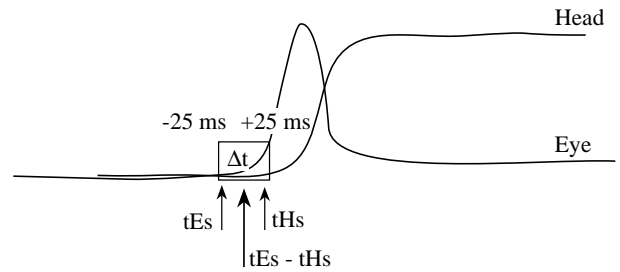


Figure 5.3-34. Stark type I $tEs - tHs > \Delta t$ and $< +\Delta t$.

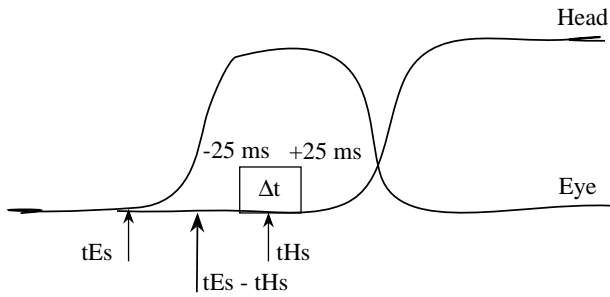


Figure 5.3-35. Stark type II $tEs - tHs < \Delta t$.

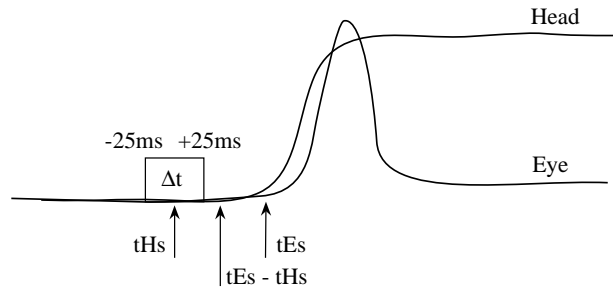


Figure 5.3-36. Stark type IIIa $tEs - tHs > + \Delta t$ and < 150 msec.

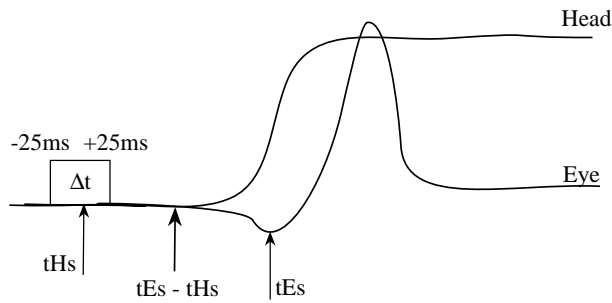


Figure 5.3-37. Stark type IIIb $tEs - tHs > 150$ msec and < 500 msec.

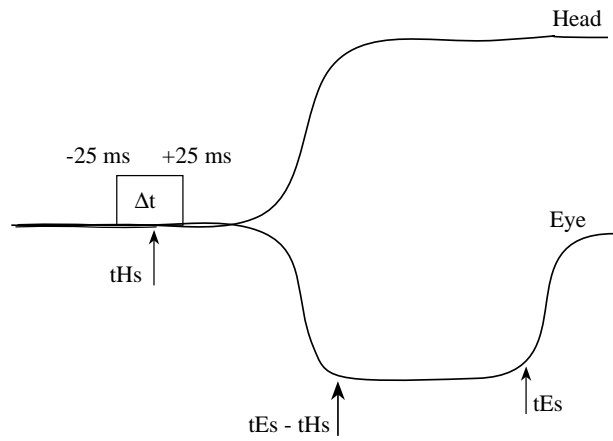


Figure 5.3-38. Stark type IV $tEs - tHs > 500$ msec.

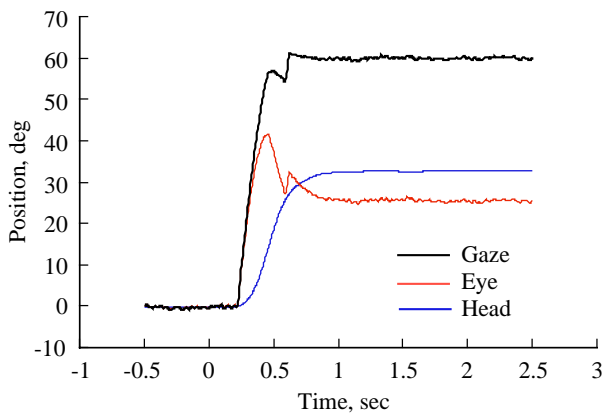


Figure 5.3-39. Preflight acquisition of target beyond the EOM.

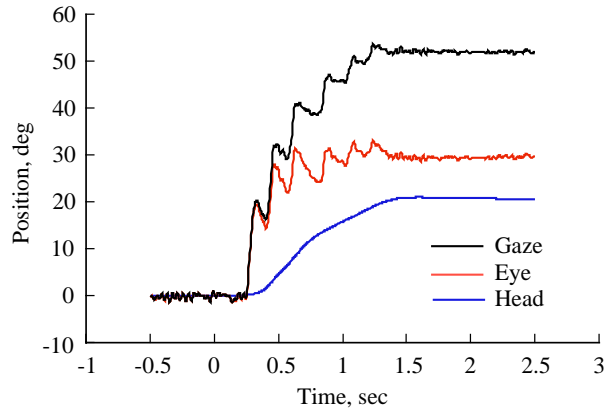


Figure 5.3-40. Postflight acquisition of a target beyond the EOM.

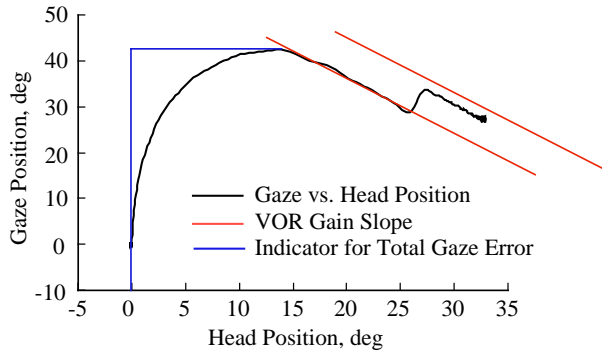


Figure 5.3-41. Gaze plane showing preflight total gaze error and VOR gain.

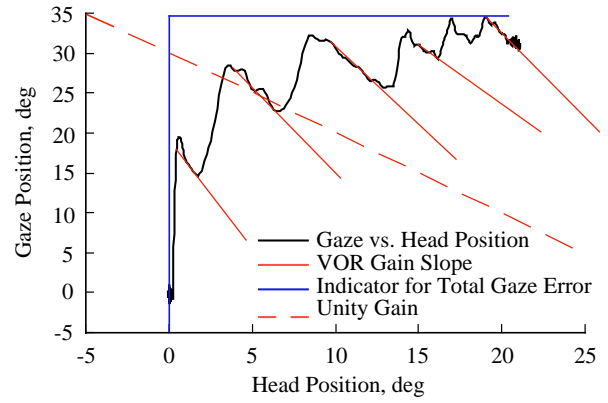


Figure 5.3-42. Gaze plane showing postflight total gaze error and VOR gain.

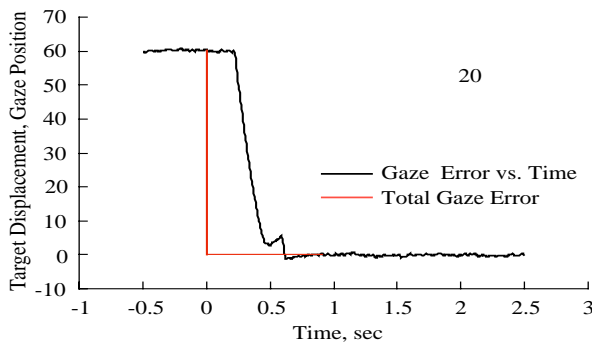


Figure 5.3-43. Preflight gaze error.

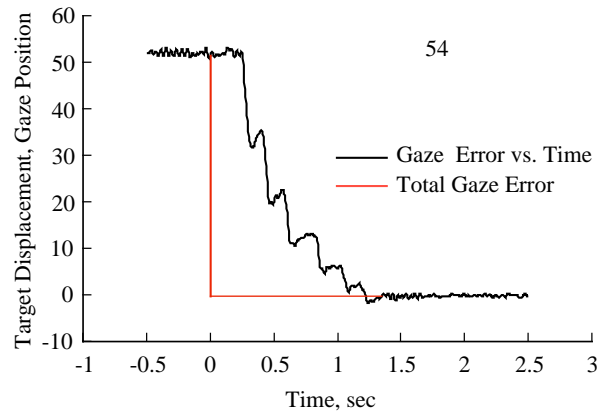


Figure 5.3-44. Postflight gaze error.

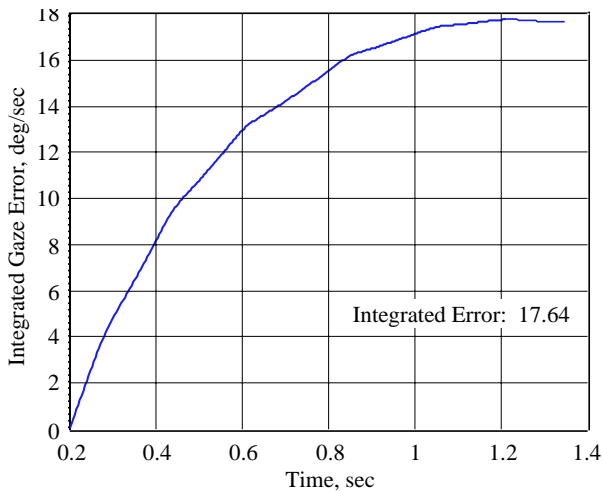


Figure 5.3-45. Integrated gaze error over time.

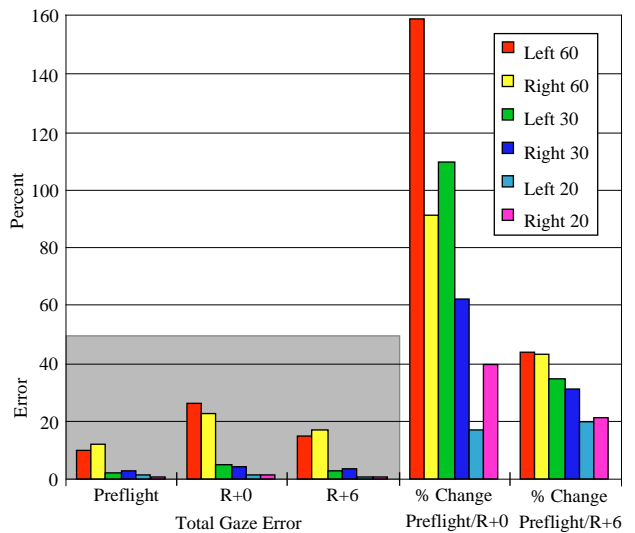


Figure 5.3-46. Changes in gaze error during flight for target displacement and recovery following flight.

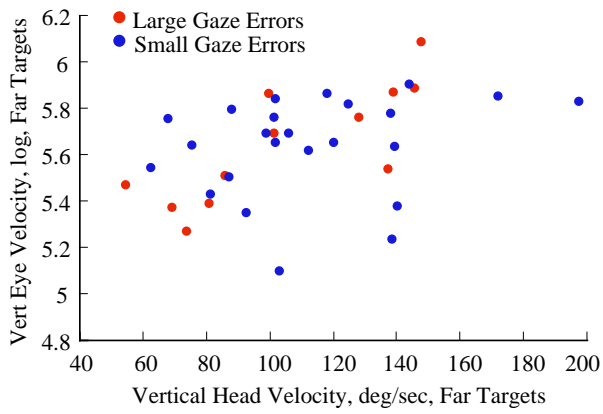


Figure 5.3-47. Postflight performance based on preflight gaze error.

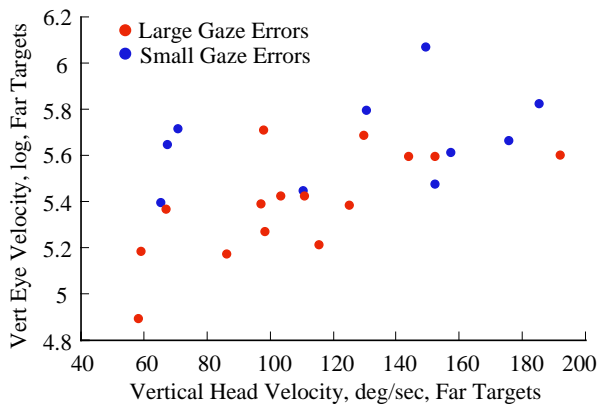


Figure 5.3-48. Postflight performance based on inflight gaze error.

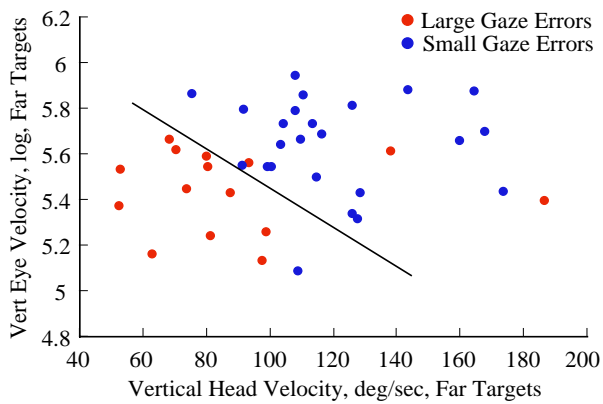


Figure 5.3-49. Postflight performance based on gaze error.

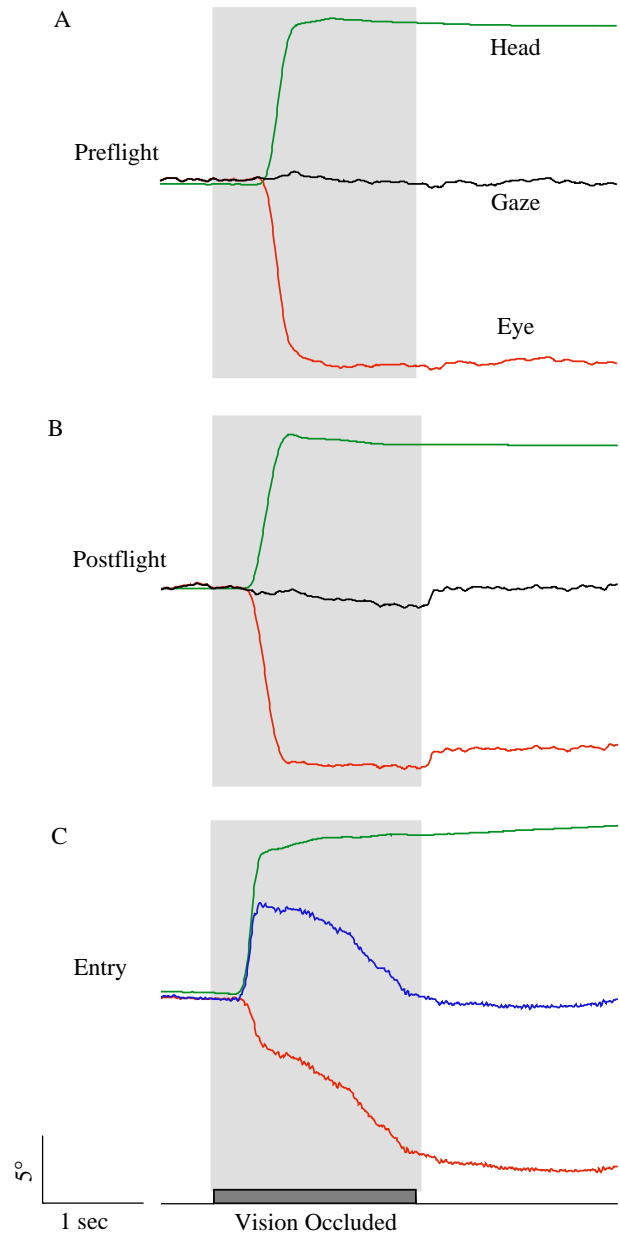


Figure 5.3-50. Gaze stabilization as a function of flight phase.

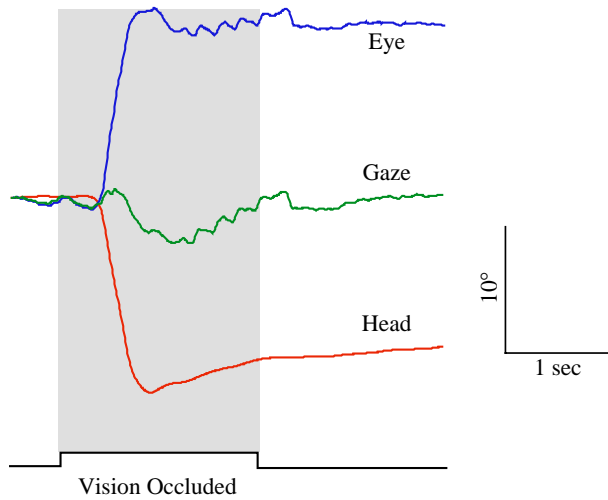


Figure 5.3-51. Postflight gaze stabilization with associated saccadic activity.

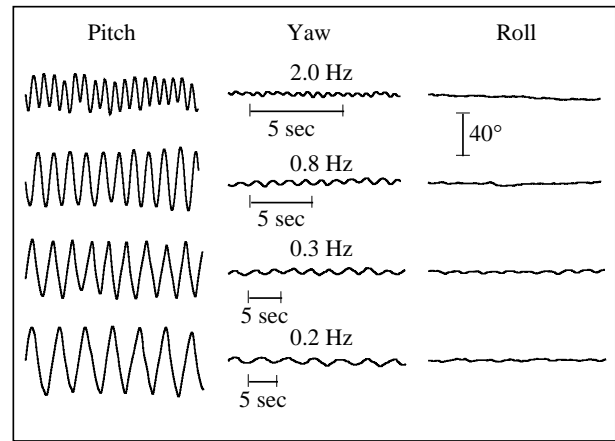


Figure 5.3-52. Sinusoidal head shakes: peak-to-peak displacements with vision during voluntary head shakes in the vertical plane.

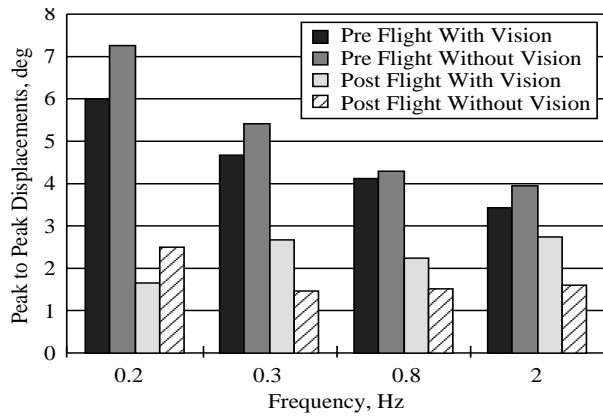


Figure 5.3-53. Displacement in the yaw plane during pitch head shakes: effects of flight phase and vision.

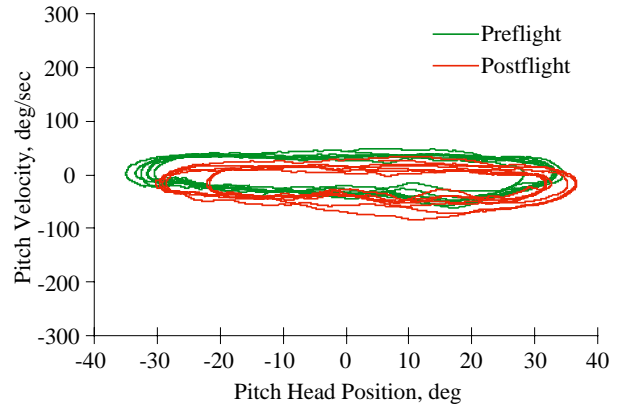


Figure 5.3-54. Phase plane for 0.2 Hz vertical head shake with vision.

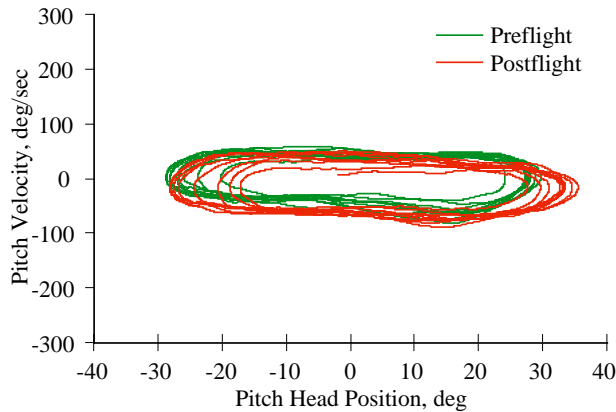


Figure 5.3-55. Phase plane for 0.3 Hz vertical head shake with vision.

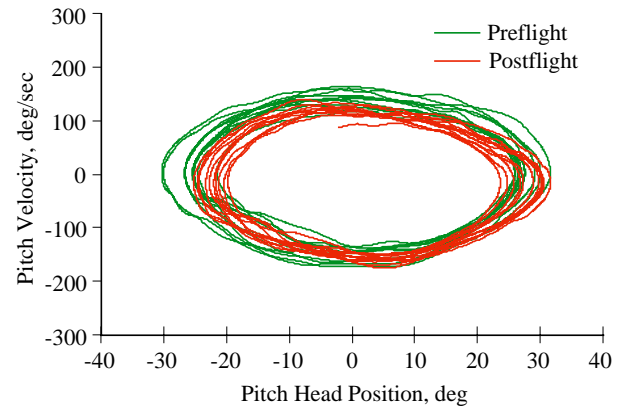


Figure 5.3-56. Phase plane for 0.8 Hz vertical head shake with vision.

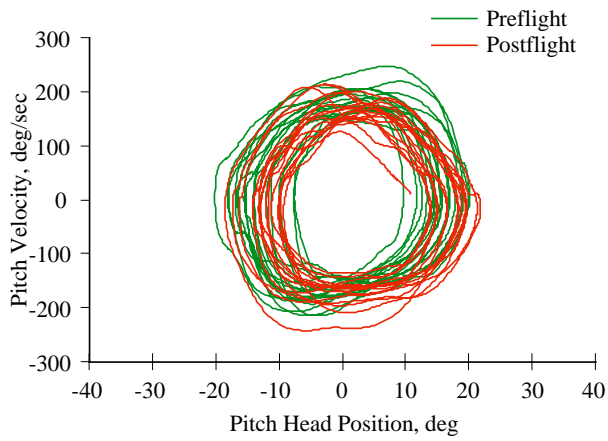


Figure 5.3-57. Phase plane for 2.0 Hz vertical head shake with vision.

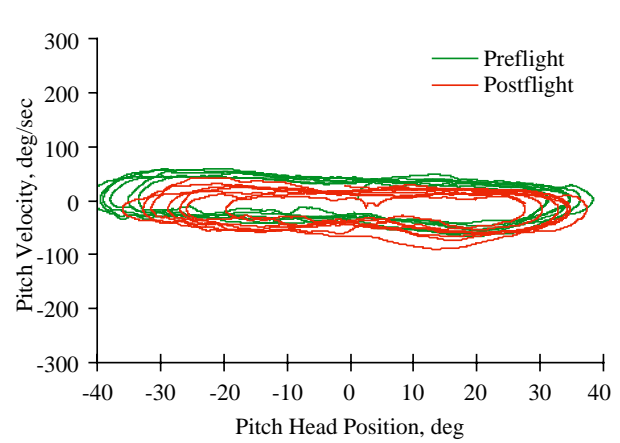


Figure 5.3-58. Phase plane for 0.2 Hz vertical head shake without vision.

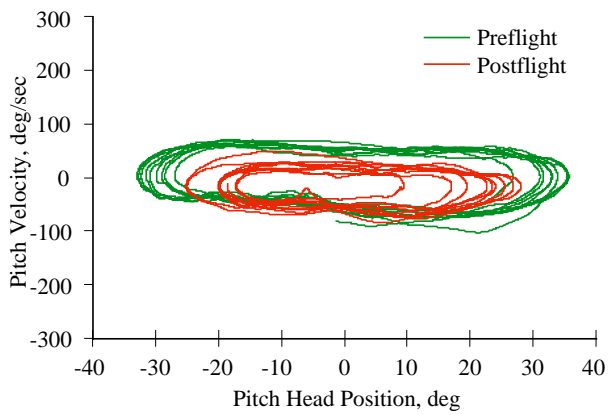


Figure 5.3-59. Phase plane for 0.3 Hz vertical head shake without vision.

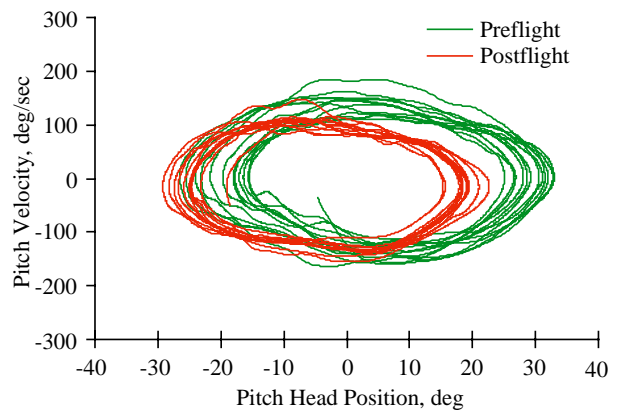


Figure 5.3-60. Phase plane for 0.8 Hz vertical head shake without vision.

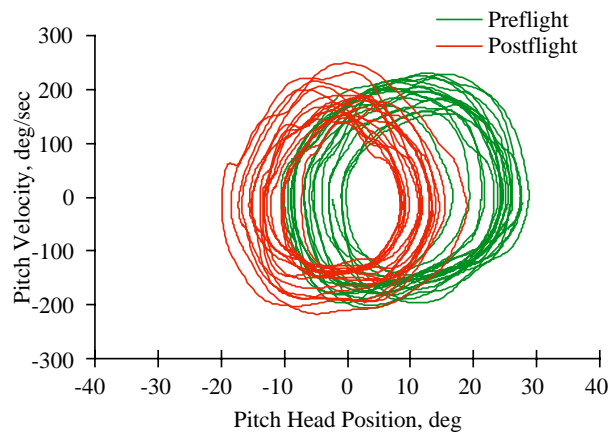


Figure 5.3-61. Phase plane for 2.0 Hz vertical head shake without vision.

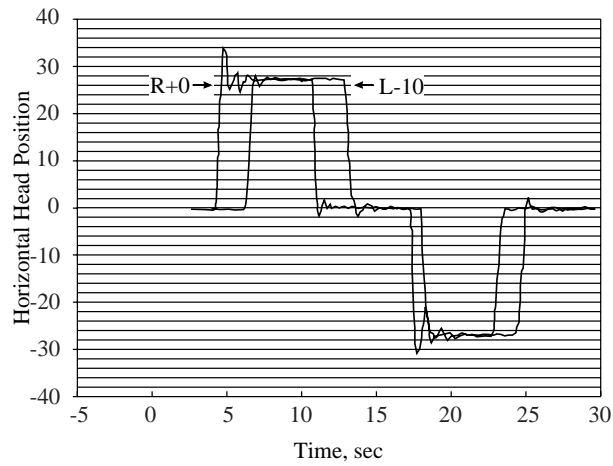


Figure 5.3-62. Horizontal head calibration, velocity:
subject 1.

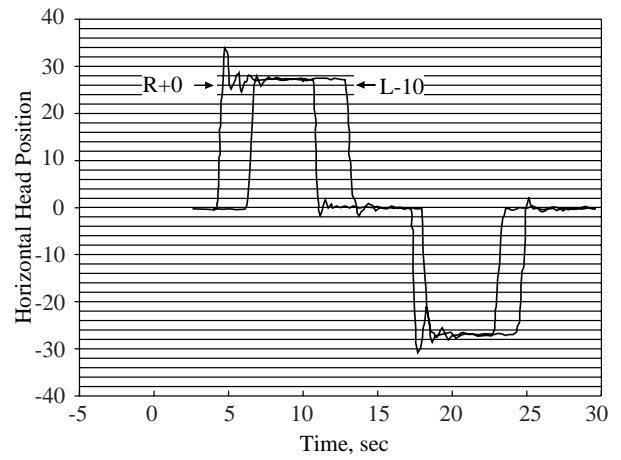


Figure 5.3-63. Horizontal head calibration position:
subject 2.

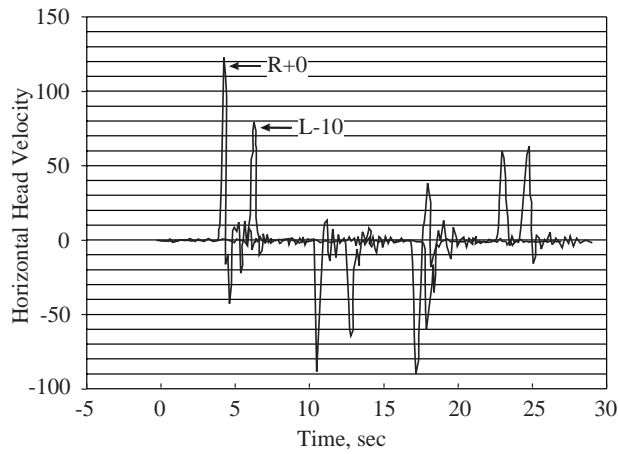


Figure 5.3-64. Horizontal head calibration velocity:
subject 1.

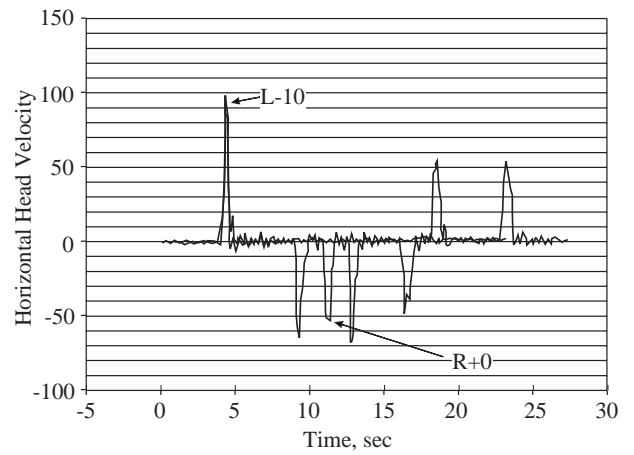


Figure 5.3-65. Horizontal head calibration velocity:
subject 2.

Section 5.4

Neurovestibular Dysfunction

Recovery of Postural Equilibrium Control Following Space Flight

(DSO 605)

*William H. Paloski and Millard F. Reschke of the Johnson Space Center, Houston, TX;
F. Owen Black of the Legacy Portland Hospitals and
R.S. Dow Neurological Sciences Institute, Portland, OR*

BACKGROUND

Human sensory-motor systems have evolved to optimize coordinated body movements and posture control in the terrestrial gravitational field. The central nervous system (CNS) has developed neurosensory systems that monitor and process sensory inputs to assess the biomechanical state of the body (spatial orientation), and neuromotor systems that create, select, and issue motor commands to correct biomechanical state errors [1-3]. Neurosensory systems respond to the sudden loss of graviceptor (otolith) stimulation during spaceflight by remodeling the sensory information integration processes used to assess spatial orientation [4,5]. Also, neuromotor systems respond to the sudden loss of the static gravitational biomechanical load by modifying the repertoire of motor command strategies and synergies used for movement control [6]. These in-flight sensory-motor adaptations optimize neural control of movement in microgravity but, unfortunately, are maladaptive for the terrestrial gravitational field. Among the operationally relevant consequences of this maladaptation is a disruption in postural equilibrium control immediately after return to Earth [7].

Terrestrial posture control systems develop to maintain biomechanical stability during normal lifetime activities. Early in life the CNS learns to maintain stable control of the body center of mass during quiet stance, as well as in anticipation of, or in response to, postural disturbances created by voluntary movements or external disturbances. To accomplish this, the CNS uses inputs from visual, vestibular, proprioceptive, and somatosensory receptors to assess the current biomechanical state of the body [1]. This state feedback is used in conjunction with internal models of body kinematics and dynamics [2] to determine the spatial orientation and relative stability of the body. Also, based on these determinations, the CNS selects and commands the most appropriate motor control strategies and synergies to return the body to the desired equilibrium state [3, 8].

Sensory feedback is critical to posture control. Normally, the CNS continuously, and subconsciously, assesses the differences between the actual biomechanical state observed by the available sensory feedback systems and

the desired biomechanical state generated by higher level brain centers. When the differences (errors) are small, closed loop control neuronal circuits may adjust the motor outputs to compensate. However, when the errors are large, an open loop control mode may be triggered. Based on previous experience as well as the magnitude, direction, and rate of change of the error state vector, the CNS selects a stereotyped response from its memorized repertoire. It then issues the set of motor commands encoded in this response memory, triggering predetermined muscles at predetermined latencies without regard for the concomitant sensory feedback. Following this open loop command volley, the CNS immediately resumes continuous assessment of the current biomechanical state.

Motor performance and biomechanics are also critical to posture control. Changes in muscle strength, muscle tone, or reflex activity, as well as changes in body mass distribution, intersegmental orientation, or support surface characteristics will alter both the kinematic and dynamic responses to a particular set of motor commands. During quiet stance, the continuous CNS adjustment of motor outputs generally compensates for moderate motor performance and biomechanical deficits. However, following sudden perturbations, the success of resulting motor command volleys in recovering postural equilibrium depends critically on motor performance and biomechanics.

During spaceflight, the continuous, omnipresent, Earth-vertical spatial reference that is normally provided by gravity and sensed by the otolith organs and other corporal graviceptors is absent. This causes incongruence between the expected and actual sensory afference resulting from body movements. This incongruence may lead to space motion sickness (SMS) [9], perceptual illusions, and malcoordination. When sustained, the incongruence may also drive central adaptive processes that result in new internal models of the reafferent signals expected from efferent motor commands. The new internal models have been described previously in terms of reinterpretation [4] or neglect [5] of gravity-mediated otolith inputs. The end result of this adaptation is that the CNS no longer seeks gravitational stimuli for use in estimating spatial orientation. While this may be advantageous for the amelioration

of SMS and is likely to optimize central neural control of coordinated body movements in the absence of gravity, it also appears to significantly disrupt control of coordinated body movements immediately after return to Earth [10]. Among the postflight effects of in-flight neurosensory adaptation to microgravity is the disruption of postural stability control, which has been demonstrated in both astronauts and cosmonauts following spaceflight [6, 7, 11-21]. The sustained absence of gravity also affects neuromotor components of the CNS. For instance, loss of gravity causes (1) weight unloading that triggers muscle disuse disturbances, (2) elimination of tonic antigravity muscle activation, (3) reduction of support reactions, and (4) changes in biomechanics characterized, for example, by altered relationships between the mass of, and the force required to move, a body segment [16].

Previous investigators in both the U.S. and Russian space programs have examined the characteristics and mechanisms of postflight postural ataxia. One class of investigations examined posture control by studying the abilities of crew members to maintain stable upright posture during quiet stance with normal and modified sensory feedback. The first such paradigm used in the U.S. program required astronauts to stand on narrow rails with their eyes either open or closed [12-14, 22, 23]. Results obtained using this paradigm demonstrated substantial postflight performance decrements during the eyes closed tests, with the magnitude of the postflight ataxia being greatest during the first postflight test. Recovery appeared to be related to mission length. Similar results were obtained early in the Russian program, where investigators used stabilogram recordings of (1) quiet standing with eyes open and eyes closed, (2) standing in the sharpened Romberg posture, and (3) standing with the head tilted either forward or backward [24-26]. Subsequent studies of postural stability during quiet stance before and after flight have employed more complex paradigms. For example, von Baumgarten et al. [27] required crew members to stand on an Earth-fixed stabilometer beneath a tilting room with eyes open, eyes closed, conflicting visual-vestibular input in which the room was tilted with a sinusoidal motion, and altered somatosensory input in which the subject stood on foam rubber placed atop the stabilometer. They found an increased reliance on visual feedback for posture control immediately after spaceflight, and impaired postural stability for up to 5 days after return to Earth.

Another class of postural investigations examined the abilities of crew members to recover stable upright posture following external perturbations of their upright stance. In the U.S. program, external postural perturbations were provided most frequently by moving the support surface upon which the subject stood. For example, Anderson et al. [11] used sudden stepwise translations of the support surface. They found that the segmental biomechanical responses were exaggerated, the latency of

the initial soleus muscle electromyographical (EMG) response was increased, and the time required to achieve a new equilibrium position was greater after spaceflight than before. Kenyon and Young [14], using sudden stepwise pitch rotations of the support surface, found that the late (long loop) EMG response was higher in amplitude after flight than before. In the Russian space program, investigators have frequently used postural perturbations at the chest, rather than the base of support, to study ataxia after flight. For example, Grigoriev and Yegorov [28] studied postflight posture control in the three prime crew members of the long duration MIR-Quant expedition. When compared to preflight values, they found that on the 6th day after flight, less force was required to perturb posture, and both the time to recover from the perturbation and overall muscle activity following the perturbation increased. Similar changes were also reported in larger groups of subjects following other long duration missions, short duration missions, and microgravity simulation experiments [6, 15, 26, 29]. On the basis of these studies, the authors concluded that support unloading played an important role in the genesis of postural ataxia in short duration (up to 30 days) exposure to real and simulated microgravity. This was attributed to a reduction in afferent inflow from the support areas and the subsequent decline in antigravity (extensor) muscle tone, as well as to a hypersensitivity of the spinal reflex mechanisms. They suggested that, for longer duration hypogravity exposures, peripheral disorders, such as muscle hypotrophy, alterations of neuromuscular transfer functions, and alterations of muscle membrane properties were also important. Finally, they suggested that on long duration spaceflights, disturbances to the processes of reorganization of motor patterns occurred, and that recovery time depended strongly on mission duration.

Postflight postural equilibrium disturbances have important implications to the potential success of emergency egress from the Shuttle immediately after landing. Despite the fact that there appears to be a rapid initial readaptation to the terrestrial environment, subjective reports from crew members indicate that, at least in certain instances, it would have been difficult to egress from the vehicle soon after wheels stop. Previous findings that the microgravity adapted individual depends more heavily on visual system inputs for posture control suggest that the severity of the postflight ataxia would increase dramatically if the crew compartment were filled with smoke or darkened by malfunctioning lights. Under these circumstances, emergency egress would be difficult or impossible. These egress difficulties are likely to be further exacerbated by the 6-degree forward pitch attitude of the vehicle, should emergency egress be required on the runway following landing. This forward pitch could add to the disequilibrium by (1) shifting the apparent (visual) vertical within the vehicle from that surrounding the vehicle, and (2) shifting the visual vertical with respect to the

gravitational (otolith) vertical. Furthermore, these egress difficulties could also be increased by the perceptions of self-motion and/or surround-motion reported to be elicited by head movements during entry and immediately after flight [4, 30]. Finally, these difficulties might be further exacerbated by changes in effector characteristics such as muscle tone and strength, and by the de facto requirement that emergency egress be performed wearing a massive, bulky launch and entry suit (LES).

A number of studies have been performed to investigate the etiology and severity of postflight postural ataxia. The results from each of these studies are generally consistent with the hypotheses under investigation in Detailed Supplementary Objective (DSO) 605. However, the combination of small population size and lack of corroborating evidence in abnormal human subjects has left considerable doubt concerning the degree to which non-vestibular factors may account for the observed postflight ataxia. A small number of subjects tested is the main problem shared by all of the previous studies of posture control changes associated with spaceflight. Interpretation of the results of experiments on two to four subjects cannot be conclusive, particularly in light of the wide variations in demographic factors such as age, gender, flight experience, and mission duration that could potentially affect the results. Furthermore, development and/or evaluation of specific countermeasures to the untoward effects of in-flight sensory-motor adaptation can only be accomplished when the influence of these demographic factors is understood.

DSO 605 was designed to build on the results of previous studies of postflight postural ataxia and to extend these results by (1) examining the components of neurosensory control of posture with a more sensitive posturography technique than previously used, (2) systematically evaluating the total postflight recovery process, (3) controlling explicitly for previous spaceflight experience, and (4) studying enough subjects to draw statistically significant conclusions. The ultimate goals of this study were (1) to characterize the recovery process for postural equilibrium control in crew members returning from Shuttle missions, and (2) to validate the dynamic posturography system as a dependent measure for future evaluation of vestibular and/or sensory-motor countermeasures.

The long term objective of this investigation was to determine the underlying mechanisms contributing to postflight postural ataxia in astronauts participating in extended duration Orbiter spaceflight missions. It was expected that this knowledge would lead to insights that would guide the development of effective countermeasures to the effects of sensory-motor adaptation to spaceflight. The following hypotheses were tested:

1. In-flight loss of gravitational otolith stimulation, coupled with concomitant reductions in biomechanical constraints to body motion, lead to adaptive changes in

the CNS that eliminate the use of gravity-mediated otolith information in estimating spatial orientation, and supplant it (partially) by increasing the weighting of visual spatial information. This will cause postflight reductions in the effectiveness of vestibular control of posture, while concomitantly increasing the dependence on visual inputs for posture control.

2. The effectiveness of posture control during quiet stance, and in response to stability threatening external disturbances, will be reduced early after spaceflight because of retention of in-flight sensory-motor adaptation. Both the magnitude and the recovery time of this post-flight postural ataxia will increase with mission duration because of the increased time for in-flight sensory-motor adaptation to microgravity.

3. Repeated exposures to microgravity result in a training effect such that the magnitude and the recovery time course of postflight postural ataxia decrease with flight experience. Astronauts having previous spaceflight experience will exhibit less severe ataxia than those flying for the first time.

METHODS

Two experiment paradigms were performed by 40 crew members before, during, and after Shuttle missions of varying duration. The first of these paradigms focused primarily on neuromotor performance by quantifying the response to sudden, stability threatening base-of-support perturbations. The second paradigm focused on neurosensory performance by quantifying postural sway during quiet upright stance with normal, reduced, and altered sensory feedback. All participating subjects performed the two paradigms on at least three occasions before flight to provide an accurate, stable set of unit gravity control data from which postflight changes could be determined. All subjects also performed the two paradigms on up to five occasions after flight to capture the full sensory-motor readaptation time course. Postflight tests began on landing day, as soon after Orbiter wheels stop as possible, and were scheduled on an approximately logarithmic time scale over the subsequent 8 days (Table 5.4-1).

Of the 40 subjects studied: 11 were from short duration (4-7 day) missions, 18 from medium duration (8-10 day) missions, and 11 from long duration (11-16 day) missions. Seventeen of the subjects were first time (rookie) fliers, and 23 were experienced (veterans).

All testing was performed using a modified version of the Equitest computerized dynamic posturography system developed by Neurocom, International (Clackamas, OR, USA) for clinical assessment of disorders in balance control. The posturography system consisted of a computer controlled, motor driven dual foot plate capable of both rotational and translational movements, and a computer controlled, motor driven visual surround capable of

Table 5.4-1. DSO 605 experiment test schedule

<i>Preflight (JSC/Bldg.37)</i>		
L-60 days (+/-5 days):	Crew Briefing and Control Session No. 1	60 min
L-30 days (+/-5 days):	Control Session No. 2	30 min
L-10 days (+/-2 days):	Control Session No. 3	30 min
<i>Postflight-Early (KSC or DFRC)</i>		
R+1 hour (or sooner):	Study Session No. 1	30 min
R+3 hours (+/-1 hr):	Study Session No. 2	20 min
<i>Postflight-Late (JSC/Bldg. 37)</i>		
R+48 hours (+/-6 hrs):	Study Session No. 3	30 min
R+96 hours (+/-12 hrs):	Study Session No. 4	30 min
R+8 days (+/-1 day):	Study Session No. 5	30 min

Key: L-n = n days before launch
 R+n = n hrs (or days) after return
 JSC = Johnson Space Center
 KSC = Kennedy Space Center
 DFRC = Dryden Flight Research Center

rotational movements about an axis colinear with the subject's ankles. Force transducers located beneath the dual foot plate were used to monitor and record the subject's weight distribution and reaction torques during testing. To improve the sensitivity of the posturography system, it was modified to monitor and record the EMG activity of various antigavity muscles as well as dynamic changes in sagittal plane hip position, shoulder position, and head angular velocity throughout the testing periods. Also, to eliminate auditory spatial orientation cues from external sources, the subject was required to don headphones, through which wide-band masking noise was provided.

Upon arrival at the test facility, the subject completed a pretest questionnaire designed to identify any uncontrolled factors that could potentially influence the test results. The subject's height was measured during the first preflight and postflight session. Prior to posture testing, the subject donned loose fitting short pants to facilitate EMG electrode placement and joint position monitoring. The skin surface at each EMG electrode site was prepared for placement of a pre-gelled disposable silver/silver chloride surface electrode, by shaving away any existing hair and scrubbing the region with an abrasive skin cleanser (Omni-Prep). Pairs of electrodes were attached to the skin surface above the medial gastrocnemius, tibialis anterior, hamstrings (primarily biceps femoris), and quadriceps (primarily rectus femoris) muscle groups. A single ground electrode was placed adjacent to the medial gastrocnemius pair. The impedance between each monitoring electrode and the ground reference electrode was then measured. If the electrode impedance was above 100 Kohms, the electrode was replaced. During electrode

placement, the subject was briefly interviewed, on camera, to determine the sensations and perceptions experienced during landing, egress, and/or previous posture testing. Before the subject stepped onto the posture platform, the operator powered up the posturography system and zeroed any sensor offsets. The subject then donned a safety harness and mounted the platform. The operator next fastened the safety harness to the safety bar that looped over the subject's head, positioned the subject on the platform, and attached the body segment position measuring devices (sway bars). Finally, the subject donned headphones used to provide the masking noise and couple the angular rate sensors to the subject's head.

Each test session began with a set of motor control tests, during which the subject attempted to recover upright postural equilibrium as quickly as possible after support surface perturbations. These were (1) three sequential backward translation trials (≈ 5.7 cm during 400 msec), (2) five sequential toes-up rotation trials (8 degrees during 400 msec), (3) three sequential forward translation trials (≈ 5.7 cm during 400 msec), and (4) five sequential toes-down rotation trials (8 degrees during 400 msec). The duration of each trial was approximately 3 seconds, and the time between trials was usually less than 5 seconds. Support surface translations and rotations were applied automatically under computer control.

Immediately following the motor control tests, the test session proceeded with a set of sensory organization tests, during which the subject attempted to maintain upright balance control under the following conditions (1) eyes open, fixed support surface, (2) eyes closed, fixed support surface, (3) sway referenced vision, fixed support surface, (4) eyes open, sway referenced support surface, (5) eyes closed, sway referenced support surface, and (6) sway referenced vision, sway referenced support surface. Each of these conditions was repeated three times during the test session in random order. The duration of each trial was 20 seconds, and the time between trials was normally less than 5 seconds. Throughout the test period, the test operator controlled the execution of the test protocols at the posturography system computer rack, while standing near enough to the platform to steady the subject when disorientation or loss of balance occurred. The operator was required to depress a foot switch to execute the test procedures. When the posturography system detected that the subject had fallen (lost balance), it automatically interrupted the test procedure and waited for the operator's command to abort or continue the test. Following the sensory organization tests, the subject was deinstrumented and stepped down from the posture platform. EMG electrodes were then removed and the electrode sites cleaned with sterile alcohol pads. While the electrodes were being removed, the subject was again briefly interviewed on camera, to determine the sensations and perceptions experienced during landing, egress, and/or the posture testing.

The posturography system support surface comprised

two 23 by 46 cm foot plates, connected together by a pin joint and supported by four temperature compensated load cell force transducers symmetrically mounted on a supporting center plate. The four load cells independently sensed the anterior and posterior normal forces applied to the support surface by each foot. A fifth temperature compensated force transducer, mounted centrally between the support surface and supporting center plate, sensed shearing forces applied to the support surface in the antero-posterior direction. During each test, outputs from the five force transducers were amplified, digitized at 103 Hz, and stored electronically. Calibration of the force transducers was verified before each test using custom calibration fixtures.

The force plate data were combined algebraically to compute the instantaneous antero-posterior and medio-lateral coordinates of the center of pressure as a function of time. These center of pressure data were subsequently low pass filtered (-3 dB point at 1 Hz) to obtain an estimate of the center of gravity position as a function of time. The center of gravity was assumed to be located at 55% of the subject's height [31]. Its position was then converted geometrically to a center of gravity sway angle.

For the sensory organization tests, the peak to peak center of gravity sway angles (p-p sway) were determined for each 20 second trial. For some comparisons, the p-p sway data were used to compute a measure of postural stability known as the equilibrium score:

$$\text{Equilibrium Score} = \left[1 - \frac{\text{p-p sway}}{12.5} \right] \times 100$$

where 12.5 was the maximum stable sway amplitude expected in a normal population

The equilibrium score varied directly with postural stability. To provide an overall assessment of the subject's postural stability at each test session, a composite equilibrium score was computed by summing the average equilibrium scores from test 1 (eyes open, fixed support surface) and test 2 (eyes closed, fixed support surface) with the individual equilibrium scores from each trial of tests 3 to 6. The resulting equilibrium scores, scaled to 1000, were compared with a large normative database compiled by the posture platform system manufacturer [32].

Sagittal plane segmental body movements were monitored throughout each test using lightweight wooden sway bars attached to hooks mounted on the subject's posterior midline at the level of the greater trochanters and the seventh cervical vertebrae. The opposite end of each sway bar was attached to a potentiometer mounted on a column fixed to the base of the platform system. Sagittal plane hip and shoulder sway displacements, relative to an Earth-fixed spatial coordinate system, were determined through geometric manipulation of the outputs of the sway bar potentiometers. These outputs were digitized at 103 Hz

and stored electronically. Calibration of the hip and shoulder sway monitoring systems was verified before each test session using a custom calibration fixture. Head movements were also monitored throughout each test. Sagittal and frontal plane head angular velocities were sensed using angular rate sensors (Watson Model ARS-C241-1AR, Watson Industries, Inc., Eau Claire, WI) attached to the subject's headset. Rate sensor outputs were digitized at 103 Hz and stored electronically. Head angular positions were determined, relative to the starting position at each trial, by digital integration of the rate sensor data.

A link segment mathematical model [33] was developed and used for analyzing intersegmental coordination during the dynamic posturographic tests (Figure 1). Inputs to the model were the five time-varying segment angles, θ_i ($i = 1, 2, 3, 4$), measured using the sway bars and angular rate sensors. The knee angle was not monitored during these tests and was assumed to remain constant. Two other time-varying angles, θ_0^* and θ_3^* , oriented fixed angular distances from θ_0 and θ_3 , respectively, indicated the locations of the centers of mass for the two non-axisymmetric segments of feet and torso/arms. θ_0^* was determined from anthropometric data tables, but θ_3^* was determined empirically. Outputs from the model included a number of kinematic and kinetic parameters commonly used to analyze postural biomechanics:

Joint Positions: By assigning the origin of the sagittal plane reference axes to the ankle joint, and assuming that the heels and toes always remain in contact with the support surface, the instantaneous horizontal (x_{ji}) and vertical (y_{ji}) positions of the ankle, knee, hip, and cervicothoracic joints, as well as the location of a fictive joint at the bottom of the foot (the point on the support surface closest to the ankle joint), were computed at each sampled data point ($k = 1, 2, \dots, n$) from:

$$x_j(k) = L \cos \theta(k)$$

$$y_j(k) = L \sin \theta(k).$$

Center of Mass Positions: The instantaneous locations of the segment centers of mass (x_{cm_i}, y_{cm_i}) were computed from:

$$x_{cm}(k) = D \cos \theta(k)$$

$$y_{cm}(k) = D \sin \theta(k).$$

Center of Mass Accelerations: From the second derivatives of the center of mass position equations:

$$\ddot{x}_{cm}(k) = -D [\alpha(k) \sin \theta(k) + \omega^2(k) \cos \theta(k)]$$

$$\ddot{y}_{cm}(k) = -D [\alpha(k) \cos \theta(k) - \omega^2(k) \sin \theta(k)].$$

Center of Gravity: The instantaneous antero-posterior position of the center of gravity (CG), which is the vertical projection of the whole body center of mass

position, was computed from:

$$CG(k) = \frac{1}{M} m \ddot{x}_{cm}(k).$$

Joint Forces: The total horizontal (F_{x_i}) and vertical (F_{y_i}) forces acting at the foot support surface interface ($i = 0$) as well as at the ankle, knee, hip, and cervico-thoracic joints ($i = 1, 2, 3, 4$), were computed from:

$$F_x(k) = M \ddot{x}_{cm}(k)$$

$$F_y(k) = M [\ddot{y}_{cm}(k) + g].$$

Ground Reaction Forces: The normal (F_n) and shear (F_s) components of the ground reaction force were computed from:

$$F_n(k) = F_{y_0}(k) \cos \theta_0(k) - F_{x_0}(k) \sin \theta_0(k)$$

$$F_s(k) = F_{x_0}(k) \cos \theta_0(k) + F_{y_0}(k) \sin \theta_0(k).$$

Joint Torques: The net torques (T_i) acting about each joint, including the fictive joint at the support surface, were computed from:

$$T(k) = J \ddot{\theta}(k) - \Delta_y(k) F_x(k) + \Delta_x(k) F_y(k).$$

Center of Pressure: The center of pressure was computed from the support surface torque by:

$$CP(k) = \frac{T_0(k)}{F_n(k)}.$$

The segmental and whole body kinematic data were also analyzed to determine what, if any, stereotypical movement patterns were employed during the execution of each task, and how these patterns were affected by adaptation to microgravity and readaptation to Earth. In particular, ankle and hip whole body sway strategies [34], and stable platform and strapped down head-trunk segmental strategies [21, 35] were sought. Temporal sequences demonstrating recovery of the p-p sway and equilibrium score measurements were created from the postflight test sessions. These sequences were then fit to multiexponential readaptation models using the Levenberg-Marquardt nonlinear least squares technique [18, 36].

EMG activities of the primary postural muscles on the left side of the body were monitored using surface electrodes to establish motor reaction times and temporal activation patterns associated with specific motor synergies/strategies. EMG potentials sensed by these electrodes were band-pass filtered (-3 dB points at 1 Hz and 100 Hz) and amplified (2000 v/v) using Grass Model 7P511 AC Preamplifiers. These processed analog signals were then digitized at 412 Hz and stored electronically.

Sensory organization test data were analyzed using the StatView and SuperANOVA statistical analysis software packages (both from Abacus Concepts, Inc., Berkeley, CA). Differences in p-p sway amplitude between the preflight and postflight test sessions were investigated using repeated measures analysis of variance (ANOVA) for each balance control test. The roles of the visual, proprioceptive, and vestibular sensory systems in balance control were assessed using a one-between (rookies, veterans), three-within (vision, proprioception, vestibular, i.e., spaceflight), full-interaction ANOVA model with specific contrasts. To meet the equal variance assumption of the ANOVA model, p-p sway amplitude data were subjected to natural logarithmic transformation prior to analysis. Anti-transforming the results of these analyses resulted in standard errors that were asymmetric about the mean. Differences in p-p sway amplitude between the mission position groups were investigated using analysis of covariance (ANCOVA) for each test condition. Postflight values were used as the dependent variable; rookie or veteran status was used as a group factor; and preflight values were used as the covariable. Use of ANCOVA with preflight values as the covariable permitted comparison of postflight means for the two groups that were independent of preflight values.

The effects of the continuous demographic variables (height, weight, and mission duration) were assessed using multiple regression analyses to determine whether any relationships existed between the demographic variables and the changes in p-p sway amplitude associated with spaceflight. For each test condition, the dependent parameter was the postflight p-p sway amplitude. The independent parameters were the preflight p-p sway amplitude and the demographic parameter of interest. Probabilities were adjusted, when necessary, to the greater of the values obtained from the Huynh and Feldt [37] and the Geisser and Greenhouse [38] corrections for violations of assumptions of the repeated measures ANOVA model. Null hypotheses were rejected when the adjusted probabilities were less than 0.05.

RESULTS AND DISCUSSION

Inability to Use Vestibular Information Following Spaceflight

Sensory organization test results from 34 crew members summarized in Tables 5.4-2 and 3, and in Figures 5.4-2 through 7 and 10, are in review for publication [7].

Typical Subject: Preflight and postflight antero-posterior (a-p) center of gravity sway time series traces for a typical subject for each of the six test conditions are presented in Figure 5.4-2. Each of the traces in this figure represent subject response to a different set of sensory orientation reference conditions. The lower center and lower

Table 5.4-2. Subject demographic information

Subject	Age, yrs	Height, cm	Weight, kg	Flt No.	Length, days	L-2, days	L-1, days	R+0, hrs
Mean	41.4	180.0	78.4	1.9	9.11	-45.0	-14.1	2.72
SEM	0.84	1.08	1.77	0.16	0.55	3.83	0.78	0.13
Min	32	165	48	1	4.09	-111	-25	1.62
Max	50	191	99	4	16.63	-22	-7	4.50

Key: Flt No. = subject flight number (1 = first-time flier, 2 = second-time flier, etc.)
 Length = mission duration
 L-2, L-1 = time before launch of preflight data collections
 R+0 = time after landing (wheel stop) of initial postflight data collection

right panels represent responses to test conditions during which vestibular inputs provided the only theoretically accurate sensory feedback. All other test conditions provided the subject with fully or partially redundant sensory orientation information from the visual, vestibular, and/or proprioceptive systems.

Before flight (Figure 5.4-2, “pre” traces), changes in visual cues had little effect on this subject’s a-p sway amplitude when the proprioceptive cues were left intact, as shown in the upper row-fixed support surface. When the proprioceptive inputs were altered, as shown in the lower row-sway referenced support surface, the subject’s a-p sway amplitude increased for all visual conditions. The greatest increases occurred when visual cues were either absent (eyes closed) or simultaneously sway referenced, forcing the subject to rely on vestibular inputs as the only veridical spatial orientation reference cues.

Immediately after spaceflight (Figure 5.4-2, “post” traces), the subject’s a-p sway amplitude increased under all test conditions when compared to preflight values. The increased amplitudes observed under sway referenced support conditions (lower row) were balance threatening. When both visual and proprioceptive cues were sway referenced, this subject’s center of gravity oscillated between his/her forward and backward stability limits.

Stabilograms corresponding to each of the time series traces in Figure 5.4-2 are shown in Figure 5.4-3. The stabilograms demonstrate that, in addition to the increased a-p sway amplitudes, the subject’s mediolateral (m-l) sway amplitudes were also increased on each test condition after flight. The increased center of gravity sway was relatively symmetric about the equilibrium point during tests 1 and 2 (upper left and upper center). However, under the other four test conditions, the a-p sway amplitudes were clearly larger than the m-l sway amplitudes.

Sensory Test Performances: Landing day data were obtained, in all six sensory organization test conditions, for 34 of the 40 subjects (Table 5.4-2). Cumulative distribution functions for the average p-p sway amplitudes observed in

these 34 subjects before and after spaceflight, under each of the six sensory organization test conditions, are presented in Figure 5.4-4. These population data are qualitatively similar to the single subject sway data presented above. Note that, with the possible exception of the most stable performers on tests 1 and 2 (Figure 5.4-4, upper left and upper center panels), the entire cumulative distribution function for each test condition was shifted to the right, toward higher center of gravity sway, and lower postural stability, values. Furthermore, the preflight and postflight sways were significantly correlated in all but test 2. The correlation coefficients ranged from 0.51 to 0.65 (Table 5.4-3).

Compared to preflight, significant sway amplitude increases were observed early after flight (2.72 ± 0.13 hrs) in all six test conditions. The mean and standard error values for these data are presented in Table 5.4-3 and plotted in Figure 5.4-5. Under the standard Romberg conditions (Table 5.4-3, tests 1 and 2), the sway amplitude increased by only 0.27 degrees (35%) with eyes open and 0.35 degrees (25%) with eyes closed. Under sensory conflict conditions, the sway amplitude increased by 0.60 degrees (60%) when the visual surround was sway referenced (test 3), by 0.94 degrees (69%) when the support surface was sway referenced and eyes were open (test 4), by 1.97 degrees (63%) when the support surface was sway referenced and eyes were closed (test 5), and by 3.12 degrees (104%) when both the visual surround and the support surface were sway referenced (test 6). While the sway was increased on all sensory organization tests after flight, the increased sway was only stability threatening under the postflight conditions during which vestibular inputs provided the only theoretically accurate sensory feedback (tests 5 and 6).

Sensory Analyses: Data from all preflight and postflight sensory organization test conditions were fit to a single ANOVA model to determine the interdependent relationships between sensory inputs in the control of postural stability (p-p sway amplitude). Significant alterations in the main effects of visual, proprioceptive, and vestibular

Table 5.4-3. Preflight and postflight data for the six experiment test conditions

Test No.	Visual Cues	Somatosensory Cues	Preflight Sway, deg		R+0 Sway, deg		r
			Mean	SEM	Mean	SEM	
1	normal	normal	0.76	+0.05/-0.04	1.03	+0.07/-0.07	0.56
2	absent	normal	1.37	+0.08/-0.07	1.72	+0.13/-0.12	ns
3	sway-referenced	normal	1.00	+0.07/-0.06	1.60	+0.11/-0.10	0.51
4	normal	sway-referenced	1.36	+0.09/-0.09	2.30	+0.15/-0.14	0.65
5	absent	sway-referenced	3.12	+0.16/-0.15	5.09	+0.32/-0.30	0.59
6	sway-referenced	sway-referenced	3.00	+0.23/-0.21	6.12	+0.38/-0.36	0.51

The columns labeled Preflight Sway present the means and standard errors of the average p-p sway amplitude observed in the 34 astronaut subjects during preflight and landing day testing. Standard errors are not symmetric about the means because the statistical analysis was performed on the data after natural logarithmic transformation. All landing day (R+0) means were found to be significantly higher than preflight means for the same test condition. Column r presents the correlation coefficients obtained between the Preflight and R+0 data. (ns = not significant) (reprinted from 7)

system contributions to balance control were demonstrated (Figure 5.4-6). For all subjects and test sessions combined, altering visual cues (Figure 5.4-6a) approximately doubled sway amplitude, from 1.31 degrees with eyes open to 2.61 degrees with eyes closed, or 2.49 degrees with vision sway referenced ($F = 295$, $df = 2, 64$, $p < 0.0001$). There was no significant difference between the eyes closed condition and the sway referenced vision condition. Mechanically altering proprioceptive cues (Figure 5.4-6b) nearly tripled sway amplitude, from 1.24 degrees with a fixed support surface to 3.25 degrees with a sway referenced support surface ($F = 924$, $df = 1, 32$, $p < 0.0001$). Altering vestibular inputs (Figure 5.4-6c) by 4 to 17 days adaptation to microgravity increased sway amplitude by 60%, from 1.61 degrees before flight to 2.56 degrees after flight ($F = 156$, $df = 1, 32$, $p < 0.0001$).

Significant interactions were also observed among the independent variables between the main effects (Figure 5.4-7). For instance, the effects of altering visual cues were exaggerated by simultaneously altering proprioceptive cues ($F = 77.8$, $df = 2, 64$, $p < 0.0001$) (Figure 5.4-7a) and/or vestibular system contributions ($F = 10.3$, $df = 2, 64$, $p < 0.0001$) (Figure 5.4-7b). Also, the effects of altering proprioceptive cues were exaggerated by simultaneously altering vestibular system contributions ($F = 20.7$, $df = 1, 32$, $p < 0.0001$) (Figure 5.4-7c).

Time Course of Recovery of Postural Equilibrium Control Following Spaceflight

Data presented in Figure 5.4-8, obtained from 13 DSO 605 crew member subjects aboard six separate Shuttle missions ranging from 4 to 10 days in duration, were previously published [18]. Normalized composite equilibrium data from the 10 subjects having landing day measurement sessions were qualitatively similar. Compared

to their preflight measurements, which were usually above the 80th percentile scores for a normative population, every subject exhibited a substantial decrease in postural stability on landing day. Four of the 10 had clinically abnormal scores, being below the normative population 5th percentile. All subjects reported similar subjective feelings of rapidly increasing stability (initial readaptation) that were corroborated quantitatively in each of the four subjects studied twice on landing day. Although there was some variability in the time required, preflight stability levels were reacheived in all subjects by 8 days after wheels stop.

Based on these results, postflight readaptation was modeled as a double exponential process (Figure 5.4-8). Normalized composite equilibrium score data were fit to this model using the Levenberg-Marquardt nonlinear least squares technique [36]. The results of this exercise demonstrated that (1) at wheels stop, the average returning crew member was below the limit of clinical normality, (2) the initial rapid phase of readaptation had a time constant on the order of 2.7 hrs and accounted for about 50% of the postural instability, and (3) the slower secondary phase of readaptation had a time constant on the order of 100 hrs and also accounted for about 50% of the postural instability.

Head-Trunk Coordination Strategies Following Spaceflight

Motor control test results from 28 astronauts aboard 14 separate Shuttle missions of 4 to 10 days in duration were analyzed. The hypothesis that postflight postural biomechanics are affected by adopted strategies aimed at minimizing head movements was investigated to better understand the mechanisms underlying postflight postural ataxia. Subjects were exposed to three sequential sudden support surface translations in the posterior direction

before flight. Ground reaction forces and segmental body motions were monitored and used to compute sagittal plane center of pressure and sway trajectories [33]. Sway responses to translational perturbations were exaggerated on R+0 compared to preflight. The center of force and hip sway trajectories were generally more labile, or underdamped, on R+0 than before flight (Figure 5.4-9), and the learning associated with successive sequential perturbations disappeared in some subjects after flight. In some subjects, head movements were exaggerated on R+0; however, in other subjects, head movements were substantially reduced compared to preflight. Under these circumstances, hip sway was generally found to be increased while shoulder sway and/or head movement in space were found to be decreased compared to preflight. The strap down and stable platform head trunk coordination strategies postulated by Nashner [35] were often observed after flight, but rarely observed before flight. The biomechanical changes appeared to follow recovery trajectories similar to those found in the sensory test performance measurements, with preflight patterns returning by R+4 or R+8 days. We conclude that postflight postural instabilities resulted in part from new constraints on biomechanical movement caused by the CNS adopting strategies designed to minimize head movement.

Effects of Previous Spaceflight Experience

Comparisons of performances on sensory organization tests between the rookie and veteran groups demonstrate significant differences between subjects having previous spaceflight experience and those having none (Figure 5.4-10). Preflight performances were statistically indistinguishable between these groups on every sensory organization test. Similarly, postflight performances on tests 1, 2, 3, and 4 were not different between rookies and veterans. On the postflight conditions in which vestibular inputs provided the only theoretically accurate sensory feedback (tests 5 and 6), however, rookies exhibited significantly higher ($p=0.02$) sway than veterans.

These observations demonstrate that experienced space travelers were better able to use vestibular information immediately after flight than first time fliers. Since experienced astronauts had previously made the transitions between unit gravity and microgravity, they may have been partially dual-adapted and able to more readily transition from one set of internal models to the other. The fact that no differences were observed between rookies and veterans on tests 1 through 4 further supports our assertion that altered processing of vestibular system inputs is the primary mechanism of postflight postural ataxia.

Effects of Mission Duration and Demographic Factors

Postflight p-p sway amplitude was not significantly affected by mission duration, subject height, or subject

weight for any test condition. There were weak, but not significant relationships between postflight sway amplitude and age on test 3 (slope = -0.04 deg/yr, $p = 0.04$, $r^2 = 0.31$) and test 6 (slope = -0.19 deg/yr, $p = 0.006$, $r^2 = 0.41$), in which vision was sway referenced with and without accurate proprioceptive cues. As there were only two female crew members studied, no gender effects could be examined.

A significant effect of mission position was found only for test 6 (sway referenced vision and support surface; $F = 4.7$, $df = 2, 30$, $p < 0.02$). Mission commanders had the most stable landing day performances on this test condition (mean \pm sem = 4.9 ± 0.61 deg), followed by mission specialists (mean \pm sem = 6.3 ± 0.44 deg), and mission pilots (mean \pm sem. = 7.4 ± 0.55 deg). The number of payload specialists studied was too small to allow their inclusion in this analysis.

CONCLUSION

DSO 605 represents the first large n study of balance control following spaceflight. Data collected during DSO 605 confirm the theory that postural ataxia following short duration spaceflight is of vestibular origin. We used the computerized dynamic posturography technique developed by Nashner et al. [39] to study the role of the vestibular system in balance control in astronauts during quiet stance before and after spaceflight. Our results demonstrate unequivocally that balance control is disrupted in all astronauts immediately after return from space. The most severely affected returning crew members performed in the same way as vestibular deficient patients exposed to this test battery. We conclude that otolith mediated spatial reference provided by the terrestrial gravitational force vector is not used by the astronauts' balance control systems immediately after spaceflight.

Because the postflight ataxia appears to be mediated primarily by CNS adaptation to the altered vestibular inputs caused by loss of gravitational stimulation, we believe that intermittent periods of exposure to artificial gravity may provide an effective in-flight countermeasure. Specifically, we propose that in-flight centrifugation will allow crew members to retain their terrestrial sensory-motor adapted states while simultaneously developing microgravity adapted states. The dual-adapted astronaut should be able to make the transition from microgravity to unit gravity with minimal sensory-motor effects. We have begun a ground based program aimed at developing short arm centrifuge prescriptions designed to optimize adaptation to altered gravitational environments. Results from these experiments are expected to lead directly to in-flight evaluation of the proposed centrifuge countermeasure.

Because our computerized dynamic posturography system was able to (1) quantify the postflight postural ataxia reported by crew members and observed by flight surgeons

and scientists, (2) track the recovery of normal (preflight) balance control, (3) differentiate between rookie and veteran subjects, and (4) provide normative and clinical databases for comparison, and because our study successfully characterized postflight balance control recovery in a large cross-section of Shuttle crew members, we recommend that this system and protocol be adopted as a standard dependent measure for evaluating the efficacy of countermeasures and/or evaluating the postflight effects of changing mission durations or activities.

REFERENCES

- Nashner LM, McCollum G. The organization of human postural movements: a formal basis and experimental syntheses. *Behav Brain Sci* 1985; 8:135-72.
- Gurfinkel VS, Levik YS. Sensory complexes and sensorimotor integration. Translated from *Fiziologiya Cheloveka* 1978; 3:399-414.
- Massion, J. Movement, posture and equilibrium: interaction and coordination. *Prog Neurobiol* 1992; 38: 35-56.
- Parker DE, Reschke MF, Arrott AP, Homick JL, Lichtenberg BK. Otolith tilt-translation reinterpretation following prolonged weightlessness: implications for preflight training. *Aviat Space Environ Med* 1985; 56:601-6.
- Young LR. Adaptation to modified vestibular input. In: *Adaptive Mechanisms in Gaze Control*. Berthoz A, Melvill Jones G, editors. Amsterdam: Elsevier; 1985.
- Kozlovskaya IB, Kreidich YV, Rakhman OV. Mechanisms of the effects of weightlessness on the motor system of man. *Physiologist* 1981; 24:59-64.
- Paloski WH, Black FO, Reschke MF, Calkins DS. Altered CNS processing disrupts balance control after spaceflight. *Exp Brain Res* 1998. (Submitted; in review)
- Nashner LM. Fixed patterns of rapid postural responses among leg muscles during stance. *Exp Brain Res* 1978; 43:395-405.
- Reason JT, Brand JJ. *Motion Sickness*. London: Academic Press; 1975.
- Reschke MF, Bloomberg JJ, Harm DL, Paloski WH, Parker DE. Neurophysiological aspects: sensory and sensory-motor function. In: *Space Physiology and Medicine*. Nicogossian AE, Huntoon CL, Pool SL, editors. 3rd ed. Philadelphia: Lea & Febiger; 1994.
- Anderson DJ, Reschke MF, Homick JL, Werness SAS. Dynamic posture analysis of Spacelab-1 crew members. *Exp Brain Res* 1986; 64:380-91.
- Homick JL, Reschke MF. Postural equilibrium following exposure to weightless space flight. *Acta Otolaryngol* 1977; 83:455-64.
- Homick JL, Reschke MF, Miller EF II. Effects of prolonged exposure to weightlessness on postural equilibrium. In: *Biomedical Results from Skylab (NASA SP-377)*. Johnston RS, Dietlein LF, editors. 1977. p 104-12.
- Kenyon RV, Young LR. MIT/Canadian vestibular experiments on Spacelab-1 mission 5: postural responses following exposure to weightlessness. *Exp Brain Res* 1986; 64:335-46.
- Kozlovskaya IB, Aslanova IF, Grigorieva LS, Kreidich YV. Experimental analysis of motor effects of weightlessness. *Physiologist* 1982; 25:49-52.
- Kozlovskaya IB, Demetrieva I, Grigorieva LS, Kirenskaya AV, Kreidich YV. Gravitational mechanisms in the motor systems: studies in real and simulated weightlessness. In: *Stance and Motion, Facts and Fiction*. Gurfinkel VS, Ioffe ME, Massion J, Roll JP, editors. New York: Plenum; 1988. p 37-48.
- Paloski WH, Harm DL, Reschke MF, Doxey DD, Skinner NC, Michaud LJ, Parker DE. Postural changes following sensory reinterpretation as an analog to spaceflight. In: *Proceedings of the Fourth European Symposium on Life Sciences Research in Space (ESA SP-307)*. Trieste, Italy; 28 May - 01 June 1990. p 175-8.
- Paloski WH, Reschke MF, Black FO, Doxey DD, Harm DL. Recovery of postural equilibrium control following space flight. In: *Sensing and Controlling Motion: Vestibular and Sensorimotor Function*. Cohen B, Tomko DL, Guedry F, editors. *Ann NY Acad. Sci*; 682: 1992. p 747-54.
- Paloski WH, Reschke MF, Doxey DD, Black FO. Neurosensory adaptation associated with postural ataxia following spaceflight. In: *Posture and Gait: Control Mechanisms*. Woolacott M, Horak F, editors. Eugene: University of Oregon Press; 1992. p 311-15.
- Paloski WH, Black FO, Reschke MF. Vestibular ataxia following shuttle flights: effects of transient microgravity on otolith-mediated sensorimotor control of posture. *Am J Otolaryngol* 1993; 1:9-17.
- Paloski WH, Bloomberg JJ, Reschke MF, Harm DL. Spaceflight-induced changes in posture and locomotion. *Proc Biomech XIVth I.S.B. Congress*. Paris, France; 1993. p 40-41.
- Berry CA, Homick JL. Findings on American astronauts bearing on the issue of artificial gravity for future manned space vehicles. *Aerospace Med* 1973; 44:163-8.

23. Homick JL, Miller EF II. Apollo flight crew vestibular assessment. In: Biomedical results of Apollo (NASA SP-368). Johnston RS, Dietlein LF, Berry CA, editors. 1975. p 323-40.
24. Bryanov II, Yemel'yanov MD, Matveyev AD, Mantsev EI, Tarasov IK, Yakovleva IY, Kakurin LI, Kozrenko OP, Myasnikov VI, Yeremin AV, Pervushin VI, Cherepakhin MA, Purakhin YuN, Rudometkin NM, Chekidra IV. Characteristics of statokinetic reactions. In: Space Flights in the Soyuz Spacecraft: Biomedical Research. Gazenko OG, Kakurin LI, Kuznetsov AG, editors. Leo Kanner Associates, Redwood City, CA. Translation of Kosmicheskiye Polety na Korablyakh 'Soyuz' Biomeditsinskiye Issledovaniya. Moscow: Nauka Press; 1976. p 1-416.
25. Yegorov AD. Results of medical studies during long-term manned flights on the orbital Salyut-6 and Soyuz complex. NASA TM-76014. U.S.S.R. Academy of Sciences; 1979.
26. Kozlovskaya IB, Kreidich YV, Oganov VS, Koserenko OP. Pathophysiology of motor functions in prolonged manned space flights. *Acta Astronautica* 1981; 8:1059-72.
27. Baumgarten von R, Benson A, Berthoz A, Bles W, Brandt T, Brenske A, Clarke A, Dichgans J, Eggertsberger R, Jürgens K, Kass J, Krafczyk S, Probst T, Scherer H, Thümler R, Vieville T, Vogel H, Wetzig J. European experiments on the vestibular system during the Spacelab D-1 mission. In: Proc Norderney Symp on Scientific Results of the German Spacelab Mission D1. Sahm PR, Jansen R, Keller MH, editors. Norderney, Germany; 27-29 August 1986. p 477-90.
28. Grigoriev AI, Yegorov AD, editors. Preliminary medical results of the 180-day flight of prime crew 6 on Space Station MIR. Proc Fourth Meeting of the US/USSR Joint Working Group on Space Biology and Medicine. San Francisco, CA; 16-22 September 1990.
29. Kozlovskaya IB, Aslanova IF, Barmin VA, Grigorieva LS, Gevlich GI, Kirenskaya AV, Sirota MG. The nature and characteristics of gravitational ataxia. *Physiologist Supplement*, 1983; 26:108-9.
30. Harm DL, Parker DE. Perceived self-orientation and self-motion in microgravity, after landing, and during preflight adaptation training. *J Vestib Res* 1993; 3:297-305.
31. Croskey MI, Dawson PM, Lueson AC, Mahron IE, Wright HE. The height of the center-of-gravity in man. *Am J Physiol* 1922; 61:171-185.
32. Anonymous. Equitest system version 4.0 data interpretation manual. Clackamas OR: NeuroCom International; 1991.
33. Nicholas SC, Gasway DD, Paloski WH. A link-segment model of upright human posture for analysis of head-trunk coordination. *J Vest Res* 1998; 8(3). (In Press)
34. Horak FB, Nashner LM. Central programming of postural movements: adaptation to altered support-surface conditions. *J Neurophysiol* 1986; 55:1365-81.
35. Nashner LM. Strategies for organization of human posture. In: Vestibular and Visual Control on Posture and Locomotor Equilibrium. Igarashi M, Black FO, editors. Basel: Karger; 1985. p 1-8.
36. Marquardt DW. *J Soc Ind Appl Math* 1963; 11:431-41.
37. Huynh H, Feldt LS. Performance of traditional F tests in repeated measures designs under covariance heterogeneity. *Commun Statist – Theor Meth* 1980; A9(1):61-74.
38. Geisser S, Greenhouse SW. An extension of Box's results on the use of the F distribution in multivariate analysis. *Annals of Mathematical Statistics* 1958; 29:885-91.
39. Nashner LM, Black FO, Wall C. Adaptation to altered support and visual conditions during stance: patients with vestibular deficits. *J Neurosci* 1982; 5:536-44.

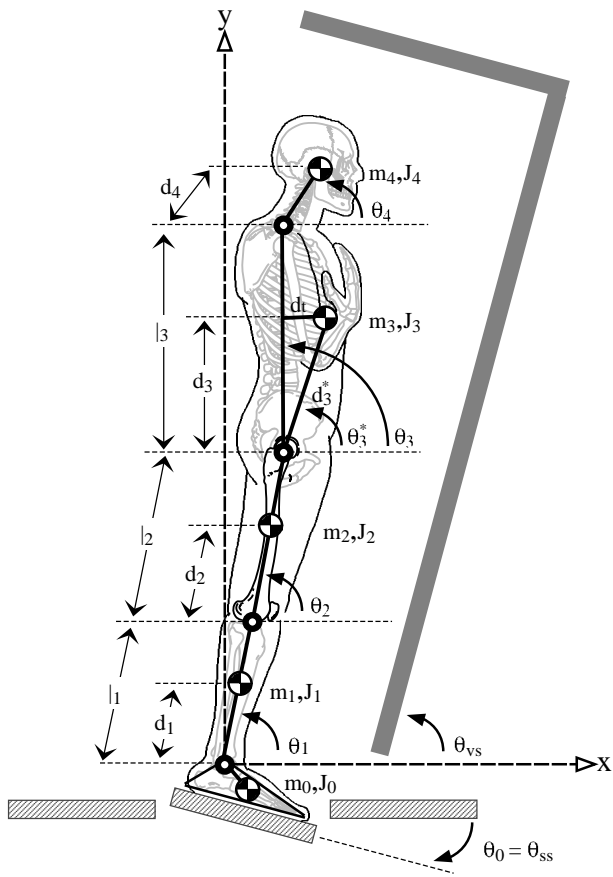


Figure 5.4-1. Link segment biomedical model. Lengths, angles, masses, etc. are defined in the text. (reprinted from 33)

	Eyes Open	Eyes Closed	Sway-Referenced Vision
Fixed Support	post pre 	 	
Sway-Referenced Support	5 cm 5 sec 	 	

Figure 5.4-2. Preflight and postflight antero-posterior (a-p) center of gravity sway time series traces for each of the six sensory organization test conditions for a typical subject. Each column in this figure represents a different visual condition. Each row represents a different proprioceptive (support surface) condition. The two traces in each panel represent different vestibular conditions. The lower traces (pre) represent the preflight performances and the upper traces (post) represent the postflight performances. (reprinted from 7)

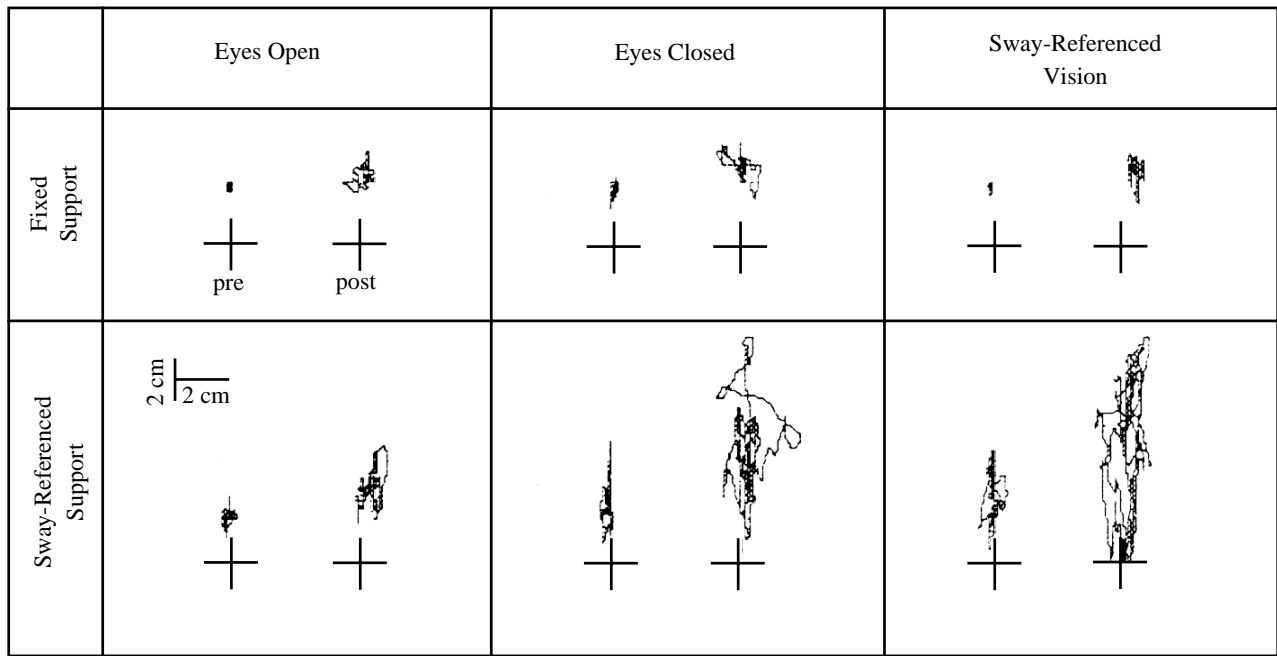


Figure 5.4-3. Preflight and postflight stabilograms corresponding to the a-p center of gravity sway traces of figure 5.4-2. Panel arrangement is similar to figure 5.4-2. Antero-posterior (body x-axis) sway is plotted on the ordinate, with the top of the plot representing the body forward direction. Medio-lateral (body y-axis) sway is plotted on the abscissa, with the right of the plot representing the body rightward direction. The cross in each plot represents the location midway between the subject's right and left medial malleoli.

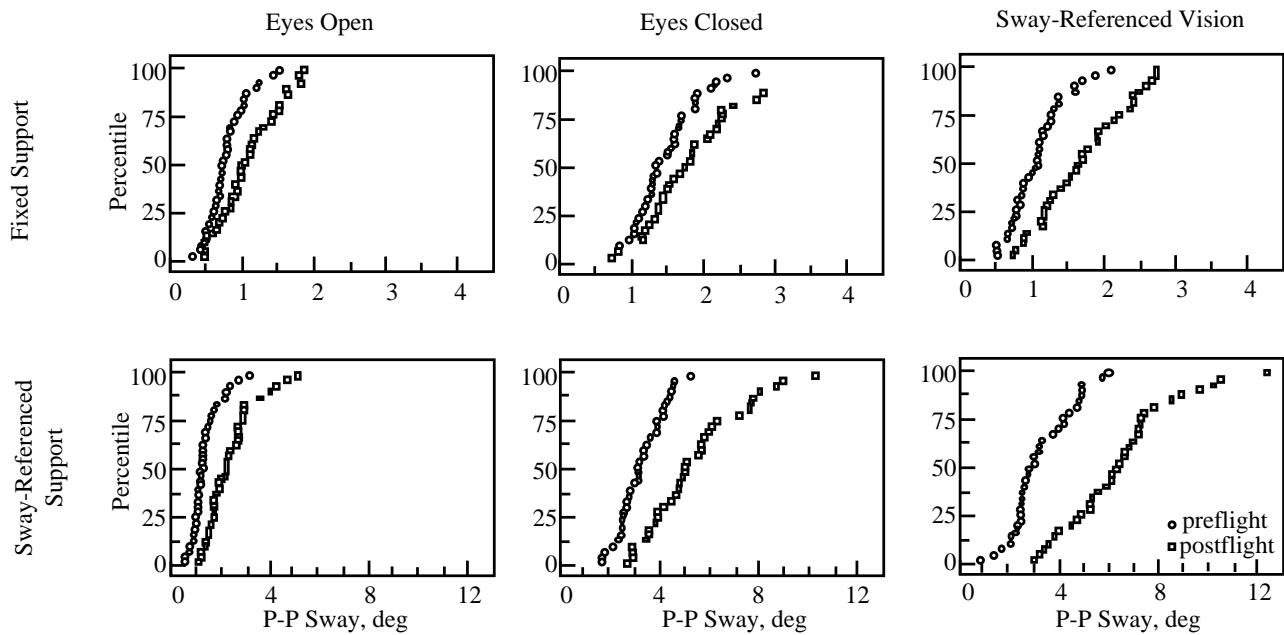


Figure 5.4-4. Preflight (circles) and postflight (squares) cumulative distribution functions of the peak to peak (p-p) a-p center of gravity sway for the 34 subjects of each of the six sensory organization test conditions. Panel arrangement is similar to figure 5.4-2. Note difference in abscissa scaling between fixed support surface conditions and sway referenced support surface conditions. (reprinted from 7)

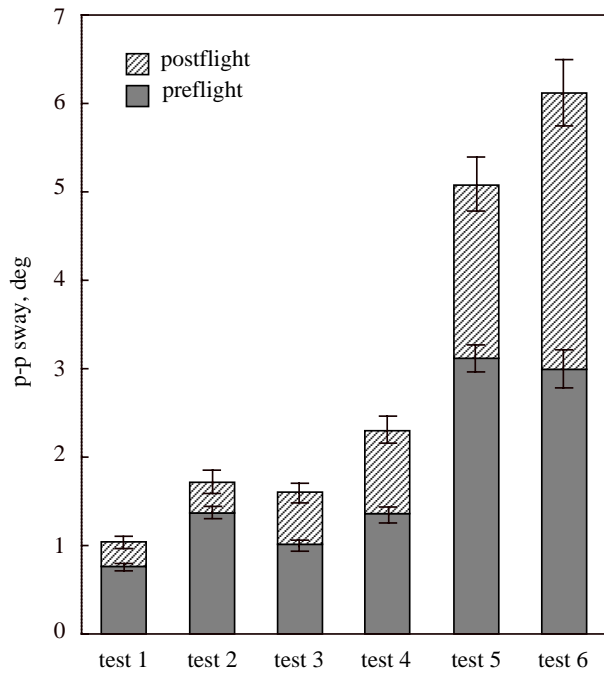


Figure 5.4-5. Mean (\pm s.e.m.) p-p a-p center of gravity sway for each of the six sensory organization tests preflight and postflight. Sway was significantly increased on every test after flight. (reprinted from 7)

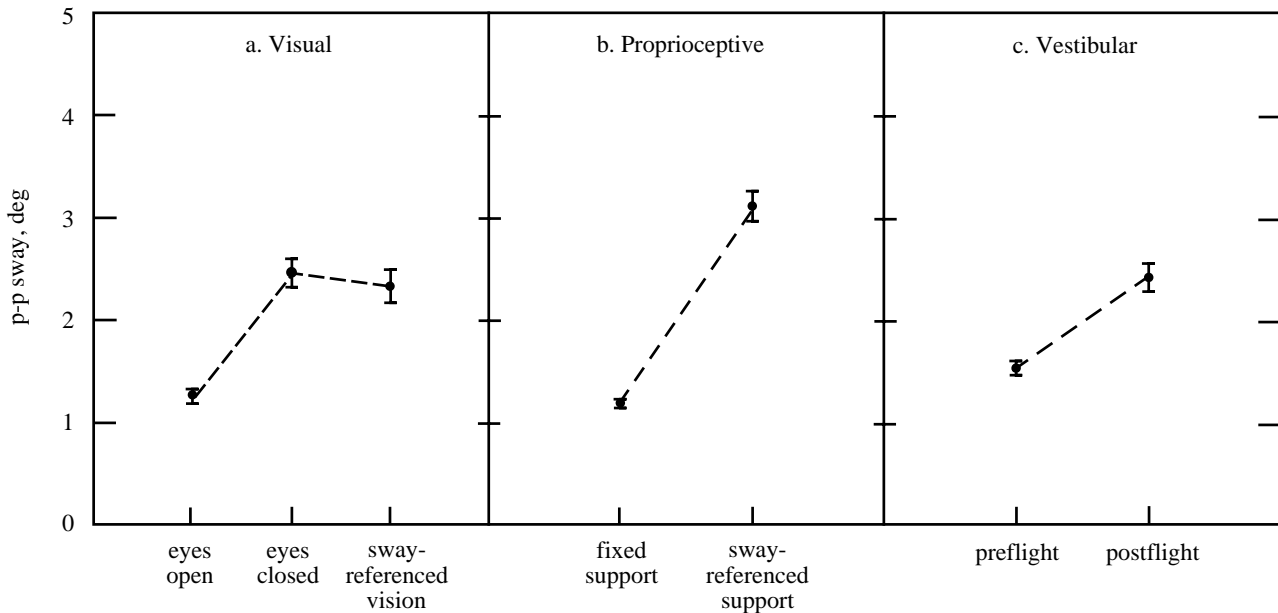


Figure 5.4-6. Mean (\pm s.e.m.) p-p a-p center of gravity sway data demonstrating the independent roles of sensory inputs to balance control. a. Sway was significantly increased when visual inputs were either absent (eyes closed) or sway referenced. Sway with absent vision was statistically indistinguishable from that with vision sway referenced. b. Sway was significantly increased when proprioceptive inputs were sway referenced. c. Sway was significantly increased when vestibular inputs were disrupted by adaptation to microgravity during space flight.

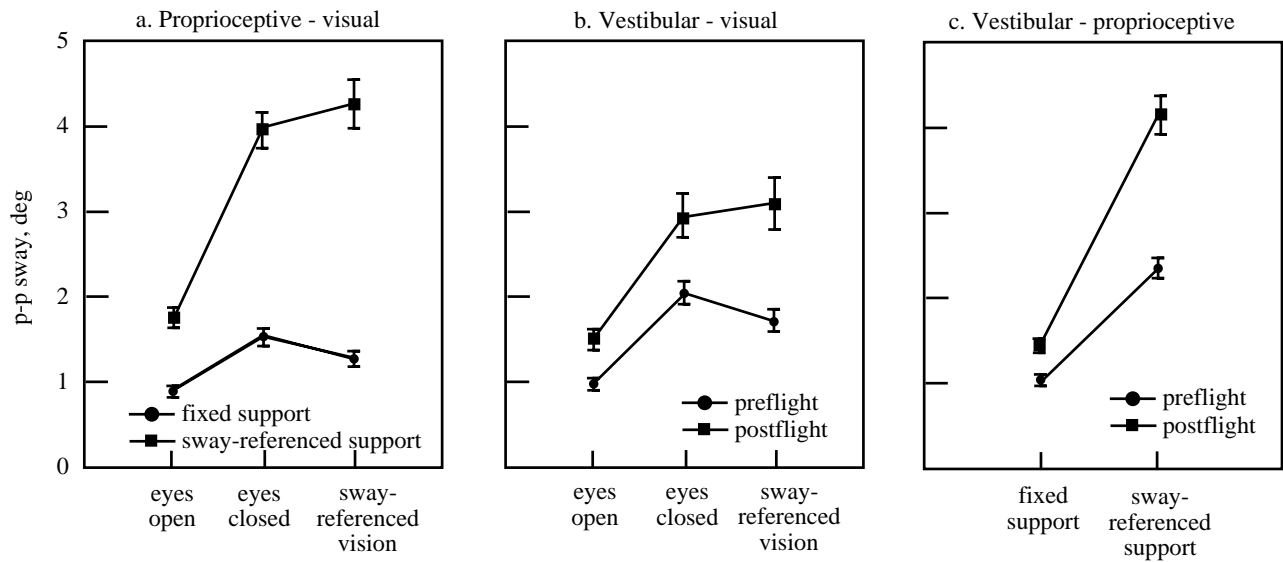


Figure 5.4-7. Mean (\pm s.e.m.) p-p a-p center of gravity sway data demonstrating the interactions among the independent variables between the main effects. a. The destabilizing effects of altering visual cues were significantly increased by simultaneously altering proprioceptive cues. b. The destabilizing effects of altering visual cues were also significantly increased by simultaneously altering vestibular cues. c. The destabilizing effects of altering proprioceptive cues were significantly increased by simultaneously altering vestibular cues.

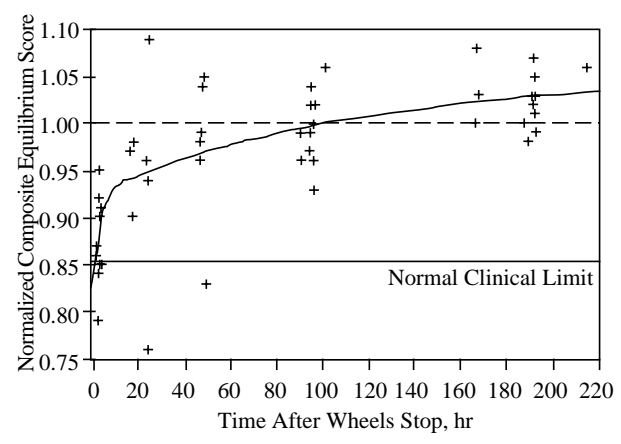
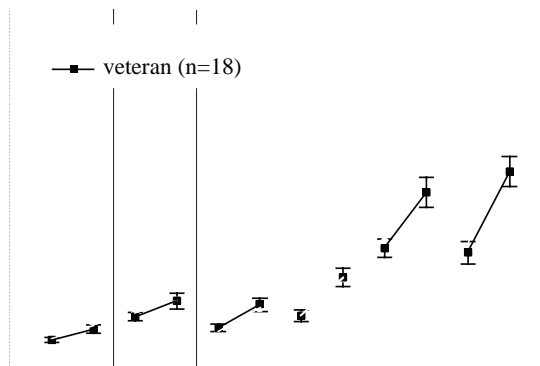
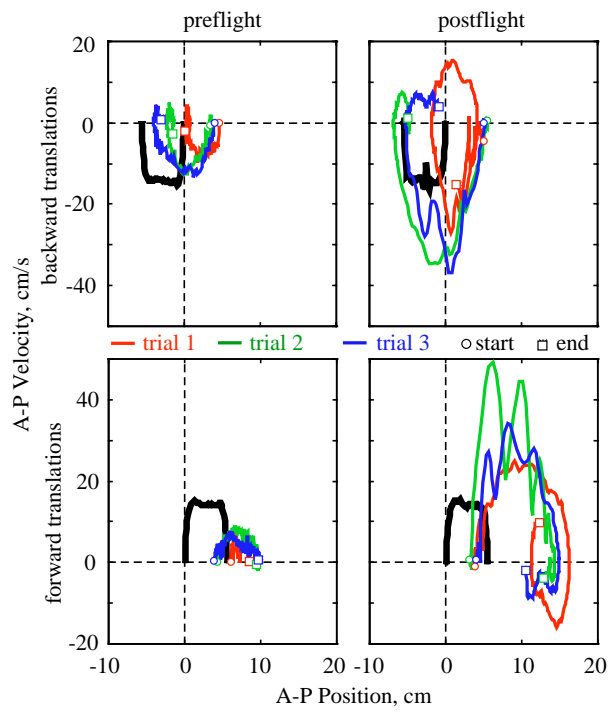


Figure 5.4-8. Model of postflight balance control recovery dynamics. (reprinted from 18)



Section 5.5

Neurovestibular Dysfunction

Effects of Space Flight on Locomotor Control

(DSO 614)

Jacob J. Bloomberg, Charles S. Layne, P. Vernon McDonald, Brian T. Peters, William P. Huebner, and Millard F. Reschke of the Johnson Space Center, Houston, TX;

Alain Berthoz of the Laboratoire de Physiologie de la Perception et de L'Action, Collège de France, Centre National de la Recherche Scientifique, Paris, France;

Stefan Glasauer of the Ludwig-Maximilians-Universität München, Klinikum Großhadern Neurologische Klinik, München, Germany; Dava Newman and D. Keoki Jackson of the Massachusetts Institute of Technology, Cambridge, MA

BACKGROUND

Locomotor Head-Trunk Coordination Strategies

In the microgravity environment of spaceflight, the relationship between sensory input and motor output is altered [1]. During prolonged missions, neural adaptive processes come into play to recalibrate central nervous system function, thereby permitting new motor control strategies to emerge in the novel sensory environment of microgravity. However, the adaptive state achieved during spaceflight is inappropriate for a unit gravity environment and leads to motor control alterations upon return to Earth that include disturbances in locomotion. Indeed, gait and postural instabilities following the return to Earth have been reported in both U.S. astronauts and Russian cosmonauts [1-17] even after short duration (5- to 10-day) flights. After spaceflight, astronauts may: (1) experience the sensation of turning while attempting to walk a straight path, (2) encounter sudden loss of postural stability, especially when rounding corners, (3) perceive exaggerated pitch and rolling head movements during walking, (4) experience sudden loss of orientation in unstructured visual environments, or (5) experience significant oscillopsia during locomotion.

Russian investigators [3, 6, 7] have studied locomotor behavior in cosmonauts following Soyuz missions lasting from 2 to 63 days. The sequential positions of various body joints and limbs were recorded and analyzed to determine kinematic features of walking, running, long jumps, and high jumps. Their results showed distinct postflight performance decrements in gait and jumping behavior. In most cases, the durations of the postflight performance decrements were related to the length of the flight. Postflight walking was characterized by an exaggerated width in leg placement, shifting the trunk to the side of the supporting leg, and failure to maintain the intended path. To enhance stability, the subjects frequently raised their arms to the side while making small steps of

irregular length. Although both anecdotal and experimental evidence indicate that significant locomotor disturbances occur following spaceflight, little is known about underlying mechanisms contributing to these problems.

Pozzo and Berthoz [18, 19] have demonstrated that during normal locomotion the head is actively stabilized relative to space with a precision of a few degrees. Based upon this result they have speculated that postural and gait motor control mechanisms may utilize a top down control scheme to ensure head stability during body movement. Such a strategy is advantageous because a stable head facilitates the maintenance of gaze stability during locomotion. Grossman et al. [20] have determined that during walking and running, the peak velocities of head rotations in yaw, pitch, and roll are generally maintained below 100°/s and are thus below the saturation velocity (350°/s) of the vestibulo-ocular reflex [21]. Grossman and colleagues [22] have characterized gaze stability during locomotion and have found that the angle of gaze is maintained relatively stable during walking and running. However, individuals with loss of vestibular function and neurological disease experience increased oscillation of the head and instability of gaze during locomotion, leading to impaired visual acuity and instability of the visual scene during locomotion [23-28]. These results underscore the importance of head stability in aiding gaze stabilization during locomotion.

Guitton et al. [29] examined visual, vestibular, and voluntary control of head movement in normal subjects and patients with bilateral vestibular deficits during passive whole body rotation about a vertical axis. Subjects were asked to maintain the position of a head-fixed laser on a stationary target, with vision, without vision in the dark, and during performance of a distraction task such as mental arithmetic. Normal subjects were most accurate when vision was provided. With vision, the vestibular deficit patients performed as well as normal subjects. Performance of the patient group deteriorated when vision was denied, indicating that vestibular information plays a

role in head movement control. Guitton et al. [29] determined that long latency voluntary mechanisms were responsible for head stabilization. However, as head frequency increased (above 2 Hz), they hypothesized that the passive inertial properties of the head-neck system would dominate the response in the higher frequency range. Keshner and Peterson [30] examined head stability during free locomotion and during passive rotations. Their results indicated that head movement during free locomotion was largely restricted to the 1 to 2 Hz range. This falls within the frequency range identified for vestibulocollic and cervicocollic reflex control of head movement characterized during passive rotation. Voluntary, reflexive, and passive mechanisms may all play a role in head movement control during locomotion [31, 32].

Angular head movements can actually contribute to gaze stabilization during locomotion. In humans, both during treadmill and free locomotion, pitch head rotations (in the sagittal plane) aid gaze stabilization by compensating for the vertical trunk translation that occurs with each step during locomotion [13, 19, 28, 33]. In a previous study, we determined that when subjects are asked to visually fixate a target while walking on a treadmill, the magnitude of these pitch head rotations was modulated, depending upon target distance [13]. When an Earth-fixed visual target at optical infinity was brought close (within 30 cm) to the eyes, pitch head movements increased in amplitude in a way consistent with the hypothesis that rotational head movements are driven in part by the requirement to aid in gaze stabilization. In related work, Paige et al. [34] showed that compensatory eye movements during vertical trunk translation were mediated by similar alterations in target distance. The goal-directed response of pitch head movements during concurrent locomotion and visual target fixation suggests that these head movements were not completely dependent on passive inertial and visco-elastic properties of the head-neck system, but could be actively modulated to respond to altered gaze control requirements. Monkeys trained to locomote around the perimeter of a circular platform were found, while running, to produce continuous eye and head nystagmus to maintain gaze stabilization during body movement [35, 36]. Thus, coordinated head and trunk movements play a central role in maintaining clear vision during natural body movements, and may have a strong influence on the organization of postural and locomotor control patterns. Accordingly, one of the objectives of DSO 614 was to determine if exposure to the microgravity environment encountered during spaceflight adaptively modified head-trunk coordination strategies during postflight locomotion.

Lower Limb Kinematics During Treadmill Walking

Both scientific and anecdotal evidence suggest profound changes in perceptual motor functioning after spaceflight

[10]. These changes pose concern for situations in which movements must be executed reliably and accurately. Locomotion, whether on Earth following completion of a U. S. Space Shuttle mission or on a remote planet surface following a lengthy flight, would be subject to compromise by changes in perceptual motor functioning resulting from in-flight adaptation to the microgravity environment.

Postflight locomotor changes of a biomechanical nature include increased angular amplitude at the knee and ankle, and increased vertical accelerations in the center of mass [37]. In addition, Chekirda et al. [6] noted both: (1) apparent change in the contact phase of walking, in which the foot appeared to be thrust onto the support surface with a greater force than that observed before flight, and (2) efforts to preserve stability in which cosmonauts spread their legs far apart, used their arms more, and used shorter steps after flight. Even with these compensatory changes, both Russian and U.S. investigators have observed disturbances in performance, including deviations from a straight trajectory [6] and a tendency toward loss of balance during walking when turning corners [1, 3].

Locomoting through a complex and cluttered environment also involves perceptual demands. A contributing factor to stable and reliable locomotion is the maintenance of stable gaze. Empirical evidence suggests that the head-neck-eye complex operates to minimize angular deviations in gaze during locomotion [19]. Since the head-neck-eye complex is situated on top of the trunk-lower limb complex, the noted postflight biomechanical changes suggest a high potential for negative impact on gaze stabilization strategies. The situation is further compounded by changes in perceptual function. For example, after spaceflight, crew members developed a stronger dependence on visual cues [38], there were changes in the ability to detect accelerations, and otolith organ sensitivity declined throughout the duration of a flight [128]. In addition, changes in vestibulo-ocular reflex (VOR) gain as a function of spaceflight were observed [39, 40], and exposure to microgravity modified eye-head coordination during target acquisition [41, 42] and ocular saccadic performance [43].

When considered together, these biomechanical and perceptual changes point toward a highly probable adaptation of head and gaze control during locomotion after spaceflight. However, strategies used for maintaining gaze stability have not been documented during postflight locomotion. To better understand the functional implications of existing flight related evidence, especially in terms of the strategies used for coordination among the various perceptuo-motor subsystems, we designed the DSO 614 investigation to examine the role of adaptive modification in head movement control during postflight locomotor performance. The investigation was designed to address this problem not only in terms of eye-head-trunk coordination, but rather as a problem from the ground up, inasmuch as lower limb coordination and support surface

dynamics influence gaze control [44]. We contend that an important element of gaze control during locomotion is the management of energy flow through the body, especially during high energy interactions with support surfaces such as those occurring at the moment of heel strike and toe off [45, 46]. The ability to attenuate the transmission of energy through the body is influenced directly by a number of factors. Among these are changes in the characteristics of the musculoskeletal shock absorbers, including the viscoelastic properties of joints [47]. Also important for the management of energy flow through the body is the pattern of joint kinematics seen during locomotion. Of specific relevance is lower limb joint configuration at the moment of heel strike with the support surface. Perry and Lafortune [48] demonstrated that absorption capacity could be reduced by excessive foot pronation, suggesting that the joint configuration of the foot-ankle at heel strike contributes directly to the potential transmission of the heel strike shock wave through the body. Changes in foot activity during the contact phase of locomotion following spaceflight were demonstrated by Chekirda et al. [7].

McMahon and colleagues [49] suggested that the degree of shock wave transmission during locomotion was extremely sensitive to the degree of knee flexion. They discovered that while tibial shock was increased with increased knee flexion, transmission of the shock wave to the head was significantly reduced. However, after a direct investigation of the role of knee angle on axial stiffness of the lower limb, Lafortune et al. [50] suggested that increased knee angle at foot impact was less effective than previously thought in attenuating impact shock. Nevertheless, Hernandez-Korwo et al. [37] noted locomotor changes in both knee and ankle angles following spaceflight.

Grossman et al. [20] recognized that locomotion induces rhythmic oscillations of the trunk and the head. The predominant frequency of these oscillations is equivalent to the step frequency. Since the head contains both the visual and vestibular systems, any irregularities in these step-dependent oscillations could influence locomotor control. Consequently, we determined that it was crucial to examine not only the head-trunk linkage [51], but all the links between the head and the support surface. Appropriate attenuation of the intersegmental energy flow during locomotion minimizes the disturbance of the visual and vestibular systems, and preserves head and gaze stability. However, we suspect that spaceflight adaptation may compromise this ability and thus lead to impaired head and gaze control. To more clearly determine the role of the lower limb joint complex in this phenomenon, we chose to focus attention on two specific locomotor events: heel strike and toe off. High energy transitions between the stance and swing phases were considered the most likely events to illustrate changes in locomotor performance, since any maladapted effort to manage energy flow would result in inappropriate energy transfer among contiguous

body segments and could cause disturbances in both lower limb coordination and head-eye coordination observed during walking after spaceflight.

Neuromuscular Activation Patterns During Locomotion

Astronauts display remarkable flexibility in adapting themselves and their movements to the unique microgravity environment of spaceflight. Despite shifts in many physiological processes, crew members rapidly develop motor control strategies to perform tasks effectively in space. Moreover, astronauts must readapt quickly upon return to Earth in order to regain appropriate coordination strategies, particularly with regard to posture and locomotion.

Spaceflight has been associated with: (1) decreases in muscle strength and tone [5, 52-54], (2) hyperactivity in H- and stretch-reflex characteristics [5, 53, 55], (3) changes in muscle strength velocity profiles [54], (4) changes in lower limb muscle activation patterns [55], (5) changes in proprioceptive and vestibular functioning [5, 53, 56], and (6) oscillopsia [57]. These neurological and physiological alterations could be expected to influence the precise neural control needed for the lower limb muscle activation patterns required for optimal locomotion.

Electromyography (EMG) has long been used to assess the neuromuscular control features associated with both normal and abnormal gait [58-66]. The phasic properties of processed EMG are highly correlated with the changes in muscle tension and joint angular accelerations that occur throughout the gait cycle [60, 67], and a linear relationship exists between muscle tension and EMG amplitude in the range of tension levels found during normal walking [68, 69].

A wide range of compensatory locomotor neuromuscular patterns have been identified in several clinical populations [70-72], suggesting that the sensorimotor system can adapt so as to allow a range of locomotor behavior. Changes in EMG measures reflecting muscle co-contraction, such as simultaneous activation of antagonist muscles, have often been interpreted as representing modifications of neuromuscular control strategies [73, 74]. The learning and development phase of a skilled movement is often associated with a high degree of muscle co-contraction. This co-contraction results in stiff, uncoordinated movement patterns. As skill level increases, segmental motions become smoother and well coordinated, reflecting a decrease in muscle co-contraction. Conversely, increases in co-contraction following spaceflight may result in less coordinated and more variable segmental motions. Additionally, the stiffness resulting from increased co-contraction can alter how the impact forces generated at heel strike are dissipated throughout the body during locomotion. The inability to efficiently manage the energy resulting from heel strike may result in increased head motion, thereby increasing the possibility of gaze

instability. Thus, muscle co-contraction is an important index of how effectively the sensorimotor system is able to control neuromuscular activation in order to produce coordinated movement. On the basis of the above properties, the use of EMG to describe changes in muscle activation patterning and co-contraction levels during locomotion seems well suited for revealing changes in neuromuscular properties resulting from spaceflight. Although much anecdotal information exists, DSO 614 was the first time that the influence of 8- to 15- day spaceflight on lower limb neuromuscular activation during postflight locomotion had been adequately evaluated.

Spatial Orientation

Prolonged stays in the microgravity environment result in changes in both the vestibular and somatosensory systems [10]. Several hypotheses have addressed the question of how the changed sensory inputs are reinterpreted. For example, the otolithic system, which on Earth measures a combination of head orientation through gravity and linear translational acceleration, should reinterpret all linear acceleration in microgravity as being translational [75]. This could lead to misperception of head tilt as translation in the first hours after return to Earth. These changes in perception of vestibular input may affect the ability to spatially orient during locomotion after spaceflight.

In the new paradigm presented here, the astronaut subjects perform a natural task involving both somatosensory and vestibular sensory inputs. Goal-directed locomotion satisfied these requirements and provided information about the spatial orientation capabilities of the subjects. Goal-directed locomotion, with or without vision, is a simple everyday task, in contrast to former investigations that required more artificial tasks such as performing eye movements with the head fixed. This portion of DSO 614 focused mainly on the question of whether exposure to the microgravity conditions encountered during spaceflight was associated with impaired spatial orientation during locomotion following return to Earth, and what role vision played in this process.

Lower Limb and Mass Center Kinematics in Downward Jumping

In addition to changes in posture and locomotor control, astronauts exhibit alterations in the ability to maintain stability following drop landings. Watt et al. [77] tested astronauts subjected to sudden “drops” and reported that all subjects were unsteady postflight, and that one subject fell over backwards consistently.

Such performance decrements may result from various changes in the sensorimotor complex resulting from microgravity exposure. Parker et al. [78] found direct evidence for reinterpretation of graviceptor inputs during spaceflight. Young et al. [79] also provided evidence for

sensory compensation during spaceflight, resulting in interpretation of utricular otolith signals as linear acceleration rather than head tilt, as well as increased dependence on visual cues for perception of orientation. The otolith-spinal reflex, which helps prepare the leg musculature for impact in response to sudden falls, is dramatically reduced during spaceflight [77]. However, postflight results were not significantly different from preflight responses, indicating a rapid course of readaptation upon return to Earth. Other work indicates that spaceflight may affect proprioception of limb position; Watt et al. [77] found a considerable decline in arm pointing accuracy while blindfolded during and immediately following spaceflight. Furthermore, the subject who fell consistently in the drop test reported that his legs were always further forward than he expected them to be.

Other possible explanations for postflight postural instability include atrophy of the antigravity muscles [80], in-flight changes in tonic leg muscle activation patterns, or microgravity-induced alterations in stretch reflexes [81, 82]. Gurfinkel [83] also reported reorganization of higher-level anticipatory postural responses to rapid movements during spaceflight. Altered patterns of leg muscle coactivation may result in changes in the modulation of limb impedance that controls the dynamic interaction of the limb with the environment. McDonald et al. [45] cited postflight changes in the phase-plane description of knee joint kinematics during gait as preliminary evidence for changes in joint impedance resulting from exposure to weightlessness.

The aim of this aspect of the study was to determine the effects of microgravity exposure on the astronauts' performance of two-footed jump landings. This study was intended to elucidate how exposure to an altered gravitational environment affects control of lower limb impedance and preprogrammed motor strategies for impact absorption. The joint kinematics of the lower extremity during the jump landings, as well as the kinematics of the whole-body mass center, were of particular interest. The results suggest that different subjects adopt one of two response modes upon return to 1-g following spaceflight, and that postflight performance differences may result largely from adaptive changes in open-loop lower limb impedance modulation. The altered jumping kinematics seen postflight may reflect decrements in limb proprioception, altered interpretation of otolith acceleration cues, and reduced requirements for maintenance of posture under microgravity conditions.

METHODS

Locomotor Head-Trunk Coordination Strategies

Twenty-three astronauts, 19 males and 4 females, ranging in age from 34 to 51 years, served as subjects in this study. All subjects gave informed consent to testing,

and all protocols were approved by the NASA/Johnson Space Center Institutional Review Board for Human Research. To measure head and trunk movements, passive retroreflective markers, with negligible mass, served as tracking landmarks. These were affixed to the vertex, occipital, right temporal positions of the head and on the seventh cervical vertebrae (C7). The movements of these markers were simultaneously recorded with four video cameras sampling concurrent video images at 60 Hz. The position of each marker in space was uniquely determined with the aid of a video-based motion analysis system (Motion Analysis Corporation, Santa Rosa, CA). Each subject wore spandex shorts, sleeveless shirt, and running shoes. Markers and electromyographic (EMG) electrodes were also placed on the lower limbs for a separate analysis of kinematic and muscle activation patterning. Vertical eye position relative to the head was recorded using standard DC-Electrooculographic (EOG) methods.

During each test session, the astronaut subjects were required to walk, at 6.4 km/h (4 mph), on a motorized treadmill (Quinton™ Series 90 Q55 with a surface area of 51 cm × 140 cm, or 20 in × 55 in) while visually fixating on a centrally located Earth-fixed target. This target consisted of a light emitting diode (LED) positioned either 30 cm or 2 m from the subject, at the height of the subject-perceived eye level. Prior to initiating the trial, the subject straddled the treadmill belt while the speed was increased to the desired speed, at which time the subject was free to begin walking. A few strides were permitted to allow the subject to become comfortable with the treadmill speed and to attain a steady gait. After a verbal ready indication from the subject, data collection was initiated, with the subject continuing to locomote while fixating the target for 20 seconds. The subject maintained fixation of the target for the full duration of the trial. To prevent potential injury through falling, each subject wore a torso harness attached to an overhead frame. During nominal treadmill performance, this harness provided no support and did not interfere with natural movements of head or limbs.

Data were collected before and after Shuttle missions of 8 to 15 days duration. Preflight testing consisted of two sessions, one each at approximately 90 and 10 days prior to launch. Postflight testing was performed 2 to 4 hours after landing and 2, 4 and 8 days following return to Earth. Data collected approximately 10 days before flight (referred to as “preflight”) and on landing day (referred to as “postflight”) were evaluated. Recovery data (R+2, 4, and 8 days) will be covered in future communications.

A variety of challenges to head-trunk coordination were used to delineate adaptive changes in goal directed response characteristics. These included:

1. Far Target Condition (FAR) – Subjects walked on the treadmill while visually fixating the target located 2 m (6.5 ft) from the outer canthus of the eyes. Two trials of 20 s in duration were performed.

2. Near Target Condition (NEAR) – Subjects walked on the treadmill while visually fixating the target located 30 cm (1 ft) from the outer canthus of the eyes. Two trials of 20 s in duration were performed.

3. Intermittent Vision Condition (IV) – To investigate how the head-trunk system dynamically responded to short term (5 seconds) alternating changes in sensory input, subjects walked on the treadmill during intermittent visual occlusion. A 20-second locomotion trial would begin with the eyes open and the subject fixating the visual target. After 5 seconds, subjects were instructed to close their eyes and continue walking while attempting to fixate on the remembered position of the target. Five seconds later, subjects were instructed to open their eyes. The 5-second eyes open/eyes closed periods alternated through the 20-second duration of the IV walking trial. Two trials of 20 seconds in duration were performed. To address safety concerns, subjects lightly placed their index finger on the forward hand rail of the treadmill to gain additional haptic cues regarding body placement. It has been recently shown [84, 85] that a light touch, insufficient to produce mechanical support, contributes significantly to control of postural equilibrium in the absence of vision. Although the light finger touch may have enhanced performance in general, all the eyes-open and eyes-closed epochs in an IV trial occurred under the same haptic conditions. The alternating 5 s epochs of eye closure were confirmed using vertical electrooculography to detect eye closure transitions in EOG baselines.

Three-dimensional translational trajectories of each body-fixed marker were calculated relative to a coordinate frame that was coincident with the surface of the treadmill. The marker trajectories were low pass filtered at 10 Hz using a finite impulse response filter with a Hamming window. Movement of the head in the sagittal plane (head pitch) was characterized by the angle between the horizontal and the line connecting the vertex and occipital markers. Vertical (z-axis) trunk translation was determined from the displacement of the marker placed on the seventh cervical vertebrae (C7).

The degree of association between vertical trunk translation and corresponding compensatory pitch head movement was characterized using the coherence function. The coherence between two signals was defined as:

$$\text{Coherence} = \frac{|\text{cross spectra of signals } x, y|^2}{(\text{power spectra } x)(\text{power spectra } y)} \quad (1)$$

The coherence value could vary between zero and unity. If a perfect linear relationship existed between the two signals at some specific frequency, the coherence

function was equal to unity at that frequency. If the two signals were completely unrelated, the coherence function was zero over all frequencies.

Compensatory pitch head movement wave forms were also subjected to Fourier analysis and the amplitude of the predominant frequency was determined. Each 20-second walking trial was divided into 4 epochs of 4 seconds duration. The frequency spectra of each 4-second epoch was then calculated separately. For each subject, over two walking trials per condition, eight individual epochs were analyzed and the predominant peak determined, allowing the mean peak amplitude to be determined for each subject.

Lower Limb Kinematics During Treadmill Walking

A total of seven subjects were tested from three Shuttle missions, of eight or nine days duration, flown between March 1992 and February 1994. Of the seven subjects, two were first-time fliers and five had flown at least once previously, six were men and one was a woman. Subject height ranged from 1.68 m (5 ft 6 in) to 1.85 m (6 ft 1 in). Subject ages ranged from 35 to 49 years with a mean of 41 years.

Before each testing session, passive retroreflective markers, serving as tracking landmarks, were affixed at vertex, occipital and temporal positions on the head, and at the acromion process, lateral epicondyle of the humerus, midpoint on the dorsal surface of the distal portion of the radius-ulnar, C7, femoral greater trochanter, lateral femoral epicondyle, lateral malleolus, shoe surface coincident with the posterior surface of the calcaneus of both feet, and the fifth metatarsophalangeal joint, on the right side of the body. The movement of these markers was recorded simultaneously with four video cameras sampling images at 60 Hz. Ambient light was adjusted to allow high contrast between the retroreflective markers and the surface to which they were attached. The position of each marker in space was determined with the aid of a video based motion analysis system (Motion Analysis Corporation, Santa Rosa, CA). Each subject wore cycling shorts, a sleeveless shirt, and the same brand of running shoe before and after flight. Foot switches, using Interlink

Electronics™ force sensing resistors, were attached to each shoe at the heel and toe and sampled at 752 Hz through a 12 bit analog/digital (A/D) board.

Subjects were required to ambulate on a treadmill and tested on the same schedule as described earlier.

Table 5.5-1 illustrates the conditions of each data collection session. Trial numbers indicate presentation order within each testing session. Additional walking trials were performed during periodic visual occlusion. Trials 1 and 10 were the standing trials used to calibrate the EOG system. Segmental kinematic data collected during these trials were used to calculate joint configurations during quiet standing. Only data from walking (6.4 km/h or 4 mph) trials during near (30 cm or 1 ft) target visual fixation collected 10 days before flight (preflight) and on landing day (postflight) were evaluated, since this comparison was most likely to reflect any spaceflight induced effects.

Subjects were instructed to maintain ocular fixation of the target at all times. During each trial, the spotter monitored subject location on the treadmill and instructed the subject to move forward or backward if necessary. For the walking trials, subjects stood off the treadmill belt while its speed was increased to the criterion. At this point the subject was free to begin walking. A few strides were permitted to allow the subject to become comfortable with the speed and to attain a steady gait. After a verbal ready indication from the subject, data collection was begun with the subject continuing to walk and fixate the target for 20 seconds.

Data resulted from a direct evaluation of lower limb joint kinematics patterns observed during treadmill walking after short duration spaceflight. Data analyses were designed to determine the potential influence of lower limb kinematics on adaptive strategies utilized for head and gaze control during postflight locomotion. Basic characteristics of the temporal form of the gait pattern were examined, since even while locomoting on a treadmill at a fixed speed, there was an opportunity to trade off step amplitude and step frequency while maintaining the same forward speed. At the same time, the relative duration of the stance and swing components of the step could be adapted. This composition was referred to as the duty factor, a ratio representing the amount of time spent in the stance phase in each step. The duty factor could be

Table 5.5-1. Experiment Conditions

Treadmill Speed	Visual Target at 2 m		Visual Target at 30 cm	
	Continuous Vision	Periodic Occlusion	Continuous Vision	Periodic Occlusion
6.4 km/h	trials 2 and 4	trials 3 and 5	trials 6 and 8	trials 7 and 9
9.6 km/h	trials 11 and 12	Not performed	Not performed	Not performed

identified by analyzing the temporal location of the toe-off between two successive foot falls. The duty factor of bipedal walking was typically reported as approximating 0.6 because the toe-off occurred at about 60% of the step. Step-to-step variation of these temporal measures is presented as a precursor to the joint kinematic analyses. Any changes in these factors could directly influence the frequency and amplitude of the rhythmic oscillations in the trunk and the head.

Several techniques were used to evaluate the lower limb locomotion system comprising the hip, knee, and ankle joints. Representing the periodic motion of these joints on the phase plane, we documented within-cycle variability over discrete epochs of the cycle, and also at two discrete events, heel strike and toe off. These analyses were performed on each joint independently, to document any disturbances in individual joint activity, and to identify where these disturbances occurred relative to gait cycle phases. To quantify cycle-to-cycle stability in gait patterns, a Poincaré map was used to take the continuous dynamics of the joint phase portraits into the discrete regime, based on the event-specific iterations at heel strike and toe off. The states of the phase portraits (angular displacement and angular velocity) of the three lower limb joints were used to define a six-dimensional state space. Such a representation allowed the exploitation of a specific analysis technique to evaluate system stability. This technique evaluated behavior of the three-joint system as a whole, so that any changes in a single joint could be assessed at the system level. Therefore, independent measures of system component variability, and a measure of system stability as a whole are presented. These measures were intended to determine changes in the nature and source of perturbations to the trunk emanating from the lower limbs during the locomotor cycle.

Marker trajectory data were processed to derive three-dimensional translation information relative to a coordinate frame coincident with the surface of the treadmill. Subjects walked toward the +X direction and the belt moved in the -X direction. The vertical axis orthogonal to the treadmill surface was +Z, and the Y axis was orthogonal to the X-Z plane (Figure 5.5-1). Marker trajectories were low pass filtered at 10 Hz using a finite impulse response filter with a Hamming window. The filtered trajectories in X and Z were then used to determine joint angular motions in the sagittal plane for the hip (thigh and knee markers), knee (thigh, knee, and ankle), and the ankle (knee, ankle, toe). Figure 5.5-1 illustrates how these joint angles were determined relative to the coordinate frame of reference. The hip (H) angle was measured with respect to the vertical, with flexion designated as positive and extension as negative. The knee (K) angle was measured from the projection of the thigh link segment to the tibial link segment, with flexion designated positive and extension as negative. The ankle (A) angle was measured as that angle between the tibial link segment and the foot

segment, with plantar flexion being greater than 90 degrees and dorsiflexion less than 90 degrees. These three joint angles were considered to be a satisfactory representation of the lower limb dynamic during the task of treadmill walking.

The equilibrium position was determined for each joint under consideration, to facilitate the modeling of lower limb oscillatory motion. This position was equivalent to the joint angles measured during quiet standing on the treadmill. Hence, the hip, knee, and ankle joint angles were used to determine the equilibrium point about which the joint motions occurred for each subject. This equilibrium point was represented as the origin (0,0) on the phase plane. All subsequent joint angular displacement data were represented with respect to this origin. Having determined the sagittal plane joint angular displacements, joint angular velocities were then determined with a fourth order central difference algorithm.

Foot switch signals allowed determination of the moments of heel strike and toe off in the right limb. However, foot switch information was not available for all subjects. In such cases reliable kinematic correlates for heel strike and toe off were determined from toe marker velocity in the Z direction. Determining heel strike and toe off in this manner matched foot switch information with an error not exceeding ± 16.7 ms.

Phase plane data, using the joint angular displacement and joint angular velocity as the states of the system, were analyzed using three different techniques to evaluate joint dynamics. The first of these techniques was employed to evaluate variability of independent joint motion over the course of the full gait cycle. The second technique was used to evaluate variability of independent joint configuration at two discrete points in the gait cycle. For both of these techniques, a measure was constructed to combine the variability in the joint angular displacement with the variability in the joint angular velocity. After normalizing each gait cycle to 60 samples, the variability in the joint angular kinematics observed over multiple cycles of one trial was quantified using the standard deviation about the mean joint angle, and the mean joint angular velocity at the moment of heel strike and at the moment of toe off. The displacement and velocity standard deviation magnitudes were then used to define the diameter of the two orthogonal axes of an ellipse. The area of this ellipse was presented as an index of the variability on the phase plane. To evaluate variability over the full gait cycle, the cycle was divided into five 20% temporal epochs, and the variability from each of the 12 samples within each epoch was summated. The phase plane variability at heel strike and at toe off was presented using those samples at which the named events occurred. The third technique used phase plane data to evaluate system stability. This technique utilized the three lower limb joints in combination. The idea of using joint kinematics as state variables and Poincaré maps to evaluate the stability of human locomotion was first introduced by Hurmuzlu [86, 87].

First return maps can be represented by the following finite difference equations in an n-dimensional state space:

$$x_{i+1}^k = f_k(x_i) \quad k=1, \dots, n \quad (2)$$

where x is a vector of state variables ($x=[x^1, x^2, \dots, x^n]^T$) and f represents the nonlinear mapping function. The equilibrium values (steady state) of equation (2) are known as fixed points of the map. Assuming that the fixed point of a map is defined as:

$$x^* = x_{i+1} = x_i \quad (3)$$

the stability of a dynamical system can be analyzed by linearizing equation (2) in the neighborhood of the fixed point to obtain:

$$\delta x_{i+1} = J \delta x_i \quad (4)$$

where δx_i and δx_{i+1} represent the perturbations associated with the i 'th and $(i+1)$ 'th elements of the state vectors, and J is a $(n \times n)$ Jacobian matrix. The entries of this matrix are the partial derivatives of the nonlinear mapping functions ($f_i, i=1, \dots, n$) with respect to the state variables, given as:

$$a_{kj} = \left. \frac{\partial f_k}{\partial x^j} \right|_{x^*} \quad j=1, \dots, n, \quad k=1, \dots, n \quad (5)$$

Such a system is considered to be stable around equilibrium if all the eigen values of the Jacobian matrix lie inside the unit circle [88, 89]. Bifurcations occur if the eigen value(s) move outside the unit circle, resulting in structural changes in the system.

Elements of the Jacobian matrix can be obtained easily if the nonlinear mapping functions (f), that return cross sections of the flow to itself, are known. However, the complexity of human locomotion does not permit simple determination of the functions (f) such as in equations (1) or (2). Although mathematical models of locomotion are available in the literature [86], the authors are not aware of any study that identifies an appropriate form of analytical equation or function. Consequently, we experimentally acquired joint kinematics of human gait and constructed the Jacobian matrix by means of least square regression techniques [85].

Following the procedures of Hurmuzlu [85, 86], we first identified the state variables of our system as the hip, knee, and ankle motions in the sagittal plane. This resulted in a six-dimensional state space of the form:

$$X_{space} = \{\Phi_H, \Phi_K, \Phi_A, \dot{\Phi}_H, \dot{\Phi}_K, \dot{\Phi}_A, \} \quad (6)$$

where Φ and $\dot{\Phi}$ represent angular rotations and velocities of the three joints used in defining the conceptual

model of the gait dynamics. These state variables were each sampled at the moment of heel strike and the moment of toe off. The same data were used to construct Poincaré maps. For each trial, a mean value for each state was calculated and designated as the equilibrium value. The steady state value of each state variable at each event, heel strike or toe off, was assumed to be the statistical average (mean) of all samples. Deviation from equilibrium was then measured at each iteration for each state by calculating the difference between the mean state value and the state value at that iteration. To approximate elements of the Jacobian matrix, a multidimensional regression was then performed among the vectors determined relative to the steady state value.

The set of equations that formulate this multidimensional fit can be written as

$$(Q_H)_{i+1} = A_{11}(Q_H)_i + \dots + a_{16}(\dot{Q}_A)_i + p_1 \quad (7)$$

$$(\dot{Q}_H)_{i+1} = A_{61}(Q_H)_i + \dots + a_{66}(\dot{Q}_A)_i + p_6$$

where Q_H, \dots, \dot{Q}_A , represents the column vectors, with a number of rows equal to the number of sampled locomotion steps (e.g., Q_H is a column vector indicating the deviation magnitude of the sagittal hip excursion relative to the steady state hip excursion), a_{ij} 's form the elements of the approximated Jacobian matrix, and p_i ($i=1, \dots, 6$) are the constants of the regression.

Finally, we calculated the eigen values ($\lambda_i, i=1, \dots, 6$) of the Jacobian matrix and statistically averaged them for each individual subject to quantify the dynamic stability exhibited by that subject during treadmill walking. According to stability theory, all eigen values should lie inside the circle, ($|\lambda_i| < 1.0, i=1 \dots 6$) for a stable system [89].

Neuromuscular Activation Patterns During Locomotion

Subjects in this study were 10 astronauts (3 women and 7 men) who had completed Shuttle missions lasting 8 to 15 days. All provided informed consent to participate, as required by the Johnson Space Center Institutional Review Board. Six of the subjects had flown on previous Shuttle missions.

Subjects walked on a motorized treadmill and followed the same testing protocol as described earlier.

After the skin was cleaned with alcohol wipes, pre-amplifier surface EMG electrodes were placed on the subjects over the bellies of the rectus femoris (RF), biceps femoris (BF), tibialis anterior (TA), and gastrocnemius (GA) in parallel to the muscle fibers. Electrodes were attached with hypoallergenic tape and covered with elastic leg wraps to prevent movement on the skin. Analog EMG data were band-passed at 30 to 300 Hz before being

digitized at 752 Hz. Foot switch information, also sampled at 752 Hz, was stored within the EMG data files.

Data analysis focused on characterizing the influence of spaceflight on terrestrial locomotion as soon as possible after landing, early in the readaptation process. Data were analyzed to compare the neuromuscular responses obtained 10 days before launch with those obtained between 2.5 and 4 hours after landing.

The first step in data analysis was to determine whether spaceflight influenced stride time, defined as heel strike to heel strike for the same leg, during locomotion. Trials of 20 to 22 strides were averaged relative to heel strike so that stride times before and after spaceflight could be compared. Stride time was a function of time spent in swing and stance phases, both of which could be controlled by the locomoting subject. Changes in the duty factor, defined as the percentage of the gait cycle spent in stance phase, could reflect changes in the neuromuscular activation patterns [90]. Each subject's stride time and duty factor were calculated for each stride. Values before and after spaceflight were compared with t-tests for correlated data.

EMG data were evaluated for each muscle and for each subject. Data across stride cycles were first time-normalized to 100% of stride by averaging the data between consecutive right heel strikes. Next, to reduce variability among subjects [62], wave forms were magnitude normalized to the mean level of activation across the wave form, so that the mean level of activation within the wave form was 100%. The mean wave forms then were divided into 5% epochs by representing the averaged data within an epoch as a single point [91, 92]. Standard deviations, and coefficients of variation across the mean wave forms, were calculated to assess activation variability. These reduction techniques produced EMG wave forms (referred to as reduced wave forms) that represented the phasic features of each muscle across the stride cycle.

The question of how spaceflight affects the lower limb neuromuscular activation during treadmill locomotion was addressed in five ways:

1. Reduced wave forms were compared before and after flight using Pearson product moment correlations for each muscle and each subject [66, 91, 92]. This analytical approach was extended to determine the degree of activation symmetry between individual muscles of both legs before and after flight.
2. Repeated measures analysis of variance (ANOVA) was used in combination with post hoc testing to compare normalized amplitudes before and after spaceflight at each 5% epoch for each right lower limb muscle.
3. Full wave-rectified EMG records, obtained from individual strides, were used to characterize the phasic pattern of activation from the right lower

limb muscles. This approach was adopted to assess the potential for changes in the time of muscle activation within the time-normalized wave forms. Changes in time of muscle activation within a stride cycle would indicate subtle, but potentially important, modifications in neural control.

4. Potential preflight versus postflight changes in coefficient of variation of the reduced EMG wave forms around the behavioral events of heel strike and toe off were assessed using repeated measures ANOVA with post hoc testing. EMG variability around these two events was evaluated because these periods in the stride cycle have large segmental decelerations (heel strike) or accelerations (toe off) and, therefore, require precise neuromuscular control.
5. Muscle co-contractions between the traditional agonist-antagonist pairs of the BF-RF and TA-GA were evaluated for potential preflight versus post-flight differences using repeated measures ANOVAs with post hoc testing. An alpha level of $p < 0.05$ was adopted for all statistical tests.

To evaluate the phasic activity of individual strides, the most significant neuromuscular control feature of each muscle during each stride was determined for each subject. For the RF, BF, and GA, this feature was the temporal onset (relative to heel strike) and duration (as a percent of stride cycle) of the largest amplitude burst of activity. For the RF and BF, the largest burst of activity occurred around heel strike. The largest burst of GA activity occurred in preparation for toe off. For the TA, the most significant neuromuscular control feature was the silent period present in most subjects shortly before toe off. This silent period usually corresponded to a large increase in gastrocnemius activity. Thus, the temporal features of the TA silent period was thought to reflect the sensorimotor system's ability to regulate ankle musculature activity, particularly around the critical time of toe off.

Muscle activation onset time was obtained by displaying the EMG activity of all strides simultaneously on the computer monitor. Visual inspection, in combination with interactive electronic cursors, was used to establish parameters of an algorithm for the identification of temporal onset of the phasic activity of interest in each stride. The algorithm was used to identify onset of muscle activation by noting the first point of a burst that exceeded a fixed amplitude threshold value (approximately two standard deviations above a quiet baseline) for at least 30 ms. A 30 ms minimum was selected on the basis of a report that muscle bursts that last less than 30 ms do not contribute to the force of the moving limbs during locomotion [93]. The algorithm was reversed to obtain muscle activation offsets. Muscle activation durations were obtained by calculating

the temporal difference between activation onset and offset. Duration of the silent period for the TA was calculated as the difference between offset and subsequent onset of muscle activity. To standardize measures across data collection sessions and subjects, temporal measures were expressed as a percentage of stride. The relationship between the ankle joint muscle activation characteristics, in preparation for toe off, was assessed by computing the temporal differences (as percent of stride cycle) between GA offset and TA onset. Paired Student *t*-tests were used to test for preflight-to-postflight changes in the activation features of each muscle for each subject. Although this statistical approach limited generalizations to other populations, it was appropriate for our goal of characterizing the range of individual responses after spaceflight.

Although previous gait investigations have revealed greater variability in motor patterns than in limb kinematics, large changes in EMG activation characteristics have a functional effect as well [66]. Following the convention of Ounpuu and Winter [64], changes in relative amplitude were considered functionally significant if: (1) the difference was statistically significant at $p < 0.05$, (2) the difference between the preflight and postflight measures was greater than the variability of each individual measure, and (3) the muscle was active (i.e., 20% of mean amplitude) during the analyzed epoch. A difference between preflight and postflight phasic patterns was considered functionally significant if the Pearson *r* value was less than or equal to 0.71 [66, 94].

It was plausible that the sensorimotor system may have had difficulty in controlling neuromuscular activation after spaceflight, in preparation for the events of heel strike and/or toe off, as a result of these two events, or a combination of preparation for and reaction to heel strike and toe off. Therefore, preflight versus postflight differences in the coefficient of variation during three epochs of the stride cycle were tested. These epochs were: (1) the 10% preceding the event, (2) the 10% following the event, and (3) the combination of the previous two epochs (i.e., 20% of the stride cycle with the event centered in the middle of the epoch). Only muscles that were active during all three epochs around the particular event were evaluated for preflight versus postflight differences.

Measures of co-contraction were obtained by initially summing the area under the curve of the reduced EMG wave forms and expressing the activity within each of the 20 epochs as a percentage of the summed area. The cross-sectional area of EMG activity for the BF-RF and GA-TA antagonist pairs was then calculated and used as an indicator of co-contraction [95].

Spatial Orientation

Tests were conducted to quantify orientation performance during free walking after spaceflight. Seven astronaut subjects, 5 male and 2 female, from spaceflights of

8 to 14 days' duration, performed two spatial orientation tasks requiring them to negotiate a path consisting of a right triangle with two sides 3 m (10 ft) in length, by walking with and without the aid of vision. Three corners were marked on the floor with targets consisting of 7 cm \times 7 cm (2.75 in \times 2.75 in) crosses (Figure 5.5-2). The task was to walk the triangular path, starting at either corner 1 or corner 3. When the path was completed, the subject was requested to turn and face the original direction. The verbal instructions given were, "walk at a comfortable pace, as accurately as possible around the path. The motion should be continuous. The goal is accuracy, with accuracy defined as your ability to straddle the path." For all experiment sessions, two spotters were present to prevent any collisions during the eyes closed tasks.

To control for directional preferences, the task was performed alternating clockwise (cw) and counterclockwise (ccw) directions, but always approaching the right angle (corner 2) of the triangle first. To minimize visual feedback, (1) vision occluded trials were performed before the eyes open trials, and (2) at the conclusion of each eyes closed trial, the subject was led in a serpentine path, with eyes still closed, to the next starting point. The subject was instructed to look at the path before starting each eyes closed trial. The subjects performed 12 trials eyes closed (6 cw and 6 ccw) and 6 trials eyes open (3 cw and 3 ccw). This protocol was performed 45 days and 15 days before, and 2 hours, 2 days, and 4 days after, spaceflight. This report will only present data from 15 days preflight and 2 hours postflight. Each subject wore a helmet with three retroreflective markers located above the head in approximately the sagittal plane (Figure 5.5-3). This helmet was also equipped with headphones that provided white noise to mask out spatial auditory cues, and blackened goggles to occlude vision.

Head kinematic data were collected with a video based motion analysis system using four CCD cameras (Motion Analysis Corporation, Santa Rosa, CA). Signals from the four cameras were fed to a video processor at a sampling frequency of 60 Hz. The outline of each target was extracted and passed to a system that tracked the three reflective head targets, producing a three-dimensional assessment of each marker.

The coordinates necessary to describe head position in all six degrees of freedom were computed from the three-dimensional positions of the head markers, and were used to: (1) identify translational position, (2) compute linear velocity, (3) express tilt, and (4) compute angular velocity of the head. The rotational head position was expressed as quaternions [96]. An interactive graphical software package assisted in determining the corners of the walked trajectory, and angular head velocity maxima, for each walk. Corner points were used to compute distance errors and mean walking velocity. To evaluate the mean walking direction for each leg of the triangle, lines of minimum least square

distance were fitted to the trajectory between the corners. The angle between two lines gave the amount of turn performed by the subject. Angular deviation from desired trajectory was computed as the difference between angle turned and required turn angle at the respective corner. Due to marker dropouts, not all parts of the trajectory were successfully recorded in all trials. The incomplete parts were marked as being invalid. Statistical analysis, performed on the mean parameter values of each subject, was based on a 3 segments \times 2 directions \times 2 visual conditions \times 2 days repeated measures design.

Lower Limb and Mass Center Kinematics in Downward Jumping

Experiment Design

The subject pool for this study consisted of 9 astronauts. In order to protect the subjects' anonymity, they will henceforth be designated by letter codes (S-1, S-2, ...S-9). The subjects ranged in age from 36 to 50 years. Of the 9 subjects, 8 were male and 1 was female. The first preflight testing (PRE1) took place 2-6 months before launch. Another preflight test (PRE2) occurred 9-15 days before launch, while the postflight tests (POST) were performed within 4 hours of Shuttle landing. Mission lengths varied between 7 and 14 days.

At each data collection session, the jumping protocol consisted of 6 voluntary two-footed downward hops from a 30 cm (1 ft) platform. Three jumps were performed while fixating continuously on a ground target 1 meter forward of the subject's initial toe position. The other three jumps were performed with the eyes closed, and subjects were instructed to look at the ground target then close their eyes and fixate on the imagined ground target position during the jump. Eyes open (EO) and eyes closed (EC) trials were alternated. Because of safety concerns related to subject instability postflight, the first jump was always performed with the eyes open. The subjects were instructed to land on both feet at the same time, although no specific instructions were given regarding the jump takeoff. A safety harness connected to an overhead frame prevented subjects from falling to the floor, but did not interfere with mobility during a normal jump.

Full-body kinematic data were collected with a video-based motion analysis system (Motion Analysis Corporation, Santa Rosa, CA). This system tracked the three-dimensional position of 14 passive reflective markers placed on the body. Markers were placed on the right side of the body at the toe, ankle, maleolus, knee, hip, shoulder, elbow, wrist, and ear. The remaining markers were located at the left heel and along the body centerline at the sacral bone, seventh cervical vertebra, occipital protuberance, and the second and third occipital condyles. For some of the subjects, foot switches located in the shoes underneath the heel and great toe of both feet were used to record the times when the feet were in contact with the ground.

Data Analysis

The motion analysis system provided the marker positions in three dimensions at a sampling rate of 60 Hz. The ankle, knee, and hip joint angles in the right leg were computed using the positions of the markers at the toe, ankle, knee, hip, and shoulder (See Figure 15.4). It was assumed that the foot, shank, thigh, and trunk were rigid segments. For all three joints, larger positive joint angles represented greater joint flexion while negative values denoted joint extension. In order to account for the possibility of variation in marker placement from session to session, average resting joint angles during quiet standing were calculated for each data collection session. These average resting angles were subtracted from the joint angle time series data for that session. Hence, the data shown here represent deviations from quiet standing posture, and positive joint angles indicate increased flexion from the rest position. Joint angular velocities were found by numerically differentiating the joint angle data using a four point centered difference. Before differentiating, the angle data were smoothed by filtering forward and backward (to eliminate phase shift) using a 3rd order Butterworth filter with a corner frequency of 15 Hz. Impact resulted in large and nearly instantaneous increases in the joint angular velocities. In order to avoid excessive smoothing of this feature, the data segments prior to and following impact were filtered and differentiated separately. Care was taken to minimize startup and ending filter transients by matching initial conditions.

The time of foot impact with the ground was extracted from the foot switch data for those subjects who were tested using the switches. For the other subjects, the impact time was calculated by determining when the downward velocity of the toe marker dropped to less than 10 mm/s. Comparisons of the two methods for finding impact time in the subjects with foot switch data yielded excellent agreement. For each jump, peak flexion angles and flexion rates after impact were computed for the ankle, knee, and hip joints as well as joint angles at the time of impact.

The position of the full-body center of mass (COM) in the sagittal plane was estimated from the marker positions, using an 8-segment body model (feet, shanks, thighs, trunk, upper arms, forearms, neck, and head). Lateral symmetry was assumed, allowing combination of the left and right segments in the arms and legs. The approximate distribution of the body mass among the body segments was found using a regression model based on the subject's weight and height [97, 98]. COM position was computed in an X-Z coordinate system, where the X value represented the fore-aft position and the Z direction corresponded to the gravitational vertical. Positive values for X and Z corresponded to forward and upward, respectively. The velocity of the COM was found using the same numerical differentiation procedure described above for the joint angular velocities.

Initial analysis of the joint and COM kinematics indicated a non-uniform pattern of postflight responses across

Table 5.5-2. Number of significant differences in preflight and postflight variables

Measure	Number of Subjects Exhibiting Significant Change		Ratio of Number of (PRE1 and PRE2 vs.POST)/ (PRE1 vs. PRE2)
	Preflight: PRE1 vs. PRE2	PRE1 and PRE2 vs. POST	
Peak Hip Angle	4	3	0.75
Peak Knee Angle	3	8	2.67
Peak Ankle Angle	5	6	1.20
Peak Hip Rate	2	7	3.50
Peak Knee Rate	2	6	3.00
Peak Ankle Rate	1	1	1.00
Peak COM Deflection	2	4	2.00
Time From Impact to Peak COM Deflection	0	4	•
Peak COM Upward Recovery Velocity	3	3	1.00

the subject pool. Therefore, preflight and postflight data sets were compared for each subject individually for peak joint flexion angles, peak joint flexion rates, and three COM-related measures: (1) maximum downward deflection, (2) time from impact to maximum downward deflection, and (3) peak upward recovery velocity. A two-way analysis of variance (ANOVA) was used to examine the effects of test session (PRE1, PRE2, POST) and vision (EO, EC). Test session effect was computed two ways: (1) PRE1 vs. PRE2, and (2) PRE1 and PRE2 together vs. POST. Tests yielding $p < 0.05$ were considered statistically significant.

Changes preflight to postflight in nine measures (3 peak joint angles, 3 peak joint rates, and 3 COM quantities) were considered for classification of the subjects into groups based on postflight performance. For each quantity, the number of subjects showing a significant change between the two preflight sessions was compared with the number demonstrating a significant difference between preflight and postflight (Table 5.5-2).

Of the nine measures, five were selected for classification purposes because they proved relatively insensitive to day-to-day variations. These measures (peak knee angle, peak hip and knee rates, peak COM deflection, and time to peak COM deflection) showed differences between pre- and postflight in at least twice as many subjects as were shown between the two preflight sessions. The five variables were tested together for the effects of test session and vision, using a two-way multivariate analysis of variance (MANOVA). Again, the contrast for test session effect was computed for pre- vs. postflight. Probabilities were based on Wilks' Lambda (likelihood ratio criterion) and Rao's corresponding approximate (sometimes exact) F-statistic. Subjects who did not exhibit

significant differences between pre- and postflight for the multivariate measure were classified as "No Change" (N-C).

The other subjects were classified as either "Postflight Compliant" (P-C) or "Postflight Stiff" (P-S) by scoring the five individual measures used in the MANOVA. For each measure, the subject received a [+1] for a significant change toward greater compliance postflight, a [-1] for a significant change toward lower compliance postflight, and a [0] for no significant change. The results for the individual measures were summed to get an overall score ranging from -5 to +5. Subjects with positive scores were designated P-C, while negative scores were labeled P-S. All statistical computations were performed using SYSTAT [97].

Model of COM Vertical Motion

A simple mechanical body model was developed to investigate the vertical motion of the COM following impact with the ground. In this single degree-of-freedom model (Figure 5.5-5), the vertical (Z) motion was assumed to decouple from the horizontal motion, which was neglected. The entire body mass was concentrated at the COM, supported by a massless, constant stiffness Hookean spring representing the legs. Similar models have been used by Alexander and Vernon [98] and McMahon and Cheng [99] to examine hopping and running. The upward restoring force exerted by the spring was proportional to the downward displacement of the COM from the uncompressed spring length Z_0 (nominally the height of the COM at the moment of impact). Energy dissipation, or damping, was modeled by a linear dashpot in parallel with the leg spring, which opposed the COM motion with a force proportional to COM velocity.

This model led to a second order linear differential equation that describes the COM motion:

$$M\ddot{z} + B\dot{z} + K(z - Z_0) = Mg \quad (8a)$$

$$\ddot{z} + \frac{B}{M}\dot{z} + \frac{K}{M}(z - Z_0) = g \quad (8b)$$

where z, \dot{z}, \ddot{z} = COM vertical position, velocity, and acceleration, respectively; g = gravitational acceleration; M = body mass; B = damping; and K = spring stiffness. The initial conditions needed to find the time solution of the equations are given by the vertical position and velocity of the COM at the moment of impact. In order to compare the pre- and postflight limb impedance properties for each subject, best fit values for each jump were determined for the coefficients $\frac{K}{M}$ and $\frac{B}{M}$ (the stiffness and damping, respectively, normalized by subject body mass). The best fit values were found using the MatLab System Identification Toolbox (The MathWorks Inc., Natick, MA). Model fitting was accomplished by minimizing a quadratic prediction error criterion, using an iterative Gauss-Newton algorithm [100]. The best fit for the rest spring length Z_0 was determined concurrently, although this parameter was nominally set by the height of the COM at impact. Unfortunately, the sampling rate was too low to provide an adequate estimate of the Z_0 value: with COM velocities greater than 2 m/s (6.5 ft/s) at impact, an uncertainty of one sampling interval in the time of impact could result in errors in Z_0 exceeding 3 cm (1.2 in). Since peak deflection of the COM following impact typically ranged from 8-15 cm (3.1-5.9 in), this level of uncertainty required simultaneous estimation of the spring length, using the MatLab identification routines.

Equation 8 can be rewritten in canonical second order form:

$$\ddot{z} + 2\zeta\omega_n\dot{z} + \omega_n^2(z - Z_0) = g \quad (9)$$

where $\omega_n = \sqrt{\frac{K}{M}}$ = natural frequency

$$\zeta = \frac{B}{2\sqrt{KM}} = \text{damping ratio}$$

The natural frequency is roughly equivalent to the bandwidth of the system and provides a measure of the speed of response, since higher natural frequencies correspond to faster transient responses. Clearly, increasing the stiffness K leads to a higher natural frequency. The damping ratio measures how oscillatory the transient response is, with lower damping ratios indicating more overshoot and oscillation or “ringing” in the system behavior. Increasing the stiffness K decreases the damping ratio, as does reducing the damping coefficient B .

RESULTS

Locomotor Head-Trunk Coordination Strategies

Figure 5.5-6 shows an example from one subject of the relationship between: (1) vertical translation of the trunk that occurred during each step, and (2) the corresponding pitch angular head movement during the NEAR target condition. During preflight testing (Figure 5.5-6a), pitch head movements acted in a compensatory fashion to oppose vertical trunk translation during locomotion. As the trunk translated upward, the head pitched forward/downward, thereby assisting maintenance of target fixation. Four hours after spaceflight (Figure 5.5-6b), there was a significant alteration in coordination between compensatory pitch angular head movements and vertical trunk translation. This was evidenced by a breakdown in the smooth, sinusoidal nature of pitch head movements into a number of sub-components.

The step-to-step variability of vertical trunk translation and corresponding compensatory pitch head movement is depicted for one subject in Figure 5.5-7. Each cycle was aligned at the point just prior to heel strike. Very little variation in vertical trunk translation occurred during locomotion, both before (Figure 5.5-7a) and after (Figure 5.5-7b) spaceflight. Pitch head movements showed more step-to-step variability and were considerably increased after flight.

Figure 5.5-8 shows the mean (± 1 S.E.) preflight and postflight coherence values relating vertical trunk translation and corresponding pitch head movement, for all subjects combined, for both NEAR and FAR target conditions. Using these data, a 2×2 (Target Distance versus Spaceflight Exposure) repeated measures ANOVA on pitch head/trunk coherence was performed. This analysis revealed significant effects for both spaceflight exposure ($F(1, 84) = 38.22, p < 0.0001$) and target distance ($F(1, 84) = 13.04, p = 0.0005$). In addition, a significant interaction occurred between target distance and spaceflight exposure ($F(1, 84) = 5.37, p = 0.0230$). There was a general postflight decrement in coordination between head and trunk in both NEAR and FAR, without a greater decrement in performance for the FAR, target condition.

Figure 5.5-9 displays preflight and postflight examples of Fourier amplitude spectra of pitch head angular displacement for the NEAR target condition for one subject. A predominant peak occurred at 2 Hz in both examples. Following spaceflight, the magnitude of the predominant 2 Hz peak was diminished in this subject, suggesting that a change in compensatory head movement control occurred during postflight locomotion.

Individual mean preflight and postflight variability in predominant peak of pitch head movements magnitude is illustrated in Figure 5.5-10 for the FAR and NEAR target conditions. For the FAR target condition, 8 subjects demonstrated a significant (paired t-test; $p < 0.05$) reduction

in predominant peak magnitude, 11 showed no change, and 4 showed a significant augmentation. For the NEAR target condition, 6 subjects demonstrated a significant (paired t-test; $p < 0.05$) reduction in predominant peak magnitude, 13 showed no change, and 4 showed a significant augmentation. The response variability illustrated in Figure 5.5-10 may reflect discrete head movement control strategies intended to maximize the central integration of veridical sensory information during the postflight recovery process.

Figure 5.5-11 shows the mean magnitude of the predominant peak (± 1 S.E.) of pitch head movements for all subjects, before and after spaceflight. The magnitude of the predominant peak was augmented during both the preflight and postflight NEAR target fixation condition. A 2×2 (Target Distance versus Space Flight Exposure) ANOVA revealed a significant effect for target distance ($F(1, 354) = 23.35, p < 0.0001$). This finding indicates that as the visual target was brought closer to the eyes, larger compensatory pitch head movements were induced to aid gaze stabilization of the near target. Results from the ANOVA showed only a marginally significant effect for spaceflight exposure ($F(1, 354) = 5.64, p = 0.018$), presumably reflecting the individual variability displayed in Figure 5.5-10.

To ascertain whether previous spaceflight experience modified head movement control strategies, data were divided into two groups based on experience. Multi-time fliers were defined as those subjects with at least one previous spaceflight exposure. Fifteen subjects were in this category. First-time fliers were defined as those experiencing their first encounter with actual spaceflight during participation in our study. Eight subjects were in this category.

In Figure 5.5-12, the mean preflight and postflight changes in the magnitude of the predominant peak from the amplitude spectra of pitch head movements for multi-time fliers and first-time fliers, for both FAR and NEAR target conditions, are compared. A 2×2 (Experience Level versus Spaceflight Exposure) ANOVA on peak amplitude revealed a significant effect for experience level for both FAR and NEAR target conditions. Inexperienced astronauts may have adopted different head movement strategies compared to their more experienced counterparts during locomotion following return to Earth.

Figure 5.5-13 displays a preflight example of pitch angular head displacement for 5 individual subjects (A-E) performing the Intermittent Vision (IV) paradigm during fixation of the NEAR target. There was a general reduction in head pitch amplitude during each eye closure period. These subjects were attempting to control the magnitude of head pitch movement during eye closure periods. Amplitude was restored within one or two cycles following restoration of vision. In addition to reducing amplitude, subjects also demonstrated a sustained forward head tilt during eye closure periods. During eye closure periods, head pitch amplitude was actively reduced and then

alter
alter

terized by calculating the Fourier amplitude spectrum of each alternating 5 second eyes open/closed epoch.

Figure 5.5-14a compares the preflight and postflight mean (± 1 S.E.) predominant frequency amplitude of pitch head movements, for all subjects, during alternating 5 second eyes open/closed epochs during locomotion. A 2×2 (Visual Condition versus Spaceflight Exposure) ANOVA revealed a significant effect for visual condition ($F(1, 166) = 52.72, p < 0.0001$), but no effect for spaceflight exposure. The entire subject population, taken as a whole, showed no difference in preflight versus postflight responses for both eyes open (EO) and eyes closed (EC) conditions. However, there was a significant ($p < 0.05$) difference across visual conditions. This confirmed the general trend of head pitch amplitude reduction when vision was denied, during both preflight and postflight testing. Figure 5.5-14b compares the preflight and postflight changes in mean (± 1 S.E.) head tilt, relative to horizontal in the sagittal plane for all subjects, during alternating 5 second eyes open/closed epochs during locomotion. A 2×2 (Visual Condition versus Spaceflight Exposure) ANOVA on head tilt revealed a significant effect for visual condition ($F(1, 166) = 67.8, p < 0.0001$), but no effect for spaceflight exposure. In addition to a reduction in predominant frequency amplitude during eye closure, there was also a static forward head pitch during the eye closure periods during both preflight and postflight locomotion.

Lower Limb Kinematics During Treadmill Walking

Temporal stride measures were evaluated for two reasons: (1) to assess the task-specific performance of the lower limb system, and (2) to evaluate a potential confound of the subject population. Subjects were asked to walk at a fixed speed of 6.4 km/hr (4 mph) on the treadmill. However, preferred walking speed was closely related to subject height. Given the range in subject height, certain subjects may have had to walk at other than their preferred speed. Evidence exists to suggest performance may not be as stable in a non-preferred state [104, 123]. Consequently, we examined several simple temporal characteristics of the gait patterns relative to subject height.

Figure 5.5-15 presents the mean stride time and standard deviation about the mean as a function of subject height. The Pearson correlation of mean stride time and subject height was significantly different from zero and remained so after flight (pre = 0.820, post = 0.681, $p < 0.05$), indicating that mean stride time increased with increasing subject height and was not influenced by flight. The Pearson correlation between standard deviation of stride time and subject height was neither significantly different from zero, nor did it change after flight (pre = -0.117, post = 0.147, $p > 0.05$), confirming that no simple

Table 5.5-3. ANOVA Results of Phaseplane Variability as a Function of Stride Epoch and Flight

	Hip	Knee	Ankle
Epoch	F(1,33)=3.4, p=.074	F(1,33)=1.5, p=.23	F<1.0
Pre vs. Post	F(1,33)=2.4, p=.134	F(1,33)=2.8, p=.10	F(1,33)=7.3, p=.011

linear relationship existed between stride time variability and subject height. Therefore, differences in subject height were assumed not to have influenced postflight results.

Figure 5.5-16 illustrates the similarity of duty factors for each subject before and after flight, and the lack of interaction with subject height. The mean duty factor both before and after flight was approximately 0.59, indicating that toe off occurred 59% of the way through the stride after heel strike. Paired t-tests of both the mean duty factor data and the within trial variability of the duty factor identified no differences ($p>0.05$) preflight versus postflight.

Figure 5.5-17 displays exemplar phase portraits, along with identification of the location of heel strike and toe off, to help illustrate the degree of variability in joint kinematics within a trial. The quantitative analyses that follow use data in this form to evaluate within-cycle fluctuations, changes in variability at discrete points within each cycle, and system stability.

Within-cycle variability on the phase plane is illustrated in Figure 5.5-18, which presents box plots of preflight and postflight data for the hip, knee, and ankle joints, constructed from the seven subjects. In all three joints, the postflight variability was clearly higher than the preflight variability, at all epochs. Moreover, there were apparent differences in variability magnitude at the different stride epochs. The knee joint had elevated variability around heel contact, whereas the ankle joint had elevated variability about the swing phase. However, the sizes of box and whiskers at many epochs, in all joints, indicate quite substantial individual differences in joint variability. Consequently, repeated measures ANOVA on each joint revealed no significant flight or epoch effects at the hip and knee joints. Only the ankle joint displayed significantly higher variability postflight at the 0.05 level. Table 5.5-3 summarizes these results. In general these data indicate that postflight treadmill walking was more variable than preflight, and that the response throughout the course of a gait cycle was joint and subject dependent.

Figure 5.5-19 documents variability on the phase plane at the moment of heel strike and toe off for each of the three lower limb joints. In most instances, variability was seen to increase after flight. However, paired t-tests of these data identified only the postflight increase in knee variability as significant ($p<0.05$) at the moment of heel strike, with only the hip joint postflight variability being significantly higher

($p<0.05$) at the moment of toe off. While the size of the box and whiskers in postflight measures on all three joints is indicative of substantial individual differences, the significant joint-specific changes at heel strike and toe off emphasize the importance of these locomotor events.

Figure 5.5-20 illustrates an index of dynamic stability calculated at the moment of heel strike and toe off during preflight and postflight performance. Paired t-test analyses identified no significant difference between preflight and postflight at either heel strike or toe off. Furthermore, the stability index magnitude across subjects was quite consistent, as seen in the width of the box and whiskers.

The stability index was based on eigen values of the Jacobian matrix. A complete loss of stability was identified specifically by the index exceeding unity. Detection of a statistically significant difference in this stability index, which never exceeded unity, did not denote a qualitative change in the system dynamics from the perspective of nonlinear dynamics. However, such a result could be used to indicate a tendency to less stable behavior. The absence of any notable change in the stability index was indicative of the preservation of lower limb intersegmental coordination.

Neuromuscular Activation Patterns

Neither stride time nor duty factor were affected by spaceflight. The group mean stride time before flight was 957.6 ms (SD 39.5), and the postflight mean was 959.1 (SD 38.2). The duty factor was 57.8% of stride cycle before flight (SD 2.2) and 58.6% (SD 1.3) afterward. Although postflight values were statistically different from preflight values for all but one subject, the magnitude of these changes was often small (1-2%). The difference was within the variability of treadmill control, and, therefore, did not have functional significance. Because treadmill belt speed could vary by up to 5% across data collection sessions, we chose to consider preflight versus postflight differences in stride time of less than 5% to be within the normal range of variation for this task. After flight, all of the subjects were able to reproduce preflight kinematic temporal features within 5%.

With few exceptions, preflight and postflight patterns of muscle activity were highly correlated, suggesting that the temporal features of lower limb neuromuscular activation 2.5 to 4 hours after landing were similar to preflight

characteristics. Pearson *r* correlations between preflight and postflight muscle activation in the left and right lower limbs are summarized in Table 5.5-4. The grand ensemble reduced wave form patterns for each muscle before and after flight, illustrated in Figure 5.5-21, reveal few differences in the phasic characteristics of the wave forms. Since there were no differences between the activation patterns of the muscles of the right and left lower limbs, the frequency distribution for preflight versus postflight activation pattern correlations was combined for the right and left lower limbs (Table 5.5-4). To make sure that our data reduction technique did not produce artificially high correlations, correlations were assessed between the mean wave forms developed from all of the digital samples contributing to those wave forms for three subjects. Correlations using all of the available data always revealed relationships as strong as or stronger than those found using the reduced wave forms.

In 70 of the 78 comparisons (90%), symmetry between the left and right lower limb muscle activation patterns, both before and after flight, exceeded a Pearson *r* value of 0.71 (Table 5.5-5). Therefore, the lower limb musculature was activated symmetrically, and this symmetry was not affected by spaceflight.

Despite observing no change in the temporal features of the overall wave form, analysis of the normalized mean amplitude of activation revealed significant functional differences before, versus after flight, around toe off and heel strike (Figure 5.5-22). Specifically, the RF, BF, and TA activation amplitudes were different around the heel strike, and RF and TA activation levels were different around toe off.

Table 5.5-4. Frequency Distribution of Preflight-to-Postflight Muscle Activation Correlation Coefficients for the Combination of the Right and Left Lower Limbs

	BF	RF	GA	TA	Total
1.00-0.91	12	9	17	14	52
0.90-0.81	5	5	1	5	16
0.80-0.71	1	3	2	1	7
0.70-0.61	1	1	0	0	2
0.60-0.51	1	0	0	0	1
0.50-0.00	0	0	0	0	0
Total no. of comparisons	20	18*	20	20	78

*Postflight RF data could not be obtained for two subjects.

Ranges of Pearson Product Moment correlations are presented in the left column.

BF - Biceps Femoris RF - Rectus Femoris
 GA - Gastrocnemius TA - Tibialis Anterior

Table 5.5-5. Frequency Distribution of Right vs. Left Lower Limb Muscle Activation Correlation Coefficients Combined for Preflight and Postflight Conditions

	BF	RF	GA	TA	Total
1.00-0.91	11	10	16	12	49
0.90-0.81	6	3	1	4	14
0.80-0.71	2	2	3	2	9
0.70-0.61	0	1	0	1	2
0.60-0.51	0	0	0	0	0
0.50-0.00	1	2	0	1	4
Total no. of comparisons	20	18*	20	20	78

*Postflight RF data could not be obtained for two subjects.

Table 5.5-6 presents muscle activation onset and duration for the RF, BF, and GA. Offset of activation and duration of the TA silent period are given in Table 5.5-7. Many of the preflight-to-postflight comparisons for individuals were statistically different, although the absolute differences were small. Figure 5.5-23 graphically represents the differences between GA activation offset and TA onset before and after flight. All but two subjects showed changes in the postflight temporal relationship between GA offset and TA onset relative to before flight. For some subjects, GA offset preceded the TA onset (i.e., the difference was negative). For other subjects the difference was positive. Moreover, the direction of the difference was changed after spaceflight for half of the subjects, indicating a complete reversal of the activation/deactivation sequence for the ankle musculature in preparation for toe off. The average preflight-to-postflight difference in this temporal relationship was 7.1 percent of the stride cycle. Because mean stride time across subjects was approximately 950 ms, each percentage point represented roughly 9.5 ms. Therefore, the average postflight difference between the GA offset and TA onset changed by approximately 67 ms (7.1% * 9.5 ms) relative to preflight values. Even accounting for slight changes in stride cycle time between the preflight and postflight measures, the magnitude of this difference indicates that at least some subjects experienced considerable changes in neuromuscular control of their ankle musculature in preparation for toe off.

Although there was a trend toward increased variability for all the active muscles around both heel strike and toe off, only the activation variability of the TA around toe off was significantly increased after spaceflight. The magnitude of co-contraction of the GA-TA muscles increased after flight, during the epochs immediately before toe off (at 45-55% of the stride cycle), but decreased just before heel strike (95% of the stride cycle).

Table 5.5-6. Onset and Duration (as Percent of Stride Cycle) of Muscle Activation Before and After Space Flight

Subject	Rectus Femoris Onset, % of Stride Time			Rectus Femoris Duration, % of Stride Time		
	Preflight	Postflight	p value	Preflight	Postflight	p value
A	87.8 (2.1)	89.8 (1.6)	0.001	29.0 (3.9)	26.8 (3.0)	0.024
B	88.4 (1.4)	89.7 (1.2)	0.001	77.0 (4.1)	74.4 (4.0)	0.021
C	87.3 (2.7)	86.9 (3.3)	0.356	24.5 (2.9)	28.0 (4.3)	0.003
D	88.0 (1.6)	86.8 (1.9)	0.019	26.4 (1.9)	27.9 (3.7)	0.050
E	90.9 (2.6)	85.3 (4.0)	<0.000	23.4 (3.2)	30.9 (4.1)	<0.000
F	93.3 (3.0)	91.1 (1.7)	0.002	16.5 (3.4)	24.6 (2.5)	<0.000
G	88.1 (2.7)	89.5 (2.9)	0.033	26.7 (3.3)	32.4 (4.0)	<0.000
H	89.0 (1.4)	88.2 (1.3)	0.024	26.6 (2.6)	33.9 (4.2)	<0.000
I	88.1 (3.1)	89.1 (2.4)	0.083	24.2 (5.1)	31.3 (12.0)	<0.000
J	91.9 (1.9)	94.5 (1.8)	<0.000	21.0 (2.4)	18.4 (1.7)	<0.000
Mean	89.3 (3.0)	89.0 (3.3)		29.5 (17.0)	32.9 (15.3)	
Median	88.9	88.9		25.45	29.45	
Subject	Biceps Femoris Onset, % of Stride Time			Biceps Femoris Duration, % of Stride Time		
	Preflight	Postflight	p value	Preflight	Postflight	p value
A	82.0 (0.5)	81.9 (0.6)	0.365	51.9 (4.2)	44.6 (10.1)	0.002
B	77.4 (1.2)	78.7 (3.4)	0.066	28.1 (4.4)	28.2 (4.5)	0.482
C	82.9 (0.7)	83.2 (0.8)	0.141	25.4 (3.3)	29.7 (4.2)	0.000
D	79.6 (1.1)	80.9 (1.4)	0.002	63.7 (2.8)	62.8 (1.9)	0.124
E	86.7 (4.3)	81.2 (1.5)	<0.000	23.6 (5.2)	33.2 (8.0)	<0.000
F	76.8 (2.3)	84.6 (6.7)	<0.000	24.6 (2.3)	24.7 (6.8)	0.480
G	84.3 (7.1)	82.4 (0.9)	0.125	43.1 (7.7)	42.2 (9.2)	0.380
H	81.5 (0.6)	80.3 (1.0)	<0.000	43.4 (6.2)	46.6 (3.0)	0.020
I	75.4 (2.2)	73.3 (5.0)	0.035	29.6 (3.7)	35.9 (5.4)	<0.000
J	77.0 (4.7)	81.4 (1.7)	<0.000	43.6 (6.5)	39.8 (11.0)	0.099
Mean	80.4 (4.7)	80.8 (4.2)		37.7 (13.6)	38.8 (11.1)	
Median	81.0	81.2		36.4	37.9	
Subject	Gastrocnemius Onset, % of Stride Time			Gastrocnemius Duration, % of Stride Time		
	Preflight	Postflight	p value	Preflight	Postflight	p value
A	94.7 (0.7)	6.6 (9.6)	<0.000	71.9 (4.8)	48.7 (10.5)	<0.000
B	25.8 (2.7)	96.3 (4.1)	<0.000	31.8 (5.4)	55.2 (5.6)	<0.000
C	22.7 (6.9)	87.7 (2.7)	<0.000	28.1 (7.9)	85.9 (3.1)	<0.000
D	27.8 (2.6)	93.8 (2.4)	<0.000	24.7 (4.3)	67.5 (5.2)	<0.000
E	94.3 (2.9)	17.3 (5.0)	<0.000	59.2 (4.6)	35.8 (6.5)	<0.000
F	91.7 (2.4)	96.5 (6.3)	<0.000	57.8 (3.6)	53.3 (6.2)	<0.000
G	99.5 (7.3)	95.3 (2.5)	0.009	52.6 (7.8)	63.5 (8.7)	<0.000
H	16.4 (4.2)	20.2 (3.2)	0.005	41.5 (7.6)	39.7 (4.3)	0.171
I	92.1 (2.4)	94.8 (2.7)	<0.000	56.8 (2.7)	55.8 (4.5)	0.200
J	0.4 (6.5)	90.9 (3.8)	<0.000	54.8 (7.3)	66.0 (4.7)	<0.000
Mean	6.6 (14.8)	99.9 (11.5)		47.9 (15.6)	57.1 (14.6)	
Median	97.8	95.7		53.7	55.5	

Numbers in parentheses are S.D. Note that 0.00% and 100.00% represent heel strike.

Table 5.5-7. Offset and Duration (as Percent of Stride Cycle) of Tibialis Anterior Activations Before and After Space Flight

Subject	Tibialis Anterior Offset, % of Stride Time			Tibialis Anterior Silent Period Duration, % of Stride Time		
	Preflight	Postflight	p value	Preflight	Postflight	p value
A	44.1 (4.1)	51.2 (1.1)	<0.001	14.7 (3.9)	8.0 (1.3)	<0.000
B	14.4 (7.7)	16.2 (11.2)	0.268	39.6 (7.2)	39.2 (11.1)	0.452
C	48.8 (3.0)	51.0 (3.3)	0.022	9.5 (3.5)	6.7 (2.8)	0.010
D	47.4 (1.4)	47.8 (1.5)	0.218	7.4 (1.4)	7.4 (3.5)	0.473
E	46.7 (2.1)	49.7 (2.5)	<0.000	9.8 (1.6)	8.3 (2.8)	0.021
F	33.2 (16.0)	46.4 (1.6)	<0.000	18.0 (15.9)	11.2 (1.6)	0.030
G	45.4 (6.2)	50.3 (2.1)	0.001	11.4 (5.8)	7.1 (1.6)	0.002
H	46.7 (2.5)	46.1 (2.5)	0.194	9.2 (2.0)	9.9 (2.6)	0.155
I	44.4 (2.9)	46.7 (2.9)	0.013	10.5 (1.9)	7.3 (2.5)	<0.000
J	49.4 (2.0)	51.1 (0.8)	0.012	5.5 (2.5)	4.3 (1.1)	0.095
Mean	42.0 (12.0)	45.4 (11.0)		86.8 (10.0)	89.2 (10.2)	
Median	46.3	48.5		89.4	91.9	

Numbers in parentheses are S.D.; 0.00% and 100.00% represent heel strike.

Co-contraction of the BF-RF muscles increased in the two epochs immediately before heel strike (90-100% of the stride cycle).

Spatial Orientation

Two different ways of describing distance errors were used: (1) the two-dimensional distance error of each corner point to the required corner at the end of a segment (arrival error), and (2) the difference between required length of a segment and actual distance covered (length error). The arrival error gave an absolute estimate of both directional and longitudinal deviations from the required path. The length error showed purely longitudinal errors in reproducing segments. Arrival error was cumulative over the walk, while length error was not. Figure 5.5-24 shows pre- and postflight walking trajectories for one subject during the eyes closed condition.

For all subjects combined, the four-way ANOVA revealed a significant effect of segment ($F(2,6)=8.74$; $p=0.017$) and a segment vision interaction ($F(2,6)=5.86$; $p=0.039$) on length error. Length error was increasing from segment 1 to 3 for the eyes closed condition, while it was largest for segment two in the eyes open condition, due to the fact that subjects tended to walk around corner 1 and 2 with open eyes. The segment effect could partly be explained by the different length of segment 3, while the interaction illustrated that errors increased more from one segment to the next in the eyes closed condition. The segment effect could partly be explained by the different length of segment 3, while the interaction illustrated that errors increased more from one segment to the next in the eyes closed condition.

Two-dimensional distance error was slightly larger after flight (0.74 ± 0.53 m) than before flight (0.61 ± 0.42 m). However, the difference was far from being significant. Only vision ($F(1,3)=12.66$; $p=0.038$) and the segment vision interaction ($F(2,6)=12.83$; $p=0.006$) had significant effects. The effect of vision was the result of much smaller errors in the eyes open condition (0.22 ± 0.11 m preflight, 0.27 ± 0.12 m postflight).

The directional error was described as the difference between: (1) the mean walking direction during each segment with respect to the previous segment, and (2) the required angle of turn from one segment to the next. Therefore, the directional error of the first segment only gave the heading error toward corner 1, while the directional errors during segments 2 and 3 gave the errors of angular turn with respect to the preceding path segment. Directional error, as defined here, was not cumulative because it was computed in relative coordinates.

Directional error was tested only for segment 2 and 3. Mean errors for the eyes closed conditions were -7.01 ± 9.77 degrees preflight, and -9.28 ± 8.23 degrees after flight, showing a trend to underestimate turns. The vision factor ($F(1,3)=14.45$; $p=0.031$) and the interaction segment-direction ($F(1,3)=36.72$; $p=0.009$) were significant.

The absolute mean directional error was tested to assess absolute errors. Here, sample day was found to be a significant factor ($F(1,3)=15.25$; $p=0.030$), caused by larger absolute errors in the postflight testing. The two-way interactions segment direction and segment vision were also significant. The segment direction interactions were due to individual differences between the clockwise and counterclockwise conditions. The effect of day on absolute directional error showed that postflight directional deviations were larger than before flight.

Mean walking velocity was computed by dividing walked length by the time needed for one segment to be walked. Subjects walked slower postflight for both eyes closed (0.73 ± 0.10 m/s preflight, 0.66 ± 0.10 m/s postflight) and eyes open (0.84 ± 0.08 m/s preflight, 0.81 ± 0.10 m/s postflight) conditions. All of the main factors, except direction, were significant, i.e., segment ($F(2,6)=21.68$; $p=0.002$), vision ($F(1,3)=28.28$; $p=0.013$) and day ($F(1,3)=12.26$; $p=0.039$). The interaction between direction and day ($F(1,3)=10.62$; $p=0.047$) was the only significant two-way interaction. Walking velocity for segment 3, with eyes closed, was slower after spaceflight.

Lower Limb and Mass Center Kinematics in Downward Jumping

Joint Kinematics

Phase plane plots, where joint angular velocities (degrees per second) are plotted against the joint angles (degrees), yield the best format for comparing the joint kinematics of several jumps. Figure 5.5-25 (top) shows phase portraits for subject S-1, comparing a time synchronized average of 12 preflight and 6 postflight jumps for the hip, knee, and ankle joints. The time of impact is marked by an open circle (○) on each plot, and the plots are traversed in the clockwise direction through the impact absorption and recovery to an upright posture. In general, after impact the peak flexion rate is reached rapidly; the peak flexion rate is the uppermost point on the phase portrait. Moving further along the phase diagram, the joint angular velocities drop to zero as the muscles act to decelerate the body's downward motion. When the joint flexion rate reaches zero, the joint is at its peak flexion angle, the rightmost point on the plot. After this point, the flexion rate becomes negative, indicating joint extension as the subject recovers to the upright resting posture. These plots depict averages of the jumps for the preflight and postflight sessions, with the time scales for each data series synchronized at the time of foot impact with the ground.

The plots for subject S-1 clearly illustrate expanded postflight phase diagrams for each joint with respect to the preflight measurements. Postflight, this subject exhibits greater peak joint flexion angles than during the preflight jump landings, indicating that the subject reached a more crouched body position postflight while absorbing the impact from the jump. Furthermore, the peak joint angular velocities seen postflight are greater than the joint rates observed preflight. In contrast, the phase-plane diagrams for subject S-9 in Figure 5.5-25 (bottom) demonstrate the opposite effect; the postflight portraits are consistently smaller than the plots of the preflight jumps. This postflight contraction of the phase diagrams denotes a decrease in peak joint flexion postflight, indicating that this subject retained a more upright posture while absorbing the impact. In addition, this subject showed smaller peak joint flexion rates in postflight testing than in the preflight jumps.

Center of Mass (COM) Kinematics

As with the joint angle data, the kinematics of the COM are plotted in a phase-plane format. Figure 5.5-26 shows the COM motion for subject S-1. Once again, the plots depict averages of the 12 preflight and 6 postflight trials. Figure 5.5-26 (left) shows the average motions of the COM in the X-Z (sagittal) plane. Figures 5.5-26 (middle) and 5.5-26 (right) present the phase-plane trajectories in the X (fore-aft) and Z (vertical) directions traversed in the clockwise direction, respectively. The open circles (○) denote the moment of impact coinciding with peak downward COM velocity. Deceleration of the COM downward motion takes place until the COM is at its lowest point and the Z velocity is zero. Then the Z velocity becomes positive as the COM recovers to the steady-state value for standing posture. The peak upward velocity occurs at the uppermost point on the trajectory. The trajectory may spiral in around the equilibrium point if there is oscillation about the final steady-state position.

Subject Classification

The joint angle phase diagrams for these two astronauts suggest that the subjects who exhibit postflight changes in joint kinematics compared to preflight values may be divided into two distinct groups. Using the analogy of a spring of variable stiffness, the first group is denoted "postflight compliant," or P-C. Just as a more compliant spring compresses more under a given load, this group generally exhibited greater joint flexion postflight than preflight, accompanied by increased postflight flexion rates. The second group is labeled "postflight-stiff," or P-S, indicating lower peak flexion and flexion rates for the jump landings following spaceflight.

The COM kinematics provide complementary information for classification of subject performance following spaceflight. If the legs are considered to be roughly spring-like in supporting the mass of the upper body, the maximum downward deflection of the COM following impact gives a measure of the stiffness of the lower limb "spring" (e.g., an increase in the downward deflection of the mass center indicates a decrease in the spring stiffness). The time from impact to the point of peak downward deflection also provides an indicator of the effective stiffness of the lower limbs. A decrease in the time between impact and maximum deflection implies an increase in the stiffness.

Table 5.5-8 contains the scoring of the five measures used to classify each subject. Positive entries indicate significant changes toward greater compliance postflight, corresponding to increases in peak joint angles or peak joint flexion rates, greater downward COM deflection, or longer times from impact to maximum COM vertical deflection. Negative entries represent significant differences in these quantities that indicate greater stiffness postflight. The statistical significance for the preflight/postflight MANOVA contrast of the five measures are shown for each subject. As previously mentioned, subjects with significant

Table 5.5-8. Subject Classification Based on Kinematic Measurements

Subject	S-1	S-2	S-3	S-4	S-5	S-6	S-7	S-8	S-9
Peak Knee Flexion	+1	+1	+1	+1	+1			-1	-1
Peak Knee Flexion Rate	+1	+1	+1	+1	+1				-1
Peak Hip Flexion Rate	+1	+1	+1	+1	+1		+1		-1
Peak COM Deflection	+1	+1	+1					-1	
Time to Peak COM Deflection	+1	+1	+1						-1
Overall Score	+5	+5	+5	+3	+3	0	+1	-2	-4
p-value	0.005	0.003	0.002	0.003	0.277	0.275	0.051	0.002	4×10^{-6}
Classification	P-C	P-C	P-C	P-C	N-C	N-C	N-C	P-S	P-S

MANOVA results were denoted P-C or P-S based on positive or negative overall scores respectively for the five classification measures; the remainder were designated “No Change” (N-C).

Four subjects (S-1, S-2, S-3, S-4) were classified P-C. All four had significantly increased peak knee flexion combined with significantly greater peak knee and hip flexion rates postflight; for three of the four (all except S-4), COM downward deflection and the time from impact to peak COM downward deflection also increased postflight. Both of the subjects designated P-S (S-8 and S-9) exhibited significantly decreased peak knee flexion postflight. Subject S-9 also showed significant decreases in peak hip and knee flexion rates after spaceflight, as well as a decrease in the average time from impact to peak COM downward deflection. Peak COM downward deflection was significantly reduced for subject S-8. The remaining three subjects (S-5, S-6, S-7) did not show a significant change between preflight and postflight, based on the multivariate criterion.

Because the measures of peak joint angle, peak joint rate, and maximum COM vertical deflection are affected by the magnitude of the impact force as well as lower limb stiffness, the changes observed cannot be attributed to limb impedance changes unless the impact loading is the same pre- and postflight. For this reason, the COM vertical velocity at the moment of impact was compared for each subject’s pre- and postflight jumps. Only two subjects (S-9 and S-2) showed significant differences between pre- and postflight impact velocities at the $p < 0.05$ level. For subject S-9, the average postflight impact velocity was

reduced by almost 20% compared to the preflight jumps. This change probably contributed to the decrease in knee flexion, joint rates and COM displacement observed for this subject. Subject S-2 also exhibited a significant postflight decrease of about 5% in impact velocity. In spite of the postflight reduction in impact loading, subject S-2 exhibited consistent increases in peak joint flexion, flexion rate and COM downward deflection. Thus, the impact velocity result actually adds support to the P-C classification for S-2. All other P-C and P-S subjects showed small, non-significant differences between pre- and postflight COM impact velocity.

In summary, the P-C subjects exhibited significant increases in postflight joint flexion and flexion rates; the P-S subjects showed the opposite effect, although the trend was less apparent in subject S-8. Figure 5.5-27a compares the average preflight and postflight values for maximum knee flexion, based on two preflight sessions of six jumps each and one postflight session of six jumps. Figures 5.5-27b and 27c contain pre- and postflight peak flexion rates for the knee and hip joints, respectively. Figures 5.5-28a and 28b show the preflight and postflight values for the two COM-related measures: peak downward COM deflection and time from impact to peak deflection. With the exception of subject S-4, all of the P-C and P-S subjects demonstrated a significant change in one or both of the COM measures, supporting their classification.

The error bars are standard errors, and significant differences between the pre- and postflight data are denoted with asterisks (*). Cases marked by a “†” indicate a significant test day effect for the contrast between the two

Table 5.5-9. Stiffness and Damping in Second Order Model

Subject	Stiffness, K/M, 1/s ²				Damping, B/M, 1/s			
	Preflight	Postflight	Percent Change	p-value	Preflight	Postflight	Percent Change	p-value
S-1	217.2	98.3	-54.7	0.0001	14.2	12.8	-9.7	0.1490
S-2	132.0	76.6	-42.0	0.0007	14.0	14.0	+0.1	0.7150
S-3	247.2	150.7	-39.1	0.0001	16.2	12.5	-22.9	0.0030
S-4	208.2	159.9	-23.2	0.0240	13.7	12.5	-8.6	0.0740
S-5	178.6	108.9	-39.0	0.0100	12.3	13.4	+9.5	0.2630
S-6	158.3	106.3	-32.8	0.1990	14.6	14.8	+1.8	0.6590
S-7	247.1	265.4	+7.4	0.3230	15.2	16.2	+6.5	0.3030
S-8	170.5	207.8	+21.9	0.0510	14.4	13.6	-5.9	0.2280
S-9	101.4	150.4	+48.3	0.1720	12.8	13.7	+7.1	0.4620

preflight sessions. Group averages for pre- and postflight data were also calculated for the P-S subjects, the P-C subjects, and all subjects taken together, and are shown at the right in Figures 5.5-27 and 28. Taken as a group, the P-C subjects show significant increases in all five measures. Grouping the two P-S subjects reveals significant decreases in peak knee flexion and maximum COM downward deflection.

Modeled COM Vertical Motion

Figure 5.5-29 shows predicted COM model responses using parameters estimated for representative pre- and postflight jumps for P-C subject S-1. Model fits for the 12 preflight (Fig. 5.5-29a upper) and 6 postflight (Fig. 5.5-29a lower) trials are staggered along the vertical axis. Figure 29b shows preflight (upper) and postflight (lower) average COM vertical trajectories; the shaded region indicates ± 1 standard deviation. Simulated model results using the pre- and postflight stiffness and damping averages are included as well. The COM motion in the preflight jump exhibited a substantial overshoot above the final equilibrium posture, indicating a fairly low damping ratio. The postflight jump showed a much slower response with little overshoot. Thus, the postflight response was consistent with a decreased natural frequency and increased damping ratio, in comparison to the preflight jump. P-S subjects, in contrast, demonstrated the opposite trend toward faster responses postflight, with greater overshoot.

Table 5.5-9 summarizes the stiffness and damping coefficients that were estimated for each subject, and shows an excellent match with the subject classification based on kinematics. Note that these values have been normalized by the subject body mass, and modeled stiffnesses are shown in Figure 5.5-30. All four P-C subjects (S-1, S-2, S-3, and S-4) and S-5 showed large (23%-55%), statistically significant decreases in postflight stiffness

compared to preflight values. Stiffness increases for P-S subjects S-8 and S-9 were not significant. The surprising lack of a significant postflight stiffness increase for subject S-9 (considering the consistent P-S changes in the joint and COM kinematics) may have been due to this subject's postflight decrease in impact velocity. The change in impact loading is explicitly accounted for in the COM motion model. In contrast with the changes in stiffness, examination of the damping coefficients revealed few differences between pre- and postflight performance, with only subject S-3 exhibiting a significant change (decrease). Furthermore, there was no apparent pattern of increases or decreases in the level of damping that corresponds to either subject classification or the changes in stiffness.

From the definitions of ω_n and z in Equation 2, a decrease in stiffness for a constant damping level should result in a lower natural frequency and a higher damping ratio. The calculated values for ω_n and z are shown in Table 5.5-10. As anticipated, the four P-C subjects, as well as S-5, all exhibited significant decreases of 13%-33% in the natural frequency, and hence reduced bandwidth postflight. Four of these subjects had increased damping ratios postflight as well, although significant changes were seen only for subjects S-1, S-2, and S-5. The P-S subjects demonstrated the opposite trend: increased natural frequency postflight, combined with decreases in the damping ratio (significant only for S-8 damping ratio).

Table 5.5-10. Second Order Response Parameters

Subject	Natural Frequency, ω_n				Damping Ratio, z			
	Preflight	Postflight	Percent Change	p-value	Preflight	Postflight	Percent Change	p-value
S-1	14.7	9.8	-33.3	0.0001	0.49	0.66	+36.5	0.0004
S-2	11.4	8.6	-24.6	0.0003	0.61	0.83	+35.4	0.0010
S-3	15.7	12.3	-21.8	0.0001	0.52	0.51	-2.5	0.7600
S-4	14.4	12.6	-12.7	0.0200	0.48	0.50	+5.6	0.2850
S-5	13.3	10.3	-22.5	0.0090	0.47	0.67	+43.0	0.0100
S-6	14.3	10.1	-18.0	0.1870	0.61	0.74	+20.7	0.1020
S-7	15.7	16.2	+3.4	0.3260	0.49	0.50	+3.0	0.5920
S-8	13.0	14.4	+10.5	0.0540	0.56	0.48	-14.7	0.0090
S-9	9.8	11.7	+20.0	0.1500	0.68	0.61	-10.4	0.2600

DISCUSSION

Locomotor Head-Trunk Coordination Strategies

Head-Trunk Coordination During Locomotion

We have characterized the deterioration in coordination between vertical trunk translation and compensatory pitch head movements during locomotion by determining the change in coherence between these two wave forms. The results demonstrated that exposure to the microgravity environment of spaceflight induced adaptive modification in coordination between vertical trunk translation and compensatory pitch head movements during locomotion. This change in head-trunk coordination strategy may account, in part, for the reported oscillopsia during locomotion following spaceflight, and may have contributed to disruption in descending control of locomotor function.

One of the interesting features of our data set concerns individual subject differences, illustrated by the individual responses shown in Figure 5.5-10. The variability between subjects may have been caused by individual susceptibility to adaptive neural modification. Alternatively, this variability may reflect the response of a control system looking for a new equilibrium point by assessing the veracity of multiple sensory inputs. Indeed, the requirement to maintain gaze stability may not fully account for the variety of head movement strategies observed during locomotion. Head movement strategies adopted during locomotion may reflect specific task constraints and the need to rely on specific sources of sensory information for the effective organization of coordinated movement. Nashner [105] described two possible head-trunk coordination strategies observed during the maintenance of dynamic postural equilibrium. The first strategy (“strap down”) calls for the head to be fixed to the trunk during body movement, so that in essence the head and trunk can be considered a single unit. Adopting this strategy means

that head-trunk control is simplified. However, the ability to resolve complex movements into their linear and angular components by the otoliths and semicircular canals becomes complex. Alternatively, the “stable platform strategy” fixes orientation of the head with respect to the gravito-inertial force vector, essentially stabilizing the head in space while the body moves underneath. The advantage of this strategy is that larger sustained rotations of the head are actively nulled, permitting simplification of the otolithic process responsible for detecting linear acceleration and static orientation of the head. The cost incurred by this strategy is that complex head-trunk patterns of coordination are required to successfully execute this control scheme.

The significant postflight reduction in predominant frequency amplitude of pitch head movements observed in some of our subjects (Figure 5.5-10) may have been caused by attempts to reduce angular head movement during locomotion and, therefore, reduce potential canal-otolith ambiguities during the critical period of terrestrial readaptation. This action may have further simplified coordinate transformation between head and trunk, presumably allowing an easier determination of head position relative to space. However, this strategy was not optimal for gaze stabilization because it resulted in a disruption in the regularity of the compensatory nature of pitch head movements during locomotion. This strategy also restricted behavioral options for visual scanning during locomotion. Consequently, there may have been tradeoffs between head movement strategies, depending on the imposed constraints. Once significant readaptation took place, a decrease in constraints on the degrees of freedom of head movement was likely to occur, returning performance to preflight levels. Importantly, head movement restriction during locomotion was also shown by patients suffering from vestibular deficits [106] and by children prior to development of the mature head stabilization response [51].

Some subjects showed a significant increase in predominant frequency amplitude of pitch head movements following spaceflight, in both the FAR and NEAR target conditions. These subjects may have been at the very early phase of their individual readaptation path prior to the establishment of a normal, or head restrictive, strategy. Therefore, the observed strategies may not have been subject specific, but rather a snapshot from a recovery curve that contained a continuum of responses. Consequently, immediately after spaceflight, some subjects experienced excessive head instability and the associated postural and gait dysfunctions. In response, a head restrictive strategy was adopted and maintained until normal control could be attained.

Various compensatory head movement strategies may play a central role in facilitating optimal sensorimotor transformations between the head and trunk, required for descending control of locomotion. Zangemeister et al. [107] demonstrated that normal locomotion, performed with the head in a retroflexed position, induced alterations in lower limb muscle activity patterns. They concluded that a functional linkage exists between otolith signals generated by various head positions and the muscle activity patterns generated in the lower limbs during locomotion. Given this functional linkage, it can be argued that if spaceflight induced adaptive modification in head-trunk coordination, this in turn could cause a disruption in the organization of coordinated body movement during post-flight terrestrial locomotion. It follows that active body movement in the unique inertial environment encountered during spaceflight may have required subjects to adaptively acquire novel head-trunk control strategies. However, these strategies may have been maladaptive for locomotion in a terrestrial environment, leading to impairment of locomotor function during the readaptation period following return to Earth.

Effects of Target Distance on Head Movement Control During Locomotion

DSO 614 results confirmed our previous findings which demonstrated that the amplitude of compensatory pitch head movements occurring during locomotion were modified by changes in the distance of the eyes from the visual target [13]. Specifically, when the target was brought closer to the eyes (30 cm vs. 2m, or 1 ft vs. 6.5 ft), the amplitude of pitch head movements increased in accordance with the greater angular gaze deviation per vertical trunk translation required to stabilize the near target. Therefore, we can conclude that the pitch head movements observed during locomotion, in the present context, were goal directed and dependent on the requirement to stabilize gaze, and were not completely a result of the passive inertial and viscoelastic properties of the head-neck system. That is not to say that passive properties did not play a role. However, the response was subject to neural mediation. We can infer that the observed changes in

head-trunk coordination following spaceflight reflected sensorimotor modification, in addition to passive mechanical changes, in the head-neck system following extended exposure to the microgravity environment. However, it is possible that as flight duration is extended from weeks to months, head control may be compromised by both changes in sensorimotor function and atrophy of the neck musculature responsible for maintaining the head upright against gravity. Investigations conducted with Russian cosmonauts, exposed to extremely long duration spaceflight of up to 175 days, indicated a decrease in neck strength of up to 40% following flight [108]. Therefore, it is likely that additional factors may have played a role in changing the dynamics of head movement control during locomotion following long duration spaceflight.

Postflight coherence decrements were observed in both the FAR and NEAR target conditions, with the decrease being greater during the FAR target condition. The apparent difference in head-trunk coordination between the FAR and NEAR ocular fixation conditions may have resulted from enhanced visual feedback of the head-trunk coordination breakdown during the NEAR target condition. During NEAR target fixation, the degree of apparent target motion was greater, resulting in a greater sensitivity to apparent target motion and oscillopsia. Greater sensitivity to target motion could then be used as feedback to enable subjects to actively modify their performance to permit better target stabilization. This would translate into enhanced head movement control during NEAR target fixation. Such enhancement in performance was observed by Dijkstra et al. [109] in standing human subjects asked to maintain postural stability in a moving visual environment. They found that a moving visual environment induced postural sway in subjects, with specific temporal characteristics linked to the presented visual information. Specifically, if the mean distance to a virtual sinusoidally moving wall was varied, the temporal relationship between the wall and induced body sway was dependent on the distance between the wall and the observer. As the distance of the subject to the wall increased, the tight relationship between body sway and wall movement decreased, suggesting a distance effect in action-perception coupling.

Effects of Transient Visual Occlusion on Head Movement Control

To investigate how the head-trunk system dynamically responded to short term (5s) alternating changes in visual input, we asked subjects to walk on the treadmill during intermittent visual occlusion (IV Condition). The results clearly demonstrated that during visual occlusion periods, in both preflight and postflight data sets, pitch head movement amplitudes were minimized. Importantly, this strategy was abandoned almost immediately once vision was restored. These results support the conclusion that the reduction in head pitch amplitude, observed in

some subjects during postflight trials performed with vision, was a goal-directed behavioral strategy produced in response to adaptive alterations in sensorimotor function and not exclusively an outcome of passive head-neck dynamics. When the subject population was considered as a whole, spaceflight had no effect on the predominant frequency amplitude of pitch head movements and static head tilt during the IV Condition. This lack of effect may have been due to enhanced locomotor stability afforded by the light finger touch on the handrail, similar to the enhanced postural stability produced, in the absence of vision, by precision contact of the subject's index finger with a stationary bar [85, 86]. Thus, the light touch could have provided an alternate path for veridical haptic information to contribute to, and enhance, postflight locomotor control.

It is reasonable to predict that both during readaptation to unit gravity and during visual occlusion, different head-trunk coordination strategies may emerge that are appropriate for maximizing input from the sensory modalities providing veridical information. Pozzo et al. [19, 28] demonstrated that during free locomotion in darkness, the mean head position was tilted downward. They hypothesized that the downward head tilt could help minimize head movements by locking the head to the trunk as well as serving to enhance otolithic sensitivity by maximizing the shear force acting on the otoconial membrane. Another rationalization that may account for the reduction in pitch head movement during visual occlusion and during postflight readaptation comes from an observation made by Bernstein [110]. He speculated that in the early stages of motor skill acquisition, subjects reduced available degrees of freedom in an attempt to simplify the control problem. As learning progressed, the restriction placed on degrees of freedom was eventually reduced and the full behavior was manifested. Recent work by Vereijken et al. [111] provided empirical evidence that support Bernstein's concepts. Our data show that restriction of head movement may simply have been a manifestation of a general phenomenon associated with the relearning of appropriate terrestrial motor strategies following spaceflight.

Enhanced Motor Response Flexibility: A Potential Training Tool?

Comparison of responses from multi-time and first-time astronauts indicates that multi-time astronauts demonstrated less postflight alteration in head control strategies than did subjects on their first flight. Postflight behavioral differences between astronauts based on their experience level were previously observed in tests of dynamic postural equilibrium control [8, 9, 112-114]. In these tests, inexperienced astronauts showed greater postflight decrement in postural stability than their more experienced counterparts. Such differences may have been the result of many factors. However, they did indicate a prolonged retention of learned strategies in experienced astronauts

that enabled quicker adaptive transition from microgravity to unit gravity. The identification of a learned enhancement in the capacity for flexible motor responses to altered sensory input and its association with a reduced decrement in postflight motor control suggests that preflight training regimes may be designed to promote development of motor response flexibility. This increased capability for motor response flexibility might aid in mitigating postflight motor disturbances. This concept is supported by the work of Kennedy et al. [115] who examined whether motor behavior could be adapted by exposing subjects to inter-sensory conflict involving vestibular input, and determining if the resultant adaptation was transferred to a different visual-vestibular conflict situation. In this study, one group of subjects was exposed to a visual-vestibular conflict (Purkinje stimulation) and allowed to adapt. A control group was not exposed to any sensory conflict training. The two groups were then exposed to a different visual-vestibular conflict situation (pseudo-Coriolis). Those subjects pre-exposed to sensory conflict experienced less dizziness and locomotor difficulties than the control group. The concept of enhanced motor flexibility or "learning to learn" was confirmed by Welch and colleagues [116], who exposed subjects to prismatic displacement of the visual scene. Using a pointing task as the dependent measure for adaptation, they found that previous exposure to prism displacement enhanced the ability to adapt to novel or previously unexposed visual displacements.

Similarly, astronauts could be exposed to visual-vestibular conflict situations during locomotion as part of a training regime designed to enhance the ability to reorganize motor control responses during sensory conflict situations. Such a training program would provide crew members with preflight experience in solving motor control problems and formulating workable solutions for each encountered situation. This solution might include learning to ignore some sensory input and becoming more reliant on others, and by attending more closely to vision and less to vestibular signals. In essence, this approach would train inexperienced crew members to rapidly reorder their motor control strategies, thereby increasing their chances for improved early postflight postural and locomotor performance.

Lower Limb Kinematics During Treadmill Walking

This aspect of DSO 614 was designed to evaluate lower limb joint kinematics during treadmill walking after spaceflight, with specific reference to head and gaze control. Basic temporal features of the gait cycle, such as stride time and duty cycle, remained unchanged following flight. However, specific and consistent changes in joint phase plane dynamics were identified at the moment of heel strike and toe off. In general, variability was greater

after flight. Although dynamic stability of the lower limb system, during transitions between stance and swing phases, did not seem to change following flight, individual responses to flight should be investigated further.

We expected joint angular dynamics to be significantly perturbed by spaceflight. However, stride epoch data indicated an overall, but statistically insignificant, increase in phase plane variability at all three joints. The lack of significance was partly attributed to the substantial individual differences. The expectation was that susceptibility of the gait cycle to disturbance would be greatest around heel strike and toe off. These events represented significant energy exchange with the support surface, either through exaggerated impact at heel strike or through an exaggerated effort to propel the body forward at toe off. Generally, variability was higher in the heel contact epoch of the knee joint, both before and after flight, and was exacerbated in much of the postflight data. Similarly, postflight variability in the ankle joint was higher for the epoch containing toe off, both before and after flight, and also was exacerbated after flight. These data lend some indirect support to the possibility that these peak energetic events were the source of postflight disturbances in gait. Since the head and eyes are located atop a multi-segmental system, any disturbance can propagate through these segments. Consequently, disturbances identified in the lower limbs may have been related to the reported oscillopsia during walking after flight [57].

Confirmation of the significance of these gait events was sought with analyses focusing on joint variability at the precise moments of toe off and heel strike. At toe off, the initiation of the swing phase, hip joint phase plane variability was significantly greater after flight than before. At the beginning of the swing phase, the hip was flexing and accelerating to maximum angular velocity, and therefore was a strong candidate for perturbations of the trunk. At the moment of heel strike, the initiation of the stance phase, the knee joint phase portrait variability was also significantly greater after flight. McMahon and colleagues demonstrated that, while exaggerated knee flexion during running was energetically inefficient, this strategy changed the joint stiffness and consequently reduced transmission of heel strike energy to the head [49]. The increased variability observed in our data may have been the result of attempts by crew members to adjust lower limb configuration about the moment of heel strike, indicating both a postflight increase in susceptibility to perturbations at heel strike, and explicit attempts to modulate head perturbations resulting from the impact force of heel strike.

In addition to changes in joint variability, we anticipated noticeable changes in system stability following spaceflight, indicating at least a decrease of system stability, if not a qualitative change in system dynamics. These changes did not occur, because increased individual joint variability was not sufficient to interfere with the

basic pattern of lower limb coordination. The absence of significant changes in the index used to evaluate system stability at both toe off and heel strike was consistent with the subjects successfully walking on the treadmill after flight. However, in light of the retained system stability, the relationship between joint coordination pattern and the observed joint variability should be investigated further. Relatedly, variability seen in the lower limbs may have been propagated through the trunk to the head, where the consequences could be more profound for the strategies engaged in maintaining head and gaze stability.

We decided to use a treadmill protocol because it permitted parallel evaluation of full body segmental kinematics and head movement control during locomotion. Only in this manner was it possible to evaluate head and gaze control strategies during locomotion. However, the use of the treadmill also subjected the locomotor performance to certain constraints. Some evidence suggests that treadmill walking is inherently less variable than over-ground walking. Nelson and colleagues observed that treadmill running was characterized by less variable vertical and horizontal velocities than over-ground running [117]. Similarly, a comparison of the mechanical energies of over-ground and treadmill walking by Woolley and Winter [118] found that the stride-to-stride variability of all work measures was significantly greater over ground, suggesting that the treadmill constrained walking more rigidly.

We found the temporal characteristics of gait patterns to be remarkably robust, as demonstrated by the lack of any significant change in either the mean duty factor, or the variability of the duty factor. Consequently, subjects seemed to maintain a consistent stance-to-swing ratio, even on landing day. The basic stride data did illustrate a linear correlation between stride time and subject height. This was not surprising, given the well documented allometric relationships found in animal locomotion [103]. However there was no such relationship between stride time variability and subject height, and no spaceflight influence on this feature could be detected. On a treadmill, the appropriate locomotory state is well defined, with a specific unvarying speed and little opportunity for directional error. Since treadmill walking is associated with low tolerance for error, variation beyond the acceptable state results in a complete failure in performance. In comparison, over-ground walking is much more forgiving, with much more opportunity for variance in speed and direction.

Some subjects opted not to attempt the treadmill protocol after spaceflight. This suggests that there may have been gross changes in locomotor control, beyond the relatively subtle changes we observed, in some individuals. Subjects from whom we acquired data on treadmill walking at the criterion speed had, by definition, attained a relatively high and consistent level of coordination. The possibility of observing qualitative coordination changes

in the lower limb may have been extremely slight, given this constraint. Moreover, subjects were additionally constrained by fixating and maintaining their gaze on a visual target, further regulating their performance.

Our data were also subject to the unique constraints of spaceflight related research. Specifically, crew members began to readapt to the presence of unit gravity between the moment of Shuttle landing and the time when postflight data were collected (usually 2 to 4 hours after landing). Postflight data were evaluated with the knowledge that the readaptation rate during this time was particularly high [8, 9]. In addition, first-time fliers often displayed more difficulty with postural control after flight than did experienced fliers [8, 9]. Although some subtle, but consistent, changes in postflight lower limb dynamics during treadmill walking were identified, our data confirmed the heterogeneous nature of human adaptation after spaceflight. The significant changes at the moment of heel strike and toe off were encouraging for the hypothesized change in the attenuation capacity of the musculoskeletal system.

Neuromuscular Activation Patterns

In general, the overall phasic activation characteristics of lower limb muscles were only minimally affected by short duration spaceflight. However, when analysis focused on muscle activation characteristics around heel strike and toe off, a variety of preflight versus postflight differences were observed. These changes in neuromuscular activation associated with spaceflight are discussed below in relation to observed changes in head and lower limb gait control strategies after spaceflight and the possible neurophysiological adaptations that contributed to these control strategies.

Perforations in the skin were made to allow for the placement of surface EMG electrodes. Correlations between muscle activation patterns during treadmill locomotion before and after flight revealed that spaceflight had a minor impact on the overall temporal activation patterns. Dickey and Winter [66], using activation pattern correlations to evaluate the effect of ischemic block on lower limb muscle activation during locomotion, considered correlations less than or equal to 0.71 to represent a significant change in the pattern of muscle activation. Gabel and Brand [92] recommended using an r^2 value of 0.50 (differences between muscle activation patterns). Using this criterion, only 4 of our 78 single limb muscle activation patterns differed after flight, compared to the preflight baseline. However, several subjects in this study had obvious postflight gait abnormalities as they entered the testing room. These included widened support base, shuffling (cautious) gait, and reluctance to move their heads relative to their trunks. Despite these problems, the phasic characteristics of muscle activation during postflight treadmill locomotion were remarkably similar to preflight patterns. This lack of difference was consistent with the observed

minimal preflight-to-postflight difference in stride duration and duty factor. However, evaluating single stride phasic muscle activation characteristics, as a percentage of stride duration for each subject, revealed many statistically significant differences between preflight and postflight locomotion. Although these changes may represent slight modifications in neuromuscular control strategies, they indicate that the sensory motor system generally could reproduce the major phasic activity of each muscle involved in locomoting effectively on a treadmill. However, our subjects did report oscillopsia after flight, suggesting they may have exchanged clear vision for dynamic postural stability during postflight treadmill locomotion. This trade-off was not particularly surprising, given that the consequences of locomotor instability during this task (ie, falling) were severe. Conversely, the safety consequences of unclear vision, while tracking an Earth-fixed target during our task, were minimal.

Given the inherent locomotion constraints on a motor-driven treadmill, this preflight-to-postflight stability could also reflect the task itself. Arsenault et al. [119] found treadmill locomotion to limit the variability in lower limb neuromuscular activation patterns normally present in over-ground locomotion. The minimal requirement for over-ground locomotion was translation from one point to another, which allowed much greater flexibility in the coordination pattern used to accomplish the task than that allowed during treadmill locomotion. The minimal requirement of upright treadmill locomotion was to coordinate body segments in a symmetrical manner that kept the subject within a limited gait width, while keeping pace with belt movement. Deviations from these requirements could result in falling. Moreover, the wide stance and shuffling gait used during over-ground locomotion after spaceflight would be ineffective during our treadmill task. In fact, some Shuttle astronauts have opted not to participate in previously scheduled treadmill testing on landing day, suggesting that these individuals were not confident in their ability to adopt the strategies necessary for successful treadmill locomotion.

Rapidity of readaptation after landing was another potential reason for the similarity between preflight and postflight neuromuscular activation patterns. Although many subjects displayed clinical abnormalities in postural control 2.5 hours after landing, they improved substantially one hour later. [8, 9] These results substantiated numerous anecdotal reports that although astronauts frequently have had problems with postural control immediately following Shuttle landing, they quickly readapt.

One discrete event in the gait cycle that required precise neuromuscular control was toe off. This fine motor skill is achieved by rapid exchanges between a large plantar flexor moment late in the stance to a large dorsiflexor moment at toe off. This exchange normally produces toe clearance during the swing phase of less than 1 cm (0.39 in), with a horizontal velocity greater than 4 m/sec

(13 ft/sec) [61]. Immediately before toe off, the GA actively contributes to the peak plantar flexor moment, with reciprocal inhibition of the TA. TA inhibition contributes to the ability of the GA to produce the necessary peak moment. Immediately before toe off, GA activity ceases and the TA is activated to produce a large dorsiflexion moment to provide appropriate toe clearance. In our study, eight of ten subjects displayed a significant change, after spaceflight, in the relationship between the offset of the GA and the subsequent onset of the TA. Moreover, the relative amplitude of the TA at toe off was reduced after flight, and GA-TA co-contraction magnitude was increased just prior to toe off. This further supported the idea that the precise neuromuscular control necessary to achieve proper toe clearance was compromised after spaceflight. These subtle changes could well explain the excessive foot scraping on the treadmill noted during postflight testing, and are consistent with the shuffling gait often noted during over-ground locomotion after flight.

The excessive foot scraping observed in our subjects may have been a maladaptive strategy that resulted from an inability of the sensorimotor system to efficiently activate ankle musculature. It may also have resulted from an exploratory behavioral mode designed to increase proprioceptive and cutaneous feedback. Pozzo et al. [28] suggested that patients with bilateral vestibular deficits, whose shoes displayed excessive wear on the soles, may have used such a strategy. Since proprioception was altered as a result of spaceflight [5, 53], it is plausible that our subjects were scraping their feet along the treadmill belt to obtain increased feedback. However, the cost of this strategy was to increase the possibility of tripping during postflight locomotion.

At heel strike, the sensorimotor system must effectively absorb the energy generated as the result of the sudden impact of the heel with the support medium, while controlling a kinematic strategy that ensures dynamic stability. During this yielding portion of the gait cycle, the hip joint angle is maintained in approximately 10 degrees of flexion while the knee joint rapidly flexes and the ankle joint plantar-flexes. This kinematic and associated neuromuscular strategy serves to keep the head, arm, and trunk segment (HAT) erect to within 1.5 degrees and attenuates potential head accelerations during locomotion [61]. This tight regulation of the HAT helps maintain the dynamic stability necessary to maintain a safe forward trajectory while contributing to stable gaze. The observed postflight differences in the EMG amplitudes of the RF, BF, and TA relative to preflight values, and increased BF-RF co-contraction around heel strike, indicated some disruption in the neuromuscular control needed to ensure optimal control during this critical behavioral event. This finding was consistent with those of McDonald et al. [45], who reported increased kinematic variability in the lower limb around heel strike during treadmill locomotion after spaceflight. Bloomberg et al. [14, 15] also reported the

presence of modified head control strategies after flight that may not have been as effective as preflight strategies in stabilizing gaze. The presence of these strategies could indicate that the energy introduced into the system, and transmitted to the head at heel strike, may not have been damped as effectively after spaceflight as before. Reductions in energy damping could have exacerbated oscillations during postflight locomotion. Subjects in this study consistently reported that the static target they were asked to visually fixate on during the locomotion task seemed to move more after flight than it did before.

Several neurophysiological changes associated with spaceflight could have been responsible for disruptions in lower limb neuromuscular control occurring around toe off and heel strike. Kozlovskaya et al. [5, 53] reported a generalized trend toward increased proprioceptive hyperreactivity after spaceflight. This was manifested by decreased tendon tap reflex thresholds, increased H reflex amplitudes, and increased vibrosensitivity of the soles of the feet. Other evidence of this phenomenon included increased tendon tap reflex amplitude after spaceflight [55]. Associated with these changes were reductions in the ability to perform graded muscle contractions and decreases in muscle stiffness, particularly in the triceps surae [54]. Shuttle crew members experienced a change in strength ratio between ankle plantar flexors and dorsiflexors. The plantar flexors lost significant strength while the dorsiflexors actually increased strength [120]. This change in relative strength was thought to result from the use of foot loops to maintain orientation relative to the work station. The foot loops were designed so that dorsiflexor activation was primarily required to maintain the proper orientation, as opposed to plantarflexor activation which was generally used to maintain the upright position on Earth. Therefore, increase in dorsiflexor strength and decrease in plantar flexor strength after spaceflight was not unexpected. Additionally, Zangemeister et al. [107] suggested that otolith input could influence TA activation characteristics during locomotion. Thus, spaceflight related adaptive modifications in neural processing of vestibular input could also negatively influence ankle joint muscle control after flight. These neurophysiological changes probably contributed to the inability of subjects in our study to achieve optimal transitions between the plantar and dorsiflexor muscle moments required around toe off, resulting in foot scraping on the treadmill after flight.

During spaceflight, dorsiflexors assumed a larger role than on Earth in regulating the orientation of the individual relative to the environment. Conversely, plantar flexors had a reduced role in orientation control compared with Earth-bound control strategies. Roll et al. [56] suggested that these in-flight adaptations in the respective roles of the ankle musculature eventually resulted in the reinterpretation of ankle proprioceptive input. With increasing mission duration, ankle proprioception was no longer interpreted as coding anterior-posterior body sway while upright, but rather, as coding either whole body axial

transportation (i.e., pushing off the support surface) or foot movement [56]. Although the adaptive ankle musculature control strategy and associated sensory input reinterpretations were appropriate in microgravity, they were maladaptive upon return to the terrestrial environment. It is quite possible that during testing on landing day, these maladaptive ankle control strategies contributed to the disordered EMG activation characteristics observed in this study.

The cautious gait shown when subjects entered the testing room after flight undoubtedly reflected the effects of sensorimotor adaptations. However, these subjects could, and did, organize effective neuromuscular activation strategies that allowed them to complete the task of treadmill locomotion. Nonetheless, subtle alterations were present, both in temporal activation features and in relative activation levels, of several muscles after spaceflight. These changes were particularly prominent around the important behavioral events of heel strike and toe off. Although the sensorimotor system could effectively develop and execute functional behavioral strategies during the goal-directed task of treadmill locomotion, changes in the neuromuscular activation characteristics observed during the task probably contributed to the observed difficulty in over-ground locomotion after landing.

Spatial Orientation

Repeating a previously seen trajectory without vision has been examined since Thomson's experiment on locomotor pointing [121]. However, most of the work has concentrated on walking toward one target. Subjects were able to reproduce previously seen distances correctly by walking two different segments, one straight ahead and the second perpendicular to it [122].

A similar task to the one presented here was called triangle completion. The subject was guided over two legs of the course, and then attempted to return directly to the point of origin [123, 124]. Walked segment length and sustaining angles were varied. Measured parameters were: (1) error in turning toward the origin after walking the first two legs, and (2) error in the distance walked to complete the third leg. A pattern of systematic regression to the mean was shown in both of these errors. Subjects tended to over-respond when the required distance or turn was small, and to under-respond when they were large. These responses were similar for both blind and normal subjects [124].

In blindfolded individuals, triangle completion has one major drawback in indicating disturbances in complex spatial understanding. Some errors made during both the guided walk and return walk were not seen in the results. Imagine a subject over-estimating the walked distance by a certain factor but making no other errors. This subject would perfectly perform the triangle completion, but fail to reach the first and second corners in our task. Therefore, we have chosen the reproduction of a previously seen path by means of locomotion. In this way, the locomotor

pointing performance allowed us to quantify misperception of linear and angular self-displacement.

Astronauts have reported anecdotally about problems in walking straight paths or going around corners when visual information was suppressed [10]. However, little is known about the influence of these modifications on spatial orientation during free locomotion following spaceflight. In DSO 614 we tried to assess this question by having subjects walk a triangular path before and after flight, with and without visual information. The subjects showed inter-individual differences, especially for directional deviations from the path in the vision occluded condition, even before spaceflight. The characteristics of these differences persisted throughout all sessions. However, the absolute directional errors turned out to be larger after flight, meaning that the subjects had larger directional errors, but in different directions. There was a trend toward larger under-estimation of the angle turned at each corner in the postflight condition. In contrast to directional errors, the length of the legs walked was similar before and after flight. If this trend was verified within additional subjects, it would suggest that the perception of self-displacement during turning, but not during linear motion, had been changed as a result of the stay in microgravity. This could have been due to a mismatch between information from otoliths and semicircular canals during whole body turns in microgravity, and could have been responsible for disturbances in locomotion experienced by returning astronauts.

Previous experiments [126] showed that angular as well as linear path integration performance heavily depended on velocity. All changes found could have been caused by the most significant finding, the lower walking velocity during postflight testing. The observed correlation between angular and linear velocity suggests that post-flight decrease in velocity, as found, for example for saccades [127], was a general effect of spaceflight.

The question of why subjects walk more slowly after spaceflight remains unanswered. It appears that a classic speed/accuracy tradeoff was achieved by walking more slowly. Another possible explanation might be that a task as simple as walking toward a previously seen target required a larger cognitive effort after spaceflight, which would slow down motor performance. This implies that mechanisms like computing self-displacement from somatosensory and/or vestibular inputs and updating of spatial information, were disturbed by spaceflight and had to be reacquired after return to Earth.

Lower Limb and Mass Center Kinematics in Downward Jumping

Pre- and postflight comparisons of the joint kinematics during jump landings indicate that the astronaut subjects may be separated into two different classes based on examination of the phase-plane descriptions, namely, P-C and P-S. The P-C group exhibited expanded phase-plane

portraits postflight in comparison to preflight baseline data, and the P-S group showed the contrary. The lower leg musculature may be thought of as contributing a resistance to joint displacements, or stiffness (modeled as a torsional spring-like element), as well as a resistance to joint angular velocity, or damping (represented by a viscous damper or dashpot). These stiffness and damping elements represent the displacement- and velocity-dependent components of the joint impedance, respectively.

Using this description, the P-C group exhibited postflight increases in the majority of both peak joint flexion angles and rates, indicating a reduction in stiffness about the joints following microgravity exposure. In these subjects, increases in joint flexion provided quantitative support for the reports of Watt et al.'s [128] astronaut subjects that their legs were bending more during drop landings postflight. These changes were also consistent with reductions in joint torques and a reduction in the bandwidth of the postural control system as a whole. In contrast, two of the subjects demonstrated an opposite, postflight-stiff response after returning from spaceflight. Their postflight contraction in the phase-plane plots indicated increases in limb stiffness and bandwidth of the postural controller.

A number of possible explanations exist for the observed changes in joint impedance during these jump landings, including loss of strength in the antigravity musculature, altered sensory feedback (muscle stretch reflexes, vestibular, or visual), and changes in open-loop modulation of limb stiffness. Since the stiffness and damping that can be exerted about a joint are directly related to the forces in the muscles acting about the joint, significant strength decreases in the antigravity muscles of the legs could well account for the expanded phase-plane portraits observed in the P-C group of astronauts. However, the P-S subjects exhibited postflight increases in stiffness, indicating increased joint torques; thus, the results from these subjects undermine the hypothesis that loss of muscle strength alone can account for the observations in this study.

Sensory Feedback

Sensory feedback pathways also contribute to the stiffness and damping of the closed-loop postural control system. Feedback quantities that could play a role in the jump landings include postural muscle stretch (modulated through spinal reflexes), vestibular sensing of head orientation and angular velocity, and visual inputs. The stretch reflexes effectively increase the stiffness about the joints by recruiting additional muscle fibers to counteract perturbations to the muscle lengths; the stretch reflexes in concert with Golgi tendon organ force feedback probably serve to modulate the tension-length behavior (impedance) of the muscles. Gurfinkel [83] reported decreases in the strength of the stretch reflex in tibialis anterior following spaceflight; Kozlovskaya et al. [5] found amplitude reductions in Achilles tendon stretch reflexes after long-duration flight. Such decreases could have the effect of

reducing the stiffness about the leg joints, and hence the stiffness of the leg "spring" supporting the body mass. However, Melvill Jones and Watt [129] demonstrated that the monosynaptic stretch response (occurring approximately 40 ms after forcible dorsiflexion of the foot) did not contribute to gastrocnemius muscle tension. Rather, the development of force was found to correspond to a sustained EMG burst with a latency of 120 ms following dorsiflexion stimuli, that they termed the "functional stretch reflex." Since the peak joint angle deflections in the jump landing occur only 100 ms after impact, stretch reflex activity is unlikely to play a major role in the impact absorption phase.

Studies by Allum and Pfaltz [130] and Greenwood and Hopkins [131] found vestibulo-spinal reflex latencies for postural muscles of 80 ms. Visual influences were found to be delayed 80 ms and 100 ms, respectively, by Allum and Pfaltz [130] and Nashner and Berthoz [132]. These latencies comprise most of the interval from impact to peak joint deflections, indicating that sensory feedback information from these sources following impact cannot be expected to contribute significantly to the impact absorption phase of jump landings. However, vestibular and visual inputs during the takeoff and flight phases of the jump may contribute to the motor activity during impact absorption. Interestingly, in the current study the eyes were closed in half of the jumps without a measurable effect on performance, indicating that vision's effect during the jump landings was minimal. This qualitative finding is intriguing in light of evidence for increased dependence on visual cues following spaceflight, for posture control and perception of body orientation and self-motion [10]. However, McKinley and Smith [133] describe jump-down behavior in normal and labyrinthectomized cats with and without vision, and conclude that normal cats that jumped from a known height did not rely on visual input to program pre-landing EMG responses, but when jump height was uncertain and visual input was absent, they speculate that vestibular input became more important. In our study, the astronaut subjects had full knowledge of the jump height after the first jump, which was always conducted with the eyes open. Furthermore, even in the EC jumps, the subjects had visual information about the jump height, even though they closed their eyes immediately before jumping. Therefore, the apparent ability to program pre-landing responses without vision may account for the lack of difference in jumps with and without vision.

Limb Stiffness

The limitations on the sensory feedback pathways indicate that the stiffness properties of the lower limbs may be largely predetermined before impact. The stiffness about the joints is determined by the level of muscle activation, and the overall impedance of the leg to COM motion is also affected by the configuration of the limbs

at impact (in general, less joint flexion results in greater vertical stiffness, due to the reduction of the moment arm about the joint centers). McKinley and Pedotti [134] found that the knee extensor muscles (rectus femoris and vastus lateralis) were activated slightly before impact, while the ankle plantarflexors (gastrocnemius and soleus) were continuously active from midflight during jumps. Furthermore, the legs reached their largest extension before impact, and were already slightly flexed again by the time of impact. Other investigators [135,136] have determined that the timing of the preparatory muscle activation and limb configuration is keyed to the expected time of impact. For downward stepping and repetitive hopping, Melvill Jones and Watt [129] found that muscular activity commenced from 80-140 ms before ground contact, and concluded that the deceleration associated with landing was due to a pre-programmed neuromuscular activity pattern rather than stretch reflex action.

Melvill Jones and Watt [137] demonstrated activation of both gastrocnemius and tibialis anterior approximately 75 ms following an unexpected fall; this reflex activity is most likely due to vestibular system otolith inputs. Such activation of antagonist muscles would contribute to stiffening of the limbs before impact. Furthermore, Watt et al. [128] showed that the amplitude of this response is markedly decreased during spaceflight. However, Watt's tests on landing day showed that the response had returned to normal almost immediately postflight, so changes in the otolith-spinal reflex may not account for the changes observed in the jumps described here. Reschke et al. [138] used the H-reflex to examine the effect of drops on the sensitivity of the lumbosacral motoneuron pool, which is presumably set by descending postural control signals. A large potentiation of the H-reflex (recorded in the soleus muscle) was found beginning approximately 40 ms following an unexpected drop. Furthermore, the investigators found that on the seventh day of spaceflight, the potentiation of the H-reflex during drops vanished. Immediately following spaceflight, 2 of 4 subjects demonstrated a significant increase in potentiation during the drop compared to preflight testing. While an increase or decrease in the sensitivity of the motoneuron pool might correspond to respective increases or decreases in the leg stiffness via a gain change in the spinal reflex pathway, the link to preprogrammed muscular activity is not clear.

In addition to the muscular commands linked to the flight and impact phases of the jump, the underlying tonic activation in the leg musculature may contribute to the impedance in the lower limbs during jump landing. Clément et al. [76] found an increase in tonic ankle flexor activity combined with a decrease in tonic extensor activity during spaceflight that, if carried over postflight, could lead to a reduction in the stiffness about the ankle joint against gravitational loads. It is well established that suppression of vestibular function results in depression of the gamma-static innervation to the leg extensors, causing

reduction in extensor tone [139]. However, because relative enhancement of the knee flexor was not observed, Clément's group viewed the changes at the ankle as a "subject initiated postural strategy" rather than a functional deafferentation of the otoliths caused by exposure to microgravity. Regardless of the origin, significant changes in leg muscle tone could well contribute to altered leg stiffness postflight.

Modeled Stiffness

The hypothesis that the joint impedance characteristics transform into lumped leg stiffness and damping parameters governing the vertical COM motion following impact provides the basis for the mechanical model postulated in this paper. These parameters are assumed to remain constant through the impact absorption and recovery to upright stance. McMahon and Cheng [101] summarized evidence indicating that the legs behave much like a linear spring of near-constant stiffness over a wide range of forces and running speeds. Based on those arguments and the generally close fits to experimental data obtained for the jumps in the present study, the simplifying assumptions of constant stiffness and damping appear reasonable. The constant leg stiffness value that best described human running in McMahon and Cheng's 1990 model was approximately 150 (N/m)/kg, falling well within the range of stiffness computed for the jump landings here.

Comparison of the pre- and postflight fits for this model indicates that variations in the model parameters can adequately predict the alterations in COM motion seen in astronaut jump landings following spaceflight. More specifically, changes in the leg stiffness alone appear to govern the differences in transient response observed upon return to earth. The postflight decreases and increases in the vertical leg stiffness found for these subjects correspond to the classifications of P-C and P-S made previously on the basis of kinematics alone.

In the model, decreases in leg stiffness lead to decreases in bandwidth, with slower and less oscillatory time responses. In contrast, increased stiffness results in faster, higher bandwidth performance with greater overshoots. These decreases and increases in leg stiffness postflight match the changes found in the transient performance for the P-C and P-S subjects, respectively. Interestingly, the model fits did not show changes in the leg damping to play a significant role in the postflight differences. This result is counterintuitive, since an increase in antagonist muscle activation to raise the limb stiffness might be expected to cause a corresponding increase in the mechanical damping properties of the muscles as well. Furthermore, changes in damping in accordance with increases or decreases in stiffness would help to prevent large deviations in the damping ratio (see equation 9), which is often desirable from a control system standpoint. Regardless, the evidence presented here indicates that the damping properties of the limbs can be modulated independently of the stiffness, or simply that the

damping characteristics are largely constant in the face of large changes in leg stiffness.

The final equilibrium positions predicted by the model lie somewhat below the actual final COM rest values, implying that the stiffness for these model fits is less than the values that would have been calculated from the final equilibria alone. In many cases, it was not possible to find parameter values that gave good predictions for both the transient portion of the response and the steady-state equilibrium. Because this study focused on impedance modulation during the impact absorption phase of the jump, the parameter estimation procedure was designed to find best fits for the transient portion of the response, often resulting in differences between the predicted and actual equilibrium positions. Interestingly, the pattern seen in Figure 5.5-29 was consistent across the subject pool: on average, predicted equilibria lay below the actual values. This result was attributed to a transition in control mode and limb posture from the impact absorption phase to the maintenance of upright posture near equilibrium. In equilibrium posture control, the flexed joints and greater compliance used in impact absorption give way to the more upright resting stance, where the alignment of the leg joints results in high vertical stiffness.

The changes in the model parameters corresponding to altered joint and mass center kinematics observed in the astronauts postflight were likely due to changes in the preprogrammed muscle activity prior to impact, which sets the limb impedance in an open-loop fashion by controlling the muscle tension-length properties and the limb configuration. The changes observed in this study in the impact absorption phase support the notion that spaceflight contributed to altered neuromuscular activity during the flight phase of the jump, even though EMG records were not available. The presumed alterations in muscle activation patterns following spaceflight could reflect changes in the relative recruitment of antagonist muscles, or differences in the timing of activation (e.g., failure to activate antigravity muscles early enough during the flight phase to stiffen the limbs for impact).

From an operational standpoint, the results of this study are important for understanding how microgravity exposure might impair astronauts' abilities to perform tasks such as an emergency egress from the Space Shuttle, or even locomotion on another planet following an extended duration spaceflight. The postflight changes in the kinematics of astronaut jump landings reported here have been attributed to changes in the control of the lower limb impedance resulting from exposure to the microgravity conditions of spaceflight. The decreased stiffness of the posture control system observed in the P-C group of subjects may reflect in-flight adaptation to the reduced requirements for posture control in the absence of gravitational forces. On the ground, the nature of the body's compound inverted pendulum structure requires the maintenance of a certain minimum stiffness for stability

in an upright position. In space, the body need not be stabilized against gravity, and the control bandwidth and stiffness may therefore be reduced without compromising postural stability. In flight, an overall reduction in postural stiffness may be observed as reduction in extensor tone and decreases in stretch reflex gain, and may be related to the loss of drop-induced H-reflex potentiation. Compliant postflight behavior may result from a residual decrement in the stiffness of the postural control system following return to Earth. In contrast, stiff postflight behavior may indicate overcompensation for reduced in-flight stiffness upon return to Earth, similar to the "rebound" effect observed by Reschke et al. [138] for the H-reflex. Thus, stiff responses postflight may be related to the observation by Young et al. [79] that some subjects were able to maintain balance only within a narrow "cone of stability" postflight, especially with the eyes closed. By using a stiffening strategy postflight, the subject minimizes deviations from equilibrium to avoid approaching the boundaries of the cone of stability. Such stiffening in turn requires a commensurate increase in postural control bandwidth.

In summary, this study provides evidence for modulation of lower limb impedance by astronauts in response to exposure to the microgravity of spaceflight. The results reported here, interpreted in light of other studies, indicate that this impedance modulation may result from a combination of altered tonic muscular activity and changes in the pre-programmed neuromuscular activity observed prior to and during impact absorption. Simulations using a simple mechanical model of the COM vertical motion indicate that changes in the lumped leg stiffness cause the differences in postflight jumping performance seen in the joint and COM kinematics. The reduced requirements for maintenance of posture under microgravity conditions probably contribute to the changes seen postflight, in concert with decrements in limb proprioception and altered interpretation of otolith acceleration cues.

REFERENCES

1. Homick JL, Reschke MF. Postural equilibrium following exposure to weightless space flight. *Acta Otolaryngol* 1977; 83:455-64.
2. Kenyon RV, Young LR. M.I.T./Canadian vestibular experiments on the Spacelab-1 mission: 5. Postural responses following exposure to weightlessness. *Exp Brain Res* 1986; 64:335-46.
3. Bryanov II, Yemel'yanov MD, Matveyev AD, Mantsev EI, Tarasov IK, Yakovleva IYa, Kakurin LI, Kozrenko OP, Myasnikov VI, Yeremin AV, Pervushin VI, Cherepakhin MA, Purakhin YuN, Rudometkin NM, Chekidra IV. Characteristics of statokinetic reactions. In: Gzenko OG, Kakurin LI, Kuznetsov AG, editors. *Space flights in the soyluz spacecraft:*

- biomedical research. Redwood City, CA: Leo Kanner Associates. Translation of Kosmicheskiye Polety na Korablyakh "Soyuz" Biomeditsinskiye Issledovaniya. Moscow: Nauka Press; 1976. p 1-416.
4. Kozlovskaya IB, Aslanova IF, Barmin VA, Grigorieva LS, Gevlich GI, Kirenskaya AV, Sirota MG. The nature and characteristics of gravitational ataxia. *Physiologist (Supplement)* 1983; 26:108-9.
 5. Kozlovskaya IB, Kriendich YV, Oganov VS, Koserenko OP. Pathophysiology of motor functions in prolonged manned space flights. *Acta Astronautica* 1981; 8:1059-72.
 6. Chekirda IF, Bogdashevskiy AV, Yeremin AV, Kolosov IA. Coordination structure of walking of Soyuz-9 crew members before and after flight. *Kosmicheskaya Biologiya i Meditsina* 1971; 5:48-52.
 7. Chekirda IF, Yeremin AV. Dynamics of cyclic and acyclic locomotion of the Soyuz-18 crew after a 63-day space mission. *Kosmicheskaya Biologiya i Aviakosmicheskaya Meditsina* 1977; 4:9-13.
 8. Paloski WH, Reschke MF, Black FO, Doxey DD, Harm DL. Recovery of postural equilibrium control following space flight. In: Cohen B, Tomko DL, Guedry F, editors. *Sensing and controlling motion: vestibular and sensorimotor function*. Ann NY Acad Sci 1992; 682:747-54.
 9. Paloski WH, Reschke MF, Doxey DD, Black FO. Neurosensory adaptation associated with postural ataxia following spaceflight. In: Woolacott M, Horak F, editors. *Posture and gait: control mechanisms*. Eugene, OR: University of Oregon Press; 1992. p 311-15.
 10. Reschke MF, Bloomberg JJ, Paloski WH, Harm DL, Parker DE. Physiologic adaptation to space flight: Neurophysiologic aspects: sensory and sensory-motor function. In: Nicogossian AE, Leach CL, Pool SL, editors. *Space Physiology and Medicine*. Philadelphia: Lea & Febiger; 1994. p 261-85.
 11. McDonald PV, Layne CS, Bloomberg JJ, Merkle L, Jones G, Pruett CJ. The impact of space flight on postflight locomotion. *Soc Neurosci Abstr* 20, Part 1 1994; 792.
 12. Layne CS, Bloomberg JJ, McDonald PV, Jones G, Pruett CJ. Lower limb electromyographic activity patterns during treadmill locomotion following space flight. *Aviat Space and Environ Med* 1994; 65:449.
 13. Bloomberg JJ, Huebner WP, Reschke MF, Peters BT. The effects of space flight on eye-head coordination during locomotion. *Soc Neurosci Abstr* 18, Part 2 1992; 1049.
 14. Bloomberg JJ, Reschke MF, Peters BT, Smith SL, Huebner WP. Head stability during treadmill locomotion following space flight. *Aviat Space and Environ Med* 1994; 65:449.
 15. Bloomberg JJ, Reschke MF, Huebner WP, Peters BT, Smith SL. Locomotor head-trunk coordination strategies following space flight. *J Vestib Res* 1997; 7:161-77.
 16. Layne CS, McDonald PV, Bloomberg JJ. Neuromuscular activation patterns during locomotion after space flight. *Exp Brain Res* 1997; 113:104-16.
 17. McDonald PV, Basdogan C, Bloomberg JJ, Layne CS. Lower limb kinematics during treadmill walking after space flight: implications for gaze stabilization. *Exp Brain Res* 1996; 112:325-34.
 18. Berthoz A, Pozzo T. Intermittent head stabilization during postural and locomotor tasks in humans. In: Amblard B, Berthoz A, Clarac F, editors. *Posture and gait: development, adaptation and modulation*. Amsterdam: Elsevier; 1988. p 189-98.
 19. Pozzo T, Berthoz A, Lefort L. Head stabilization during various locomotor tasks in humans. 1. Normal subjects. *Exp Brain Res* 1990; 82:97-106.
 20. Grossman GE, Leigh RJ, Abel LA, Lanska, DJ, Thurston SE. Frequency and velocity of rotational head perturbations during locomotion. *Exp Brain Res* 1988; 70:470-76.
 21. Pulaski PD, Zee DS, Robinson DA. The behavior of the vestibulo-ocular reflex at high velocities of head rotation. *Brain Research* 1981; 222:159-65.
 22. Grossman GE, Leigh RJ, Bruce EN, Huebner WP, Lanska DJ. Performance of the human vestibulo-ocular reflex during locomotion. *J Neurophysiol* 1985; 62:264-72.
 23. Taguchi K, Hirabayashi C, Kikukawa. Clinical significance of head movement while stepping. *Acta Otolaryngol (Stockh)* 1984; 406:125-28.
 24. Gresty M, Leech J. Coordination of the head and eyes in pursuit of predictable and random target motion. *Aviat Space Environ Med* 1977; 48:741-44.
 25. Takahashi M, Hoshikawa H, Tsujita N, Akiyama. Effect of labyrinthine dysfunction upon head oscillation and gaze during stepping and running. *Acta Otolaryngol (Stockh)* 1988; 106:348-53.
 26. Grossman GE, Leigh RJ. Instability of gaze during locomotion in patients with deficient vestibular function. *Annals of Neurology* 1990; 27:528-32.
 27. Takahashi M. Head stability and gaze during vertical whole-body oscillations. *Annals of Otology, Rhinology and Laryngology* 1990; 99:883-88.
 28. Pozzo T, Berthoz A, Lefort L, Vitte E. Head stabilization during various locomotor tasks in humans. II. Patients with bilateral peripheral vestibular deficits. *Exp Brain Res* 1991; 85:208-17.
 29. Guitton D, Kearney RE, Wereley N, Peterson BW. Visual, vestibular and voluntary contributions to human head stabilization. *Exp Brain Res* 1986; 64:59-69.

30. Keshner EA, Peterson BW. Multiple control mechanisms contribute to functional behaviors of the head and neck. In: Berthoz A, Graf W, Vidal PP, editors. *The head-neck sensory motor systems*. New York: Oxford University Press; 1992. p 381-86.
31. Keshner EA, Peterson BW. Mechanisms controlling human head stabilization. I. Head-neck dynamics during random rotations in the horizontal plane. *J Neurophysiol* 1995; 73:2293-301.
32. Keshner EA, Cromwell RL, Peterson BW. Mechanisms controlling human head stabilization. II. Head-neck characteristics during random rotations in the vertical plane. *J Neurophysiol* 1995; 73:2302-12.
33. Hirasaki E, Takeshi K, Nozawa S, Matano S, Matsunaga T. Analysis of head and body movements of elderly people during locomotion. *Acta Otolaryngol (Stockh)* 1993; 501:25-30.
34. Paige GD. The influence of target distance on eye movement responses during vertical linear motion. *Exp Brain Res* 1989; 77:585-93.
35. Solomon D, Cohen B. Stabilization of gaze during circular locomotion in light. I. Compensatory head and eye nystagmus in the running monkey. *J Neurophysiol* 1992; 67:1146-57.
36. Solomon D, Cohen B. Stabilization of gaze during circular locomotion in darkness. II. Contribution of velocity storage to compensatory eye and head nystagmus in the running monkey. *J Neurophysiol* 1992; 67:1158-70.
37. Hernandez-Korwo R, Kozlovskaya IB, Kreydich YV, Martinez-Fernandez S, Rakhmanov AS, Fernandez-Pone E, Minenko VA. Effect of seven-day space flight on structure and function of human locomotor system. *Kosm Biol Aviakosm Med* 1983; 17:37-44.
38. Anderson, DJ, Reschke MF, Homick JL, Werness SAS. Dynamic posture analysis of Spacelab-1 crew members. *Exp Brain Res* 1986; 64:380-91.
39. Berthoz A, Grantyn A. Neuronal mechanisms underlying eye-head coordination. *Prog Brain Res* 1986; 64:325-43.
40. Vieville T, Clément G, Lestienne F, Berthoz A. Adaptive modifications of the optokinetic vestibulo-ocular reflexes in microgravity. In: Keller EL, Zee DS, editors. *Adaptive processes in visual and oculomotor systems*. New York: Pergamon Press; 1986. p 111-20.
41. Kozlovskaya IB, et al. The effects of real and simulated microgravity on vestibulo-oculomotor interaction. *The Physiologist* 1985; 28(6):51-56.
42. Thornton WE, Moore TP, Uri JJ, Pool SL. Studies of the vestibulo-ocular reflex on STS 4, 5 and 6. *NASA Technical Memorandum* 1988; 100(461):42.
43. Uri JJ, Linder BJ, Moore TP, Pool SL, Thornton WE. Saccadic eye movements during space flight. *NASA Technical Memorandum* 1989; 100(475):9.
44. Jones GM, Gordon C, Fletcher W, Weber K, Block E. Adaptation in the non-visual control of locomotor trajectory. *Third International Symposium on the Head/Neck System*. Vail, CO, 1995.
45. McDonald PV, Basdogan C, Bloomberg JJ, Layne CS. Lower limb kinematics during treadmill walking after space flight: implications for gaze stabilization. *Exp Brain Res* 1996; 112:324-34.
46. McDonald PV, Bloomberg JJ, Layne CS. A review of adaptive change in musculoskeletal impedance during space flight and associated implications for postflight head movement control. *J Vestib Res* 1997; 7:239-50.
47. Voloshin AS, Wosk J, Brull M. Force wave transmission through the human locomotor system. *Transactions of the American Society of Mechanical Engineers Journal of Biomechanical Engineering* 1981; 103:48-50.
48. Perry SD, Lafortune MA. Effect of foot pronation on impact loading. *International Society of Biomechanics 14th Congress*. Paris, France, 1993.
49. McMahan TA, Valiant GA, Frederick EC. Groucho running. *J Appl Physiol* 1987; 62:2326-37
50. Lafortune MA, Hennig EM, Lake MJ. Dominant role of interface over knee angle for cushioning impact loading and regulating initial leg stiffness. *J Biomech* in press. 1996.
51. Assaiante C, Amblard B. Ontogenesis of head stabilization in space during locomotion in children: influence of visual clues. *Exp Brain Res* 1993; 93:499-515.
52. Thornton WE, Rummel JA. Muscular deconditioning and its prevention in space flight. In: Johnston RS, Dietlein LF, editors. *Biomedical results of Skylab, NASA SP-377*. U.S. Government Printing Office: Washington, DC; 1977. p 191-97.
53. Kozlovskaya IB, Kreidich YV, Rakhman OV. Mechanisms of the effects of weightlessness on the motor system of man. *Physiologist* 1981; 24:59-64.
54. Grigoryeva LS, Kozlovskaya IB. Effect of weightlessness and hypokinesia on velocity and strength properties of human muscles. *Kosm Biol Aviakosm Med* 1987; 21(1):27-30.
55. Harris BA, Billica RD, Bishop SL, Blackwell T, Layne CS, Harm DL, Sandoz GR, Rosenow EC. Physical examination during space flight. *Mayo Clin Proc* 1997; 72:301-08.
56. Roll JP, Popov K, Gurfinkel VS, Lipshits M, Andre-Deshays C, Gilhodes JC, Quoniam C. Sensorimotor and perceptual function of muscle proprioception in microgravity. *J Vestib Res* 1993; 3:259-73.
57. Hillman EJ, Bloomberg JJ, McDonald PV, Cohen HS. Dynamic visual acuity while walking in normals

- and labyrinthine deficient patients. *J Vestib Res* 1998; In press.
58. Milner M, Basmajian JV, Quanbury AO. Multifactorial analysis of walking by electromyography and computer. *Arch Phys Med Rehabil* 1971; 50:235-58.
 59. Dubo HIC, Peat M, Winter DA, Quanbury AO, Hobson DA, Steinke T, Reimer G. Electromyographic temporal analysis of gait: normal human locomotion. *Arch Phys Med Rehabil* 1976; 57:415-20.
 60. Winter DA. Pathologic gait diagnosis with computer-averaged electromyographic profiles. *Arch Phys Med Rehabil* 1984; 65:393-98.
 61. Winter DA, MacKinnon, Ruder GK, Wieman C. An integrated EMG/biomechanical model of upper body balance and posture during human gait. In: Allum JHJ, Allum-Mecklenburg DJ, Harris FP, Probst R, editors. *Progress in Brain Research* 1993; 97:359-67.
 62. Winter DA, Yack HJ. EMG profiles during normal human walking: stride-to-stride and inter-subject variability. *Electroencephalogr Clin Neurophysiol* 1987; 67(5):402-11.
 63. Shiavi R, Bugle HJ, Limbird T. Electromyographic gait assessment, part 1: adult EMG profiles and walking speed. *J Rehabil Res Dev* 1987; 24(2):13-23.
 64. Ounpuu S, Winter DA. Bilateral electromyographical analysis of the lower limbs during walking in normal adults. *Electroencephalogr Clin Neurophysiol* 1989; 72:429-38.
 65. Kameyama O, Ogawa R, Okamoto T, Kumamoto M. Electric discharge patterns of ankle muscles during normal gait cycle. *Arch Phys Med Rehabil* 1990; 71: 969-74.
 66. Dickey JP, Winter DA. Adaptations in gait resulting from unilateral ischaemic block of the leg. *Clinical Biomechanics* 1992; 7(4):215-25.
 67. Crosby PA. Use of surface electromyography as measure of dynamic force in human limb muscles. *Med Biol Eng Comput* 1978; 16:519-24.
 68. Komi PV. Relationship between muscle tension, EMG and velocity of contraction under concentric and eccentric work. In: Desmedt JE, editor. *New developments in electromyography and clinical neurophysiology*, vol. 1. Karger & Basel; 1973. p 596-606.
 69. de Jong RH, Freund FG. Relation between electromyogram and isometric twitch tension in human muscle. *Arch Phys Med Rehabil* 1967; 48:539-42.
 70. Bogardh E, Richards CL. Gait analysis and relearning of gait control in hemiplegic patients. *Physiotherapy Canada* 1981; 33:223-30.
 71. Peat M, Woodbury MG, Ferkul D. Electromyographic analysis of gait following total knee arthroplasty. *Physiotherapy Canada* 1984; 36:68-72.
 72. Richards CL, Wesse J, Malouin F. Muscle activation patterns in gait of rheumatoid arthritic patients. *Physiotherapy Canada* 1985; 37:220-28.
 73. Moore SP, Marteniuk, RG. Kinematic and electromyographic changes that occur as a function of learning a time-constrained aiming task. *J Mtr Beh* 1986; 18:397-426.
 74. Normand MC, Lagesse PP, Rouillard CA, Tremblay LE. Modifications occurring in motor programs during learning of a complex task in man. *Brain Res* 1982; 241:87-93.
 75. Young LR, Oman CM, Watt DGD, Money KE, Lichtenberg BK. Spatial orientation in weightlessness and readaptation to earth's gravity. *Science* 1984; 225: 205-8.
 76. Clément G, Gurfinkel VS, Lestienne F, Lipshits MI, Popov KE. Adaptation of posture control to weightlessness. *Exp Brain Res* 1984; 57:61-72.
 77. Watt DGD, Money KE, Bondar RL, Thirsk RB, Garneau M, Scully-Power P. Canadian medical experiments on Shuttle flight 41-G. *Canadian Aeronautics and Space Journal* 1985; 31(3):215-26.
 78. Parker DE, Reschke MF, Arrott AP, Homick JL, Lichtenberg BK. Otolith tilt-translation reinterpretation following prolonged weightlessness: implications for preflight training. *Aviat Space Environ Med* 1985; 56:601-6.
 79. Young L, Oman C, Watt D, Money K, Lichtenberg B, Kenyon R, Arrott A. M.I.T./Canadian vestibular experiments on the Spacelab-1 mission: 1. Sensory adaptation to weightlessness and readaptation to one-g: an overview. *Exp Brain Res* 1986; 64:291-98.
 80. Martin TP, Edgerton VR, Grindeland RE. Influence of spaceflight on rat skeletal muscle. *J Appl Physiol* 1988; 65:2318-25.
 81. Gurfinkel V. The mechanisms of postural regulation in man. *Soviet scientific reviews, section F: physiology and general biology reviews* 1994; 7(5):59-89.
 82. Layne CS, McDonald, PV, Pruett CJ, Jones G, Bloomberg JJ. Preparatory postural control after space flight. *Society of Neuroscience Abstracts* 1995; 21:138.
 83. Gurfinkel V. The mechanisms of postural regulation in man. *Soviet scientific reviews, section F: physiology and general biology reviews*; 7(5):59-89.
 84. Jeka JJ, Lackner JR. Fingertip contact influences human postural control. *Exp Brain Res* 1994; 100: 495-502.
 85. Holden M, Ventura J, Lackner JR. Stabilization of posture by precision contact of the index finger. *J Vestibular Res* 1994; 4:285-301.

86. Hurmuzlu Y, Basdogan C. On the measurement of dynamic stability of human locomotion. *Journal of Biomechanical Engineering, Transactions of the American Society of Mechanical Engineers* 1994; 116:30-36.
87. Hurmuzlu Y, Basdogan C, Carollo JJ. Presenting joint kinematics of human locomotion using phase plane portraits and Poincaré Maps. *J Biomech* 1994; 27:1495-99.
88. Parker TS, Chua LO. *Practical numerical algorithms for chaotic systems*. New York: Springer; 1989.
89. Guckenheimer J, Holmes P. *Nonlinear oscillations, dynamical systems, and bifurcations of vector fields*. New York: Springer-Verlag; 1983.
90. Kadaba MP, Wootten ME, Gainey J, Cochran GVB. Repeatability of phasic muscle activity: Performance of surface and intramuscular wire electrodes in gait analysis. *J Orthop Res* 1985; 3:350-59.
91. Yang JF, Winter DA. Electromyographic amplitude normalization methods: improving their sensitivity as diagnostic tools in gait analysis. *Arch Phys Med Rehabil* 1984; 65:517-21.
92. Yang JF, Winter DA. Surface EMG profiles during different walking cadences in humans. *Electroencephalogr Clin Neurophysiol* 1984; 60:485-91.
93. Bogey RA, Barnes LA, Perry J. Computer algorithms to characterize individual subject EMG profiles during gait. *Arch Phys Med Rehabil* 1992; 73:835-41.
94. Gabel RH, Brand RA. The effects of signal conditioning on the statistical analyses of gait EMG. *Electroencephalogr Clin Neurophysiol* 1994; 93:188-201.
95. Dietz V, Zijlstra W, Duysens J. Human neuronal interlimb coordination during split-belt locomotion. *Exp Brain Res* 1994; 101:513-20.
96. Tweed DW, Cadera, Vilis T. Computing three-dimensional eye position quaternions and eye velocity from search coil signals. *Vision Res* 1990; 30:97-110.
97. McConville J, Churchill T, Kaleps I, Clauser C, Cuzzi J. Anthropometric relationships of body and body segment moments of inertia. Anthropology Research Project, Inc., Aerospace Medical Division, AFSC Technical Report AFAMRL-TR-80-119. 1980.
98. Young J, Chandler R, Snow C. Anthropometric and mass distribution characteristics of the adult female. Civil Aeromedical Institute, Federal Aviation Administration, Report FAA-AM-83-16.
99. Wilkinson L. SYSTAT: the system for statistics. Evanston, IL: SYSTAT, Inc.; 1989.
100. Alexander R McN, Vernon A. Mechanics of hopping by kangaroos (Macropodidae). *J Zoology* 1975; 177:265-303.
101. McMahon TA, Cheng GC. The mechanics of running: how does stiffness couple with speed? *J Biomechanics* 1990; 23(Suppl. 1):65-78.
102. Ljung L. *System identification toolbox user's guide*. Natick, MA: The MathWorks, Inc.; 1993.
103. Kugler PN, Turvey MT. *Information, natural law, and the self assembly of rhythmical movement: theoretical and experimental investigations*. Hillsdale, NJ: Erlbaum; 1987.
104. Turvey MT, Schmidt RC, Rosenblum LD, Kugler PN. On the time allometry of co-ordinated rhythmic movements. *J Theor Biol* 1988; 130:285-325.
105. Nashner LM. Strategies for organization of human posture. In: Igarashi M, Black FO, editors. *Vestibular and visual control on posture and locomotor equilibrium*. Houston, TX: Karger & Basel; 1985. p 1-8.
106. Keshner EA. Postural abnormalities in vestibular disorders. In: Herdman SJ, editor. *Vestibular rehabilitation*. Philadelphia: FA Davis; 1994. p 47-67.
107. Zangemeister WH, Bulgheroni MV, Pedotti A. Normal gait is differentially influenced by the otoliths. *J Biomed Eng* 1991; 13:451-58.
108. Kozlovskaya IB. Personal communication. 1996.
109. Dijkstra TMH, Schöner G, Gielen CCAM. Temporal stability of the action-perception cycle for postural control in a moving visual environment. *Exp Brain Res* 1994; 97:477-86.
110. Bernstein N. *The coordination and regulation of movements*. New York: Pergamon Press; 1967.
111. Vereijken B, Van Emmerik REA, Whiting HTA, Newell KM. Free(z)ing degrees of freedom in skill acquisition. *J of Mot Behav* 1992; 24:133-42.
112. Paloski WH, Harm DL, Reschke MF, Doxey DD, Skinner NC, Michaud LJ, Parker DE. Postural changes following sensory reinterpretation as an analog to spaceflight. Fourth European Symposium on Life Sciences Research in Space; Trieste Italy, May 28-June 1, 1990.
113. Paloski WH, Black FO, Reschke MF. Vestibular ataxia following shuttle flights: effects of transient microgravity on otolith-mediated sensorimotor control of posture. *Am J Otolaryngology* 1993; 1:9-17.
114. Paloski WH, Bloomberg JJ, Reschke MF, Harm DL. Spaceflight-induced changes in posture and locomotion. *Proc Biomech XIVth I.S.B. Congress; Paris France, 1993*. p 40-41.
115. Kennedy RS, Berbaum KS, Williams MC, Brannen J. Transfer of perceptual-motor training and space adaptation syndrome. *Aviat Space and Environ Med* 1987; 58:A29-33.

116. Welch RB, Bridgeman B, Sulekha A, Browman KE. Alternating prism exposure causes dual adaptation and generalization to a novel displacement. *Perception and Psychophysics* 1993; 54:195-204.
117. Nelson RC, Dillman CJ, Lagasse P, Bickett P. Biomechanics of overground versus treadmill running. *Med Sci Sports Exerc* 1972; 4:233-40.
118. Woolley SN, Winter DA. Mechanical energies in overground and treadmill walking. 3rd Annual Conference of the American Society of Biomechanics; University Park PA, 1979.
119. Arsenault AB, Winter DA, Marteniuk RG. Treadmill versus walkway locomotion in humans: an EMG study. *Ergonomics* 1986; 29(5):665-76.
120. Hayes JL, McBrine JJ, Roper ML, Stricklin MD, Siconolfi SF, Greenisen MC. Effects of space shuttle flights on skeletal muscle performance. *FASEB J* 1992; 6(5):A1770.
121. Thomson JA. How do we use visual information to control locomotion? *Trends Neurosci* 1980; 3:247-50.
122. Loomis JM, Da Silva JA, Fujita N, Fukushima SS. Visual space perception and visually directed action. *J Exp Psychol: Human Perception and Performance* 1992; 18:906-21.
123. Worchel P. Space perception and orientation in the blind. *Psychological monographs: general and applied*. 1951. 65L1-27 (Whole No. 332).
124. Loomis JM, Klatzky RL, Golledge RG, Cicinelli JG, Pellegrino JW, Fry PA. *Journal of Experimental Psychology: General* 1993; 122(1):73-91.
125. Fujita N, Klatzky RL, Loomis JM, Golledge RG. The encoding-error model of pathway completion without vision. *Geographical Analysis* 1993; 25(4): 295-314.
126. Mittelstaedt ML, Glasauer S. Idiopathic navigation in gerbils and humans. *Zool Jb Physiol* 1991; 95:427-35.
127. Glasauer S, Reschke M, Berthoz A, Michaud L, Huebner W. The effect of space flight on gaze control strategy. *Proc 5th Eur Symp on Life Science Research in Space* 1984; Arcachon France. ESA SP-366 1994; p 339-44.
128. Watt DGD, Money KE, Tomi LM. M.I.T./Canadian vestibular experiments on the Spacelab-1 mission: 3. Effects of prolonged weightlessness on a human otolith-spinal reflex. *Exp Brain Res* 1986; 64:308-15.
129. Melvill Jones G, Watt DGD. Muscular control of landing from unexpected falls in man. *J Physiol* 1971; 219:729-37.
130. Allum JHJ, Pfaltz CR. Visual and vestibular contributions to pitch sway stabilization in the ankle muscles of normals and patients with bilateral peripheral vestibular deficits. *Exp Brain Res* 1985; 58:82-94.
131. Greenwood R, Hopkins A. Muscle responses during sudden falls in man. *J Physiol* 1976; 354:507-18.
132. Nashner LM, Berthoz A. Visual contributions to rapid motor responses during postural control. *Brain Res* 1978; 150:403-07.
133. McKinley P, Smith J. Visual and vestibular contributions to replacing EMG during jump-downs in cats. *Exp Brain Res* 1991; 52:439-48.
134. McKinley P, Pedotti A. Motor strategies in landing from a jump: The role of skill in task execution. *Exp Brain Res* 1992; 90:427-40.
135. Dyhre-Poulsen P, Laursen AM. Programmed electromyographic activity and negative incremental muscle stiffness in monkeys jumping down. *J Physiol* 1984; 350:121-36.
136. Thompson HW, McKinley PA. Effect of visual perturbations in programming landing from a jump in humans. *Society for Neuroscience Abstracts* 1988; 14:66.
137. Melvill Jones G, Watt DGD. Observations on the control of stepping and hopping movements in man. *J Physiol* 1971; 219:709-27.
138. Reschke MF, Anderson DJ, Homick JL. Vestibulo-spinal response modification as determined with the H-reflex during the Spacelab-1 flight. *Exp Brain Res* 1986; 64:367-79.
139. Molina-Negro P, Bertrand RA, Martin E, Gioani Y. The role of the vestibular system in relation to muscle tone and postural reflexes in man. *Acta Otolaryngol* 1980; 89:524-33.

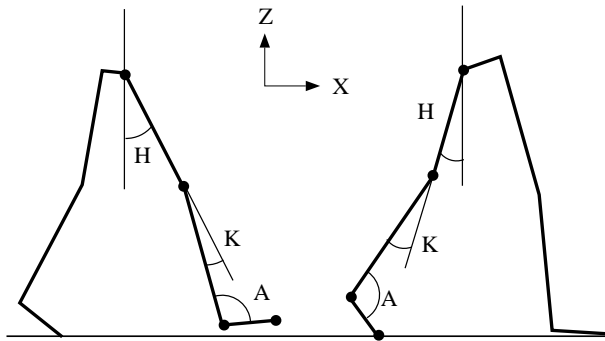


Figure 5.5-1. The convention for joint angle measurements (H = hip angle K = knee angle; A = ankle angle).

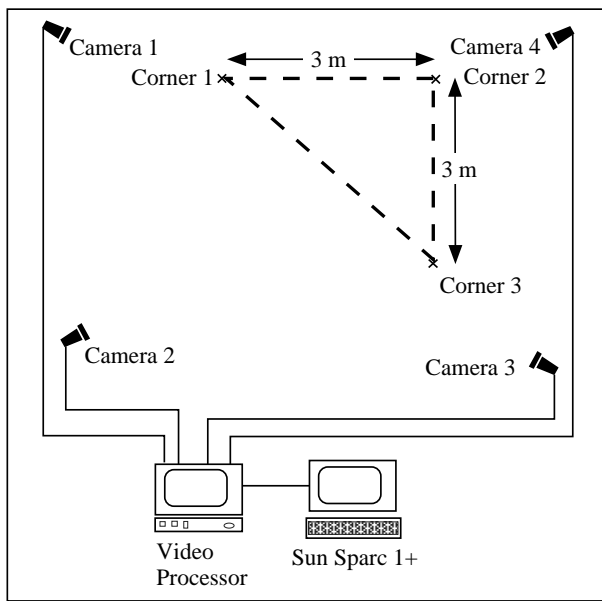


Figure 5.5-2. Map view of the experiment set up. Four cameras connected to a video processor recorded subject path. Three corners of the triangular path (dashed lines) were marked on the floor by white crosses.

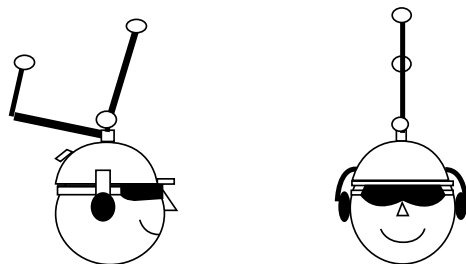


Figure 5.5-3. Subject head sets were used in the locomotor spatial orientation study. Three reflective markers were fixed to the helmet. Head phones and blackened goggles were used to mask auditory cues and occlude vision.

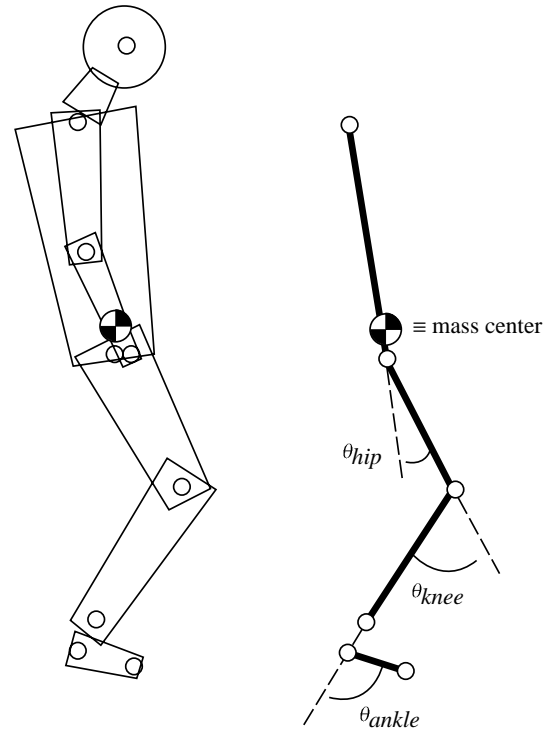


Figure 5.5-4. Sagittal plane body model. The joint angle convention is shown at right. The eight segments used for COM calculation (feet, shanks, thighs, trunk, forearms, upper arms, neck and head) are shown schematically on the left. Reflective marker positions are denoted by "O".

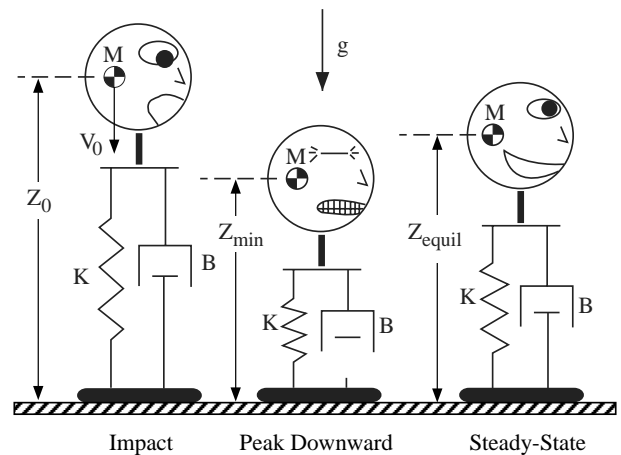
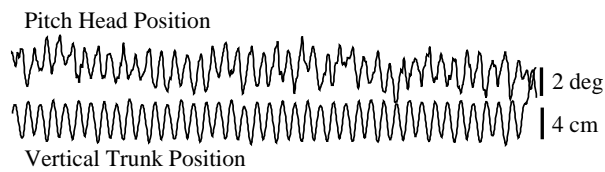
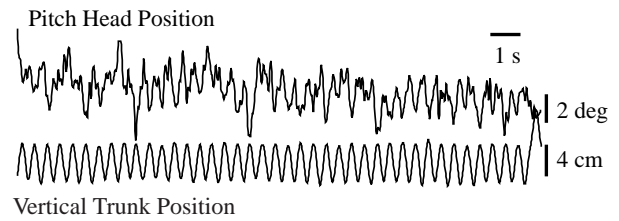


Figure 5.5-5. One degree of freedom, second order model of vertical (Z) COM motion following impact. Body mass (M), located at the COM, is supported by linear spring (K) and dashpot (B). The unloaded length of the spring is Z_0 (nominally the height of the COM at impact), minimum spring length is Z_{min} , and the spring length at the final equilibrium is Z_{equil} .



a. Preflight



b. Postflight

Figure 5.5-6. Waveforms from one subject showing the relationship between vertical translation of the trunk and corresponding pitch angular head movement for the NEAR target condition during pre- (a) and postflight (b) locomotion.

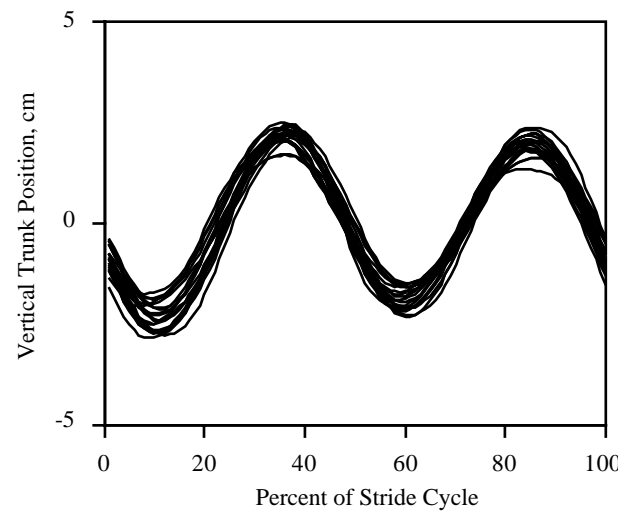
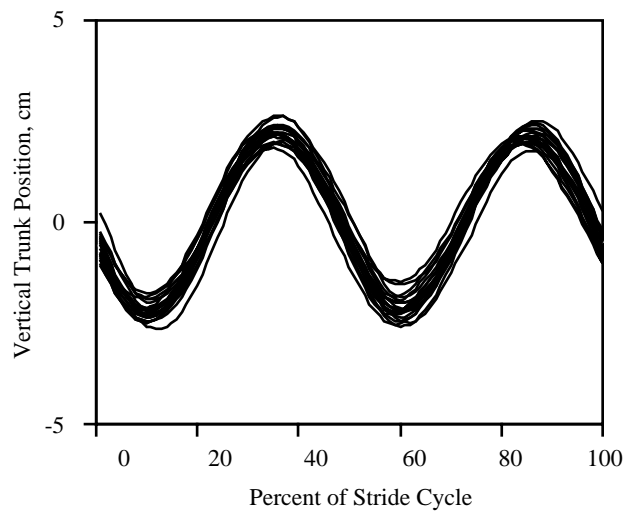
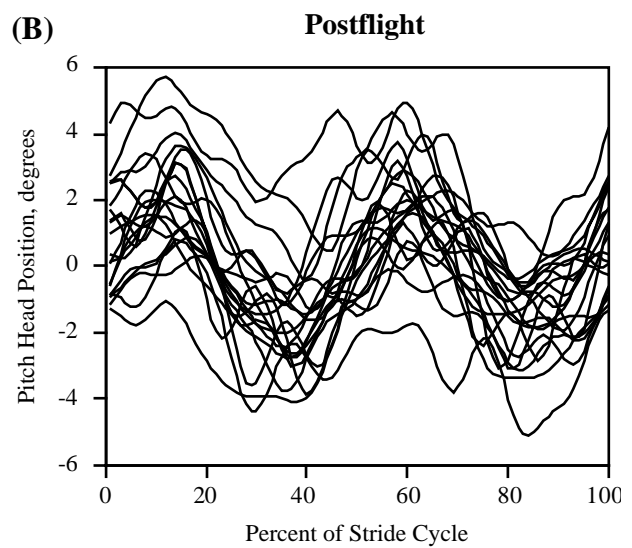
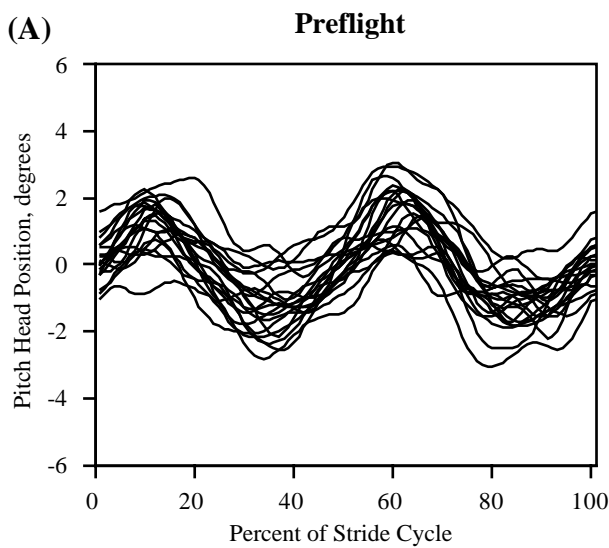


Figure 5.5-7. To show the step-to-step variability, each cycle in the waveforms depicting vertical trunk translation and compensatory pitch head movements were aligned at the point of heel strike in one subject. (a) Preflight and (b) Postflight pitch head movements and corresponding vertical trunk translations during locomotion. Note the increased variability in postflight pitch head movements despite little change in vertical trunk translation.

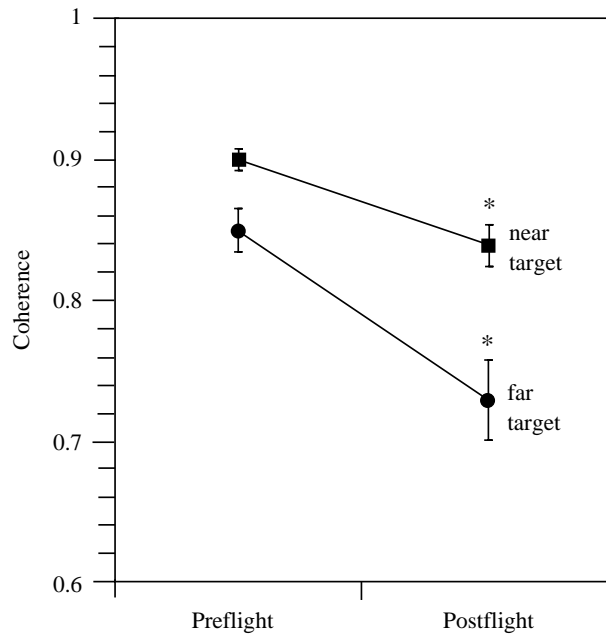


Figure 5.5-8. Mean (± 1 S.E.) pre- and postflight coherence values relating vertical trunk translation and corresponding pitch head movement for all subjects combined, for both FAR and NEAR target conditions. * denotes a significant difference ($p < 0.05$) between pre- and postflight mean coherence values.

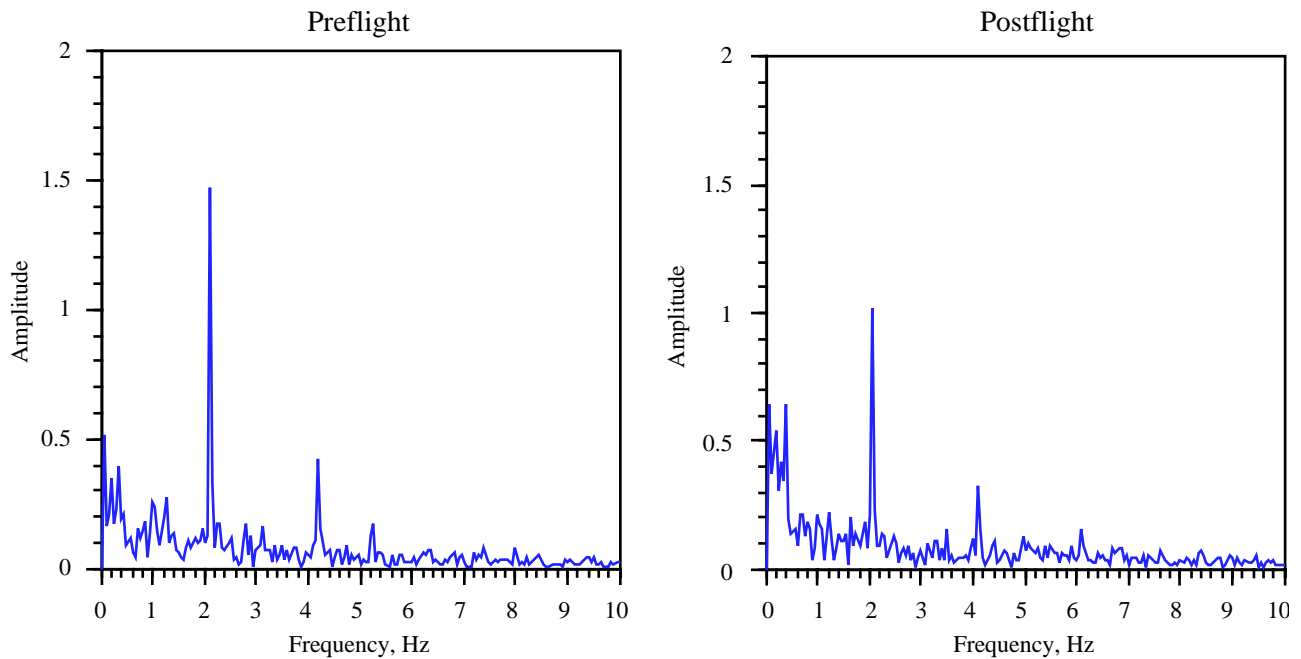


Figure 5.5-9. One pre- and postflight example of Fourier amplitude spectra of pitch head angular displacement for the NEAR target condition for one subject during locomotion. Note the decrease in the amplitude of the predominant frequency component at 2 Hz.

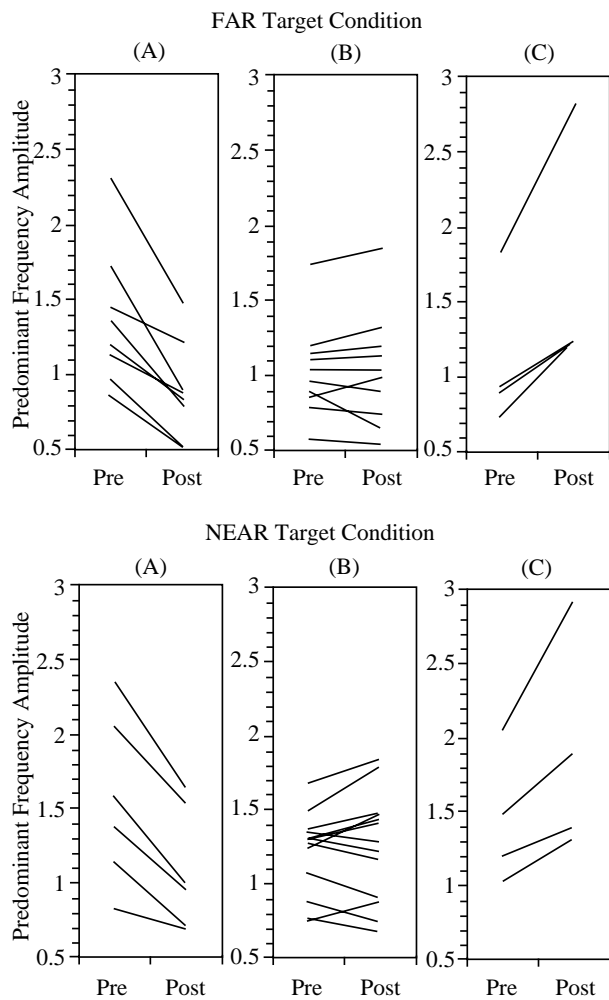


Figure 5.5-10. Individual mean pre- and postflight changes in the magnitude of the predominant peak of pitch head movements for the FAR (top) and NEAR (bottom) target conditions. Individually, subjects show significant ($p < 0.05$) reduction (a), no significant change (b), and augmentation (c) and in predominant peak of pitch head movements during locomotion.

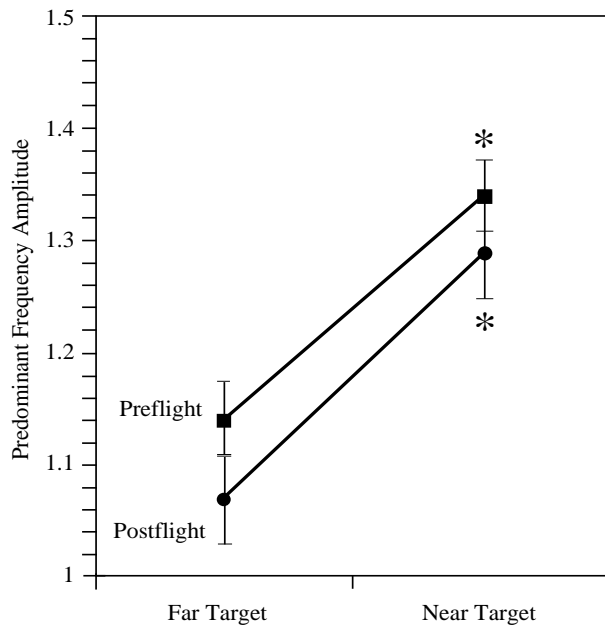


Figure 5.5-11. Mean (± 1 S.E.) magnitude of the predominant peak of pitch head movements for all subjects for the FAR and NEAR target conditions during both pre- and postflight testing. Note the increase in magnitude of predominant peak during visual fixation of the NEAR target. * denotes a significant difference between FAR and NEAR target conditions during both pre- and postflight testing.

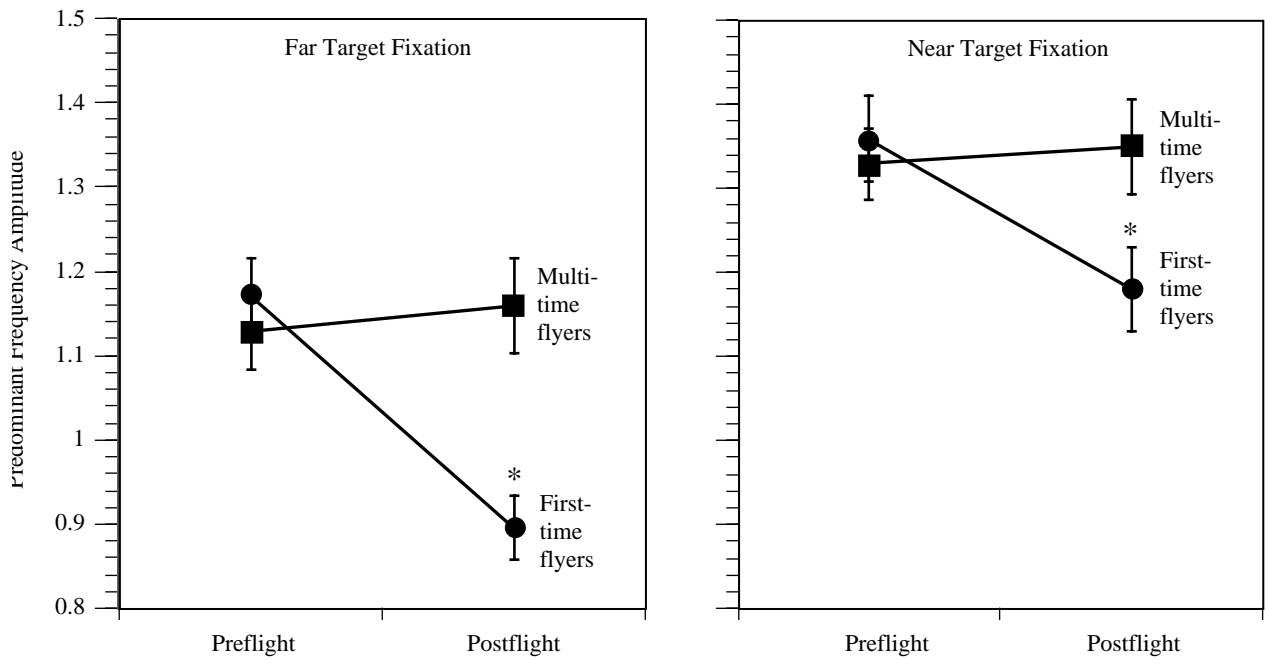


Figure 5.5-12. Comparison between first- and multi-time fliers of the mean (± 1 S.E.) magnitude of the predominant peak of pitch head movements during the FAR and NEAR target conditions. *Note that in both target conditions, first-time fliers display significant ($p < 0.05$) reduction in the predominant peak of pitch head movements while multi-time fliers show no significant changes in pitch head response following space flight.

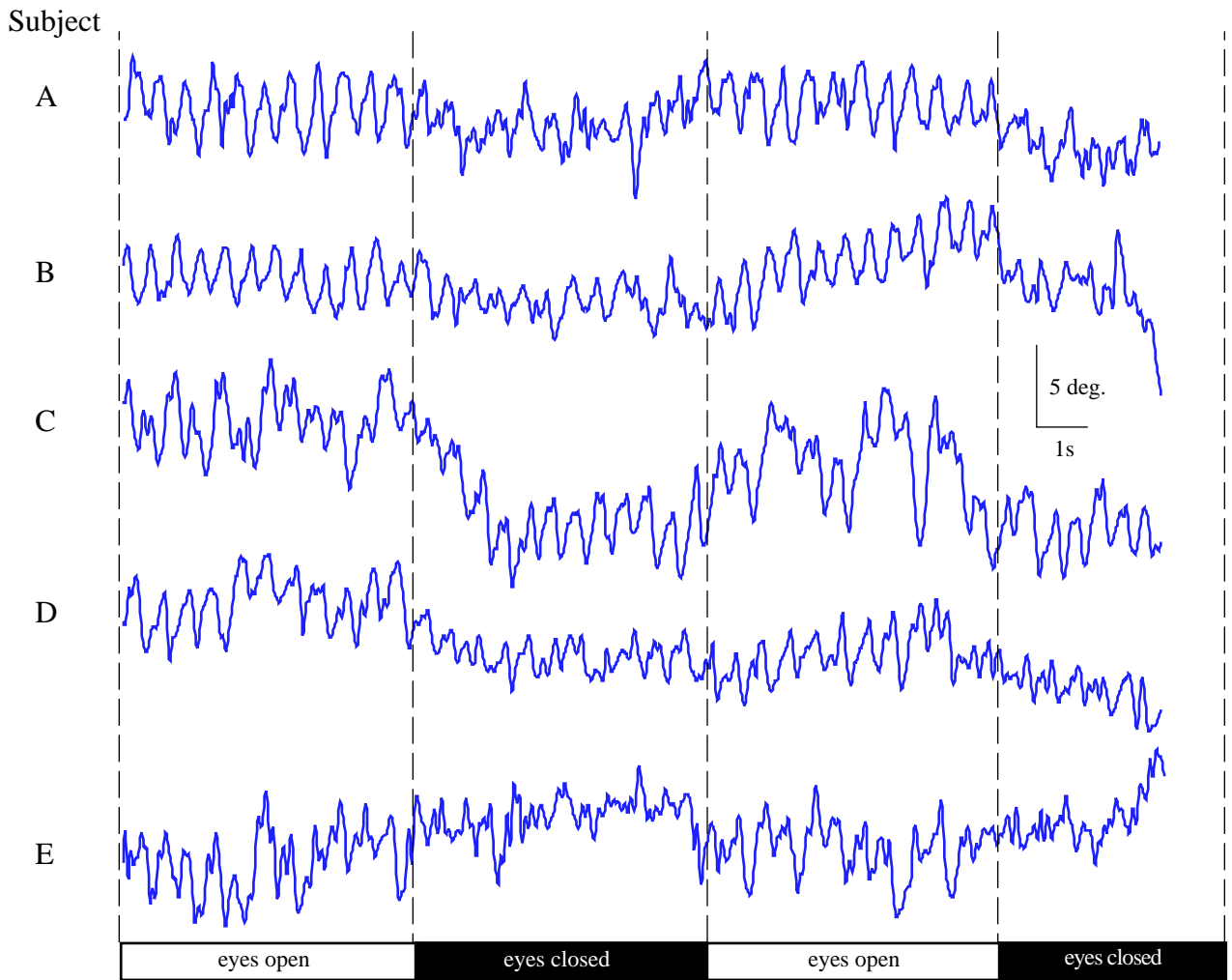


Figure 5.5-13. Waveforms showing pitch angular head displacement for 5 individual subjects (A-E) during the eyes open and eyes closed epochs of the IV condition obtained during one preflight trial. Note the reduction in amplitude and breakdown in waveform regularity during the Eyes Closed epochs.

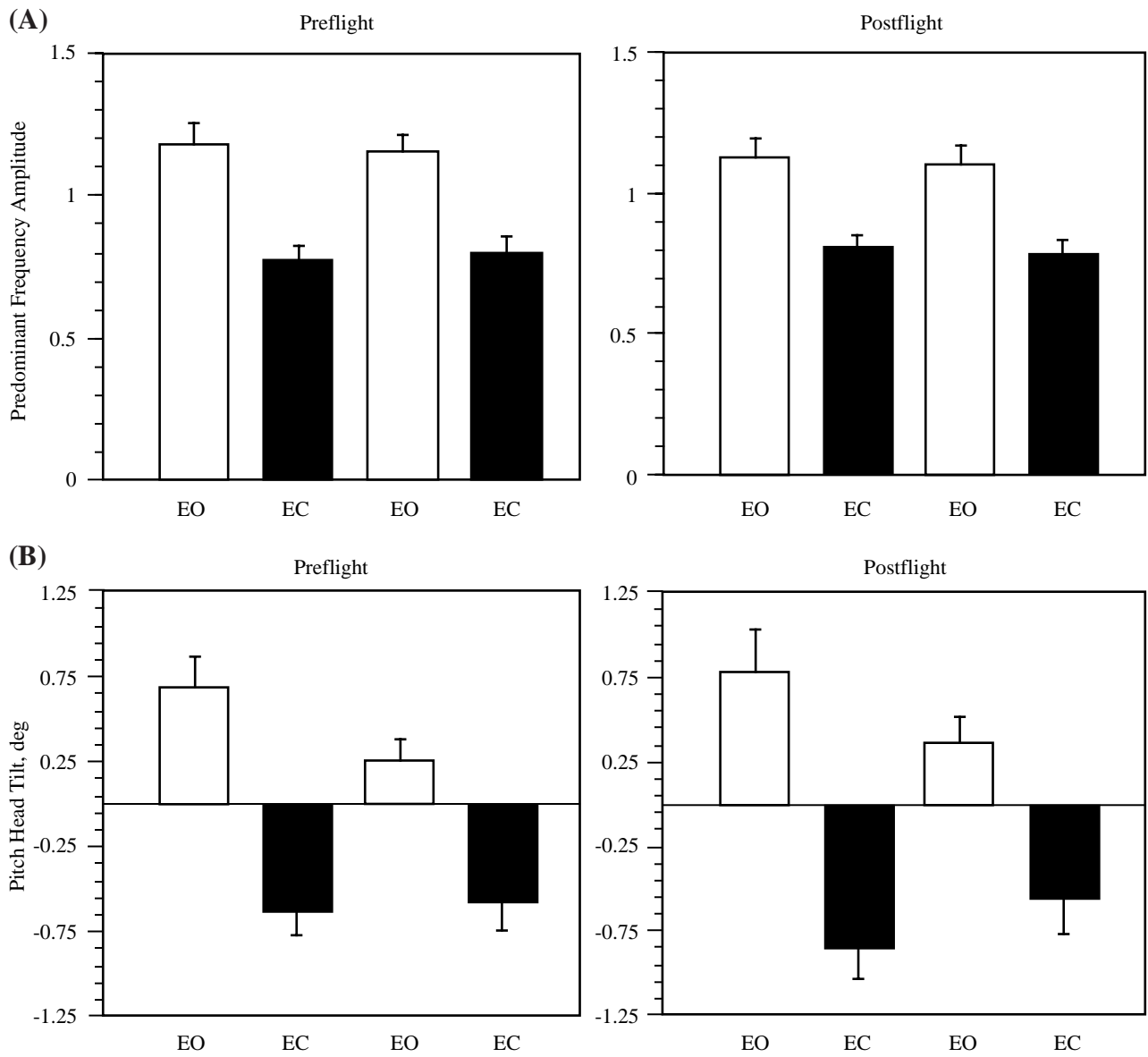


Figure 5.5-14. (a) Pre- and postflight mean (± 1 S.E.) predominant frequency amplitude for all subjects during the alternating 5 second eyes open/closed epochs of the IV condition. (b) Pre- and postflight mean (± 1 S.E.) head tilt relative to vertical in the sagittal plane for all subjects during the alternating 5 second eyes open/closed epochs. EO (eyes open); EC (eyes closed). During eye closure periods, both during pre- and postflight testing, pitch head movements were reduced and the head tilted forward.

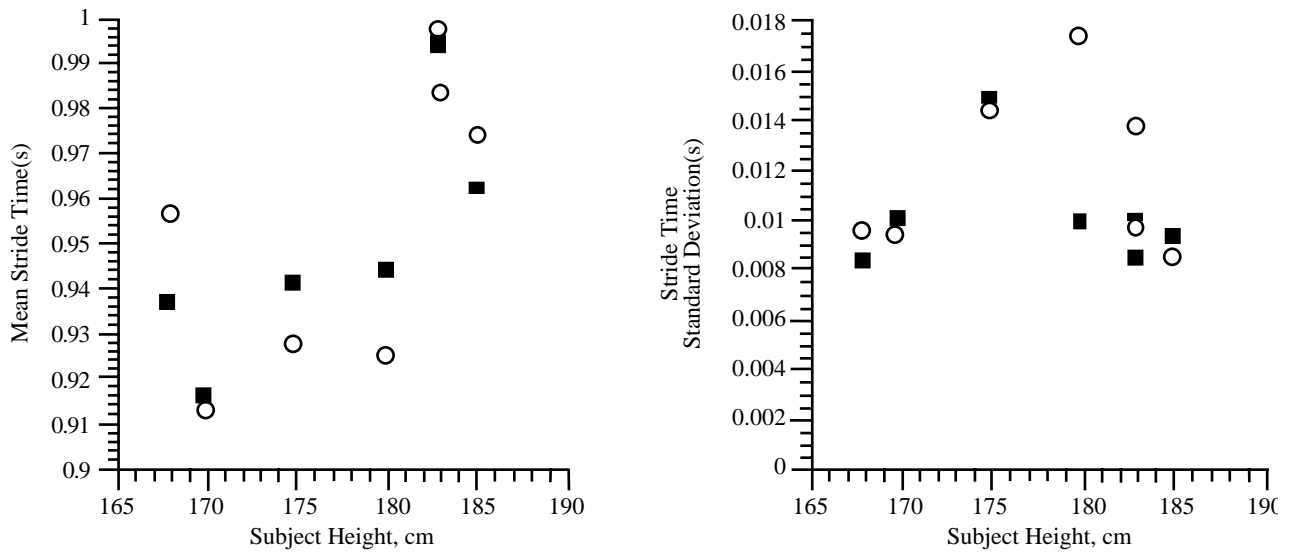


Figure 5.5-15. Mean and standard deviation of the preflight (filled square) and postflight (circle) trial stride time for each of the seven subjects plotted as a function of subject height.

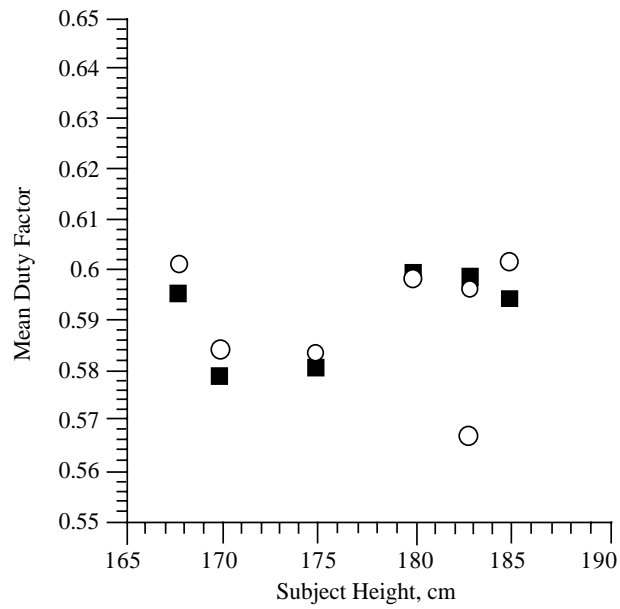


Figure 5.5-16. Preflight (filled square) and postflight (circle) mean duty factor presented for each subject as a function of subject height.

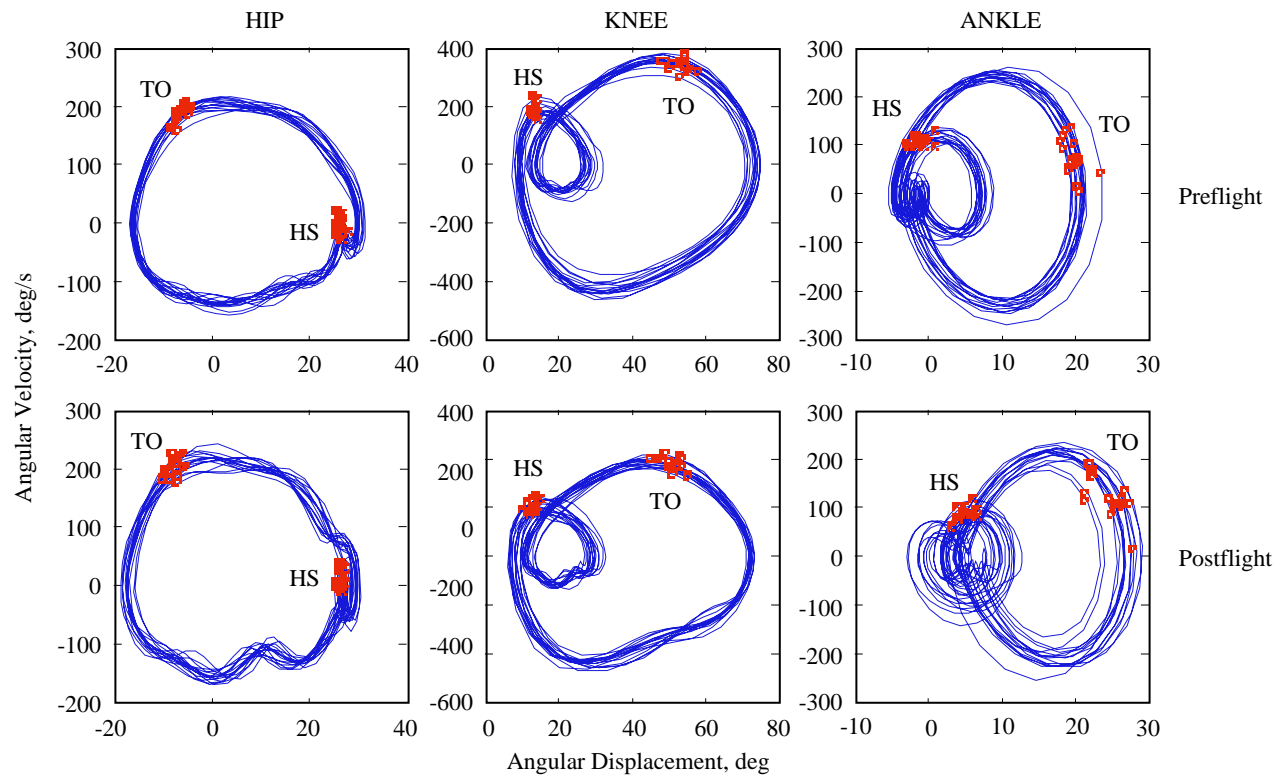


Figure 5.5-17. Exemplar phase portraits of three lower limb joints. These data are from one subject and illustrate 15 consecutive cycles from one preflight and one postflight trial. The location of heel strike (HS) and toe off (TO) for each cycle is indicated.

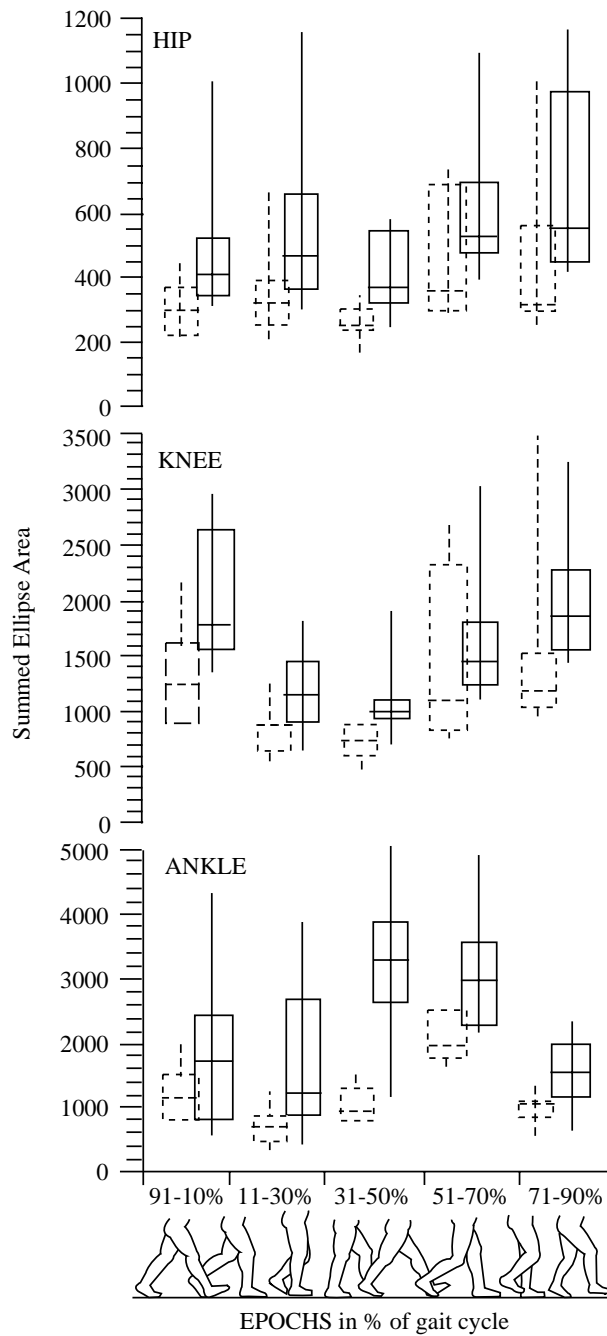


Figure 5.5-18. Box plots of phase plane variability as a function of stride epoch, from right heel strike to right heel strike. Epochs represent 91%-10%, 11%-30%, 31%-50%, 51%-70%, and 71%-90% of gait cycle. Dashed lines indicate preflight, solid lines indicate postflight. Boxes represent the 25th, 50th, and 75th percentile. Whiskers represent the 10th and 90th percentile.

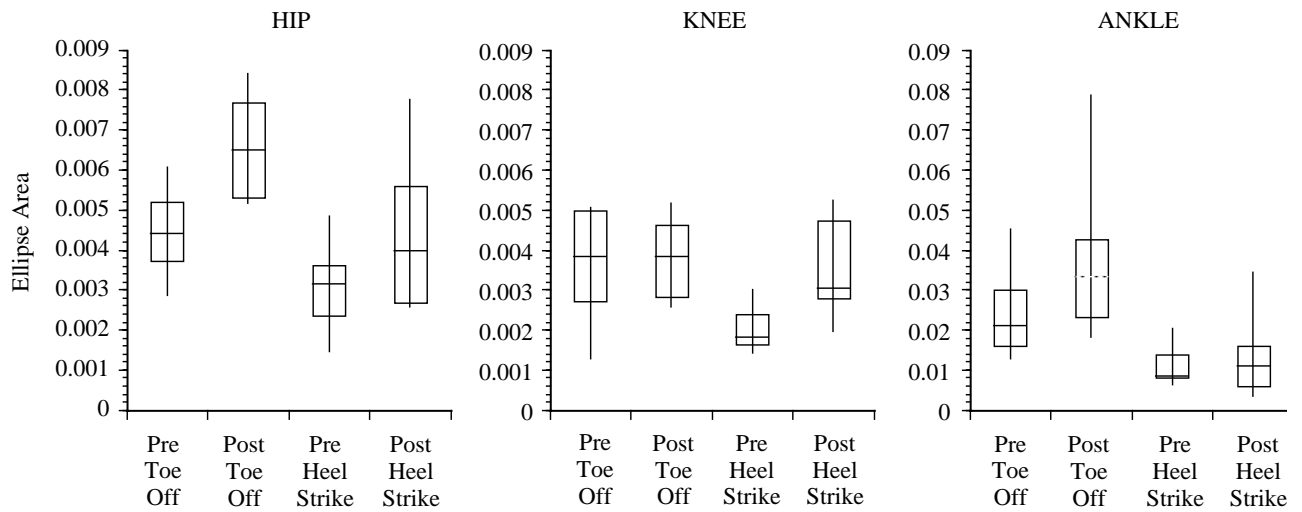


Figure 5.5-19. Box plots of phase plane variability of the preflight and postflight toe off and heel strike events for the hip, knee, and ankle angles.

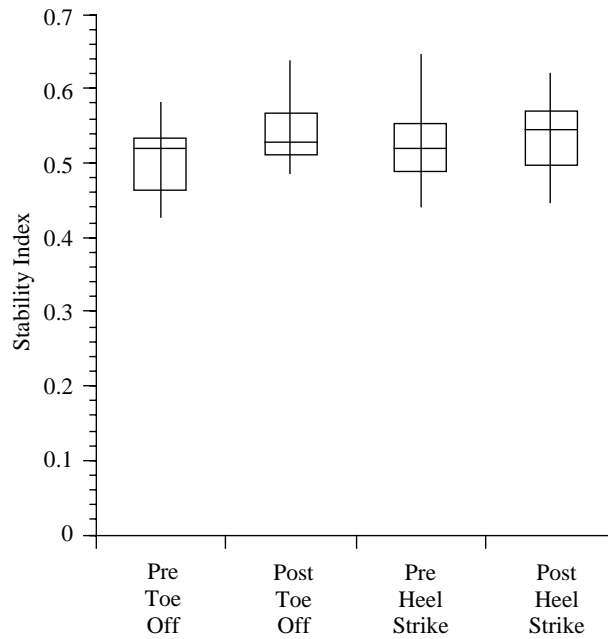
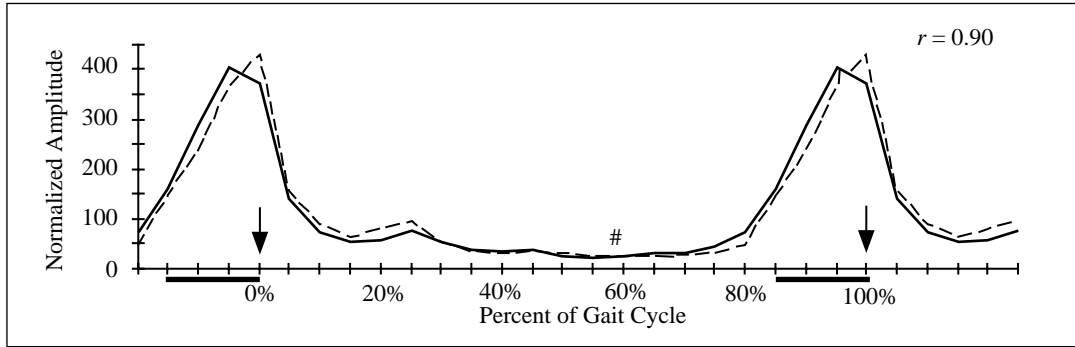
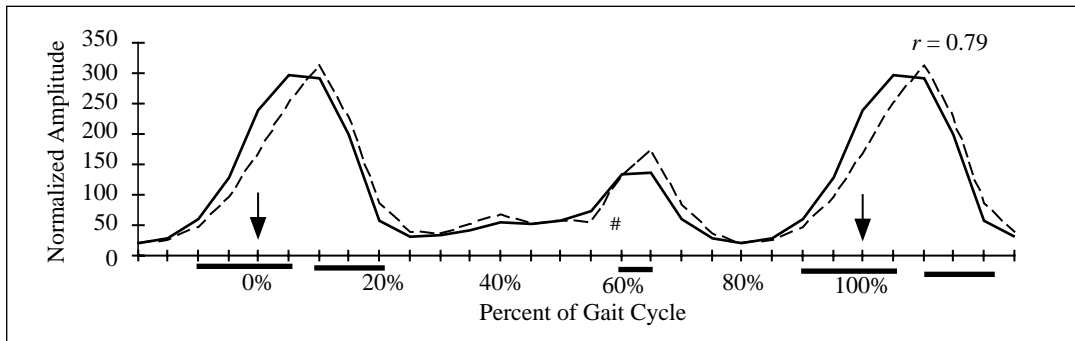


Figure 5.5-20. Box plots of the system stability index for the preflight and postflight toe off and heel strike events.

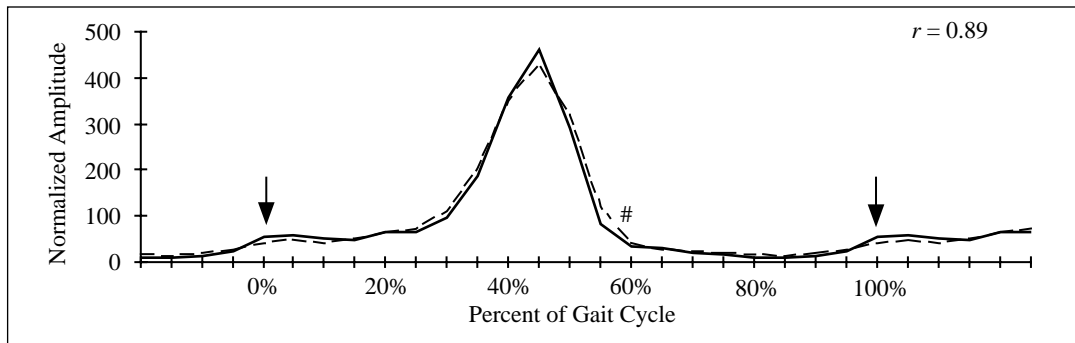
A. *Biceps Femoris*



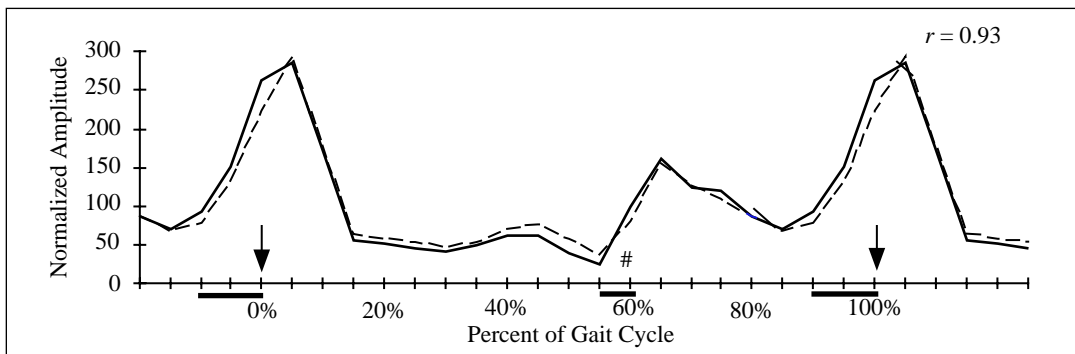
B. *Rectus Femoris*



C. *Gastrocnemius*



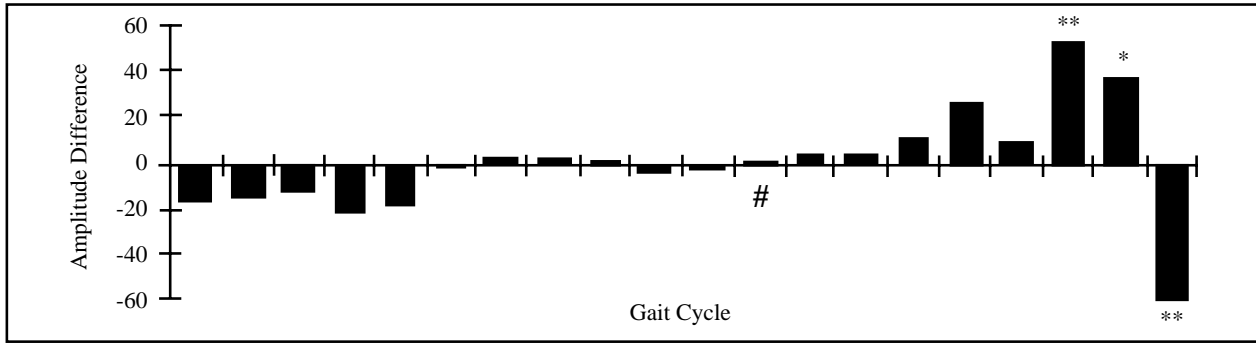
D. *Tibialis Anterior*



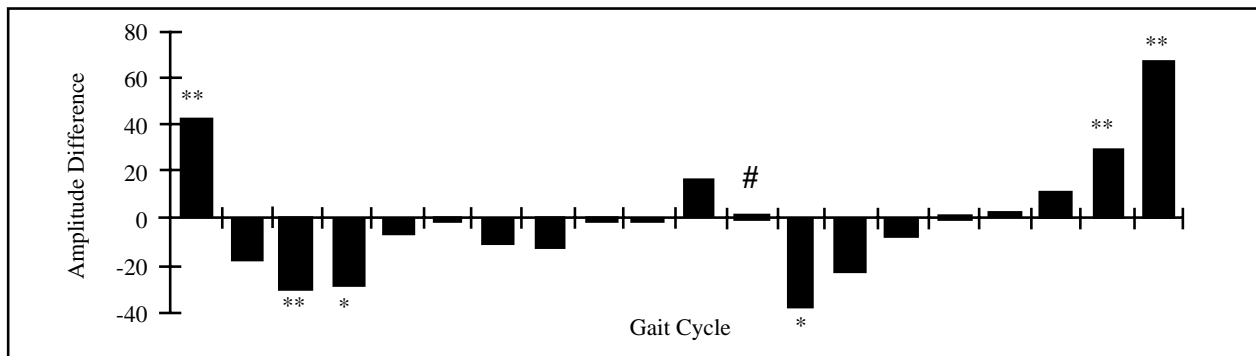
Indicating significant differences in normalized amplitude ——— Mean Waveform Preflight
 Indicating heel stroke - - - Mean Waveform Postflight
 # Indicating toe off

Figure 5.5-21. Grand ensemble average preflight and postflight waveforms for biceps femoris (A), rectus femoris (B), gastrocnemius (C) and tibialis anterior (D).

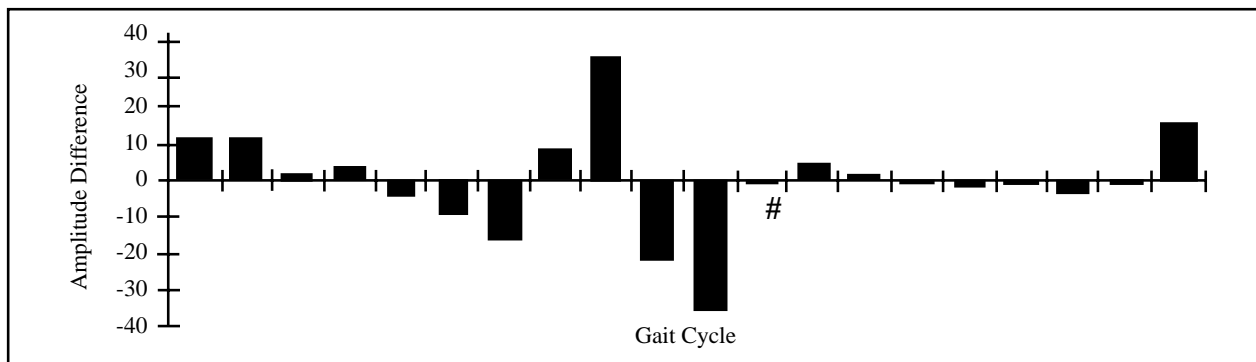
A. *Biceps Femoris*



B. *Rectus Femoris*



C. *Gastrocnemius*



D. *Tibialis Anterior*

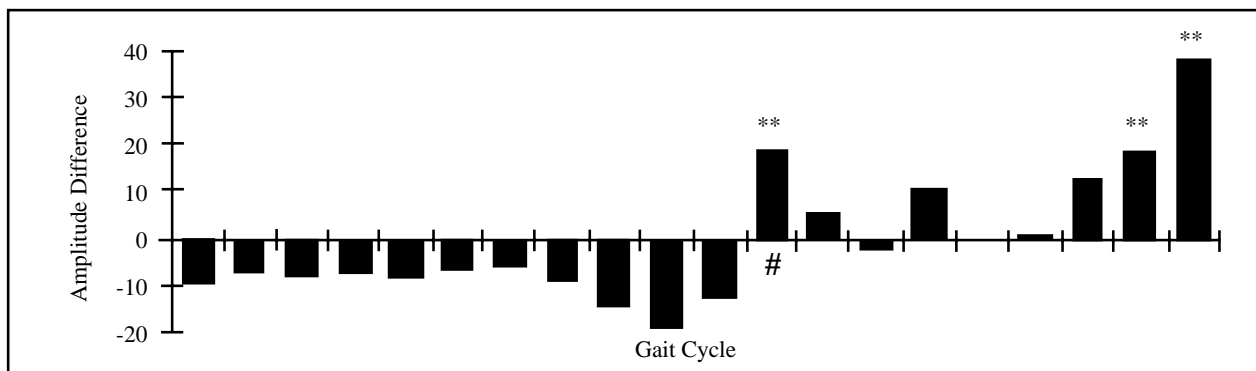


Figure 5.5-22. Differences in relative amplitude between preflight and postflight grand ensemble reduced wave forms at each 5% gait cycle epoch for: *biceps femoris* (A), *rectus femoris* (B), *gastrocnemius* (C) and *tibialis anterior* (D). Analysis epochs began at heel strike. # = Toe off. * = a significant statistical difference. ** = a significant functional difference.

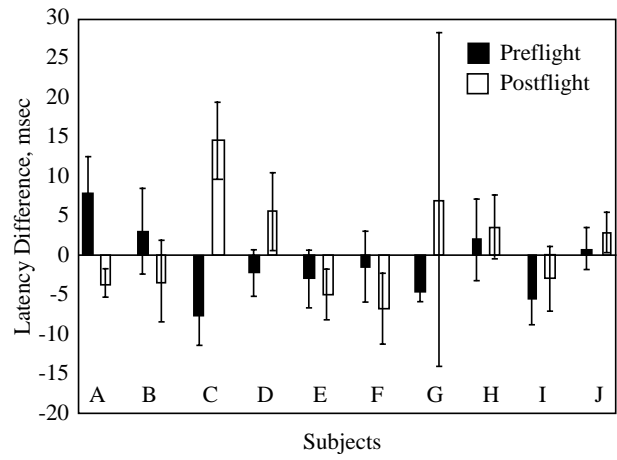
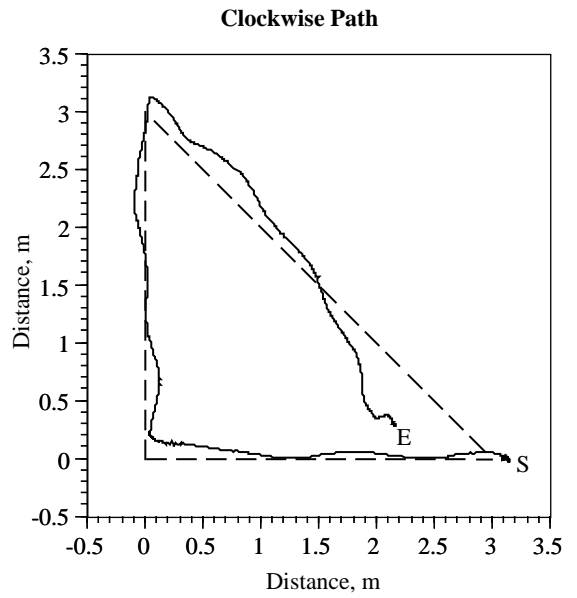
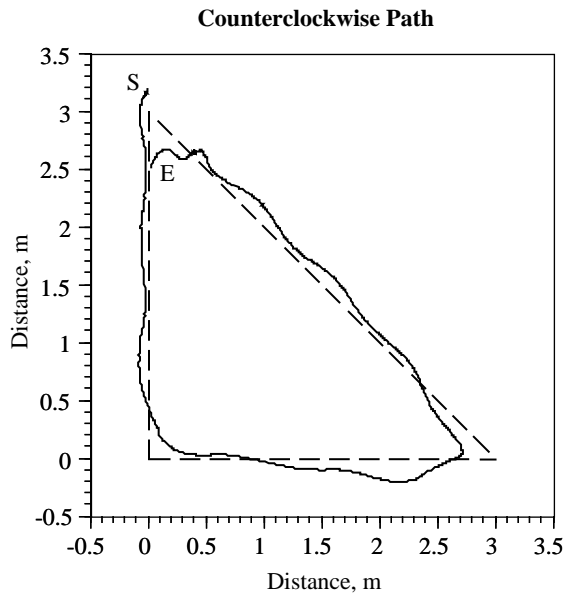
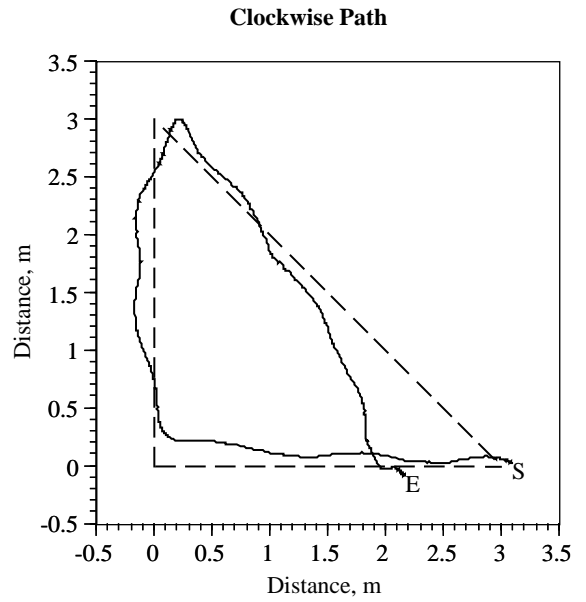
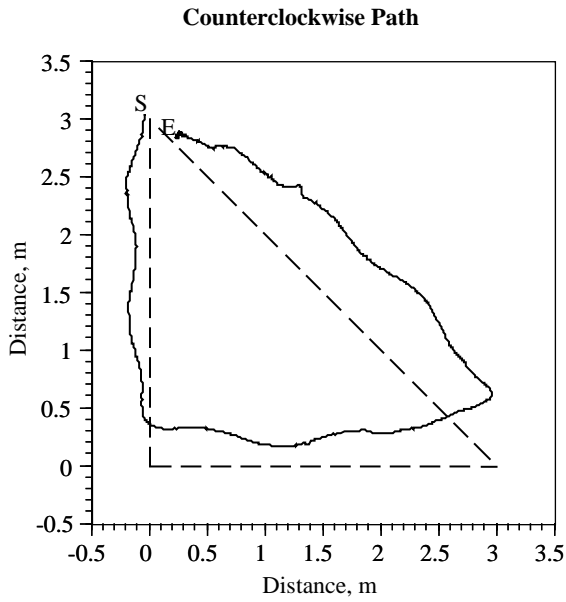


Figure 5.5-23. Preflight versus postflight latency average (± 1 S.D.) difference for each subject between GA offset and TA onset. Negative values indicate that the offset of the GA preceded the onset of the TA. GA = gastrocnemius. TA = tibialis anterior.

Preflight Locomotor Path Integration (without vision)



Postflight (R+0) Locomotor Path Integration (without vision)



— — Designated Path
 ——— Subjects Path

S Starting Point
 E Ending Point

Figure 5.5-24. Example of preflight and postflight walking trajectories (eyes closed condition). Dashed line = Map view of the path. Solid line = Trajectory performed by the subject.

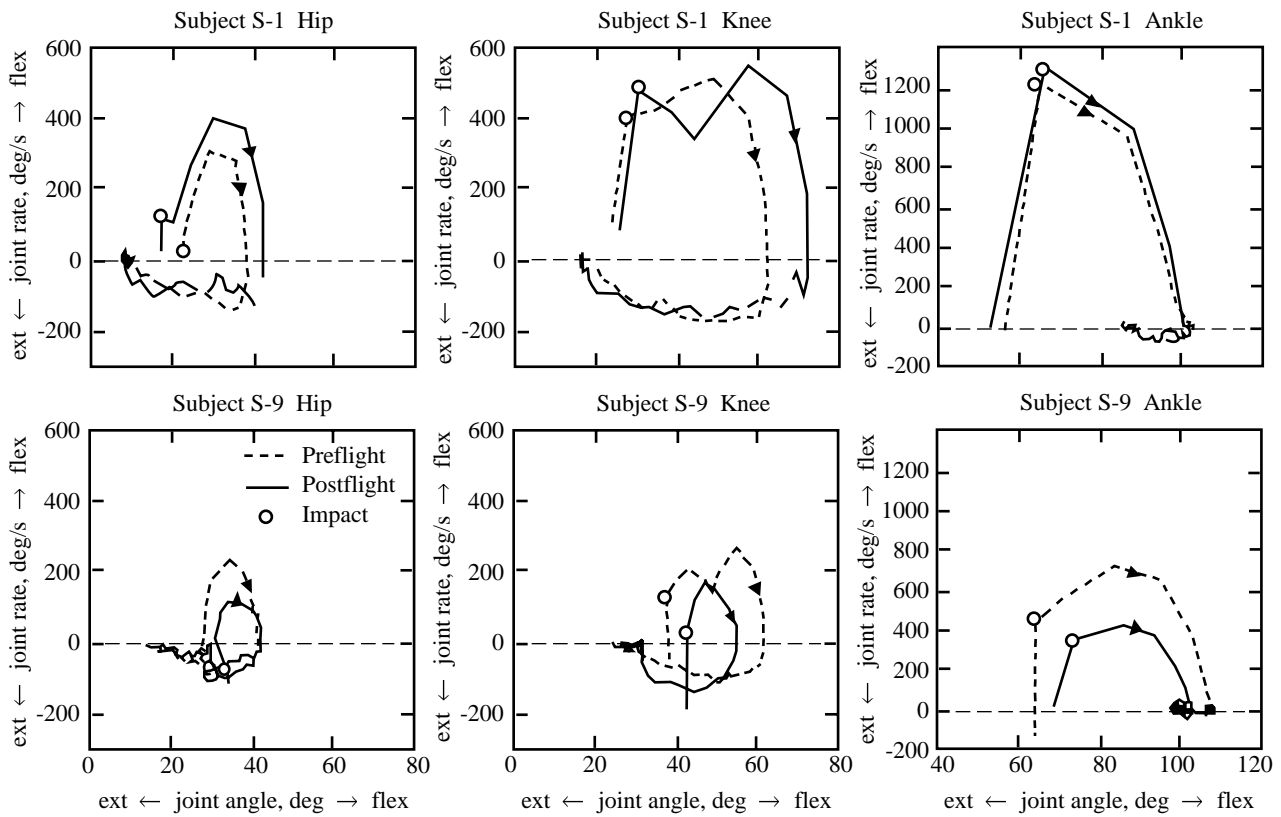


Figure 5.5-25. Comparison of preflight (dashed) and postflight (solid) joint angle phase-plane portraits for hip, knee and ankle. (Top) For subject S-1, the postflight phase is expanded with respect to the preflight diagram. (Bottom) In contrast, subject S-9 demonstrates postflight contraction of the phase portrait in comparison to preflight results.

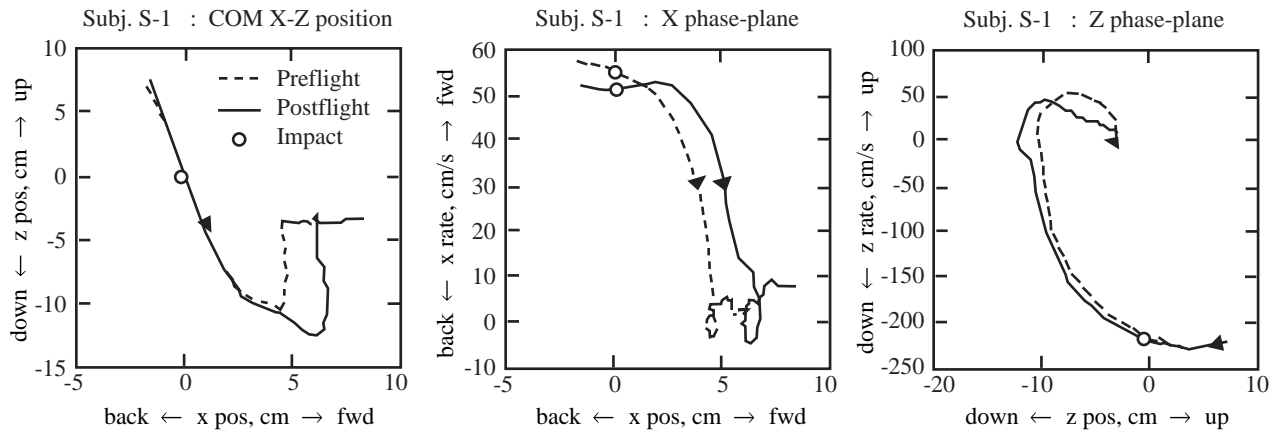
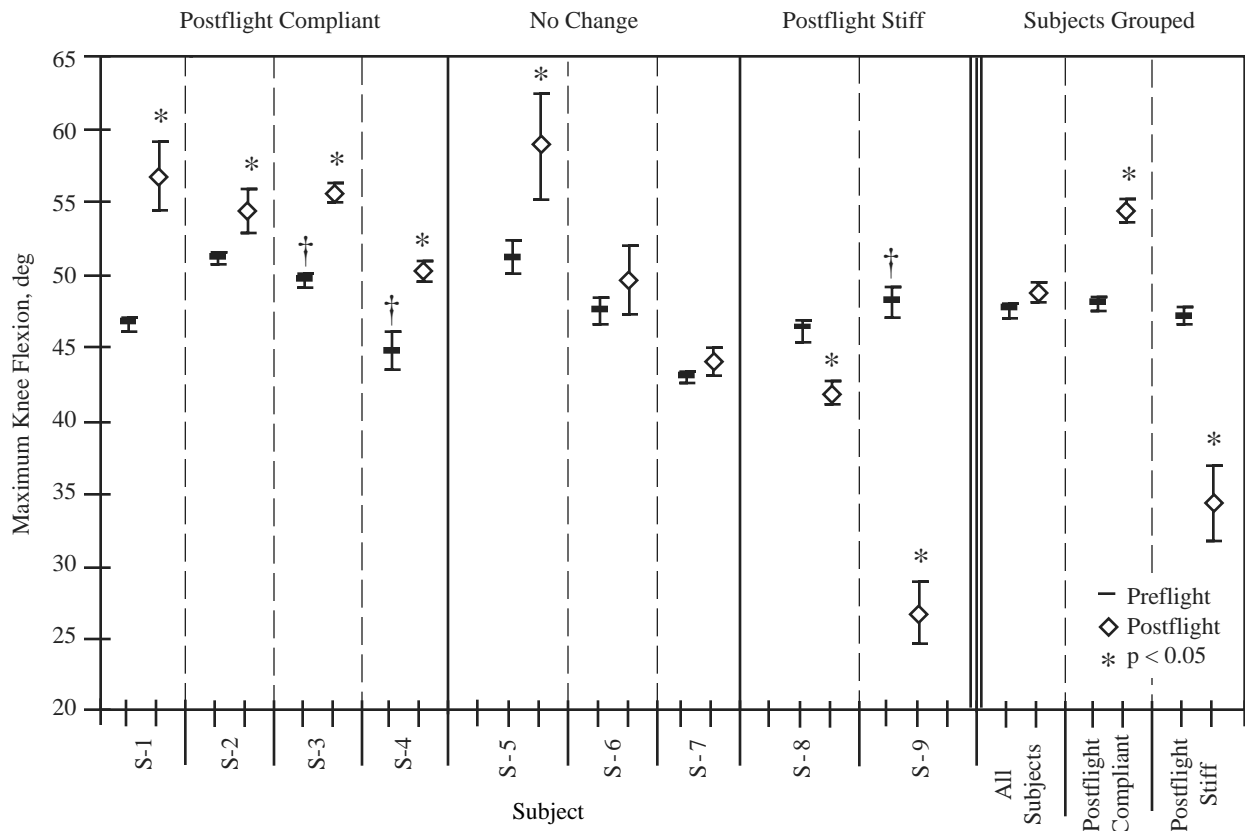
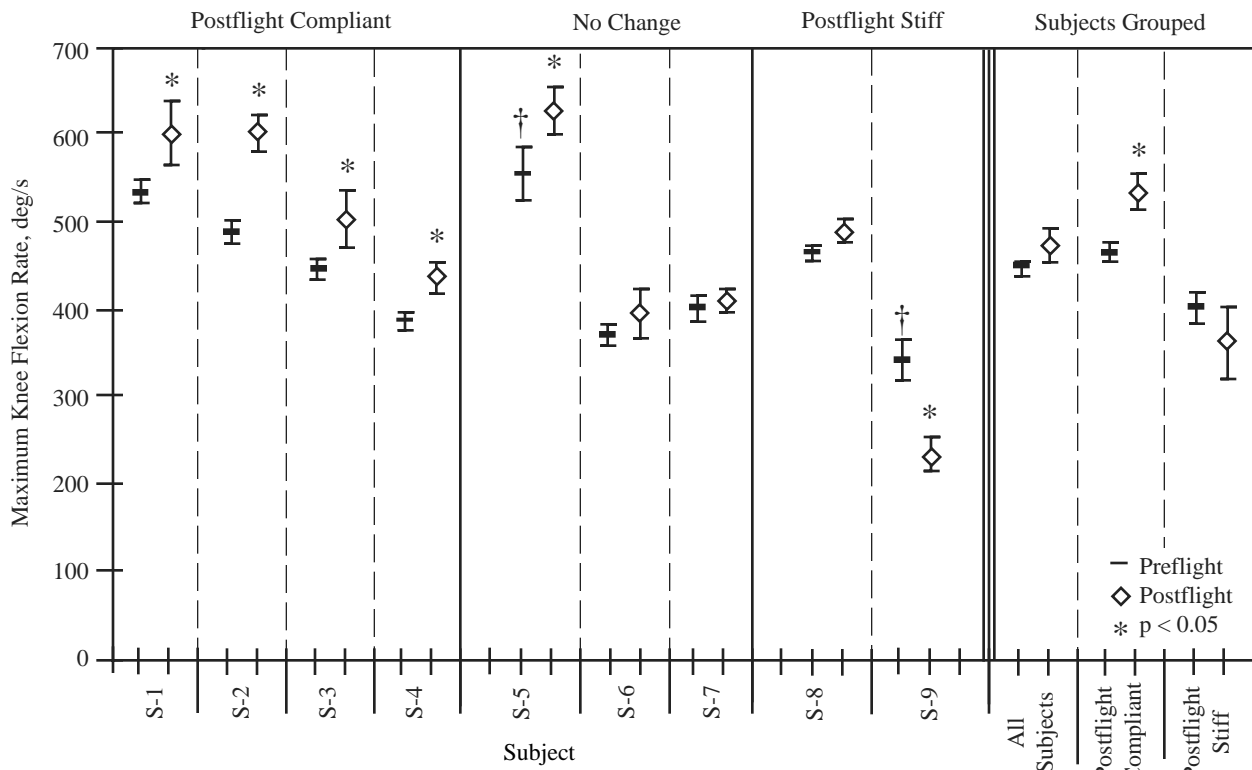


Figure 5.5-26. Comparison of preflight (dashed) and postflight (solid) COM motion for postflight-compliant subject S-1. (Left) The trajectory of the COM in the sagittal (X-Z) plane; peak deflection of the COM is greater postflight. (Middle) Phase-plane motion of the COM in the X (horizontal) direction is shown. (Right) Z (vertical) motion is shown in the phase-plane diagram, indicating greater downward deflection and slower upward recovery postflight.

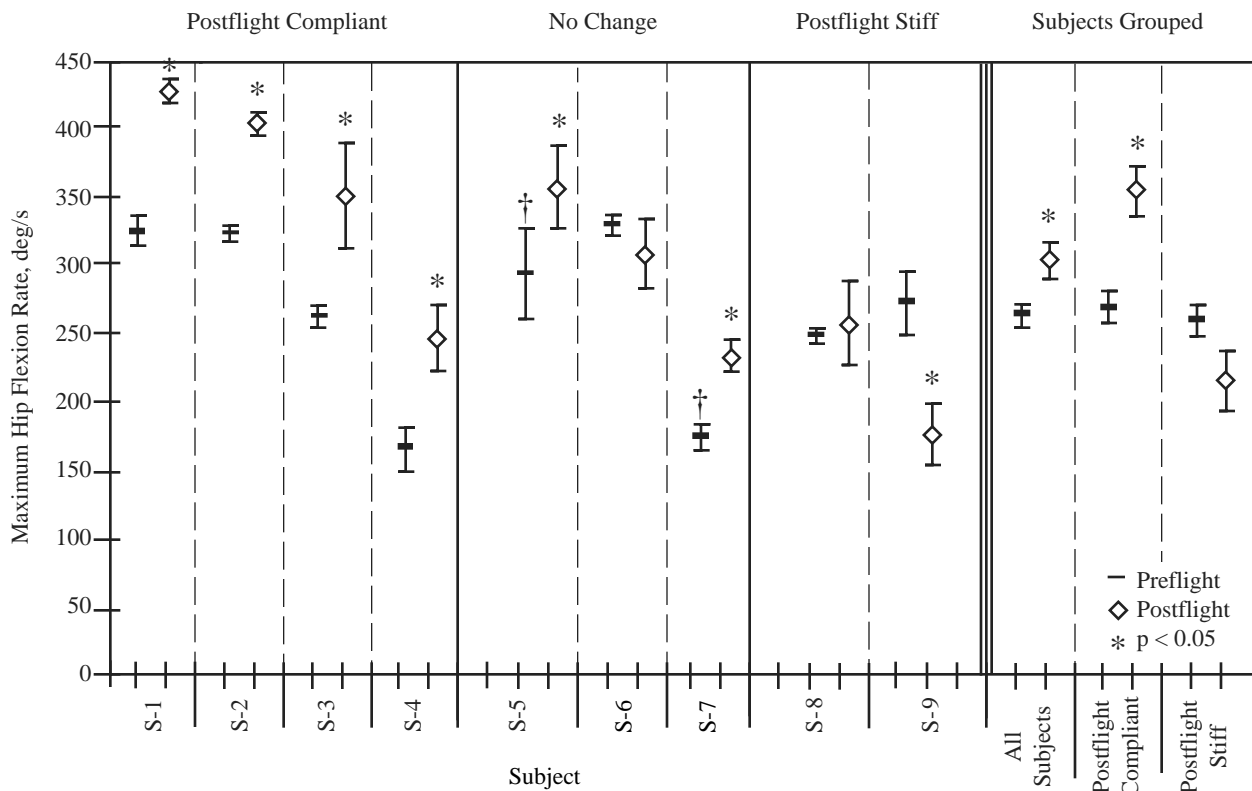


a. Joint flexion angles following impact from a 30 cm jump for the knee: postflight vs. preflight

Figure 5.5-27. Average preflight and postflight maximum values for nine astronaut subjects. Levels of statistical significance are denoted by $*p < 0.05$ and error bars indicate the standard error of the mean. A cross “†” indicates a significant test day effect for the contrast between the two preflight sessions.

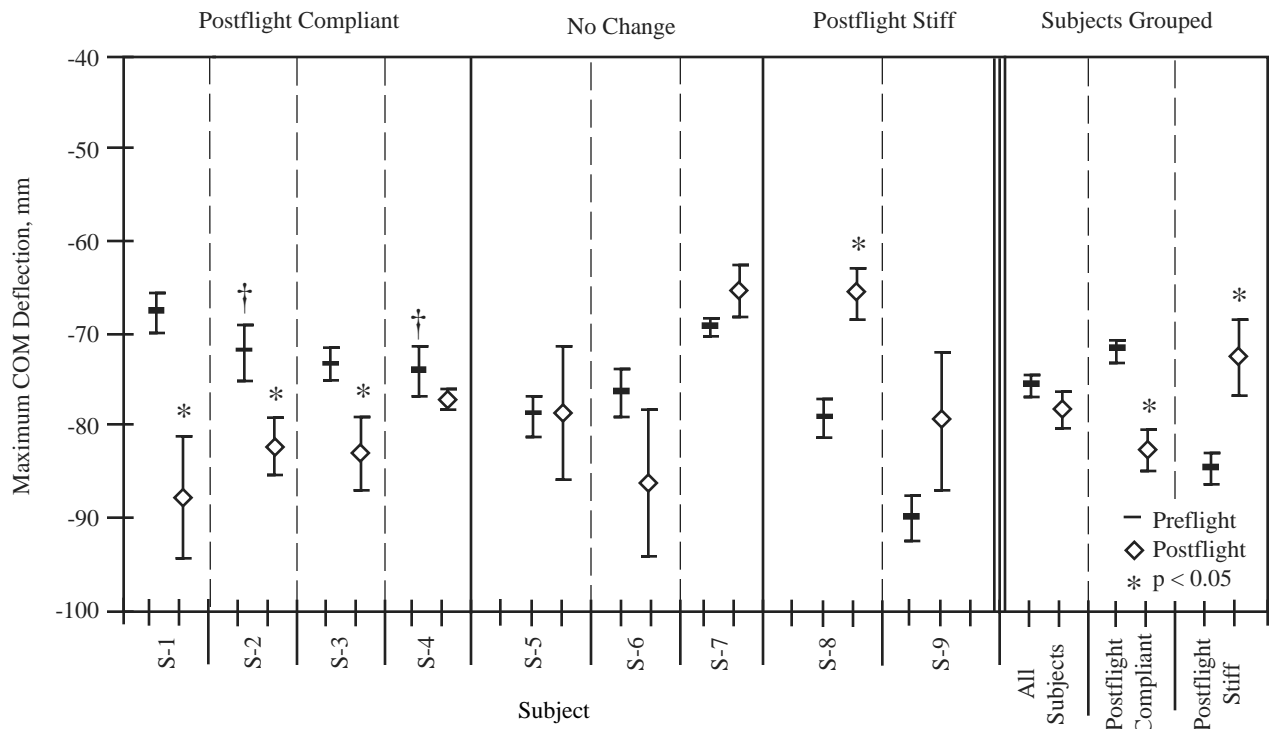


b. Peak joint flexion rate following impact for the knee: postflight vs. preflight

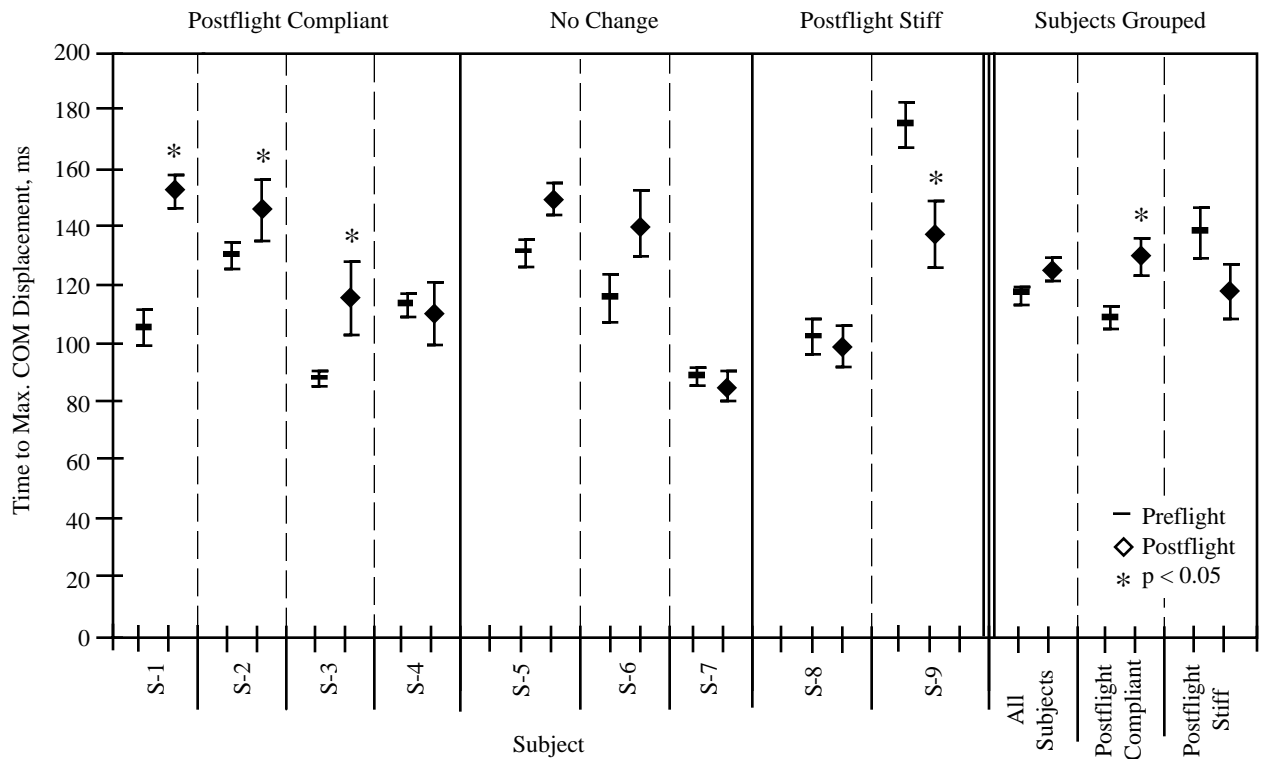


c. Peak joint flexion rate following impact for the hip: postflight vs. preflight

Figure 5.5-27. Concluded.

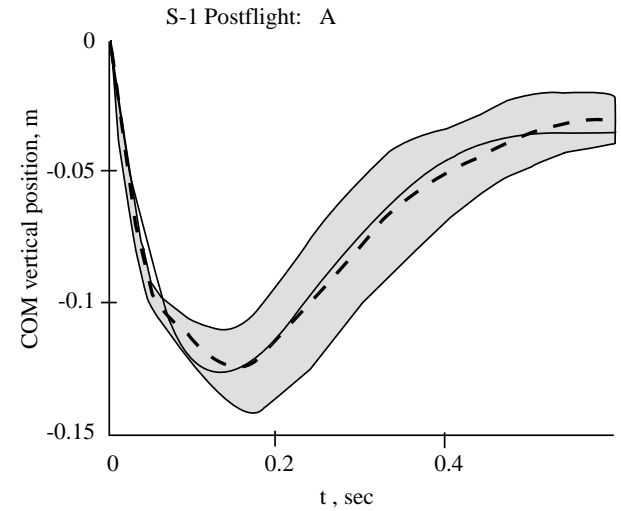
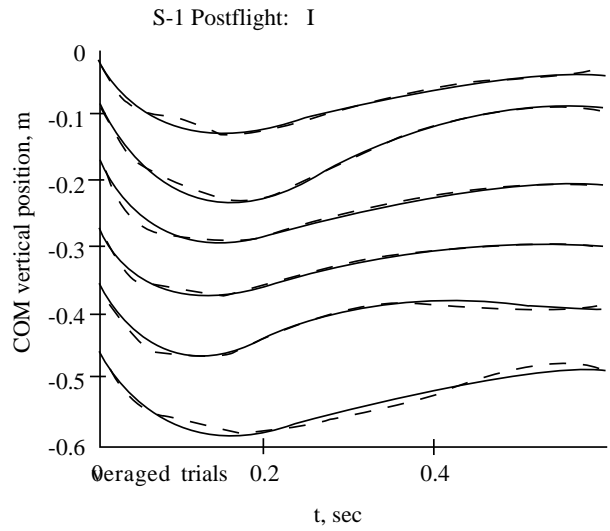
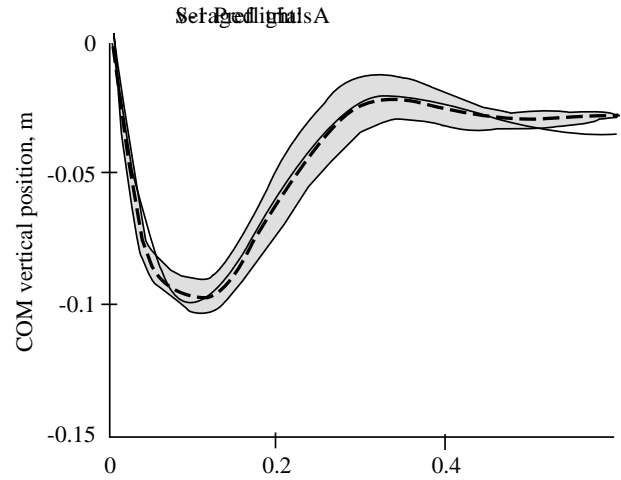
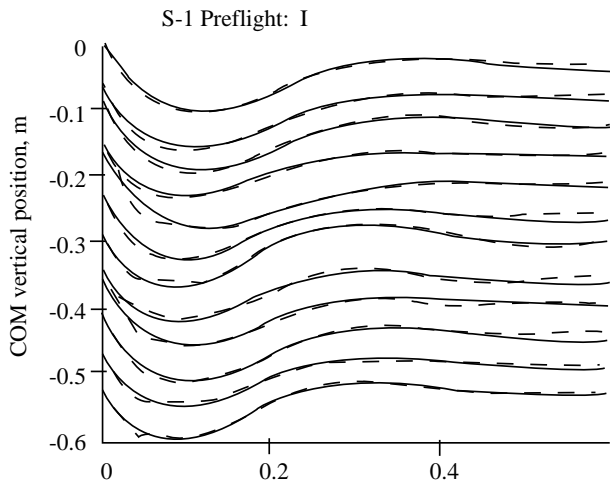


a. Maximum downward deflection of the COM following impact: postflight vs. preflight



b. Time from impact to maximum COM downward displacement: postflight vs. preflight

Figure 5.5-28. COM displacement. Levels of statistical significance are denoted by * $p < 0.05$ and error bars indicate the standard error of the mean. A cross “†” indicates a significant test day effect for the contrast between the two preflight sessions.



a. 12 individual preflight trials (upper) and 6 postflight trials (lower)

b. Corresponding averages for trials shown in (a). The origin represents time synchronization of jump landings at impact. The shaded region denotes ± 1 standard deviation.

Figure 5.5-29. Modeled COM vertical motion using stiffness and damping estimated for representative pre- and postflight for P-C subject S-1. Dashed lines are experimental data and solid lines represent model fits.

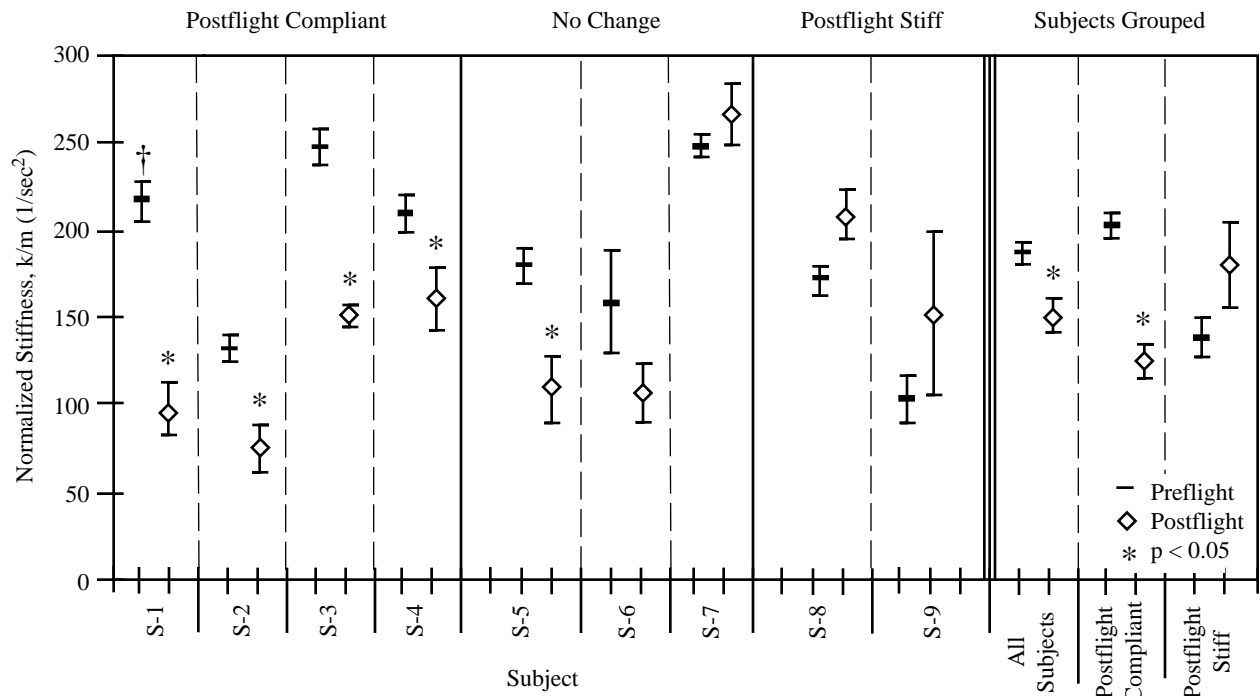


Figure 5.5-30. Mean preflight and postflight model vertical stiffness. Levels of statistical significance are denoted by * $p < 0.05$ and error bars indicate the standard error of the mean. A cross “†” indicates a significant test day effect for the contrast between the two preflight sessions.

Section 6

Assessment of Human Factors

EXTENDED DURATION ORBITER MEDICAL PROJECT

Assessment of Human Factors

*Frances E. Mount and Tico Foley
Johnson Space Center, Houston, TX*

INTRODUCTION

Human Factors Engineering, often referred to as Ergonomics, is a science that applies a detailed understanding of human characteristics, capabilities, and limitations to the design, evaluation, and operation of environments, tools, and systems for work and daily living. Human Factors is the investigation, design, and evaluation of equipment, techniques, procedures, facilities, and human interfaces, and encompasses all aspects of human activity from manual labor to mental processing and leisure time enjoyments. In spaceflight applications, human factors engineering seeks to: (1) ensure that a task can be accomplished, (2) maintain productivity during spaceflight, and (3) ensure the habitability of the pressurized living areas.

DSO 904 served as a vehicle for the verification and elucidation of human factors principles and tools in the microgravity environment. Over six flights, twelve topics were investigated (Table 6-1). This study documented the strengths and limitations of human operators in a complex, multifaceted, and unique environment. By focusing on the man-machine interface in space flight activities, it was determined which designs allow astronauts to be optimally productive during valuable and costly space flights. Among the most promising areas of inquiry were procedures, tools, habitat, environmental conditions, tasking, work load, flexibility, and individual control over work.

SPACE HUMAN FACTORS TOPICS

Ergonomic Evaluations of Microgravity Gloveboxes

Confined work stations, where the operator has limited visibility and access to the work area, may cause prolonged periods of unnatural posture. The confined work stations may have a significant impact on posture, fatigue level, and performance, especially if the task is tedious and repetitive or requires static muscle loading [1]. Although task performance at gloveboxes, which is a good example of the confined work station concept, is

Table 6-1. EDOMP Human Factors Engineering Detailed Supplementary Objective (904) Topics

<i>Topic</i>	<i>Description</i>	<i>STS Flight</i>
1.	Comfort and accessibility of the glovebox at the general purpose workstation	50, 58, 73
2.	Procedures and operation of the Lower Body Negative Pressure Device	50, 58
3.	Management, stowage, deployment, and restraint of electric power and data cables	40
4.	Obstacles and facilitators for task procedures and timelines baselined on Earth	40
5.	Advantages and difficulties using a computer touchscreen in microgravity	70
6.	Electronic and paper procedures in microgravity	57
7.	Perceptions and effects of mechanical vibration on task performance in flight	40
8.	The noise environment	40, 50, 57
9.	The lighting environment	57
10.	Crew member translation and equipment manipulation through the tunnel joining the Shuttle middeck and the pressurized SpaceHab or Spacelab	40, 47, 57
11.	Assessment of crew neutral body posture	47, 57
12.	Questionnaire responses	57

affected by such factors as constrained arm movements, postural limitations, and visual constraints, human factors guidelines have not been well established [1].

Various gloveboxes have been designed for use aboard the Space Shuttle and the International Space Station (ISS). Although the overall technical specifications are similar, the crew interfaces, such as shape and location of glove ports, are unique for each. The design of these gloveboxes was primarily driven by task requirements with minimal or no consideration of the human interface. Three glovebox designs were flown on various Spacelab missions: (1) the Material Sciences Glovebox (GBX), supporting crystal growth and other material science experiments, (2) the biorack (BR), a facility to support investigations on cells, tissues, plants, bacteria, small animals, and other biological samples, and (3) the General Purpose Work Station (GPWS), a multi-functional facility that supported animal experimentation and microscope use. Three different glovebox designs are planned for the ISS in microgravity sciences, life sciences, and the maintenance work area.

Because the human factors requirements of gloveboxes for microgravity use had not been well documented, a goal of DSO 904 was to assess the GBX during STS-50 [United States Microgravity Laboratory-1 (USML-1)]. Both crew questionnaire data and objective postural data from video downlinks were collected. Seven crew members performed various science experiments using the GBX, and rated it as not acceptable, based on the following: (1) it was found to be too small for moving around inside, (2) range of motion was limited, (3) hand positioning was sometimes difficult, (4) mounting hardware inside was hard to do, (5) neck and shoulder pain often occurred, and (6) the viewing window would have been more efficient if larger and slanted forward slightly [2].

The General Purpose Work Station (GPWS), a multi-functional facility accommodating two operators, was evaluated during STS-58 via questionnaires and postural analyses of video downlinks [3]. The GPWS, primarily used to support biological experiments involving animals [4, 5, 6], was larger than the GBX, its gauntlet interface was much more flexible than the snug glove ports of the GBX, and it was less likely to restrain the user from performing natural upper body movements. No neck or shoulder discomfort was reported by any of the crew members, even though they worked in a hunched shoulder posture 47% of the time. Although all aspects of the GPWS design were rated acceptable, reaching for loose items was difficult at times because the interior volume was too crowded [3, 7].

After modifications resulting from data gathered on STS-50, the glovebox work station was redesigned and flown on STS-73 (USML-2). This flight also provided the opportunity to evaluate the Advanced Lower Body Extremities Restraint Test (ALBERT) as a possible aid to

combat poor posture and the resultant discomfort. Four crew members, two males and two females, participated in the study and represented diverse anthropometric percentiles. A Posture Video Analysis Tool (PVAT) [8], was used to identify posture categories and to determine, using the available video footage, the mean percentage of time the crew spent in each of seven posture categories (Figure 6-1). The modified GBX design received more positive comments than the original design.

The results of this study indicated that future gloveboxes should: (1) provide flexible arm holes to allow a maximum range of arm movements for repetitive fine motor tasks, (2) have a height appropriate for a 95th percentile U. S. male, and (3) provide height adjustable foot restraints to accommodate a wide range of users. Future foot restraints should (1) provide knee support for tasks requiring force applications, (2) provide two mechanical modes, loose for adjustment without removing hands from the work area, and lock down to keep the restraint position fixed and rigid, (3) not exceed five operations for adjustments to height, in-out distance, and orientation, (4) provide simple adjustment mechanism operation to encourage the user to find a best fit, and (5) provide scales or markings to facilitate readjustment to a previously determined configuration.

Glovebox design should be further evaluated to determine the best orientation of the viewing window relative to the arm holes, minimum work volume in an enclosed work area, and appropriate arm hole designs for force and torque tasks. Foot restraint design should be further evaluated to determine the best knee support designs to accommodate each of a variety of directions and magnitudes of force and the best method to accommodate a 95th percentile U. S. male.

Lower Body Negative Pressure (LBNP) System

The LBNP human factors and interfaces under investigation in DSO 904 included stowage and assembly, ease and comfort, and operation of the controls and displays. Although the LBNP system had previously undergone many usability analyses [9], fundamental human machine design issues had not been systematically investigated. The goal of this human factors evaluation of the LBNP was to identify human machine design and operational procedure improvements.

Seven Shuttle astronauts participated in the investigation. Data collection methods included: (1) examination of still photographs, (2) administration of questionnaires during and after flight, (3) participation in structured debriefings, (4) application of human factors design principles, and (5) analysis of mission video. Data from in-flight questionnaires enabled the crew to record comments and evaluations while the experience was still in progress. Postflight questionnaires, subtask rating scales, and structured debriefs provided additional information for

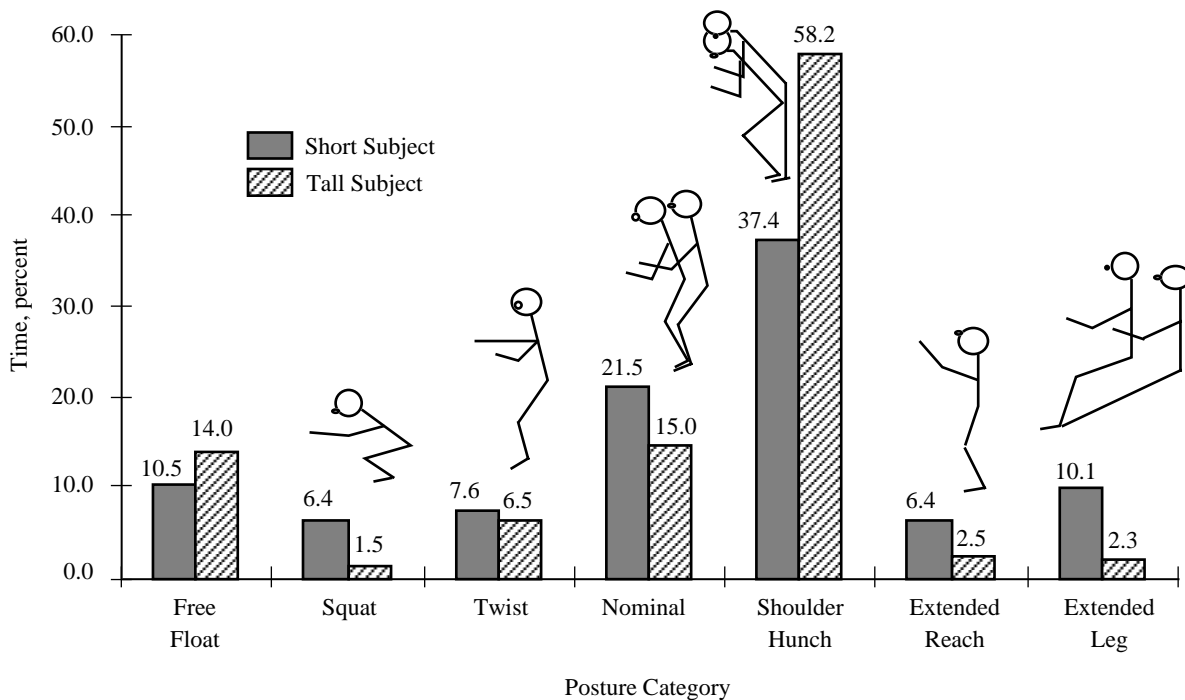


Figure 6-1. Percentage of time primary crewmembers spent in each posture category.

comparative summary analyses. Analysis of the video images provided information about procedures, training, and operations.

There were no appreciable problems during the performance of timelined activities on STS-58. This was attributed to the numerous opportunities the crew members had to work with the equipment and to the effectiveness of the training program. The following observations concerning crew patterns of performance during LBNP operations were noted from observation and video analysis: (1) in microgravity, procedures requiring crew coordination took longer than those that required only one crew member, (2) in microgravity, gross motor movements took longer than fine motor movements, (3) LBNP egress/ingress abilities increased from flight day 1 through flight day 4 and then stabilized, (4) there was no evidence of performance degradation that could be specifically attributed to microgravity, (5) performance of LBNP protocols did not change during the mission, and (6) crew proficiency was impeded by malfunctions, waist seal configuration, and interruptions by the ground control.

Review of preflight training video and mission video, and discussions with crew members indicate that there was an effective preflight training of LBNP set up, stowage and operation. No problems affecting the timeline or completion of the LBNP objectives were noted. Because the LBNP design did not meet all applicable human engineering standards, the following minor changes are recommended: (1) provide color-coded knee

pad and foot rest buckles to minimize installation errors, (2) increase strap lengths to facilitate positioning of struts in bag, (3) provide instructions on the LBNP checklist for rewinding data tapes to minimize destruction of the tapes by the Analog Data Recorder, (4) provide adjustment capability for the waist seal, and (5) provide restraints to secure the floating cables and other equipment.

Stowage, Restraints, Deployment and Cables

Human factors studies were conducted during the three Skylab missions [10-13], on STS-9 [14], and on STS-51B (Spacelab-3) [15]. However, the problems of stowage, restraints, deployment, and cables were not fully understood or resolved. Accordingly, a primary objective of DSO 904 was to understand the effects of microgravity on stowage systems, on restraints for equipment and crew members, and on cable management. A secondary objective was to determine if any increased task completion times resulted from problems in these areas.

These objectives were first implemented on STS-40 [Space & Life Sciences-1 (SLS-1)], with all seven crew members serving as subjects. Of the four males and three females, three subjects had previous Shuttle flight experience. A questionnaire with both closed-ended and open-ended questions was administered on day 2 or day 8 during, or within 3 weeks after, flight. The questionnaires covered medical experiments E022 (Influence of Weightlessness Upon Human Autonomic Cardiovascular

Table 6-2. Approximations of Microgravity Experiment Crew Time Usage (STS-40/SLS-1)

Experiment	Crew Member Minutes				
	1-g Time	Microgravity Estimate	FD-2 Actual Time	FD-5 Actual Time	FD-9 Actual Time
E198+setup	140	222	200		210
E198	140	168		155	
E294	192	384	330	370	370
E066 Calibration	25	27	25	30	30

Control), E066 (In-flight Study of Cardiovascular Deconditioning), and E072 (Vestibular Experiments in Spacelab) that had been independently planned as part of the crew members' flight activities. Crew members were monitored during waking hours via video downlink as well as crew and ground audio. Several problems were identified with stowage, ranging from locker design to practices associated with stowing individual items. Stowage planning and training were not always adequate. Crew members reported that they would prefer to train with stowage in the flight configuration, using the actual foam for stowage. Lost time also resulted from equipment for a given experiment not being stowed together. Crew members recommended adding more Velcro to loose items, as well as to rack faces and the work bench, and removable Velcro to replace areas soaked with spilled liquids. Access to some lockers in the floor and ceiling was difficult, partly due to the lack of nearby hand holds. Crew members generally agreed that loose cables did not interfere with translation or other procedures.

The results of this study indicated that: (1) Restraints should vary according to task requirements; when the task involves exerting significant forces or torques, more robust restraints are needed than for tasks generating less reaction forces. (2) Rigid devices should be available for both foot restraints and three point restraints. (3) Stowage lockers should be designed to be opened with one hand. (4) Equipment in stowage lockers should be restrained so that it neither jams the locker nor drifts out when the locker is opened and another item removed. (5) Quick, simple methods for restraining small items should be supplied; these could include Velcro, adhesive surfaces, vacuum, or elastic bands. (6) Cables should be sized to minimize extra length. And, (7) easy to use techniques and equipment should be provided to restrain cables.

Crew Productivity — Task and Timeline Analysis

Prior to EDOMP there were some attempts to quantify human performance, productivity, and adherence to mission timelines [16-20]. DSO 904 described variations

in tasks performed in microgravity from an integrated mission operations perspective, and derived adaptive strategies and a preliminary set of guidelines for optimizing crew productivity on future spaceflight missions.

Experiments E066 (In-flight Study of Cardiovascular Deconditioning), E198 (Pulmonary Function During Weightlessness), and E294 (Cardiovascular Adaptation to Zero Gravity) involving medical procedures [21] that were part of the planned schedule for the SLS-1 mission were selected for evaluation because they were of particular relevance to crew member ability to adhere to the timeline. Five Shuttle astronauts served either as subject, investigator, or both. Information was obtained from preflight crew interviews, mission monitoring, mission video, postflight questionnaires, and postflight debriefs. Response variables included preflight and postflight Procedures Completion Times, task performance correlates, and task interruptions. Although the experiments took approximately the amount of time budgeted, malfunction procedures took longer in microgravity than estimated beforehand (Table 6-2). Interruptions were caused by malfunctions or other problems with the Gas Analyzer Mass Spectrometer (GAMS II) (which necessitated a repeat of E198), the Orbiter refrigerator/freezer, the indicators on E066, the electromyogram (EMG) amplifier for the rotating dome, the operation of temperature strips, experiment E022 calibration, unclear intravenous (IV) pump procedures, incorrect E066/E294 measurement procedures, high noise levels caused by some experiment-specific equipment, the text and graphics system (TAGS), and reconfiguration of the communications loop.

Questionnaire responses indicate that a more thorough preflight training regimen might have eliminated confusing procedural steps containing prompts and values that were not always accurate. Additionally, communication problems often necessitated repetition of the procedure, important blocks of information were not distinguishable from other information, and steps that had to be completed were embedded in text that did not require action. Flight experiment E294 was a difficult procedure that never worked as planned. The cuff could not find

pressures, the batteries often failed, and switch guards were never used. To some extent, frustration was also experienced due to the requirements for complete exhalation and the need to crane the neck to see the screen.

Touchscreen Usability in Microgravity

Prior to EDOMP, the usability of touchscreens had not been tested in the microgravity environment. DSO 904 was designed to identify touchscreen requirements, develop display guidelines, and compare performance with input devices currently used in spaceflight. Five STS-70 crew members performed two ground baseline and two in-flight data collection sessions with the touchscreen and the standard portable onboard input device, the IBM Thinkpad Trackpoint II™ (Figure 6-2). The touchscreen was an Elo TouchSystems AccuTouch®(model E274) resistive membrane touchscreen integrated with a 9.4 inch (24 cm) active matrix color thin film transistor (TFT) liquid crystal display (LCD) monitor (model LMT 5020).

Most of the subjects preferred the touchscreen on the ground and the Trackpoint in flight. Hand fatigue was almost immediately experienced when using the touchscreen in flight, although none of the subjects had complained of hand fatigue during the two sessions of baseline data collection. Subjects also reported wrist fatigue while using the Trackpoint in flight. Analysis of variance (ANOVA) indicated that: (1) there was no reaction time difference between the two ground sessions nor between the two flight sessions, (2) subjects produced fewer errors with each successive session in each environment, (3) the touchscreen was faster than the Trackpoint, (4) the Trackpoint was more accurate than the touchscreen, and (5) touchscreens performed better for those tasks with larger touch areas, but not for precise positioning (Figure 6-3).

The following recommendations derive from the DSO 904 results: (1) A touchscreen interface could be used for displays containing medium to large objects and simple actions, such as single and double click pointing. (2) For fine positioning or text editing, a touchscreen interface should be avoided, or at least supplemented with another input device. (3) Crew restraints should be provided, especially for dragging and drawing tasks. (4) Rest periods should be provided for touch-intensive tasks, since users may tend to exert more pressure than necessary. And, (5) The minimum object size for touchscreen interfaces should be 10 mm × 10 mm.

Electronic Procedures

Prior to EDOMP, all Shuttle onboard tasks were performed using hard copy procedures, resulting in the use of considerable launch weight and valuable stowage space [22], and causing unique problems during flight. A goal of DSO 904 was to determine human factors requirements

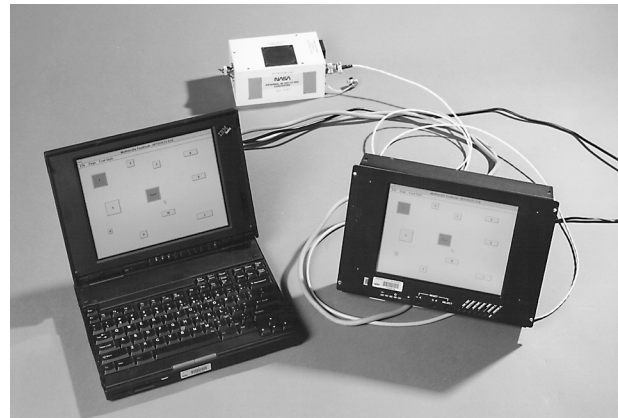


Figure 6-2. Laptop computer and touchscreen.

for electronic procedures systems in spaceflight environments. Building on the results of previous studies [23-27], performance measures were taken for the same task using both computer and paper procedures, with advantages and disadvantages of each being noted. One STS-57 (Space-Hab 1) crew member participated in a propulsion task and one crew member participated in a soldering task. After each task session, subjective data were gathered through the use of a computer-based questionnaire program, providing information on what to include and what to avoid in the design of future electronic procedures systems.

Computer procedures were very favorably rated in the questionnaire. The format was considered to be very user friendly and resulted in the task being easily performed, with the primary advantage of computer procedures being that the current step was highlighted automatically, releasing the crew member from the burden of place-keeping in the procedures. This investigation was the first step in confirming that electronic procedures are a feasible alternative and can offer many benefits over paper presentation.

Vibration Evaluation in Microgravity

For several years, the major concern about vibration in the Shuttle while in orbit was its effect on experiments, particularly materials science studies [28]. A survey of 33 astronauts demonstrated that although more than half reported vibration in flight, they did not consider it to be a problem [29]. However, general concern about vibration led to the development of a Space Acceleration Measurement System (SAMS) that could measure and store acceleration data during spaceflight. A goal of DSO 904 was to determine the effect of vibration on crew comfort and task performance. This was accomplished by postflight crew questionnaires, by ground personnel monitoring the mission during crew waking hours, by analysis of videotape, and by correlation with quantitative acceleration data from SAMS [30].

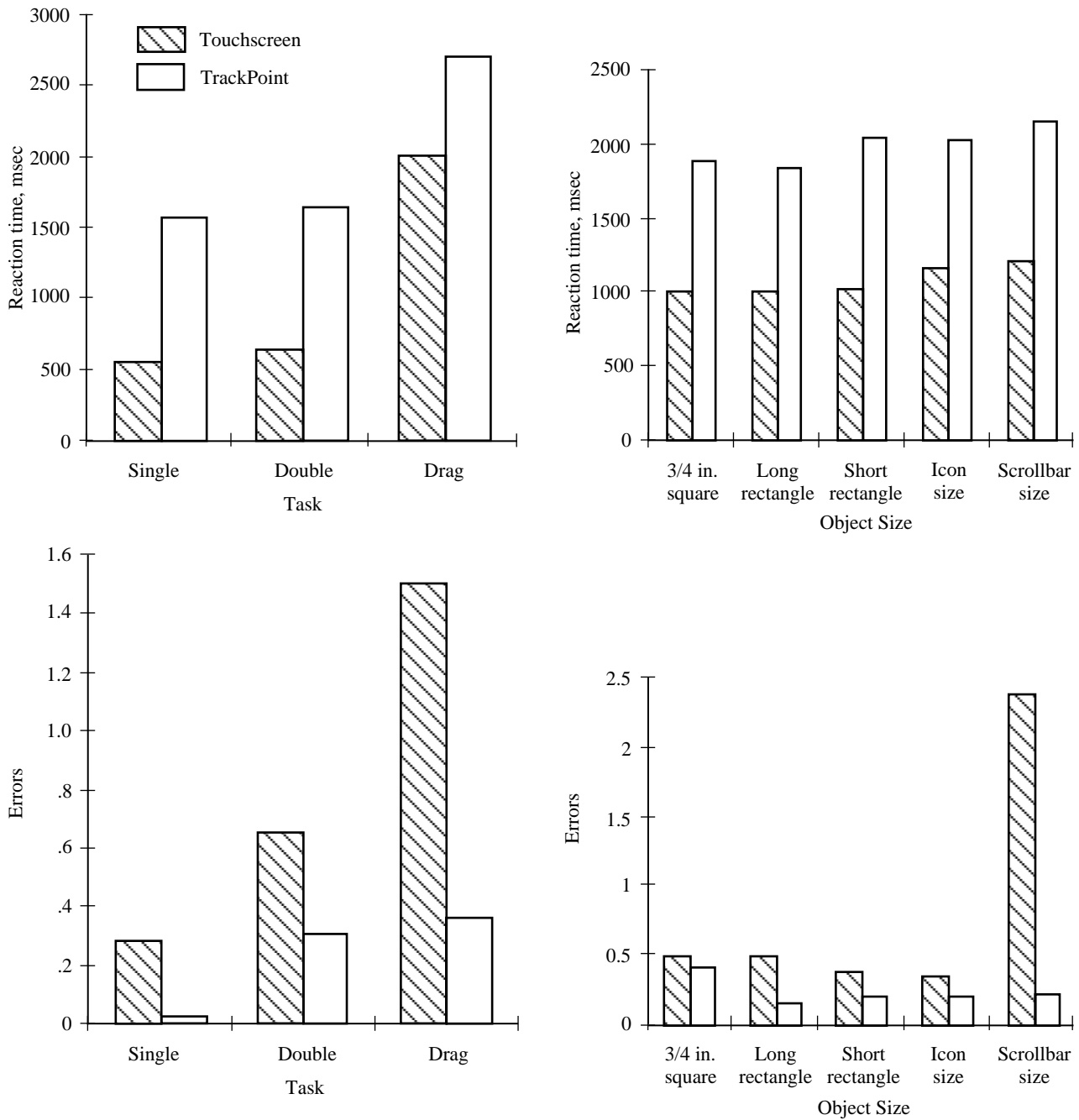


Figure 6-3. Comparison of touchscreen to trackpoint with respect to reaction time and error rate, versus task type and object size.

All seven crew members of STS-40/SLS-1 (four male, and three female) participated in the study. Vibration was perceptible by all, and sometimes annoying to five of the seven subjects during flight. Vibrations occurred at times when primary jets were firing, or when the treadmill or ergometer were in use. Treadmill and ergometer use was accompanied by significant noise, which could have interacted with vibration to be perceived as an annoyance, a stressor, or even pain. Crew

members did not report vibration interfering with any task, but did recommend that some of the more sensitive tasks, such as inserting a venous catheter, not be performed when high levels of vibration were present.

Acoustic Noise Environment

U. S. and Russian crew members have often complained about in-flight noise levels that regularly disrupt

Table 6-3. Comparison of Measured Sound Levels for STS-40, STS-50 and STS-57

FLIGHT DECK			
<i>Flight</i>	<i>Source Location</i>	<i>Conditions</i>	<i>dB(A)</i>
	Design Limit		63
STS-40	Flight Deck (Center)	nominal systems (ECLSS)	61.8
STS-50	Flight Deck (Center)	nominal systems (ECLSS)	64.0
STS-57	Flight Deck (Center)	ECLSS + SAREX	72
		ECLSS + A/G	62
MIDDECK			
<i>Flight</i>	<i>Source Location</i>	<i>Conditions</i>	<i>dB(A)</i>
	Design Limit		68
STS-40	Middeck (Center)	nominal systems (ECLSS)	63
		ECLSS + AEM	64.7
	Middeck (1 foot from AEM)	ECLSS + AEM + OR/F	67.6
STS-50	Middeck (Center)	nominal systems (ECLSS)	59.9
		ECLSS + EVIS + Bike	67.9
		ECLSS + Vacuum Cleaner	79.9
STS-57	Middeck (Center)	nominal systems (ECLSS)	63
		nominal systems (ECLSS)	62
SPACELAB/SPACEHAB			
<i>Flight</i>	<i>Source Location</i>	<i>Conditions</i>	<i>dB(A)</i>
	Design Limit		68
STS-40	Spacelab (Center)	SR/F—one compressor on	69.7
	Spacelab (4 feet from SR/F)	SR/F—both compressors on	72.6
STS-50	Spacelab (Center)	nominal systems (ECLSS)	61.6
	Spacelab (Center)	nominal systems (ECLSS)	61.2
	Spacelab (operator)	ECLSS + DPM	64.7
	Spacelab (operator)	ECLSS + GBX on	61.0
	Spacelab (operator)	ECLSS + STDCE	63.8
STS-57	SpaceHab (Center)	ECLSS, fans off	63
	SpaceHab (Center)	ECLSS, fans on	66

sleep, make communication difficult, and increase tension in an already demanding environment [29]. Some crew members have worn ear plugs, which may have protected against hearing loss, but was not an acceptable solution to the overall problems of noise. An objective of DSO 904 was to assess acoustic noise levels in order to document impacts on crew performance, collect in-flight sound level measurements, compare noise levels across missions, obtain preflight and postflight audiometry measures from crew members, and evaluate Shuttle acoustic criteria [31].

Twenty astronauts (4 males and 3 females on STS-40/SLS-1, 5 males and 2 females on STS-50/USML-1, and 4 males and 2 females on STS-57/SH-1) participated

in this study. A questionnaire, consisting of forced choice questions with prompts and spaces for further comments, was administered during the flight and again within a month after landing. Crew members subjectively evaluated the overall noise environment and the noise in the flight deck, middeck, and Spacelab or SpaceHab under nominal background noise conditions and with selected noisy equipment operating. Audiometric data acquired 10 days prior to launch were compared with audiograms obtained within 2 hours after landing [32, 33].

Crew member perceptions of noise on board the Shuttle and within the laboratories differed from one mission to the next (Table 6-3). In all cases the major noise source was from the Environmental Control and

Life Support System (ECLSS). All seven crew members on board STS-40 rated the Spacelab noise environment in need of mandatory improvements. Three of the STS-40 crew members found that the noise became more bothersome as the flight progressed, and all STS-40 crew members predicted that this noise level would be unacceptable for 30-day or 6-month missions. On the other hand the STS-50 crew members did not find the noise levels to have gotten worse during their flight and only one thought the noise might be unacceptable for a 6-month mission. Astronauts also noticed that the in-flight noise levels interfered with communication. About half of them reported occasional or frequent difficulty hearing their crew mates within the same module, and that it was almost impossible to hear someone in another module. Figure 6-4 depicts a computer simulation graphic illustrating that, even at only the background noise level, a crew member cannot communicate effectively with someone at the other end of the Spacelab.

Payload operations exceeded the acoustic design limit on each of the flights and in each of the modules (Table 6-3). On STS-40 the Spacelab refrigerator/freezers (SR/F) emitted excessive noise: 69.7 decibels (A) [dB(A)] when one compressor was operating, and 72.6 dB(A) for both compressors operating. On STS-50 the vacuum cleaner contributed significantly to a noise environment of almost 80 dB(A), a difference of 20 dB over the background sound level. Operation of the short wave amateur radio (SAREX) resulted in sound level readings of 72 dB(A). In comparison, the air-to-ground (A/G) communications loop measured 10 dB quieter than SAREX. In every case where comparisons were available on the same flight in the same module, it was shown that payload operation added 3 to 4 dB to the background noise. An analysis of variance comparing individual crew member hearing levels before and after STS-40 indicated that hearing thresholds were significantly higher following flight ($p < 0.025$).

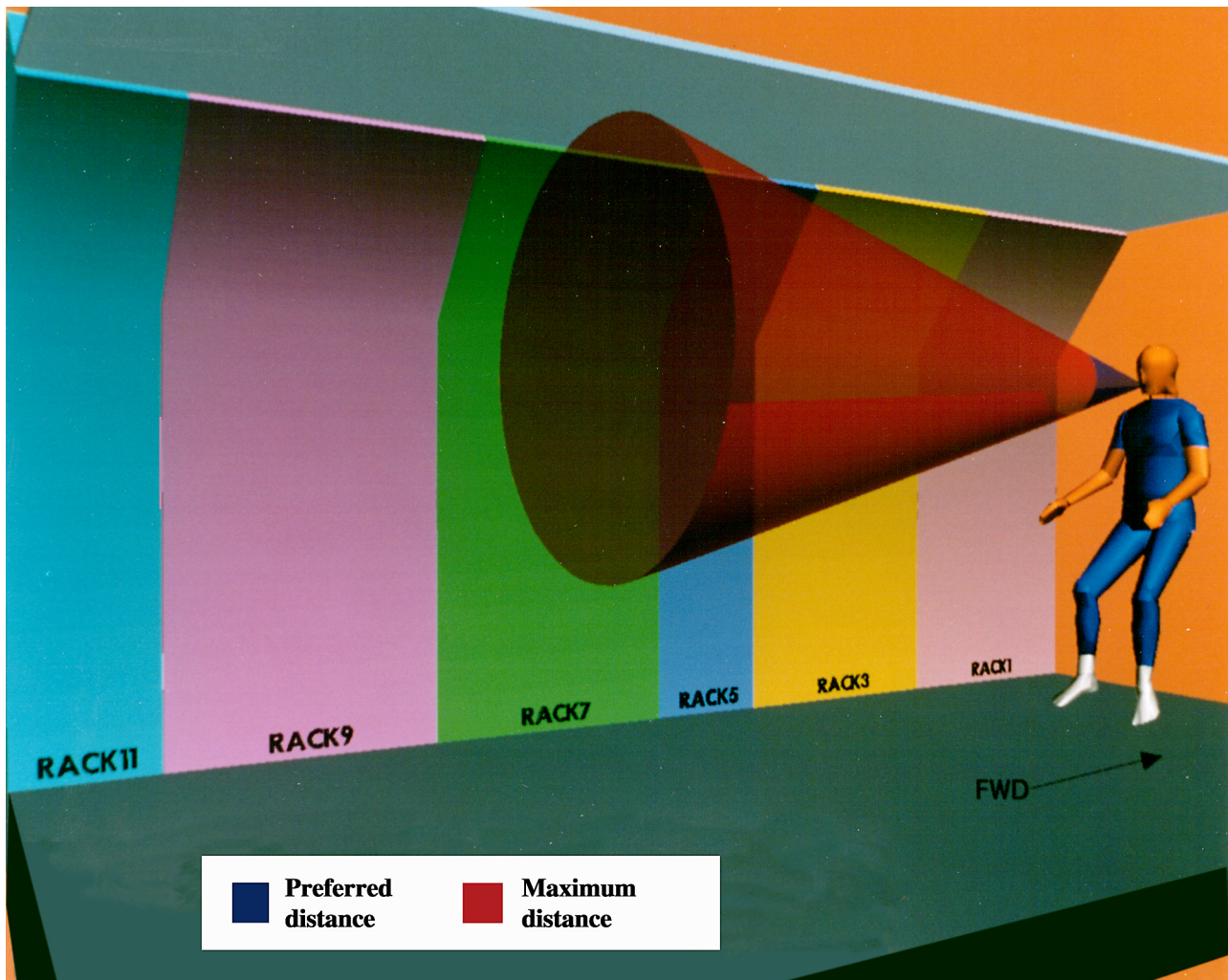


Figure 6-4. Simulation of crew member preferred and maximum communication distances in the Spacelab under typical background noise conditions.

Lighting Assessment

The objective of this study was to determine if required lighting levels within the Orbiter and SpaceHab had been maintained in compliance with NASA-STD-3000 for performing IVA tasks and other crew operations [34]. To accomplish this objective, crew members measured the luminance levels of surfaces within the Orbiter middeck, Orbiter flight deck, and SpaceHab with a hand-held Minolta Spotmeter M. Luminance levels were measured and recorded in units of exposure values (EV) which were translated into both English and SI units. The results (calculated luminance values in footlamberts and candela/square meter) from specific locations, along with crew notes regarding measurement conditions, are shown in Figures 6-5 and 6-6. All reflected light levels measured across the work surfaces in the middeck, flight deck, and SpaceHab were within the required brightness ratio and were rated reasonably acceptable or completely acceptable by crew members.

Translation Through a Transfer Tunnel

This study was designed to evaluate translation times and techniques used by astronauts to move themselves and equipment through a transfer tunnel (STS-40 and 47) or a shorter SpaceHab tunnel (STS-57) connecting the middeck and a pressurized module in the payload bay [33, 35, 36]. The tunnel presented the opportunity to study translation in a unique sense. There was a beginning and an end, making it easier to investigate translation times and techniques (Figure 6-7). Since the tunnel had a minimal and narrow passageway, crew members had to hold equipment they were moving either in front or behind during transit, thus limiting field of view and impeding the use of both hands and feet for translation mobility and stability.

Crew members found the design of the tunnel and the placement of hand holds to be acceptable, and perceived that it did take longer to move through the tunnel

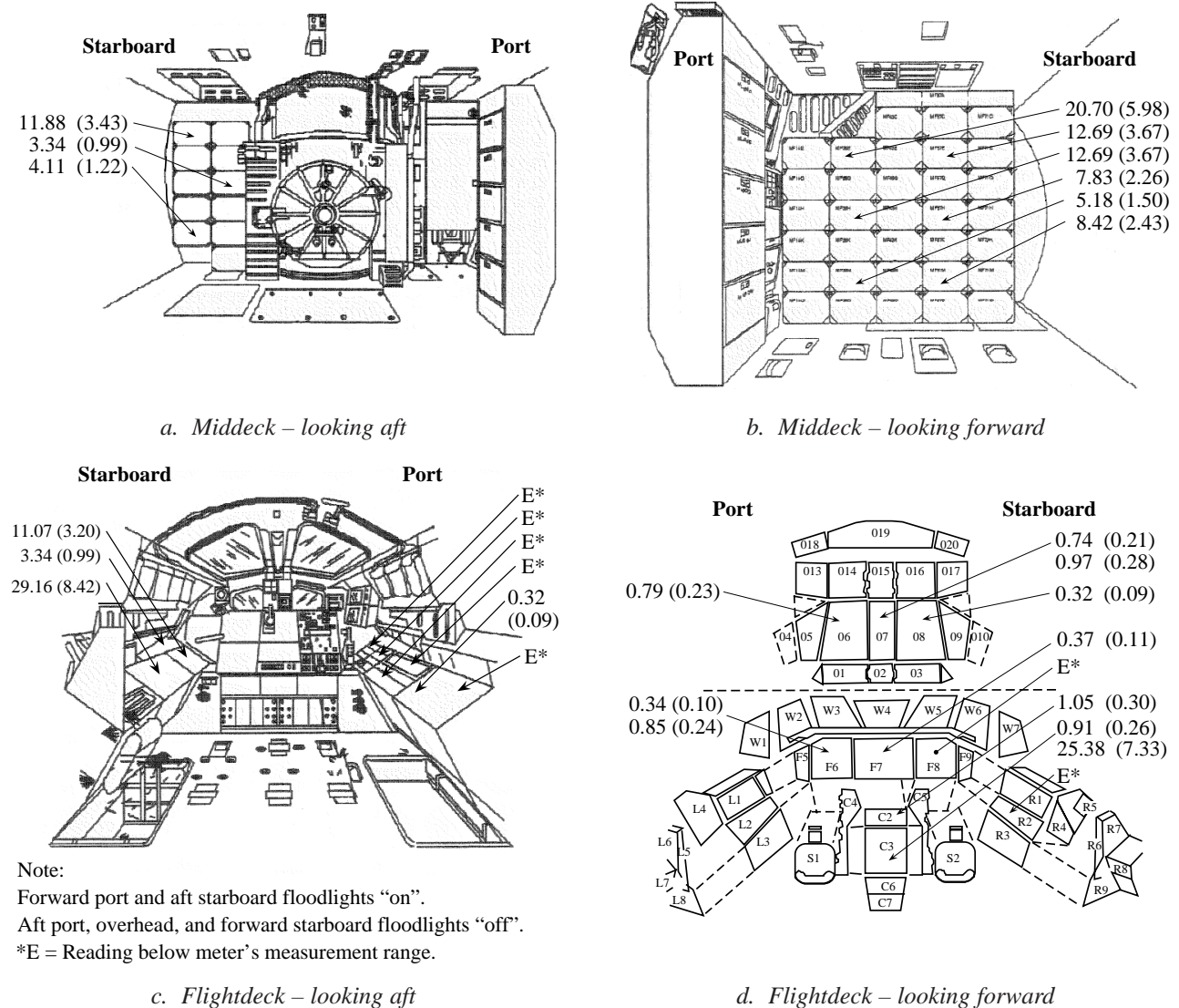
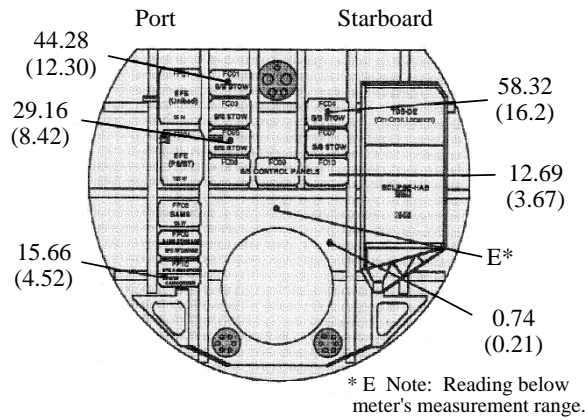
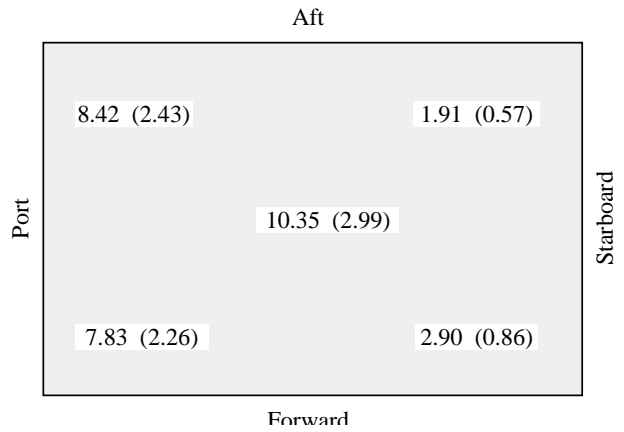


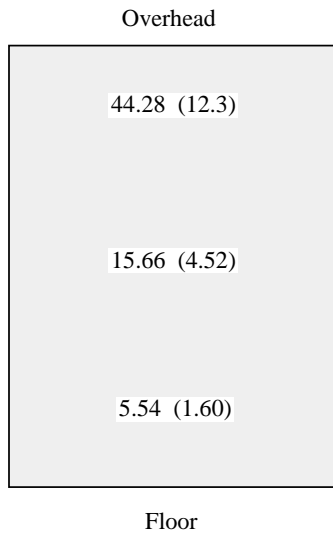
Figure 6-5. Luminance measurements in the Orbiter.



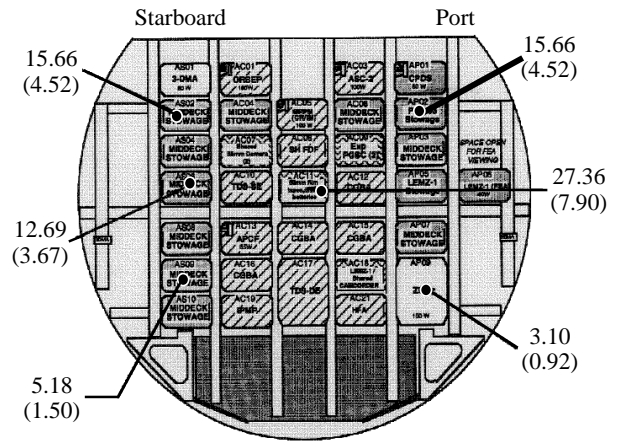
a. SpaceHab – looking forward



b. SpaceHab – looking at floor



c. SpaceHab – rack surfaces



d. SpaceHab – aft lockers

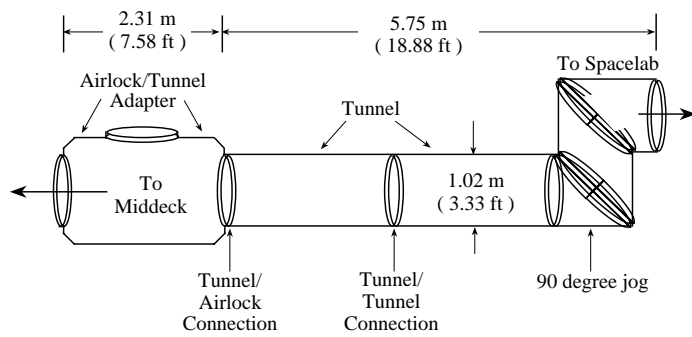
Note: Units are in candela/square meter (foot lamberts).

Figure 6-6. Luminance measurements in the SpaceHab.

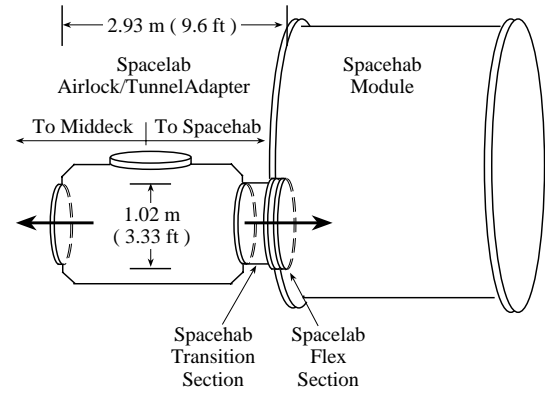
with equipment than without. Most of the astronauts did not notice any difference in the time it took to travel one way through the tunnel compared with traveling the other way. On the last mission day there was little overall difference in the time it took to translate to the Spacelab compared with how long it took to travel back to the middeck without equipment. However, traveling to the Spacelab with equipment took longer than any of the other trips. The overall average translation time was about 14.8 seconds (s) for the 8.25 meter (m) tunnel length. The average translation rate was calculated to be about 0.56 m/s (1.81 ft/s), with a range of 0.33 m/s (1.06

ft/s) to 0.80 m/s (2.57 ft/s). These rates were comparable to those reported for Skylab for ordinary translations.

At the beginning of the mission, crew members took longer to move through the SpaceHab tunnel than later in the mission. There was a larger decrease in the times for translation with equipment and for the translations from the SpaceHab to the middeck. On both days it took longer to go to the middeck with the airlock obstructions at the end of the travel than it did to go to the SpaceHab. The obvious differences in tunnel sections, like the packed air lock and the 90-degree jog, affected translation ease and translation techniques. It was noted that the



a. The Spacelab Transfer Tunnel



b. The SpaceHab Transfer Tunnel

Figure 6-7. Transfer Tunnels and their interior dimensions.

smoother parts of the tunnel were easier to navigate. Also, the jog was seen as beneficial by some crew members because it prevented them from entering the Spacelab too fast. Other crew members saw the jog as an impediment. Crew members suggested improved mobility aids. Padding and an additional center handrail within the tunnel would reduce bumps and bruises. Footloops and handholds at and beyond the exits of the transfer tunnel would facilitate stopping after translation.

Neutral Body Posture (NBP)

Physiological effects of the microgravity space environment have been of particular interest for posture studies, and have been known to affect the body's center of gravity, reach, flexibility, and dexterity in conducting work activities [36]. Possible factors influencing posture include body size, physical condition, previous injury, and mission duration [37, 38]. The European Space Agency (ESA) [38] has raised some questions about the appropriateness of the NASA microgravity neutral body posture model [34] (Figure 6-8). ESA researchers, after investigating photographs and video taken during Skylab missions, concluded that only 36% of the data they reviewed matched this model. ESA suggested that discrepancies may be due to variations among subjects, and predisposed postures due to orientation of the subjects to a work area or task. Therefore, a goal of DSO 904 was to collect additional data on body posture under microgravity conditions [39, 40].

Six crew members from each of two Shuttle flights (STS-47 and 57) participated in this evaluation. Each subject was instructed to don shorts and a tank top, to be blindfolded, and to assume a relaxed posture that was not oriented to any work area or task, while data were being taken. A blindfold facilitated acquiring a relaxed and non-oriented posture, while the clothing allowed good

visibility of the body segments, body joints, and limb angles. Responses during the STS-47 flight indicated that each crew member observed a microgravity neutral body posture in themselves that was quite comfortable and consistent throughout the mission. In general, most crew members indicated that posture did not change over the course of the mission. However, one crew member felt that the body adapted over time to the microgravity environment, resulting in a gradual attainment of the microgravity posture for that person. Data were acquired on day 6 of STS-57 after crew members became fully adapted to the microgravity environment, having recovered from any effects that motion sickness may have induced. No crew member exhibited a neutral body posture predicted by the model. Rather, arm and shoulder positions were less bent, and there were straighter leg positions at the hip and knee than expected. Also, the arms were closer to the torso sides and generally held lower toward the waist than predicted by the model (Figure 6-9).

Crew members indicated that they had difficulty relaxing, particularly in the lower back area, in the microgravity environment. This may have been due in part to a difficulty in straightening the back in microgravity because of the lack of gravity to push against. Crew member responses identified the need to design specifically for microgravity and to pay particular attention to the tasks being performed in designing foot restraints and handholds at workstations.

These studies suggest that the NASA NBP model was too generalized, and should be modified with additional data to provide more representative spaceflight crew postures. This would also tend to indicate that ESA's concerns with the original determination were well-founded and that further study should be made of microgravity posture as manifested by a more normally distributed participant population.

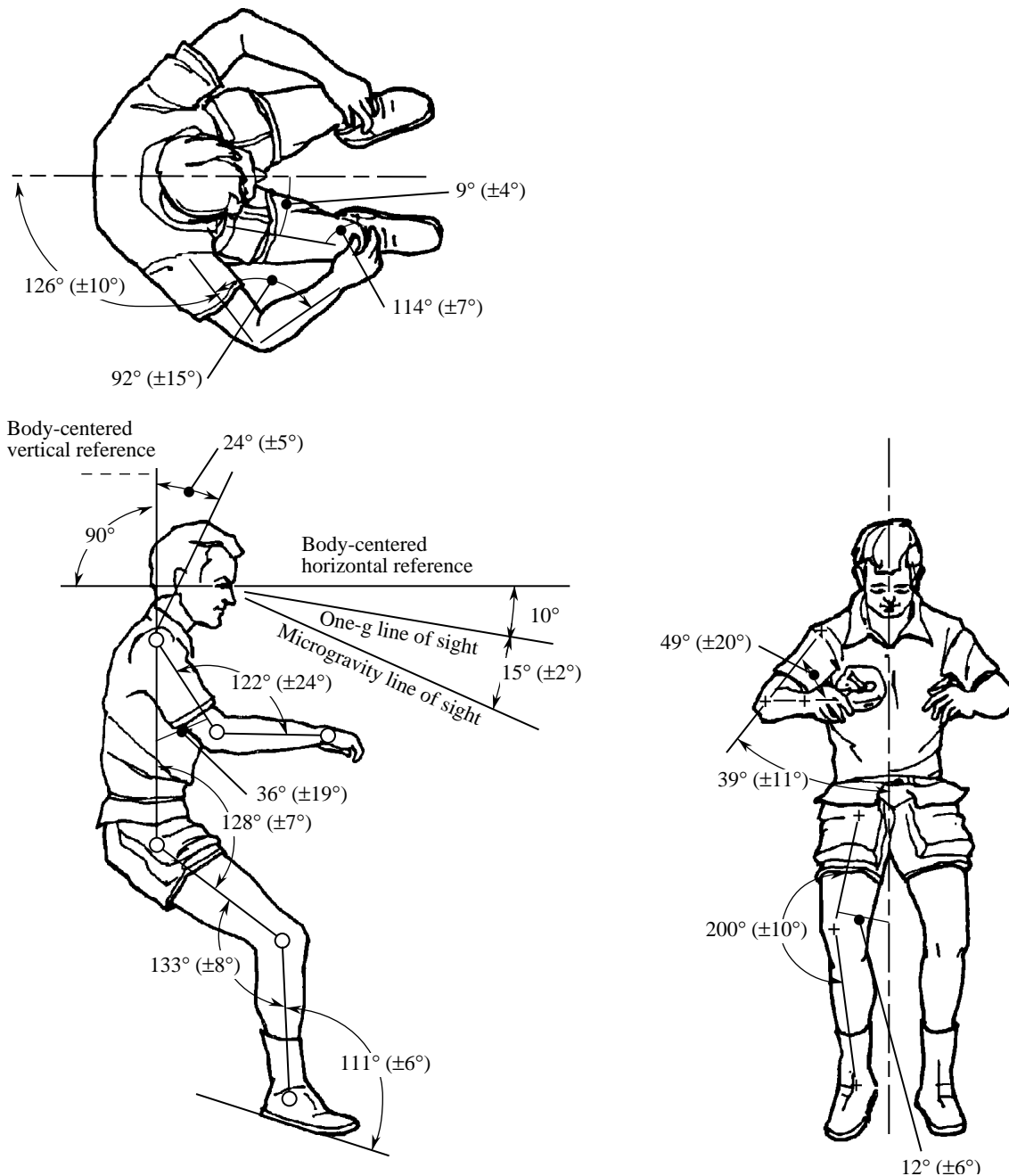


Figure 6-8. The Neutral Body Posture model. [34]

Questionnaires

An important element of spaceflight human factors assessment (HFA) is data collection methodology. Computer-based HFA questionnaires were evaluated on SpaceHab-1 (STS-57). These questionnaires were compared with data collection using written paper formats or voice recordings. The concept of an electronic questionnaire was explored as a possible means of eliciting and acquiring more explicit comments from the crew. In addition to entering comments, crew members were

asked to make one of the following inputs: 7-point scale rating, percentage estimate, or yes/no response.

The SpaceHab crew debriefing helped to identify areas in which the HFA questionnaire could be improved. For example, the crew members suggested including more specific questions. The use of a computer did not appear to elicit more crew comments than did written responses. Furthermore, it appears that using a computer may have introduced additional overhead, both in terms of timeline and required work volume. Using a computer-based questionnaire may have resulted in a



Figure 6-9. Female crew member with leg and foot posture deviating from the MSIS model.

competition for resources, such as electrical power, a place to attach the computer and foot restraints, or the availability of the computer itself. When the computer and the crew members were not available at the same time, data collection opportunities were lost.

On orbit, an electronic questionnaire offered advantages over traditional hard copy questionnaires in reduced weight, fewer free floating objects to keep track of, and greater ease in uploading changes and downloading results.

Based on findings from the HFA questionnaire and other evaluations, it is clear that questionnaires do provide a means of obtaining useful data for the evaluation of crew interface and design issues. However, as would be expected, the utility of the data collected is highly dependent upon the ability to gain access to the user of the system (in this case the SpaceHab crew). While the implementation of a questionnaire through electronic means proved to be a viable alternative, its use must be carefully examined since its operation requires additional timeline, power, and working volume requirements.

SUMMARY

Building on the experiences of Skylab, the DSO 904 studies contained herein report the first systematic formal inquiries made regarding the workplace and habitation environments aboard the Space Shuttle. The cases extending Skylab studies represented a tripling of the sample size available for guiding design of microgravity work places, tools, and tasks. The addition of female subjects added important data to the Man-Systems Integration Standards (MSIS) database, providing a basis for greater variety in representative crew members for designing microgravity equipment and tools. In studying the human-machine interface, an emphasis was placed on crew member productivity and comfort. Hardware and software designs influence ability to perform tasks and minimize errors.

Following the summary of the data collection and results for each area of inquiry, there is a list of recommendations and countermeasures that will allow designers of future spacecraft hardware and developers of spaceflight procedures to better meet the goals of human factors engineering applied to the microgravity environment of space.

The expansion of the database to document the variability among individuals, a larger sample size, and a variety of tasks will permit better design of the workplace, tools, and recreational and daily living areas for long duration spaceflights. With motivation and endurance, crew members can withstand or ignore slight discomforts and overcome task inefficiencies for short periods of time. However, as spaceflight missions get longer, it is more important to design for continued high levels of performance.

Information collected from these studies, and from Earth-based evaluations of the Shuttle and SpaceHab, will be incorporated into a database of space and life sciences research and used in the development of human factors standards for spaceflight. Additionally, the information will be used to update the *Man-Systems Integration Standards (MSIS)*, NASA-STD-3000 [34] and to suggest improvements in Orbiter hardware design, training requirements, procedure definition, and timeline development, as well as for design of the International Space Station and other space vehicles.

An assumption that no software or hardware countermeasures or enhancements are necessary can only be substantiated if both the environment and the human response are better known. Specific studies of these areas will be recommended for future flights.

REFERENCES

1. Eastman Kodak. Ergonomics Design for People at Work. Volume 1. New York: Van Nostrand Reinhold Company; 1983.

2. Whitmore M, McKay TD, Mount FE. Evaluations of a microgravity workstation design: Spacelab glove-box. In: Aghazadeh F, editor. *Advances in industrial ergonomics and safety VI*, proceeding of the Industrial Ergonomics and Safety Conference '94. Bristol, PA: Taylor & Francis; 1994.
3. Whitmore M, Mount FE. Microgravity maintenance workstation development. *International Journal of Industrial Ergonomics* 1995; 15:189-97.
4. Dalton BP, Jahns G, Hogan R. Space life sciences development towards successive life sciences flights. Technical Paper #IAF/IAA-92-0280. Paris, France: International Astronautical Federation; 1992.
5. Dalton BP, Schmidt GK, Savage PD. The general purpose work station, a spacious microgravity workbench. SAE Technical Paper Series No. 921394; 1992.
6. Wagner PA. The Development of a Space Shuttle General Purpose Workstation (GPWS). SAE Technical Paper Series No. 831090; 1992.
7. Pandya A, Hancock L. GPWS ergonomic evaluations. GRAF White Paper; 1995.
8. Whitmore M, McKay TD. PVAT: development of a video analysis tool. Poster presented at the Association for Computing Machinery's Computer Human Interaction '94 Conference; 1994.
9. Diaz MF. Human factors assessment of the STS-50 lower body negative pressure system. JSC Technical Report #26517. Houston, TX: National Aeronautics and Space Administration; 1993.
10. Dalton M. Skylab experience bulletin no. 7: an overview of IVA personal restraint systems. #JSC-09541. Houston, TX: National Aeronautics and Space Administration; 1974.
11. Dalton M. Skylab experience bulletin no. 12: temporary equipment restraints. #JSC-09546. Houston, TX: National Aeronautics and Space Administration; 1975.
12. Dalton M. Skylab experience bulletin no. 18: evaluation of Skylab IVA architecture. #JSC-09552. Houston, TX: National Aeronautics and Space Administration; 1975.
13. Sova V. Skylab experience bulletin no. 15: cable management in zero-g. #JSC-09549. Houston, TX: National Aeronautics and Space Administration; 1974.
14. STS-9 flight crew report: Columbia Spacelab 1. Houston, TX: National Aeronautics and Space Administration; 1984.
15. Wichman H, Donaldson SI. Crew performance in Spacelab. Proceedings of the Human Factors Society 35th annual meeting. Santa Monica, CA; Human Factors Society; 1991. p 571-4.
16. Compton WD, Benson CD. Living and working in space: a history of Skylab. Washington, DC: National Aeronautics and Space Administration; 1983.
17. Johnston RS, Dietlein LF, Berry CA, editors. Biomedical results of Apollo, NASA SP-368. Washington, DC: U.S. Government Printing Office; 1975.
18. Johnston RS, Dietlein LF, editors. Biomedical results from Skylab. NASA SP-377. Washington, DC: National Aeronautics and Space Administration; 1977.
19. Nicogossian AE, Parker JF Jr. Space physiology and medicine. NASA SP-447. Washington, DC: National Aeronautics and Space Administration; 1982.
20. Kubis JF, McLaughlin EJ, Jackson JM, Rusnak RR, McBride TR, Saxon SV. Biomedical results from Skylab. NASA SP-377. Washington, DC: National Aeronautics and Space Administration; 1977.
21. National Aeronautics and Space Administration. Spacelab Life Sciences 1, first space laboratory dedicated to life sciences research. NP 120. Houston, TX: National Aeronautics and Space Administration; 1989.
22. Mount FE. Elaborated and concise hypertext: effects on comprehension. Unpublished thesis, University of Houston; 1993.
23. Desaulniers DR, Gillan DJ, Rudisill M. The effects of context in computer based procedure displays. NASA Technical Report. Houston, TX: Lockheed Engineering and Sciences Company; 1989.
24. Johns GJ. Dynamic Display of crew procedures for Space Station, volume I, baseline definition, and volume II, functional requirements. MITRE Report No. MTR-88D033. McLean, Virginia: The MITRE Corporation; 1988.
25. Kelly CM. Conceptual definition for a flight data file automated control and tracking system. MITRE Report No. MTR-88D0017. McLean, Virginia: The MITRE Corporation; 1988.
26. O'Neal MR. The effects of format and contingency on procedure reading time. NASA Technical Report #25705. Houston, Texas: Lockheed Engineering and Sciences; 1992.
27. O'Neal MR, Manahan M. Spacecraft crew procedures: from paper to computers. Published in Proceedings: Fourth Annual Workshop on Space Operations, Applications, and Research (SOAR '90). NASA Conference Publication 3103; 1990. p 595-600.
28. Regel LL. Materials processing in space: theory, experiments, and technology. Bradley JES, translator; Sagdeev RZ, editor. New York: Consultants Bureau; 1990 (Original work published 1987).

29. Willshire KF, Leatherwood JD. Shuttle astronaut survey. Langley, VA: Langley Research Center; 1985.
30. Koros AS. Crewmember evaluation of vibration on STS-40/SLS-1. Houston, TX.: National Aeronautics and Space Administration; 1991.
31. Koros AS. Objective and subjective measures of noise on STS-40/SLS-1. Houston, TX: National Aeronautics and Space Administration; 1991.
32. Koros AS, Adam SC, Wheelwright CD. A human factors evaluation: noise and its effects on Shuttle crewmembers during STS-50/USML-1. NASA Technical Memorandum 104775. Houston, TX: National Aeronautics and Space Administration; 1993.
33. Mount FE, Adam SC, McKay T, Whitmore M, Merced-Moore D, Holden T, Wheelwright CD, Koros A Sr., O'Neal M, Toole J, Wolf S. Human factors assessment of the STS-57 SpaceHab-1 mission. NASA Technical Memorandum 104802. Houston, TX: National Aeronautics and Space Administration; 1994.
34. National Aeronautics and Space Administration. Man-systems integration standards, rev. B, vol. 1. NASA-STD-3000. Houston, TX.: National Aeronautics and Space Administration; 1995.
35. Callaghan TF. Human factors investigation of translation through the STS-40/SLS-1 Spacelab transfer tunnel. Houston, TX: National Aeronautics and Space Administration; 1991.
36. Adam S, Callaghan T. Human factors investigation of translation through the STS-47/Spacelab-Japan transfer tunnel. Houston, TX: National Aeronautics and Space Administration; 1992.
37. Nicogossian AE, editor. Space physiology and medicine, 2nd edition. Philadelphia: Lea & Febiger; 1989.
38. Tafforin C. Analyse Éthologique de l'adaptation du comportement moteur de l'homme a la microgravité [Ethological analysis of the adaptation of the astronaut's motor behavior in microgravity]. Unpublished doctoral dissertation, Université Paul Sabatier, Toulouse, France; 1990.
39. Wilson GF, Stealey SL, Mount FE. Neutral body posture (NBP) evaluation from Space Transportation System (STS)-47/Spacelab-Japan (SLJ). Houston, TX: National Aeronautics and Space Administration; 1993.
40. Mount FE, Whitmore M, Stealey SL. Evaluation of neutral body posture (NBP) on Shuttle mission STS-57/SpaceHab-1. Houston, TX: National Aeronautics and Space Administration; 1994.

Section 7

Facilities

Facilities

An expansion of medical data collection facilities was necessary to implement the Extended Duration Orbiter Medical Project (EDOMP). The primary objective of the EDOMP was to ensure the capability of crew members to reenter the Earth's atmosphere, land, and egress safely following a 16-day flight. Therefore, access to crew members as soon as possible after landing was crucial for most data collection activities. Also, with the advent of EDOMP, the quantity of investigations increased such that the landing day maximum data collection time increased accordingly from two hours to four hours. The preflight and postflight testing facilities at the Johnson Space Center (JSC) required only some additional testing equipment and minor modifications to the existing laboratories in order to fulfill EDOMP requirements. Necessary modifications at the landing sites were much more extensive.

LANDING SITE MEDICAL FACILITIES

Background

Before the full implementation of EDOMP, crew members egressed through a white room with a truck-mounted set of stairs that docked with the Orbiter. Although crew members could de-suit in the white room, space was restricted and the medical care capability was limited. Also, the entire crew was detained until their collective physiological recovery permitted descending the white room stairs. This arrangement limited the capability of immediate medical care and prolonged the duration between wheels stop and medical data collection. Although clinic space at both landing sites was adequate for the landing day physicals, it was not adequate to also accommodate EDOMP investigations.

Edwards Air Force Base (EAFB) was initially the prime landing site for Extended Duration Orbiter (EDO) flights of 13 to 16 days duration. One concern of long duration flights was the crew's ability to perform precision landing maneuvers, especially with a heavy payload such as a Spacelab. Landing at EAFB provided more latitude with multiple runways and expanded landing area compared to the shorter, narrower runway at Kennedy Space

Center (KSC). However, the advantage of landing at KSC was an expedited Orbiter processing turnaround, since the need to transport the Orbiter from EAFB to KSC after flight was eliminated.

Edwards Air Force Base (EAFB)

The facilities at the Dryden Flight Research Center (DFRC) of EAFB were expanded prior to those at KSC because of the large number of Shuttle landings there early in the program. Even after EAFB became the contingency landing site, a fully staffed and fully functional data collection facility was necessary to ensure that no data were lost following a flight. Because the clinic at DFRC was not suitable for expansion, a new facility named the Postflight Science Support Facility (PSSF) was built (Figure 7-1). A site was chosen based on proximity to the runway and within the NASA area at EAFB. The design was based on requirements for EDOMP investigations, flight physical examinations, and Spacelab postflight data collection (Figure 7-2).

Kennedy Space Center (KSC)

The facility at KSC, used for the landing day physical examinations, was in the Operations and Checkout



Figure 7-1. PSSF at Dryden.



Figure 7-2. Examination room at PSSF.

Building which lent itself to rearrangement of internal space. The driving factors became: (1) to design a layout where the EDOMP data collection did not impede the physical examinations and allowed extra privacy for crew members, and (2) to provide space within the total available area to meet the requirements of the principal investigators. As with the PSSF, the needs for Spacelab data collection were factored into the design. The design also had to provide enough flexibility to accommodate requirements changes from mission to mission based on the total complement of investigations and the number of crew member participants. Space was made available on the second floor, and walls (some removable) were installed to separate the spaces (Figures 7-3a and 7-3b). Some investigations that involved large equipment were always performed in the same location. Other investiga-

tions, that used smaller portable equipment and did not require much space, had fewer restrictions on their room location and enhanced the flexibility for each flight.

Experience proved that some testing equipment was too bulky and the electronics too sensitive to endure the rigors of frequent shipping. Additional units of devices such as the Posture Platform (DSO 605), the Underwater Weighing Tank (DSO 608), and the Treadmill were purchased and housed both at KSC and the EAFB PSSF. At KSC, a design change created a docking port for the Crew Transport Vehicle (CTV) (described in the next section) at the second floor of the Baseline Data Collection Facility (BDCF). The CTV docking port enabled crew members to exit directly into the BDCF, thus minimizing crew activity before testing and enhancing the landing day schedule.

Crew Transport Vehicle (CTV)

An important contribution to obtaining crew medical data in a timely manner was the addition of Crew Transport Vehicles at KSC and EAFB (Figures 7-4a and 7-4b). Prior to EDOMP, medical data collection was initiated from 1.25 hours to 2.5 hours after wheels stop. This delay allowed a partial physiological recovery from spaceflight to occur and prevented investigators from gaining data that would provide answers relative to the physiological condition of their subjects at landing. The primary objective of the EDOMP was to ensure that the crew could safely land the Orbiter and perform an emergency egress after a 16-day mission. Some of the considerations that drove the decision on what type of vehicle to purchase and develop for immediate access were: (1) potential medical emergency activities, which were possibly more likely with a 16-day flight than with



a. Entry to the Baseline Data Collection Facility (BDCF) at KSC



b. Examination room at the BDCF

Figure 7-3. Baseline Data Collection Facility (BDCF) at KSC.

the typical 5- to 7-day flight, (2) the number of people required in the CTV at landing, (3) capability and interface with the Orbiter or white room, (4) accommodations for interfacing with the BDCF and PSSF, and (5) accommodations for physiological data collection.

Several variations of available vehicles were considered. These included the airport passenger transporter (APT) with 568 square feet, and the aircraft service vehicle (ASV) with 360 square feet of available space. The ASV was determined to be insufficient primarily because of its size. The APT was selected and modified to meet the unique requirements. Both CTVs (KSC and EAFB) were fully self-contained, single operator, self-propelled units with internal environmental control systems. Each CTV could be raised by as much as 11 feet via a self-contained lift system to dock with the Orbiter hatch or the BDCF (Figure 7-4a). A telescoping gangway was provided for docking ingress and egress, and a stairway in the rear of the vehicle provided an alternate exit. The passenger seats were removed and provisions for large recliner-type chairs, a refrigerator, restroom, emergency medical equipment, and other improvements were added (Figure 7-4c).

Although the two CTVs were originally different models of a Plane Mate APT, after modification they provided similar capabilities. The CTVs have been used since June 1991 (STS-40) and have proven to be very effective. Use of the CTVs contributed to enhanced emergency medical capability, improved crew comfort, enhanced medical data collection capability, and reduced time from wheels stop to data collection.

JOHNSON SPACE CENTER (JSC)

Throughout the Space Program, JSC has been the focal point for pre- and postflight medical testing, with a significant amount of crew training and hardware development and testing also being performed there. Therefore, implementation of the EDOMP at JSC primarily involved modification and relocation of existing facilities, such as adding test and analysis equipment and utilizing any unused or under-used space to better accommodate the laboratories. EDOMP support required a wide range of activities. The activities performed at JSC were ground-based testing, flight protocol development, flight hardware development and testing, crew training, baseline data collection (pre- and postflight), planning and directing medical activities to be performed at landing sites, and analysis and archiving of data.

Because flight opportunities are relatively few, as are the number of crew members available for a particular investigation, ground-based testing of non-astronaut populations was critical to gaining as much knowledge as possible before implementation of a flight investigation. With the science knowledge gained from ground-based testing, flight protocols could be developed that



a. CTV docked to the BDCF at KSC



b. CTV at Dryden



c. Interior of CTV

Figure 7-4. Crew Transport Vehicles (CTVs).

would provide maximal data and also take into account flight constraints such as limited stowage, power, and crew time.

Development of hardware to support these flight protocols was essential to the success of each investigation. In many cases commercial off-the-shelf items were modified and certified for flight, but often hardware had to be designed specifically for the unique investigation in the environment of space. All hardware was developed, certified, and processed at JSC.

Crew training was performed at JSC, mostly in the disciplines' laboratories. Numerous training sessions were held in the Shuttle Crew Compartment Trainer (CCT) and the Full Fuselage Trainer (FFT). Access to these trainers was advantageous when precision was required in flight or where positioning of equipment and crew members was critical.

Preflight as well as postflight baseline data collection sessions were performed at JSC, typically in the disciplines' laboratories. Strict adherence to the standards for clinical testing was observed.

The success of landing day activities depended primarily on the planning and oversight of medical activities performed at the landing sites; this was performed by JSC personnel. Preparation of and adherence to a landing day schedule were required so that all crew members received their designated testing within the guidelines of numerous constraints. The constraints of each investigation had to be considered with respect to all other investigation constraints. For example, exercise would perturb results of a neurological or cardiovascular test, or drinking or eating certain foods would nullify an exercise test. This, combined with adhering to other landing day constraints, required a well-planned schedule which was ultimately approved by the crew, the flight surgeon, and each of the investigators.

All data and samples from flight and landing day were transported to JSC where they were analyzed and stored. Each laboratory was equipped with instruments and hardware to perform appropriate analyses, as well as personnel trained in these methods. After analysis, the refined data were incorporated into the EDOMP data archive.

Section 8

Hardware

Hardware

INTRODUCTION

The full complement of EDOMP investigations called for a broad spectrum of flight hardware ranging from commercial items, modified for spaceflight, to custom designed hardware made to meet the unique requirements of testing in the space environment. In addition, baseline data collection before and after spaceflight required numerous items of ground-based hardware.

Two basic categories of ground-based hardware were used in EDOMP testing before and after flight: (1) hardware used for medical baseline testing and analysis, and (2) flight-like hardware used both for astronaut training and medical testing. Individual hardware items are listed in Table 8-1. To ensure post-landing data collection, hardware was required at both the Kennedy Space Center (KSC) and the Dryden Flight Research Center (DFRC) landing sites. Items that were very large or sensitive to the rigors of shipping were housed permanently at the landing site test facilities. Therefore, multiple sets of hardware were required to adequately support the prime and backup landing sites plus the Johnson Space Center (JSC) laboratories.

Development of flight hardware was a major element of the EDOMP. The challenges included obtaining or developing equipment that met the following criteria: (1) compact (small size and light weight), (2) battery-operated or requiring minimal spacecraft power, (3) sturdy enough to survive the rigors of spaceflight, (4) quiet enough to pass acoustics limitations, (5) shielded and filtered adequately to assure electromagnetic compatibility with spacecraft systems, (6) user-friendly in a microgravity environment, and (7) accurate and efficient operation to meet medical investigative requirements.

Even more challenging was the short timeframe afforded hardware development projects, the compressed flight integration schedules, and the rapid turn-around time between flights during which hardware modifications were frequently made. All of these were necessary in order to meet the dynamic requirements of the EDOMP. Given the critical need for quick answers to the many physiological concerns associated with longer duration Shuttle missions, hardware development schedules were highly compressed. Frequently, investigations were manifested for flight prior to completion of the hardware and/or well after standard Shuttle Program manifesting deadlines. Quite often lessons learned through flight experience that could improve data

Table 8-1. Ground-Based EDOMP hardware.

LIDO Isokinetic Dynamometer
Mass Spectrometer
Quinton Treadmill
Q-plex Metabolic Analyzer
Safe Stress System
Cycle Ergometer
Underwater Weighing System
Bioelectric Response System
Data Acquisition/Analysis Systems
EMG System
Visual-Vestibular Data System
Dual Axis Laser Tracking System
Equitest Posture Platform System
Video-Based Motion Analysis System
Doppler/Ultrasound System
Finapres Blood Pressure Monitor
Automated Blood Pressure Monitor
Holter Recorders and Analysis System
Barocuff System
Lower Body Negative Pressure Device
Lifepak Monitor
Strip Chart Recorder
Peripheral Venous Pressure Monitor
Downlink Data Acquisition System
12-Lead ECG
CO Rebreathing System
Video Recorders

acquisition and quality were incorporated in time for the next flight.

Despite these scheduling pressures, flight hardware items were fully certified for safety and compatibility with the Orbiter. While the processing of many items benefited from streamlined reliability testing, hardware considered safety-critical underwent the full scope of reliability tests. The success of EDOMP in pursuing such an aggressive hardware strategy was made possible not only by the dedication of project personnel, but by the cooperation and contributions of the entire JSC flight processing community. In the Extended Duration Orbiter Medical Project, JSC truly achieved a “faster, better, cheaper” flight program.

SPECIFIC FLIGHT HARDWARE AND GROUND SUPPORT ITEMS

Ambulatory Cardiovascular Monitoring Assembly

This assembly supported Detailed Supplementary Objectives (DSOs) 602 and 603. It consisted of a commercial off-the-shelf (COTS) automatic blood pressure monitor (ABPM) (Accutracker II, manufactured by Suntech) and a COTS 9-channel data recorder (TEAC Model HR40G) (Figure 8-1a). The assembly was designed to record blood pressure and heart rate during reentry, landing, and seat egress. A special plug was fabricated for the Biomedical Instrumentation Port (BIP) in the Launch and Entry Suit (LES). The BIP plug allowed placement of the electrodes and blood pressure cuff underneath the LES, while the remainder of the hardware remained in a pocket outside the pressure garment. The BIP plug contained the necessary electrical and pneumatic pass-through connections for the ABPM, and yet provided a hermetic seal of the BIP. Beginning with STS-59 in 1994, four skin temperature sensors (HOBO-TEMP, manufactured by Onset, Inc.) were added to this complement for DSO 603, to document the thermal environment inside the LES (Figure 8-1b).

Modifications to the commercial ABPM were minor and included the development of a custom software routine and changes to the Blood Pressure Cuff and ECG cable, allowing connection through the BIP plug. Additional shielding was also provided to reduce the electromagnetic signature of the device. The TEAC Data Recorder was modified to replace the manufacturer's input connector with dual LEMO connectors, allowing inputs from both the ABPM and a 3-axis accelerometer system, while reducing dimensions of the overall assembly. In addition to the hardware modifications, a custom Nomex softgoods kit was developed to contain the hardware within the LES pocket and to organize the cables in such a way that they would not interfere with crew activities or make donning the hardware difficult during flight. A major emphasis was placed on making the assembly as small and unobtrusive as possible to minimize interference in the event that the crew was required to make an emergency egress from the Orbiter.

Lower Body Negative Pressure (LBNP) System

The LBNP system supported DSOs 478 and 623. It was used to track orthostatic deconditioning in flight by using staged application of negative differential pressures of up to -50 millimeters of mercury (mmHg), and to counteract orthostatic intolerance by stimulating physiological responses that encouraged a redistribution of body fluids. LBNP was used in flight as early as 1973 when astronauts on Skylab 2 underwent experimental protocols in the first



Figure 8-1a. Ambulatory Cardiovascular Monitoring Assembly.

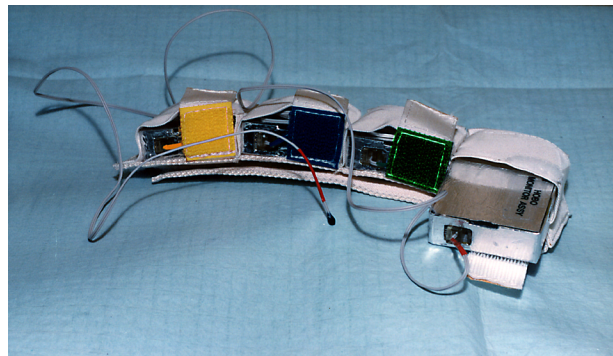


Figure 8-1b. HOBO Temperature Monitoring Device.

generation LBNP chamber [1]. This device, although effective and still in use for ground-based studies, was much too large and heavy to be practical for use on the Shuttle. A second generation LBNP device had been developed for the Spacelab, but was too bulky for stowage and use in the Shuttle middeck. The challenge was to develop a collapsible device, capable of being easily assembled and yet stowed in a single middeck locker. The challenge was met, and the first version of this collapsible system flew on STS-32 in January, 1990. Although hardware operation was successful, the astronauts using the device experienced significant discomfort. During the LBNP protocol the astronaut's body was supported by a bicycle-style seat suspended from the chamber opening. The atmospheric pressure outside the chamber pushed the crew member against the seat, analogous to hanging from a bicycle seat without being able to touch the floor. Crew suggestions following this flight led to an anthropometric redesign of the chamber and the seat.

The main component of the LBNP system was the LBNP Device (Figure 8-2a), which formed a chamber in which the subject was exposed to the varying levels of negative pressure. The LBNP Device consisted of inner and outer cylindrical Nomex bags with an airtight urethane coated nylon bag sandwiched between the two. Woven into the inner Nomex bag was a skeletal support structure of four struts and seven rings fabricated of 304 stainless steel. The struts could be disengaged and folded, allowing the chamber to collapse into a compact cylinder stowable in a Shuttle middeck locker. As mentioned earlier, during the first flight of the LBNP, crew members commented that the device was not comfortable. In an attempt to eliminate discomfort, the LBNP Device was modified. The addition of a ring canted at a 30-degree angle to the open end of the cylinder, and the replacement of the bicycle seat with a flat, tractor-like seat pan allowed the subject to assume a more natural neutral body position within the LBNP Device, and distributed the forces previously centered on the groin across the subject's buttocks. In addition to the seat pan, other modifications to the LBNP Device included: (1) a back rest, to provide support and cushioning to the lower back, (2) a foot rest, allowing the subject a leverage point, and (3) the addition of an iris assembly, which reduced the cross-sectional area at the top of the bag exposed to standard cabin pressure, thereby reducing the suction forces translated to the subject and to the neoprene waist seal.

Maintaining proper waist seal integrity and eliminating leakage was critical to the success of LBNP. Original versions of the waist seal, although basically successful, presented difficulties when subjects of widely varying waist sizes were required to use the same device. This led to the development of removable neoprene waist seals that zipped onto the LBNP Device and could be fabricated to fit different subjects.

Operation of the system was managed by the LBNP Controller (Figure 8-2b). The Controller was a self-contained, programmable integrated logic circuit (ILC) control unit that provided automated pressure control, as well as signal conditioning for ECG, blood pressure, and LBNP Device pressure waveforms. The Controller connected directly to the LBNP Device via a quick-disconnect mounted on the front of the LBNP Device. In order to create a vacuum, a stainless steel flex hose attached to quick-disconnects (QD) mounted on the LBNP Controller and on an Orbiter vacuum source. For middeck operation, the vacuum source was the Waste Collection System (WCS), accessed via a QD mounted on a panel below the Orbiter toilet. For Spacelab operation, the LBNP used the Spacelab Vacuum Vent, accessed through a custom panel fabricated by Marshall Space Flight Center (MSFC). Regulation of the internal vacuum was provided by two solenoid valves, as illustrated in Figure 8-2c. These valves were: (1) a normally open valve on the Controller's vent port, and (2) a normally closed

valve located on the vacuum inlet port. To decrease pressure in the LBNP Device, the normally open vent solenoid was energized, forcing the vent valve closed, and shutting off the LBNP chamber from the cabin. This provided a sealed environment in which to pull a vacuum. At the same time, the normally closed vacuum valve was commanded to the open position to begin evacuation of the LBNP Device. A pressure transducer, located inside the LBNP Controller, was connected directly to the LBNP Device via a dedicated sample port. The pressure transducer sent signals to the Controller's microprocessor, which compared the actual pressure in the LBNP Device to the expected (programmed) pressure. This, in conjunction with the microprocessor's internal clock, allowed the Controller to regulate and control the pressure in the LBNP Device throughout the entire protocol. If power was terminated to the Controller unit, the solenoid valves would automatically default to the vent positions, allowing the LBNP Device chamber to return to ambient cabin pressure.

For simplicity, the Controller was limited to three protocols stored in memory. However, the capability existed to modify the Controller's software and external controls to allow much greater flexibility in executing alternate protocols. The three available protocols used during EDOMP were called "Ramp," "Soak," and "Alternate." The Ramp protocol tested the cardiovascular status of a crew member. The Soak was the treatment protocol and was to be performed within 24 hours of landing to obtain maximal benefits. The Alternate was a modified soak protocol that could be used for contingencies when the LBNP session was interrupted. LBNP sessions were initiated by pushing the appropriate button on the Controller. The Controller then executed the protocol, evacuating the chamber by -10 mmHg increments every 5 minutes until -50 mmHg was reached. The Ramp test ended after 5 minutes at -50 mmHg. During the Soak treatment protocol, the Controller performed a Ramp test before repressurizing the bag to -30 mmHg, where the subject "soaked" for approximately 4 hours. A final ramp to -50 mmHg was performed at the end of the soak to test its efficacy. In the Alternate protocol, the Controller decompressed the LBNP Device to -30 mmHg without performing a ramp test, and held it there for approximately 4 hours before returning to ambient (again without a ramp). A "Pause" feature was also provided. When the Pause button was depressed, the Controller would interrupt the protocol in progress, hold the last target pressure, and display a clock to indicate the time since the pause was initiated.

During all LBNP protocols, blood pressure, electrocardiogram (ECG), and heart rate were monitored with the use of an ABPM, identical to the ones used in the Ambulatory Cardiovascular Monitoring Assembly. The ABPM was connected to the LBNP Controller via a data cable, and analog data from the ABPM were processed by signal conditioning circuitry in the Controller. Analog data,

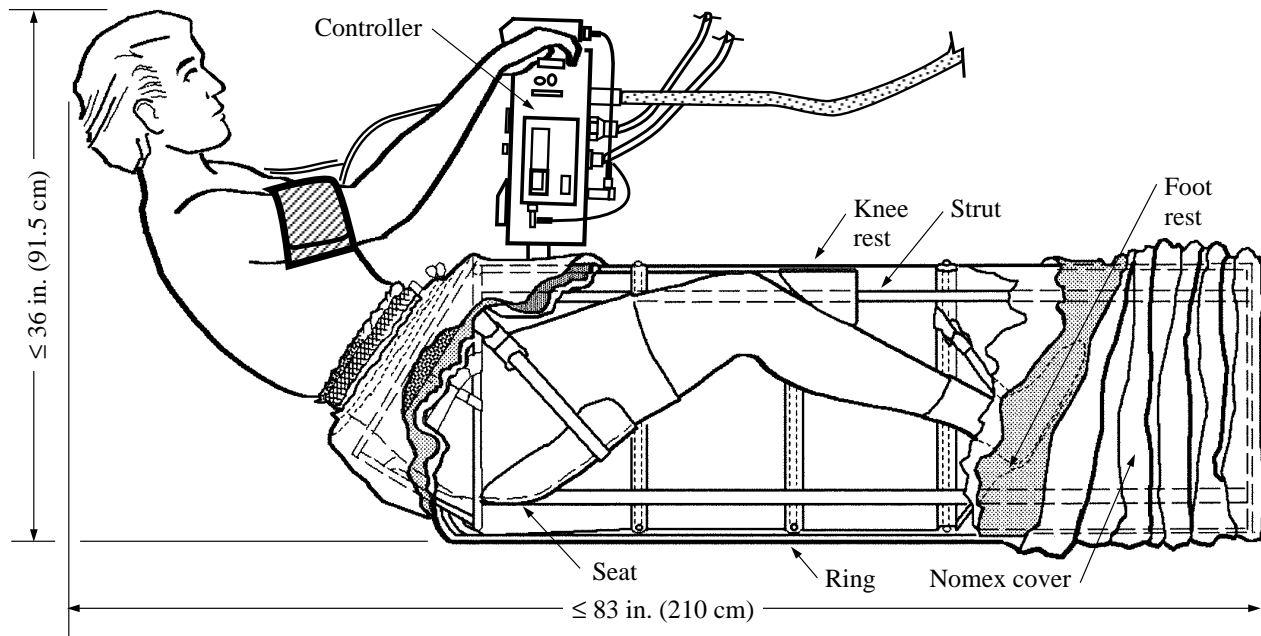


Figure 8-2a. Lower Body Negative Pressure (LBNP) Device.



Figure 8-2b. LBNP Controller.

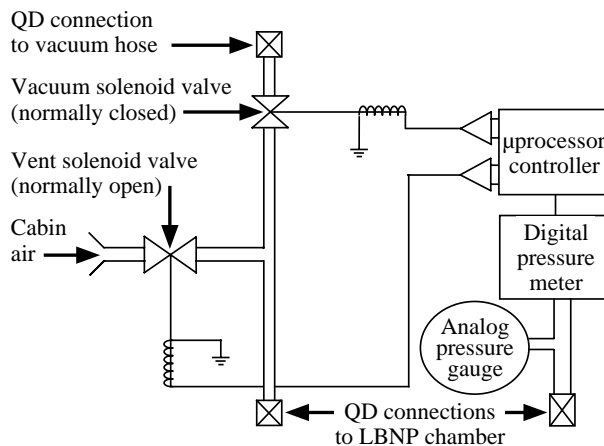


Figure 8-2c. LBNP Controller Schematic.

including continuous ECG, Korotkoff sounds, cuff pressure, LBNP vacuum pressure, and voiced comments were recorded onboard for postflight analysis using a 9-channel TEAC data recorder connected to the LBNP Controller.

For safety reasons, ground-based subject monitoring via telemetry was required during portions of the LBNP test and treatment protocols. Because LBNP was performed both in the middeck and in the Spacelab, the LBNP Controller had to be designed for two operational telemetry interfaces. In the middeck, data were down-linked via the Orbiter Bioinstrumentation System (OBS). In this configuration, conditioned analog data were sent

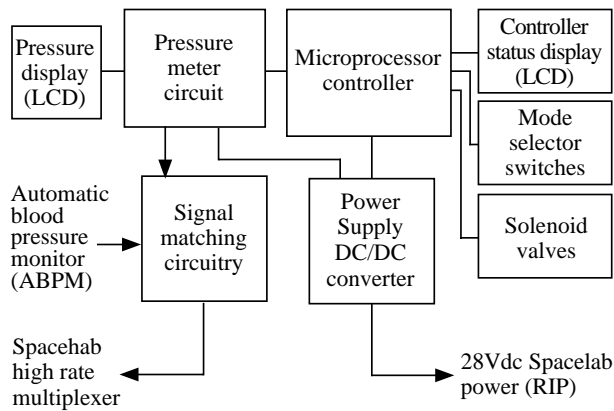


Figure 8-2d. Controller Data Flow Diagram.

via a data cable directly from the LBNP Controller to the OBS, which then digitized and downlinked the data as a part of the S-band communications. The two available OBS channels could be used to downlink any two of three available waveforms: ECG, blood pressure (K-sounds superimposed on cuff pressure), and LBNP pressure.

For Spacelab (Figure 8-2d), the analog signals were sent, via a data cable, to the Data Acquisition System (DAS) described in the next section, which processed data for the Spacelab telemetry system.

Onboard the Shuttle, the LBNP Controller provided real-time feedback to the crew members through a 20-character, 2-line liquid crystal display (LCD) that supplied continuous updates on chamber pressure and displayed a countdown to the next pressure change. An aneroid pressure gauge mounted on the LBNP Controller provided a redundant means of monitoring pressure in the LBNP Device. The ABPM tracked subject heart rate and blood pressure and provided the subject and operator with a digital readout of critical test termination criteria, such as a sudden drop in blood pressure. ABPM heart rate and blood pressure data were recorded on a hard-copy logbook by an astronaut trained to monitor subjects during testing. As a matter of course, a manual sphygmomanometer was also provided for use in the event of failure of or questionable data from the ABPM.

Data Acquisition System (DAS)

The DAS was a custom-designed flight data system for use during biomedical experiments such as LBNP that required access to the Spacelab telemetry stream. The DAS converted the analog signals from the LBNP Controller into digital data, and put the information into a serial data format compatible with the Spacelab High Rate Multiplexer (HRM). The DAS employed parallel processing technology, and consisted of analog signal processing circuitry, a network of analog to digital

converters, an Intel 486-based single-board computer, and a custom designed interface board with an imbedded processor and special output drivers that sent the digital data to the Spacelab HRM. The entire system fit into a compact enclosure measuring $13 \times 7.5 \times 5.5$ inches. The DAS also conditioned the analog signals and routed them to a redundant low rate data system called the Remote Acquisition Unit (RAU). The RAU provided a user time clock signal to the DAS for data synchronization. Both high and low rate data streams were multiplexed into the Orbiter's telemetry system for downlink via the S-band (low rate) and Ku-band (high rate) transmitters, and routed to flight surgeons and scientists monitoring the test on the ground.

Operations Acquisition System In-situ (OASIS)

To maximize benefits from the data sent to the ground by the LBNP Controller and DAS, a new system was developed for data acquisition from the Shuttle downlink telemetry. The OASIS was a portable, ground-based data processing system used to decode, display, and store information received from the Space Shuttle telemetry stream during LBNP operations in the middeck or the Spacelab. The OASIS could be used anywhere that access to telemetry data was available, such as the Science Monitoring Area (SMA) at JSC, the Payload Operations Control Centers (POCC) at MSFC and JSC, or during preflight testing in the Operations and Checkout Building at KSC. The OASIS made use of a custom designed Dual Serial Receiver board, together with special data acquisition cards in a personal computer (PC) system running customized software (developed under a LabViews platform). The OASIS system used two PCs (laptops with expansion chassis or desktop) to perform all of the functions that had previously required two racks of electronic equipment, a MicroVax computer, and a network of MacIntosh workstations. Virtual instrumentation displays on the PC monitors could be customized to perform data analysis in real or near real time, and display selected information to the investigators and medical personnel monitoring the experiment (blood pressure and heart rate trend analysis, pulse pressure monitoring, power spectral analysis of ECG, etc.). Alarms could be programmed to alert when heart rates or blood pressures approached predetermined test termination criteria. The multi-tasking capabilities of the PC workstations were optimized to display data in multiple windows simultaneously.

American Echocardiograph Research Imaging System (AERIS)

The AERIS (Figure 8-3) was a clinical ultrasound/Doppler medical imaging device (Biosound Genesis II), highly modified and repackaged for spaceflight, and

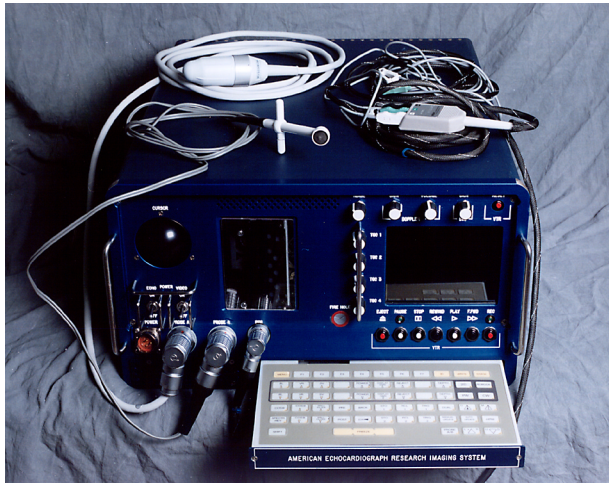


Figure 8-3. American Echocardiograph Research Imaging System (AERIS).

used to record images of the heart during LBNP studies. The AERIS was capable of: (1) displaying one- and two-dimensional images of the heart and other soft tissues, (2) performing noninvasive Doppler blood flow measurements, (3) recording on 8 mm video tape all ultrasound images or route image to an on-board camcorder, and (4) measuring or deriving the cardiac parameters of stroke volume, cardiac output, wall motion, and chamber dimensions.

A number of modifications were performed to make the AERIS useable during spaceflight. An external enclosure and an internal card cage were fabricated that could withstand launch vibration loads and protect internal circuit boards. The device was modified to fit into a single middeck locker. The original power supply was converted from alternating current (AC) to 28 volts direct current (VDC), the standard Orbiter power. The cathode ray tube (CRT) display was replaced with a color LCD flat panel display, and a small 8mm video tape recorder (VTR) was installed to provide recording and playback capabilities. After the first flight of AERIS on STS-50 [United States Microgravity Laboratory-One (USML-1)], a number of improvements were made to enhance cooling efficiency in zero gravity and improve device reliability.

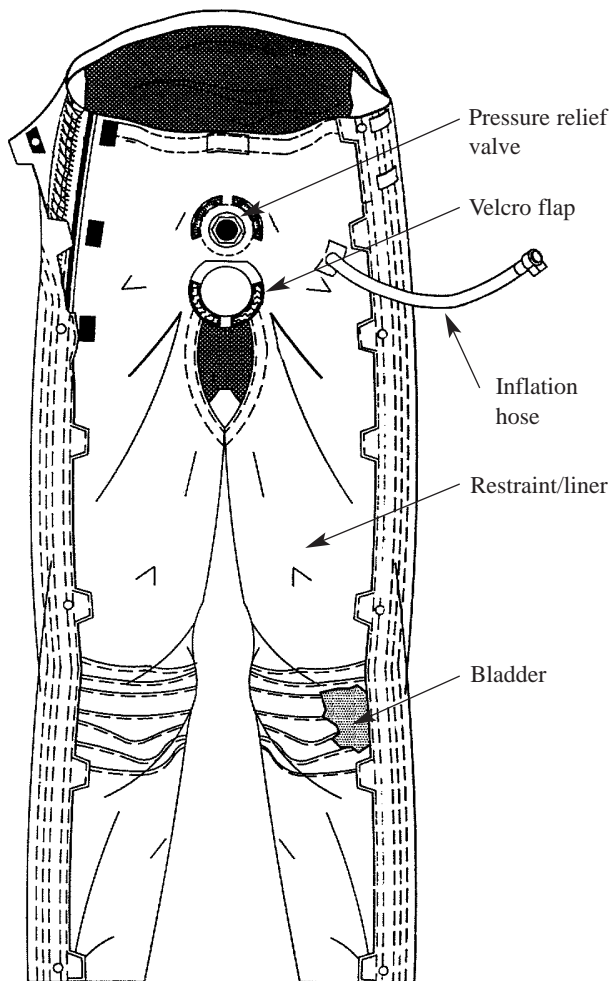


Figure 8-4. Re-entry Anti-gravity Suit (REAGS).

Re-entry Anti-gravity Suit (REAGS)

EDOMP initiated the research and development of a new anti-gravity suit (g-suit) that would improve crew comfort when inflated and provide the physiological protection needed for the Shuttle reentry profile of <2-g (Figure 8-4). Prior to the REAGS, the Shuttle g-suit (model CSU-13) was a five-bladder suit that included abdominal coverage and was designed to provide protection during the high gravity environments.

A 30-month study, conducted with the United States Air Force Armstrong Laboratory, culminated in the fabrication and functional verification of an improved garment that was ready to enter operational status concurrent with the Advanced Crew Escape Suit (ACES). The REAGS garment employed fuller leg coverage than the CSU-13, and deleted the abdominal bladder. It provided greater gravity protection than the CSU-13, at lower pressure, and without the discomfort associated with the abdominal bladder used in the older g-suit. The first Shuttle flight to use the REAGS was STS-71 in July 1995. Later modifications, such as the use of Gortex fabric and a lightweight zipper, were made to reduce the bulky nature of the suit when used in combination with the Liquid Cooling Garment (LCG).

Bar Code Reader

The Bar Code Reader (Figure 8-5) was a modified COTS device (Trakker Scanner by Intermec) used to



Figure 8-5. Bar Code Reader.

simplify repetitive logging of data or samples (food consumed, blood and urine samples, etc.). It was a rechargeable, battery-operated device first used in support of DSO 610. It was used to log each urine sample by scanning the bar code labels on the urine collection devices and the thymol and thimerosal syringes. The laser scanner inside the Bar Code Reader would scan the label when the crew member pushed one of the orange buttons on the side, and the scanned data record along with the current Mission Elapsed Time (MET) would be logged into battery-backed static memory. The Bar Code Reader was also equipped with an alpha-numeric keypad so that information could be entered manually if a label had been damaged or was missing or dirty. The Bar Code Reader was also programmed to scan food items and drinks, and to record exercise sessions. After flight, the Bar Code Reader data were downloaded onto a computer.

Urine Collection Kit

The Urine Collection Kit was designed for the in-flight collection of urine used in metabolic and renal stone studies (DSOs 610 and 612). The kit (Figure 8-6) consisted of a Urine Collection Device (UCD) contained within one 12 × 5 inch ziplock bag, placed into a second 12 × 6 inch ziplock bag. The UCD was a polyvinyl chloride (PVC) bag with an inlet and an outlet port. A syringe was used to draw aliquots of urine through the outlet port for in-flight or postflight analysis. The UCD had a plastic clamp which slipped over the inlet port for added protection against leakage after use. To contain odors and any leaks, the urine kits were placed in a large Nomex bag with a watertight polyurethane-coated nylon lining and a watertight zipper. The zippered opening of this bag had an absorbent filter paper as further protection against any urine leaks.



Figure 8-6. Urine Collection Kit.

In-flight Urine Collection Absorber (IUCA)

The IUCA, used to support DSO 328, consisted of an absorbent filter paper placed into the funnel of the Shuttle Waste Collection System urinal. The filter paper was cone-shaped and would therefore fit different funnels. After the crew member collected urine on an IUCA, it was placed into an ordinary plastic ziplock bag, then into a second ziplock-style bag made of metallized plastic, and finally into a Nomex bag, lined with waterproof polyurethane-coated nylon. The top of this Nomex bag rolled over for closure and tied down with straps. A small rectangular piece of Spandex at the top of this Nomex bag contained some absorbent filter paper to absorb any leaks. The Nomex bag, containing approximately ten IUCAs, was returned to JSC for postflight analysis.

Saliva Collection Kit

Collection of saliva is a noninvasive technique that was used frequently for pharmacologic and metabolic studies. Although several kit configurations were developed to support DSOs 612 and 622, each consisted basically of a Nomex pouch in which a quantity of collection vials was secured by means of foam inserts or elastic straps. Each vial, containing a sterile dental cotton roll, was labeled and color coded, and contained a space for the crew member to record sampling time. The kit also contained a marker, a pair of tweezers (to facilitate removal of the cotton roll from the vial), and inert Parafilm strips that the crew members could chew to stimulate salivation if necessary.

Two different types of collection vials were used. Plastic Salivette vials (developed for NASA by Sarstedt) were used for drug pharmacokinetics studies. After flight, each vial was placed into a plastic adapter that

allowed it to fit into a standard centrifuge test tube holder. The saliva samples were then removed from the vials by centrifugation for subsequent analysis. For studies involving the calculation of total body water, saliva samples were typically collected following ingestion of a tracer such as water labeled with "heavy oxygen" (^{18}O) and deuterium (^2H). In this case, glass lyophilization vials were used in place of the plastic Salivettes because the concentrations of isotopes involved were extremely low, and the plastic vials were porous enough that contamination of the samples via evaporation of the tracer dose and transport through the vial walls was possible. When the glass vials were used, each vial was wrapped in protective Teflon shrink-wrap and adhesive Teflon tape. This reduced the chance of breakage and would have contained the glass fragments if breakage occurred.

Breath Sample Kits

The Breath Sample bags used for DSO 622 were commercial off-the-shelf Mylar bags (QuinTron, Menomonee Falls, WI) with one-way valves. The bags were prepackaged with a reagent that changed color when exposed to gaseous hydrogen. The digestion process was tracked based on the production of gaseous hydrogen. At specific times after ingesting acetaminophen, the subject would collect a breath sample by blowing into the breath sample bag. After flight, the amount of hydrogen at each sample period was determined by the amount of color change resulting from the reaction of the reagent with hydrogen.

Doubly Labeled Water (DLW) Dose Kits

For DSO 612, energy utilization was measured through the use of DLW, which contains the non-radioactive tracers, ^2H and ^{18}O . After ingestion, the tracers were measured in saliva and urine. The DLW Dose Kit contained water with ^2H and ^{18}O . The crew member drank one DLW dose per flight from a standard drink container that had been stored in double ziplock bags to contain any leaks. Kits were stowed in the fresh food lockers and returned postflight for final weighing to see how much water was not ingested.

Performance Test Unit

The Psycho-Log 24 (Data Source, Valflaunes, France) was a self-contained, portable device for measuring a variety of psychomotor functions for DSO 484. It measured approximately $6 \times 4 \times 2$ inches and weighed 11 oz. It could be programmed to administer visual analog scales, a log of sleep and wake times, visual and auditory reaction time tests, a mental arithmetic test, and letter cancellation tests.

Actilume

The Actilume (Ambulatory Monitoring, Inc., Ardmore, NY), used for DSO 484, was a microprocessor-based activity monitoring device ($3 \times 1.5 \times \text{in.}$) worn on the wrist. It contained an accelerometer that measured locomotor activity in three dimensions and a photo sensor to measure illuminance. In addition, external probes such as a skin temperature probe and an external photo sensor could be attached to measure additional variables. A flexible membrane button could be depressed to mark events. The locomotor activity data could be used to estimate sleep variables by using either a pre-programmed or customized scoring algorithm.

Glucometer Kit

The Glucometer Kit, used in support of DSO 612, contained a battery-operated blood glucose meter (ONE TOUCH® II). This was a hand-held device that could measure and display blood sugar levels from a single drop of blood. The kit also included lancets, test strips, control reagents, alcohol wipes, gauze, a Sharps Waste Container, and Band-Aids. The ONE TOUCH II Blood Glucose Meter was commercially available and required only minor modifications for spaceflight.

Drug Administration Kit

The Drug Administration Kit, used for DSOs 612 and 621, consisted of a 12×12 inch ziplock bag that contained one or more Nomex pouches designed to hold drug capsules. Each pouch consisted of two rows of six small Teflon-lined pockets, each with its own Nomex and Velcro closure. Each pocket contained a predetermined dose of the appropriate drug. One pouch, identified with the subject name and color code dot on a label inserted into a Teflon window, was flown for each crew member participating in the investigation.

Heart Rate Watch Assembly

Heart rate data, collected for DSOs 476, 608, and 624 during in-flight exercise, were displayed and stored using this equipment (Figure 8-7). The Heart Rate Watch Monitor (POLAR Vantage XL) Assembly was made up of three parts: the battery-operated wrist monitor, the battery-operated sensor/transmitter, and the chest band. The wrist monitor displayed the time of day, elapsed time, and heart rate, and stored the heart rate data. The chest band was an adjustable elastic belt containing conductive electrodes and transmitter connectors. The sensor/transmitter was activated as it was snapped onto the chest band. The POLAR Vantage XL was commercially available and required only minor modifications for spaceflight.



Figure 8-7. Heart Rate Watch Assembly.



Figure 8-8a. Biotest Microbial Air Sampler (MAS) with Accessories.

Microbial Air Sampler (MAS)

Three types of microbial air samplers (Biotest RCS, Biotest RCS Plus, and Burkard) were tested during the EDOMP for DSO 611. All three were battery-operated, hand-held devices that impacted a measured volume of air onto the surface of an agar medium. The purpose of DSO 611 was twofold: (1) to determine types and levels of bacteria and fungi in spacecraft air and on spacecraft surfaces during the course of long duration missions, and (2) to test the hardware for compatibility with spaceflight requirements. The agar strips and other accessories for the Biotest units were stowed in Nomex pouches attached to a Nomex belt, which could be worn by the crew member for convenience and mobility when sampling (Figure 8-8a). The Burkard unit (Figure 8-8b) required agar dishes rather than strips and was stowed in a Nomex kit which the crew member could easily transport to each sampling site and attach to a wall if desired. The MAS units were commercially available and required minor modifications for spaceflight.



Figure 8-8b. Burkard Microbial Air Sampler (MAS).

Combustion Products Analyzer (CPA)

The CPA (Figure 8-9), used for Development Test Objective (DTO) 645, was a battery-powered, portable, real-time monitoring instrument used for the measurement of four gases that could result from thermodegradation of synthetic materials used in spacecraft. The CPA was developed specially for NASA by Enterra Instrumentation Technologies (Exton, Pennsylvania). The gases to be monitored were carbon monoxide, hydrogen chloride, hydrogen fluoride, and hydrogen cyanide. The CPA contained four electrochemical sensors (one for each gas) and a diaphragm pump to pull air over the sensors. The immobilized electrolyte in each sensor permitted the instrument to function in space and eliminated the



Figure 8-9. Combustion Products Analyzer (CPA).

possibility of electrolyte leaks. The sample inlet system was equipped with a particulate filter that prevented clogging from airborne particulate matter. Other features included a digital readout that displayed gas concentration and various warning signals such as low battery and low flow. The instrument could be set to scan the concentrations of all four gases, or it could monitor one gas continuously. The CPA was flown on the Orbiter for contingency use only. The CPA was to be unstowed and powered on only in the event of a combustion incident. Data obtained by the CPA would provide valuable information to the crew and ground personnel for management of the response to the combustion incident.

Archival Organic Sampler (AOS)

The AOS used for DSO 611 was a passive collection device that was used to detect the presence of volatile organic compounds in spacecraft air (Figure 8-10). Stored in individually sealed aluminum canisters to prevent contamination before and after deployment, each AOS contained a chamber filled with a sorbent medium (typically Tenax) retained by a stainless steel screen. Air passively entered the AOS through a precision-drilled orifice located in the center of a stainless steel plate. The sample rate of an AOS could be varied by exchanging the orifice plate for one with a smaller or larger orifice.

Before flight, each AOS was thermally cleaned, proofed (verified clean) using gas chromatography/mass spectrometry (GC/MS), and sealed inside an individual canister. Up to 12 of the devices could be flown on a mission to support multiple sampling locations and sessions. During flight, a crew member opened and deployed these devices to predetermined sampling locations in the Orbiter. One sampler served as a control and was not opened or deployed. Each AOS was exposed to the cabin atmosphere



Figure 8-10. Archival Organic Sampler (AOS).



Figure 8-11. Formaldehyde Monitor.

for 24-48 hours. At the end of the sampling period, each AOS was re-sealed inside its canister and stowed for return. Upon return to the JSC Toxicology Laboratory, each AOS was thermally desorbed and analyzed using GC/MS.

Formaldehyde Monitor Kit

The Formaldehyde Monitor Kit, used for DSO 488, consisted of formaldehyde monitor badges (Air Quality Research, Durham, NC) (Figure 8-11), which were passive collection devices modified for use either as personal samplers and worn by crew members near their breathing zones, or deployed on the wall as area samplers. Sampling of the spacecraft atmosphere began when a crew member exposed the badge by removing a seal covering the sampling orifice on its face. Sampling was stopped by placing a second seal over the sampling orifice. The crew member recorded the start and stop time on the badge. Personal sampling was performed during waking hours. Area samplers were deployed for approximately 24 hours at locations that provide adequate movement of air across the face of the sampler. Positive and negative control monitors were also used. The monitors used as positive controls were dosed with known quantities of formaldehyde before delivery for the mission. The negative controls were monitors that were not exposed to the cabin atmosphere during the flight. Exposed monitors and controls were analyzed after flight.

Shuttle Particle Sampler (SPS) and Shuttle Particle Monitor (SPM)

DSO 471 was conducted as part of EDOMP to measure and characterize airborne particulate matter during two Shuttle missions, STS-32 and STS-40. Specifically,

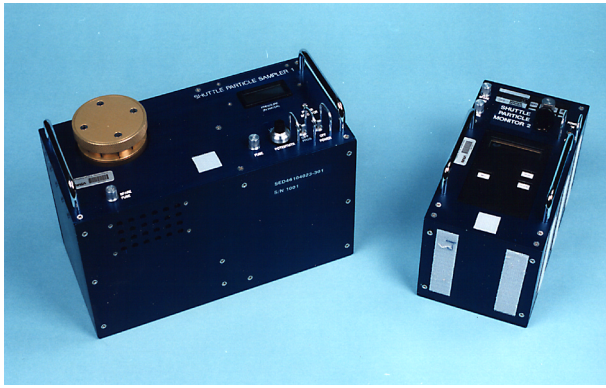


Figure 8-12. Shuttle Particle Sampler (SPS) and Shuttle Particle Monitor (SPM).

the objective was to characterize the concentration, size distribution, composition, and potential sources of airborne particulate matter in the Shuttle flight deck and middeck areas. The instrumentation developed for this experiment consisted of (1) two SPS units which collected particles in four size fractions during two 24-hour sampling periods, and (2) the SPM which continuously monitored and stored particle concentrations during the mission (Figure 8-12). The SPS and SPM hardware were developed jointly by NASA and the Particle Technology Laboratory at the University of Minnesota.

The SPS was $12.5 \times 6 \times 9$ in. in size and weighed 20.7 lbs. The SPS was self-contained and included a particle collector, vacuum pump, filter, control circuitry, and battery pack. Functionally, the SPS sorted and collected particles in four size fractions: $<2.5 \mu\text{m}$, 2.5 to $10 \mu\text{m}$, 10 to $100 \mu\text{m}$, and $>100 \mu\text{m}$. Those particles $>100 \mu\text{m}$ were collected on a 150-mesh screen with $100 \mu\text{m}$ openings, located in the sampler inlet cap. Particles in each of the other three size fractions were collected on 37 mm diameter filters made of Teflon membrane material. Two virtual impactor stages, each consisting of six parallel nozzles, were used to size-fractionate the sampled particles on the basis of their aerodynamic diameter. The samples collected with the SPS underwent a variety of analyses. All filters were weighed before and after sampling to determine the mass concentration of particles collected. Fine particle fractions were then analyzed for elemental composition by x-ray fluorescence. Course particles were analyzed by scanning electron microscopy to determine single particle morphology.

The SPM measured $10.5 \times 5 \times 6.5$ in. and the unit weighed 10 lbs. The SPM consisted of four primary components: a MiniRam photometer, a data logger, and two battery packs. The MIE Model PDM-3 MiniRAM (MIE, Bedford, MA) provided a real time, in-situ measure of the particle concentration based on the nephelometric principle. The minimum, maximum, and average particle

concentration during each 15-minute sampling period was automatically collected and stored in the data logger.

Visual-Vestibular Data System (Superpocket)

The Superpocket System, a physiological signal acquisition system, was used with DSO 604 Operational Investigation-3 (OI-3) to record electro-oculogram (EOG) and head movement data on orbit and during Shuttle entry. The Superpocket System consisted of a target, the data acquisition and control system, cables, batteries, a TEAC data recorder, and the Goggle Assembly. The Goggle Assembly consisted of a laser pointer, a polymer dispersed liquid crystal (PDLC) light occluding lens, EOG electrodes, and rate sensors (Figure 8-13). A remote control device was used to operate the laser and the PDLC lens. A Subject Preparation Kit included electrodes, electrode gel, and accessories. The system was designed to fit into one middeck locker and did not require Orbiter power.

The Superpocket System recorded up to twelve analog channels and one voice channel for subject commentary. The EOG signals were amplified 4000 times with a bandwidth of 0 to 700 Hz. Full scale after amplification was four to five times the effective range of EOG, allowing relatively strong drifts during recording. Each analog channel arriving in the Superpocket electronic box was filtered with an anti-aliasing, fourth order Bessel filter and sampled every 7ms with a resolution of 12 bits. These twelve channels were multiplexed on two pulse-code-modulation channels and recorded on the TEAC data recorder. The subject was instrumented with EOG electrodes above and below the eye. Electronic Light Occluding Goggles (ELOGs), fabricated from off-the-shelf ski goggles, were also worn to either allow vision

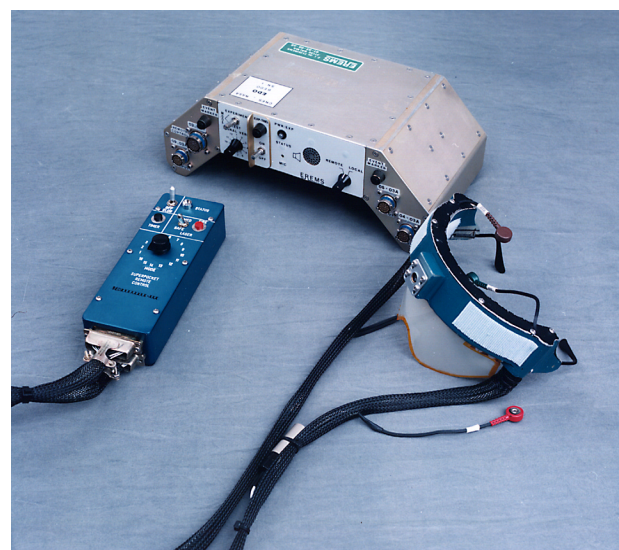


Figure 8-13. Superpocket System.

or occlude vision during testing. The lens was covered with a PDL film which was opaque in its natural form and clear when power was applied. The ELOGs were adjustable to fit any crew member. The goggles were placed over the subject's eyes and the recording session was started by pressing a button on the remote control. The Superpocket System data acquisition and control module was developed by the French Space Agency, Centre Nationale d'Etudes Spatiales (CNES) and modified under the direction of the NASA/JSC Neurophysiology Laboratory. All other components were developed by NASA/JSC.

Locker-Mounted Video Camera System

The Locker-Mounted Video Camera (Figure 8-14) was used to provide DSO 620 investigators with an objective view of crew member balance and equilibrium immediately after landing and wheels stop. The system was designed to fit into one middeck locker and required a special locker door with an opening for the camera. The Locker-Mounted Video Camera System consisted of a commercially available video camera (Sony CCD-TR7), an aluminum camera mount held in position in the locker by dense polyethylene foam, a light attached to the video camera to illuminate the immediate area of the video recording, and accessories, including a headband, marker harness, two batteries, video tape, Velcro visual targets, and a remote control.

For operation, the remote control was attached to the video camera with a quick-disconnect type connector. In preparation for performing the DSO after landing, the crew member performed a quick check of the remote control and camera while on orbit. After wheels stop, the crew member donned the headband and harness, and with the remote control, activated the camera for data recording.

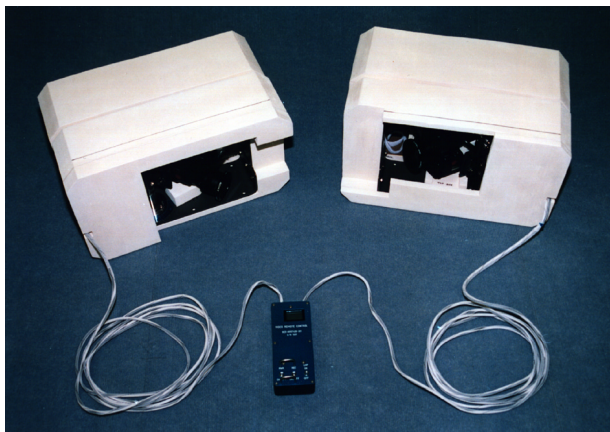


Figure 8-14. Locker-Mounted Video Camera System.

Cycle Ergometer (CE)

The CE, used in conjunction with DTOs 651, 658, 682, DSOs 608, 618, 476, and as an operational exercise device, was developed as part of a suite of exercise equipment to be used for maintaining cardiovascular and musculoskeletal fitness during EDO flights. An additional goal was to evaluate candidate exercise hardware that might eventually be used on the International Space Station. The CE system was conceived to maximize comfort, minimize acoustic noise and vibration, and yet provide reproducible, quantifiable workloads for comparison of exercise profiles in flight and on the ground.

The CE system consisted of the Cycle Ergometer (load module), a mounting frame, and an accessories case containing pedals, cycling shoes, etc. Innovision, A.G. of Odense, Denmark, developed the CE load module under contract to KRUG Life Sciences, Inc.

The workload mechanism in the load module consisted of a conventional flywheel and braking-band system, with the resistance being controlled by a stepper motor that regulated braking-band tension. In the event that power was not available, workload could also be adjusted using a manual knob to increase or decrease tension on the braking band. An external control panel was used to display deviation from the desired pedal cadence (from 50 to 120 rpm in increments of 5 rpm) and to set the desired workload (from 0 to 350 W in 25 watt increments). The CE also had a serial data port, which provided the capability to receive commands and be controlled from an external computer, allowing predefined protocols to be executed automatically. Data such as achieved work load and RPM could be continuously recorded on the computer during execution of the protocols. The CE was designed to operate on 28 VDC power at 15 watts.

A major design challenge was the mounting frame, which had to include structural elements for attachment to the Orbiter during launch, as well as a means of subject restraint. During the development phase, testing on board the KC-135 showed that a recumbent cycling position was extremely comfortable and stable in zero gravity, and required only a seat back to offset the loads generated by the legs while pedaling. The use of handlebars and/or an upright seat was less comfortable and caused arm fatigue as the operator attempted to stabilize him/herself by gripping the handlebars tightly. Thus the recumbent position was chosen for the CE.

For launch, the CE interface frame had to mate to the middeck floor using the same attachment points used by the Shuttle Treadmill (mounting studs of the type used in military cargo aircraft). However, the launch location was not suitable for on-orbit exercise for a variety of reasons. Instead, it was decided that the attachment points used during launch and landing for mission specialist seats (which are normally removed and stowed for on-orbit activities) were ideally placed for exercise using the

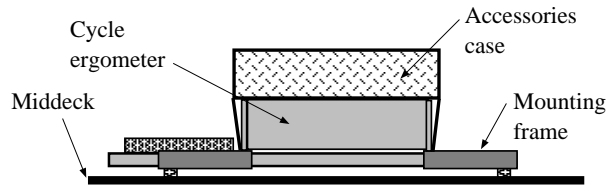


Figure 8-15a. Cycle Ergometer in Launch and Landing Configuration.

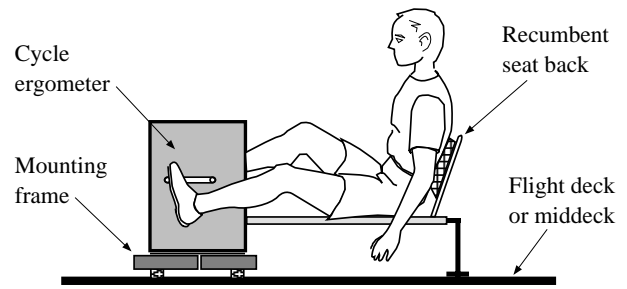


Figure 8-15c. Crew Member Exercising on Cycle Ergometer.

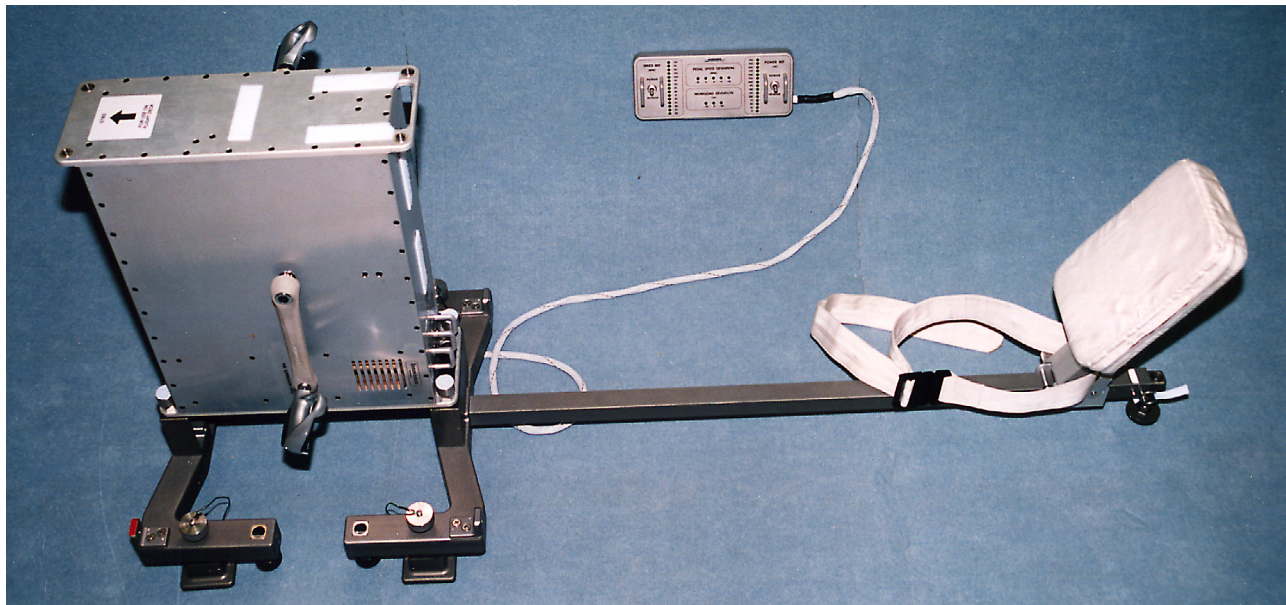


Figure 8-15b. Cycle Ergometer in Deployed Configuration.

CE. This offered the added advantage of allowing the CE to be used either on the flight deck or the middeck. However, since the footprint of attachment points for the treadmill is different from that of the mission specialist seats, a novel approach to design of the CE mounting frame was required. The result was a light weight, two-piece frame that was could be easily reconfigured by crew members in orbit. For the launch configuration, the CE load module lay flat on its side (to lower the center of gravity) on the two halves of the mounting frame. The load module and seat back stem became structural members for launch (Figure 8-15a).

For operation on orbit, the positions of the two mounting frame halves were reversed, and the CE load module was placed upright on top of them. The pedals, control panel, and power cable were connected to the CE. The seat back was positioned on the seat stem, and was set at a comfortable angle and distance from the pedals (Figure 8-15b). The exercising position is shown in Figure 8-15c.

Evaluation of the CE (as DTO 651) occurred on three flights and included hardware setup and operation, as well as determination of physiological responses during CE exercise. The results showed the CE to be an effective exercise device for use during spaceflight.

Ergometer Vibration Isolation System (EVIS)

Vibration on the orbiting Shuttle, which can be caused by many sources, disturbs sensitive microgravity experiments. The need to preserve the microgravity environment and ensure success of these experiments must sometimes be considered when devising means whereby the astronauts can receive adequate in-flight exercise to reduce muscle atrophy, loss of aerobic capacity, and general deconditioning. As mission duration increases, the need for regular exercise becomes even more important. Thus, the need for an effective method to minimize exercise-induced vibration was high priority for the EDOMP.

EVIS, developed to isolate the vibration caused by cycle ergometer exercise, was flown on STS-50 and evaluated by DTO 658. The EVIS employed isolators (composed of linear bearings, springs and dashpots) at four corners of a special one-piece CE mounting frame to inhibit transfer of forces to the spacecraft structure, and four active "throw-mass" type stabilizers to counteract the forces induced by exercise and stabilize the ergometer. The stabilizers used linear motors to drive the throw masses. Accelerometers and sophisticated control feedback circuitry were used to detect the forces and control the motion of the stabilizers. Because of the significant amount of power required by the stabilizer motors, power for EVIS was provided by the Orbiter 120 VAC 400 Hz system, internally rectified to DC within the EVIS electronics (the CE was powered by 28 VDC as described above). Isolation was provided in all three axes; however, through modeling and analysis it was decided that the primary axis of stabilization should be that in which the primary motion of the legs occurred (i.e., parallel to the seat stem in Figure 8-15c). Data were collected by the Space Acceleration Measurement System (SAMS) payload during ergometer runs with and without EVIS. Results indicated that EVIS reduced the vibration significantly. However, the results from this DTO also showed that a passive system, without the active stabilizers, was capable of significantly reducing the level of vibration transmitted to the Orbiter during cycle exercise. In addition, analysis of video collected during tests revealed that the motion most in need of stabilization during ergometry was not translation in the plane of the seat stem, but rather roll about an axis parallel to the seat stem. Given the simplicity and reduced weight, volume, and power requirements of a passive (as compared with active) system, EVIS was not recommended for further development for ergometry. However, the EVIS control system and stabilizers became the basis for a vibration isolation and stabilization system that would later be developed for the International Space Station treadmill.

Passive Cycle Isolation System (PCIS)

PCIS evolved from the lessons learned from EVIS. PCIS hardware (Figure 8-16) worked by allowing the ergometer to free-float using low force isolators connected to the Orbiter.

PCIS consisted of four isolators that were installed between the CE mounting frame and the Orbiter floor. The isolators were of a much simpler construction than the EVIS isolators used previously. Each isolator was composed of wire rope wound into several loops to form a sphere of about 5 inches in diameter. During exercise, the isolators responded independently to the motion of the crew member, allowing the system to rock back and forth. Each isolator experienced the full spectrum of

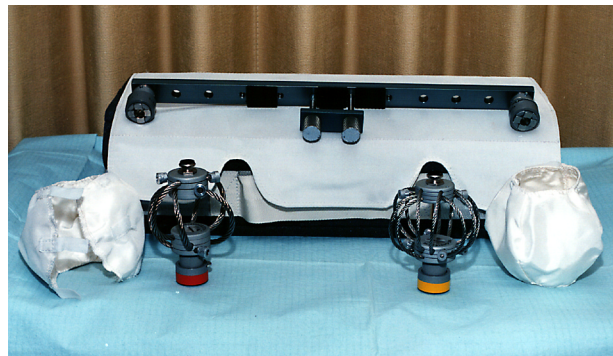


Figure 8-16. Passive Cycle Isolation System (PCIS).

disturbances, including torque, translation, compression, and extension forces. The restoring force produced by the isolator was a function of the stiffness of the wire loops comprising the sphere. The wire ropes essentially functioned as both springs and dampers, isolating the motion of the ergometer and acting as energy absorbers by bleeding off a small amount of energy.

PCIS was first flown through DTO 682 on STS-62 in February, 1994. Although the isolators performed as expected to reduce loads transmitted to the spacecraft, it was also seen that additional stabilization was required for effective exercise.

Inertial Vibration Isolation System (IVIS) for the Cycle Ergometer

IVIS was another product of the lessons learned from the EVIS experiment. IVIS was conceived to provide the roll stabilization lacking in EVIS and PCIS. The IVIS consisted of two aluminum boxes that mechanically interfaced with the cycle ergometer (Figure 8-17). Each box contained a throw mass, mounted on linear bearings, and a system of linkages to drive the throw mass. The IVIS boxes were geared directly to the pedal shaft. As the astronaut pedaled the ergometer, the throw masses moved inside the IVIS boxes to create a counter-torque which was applied to the ergometer. This counter-torque acted to nullify the major torque created by the motion of the cyclist's legs and upper body. The torque created when riding the cycle was dependent on cycling speed and workload. Weight and cycling style were major factors in cycling disturbance, so the ability to allow for gross adjustments was added. Therefore, IVIS boxes were equipped with a gain setting selection of low, medium, or high, signifying the amount of counter-torque to be delivered through the system. The masses traveled a maximum of 3.5 inches in the high gain setting to provide an oscillating torque on the ergometer, opposing the exercise-induced torque. When the gain was properly set, the torque produced by the IVIS boxes was equal and opposite to the torque produced by the cyclists.

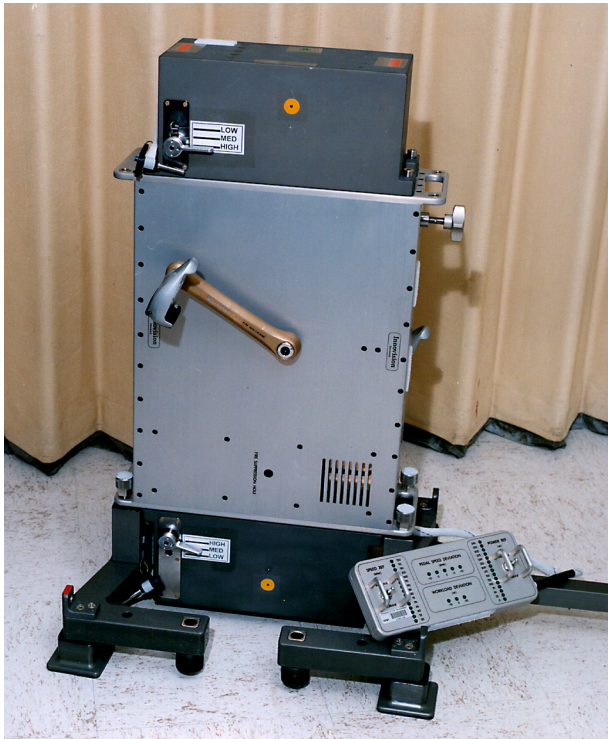


Figure 8-17. Cycle Ergometer with Inertial Vibration Isolation System (IVIS) Boxes attached.

IVIS was conceived to work in tandem with PCIS. The combined systems were first flown on STS-65, International Microgravity Laboratory-2 (IML-2) in July, 1995 and yielded excellent results. The Space Acceleration Measurement System (SAMS), which was used to record vibration and disturbances during Shuttle missions, and the MMD (see below) confirmed this finding. Video analysis and crew comments also attested to its effectiveness. The PCIS and IVIS combination was also flown in October, 1996 on STS-73, United States Microgravity Laboratory-2 (USML-2), and again yielded excellent protection against microgravity disturbances, as confirmed by the MMD.

Microgravity Measuring Device (MMD)

The MMD, a compact, lightweight acceleration measuring system with the capability to measure, display, and store in-flight acceleration data, was connected to an Orbiter-supplied Payload General Support Computer (PGSC) as the user interface and data storage device. The MMD was ideal for use on missions where real-time acceleration data could enable the crew to make assessments regarding onboard activities and the impact on the microgravity environment. The MMD also provided the capability to send acceleration data files to the ground via telemetry (downlink), thus allowing investigators to observe and evaluate any disturbances to which their payloads were subjected.

Although the MMD was originally developed to support activities for the Wake Shield experiment, one unit was modified for middeck application (Figure 8-18). The primary objective was a performance assessment of PCIS and IVIS with the cycle ergometer. During exercise on the CE with the PCIS and IVIS, crew members observed real-time acceleration data measured on the MMD and displayed on the PGSC. The secondary objective was to evaluate the ease of use of MMD. The MMD was flown as DTO 913 on two microgravity missions: STS-65 (IML-2) and STS-73 (USML-2). The STS-65 crew reported that the MMD was easily set up and stowed and that the software written to drive the data display and acquisition was straightforward and user friendly. The crew members provided some input to assist engineers in fine-tuning the device before it was flown on STS-73. The MMD again performed quite satisfactorily on STS-73. Crew members collected data that were downlinked to the ground, allowing payload investigators to view the acceleration environment on board the Orbiter during exercise and other activities.

EDO Treadmill

Radically different from its predecessor, the Shuttle treadmill, the EDO Treadmill (Figure 8-19) incorporated significant design changes intended to reduce acoustic noise output, increase comfort, and provide the ability to quantify workload. In comparison with the Shuttle treadmill, the EDO Treadmill, tested under DTO 659, had a longer running surface, a more comfortable and stable crew restraint harness, electronically adjustable devices to apply restraint force, and the capability to display effective weight (restraint force) of a subject. A control

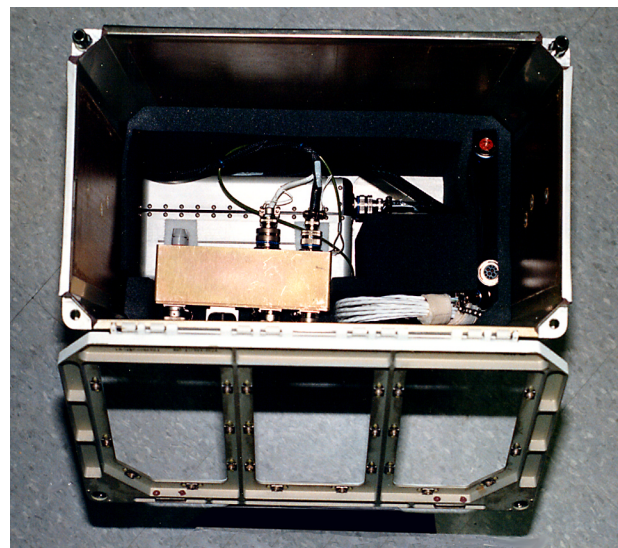


Figure 8-18. Microgravity Measuring Device (MMD) mounted in Middeck Locker.

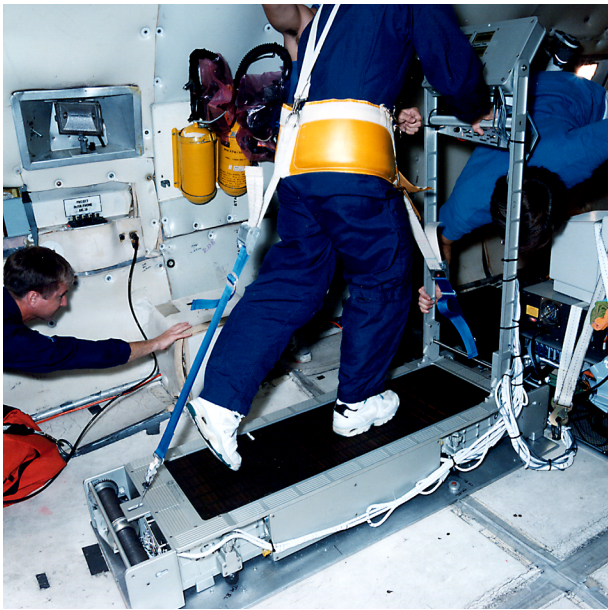


Figure 8-19. Subject Using EDO Treadmill on KC-135.

panel provided a means of adjusting restraint force, and displaying feedback on several exercise parameters such as speed and distance traveled. The EDO Treadmill was a passive (non-motorized) device and could be used with or without Orbiter power, though control panel functions were not available in the unpowered mode.

Major components of the EDO Treadmill included the tread running surface, Subject Load Devices (SLDs), a Device Interface Box (DIB) containing the majority of the electronics, a folding handrail with control panel and integral credit card memory (CCM) data storage system, and an accessory bag containing the subject harness, exercise clothing, shoes, and other accessories.

The running surface was 44 inches long and 13 inches wide, and consisted of a flexible belt to which rigid tread segments were attached, allowing flexion in only one direction. The tread belt was supported by two large diameter rollers at the forward and aft ends of the treadmill, and by two longitudinal support members with a series of small rollers running the length of the running surface. This was a complete change from the older treadmill design, which had incorporated hollow metal segments with wheels at both ends that moved around a “race track” in the side walls of the treadmill. The new design dramatically decreased the noise level of the treadmill during use and provided a more natural “feel” for the subject when running. Load cells installed under the longitudinal support members provided information on the restraint force and on foot strike forces.

One of the most difficult challenges in designing a device for running in microgravity was development of a

comfortable, effective subject restraint system. Because of the absence of gravity, a load must be applied to the subject in order to allow jogging or running. The new treadmill featured two SLDs and a subject-worn harness that attached to the treadmill at three points. The SLDs attached to the forward and aft faces of the treadmill and produced restraint forces using adjustable torsion springs coupled to cable-feed pulleys. The amount of load applied by the SLDs was controlled by the subject, using a keypad on the control panel. When the subject entered the desired restraint force, a microprocessor in the control panel sent commands that were relayed to the SLDs. A motor control circuit in each SLD then increased or decreased the preload on the torsion springs to achieve the desired restraint force. A linear potentiometer in each SLD provided feedback on motor position, which was proportional to the load supplied by the SLDs. Each SLD also contained a load cell to measure actual restraint force applied by the cable. Together, the two SLDs provided a restraint force of up to 220 pounds in the axis normal to the tread surface. The control panel displayed the actual versus desired load, allowing the crew member to adjust to a specific load. Subject load could also be varied by means of adjusting the length of the harness strap connected to the SLD cable.

The control panel displayed speed, distance, heart rate, percentage grade (calculated by differential force between the forward and aft SLDs), elapsed time and restraint force. A scrollable menu function allowed complete subject interaction with treadmill parameters. The display panel was the subject’s interface to the treadmill electronics.

The CCM access slot in the control panel was used to input and output data to and from the treadmill microprocessor. Data such as actual restraint force, average speed, duration of exercise, foot-strike forces, and heart rate could be stored directly on a subject-unique CCM card. In addition to storing data, the card could be programmed preflight with specific exercise profiles. By reading data stored on the card, the SLDs could be automatically commanded to load the subject to a specific weight, and target speeds and times could be displayed on the control panel.

In October, 1994, crew members on STS-64 first ran on the EDO Treadmill in flight. During this 9-day mission, the treadmill was used on the middeck. Crew comments were very favorable, and one crew member ran “around the world” (for one complete 90 minute orbit) on two separate occasions during the mission. In July, 1995, when the Orbiter docked with Russian Space Station Mir during STS-71, Russian and U. S. crew members returning from the Mir also used the treadmill after over 100 days’ exposure to microgravity. During this flight, the treadmill was installed in the Spacelab module.

The EDO Treadmill became the basis for the treadmill being developed for the International Space Station.

EDO Rower (MK-1 and MK-2)

Two rower ergometers, tested through DTOs 653 and 673, were developed to provide Space Shuttle crew members with an exercise alternative to the treadmill and ergometer. The rowers were the final element in the suite of EDO exercise hardware and were designed to be quiet and effective, while requiring minimal stowage space and electrical power. The flexibility of using a rower as an aerobic device (with traditional rowing) as well as its use with accessories for anaerobic resistive exercises, made it a suitable option for many in-flight applications.

The first generation rower, known as the MK-1 device, was flown on STS-42, STS-53, STS-54, and STS-56. It made use of a magnetic eddy current braking mechanism to vary the workload. A solid copper flywheel rotated between the legs of a forked armature with fixed magnets attached to each leg. A simple sliding lever moved the armature to control how much of the surface of the flywheel was covered by the magnets (and thus the resistive force). A chain and sprocket with a free-wheeling clutch coupled the flywheel to the rope spool, and a power spring provided the recoil force. A tiny DC generator coupled to a voltmeter gauge graduated in arbitrary units provided a relative indication of flywheel speed. The combination of workload setting, flywheel speed, and rowing cadence could be used to compare relative workloads preflight and in flight; however, such comparisons were largely subjective unless sophisticated means such as monitoring oxygen consumption ($\dot{V}O_{2max}$) were employed. The inability to precisely quantify workload was a major limitation of the MK-1 rower.

For launch and landing, the rower was stowed in a middeck locker. For use, it attached to the seat studs on the Orbiter middeck floor. No seat was required for rowing in zero gravity; the crew member merely restrained his/her feet on the foot plates, grasped the handles, and rowed with a conventional motion.

The second generation rower, the MK-2 (Figure 8-20), was designed with features to compensate for the shortcomings of the MK-1. It flew for the first time on STS-64 in September, 1994. Among other modifications, the ability to quantify workload was incorporated into the new design.

MK-2 rower components included the rower ergometer unit, foot plates, and rowing handle. The rower ergometer unit consisted of two compartments: mechanical and chain drive. The mechanical compartment components generated and controlled workload, which was delivered to the subject through the rowing handle. The rowing handle was attached to a rope that ran from the subject through a pulley system and wound around a rope drum. One pulley was fitted with a load cell to measure force. The rope drum had an integral power spring to provide recoil torque and baseline workload. As with the MK-1 rower, a roller ramp clutch



Figure 8-20. Subject Using MK-2 Rower on KC-135.

allowed the rope drum to deliver torque during each rowing stroke and to free-wheel during the recovery phase of each stroke. An optical encoder disc, attached to the rope drum, determined rope velocity and direction. The internal flywheel was used to provide inertial resistive load. A tension belt around the flywheel provided a variable load, controlled by embedded firmware. Tension in the flywheel belt was controlled by a servo motor/drive screw mechanism. Workload could be adjusted manually by use of a control knob extending outside the rower casing when powered operation was not possible. A position indicator gave the location of the traveler on the drive screw and was used as an indicator of the current workload setting.

In the chain drive compartment, a 1:3 rope drum-to-flywheel gear ratio increased the effective load from the flywheel and tension belt assembly. Chain drive was used to deliver torque from the rope drum to the flywheel. An idler pulley chain tightener assembly maintained proper chain tension and indicated the amount of chain wear. To ensure crew member safety, the chain drive compartment was completely sealed. Adjustable foot plates were padded and included straps to allow crew members to exercise without shoes. The plates, adjustable in inclination and foot length to accommodate all crew members, could be put on either end of the rower ergometer casing to allow flexibility in on-orbit operations. The rowing handle was fully padded for rowing and some resistive exercises. A quick release snap on the rope allowed the rowing handle to be easily interchanged.

The rower ergometer was designed so that it could be launched either in a locker or mounted to the floor in

place of a seat if fewer than seven astronauts were on a flight and the seat was not required. In this case, the rowing ergometer attached to stud fittings in the vacant seat position.

CONCLUSION

As can be seen from the foregoing descriptions, EDOMP hardware ran the gamut from the simplest COTS items to complex, integrated systems employing state of the art technology. The development task involved mastery of a number of scientific and technical disciplines. As noted before, the hardware development schedules for all of the EDOMP equipment were extremely compressed; indeed, it could be said that the entire project was on the "fast track." While there were occasional malfunctions

and hardware failures, it is significant to note that the failure rates were no greater than in programs with much higher costs and longer development times.

In addition to the data collected and countermeasures developed, a major benefit of the EDOMP effort was the stable of hardware that is now available for use in ongoing research and operations. In addition to the EDOMP-derived hardware now used in an operational capacity on the Space Shuttle and Mir station, many items have become the basis for crew health care systems and human research equipment that will fly on the International Space Station, and perhaps on future flights to the Moon and Mars. This will be the ultimate legacy of EDOMP.

The success of EDOMP is a tribute to the ingenuity, dedication, and persistence of the engineers and technicians who designed, built, tested, and processed the hardware for flight.

Section 9

Project Summary and Conclusions

EXTENDED DURATION ORBITER MEDICAL PROJECT

Project Summary and Conclusions

*Charles Sawin, EDOMP Project Scientist
Johnson Space Center
Houston, TX*

A top level summary of activities conducted throughout the course of the EDOMP in response to initial concerns at the outset of the program is shown in Table 9-1. Significant findings from the investigations are summarized, together with resulting countermeasures

that were implemented and flight rules that were developed in response to these findings. Subsequent paragraphs provide more information; details will be found in the referenced sections.

Table 9-1. Initial EDOMP concerns that led to significant findings and resulted in countermeasures and flight rules for space shuttle missions

<i>Initial Concerns at Onset of EDOMP</i>	<i>Significant Findings</i>	<i>Countermeasures</i>	<i>Flight Rules</i>
Preservation of capability for egress	Multiple factors noted below contributed to overall capability	All noted below except instrumentation monitoring	Mandatory g-suit and exercise as noted below
Anticipated degradation of landing proficiency	Time required to foveate images increased by up to 100% at landing	Commanders altered their instrument monitoring on final approach	
Orthostatic intolerance	<ul style="list-style-type: none"> • Baroreceptor function: less hypotensive buffering capacity • Significant changes in sympathetic tone <ul style="list-style-type: none"> – Non-fainters demonstrated higher catecholamine levels • Heart rate, diastolic blood pressure and premature ventricular contractions significantly reduced in flight • Plasma volume restoration did not prevent syncopal episodes • Florinef evaluated as countermeasure (CM); unacceptable due to side effects 	<ul style="list-style-type: none"> • Alternative isotonic fluid loads developed 	

Table 9-1. Continued

<i>Initial Concerns at Onset of EDOMP</i>	<i>Significant Findings</i>	<i>Countermeasures</i>	<i>Flight Rules</i>
Orthostatic intolerance (continued)	<ul style="list-style-type: none"> • Re-entry Antigravity Suit (REAGS) developed: better protection at lower pressures relative to CSU-13 • Addition of Liquid Cooling Garment (LCG) reduced incidence of orthostatic intolerance to pre-<i>Challenger</i> level • LCG decreased postflight incidence of nausea by 50% • Lower Body Negative Pressure evaluated as CM 	<ul style="list-style-type: none"> • Development and verification of REAGS • Addition of LCG to ACES ensemble • Mission implementation impact greatly outweighed physiological benefit 	<ul style="list-style-type: none"> • Mandatory preinflation of g-suit
Neuromuscular/neuro-vestibular alterations	<ul style="list-style-type: none"> • Exposure to simulated flight spatial environments facilitated “dual adaptation” and decreased incidence and severity of space motion sickness • Decreased ability to jump 30 cm postflight 	<ul style="list-style-type: none"> • Preflight Adaptation Trainer dual adaptation training 	
Maintaining aerobic capacity	<ul style="list-style-type: none"> • Cycle ergometer and rower shown to be adequate for maintaining aerobic capacity within 6-12% preflight • Exercise decrements minimized by 3× per week, 20 m sessions @ 60-80% preflight maximum levels 	<ul style="list-style-type: none"> • Cycle ergometer and rower developed and qualified for use as flight exercisers 	<ul style="list-style-type: none"> • Mandatory exercise on flights greater than 10 days
Muscle strength loss	<ul style="list-style-type: none"> • Ground-based and in-flight energy requirements determined to be equivalent • Significant strength losses in trunk musculature 		
Other	<ul style="list-style-type: none"> • Significant changes in pH, calcium, and citrate increased risk of renal stone formation • Bacterial levels increased moderately; fungal levels decreased 	<ul style="list-style-type: none"> • Daily fluid intake recommended to be greater than 2.5 liters 	

Table 9-1. Concluded

<i>Initial Concerns at Onset of EDOMP</i>	<i>Significant Findings</i>	<i>Countermeasures</i>	<i>Flight Rules</i>
Other (continued)	<ul style="list-style-type: none"> • Volatile organic compounds generally below allowable limits 		<ul style="list-style-type: none"> • Combustion Products Analyzer developed and flown on all Shuttle missions

CARDIOVASCULAR DECONDITIONING

Early mechanism studies determined vagally mediated, carotid baroreceptor-cardiac reflex responses for astronauts before and after short Shuttle missions. The investigators determined operational points that were a measure of baroreflex buffering capacity for blood pressures above and below resting levels. Low operational points indicate less hypotensive buffering capacity; conversely, high operational points imply less buffering capacity for the hypertensive stimuli. Astronauts who were unable to maintain their systolic pressures on landing day exhibited relatively slower heart rates, greater gain of vagally mediated baroreflex responses preflight, and greater weight loss and reductions of baroreflex operational points postflight than astronauts who maintained stable systolic pressures. Attempts were made to divide subjects into “more resistant” and “less resistant” groups relative to their orthostatic stability. A limitation of the baroreflex technique was that it documented changes of vagal baroreflex mechanisms but did not define sympathetic mechanisms. Investigations were extended to include catecholamine determinations and Valsalva maneuvers on missions of 8-14 days. Power spectral density analyses of R-R interval data were accomplished to determine shifts in sympathetic/ parasympathetic autonomic nervous system function. Both norepinephrine and epinephrine levels were significantly increased on landing day but returned to normal within 3 days after landing. Therefore, space flight provoked functionally significant changes in sympathetic and vagal cardiovascular control. A third study provided normative baseline data for microgravity decreases in heart rate and arterial pressure in crew subjects. Heart rate, arterial pressure, and cardiac rhythm disturbances were monitored for 24-hour periods before, during, and after space flight while astronauts performed their normal routines. Heart rate, diastolic pressure, variability of heart rate and diastolic pressure, and premature ventricular contractions (PVCs) all were significantly reduced in flight. Systolic pressure and premature atrial contractions (PACs) also tended to

be reduced in flight. These data were obtained by use of Holter monitors in conjunction with automatic auscultative blood pressure devices during 24-hour monitoring. Although there was a trend toward a reduced frequency of PACs and PVCs during flight, the only significant difference on any day was a reduction in PVCs during the early stages of flight relative to the averaged preflight frequency. Reductions in diastolic pressure seen during flight may reflect reductions in sympathetic activity and peripheral vascular resistance. These results suggest that space flight itself had a benign effect on the cardiovascular system. Finally, results from these studies did not support the idea that loss of plasma volume was the primary cause of postflight orthostatic hypotension, rather they supported previous findings from bed rest studies, which showed that restoration of plasma volumes did not fully restore post bed rest orthostatic tolerance.

Potential new or improved countermeasures were evaluated, including (1) improved use of existing anti-g suits, (2) a potential new anti-g suit, (3) use of a liquid cooling garment (LCG), (4) ingestion of hypotonic and hypertonic solutions prior to landing, (5) use of lower body negative pressure (LBNP) during flight, and (6) the use of fludrocortisone (Florinef) as a plasma volume expander during the last days of flight.

Studies were conducted to determine if early inflation of the standard five-bladder anti-g suit prior to centrifuge simulation of Shuttle landing would provide better protection against orthostasis than the standard symptomatic inflation regimen. Preinflation protected eye-level blood pressures better and resulted in lower maximum heart rates during these simulations. The second portion of these studies led to development of an improved anti-g suit, which was designated the Reentry Anti-G Suit (REAGS). This suit provided more complete lower torso coverage but deleted the abdominal bladder found in the standard CSU-13 B/P suit. Although REAGS was shown to provide greater protection at lower absolute inflation pressures, it was not incorporated into the Launch and Entry Suit (LES) because it decreased mobility and increased bulkiness of the total garment.

NASA evaluated an LCG as a countermeasure to the thermal load imposed by the LES. This thermal load is believed to be largely responsible for the increased incidence of orthostatic intolerance noted following resumption of Shuttle flights after the Challenger accident. The metabolic heat produced by an average astronaut is about 100 watts. Prior to use of the LCG, the only means of dissipating body heat was via cabin air circulated across the chest area within the LES. This provided modest benefit in a cool cabin and no benefit post landing when cabin air temperatures often reached 80-90 °F (27-32 °C). The LCG employs a thermoelectric cooler to chill water before its circulation through a full torso coverage, tube-filled garment. The LCG is presently worn both for launch and landing; it has proven extremely effective, both for general comfort and orthostatic protection. The frequency of occurrence of orthostatic symptoms has decreased to pre-Challenger levels (approximately 5%) since incorporation of the LCG; also the incidence of postflight nausea has decreased 50%.

Fluid loading with hypotonic and hypertonic solutions was evaluated by ground-based studies. Hypertonic solutions resulted in diarrhea for many subjects. Hypotonic solutions were totally ineffective. Various isotonic solutions provided increased plasma volume and were judged suitable for use in the fluid load countermeasure.

LBNP treatment protocols did not provide significant protection from orthostatic tolerance on participants in these missions. The high crew-time overhead associated with the LBNP soak protocol greatly offset potential benefits judged by improved orthostatic tolerance. The LBNP countermeasure was judged impractical for Shuttle missions.

A common clinical prescription for orthostatic intolerance, fludrocortisone or Florinef, was evaluated in several ground-based studies and then during flight. Pharmacological countermeasures are complex because absorption kinetics are different in the microgravity environment of orbital flight. Dosage regimens that proved effective in subjects after bed rest were not beneficial in flight trials. When an effective dose was tried during flight (0.1 mg, twice a day for the last 5 flight days), the side effects (head fullness, headache, congestion, etc.) made it unacceptable.

REGULATORY PHYSIOLOGY

It was uncertain how the effects of limited physical activity, combined with the potential for increased stress would affect nutritional requirements. Earlier space flight studies indicated changes in protein turnover that were consistent with a stress reaction during Shuttle flights. Energy expenditure requirements were studied during space flights of 8-14 days duration. Methods employed were developed from the doubly labeled water (DLW)

technique modified to account for baseline isotopic differences associated with the Shuttle potable water system, whose water is a product of fuel cells that operate with liquid oxygen and hydrogen. Baseline metabolic studies were accomplished approximately 2 months before flight, while flight studies typically began on the third flight day to avoid confounding effects associated with space motion sickness. The energy requirements associated with physical activity in microgravity were largely unknown, and the relatively close confines of spacecraft tended to limit the extent of physical activity. During flight, energy intake (8.8+/-2.3 Mj/day) was less than total energy expenditure or TEE (11.7+/-1.9 Mj/day). Body weight was less at landing than at 2 days before launch. No differences were found between ground-based and in-flight energy expenditures. Interpretation of body weight changes during space flight was confounded by the fluid loading countermeasure, although typically most fluid load was lost through a combination of diuresis and perspiration. Total weight loss, recorded at landing, reflected a combination of tissue and water loss.

We have observed low dietary intake during space flight. Furthermore, it has previously been shown that relative proportions of energy sources shifted during flight, with the carbohydrate component increasing, protein remaining stable, and fat declining.

Exposure to the microgravity environment of space produced a number of physiological changes of metabolic and environmental origin that increased the potential for renal stone formation. Metabolic, environmental, and physicochemical factors that influence renal stone risk potential were examined. Decreased fluid intake and vomiting associated with space motion sickness in some people during early phases of space flight probably contributed to decreases in urine volume, which added to the risk of stone formation. Urinary calcium levels increased during flight, reflecting the overall negative calcium balance during space flight. Total fluid intake from foods and liquids was approximately 2 liters per day or less. Statistically significant changes were shown for pH, calcium, and citrate in the direction of increased stone-forming risk. At landing, crew members exhibited hypercalciuria, hypocitraturia, decreased magnesium excretion, and decreased urinary pH and volume. A decrease in pH typically increases stone-forming potential by decreasing the solubility of uric acid and increasing the availability of uric acid crystals, which in turn can act as a nidus for calcium oxalate stones.

FUNCTIONAL PERFORMANCE EVALUATION

Both physical and psychological benefits were received from in-flight exercise sessions. As a result of these investigations a flight rule was established requiring exercise on missions greater than 10 days in duration. A

key objective was to determine the optimal combination of a crew member's fitness before flight and continued exercise in flight to result in minimal performance decrements. Conducting well-controlled investigations proved extremely difficult because of multiple conflicting priorities during each mission. In general, moderate to more intense levels of cycle exercise resulted in improved sub-maximal exercise responses after flight. This response required exercising more than 3 times per week for greater than 20 minutes per session at intensities of 60-80% preflight maximum work loads. Changes in muscle morphology were studied by pre- and postflight biopsy of the *vastus lateralis* muscle in the thigh. Significant changes were evident after 6-9 day Shuttle missions, including a 15% reduction in the cross sectional area of Type I and a 22% reduction in cross sectional area of Type II muscle fibers.

Muscle function was measured by a LIDO[®] dynamometer. Large decrements in trunk flexor and extensor strength, both concentric and eccentric, and significant losses in concentric quadriceps extension were seen. Muscle strength typically recovered within 7-10 days with the exception of concentric back extension. Significant additional effort is still required to define an optimal exercise program which gives consideration to (1) aerobic vs. resistive, (2) upper body vs. lower body, (3) eccentric (force while lengthening) vs. concentric (force while shortening), and (4) high-intensity interval vs. low-intensity continuous protocols.

ENVIRONMENTAL HEALTH

The Environmental Health activity developed an overall strategy for safeguarding crew members from potential airborne hazards anticipated on missions of extended duration. Degradation of air quality had the potential to affect crew performance during all mission phases, and increased risk was anticipated with extended duration flights. Second, there was the potential to reach unacceptable levels of volatile organic compounds, or excessive airborne particulate matter, and finally the potential for excessive levels of microorganisms.

Data collected during the program indicated that volatile organic compounds (VOCs) in the cabin atmosphere were generally below allowable limits. Most pollutants reached equilibrium concentrations within the first few days of a mission. Exceptions to this were hydrogen, methane, and dichloromethane. Formaldehyde was found to be present at levels exceeding the allowable limits for each of three missions monitored. Although accidental air contamination problems originated from a variety of sources, the dominant source was thermodegradation of electronic devices. Nine such incidents occurred during 20 missions; four were the result of electronic burns. The necessity for real-time monitoring of critical combustion

products resulted in the development of the Combustion Products Analyzer that now flies on each Shuttle mission.

Quantification of airborne bacteria and fungi showed in general that bacterial levels increased moderately as the mission proceeded, whereas the fungal levels tended to decrease. Fungal levels likely decreased in response to the low humidity on typical Shuttle missions.

NEUROVESTIBULAR DYSFUNCTION

Flight surgeons frequently observed disequilibrium in crew members during the first few hours after space flight. These observations were in large part attributed to functional changes in the neurovestibular system. Neurovestibular investigations were designed to use sophisticated devices to evaluate these changes: specifically, a commercially available Neurocom Equitest Posture Platform, electrooculograms, a specially designed Tilt Translation Device, and a Device for Orientation and Movement Environments.

Four primary goals were (1) to establish a normative data base of vestibular and associated sensory changes in response to space flight, (2) to determine the underlying etiology of neurovestibular and sensory motor changes associated with exposure to microgravity and the subsequent return to Earth, (3) to provide immediate feedback to flight crews regarding potential countermeasures that could improve performance and safety during and after flight, and (4) to design appropriate countermeasures that could be implemented for future missions.

Perception of spatial orientation is determined by integrating information from several sensory modalities. This involves higher levels of processing within the central nervous system to control eye movements, stabilize locomotion, and maintain posture. Operational problems occur when reflex responses to perceived spatial orientation lead to inappropriate compensatory actions.

Target acquisition protocols used a cruciform tangent system where targets were permanently fixed at predictable angular distances in both the horizontal and vertical planes. The subject was required to use a time optimal strategy for all target acquisition tasks: to look from the central fixation point to a specified target indicated by the operator (right red, left green, up blue, etc.) as quickly and accurately as possible using both head and eye movement to acquire the target. During flight, measurements were obtained using a cruciform target display that attached to the Shuttle mid-deck lockers. In all cases, surface electrodes on the face enabled quantifying eye movements that were obtained with both horizontal and vertical electrooculography. Pursuit tracking, (i.e., visually moving from a central focal point to illuminated targets) was performed before flight and after flight, using two separate protocols: (1) smooth pursuit by the eyes only, and (2) pursuit tracking with the head and eyes together. The sinusoidal pursuit tracking

tasks were performed at moderate (0.33 Hz) and high (1.4 Hz) frequencies to investigate the relative contributions of eye and head movement in maintaining gaze. Significant difficulties were observed postflight, including multiple saccades; consequently, the time required to foveate the target increased by as much as 1 to 1.5 seconds relative to pre-flight times.

Two protocols investigating postural stability were performed before, during, and after Shuttle missions of varying duration. These tests used a clinical Neurocom Equitest posture platform which permitted challenging the subject's ability to maintain balance by six different sequential tests. The effect of space flight on neural control of posture was inferred from differences between preflight and postflight performance. The effect of mission duration was inferred from statistical comparison between the performance of subjects on short, medium, and long duration missions. Astronauts with previous flight experience demonstrated better postural stability which suggested retained neurosensory learning. Multiple protocols were employed to determine if exposure to the microgravity environment induced alterations in eye-head-trunk coordination during locomotion. The normally phased relationship between head pitch and vertical trunk position was not evident when observed 4 hours after flight. This alteration resulted in decreased capability to foveate targets. Findings reinforced the criticality of vision if astronauts were to be able to compensate for vestibular function changes associated with exposure to microgravity environments.

HUMAN FACTORS

These studies documented the strengths and limitations of human operators in a complex environment. Promising areas of inquiry included tools, habitat, environmental conditions, tasking, work load, flexibility, and individual control over work.

Gloveboxes

Task performance within gloveboxes was affected by such factors as constrained arm movements, postural limitations, and visual constraints. The design of gloveboxes was primarily driven by task requirements with little or no consideration of the human interface. Three glovebox designs were flown on various Spacelab missions: (1) Material Sciences Glovebox (GBX), supporting crystal growth and other material science experiments; (2) the biorack, a facility to support investigations on cells, tissues, plants, bacteria, small animals, and other biological samples; and (3) the General Purpose Work Station (GPWS), a multifunctional facility that supported animal experimentation and microscope use. The GBX was generally rated unacceptable because of its small size,

limited range of motion, hand positioning, and resulting shoulder and neck pain. The GPWS was rated acceptable, although reaching loose items proved difficult at times. The biorack was not broadly evaluated.

Lower Body Negative Pressure (LBNP)

LBNP investigations included consideration of stowage and assembly, and operation of the controls and displays. Data from in-flight questionnaires enabled the crew to record comments and evaluations while studies were in progress. Postflight debriefs and video image analyses provided additional information.

Stowage, Restraints, Deployment and Cables

Crew members were monitored during waking hours via video downlink. Several problems were identified with stowage, ranging from locker design to practices associated with stowing individual items. It was determined that quick, simple methods for restraining small items should be supplied; these should include Velcro, adhesive surfaces, vacuum, or elastic bands.

Touchscreen Usability in Microgravity

Most of the subjects preferred the touchscreen on the ground and the Trackpoint in flight. Hand fatigue was experienced almost immediately when using the touchscreen in flight.

Vibration in Flight

The Space Acceleration Measurement System was used to measure and store acceleration data during flight. Vibration was perceptible to all subjects and annoying to some. Vibrations occurred at times when primary jets were firing, or when the treadmill or ergometer was in use.

Acoustic Noise Environment

Crew member perceptions of noise on Shuttle differed from one mission to another. In all cases, the major noise source was the Environmental Control and Life Support System. The Spacelab refrigerator/freezers emitted excessive noise (70 dB(A) with one compressor operating and 73 dB(A) with both compressors operating). The vacuum cleaner contributed significantly to the noise environment, operating at nearly 80 dB(A). The SAREX, or short wave amateur radio, resulted in sound level readings of 72 dB(A).

FACILITIES

Medical data collection facilities at both Dryden Flight Research Center (DFRC) and Kennedy Space Center (KSC) required design changes in order to implement the

EDOMP. While modifications to the KSC facility were feasible, expanding the clinic at DFRC was not; therefore, a new facility named the Postflight Science Support Facility was built.

Obtaining rapid access to the crew post landing was crucial for most studies. This resulted in the need for a crew transport vehicle (CTV) at both landing sites. Considerations leading to acquisition of the CTVs included (1) medical emergency activities could be more likely after longer duration flights, (2) medical/support personnel were required at hatch opening, and (3) accommodations were required which maintained crew privacy and allowed collection of physiological data as soon as possible after landing. The vehicles selected were airport passenger transporters because of their 568 sq. ft. interior, flexibility of design, and single operator capability. The addition of CTVs to the landing day complement contributed significantly to enhanced emergency medical capability, improved crew comfort and privacy, and reduced the time required to initiate biomedical data acquisition. At KSC a docking port was created for the CTV on the second floor of the Baseline Data Collection Facility; this feature further utilized the capabilities and benefits of the CTV.

HARDWARE

Development of flight hardware was a major element of the EDOMP, requiring a team effort among scientists, engineers, crew members, flight integration specialists, and others. Examples of EDOMP flight hardware that have been used on subsequent Shuttle flights, on Mir, and in development of ISS hardware are:

(1) Entry Blood Pressure Monitor. This hardware has been worn by long duration crew members upon their return from Mir. The automatic blood pressure monitor (ABPM) selected for the ISS blood pressure/ECG unit will be similar to the EDOMP ABPM.

(2) LBNP System. The designers of the LBNP system to be used on ISS are utilizing many features of the EDOMP system and are including modifications which resulted from experience gained during EDOMP flights.

(3) Data Acquisition System (DAS). The Generalized Controller Module, an imbedded processor control system that was developed for EDOMP and used in the DAS, has become the core of control systems for many subsequent projects. In addition, a modular concept for data acquisition and control systems was developed that reduced development time and cost.

(4) Bar Code Reader (BCR). Use of the BCR continued on Mir.

(5) Heart Rate Watch. Use of this hardware continued on Mir; a heart rate watch with enhanced capabilities will be used on ISS.

(6) Microbial Air Sampler (MAS). A MAS has been selected for use on ISS.

(7) Combustion Products Analyzer (CPA). Use of the CPA continued on subsequent Shuttle flights and on Mir; a CPA has been selected for use on ISS.

(8) Formaldehyde Monitor Kit (FMK). Use of the FMK continued on Mir.

(9) Cycle Ergometer, Ergometer Vibration Isolation System, and Passive Cycle Isolation System. This complement of hardware became the operational (or standard) exercise device for Shuttle flights. An improved version of this ergometer, with an Inertial Vibration Isolation System and upgraded electronics, will become the operational cycle ergometer in the U.S. segment of ISS.

(10) EDO Treadmill. This treadmill became the basis for the ISS treadmill.

CONCLUSIONS

Cardiovascular research received a high priority during this program because of concerns regarding decreased orthostatic tolerance and egress capability. Microgravity exposure up to 16 days was shown to be a relatively benign environment in that resting blood pressures and heart rates were below ground-based control levels. Electrocardiographic abnormalities were low for the group evaluated before flight and were even less during flight for these subjects. Multiple factors associated with orthostatic tolerance were evaluated in integrated cardiovascular investigations. Lower epinephrine responses of a group of astronauts who were relatively more susceptible to presyncope showed high correlation with their lower total peripheral vascular resistance. Further, it was shown that plasma volume replenishment per se did not prevent presyncopal episodes during laboratory stand tests. These data were consistent with multiple observations of alterations in autonomic control during space flight.

Notable advances were made in the development or improvement of cardiovascular countermeasures. Centrifuge studies conducted with the United States Air Force Armstrong Laboratory led to guidelines for use of anti-g suits. The resulting mandatory preinflation schedule optimized protection during reentry. The liquid cooling garment was integrated into the Launch and Entry Suit to solve thermal problems, thereby improving orthostatic tolerance and crew comfort. Alternative isotonic fluid loads were verified and optimized by determining total volume in relation to the subject's preflight body weight. Finally, although fludrocortisone treatment could restore plasma volume using certain protocols late in the mission, the side effects precluded its use as an operational countermeasure. Present guidelines that require use of the liquid cooling garment and the anti-g suit preinflated before reentry, together with revised fluid loading, have greatly reduced the incidence of orthostatic intolerance.

Nutritional assessments showed that ground-based and flight energy expenditures were comparable. Energy intake during flight was decreased relative to preflight levels, and a preference was noted for carbohydrates versus fat in choice of foods by astronauts. Renal stone risk profiles were established for large numbers of astronauts by collecting urine samples before and after flight.

Assessment of exercise protocols for maintenance of aerobic capacity and orthostatic tolerance led to the conclusion that aerobic capacity did not correlate with orthostatic tolerance in our subjects. Minimal losses in aerobic function were seen for crew members who exercised more than three times weekly at levels reaching 60-80% of preflight maximum work loads. Muscle biopsies were used to determine morphological changes following medium duration space flights. The most striking finding was that changes in morphology became evident following flights of only 5 days in duration. Muscle performance was evaluated in several astronauts, and significant decrements were noted in major postural muscles. It was determined that heavy resistive exercise should be evaluated for protection of major muscle function. Higher intensity aerobic interval exercise protocols were recommended and are being implemented. Finally, treadmill exercise appeared to be important for maintenance of neuromuscular patterns required for walking or running.

Environmental monitoring indicated that VOCs in the cabin atmosphere were generally below allowable limits. The need for real-time monitoring of critical combustion

products led to the development of the Combustion Products Analyzer. Quantification of airborne bacteria and fungi showed no safety concerns.

Neuroscience investigations dealt with complex, integrated systems where it was difficult to factor out underlying mechanisms associated with changes known to occur in the vestibular system. Studies were conducted to evaluate changes in visual target acquisition, postural and locomotion changes, assessment of perceived self orientation or motion, and eye-head-trunk coordination during locomotion. Exposure to simulated flight spatial environments using ground-based training devices reduced the occurrence of space motion sickness during actual space flights. Time required to foveate images increased by as much as 100% following space flight. This resulted in some Shuttle commanders altering their pattern of instrument monitoring during final approach and landing, to minimize potential hazard.

Valuable new information was gained with respect to development of productive work stations that support scientific requirements. Vibration and acoustic environments were monitored for excessive or stressful levels.

In summary, the EDOMP was a highly successful 5-year, operational research program that yielded many improvements, such as enhanced crew member safety and decreased risks to mission success.

Appendix A

EXTENDED DURATION ORBITER MEDICAL PROJECT

Appendix A

EDOMP Medical DSOs Listed by Discipline

<i>Discipline</i>	<i>DSO No.</i>	<i>Short Title</i>	<i>Principal Investigator</i>
Biomedical Physiology	328	In-flight Urine Collection Absorber (IUCA) Evaluation	H. W. Lane, Ph.D.
	484	Circadian Shifting	L. Putcha, Ph.D.
	490	Promethazine/P.I.L.O.T.	L. Putcha, Ph.D.
	610	In-flight Assessment of Renal Stone Risk Factor	P. A. Whitson, Ph.D.
	612	Energy Utilization	H. W. Lane, Ph.D.
	613	Endocrine Regulation	P. A. Whitson, Ph.D.
	622	Gastrointestinal Function	L. Putcha, Ph.D.
Cardiovascular Physiology	463	In-flight Holter Monitoring	J. B. Charles, Ph.D.
	466	Pre-and Postflight Cardiovascular Assessment	J. B. Charles, Ph.D.
	476	In-flight Aerobic Exercise	J. B. Charles, Ph.D.
	478	In-flight LBNP	J. B. Charles, Ph.D.
	479	Hyperosmotic Fluid Countermeasure	J. B. Charles, Ph.D.
	601	Changes in Baroreceptor Reflex Function	J. M. Yelle, M.S.
	602	Blood Pressure Variability During Space Flight	J. M. Yelle, M.S.
	603	Orthostatic Function During Entry, Landing, and Egress	J. B. Charles, Ph.D.
	607	LBNP Following Space Flight	S. M. Fortney, Ph.D.
	621	In-flight Use of Florinef	J. M. Yelle, M.S.
	623	LBNP Countermeasure Trial	J. B. Charles, Ph.D.
	625	Measurement of Blood Volume	J. M. Yelle, M.S.
	626	Extended Stand Test	J. M. Yelle, M.S.
Environmental	471	Airborne Particulate Sampler	D. L. Pierson, Ph.D.
	488	Measurement of Formaldehyde/Passive Dosimetry	J. James, Ph.D.
	611	A) Archival Organic Sampler B) Microbial Air Sampler	J. James, Ph.D. D. L. Pierson, Ph.D.
Exercise Physiology and Musculoskeletal	331	LES and Locomotion	M. C. Greenisen, Ph.D.
	475	Muscle Biopsy	M. C. Greenisen, Ph.D.
	476	In-flight Aerobic Exercise	S. F. Siconolfi, Ph.D.
	477	Muscle Performance	J. C. Hayes, M.S.
	606	Muscle Size and Lipids (MRI/MRS)	A. LeBlanc, Ph.D.
	608	Aerobic and Anaerobic Metabolism in Space	S. F. Siconolfi, Ph.D.
	617	Muscle Performance II	J. C. Hayes, M.S.
	618	Intense Exercise	A. D. Moore, Ph.D.
624	Submaximal Exercise	A. D. Moore, Ph.D.	
Neurophysiology	604	Visual Vestibular Integration and Adaptation	M. F. Reschke, Ph.D., D. L. Harm, Ph.D.
	605	Postural Equilibrium Control	W. H. Paloski, Ph.D.
	614	Head and Gaze Stability	J. J. Bloomberg, Ph.D.
	620	Seat Egress Ability	J. J. Bloomberg, Ph.D.

<i>Discipline</i>	<i>DTO No.</i>	<i>Short Title</i>	<i>Principal Investigator</i>
Hardware	651	EDO Cycle Ergometer	M. C. Greenisen, Ph.D.
Evaluations	652	Vibration Recordings on Treadmill	S. M. Whelan, M.Ed.
(Development	653	MK1 Rower	M. C. Greenisen, Ph.D.
Test Objectives	658	Ergometer Vibration Isolation System (EVIS)	R. B. Connell, M.S.
[(DTO)]	659	EDO Treadmill	M. A. Bowman
	670	Passive Cycle Isolation System (PCIS)	R. B. Connell, M.S.
	673	EDO Rower	R. B. Connell, M.S.
	682	Inertial Vibration Isolation System (IVIS)	R. B. Connell, M.S.
	913	Microgravity Measurement Device (MMD)	R. B. Connell, M.S.

Appendix B

EXTENDED DURATION ORBITER MEDICAL PROJECT

Appendix C

EXTENDED DURATION ORBITER MEDICAL PROJECT

Appendix C

EDOMP Publications

<i>DSO No.</i>	<i>Title</i>	<i>Publications</i>
466	Variations in Supine and Standing Heart Rate, Blood Pressure, and Cardiac Size as a Function of Space Flight Duration and Time Postflight	<p>Mukai CN, Bennett BS, Elton KF, Lathers CM, Charles JB. Acute hemodynamic responses to 0g induced by parabolic flight. <i>Aviat Space Environ Med</i> 1989; 60:509.</p> <p>Lathers CM, Charles JB, Elton KF, Holt TA, Mukai C, Bennett BS, Bungo MW. Hemodynamic changes to brief weightlessness. <i>J Clin Pharm</i> 1989; 29:833.</p> <p>Mukai CN, Lathers CM, Charles JB, Bennett BS, Igarashi M, Patel S. Acute Hemodynamic Responses to Weightlessness During Parabolic Flight. <i>J Clin Pharm</i> 1991; 31:993-1000.</p> <p>Charles JB, Lathers CM. Cardiovascular adaptation to space flight. Eds. C.M. Lathers and J.B. Charles. <i>J Clin Pharm</i> 1991; 31:1010-1023.</p> <p>Lathers CM, Charles JB, Bungo MW. Comparison of cardiovascular function during head-down bedrest and space flight. <i>J Clin Pharm</i> 1991; 31:842.</p> <p>Mulvagh SL, Charles JB, Riddle JM, Rehbein TL, Bungo MW. Echocardiographic evaluation of the cardiovascular effects of short-duration spaceflight. <i>J Clin Pharm</i> 1991; 31:1024-1026.</p> <p>Lathers CM, Charles JB. Autonomic nervous system function: Evaluation in patients and bedrest subjects (model for weightlessness). <i>J Clin Pharm</i> 1992; 32.</p> <p>Lathers CM, Charles JB. Comparison of cardiovascular function during bedrest and space flight. <i>J Clin Pharm</i> 1993; 33.</p> <p>Lathers CM, Charles JB, Mukai CN, Riddle JM, Jacobs FO, Bennett BS, Lewis D, Fortney SM, Frey MA, Stricklin MD, Schneider VS. Effect of 17 weeks bedrest on cardiovascular parameters during LBNP. <i>J Clin Pharm</i> 1993; 33.</p> <p>Lathers CM, Charles JB. Orthostatic hypotension in patients, bedrest subjects, and astronauts. <i>J Clin Pharm</i> 1993; 33.</p> <p>Simanonok KE, Charles JB. Space sickness and fluid shifts: A hypothesis. <i>J Clin Pharm</i> 1994; 36:652-663.</p>
475	Muscle Biopsy	<p>Moore AD, Charles JB, Lee SMC, Siconolfi SF, Greenisen MC. Does bed rest produce changes in orthostatic function comparable to those induced by space flight? <i>Acta Astronautica</i> 1994; 33:57-67.</p>

<i>DSO No.</i>	<i>Title</i>	<i>Publications</i>
475	<i>(continued)</i>	<p>Zhou MY, Klitgaard H, Saltin B, Roy RR, Edgerton VR, Goknick PD. Myosin heavy chain isoforms of human muscle after short-term spaceflight. <i>J Appl Physiol</i> 1995; 78:1740-49.</p> <p>Day MK, Allen DL, Mohajerani L, Greenisen MC, Roy RR, Edgerton VR. Adaptations of human skeletal muscle to space flight. <i>J Gravit Physiol</i> 1995; II (I):47-50.</p> <p>Edgerton VR, Zhou M-Y, Ohira Y, Klitgaard H, Jiang B, Bell G, Harris B, Saltin B, Gollnick P, Roy RR, Greenisen M. Human fiber size and enzymatic properties after 5 and 11 days of space flight. <i>J Appl Physiol</i> 1995; 78:1733-39.</p>
476	In-flight Aerobic Exercise	<p>Siconolfi SF, Charles JB, Moore AD, Barrows LH. Comparing the effects of two in-flight aerobic exercise protocols on standing heart rates and VO_{2peak} before and after space flight. <i>J Clin Pharm</i> 1994; 34:590-595.</p> <p>Bishop PA, Lee SM, McBrine JJ, Siconolfi SF, Greenisen MC. Validation and evaluation of a lightweight portable device for measuring VO_2. <i>Am Ind Hyg Assoc J</i> 1995; 56(1):50-54.</p> <p><i>In work:</i></p> <p>Siconolfi SF, Charles JB, Moore AD, Gilbert, JH, Suire SS. Effects of different in-flight exercise modalities and fitness on post space flight orthostatic heart rates. <i>Med Sci Sports Exer</i> (submitted for review 1997).</p> <p>Siconolfi SF, Moore AD, Gilbert JH, Suire SS, Barrows LH, Charles JB, Sawin CF. Effects of different exercise modalities and protocols during space flight on aerobic capacity. <i>Med Sci Sports Exer</i> (submitted for review 1997).</p> <p>Siconolfi SF, Gretebeck RJ, Wong WW, Pietrzyk RA, Suire SS. Assessing total body and extracellular water from bioelectrical response spectroscopy. <i>J Appl Physiol</i> (submitted for review 1996).</p>
477	Muscle Performance	<p>Day MK, Aleen DL, Mohejerani L, Greenisen MC, Roy RR, Edgerton VR. Adaptations of human skeletal muscle to space flight. <i>J Gravitational Biol</i> 1995, II(I); 47-50.</p> <p><i>In work:</i></p> <p>Hayes JC, McBrine JJ, Roper ML, Siconolfi SF, Harris BA. Effect of space shuttle flight on isokinetic skeletal muscle strength. <i>J Appl Physiol</i> 1998.</p> <p>Hayes JC, Roper ML, McBrine JJ, Siconolfi SF, Harris BA. The effect of space shuttle flight on skeletal muscle strength. <i>J Appl Physiol</i> (submitted for review).</p> <p>McBrine JJ, Hayes JC, Siconolfi SF. Effects of in-flight exercise on skeletal muscle performance.</p>

<i>DSO No.</i>	<i>Title</i>	<i>Publications</i>
478	In-flight Lower Body Negative Pressure (LBNP)	Charles JB, Lathers CM. Summary of lower body negative pressure experiments during space flight. <i>J Clin Pharm</i> 1994; 36:571-583. Lathers CM, Charles JB, Schneider VS, Frey MAB, Fortney S. Use of lower body negative pressure to assess changes in heart rate response to orthostatic-like stress during 17 weeks. <i>J Clin Pharm</i> 1994;34:563-570.
484	Assessment of Circadian Shifting in Astronauts by Bright Light	Whitson PA, Putcha L, Chen YM, Baker E. Melatonin and cortisol assessment of circadian shifts in astronauts before flight. <i>J Pineal Research</i> 1995; 18: 141-147. <i>In work:</i> Putcha L, Nimmagudda RR, DeKerlegand D, Stewart K. Light, sleep and melatonin levels during space flight. (Submitted to <i>Chronobiology Int</i> , 1997).
492	Portable Clinical Blood Analyzer	Smith SM, Davis-Street JE, Fontenot TB, Lane HW. Assessment of a portable clinical blood analyzer during space flight. <i>Clinical Chemistry</i> (in press).
601	Changes in Baroreceptor Reflex Function	Eckberg DL, Fritsch JM. Human autonomic responses to actual and simulated weightlessness. <i>J Clin Pharm</i> 1991; 31:951-954. Fritsch JM, Charles JB, Bennett BB, Jones MM, Eckberg DL. Short-duration spaceflight impairs human carotid baroreceptor-cardiac reflex responses. <i>J Appl Physio</i> 1992; 73(2):664-671. Fritsch-Yelle JM, Charles JB, Jones MM, Beighton LA, Eckberg DL. Spaceflight alters autonomic regulation of arterial pressure in humans. <i>J Appl Physiol</i> 1994; 77:1776-1783.
602	Blood Pressure Variability During Space Flight	Fritsch-Yelle JM, Charles JB, Jones MM, Wood ML. Microgravity decreases heart rate and arterial pressure in humans. <i>J Appl Physiol</i> 1996 March; 80(3):910-914.
604 OI-1	Visual-Vestibular Integration as a Function of Adaptation: Motion Perception Reporting	Harm DL, Parker DE. Perceived self-orientation and self-motion in microgravity, after landing and during preflight adaptation training. <i>J Vestib Res</i> , 1993; 3:297-305. Harm DL, Parker DE. Preflight adaptation training for spatial orientation and space motion sickness. <i>J Clin Pharm</i> 1994; 34:618-627. Harm DL, Zografos LM, Skinner NC, Parker DE. Changes in compensatory eye movements associated with simulated stimulus conditions of space flight. <i>Aviat Space & Environ Med</i> 1993; 64:820-26. Parker DE, Harm DL. Mental rotation: a key to effective performance in the virtual environment? <i>Presence</i> 1993; 1:329-333. Reschke MF, Bloomberg JJ, Harm DL, Paloski WH. Space flight and neurovestibular adaptation. <i>J Clin Pharm</i> 1994; 34:609-617.

<i>DSO No.</i>	<i>Title</i>	<i>Publications</i>
604 OI-1	<i>(continued)</i>	<p>Reschke MF, Bloomberg JJ, Harm DL, Paloski WH. Chapter 13, Neurophysiological aspects: sensory and sensory-motor function. In AE Nicogossian (Ed.), Space Physiology and Medicine, 3rd Ed., Philadelphia: Lea & Febiger, 1994.</p> <p>Reschke MF, Harm DL, Parker DE, Sandoz GR, Homick JL, Vanderploeg JM. Chapter 12, Neurophysiological aspects: space motion sickness. In AE Nicogossian (Ed.), Space Physiology and Medicine, 3rd Ed., Philadelphia: Lea & Febiger, 1994.</p> <p>Reschke MF, Harm DL, Bloomberg JJ, Paloski WH. Chapter 7, Neurosensory and sensory-motor function. In AM Genin and CL Huntoon (Eds.) Space Biology and Medicine, Vol. 3: Humans in Spaceflight, Book 1: Effects of Microgravity. Washington, DC: American Institute of Aeronautics and Astronautics (AIAA), 1997; 135-194.</p> <p><i>In work:</i></p> <p>Harm DL, Parker DE, Reschke MF, Skinner NC. Astronaut's microgravity "rest frame" selection correlates with pre- and postflight vection latencies. Brain Res Bull 1998; in press.</p>
604 OI-3	Visual-Vestibular Integration as a Function of Adaptation	<p>Reschke MF, Bloomberg JJ, Harm DL, Paloski WH. Space flight and neurovestibular adaptation. J of Clin Pharm 1994; 34:609-617.</p> <p>Huebner WP, Paloski WH, Reschke MF, Bloomberg JJ. Geometric adjustments to account for eye eccentricity in processing horizontal and vertical eye and head movement data. J of Vestib Res 1995; 5(4): 299-322.</p> <p><i>In work:</i></p> <p>Wood SJ, Paloski WH, Reschke MF. Spatially-directed eye movements during roll-tilt relative to perceived head and earth orientations. Exp Brain Res 1998; in press.</p>
605	Postural Equilibrium Control During Landing/Egress	<p>Black FO, Paloski WH, Doxey-Gasway DD, Reschke MF. Vestibular plasticity following orbital space flight: Recovery from postflight postural instability. Acta Otolaryngologica (Stockholm) 1995; Suppl 520:450-454.</p> <p>Paloski WH, Reschke MF, Black FO, Doxey DD, Harm DL. Recovery of postural equilibrium control following space flight. Annals of the New York Academy of Sciences 1992; 656:747-754.</p> <p>Paloski WH, Black FO, Reschke MF, Calkins DS, Shupert CS. Vestibular ataxia following shuttle flights: Effects of microgravity on otolith-mediated sensorimotor control of posture. Am J Otology 1993; 14:9-17.</p> <p>Reschke MF, Bloomberg JJ, Harm DL, Paloski WH. Space flight and neurovestibular adaptation. J Clin Pharm 1994; 34:609-617.</p>

<i>DSO No.</i>	<i>Title</i>	<i>Publications</i>
605	<i>(continued)</i>	<p><i>In work:</i></p> <p>Black FO, Paloski WH, Reschke MF, Igarashi M, Guedry F, Anderson DJ. Disruption of balance control recovery by inertial stimulation following the IML-1 spacelab mission. <i>J Vestib Res</i> 1998; in review.</p> <p>Nicholas SC, Doxey-Gasway DD, Paloski WH. A link-segment model of upright human posture for analysis of head-trunk coordination. <i>J Vestib Res</i> 1998; 8(3). In press.</p> <p>Paloski WH, Black FO, Reschke MF, and Calkins CS. Altered CNS processing disrupts balance control after space flight. <i>Exp Brain Res</i> 1998; in review.</p>
606	Muscle Size and Lipids (MRI/MRS)	Jaweed MM, Narayan P, Jackson E, Slopis J, Butler I. Isometric force and fatigue characteristics of the gastrocnemius-soleus muscle in astronauts after 9 days of space mission. <i>Archives of Physical Medicine and Rehabilitation</i> 1992; 72:803.
607	Cardiovascular Responses to Lower Body Negative Pressure Following Space Flight	<p><i>In work:</i></p> <p>Fortney SM, Charles JB, Whitson P, Dussack L, Wood M. Cardiovascular responses to lower body negative pressure after spaceflight. In preparation.</p>
608	Effects of Space Flight on Aerobic and Anaerobic Metabolism During Exercise	<p>Siconolfi SF, Charles JB, Moore AD, Barrows LH. Comparing the effects of two in-flight aerobic exercise protocols on standing heart rates and VO_{2peak} before and after space flight. <i>J Clin Pharm</i> 1994; 34:590-595.</p> <p>Bishop PA, Lee SM, McBrine JJ, Siconolfi SF, Greenisen MC. Validation and evaluation of a lightweight portable device for measuring VO_2. <i>Am Ind Hyg Assoc J</i> 1995; 56(1):50-54.</p> <p>Siconolfi SF, Gretebeck RJ, Wong WW. Assessing total body mineral, bone mineral content, and total body protein from total body water and bone density. <i>J Appl Physiol</i> 1995; 79:1837-1843.</p> <p>Siconolfi SF, Gretebeck RJ, Wong WW, Pietrzyk RA, Suire SS. Assessing total body and extracellular water from bioelectrical response spectroscopy. <i>J Appl Physiol</i> 1997; 82(2):704-710.</p> <p>Siconolfi SF, Nusynowitz ML, Suire SS, Moore AD, Leig J. Determining blood and plasma volumes using bioelectrical response spectroscopy. <i>Med Sci Sports Exer</i> 1996; 28(12):1510-1516.</p> <p><i>In work:</i></p> <p>Siconolfi SF, Charles JB, Moore AD, Gilbert, JH, Suire SS. Effects of different in-flight exercise modalities and fitness on post space flight orthostatic heart rates. <i>Med Sci Sports Exer</i> (submitted for review 1997).</p> <p>Siconolfi SF, Moore AD, Gilbert JH, Suire SS, Barrows LH, Charles JB, Sawin CF. Effects of different exercise modalities and protocols during space flight on aerobic capacity. <i>Med Sci Sports Exer</i> (submitted for review 1997).</p>

<i>DSO No.</i>	<i>Title</i>	<i>Publications</i>
608	<i>(continued)</i>	<p>Siconolfi SF, Gretebeck RJ, Wong WW, Moore AD, Gilbert JH. Assessing total body mineral and protein from body density and water from bioelectrical response spectroscopy (first review by J Appl Physiol 1997).</p> <p>Siconolfi SF, Gretebeck RJ, Wong WW, Moore AD, Gilbert JH. Validity of assessing percent body fat from body density and water or mineral (first review by J Appl Physiol 1997).</p> <p>Siconolfi SS, Gretebeck RJ, Wong WW, Ellis KJ. Multi-component models for body composition with a reference male and female (first review by J Appl Physiol 1997)</p>
610	In-flight Assessment of Renal Stone Risk	<p>Whitson PA, Pietrzyk RA, Pak CY, Cintron NM. Alterations in renal stone risk factors after space flight. J Urology 1993; 150:803-807.</p> <p>Whitson PA, Pietrzyk RA, Pak CYC. Renal stone assessment during space shuttle missions. J Urology 1997; 158:2305-2310.</p>
611	Air Monitoring Instrument Evaluation and Atmosphere Characterization	<p>James JT, Limero TF, Leano HJ, Boyd JF, Covington PA. Volatile organic contaminants found in the habitable environment of the space shuttle: STS-26 to STS-55. Aviat Space Environ Med 1994; 65:851-57.</p> <p>Mehta Satish K, Mishra SK, Pierson Duane L. Evaluation of three portable samplers for monitoring airborne fungi. Applied and Environmental Microbiology May, 1996; 62(5):1835-1838.</p> <p>Pierson DL, Chidambarum M, Heath JD, Mallory L, Mishra SK, Sharma B, Weinstock GM. Epidemiology of <i>Staphylococcus aureus</i> during space flight. FEMS Imm & Med Micro 1996; 16:273-281.</p>
612	Energy Utilization	<p>Gretebeck RJ, Siconolfi SF, Rice B, Lane HW. Physical performance is unaffected by the diet provided for U. S. astronauts during space flight. Aviat Space Environ Med 1994; 65(11):1036-40.</p> <p>Lane HW, Rice B, Kloeris V, Frye S, Siconolfi SF, Spector E, Gretebeck RJ. Effects of a space shuttle diet on body weight and composition in healthy active women. J American Dietetic Assoc 1994; 94:87-88.</p> <p>Lane HW, Gretebeck RJ. Metabolic energy required for flight. Advances in Space Research 1994; 14 (11):147-155.</p> <p>Gretebeck RJ, Schoeller D, Gibson EK, Lane HW. Energy expenditure during antiorthostatic bed rest (simulated microgravity). J Appl Physiol 1995; 78:2207-2211.</p> <p>Schoeller DA, Gretebeck RJ, Gibson EK, Schulz LO, Lane HW. Doubly labeled water in subjects exposed to a new source of water. J Physiol Feb, 1997.</p>

<i>DSO No.</i>	<i>Title</i>	<i>Publications</i>
612	<i>(continued)</i>	Lane HW, Gretebeck RJ, Schoeller DA, Davis-Street JE, Socki RA, Gibson EK. Comparison of ground-based and space flight energy expenditure and water turnover in middle-aged healthy male U. S. astronauts. <i>Am J Clin Nutri</i> 1997; 63(1):4-12.
613	Changes in the Endocrine Regulation of Orthostatic Tolerance Following Space Flight	Whitson PA, Charles JB, William WJ, Cintron NM. Human sympathoadrenal response to standing after space flight. <i>J Appl Physiol</i> 1995; 79(2):428-433.
614	The Effect of Prolonged Space Flight on Head and Gaze Stability During Locomotion	<p>Bloomberg JJ, Reschke MF, Huebner WP, Peters BT. The effects of target distance on eye and head movement during locomotion. <i>Annals New York Acad of Sci</i> 1992; 656:699-707.</p> <p>Bloomberg JJ, Reschke MF, Huebner WP, Peters BT, Smith SL. Locomotor head-trunk coordination strategies following space flight. <i>J of Vestib Res</i> 1997; 7(2/3):161-177.</p> <p>Conley MS, Meyer RA, Bloomberg JJ, Feeback DL, Dudley GA. Non-invasive analysis of human neck muscle function. <i>Spine</i> 1995; 23:2505-2512.</p> <p>Glasauer S, Amorim MA, Bloomberg JJ, Reschke MF, Peters BT, Smith SL, Berthoz A. Spatial orientation during locomotion following space flight. <i>Acta Astronautica</i> 1995; 36:423-431.</p> <p>Layne CS, McDonald PV, Bloomberg JJ. Neuromuscular activation patterns during locomotion after space flight. <i>Exp Brain Res</i> 1997; 113: 104-116.</p> <p>McDonald PV, Basdogan C, Bloomberg JJ, Layne CS. Lower limb kinematics during treadmill walking after space flight: Implications for gaze stabilization. <i>Exp Brain Res</i> 1996; 112:325-224.</p> <p>McDonald PV, Bloomberg JJ, Layne CS. A review of adaptive change in musculoskeletal impedance during space flight and associated implications for postflight head movement control. <i>J. Vestib Res</i> 1997; 7(2/3): 239-250.</p> <p>Newman DJ, Jackson DK, Bloomberg JJ. Altered astronaut lower-limb and mass center kinematics in downward jumping following space flight. <i>Exp Brain Res</i> 1997; 117:30-42.</p> <p>Reschke MF, Bloomberg JJ, Harm DL, Paloski WH. Space flight and neurovestibular adaptation. <i>J of Clin Pharm</i> 1994; 34:609-617.</p>
617	Evaluation of Functional Skeletal Muscle Performance Following Space Flight	<p><i>In work:</i></p> <p>Hayes JC, McBrine JJ, Siconolfi SF. Analysis of velocity spectrum skeletal muscle performance following space flight (in preparation).</p>
618	Effects of Intense Exercise During Space Flight on Aerobic Capacity and Orthostatic Function	Moore AD, Lee SMC, Greenisen MC, Bishop P. Validity of a heart rate monitor during work in the laboratory and on the space shuttle. <i>American Industrial Hygiene Association Journal</i> . 1997; 58:299-301.

<i>DSO No.</i>	<i>Title</i>	<i>Publications</i>
622	Gastrointestinal Function During Extended Duration Space Flight	<p>Lane HW, LeBlanc AD, Putcha L, Whitson PA. Review: Nutrition and human physiological adaptations to space flight. <i>Am J Clin Nutri</i> 1993; 58:583-588.</p> <p>Nimmagudda RR, Putcha L. A method for preserving saliva samples at ambient temperatures. <i>Biochemical Archives</i> 1997; 13:171-178.</p> <p>Tietze KJ, Putcha L. Factors affecting drug bioavailability in space. <i>J Clin Pharm</i> 1994; 34:671-676.</p> <p><i>In work:</i></p> <p>Putcha L, DeKerlegand D, Kovachevich I. Gastrointestinal function changes during short and long duration space flight. (Submit to <i>Gut</i>).</p> <p>Putcha L, DeKerlegand D, Hutchinson K, Hargens A. Effect of antiorthostatic bed rest on gastrointestinal motility and absorption. (Submit to <i>J Appl Physiol</i>).</p> <p>Putcha L, Nimmagudda RR, Ramanathan R, Bourne DWA. Hepatic function during antiorthostatic bed rest and during space flight. (Submit to <i>J Appl Physiol</i>).</p>
626	Cardiovascular and Cerebrovascular Responses to Standing Before and After Space Flight	<p>Fritsch-Yelle JM, Whitson PA, Bondar RL, Brown TE. Subnormal norepinephrine release relates to presyncope in astronauts after spaceflight. <i>J Appl Physiol</i> 1996; 81(5):2134-2141</p>
904	Assessment of Human Factors	<p>Mount FE, Foley T. Human factors engineering (DSO 904): evaluations of space shuttle crew habitability and productivity. NASA publication in work.</p>